SOVIET PHYSICS

JETP

A translation of the Journal of Experimental and Theoretical Physics of the USSR.

SOVIET PHYSICS—JETP VOL. 4, NO. 6, PP 777-979 JULY, 1957

Electrodynamics of Charged Scalar Particles

L. P. GOR'KOV AND I. M. KHALATNIKOV

Institute for Physical Problems, Academy of Sciences, USSR

(Submitted to JETP editor November 23, 1955)

J. Exptl. Theoret. Phys. (U.S.S.R.) 31, 1062-1078 (December, 1956)

The behavior of the Green's function in the region of high momenta for the electrodynamics of spin-zero charged particles is investigated on the basis of the Kemmer formalism.

THE asymptotic behavior of the Green's function for high momenta has been found for spin-1/2 electrodynamics by Landau, Abrikosov, and Khalatnikov[1] by means of the direct solution of the integral equations. The same problem has been treated by Gell-Mann and Low[2], who made use of the renormalizability of the theory. The present work is a similar attempt for the electrodynamics of spin-zero particles in the Kemmer formalism.

1. β-FORMALISM

Two equivalent formulations can be used for the description of particles with spin zero and one: the second order Klein-Gordon equation and the matrix formalism of Kemmer. The latter is characterized by a deep analogy with the Dirac equation for the electron. In the β-formalism, the wave function of the spin-zero or spin-one particles satisfies a first order equation

$$(\hat{p} - m_1)\Psi(x) = 0,$$

where* $\hat{p} = p_k\beta_k$, p is the momentum operator, and the β-matrices satisfy the following commutation relations

$$\beta_\mu\beta_\sigma\beta_\nu + \beta_\nu\beta_\sigma\beta_\mu = \beta_\nu\delta_{\mu\sigma} + \beta_\mu\delta_{\sigma\nu}. \qquad (1)$$

The algebra determined by Eq. (1) has two nontrivial irreducible representations, a five-dimensional and a ten-dimensional one; the first corresponds to spin-zero particles, and the second to spin-one particles. From the point of view of the Klein-Gordon equation, the five-component function for the spin-zero particles consists of one scalar component and its four derivatives with respect to space and time. The components of the wave function are therefore not dynamically independent. This is related to the fact that the β-matrices determined by relations (1) have no inverses.

The interaction of mesons with an electromagnetic field can be described both in the Klein Gordon formalism and in the β-formalism. A very significant disadvantage of the scalar formulation is the extremely complicated structure of the perturbation theory series, due to diagrams with vertices connected by two photon lines. The Kemmer formalism is more convenient, since the class of diagrams possible in its perturbation theory is the same as that in the electrodynamics of electrons, so that the rules for constructing the matrix elements from the diagrams, as has been shown by Peasly,[4] are similar to Feynman's rules for electrodynamics[3] with the difference that the γ-matrices are everywhere replaced by the β-matrices, and the Feynman propagation factor

---

* In the following we shall use the notation of Feynman[3].

$(p - m_1)^{-1}$ is equal to

$$(\hat{p} - m_1)^{-1} = \{\hat{p} + m_1 + (\hat{p}^2 - p^2)/m_1\}(p^2 - m_1^2)^{-1}. \tag{2}$$

In addition, a meson closed loop enters the matrix element with the sign opposite to that in ordinary electrodynamics. The whole formalism is equally applicable to spin zero and to spin one. The difference between the two spins occurs in considering the convergence of the perturbation theory integrals.

It is well known[5] that all existing field theories may be divided into the renormalizable and nonrenormalizable ones. In the renormalizable theories there exist several types of irreducible divergent diagrams, and the infinite expressions due to these can be included in the physical constants of the theory in a unique way. In a nonrenormalizable theory the number of different kinds of divergent diagrams is infinite. The electrodynamics of vector mesons belongs to this class, which can be seen immediately from expression (2) for $G_0(p)$, since for large values of the momentum p this factor is approximately unity. We will therefore consider only spin-zero mesons, using the five-dimensional representation of the β-matrices. For spin zero the situation is simplified, since a large number of the matrix expressions vanish due to the properties of the five-dimensional representation of the β-matrices.

We shall define two matrices[6]

$$X = (\beta_\lambda\beta_\lambda - 1)/3; \quad Y = (4 - \beta_\lambda\beta\ )/3; \quad X + Y = 1. \tag{3}$$

For spin zero

$$XY = 0, \tag{4}$$

$$X\beta_\nu\beta_\mu = \delta_{\mu\nu}X. \tag{5}$$

We present several useful expressions which follow immediately from (1), (3)-(5):

$$X\beta_\mu = \beta_\mu Y; \quad \beta_\mu(\hat{p}^2 - p^2)\beta_\nu = X(p_\mu p_\nu - \delta_{\mu\nu}p^2); \tag{6}$$

$$X(\hat{p}^2 - p^2) = 0; \quad \beta_\mu\beta_\mu = 3X + 1; \quad \beta_\mu\beta_\sigma\beta_\mu = \beta_\sigma;$$

$$\beta_\mu\beta_\sigma\beta_\tau\beta_\mu = \delta_{\sigma\tau}; \quad \beta_\mu\beta_\sigma\beta_\tau\beta_\rho\beta_\mu = X\beta_\sigma\delta_{\rho\tau} + \beta_\rho X\delta_{\sigma\tau}.$$

In calculating traces, we must bear in mind that the trace of a product of an odd number of β-matrices vanishes. In addition,

$$\mathrm{Sp}\,1 = 5; \quad \mathrm{Sp}\,X = 1; \quad \mathrm{Sp}\,\beta_\lambda\beta_\mu = 2\delta_{\lambda\mu}; \quad \mathrm{Sp}\,\beta_\lambda\beta_\mu\beta_\nu\beta_\rho = \delta_{\lambda\mu}\delta_{\nu\rho} + \delta_{\lambda\rho}\delta_{\mu\nu}. \tag{7}$$

Consideration of the perturbation theory expressions shows[6] that in the electrodynamics of a spin-zero meson there exist in general five irreducibly divergent diagrams: 1) and 2) the self-energy diagrams of the meson and photon, which are quadratically divergent; 3) the vertex part, which is logarithmically divergent; 4) a Compton type diagram, which is logarithmically divergent; 5) the diagram corresponding to scattering of a meson by a meson, which is logarithmically divergent.

Scattering of light by light gives a finite expression when summed over all permutations of the emitted quanta.

2. FUNDAMENTAL EQUATIONS

The character of the divergence which appears in the theory is determined by the asymptotic behavior of the Green's function for high momenta. Two of the articles already cited[1,2] are devoted to the problem of finding the asymptotic behavior of the Green's functions in electrodynamics and in pseudoscalar theory. In solving the corresponding problem in the electrodynamics of spin-zero particles, we shall henceforth base our considerations on the idea of a smeared out interaction[1], according to which the interaction which is usually described by a δ-function is assumed smeared out and nonvanishing in some finite region whose linear dimensions are about a. In calculating radiation effects, integration over virtual quanta is cut off at momenta $\sim \Lambda$ where $(\Lambda \sim 1/a)$, and the integrals are then finite. The transition to the exact interaction corresponds to $\Lambda \to \infty$.

Let us write the integral equations which are satisfied by the quantities entering into the theory. The equation for the meson Green's function $G(p)$ can be written, in complete analogy with the usual electrodynamics, in the following way[7]

$$G(p)\left\{\hat{p} - m_1 - (e_1^2/\pi i) \times \int B_\mu(p, p-k, k)\, G(p-k)\,\beta_\nu D_{\mu\nu}(k)\, d^4k\right\} = 1. \tag{8}$$

Here m_1 is the "bare" mass, e_1 is the "bare" meson charge, and $B_\mu(p, p-k, k)$ is the operator of the vertex part. The photon propagation factor $D_{\mu\nu}(k)$ as has previously been noted[1], can be written as the sum of the transverse and longitudinal parts

$$D_{\mu\nu}(k)=\left(\delta_{\mu\nu}-\frac{k_\mu k_\nu}{k^2}\right)\frac{d_t(k^2)}{k^2}+\frac{k_\mu k_\nu}{k^2}\frac{d_l(k^2)}{k^2}, \quad (9)$$

of which only the transverse part has physical meaning for the interaction; it must therefore be determined from the equations, whereas the longitudinal part may be chosen arbitrarily. The equation for the transverse part of the photon Green's function is of the form

$$D^t_{\mu\sigma}(k)\left\{k^2\delta_{\sigma\nu}-\frac{e_1^2}{\pi i}\int \mathrm{Sp}\,[G(p)B_\sigma(p,p-k,k) \quad (10)$$

$$\times G(p-k)\beta_\nu]\,d^4p\right\}=\delta_{\mu\nu}-\frac{k_\mu k_\nu}{k^2}.$$

The gauge invariance of the theory should follow directly from the transverse nature of the polarization tensor in this equation. Let us also note that the different sign for the integral term in Equation (10), as compared with the electro-dynamics of an electron, is related to the Bose statistics for spin-zero particles. Equations (8) and (10) for the Green's functions of an interacting meson and photon are exact and contain no approximations. The situation with respect to the equations for the operators of the vertex parts and the Compton diagrams is much more complicated. It is in general impossible to obtain exact integral equations for them in closed form. It turns out, however, that for certain conditions it is possible to write an approximate integral equation for the operator of the vertex part. In order to do this, let us go over to a consideration of the expressions furnished by perturbation theory. We shall write the expression for the meson Green's function obtained from perturbation theory to first order in e_1^2 in the high momentum region (for the space-components, $-p^2 >> m^2$) up to terms containing a large logarithm

$$G^{-1}(p)=\hat{p}-m_1+\left(\frac{3X}{m_1}\right)\left(\frac{e_1^2}{\pi i}\right)\int\frac{d^4k}{k^2} \quad (11)$$

$$-\left(\frac{e_1^2}{8\pi}\right)(\hat{p}+2m_1)\ln\left(\frac{\Lambda^2}{-p^2}\right)$$

$$+\left(\frac{e_1^2}{16\pi}\right)\Big[\hat{p}-m_1$$

$$+\left(\frac{3X}{m_1}\right)(p^2-m_1^2)\Big]\ln\left(\frac{\Lambda^2}{-p^2}\right)(d_l-1).$$

Calculation of the matrix elements for the first order correction to the vertex part leads to the following asymptotic expression for $B_\sigma(p,\,p-l,\,l)$ for large space components, the largest of which we shall call f:

$$B_\sigma(p,p-l,l)=\beta_\sigma-\frac{e_1^2}{8\pi}\beta_\sigma\ln\left(\frac{\Lambda^2}{-f^2}\right) \quad (12)$$

$$+\frac{e_1^2}{16\pi}\left[\beta_\sigma+\frac{3X}{m_1}(2p-l)_\sigma\right]\ln\left(\frac{\Lambda^2}{-f^2}\right)(d_l-1).$$

As can be seen from these expressions, not only the longitudinal, as for ordinary electrodynamics, but also the transverse part of the photon Green's function leads to terms logarithmic in the meson self-energy and vertex parts. The last (third) term in Eq. (12) shows, in view of the Ward identity, that the logarithmic divergence in the radiation corrections to the Compton effect occur only in combination with the factor $d_l - 1$. This result can also be obtained by considering the matrix element of the first correction to the Compton effect (Appendix I). Thus with the choice $d_l = d_t$ the Compton diagrams are finite in first order perturbation theory, and give no logarithmic contribution. It is interesting to note that this situation follows from the use of the β-formalism; to one diagram for the correction to the Compton effect in the Kemmer formalism corresponded several diagrams in the second order equations, each of which diverges separately. Only for the special choice $d_l = d_t$ is their β-matrix sum finite.

Except for the quadratically diverging integrals in the meson and photon mass, the perturbation theory series thus contains only logarithmic terms in the limiting momentum. Use of perturbation theory effectively implies a condition $e_1^2\ln(\Lambda^2/m^2) << 1$. We shall, following an earlier work[1], use the much weaker condition $e_1^2 << 1$. Subjecting the theory to such a limitation means that in the asymptotic region we must sum only over those diagrams whose contribution to the matrix elements contains the large logarithm raised to a power equal to the perturbation theory order. In this approximation the Compton diagrams in all perturbation theory orders are the same as in the zeroth approximation (for $d_l = d_t$; this assumption, based at this point on calculations to the first approximation in e_1^2 is later verified by the expression obtained for the operator of the vertex part). For the vertex part $B_\sigma(p,\,p-l,\,l)$ we can write the approximate integral (so-called three-vertex) equation

$$B_\sigma(p,p-l,l)=\beta_\sigma+(e_1^2/\pi i) \quad (13)$$

$$\times\int B_\mu(p,p-k,k)G(p-k)B_\sigma(p-k,p-k-l,l)$$

$$\times G(p-k-l)B_\mu(p-k-l,$$

$$p-l,-k)D(k)\,d^4k.$$

This equation expresses the fact that in summing the radiation corrections to the vertex part, only diagrams with nonintersecting photon lines are accounted for, and is derived on the assumption that the longitudinal part of the photon Green's function is chosen equal to its transverse part ($d_l = d_t$). In other words

$$D_{\mu\nu}(k) = \delta_{\mu\nu} D(k) = \delta_{\mu\nu} d_t(k^2)/k^2.$$

Direct calculations show that the second order diagram in e_1^2 with two intersecting photon lines gives no contribution in this approximation (Appendix I). Let us note also that the matrix element for scattering of a meson by a meson is not "linked" with the fundamental equations and can be considered separately.

In the following sections Equations (8), (10), and (13) will be used to find the asymptotic forms of the photon and meson Green's functions.

3. PHOTON GREEN'S FUNCTION

Let us now go on to a solution of the above equations. We should note that the matrix composition of the exact Green's functions for the meson and vertex parts will not in general, as can be seen, for instance, from expression (11), be the same as the corresponding expressions for these quantities in the zeroth approximation for noninteracting fields. Considerations of relativistic invariance, although they narrow the possible matrix combinations, still leave a sufficient number of different invariant combinations both in the meson Green's function and, especially, in the vertex part. The reason for this is the triple (and not double, as in ordinary electrodynamics) permutation rules, so that a large number of invariants are independent. For $d_l = d_t$, however, a consideration of the perturbation theory formulas (11) and (12) allow us to assume that in the high-momentum region the meson Green's function $G(p)$ and the vertex part $B_\sigma(p, p-l, l)$ can be written in the following form:

$$G^{-1}(p) = \left\{\hat{p} - m_1(p^2) - \frac{X\epsilon}{m_1}\right\}\left(\frac{1}{\beta(p^2)}\right); \tag{14}$$

$$B_\sigma(p, p-l, l) = \beta_\sigma \alpha(f^2).$$

Here $\beta(p^2)$, $\alpha(f^2)$, and $m_1(p^2)$ are slowly (logarithmically) varying functions of their arguments, $m_1(p^2)$ is proportional to the "bare" mass m_1 of the meson. and f is the largest of the three arguments in $B_\sigma(p, p-l, l)$. The quantity ϵ in the expression for $G(p)$ is of order $\sim e_1^2\Lambda^2$, where Λ is the upper limit of the interaction, and is the quadratic correction to the mass. We note that the operator which is the inverse of $(\hat{p} - m_1 - XA/m_1)$ is equal to

$$\left(\hat{p} - m_1 - \frac{XA}{m_1}\right)^{-1} \tag{14a}$$

$$= \left\{\hat{p} + m_1 + \frac{1}{m_1}(\hat{p}^2 - p^2) + \frac{YA}{m_1}\right\}\frac{1}{p^2 - m_1^2 - A}.$$

We have already seen in Eq. (11) that ϵ comes from the transverse part of the photon Green's function. It is significant that the quantity ϵ drops out of all further calculations, so that it effects only a change in mass. In our approximation ϵ may be considered constant. We make the following additional remark: in integral equations (8), (10), and (13) the high momentum region is of fundamental importance. Therefore in order to calculate these integrals we must know the behavior of all the functions in the high momentum region. This makes it possible to determine the variation of all quantities in the asymptotic region, for this approximation, without considering regions of momentum small compared to the meson mass. In addition, after all intermediate operations the integrands can be written as the sum of various combinations of matrices multiplied by a scalar function whose argument is of the form $(k-a)^2$, where a may be any of the vectors in Eqs. (8), (10), and (13). These functions have no singularities in the upper half plane. If a is a spacelike vector, then integration over k may be replaced by integration over four-dimensional Euclidean space by replacing k_0 by ik_0. Therefore in solving the equations which determine $G(p)$, $B_\sigma(p, p-l, l)$, $D(k)$, we may limit ourselves to the region of spacelike vectors. For timelike arguments, these functions may be obtained by analytic continuation through the upper half plane. In those regions of integration over k which give the main contribution (logarithmic) to arguments of the form $(k-a)^2$, we may neglect a in comparison with k, and therefore all the functions will depend on k^2; the transition to integration over Euclidean space is accomplished particularly simply:

$$d^4k \rightarrow i/4\,(-k^2)\,d(-k^2). \tag{15}$$

The importance of this transformation was first noted by Landau and co-workers[1]. Turning to Equation (13), let us replace $G(p)$ and $B_\sigma(p, p-l, l)$ by the corresponding expressions from (14). It is easy to see that the integral diverges logarithmically in the region $-f^2 \ll -k^2 \ll \Lambda^2$, where f is the largest of the arguments of the vertex part.

Bringing similar terms into the numerator, going over to integration over Euclidean space, and averaging over angles, the integral on the right side becomes

$$-\beta_\sigma \frac{e_1^2}{8\pi} \int\limits_{-k^2 \gg -f^2}^{-k^2 \ll \Lambda^2} \alpha^3(-k^2)\,\beta^2(-k^2)\,d(-k^2)\,\frac{d-k^2}{-k^2}$$

in agreement with the assumption that the right side of Eq. (13) is again proportional to B_σ. This also verifies the validity of both expressions (14), since $G(p)$ and $B_\sigma(p,\ p-l,\ l)$ are related by the Ward identity

$$\partial G^{-1}(p)\,/\,\partial p_\sigma = B_\sigma(p, p, 0).$$

The function α satisfies the following equation:

$$\alpha(\xi) = 1 - \frac{e_1^2}{8\pi}\int\limits_{\xi}^{L} \alpha^3(z)\,\beta^2(z)\,d(z)\,dz. \tag{16}$$

Here we have introduced the new variable $z = \ln(-k^2/m^2)$ so that $\epsilon = \ln(-f^2/m^2)$ and $L = \ln(\Lambda^2/m^2)$.

The equation which determines the function $\beta(p)$ should be obtained from (8); however, since the integral contains a quadratically diverging part, in order to obtain the logarithmic terms in it, it is necessary to have not only expressions (14) for $B_\mu(p,\ p-k,\ k)$, but the contributions to it up to terms of the order of about p^2/k^2 inclusive. For simplicity, we shall use the Ward identity, which we write in the form

$$\alpha(\xi)\,\beta(\xi) = 1. \tag{17}$$

With the aid of this expression, Eq. (16) can be written

$$\alpha(\xi) = 1 - \frac{e_1^2}{8\pi}\int\limits_{\xi}^{L} \alpha(z)\,d(z)\,dz. \tag{18}$$

Eq. (10) for the photon Green's function contains a quadratically diverging integral. The quadratically diverging part can be separated, and represents the photon mass. Because of the gauge invariance of the theory, the interaction should be smeared out in such a way that this quantity remain zero. The remaining part again contains logarithmic integrals, and in order to calculate these it is necessary to know the logarithmic corrections to the vertex parts $B_\sigma(p,\ p-l,\ l)$ in the region $p \gg l$ accurately to terms of second order in l/p inclusive. To obtain this information we again refer to Eq. (3), replacing the variable $p-k$ by k:

$$\begin{aligned} &B_\sigma(p, p-l, l) \\ &= \beta_\sigma + \frac{e_1^2}{\pi i}\int B_\mu(p, k, p-k)\,G(k)\,B_\sigma(k, k-l, l) \\ &\times G(k-l)\,B_\mu(k-l, p-l, k-p)\,D(p-k)\,d^4k. \end{aligned} \tag{19}$$

Inserting Eq. (14) for the appropriate factors, and multiplying out the numerator of the integrand, we see that the appropriate terms occur on the right side for the region of integration $p \gg k \gg l$ in expanding $B_\sigma(k,\ k-l,\ l)$ and the denominators of $G(k)$ and $G(k-l)$. Expanding the rest of the factors, as can be easily seen, leads to higher order terms. In order to clarify the form of the corrections in this region, let us consider the additions which come from expanding the denominators in $G(k)$ and $G(k-l)$ in powers of l/k, $(m_1^2+\epsilon)/k^2$. It turns out that the corresponding term is of the form

$$\frac{e_1^2}{24\pi}(\hat{l}l_\sigma - \beta_\sigma l^2)\ (p^{-2})\,\alpha^2(\xi)\,d(\xi)\int\limits_{\eta}^{\xi}\beta^2(z)\,\alpha(z)\,dz,$$

$$\xi = \ln(-p^2/m^2), \quad \eta = \ln(-l^2/m)^2.$$

We shall try to obtain $B_\sigma(p,\ p-l,\ l)$ in the region $p \gg l$ in the form

$$\begin{aligned} B_\sigma(p, p-l, l) &= \beta_\sigma\alpha(p^2) \\ &+ (l\hat{l}_\sigma - \beta_\sigma l^2)\ (p^{-2})\,\alpha^2(p^2)\,d(p^2)\,S_0(p^2, l^2). \end{aligned} \tag{20}$$

We then obtain the following equation (in closed form) for the function $S_0(\xi,\eta)$:

$$\begin{aligned} S_0(\xi,\eta) = &-\frac{e_1^2}{8\pi}\int\limits_{\eta}^{\xi}\alpha^2(z)\,\beta^2(z)\,d(z)\,S_0(z,\eta)\,dz \\ &+ \frac{e_1^2}{24\pi}\int\limits_{\eta}^{\xi}\alpha(z)\,\beta^2(z)\,dz. \end{aligned} \tag{21}$$

Corrections of other forms do not occur.

If we insert (20) into expression (10) for the polarization tensor, we obtain an equation which determines the function $d_t = d_l$

$$d_t^{-1}(\eta) = 1 + 2S_0(L, \eta), \tag{22}$$

where L is the logarithm of the cut-off parameter.

Equations (18), (21) and (22) must be solved simultaneously. With the aid of the Ward identity, Eq. (21) can be written

$$S_0(\xi,\eta) = -\frac{e_1^2}{8\pi}\int_\eta^\xi d(z)\,S_0(z,\eta)\,dz + \frac{e_1^2}{24\pi}\int_\eta^\xi \beta(z)\,dz.$$

Differentiating this by ξ, we obtain

$$\partial S_0(\xi,\eta)/\partial\xi = -(e_1^2/8\pi)\,d(\xi)\,S_0(\xi,\eta) + (e_1^2/24\pi)\,\beta(\xi).$$

But

$$d\beta(\xi)/d\xi = -(e_1^2/8\pi)\,d(\xi)\,\beta(\xi), \tag{23}$$

and therefore

$$\partial[S_0(\xi,\eta)\,\beta^{-1}(\xi)]/\partial\xi = e_1^2/24\pi$$

and with the conditions $S_0(\xi,\xi) = 0$, we obtain

$$S_0(\xi,\eta) = (e_1^2/24\pi)(\xi-\eta)\,\beta(\xi).$$

Since $\beta(L) = 1$, we have $S_0(1,\eta) = (e_1^2/24\pi) \times (L-n)$. It is interesting to note that $S_0(L,\eta)$ is exactly identical with the same function in spinor electrodynamics. We note in this respect that in addition to the polarization of spin-zero particles by the photon, there actually occurs also a polarization of the spin 1/2 particles. Therefore, instead of (10), we should have written the photon Green's function equation in the form

$$D^t_{\mu\sigma}(k)\left\{k^2\delta_{\sigma\nu} - \left(\frac{e_1^2}{\pi i}\right) \times \int \mathrm{Sp}\,[G^0(p)\,B_\sigma(p, p-k, k)\,G^0(p-k)\,\beta_\nu]\,d^4p + \left(\frac{e_1^2}{\pi i}\right)\int \mathrm{Sp}[G^{1/2}(p)\,\Gamma_\sigma(p, p-k, k) \times G^{1/2}(p-k)\,\gamma_\nu]\,d^4p\right\} = \delta_{\mu\nu} - \frac{k_\mu k_\nu}{k^2}.$$

Making use of previously derived results[1], we can write down immediately

$$d_t^{-1}(\eta) = 1 + 8\nu S(L,\eta).$$

The quantity ν, here introduced, plays the role of the effective number of different particles. Spin-1/2 gives 1 for ν, and spin zero, 1/4. Thus

$$d_t(\eta) = [1 + (e_1^2/3\pi)\,\nu\,(L-\eta)]^{-1}$$

or

$$d_t(k^2) = [1 + (e_1^2/3\pi)\,\nu \ln(\Lambda^2/-k^2)]^{-1}. \tag{24}$$

We note that this formula is valid not only for $k >> m$, but also for $k \gtrsim m$, since in the calculation both m_1 and ϵ drop out. For $-k^2 << m^2$

$$d_t(k^2) = [1 + (e_1^2/3\pi)\,\nu \ln(\Lambda^2/m^2)]^{-1}$$

which corresponds to the fact that the logarithmic region of integration in Eq. (10) lies* above m.

The physical charge is given by

$$e^2 = e_1^2[1 + (e_1^2/3\pi)\,\nu \ln(\Lambda^2/m^2)]^{-1}. \tag{25}$$

The expression we obtain for the "bare" charge e_1^2 is then

$$e_1^2 = e^2[1 - (e^2/3\pi)\,\nu \ln(\Lambda^2/m^2)]^{-1}. \tag{26}$$

For a sufficiently large radius of interaction $(e^2/3\pi)\nu\ln\Lambda^2/m^2 \sim 1$, and the bare charge e_1^2 becomes of the order of unity in contradiction to the original assumption of weak interaction ($e_1^2 << 1$). As has been shown by Pomeranchuk[8], this restriction is not of importance, as Eq. (25) is the exact result for large Λ^2. From this we obtain the fundamental conclusion that in the point-interaction limit ($\Lambda \to \infty$) the physical charge vanishes (for more details see Pomeranchuk[8]).

The interaction $e_1^2 d_t$ can be written in a form containing only renormalized quantities

$$e_1^2 d_t(k^2) \equiv e^2 d_{tc}(k^2) = e^2[1 - (e^2/3\pi)\,\nu \ln(-k^2/m^2)]^{-1}. \tag{27}$$

4. MESON GREEN'S FUNCTION

With the function $d(p^2)$ obtained, it is easy to derive the formula for $\beta(p^2)$ from Eq. (18):

$$\beta(p^2) = [1 + (e_1^2/3\pi)\,\nu \ln(\Lambda^2/-p^2)]^{3/8\nu}. \tag{28}$$

The function $\alpha(p^2) = 1/\beta(p^2)$. We note that the function $\beta(p^2)$ can be written as the product of a constant and a function independent of the cut-off parameter,

$$\beta(p^2) = (e_1/e)^{3/4\nu} \times [1 - (e^2/3\pi)\,\nu \ln(-p^2/m^2)]^{3/8\nu} = [e_1^2 d_t(p^2)/e_1^2]^{-3/8\nu}. \tag{29}$$

---

* We are here neglecting the difference between the meson and electron masses.

In this form $\beta(p^2)$ decreases as $-p^2$ increases, and becomes small at the same point where the denominator of expression (27) vanishes. Equation (29) expresses the so-called renormalizability of the function $\beta(p^2)$.

Let us write down the meson Green's function $G(p)$ for large momenta

$$G(p) = \Big\{\hat{p} + m_1(p^2) + \frac{1}{m_1(p^2)}(\hat{p}^2 - p^2) - \frac{Y\varepsilon}{m_1}\Big\}\frac{\beta(p^2)}{p^2}.$$

In the β-formalism $G(p)$ consists of a scalar, a vector, and a tensor component. The dependence of each of these components on the radius of cut-off Λ is different. Using a special and simply derivable representation of the β-matrices, which establishes the relation between the Klein-Gordon equation and the Kemmer equation*, we can separate out the scalar component

$$G_{55}(p) \approx \beta(p^2)\, m_1(p^2) / p^2, \tag{30a}$$

The vector component

$$G_{i5}(p) \approx \beta(p^2)(p_i / p^2) \tag{30b}$$

and the tensor component

$$G_{ik}(p) \approx \frac{\beta(p^2)}{m_1(p^2)}\left(\frac{p_i p_k}{p^2} - \delta_{ik}\right) \tag{30c}$$

in the region $-p^2 \gg m^2$. In these expressions, in addition to $\beta(p^2)$, the function $m_1(p^2)$ also enters. We shall not try to find an equation for $m_1(p^2)$, but shall make use of the fact that, as can be seen from the expression for the meson Green's function in coordinate space[9],

$$G(x, x') = \langle T(\Psi(x), \overline{\Psi}(x'))\rangle_0 - (i/m_1)(1 - \beta_0^2)\,\delta(x - x')$$

the component $G_{55}(p)/m_1$ for our representation of the β-matrices is the meson propagation kernel in the scalar formulation of the theory. The asymptotic behavior of this quantity can be determined by the method of Gell-Mann and Low[2]. The applicability of this method to one or another theory of interacting fields depends on whether or not this theory refers to quantities renormalized in the sense of Z-factors. Let us bear in mind that the requirement of the renormalizability means the following. Assume that certain functions, say $f_i(p^2)$, referring to the particle Green's function and the vertex parts appear in the theory. We construct some combination $H(p^2)$ of these functions, such that $g_1 H(p^2)$ represents an interaction, where g_1 is the bare coupling constant. Let Λ be the interaction cut-off radius, chosen so that $f_i(\Lambda^2) = 1$. The requirement of renormalizability means that the function $f_i(p^2)$ differs only by some factor from a function independent of the cut-off radius

$$f_i(p^2/\Lambda^2, g_1) = f_{ic}(p^2/m^2, g)/f_{ic}(\Lambda^2/m^2, g) \tag{31}$$

(for large values of $-p^2$, the function f_i depends only on the ratio $-p^2/\Lambda^2$). The renormalized interaction constant is determined by the condition

$$g_1 = g H_c(\Lambda^2/m^2, g).$$

It can then be shown[2] that the following relation holds:

$$g_1 H(-p^2/\Lambda^2, g_1) = F(-\varphi(g_1)\, p^2/\Lambda^2),$$

where F and φ are inverse functions: $F[\varphi(x)] = x$.

Equation (31) is not trivial. We shall see later that in the Kemmer formalism for $d_l \neq d_t$ by no means do all functions satisfy Eq. (31). In the scalar formulation, however, this relation holds; Eq. (29) shows that this is valid both with relation to the function $\beta(p^2)$ in our approximation and for the condition $d_l = d_t$. We shall present all the calculations anew in this case, using only (31). We then have

$$e_1^2 d_t(k^2) = F(-\varphi(e_1^2)\, k^2/\Lambda^2). \tag{32}$$

Inverting this expression and taking logarithms, we obtain

$$\ln\varphi(e_1^2 d_t) - \ln\varphi(e_1^2) = \ln(-k^2/\Lambda^2).$$

Expanding the left side of this equation in powers of $e_1^2(d_t - 1)$ and taking only the first term, we obtain

$$\frac{1}{\varphi(e_1^2)}\frac{d\varphi(e_1^2)}{de_1^2}\, e_1^2(d_t - 1) = \ln\frac{-k^2}{\Lambda^2}. \tag{33}$$

The quantity $d_t - 1$ may be found by perturbation theory. Vacuum polarization for spin 1/2 particles gives the following value for $d_t - 1$ in the first approximation: $(e_1^2/3\pi)\ln(-k^2/\Lambda^2)$, vacuum polarization for spin zero particles:

---

* This representation is $(\beta_\mu)_{\alpha\tau} = \delta_{\mu\alpha}\delta_{5\tau} + \delta_{\mu\tau}\delta_{5\alpha}$; $(\mu = 1 \ldots 4;\ \alpha\tau = 1 \ldots 5)$.

$$(e_1^2/12\pi)\ln(-k^2/\Lambda^2);$$

introducing again the quantity ν, we obtain $d_t - 1 = (e_1^2/3\pi)\nu\ln(-k^2/\Lambda^2)$. . Inserting this expression in (32) gives a differential equation for the function $\varphi(x)$

$$\varphi^{-1}(x)\,d\varphi(x)/dx = (3\pi/\nu)\,x^{-2},$$

whose solution is $\varphi(x) = \exp(-3\pi/\nu x)$, and for the inverse function $F(x)$

$$F(x) = -(3\pi/\nu\ln x),$$

which leads again to Eq. (24), which was obtained by solving the integral equations.

If the functions $\beta(p^2)$ and $m_1(p^2)/m_1$ are renormalizable, then it follows from Eq. (32) that they can be written in the following form:

$$\beta(p^2) = H[e_1^2 d_t]/H[e_1^2]; \tag{34}$$

$$m_1(p^2)\beta(p^2)/m_1 = Q[e_1^2 d_t]/Q[e_1^2].$$

At the same time, perturbation theory, according to (11), leads to the following expression:

$$\beta(p^2) \approx 1 - (e_1^2/8\pi)\ln(-p^2/\Lambda^2); \tag{35}$$

$$m_1(p^2)\beta(p^2)/m_1 \approx 1 - (e_1^2/2\pi)\ln(-p^2/\Lambda^2).$$

Taking logarithms in expression (34), expanding in powers of $e_1^2(d_t - 1)$ and comparing with (35), we obtain the following equations for the functions $H(x)$ and $Q(x)$, $H^{-1}(x)\,dH(x)/dx = -(3/8\nu)\,x^{-1}$; $Q^{-1}(x)\,dQ(x)/dx = -(3/2\nu)\,x^{-1}$, whose solutions are

$$H(x) = x^{-3/8\nu}; \quad Q(x) = x^{-3/2\nu},$$

which gives the previous expression (28) for the function $\beta(p^2)$, and for $m_1(p^2)$ gives the following result:

$$m_1(p^2) = m_1[1 + (e_1^2/3\pi)\nu\ln(\Lambda^2/-p^2)]^{9/8\nu} \tag{36}$$

or

$$m_1(p^2) = [e_1^2 d_t/e_1^2]^{-9/8\nu}$$

$$= (e_1/e)^{9/4\nu}[1 - (e_1^2/3\pi)\nu\ln(-p^2/m^2)]^{9/8\nu}.$$

Knowing the functions $m_1(p)$ and $\beta(p^2)$ we can write an expression for all components of the meson Green's function for $-p^2 \gg m^2$.

For the scalar component

$$G_{55}(p) \approx m_1[1 + (e_1^2/3\pi)\nu\ln\Lambda^2/-p^2]^{3/2\nu}(1/p^2), \tag{37a}$$

For the vector component

$$G_{i5}(p) \approx [1 + (e_1^2/3\pi\nu)\ln\Lambda^2/-p^2]^{3/8\nu}(p_i/p^2) \tag{37b}$$

and, finally, for the tensor component

$$G_{ik}(p) \approx \frac{1}{m_1}[1 + (e_1^2/3\pi)\nu\ln\Lambda^2/-p^2]^{-3/4\nu}\left(\frac{p_i p_k}{p^2} - \delta_{ik}\right). \tag{37c}$$

Thus when used for all the components of the meson Green's function, method (2) leads to the same results as the direct solution of the integral equations. We emphasize, however, that in the β-formalism, the use of this method requires preliminary proof of the renormalizability by solving the integral equations. Equation (31) is satisfied for all the functions only in the approximation we are considering and for the special choice $d_l = d_t$. For arbitrary d_l, Eq. (31) is not satisfied even in the first approximation. We are not, of course, referring to the function $m_1(p^2)$.

5. GAUGE TRANSFORMATION FOR THE MESON GREEN'S FUNCTION

The equations of electrodynamics remain invariant under the following transformation of the four-dimension potential

$$A_\mu(x) \to A_\mu(x) + \partial\varphi(x)/\partial x_\mu$$

with the simultaneous transformation of the particle wave function according to

$$\psi(x) \to e^{ie\varphi(x)}\psi(x),$$

and therefore an electromagnetic field operator can be separated into its transverse and longitudinal parts. The longitudinal part of the electromagnetic field operator may be arbitrary in view of gauge invariance, and does not interact (commutes) with all other quantities. For the photon Green's function this separation leads to expression (9). Gauge transformation of charged particle Green's functions has been studied by Landau and Khalatnikov[10] and is given by the following formula

$$G(x, x') = G_0(x, x')\exp\{ie_1^2(\Delta_F(0) - \Delta_F(x - x'))\},$$

where $G_0(x, x')$ is the corresponding Green's function in the absence of scalar quanta, and

$$\Delta_F(x-x') = i\langle T(\varphi(x), \varphi(x'))\rangle_0.$$

In momentum space it is more convenient to make use of another result of the same work[10], which was obtained for the infinitesimal gauge transformation

$$\delta G(p) = \frac{ie^2_1}{\pi}\int\{G(p)-G(p-k)\}\frac{\delta d_l(k^2)\,d^4k}{(k^2)^2}.$$

Restricting ourselves to slowly varying functions $d_l(k2)$, we see that this integral diverges logarithmically in the region $-k^2 \gg \mp p^2$. Let us write this relation for the scalar component $G_{55}(p)$:

$$\delta G_{55}(p) = \frac{ie_1^2}{\pi}\int\limits_{\gg p^2} G_{55}(p)\frac{\delta d_l(k^2)\,d^4k}{(k^2)^2}.$$

Transforming this to integration over Euclidean space and writing $Z = \ln(-k^2/m^2)$, we obtain

$$\delta G_{55}(p) = -\frac{e_1^2}{4\pi}G_{55}(p)\int\limits_{\ln(-p^2/m^2)}^{\ln(\Lambda^2/m^2)}\delta d_l(z)\,dz.$$

This relation should be integrated with the boundary condition that for $d_l = d_t\, G_{55}(p)$ it gives Eq. (37a). The result is then

$$G_{55}(p) \approx m_1[d_t(-p^2)]^{-9/8\nu} \tag{38a}$$

$$\times\exp\left\{-\frac{e_1^2}{4\pi}\int\limits_{\ln(-p^2/m^2)}^{\ln(\Lambda^2/m^2)}d_l(z)\,dz\right\}(1/p^2).$$

In exactly the same way we can obtain expressions for the vector components $G_{i5}(p)$ for $-p^2 \gg m^2$

$$G_{i5}(p) \approx [d_t(-p^2)]^{-9/8\nu} \tag{38b}$$

$$\times\exp\left\{-\frac{e_1^2}{4\pi}\int\limits_{\ln(-p^2/m^2)}^{\ln(\Lambda^2/m^2)}d_l(z)\,dz\right\}(p_i/p^2).$$

This shows that the difference between the exact functions and the interacting field functions does not arise only from the gauge transformation, which is not the case in electron electrodynamics. We note that according to (30), (36), and (38) the function $m_1(p^2)$ does not depend on d_l, since the vector and scalar components of $G(p)$ transform in the same way under a gauge transformation. This, furthermore should have been expected, since the function $m_1(p^2)$ gives a contribution to the experimental meson mass m

$$m^2 = m_1^2(m^2) + \varepsilon.$$

The tensor component of the meson Green's function for arbitrary d_l cannot now be written in the form of Eq. (30c). For $-p^2 \gg m^2$, however, it can always be represented in the form

$$G_{ik}(p) \approx \frac{1}{m_1}\left[\left(\frac{p_ip_k}{p^2}-\frac{1}{4}\delta_{ik}\right)\lambda(p^2) - \frac{3}{4}\delta_{ik}\mu(p^2)\right]. \tag{38c}$$

Let us write the equation for an infinitesimal gauge transformation of the tensor component

$$\left[\left(\frac{p_ip_k}{p^2}-\frac{1}{4}\delta_{ik}\right)\delta\lambda(p^2) - \frac{3}{4}\delta_{ik}\delta\mu(p^2)\right]$$
$$= \frac{ie_1^2}{\pi}\int\left\{\left(\frac{p_ip_k}{p^2}-\frac{1}{4}\delta_{ik}\right)\lambda(p^2) - \frac{3}{4}\delta_{ik}\mu(p^2) - \left(\frac{k_ik_k}{k^2}-\frac{1}{4}\delta_{ik}\right)\lambda(k^2) + \frac{3}{4}\delta_{ik}\mu(k^2)\right\}\frac{\delta d_l(k^2)\,d^4k}{(k^2)^2},$$

from which we obtain, after averaging over angles

$$\delta\lambda(\xi) = -\frac{e_1^2}{4\pi}\lambda(\xi)\int\limits_{\xi}^{L}\delta d_l(z)\,dz, \tag{39a}$$

$$\delta\mu(\xi) = -\frac{e_1^2}{4\pi}\int\limits_{\xi}^{L}[\mu(\xi)-\mu(z)]\,\delta d_l(z)\,dz, \tag{39b}$$

$$\xi = \ln(-p^2/m^2),\quad L = \ln(\Lambda^2/m^2).$$

With the boundary condition (37c) we obtain the following expression for the function $\lambda(p)$:

$$\lambda(p^2) = \exp\left\{-\frac{e_1^2}{4\pi}\int\limits_{\ln(-p^2/m^2)}^{\ln(\Lambda^2/m^2)}d_l(z)\,dz\right\}. \tag{40}$$

Differentiating Eq. (39) by ξ

$$\delta\frac{d\mu(\xi)}{d\xi} = -\frac{e_1^2}{4\pi}\frac{d\mu(\xi)}{d\xi}\int\limits_{\xi}^{L}\delta d_l(z)\,dz$$

and making use of boundary condition (37c) for $d_l = d_t$, we obtain

$$\mu(\xi) = 1 - \frac{e_1^2}{4\pi}\int\limits_{\xi}^{L}\lambda(z)\,d_t(z)\,dz. \tag{41}$$

For $d_l = d_t$ as follows from Eq. (41), $\mu(\xi) = \lambda(\xi)$; for $d_l = 0$, the function $\lambda(\xi)$ becomes unity, and $\mu(\xi)$ is given by

$$\mu(\xi) = 1-(3/4\nu)\ln\{1+(e_1^2/3\pi)\nu(L-\xi)\}. \tag{42}$$

Thus for $d_l \neq d_t$, the function $\mu(\xi)$ no longer satisfies the renormalizability relation

6. CONCLUSION

The above considerations show that spin-zero electrodynamics in the β-formalism exhibit certain formal similarities with spin 1/2 electrodynamics. Beyond this, the general situation is more complicated. In order to derive the integral equations, it is necessary to make wide use of the results of perturbation theory. The problem is simplified with the choice $d_l = d_t$, in which case it is possible to write the three-vertex equation for the vertex parts. For this choice of d_l in the approximation we are considering it becomes possible to restrict ourselves to finding only the photon and meson Green's functions, and the vertex part; the Compton diagrams give contributions equal to their zeroth approximation. In this case, use of the three-vertex equation leads to the correct expression for the photon Green's function, which follows from a comparison with a result obtained by a separate method using only perturbation theory and the requirement of renormalizability. Both methods give the same results for the meson Green's function, since expression (28), which is found directly from the equations, satisfies the renormalizability relation (31).

For $d_l \neq d_t$ Eq. (13) for the vertex part is not applicable; the expression for the meson Green's function in this case can be obtained by a gauge transformation of the expression obtained for the condition $d_l = d_t$ to arbitrary d_l. It is interesting that the difference between the exact meson Green's function and its zero-approximation form does not arise only from the guage transformation, as it does in ordinary electrodynamics.

The authors are deeply grateful to Academician L. D. Landau for many valuable suggestions.

APPENDIX I

a) Correction to the Compton effect in the first approximation in e_1^2. Let us consider the matrix element for the Compton type diagram (Fig. 1)

$$C_{\sigma\tau}(p,\ p-q_1-q_2;\ q_1,\ q_2) = -\frac{e_1^2}{\pi i}\int \beta_\mu G(p-k)\,\beta_\sigma G(p-k-q_1) \times \beta_\tau G(p-k-q_1-q_2)\,\beta_\nu D_{\mu\nu}(k)\,d^4k.$$

Here $(q_1;\sigma)$ and $(q_2;\tau)$ are the momenta and polarizations of the two omitted quantities. Writing out the products of the various factors according to Eq. (6), we obtain

$$\begin{aligned} C_{\sigma\tau}(p,\ p-q_1-q_2;\ q_1,\ q_2) &= -\frac{e_1^2}{\pi i}\int\Big\{\beta_\mu(\hat{p}_1+m_1)\beta_\sigma(\hat{p}_2+m_1)\beta_\tau(\hat{p}_3+m_1)\beta_\nu \\ &+ (p_{1\mu}p_{1\sigma}-\delta_{\mu\sigma}p_1^2)\,X\beta_\tau(\hat{p}_3+m_1)\,\beta_\nu \\ &+ \beta_\mu X(p_{2\sigma}p_{2\tau}-\delta_{\sigma\tau}p_2^2)(\hat{p}_3+m_1)\,\beta_\nu \\ &+ \frac{X}{m_1}(p_{1\mu}p_{1\sigma}-\delta_{\mu\sigma}p_1^2)\,p_{2\tau}(\hat{p}_3+m_1)\,\beta_\nu \\ &+ \frac{X}{m_1}p_{1\mu}(p_{2\sigma}p_{2\tau}-\delta_{\sigma\tau}p_2^2)(\hat{p}_3+m_1)\,\beta_\nu \\ &+ \beta_\mu(\hat{p}_1+m_1)\,\beta_\sigma(\hat{p}_2+m_1)\,\frac{X}{m_1}(p_{3\tau}p_{3\nu}-\delta_{\tau\nu}p_3^2) \\ &+ \frac{X}{m_1}(p_{1\mu}p_{1\sigma}-\delta_{\mu\sigma}p_1^2)(p_{3\tau}p_{3\nu}-\delta_{\nu\tau}p_3^2)\Big\} \\ &\times\frac{[\delta_{\mu\nu}+(k_\mu k_\nu/k^2)(d_l-1)]\,d^4k}{(p_1^2-m_1^2)(p_2^2-m_1^2)(p_3^2-m_1^2)\,k^2} \end{aligned}$$

(for simplicity we have written $p_1 = p - k;\ p_2 = p - k - q_1;\ p_3 = p - k - q_1 - q_2$).

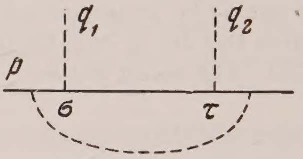

FIG. 1

The highest power of the virtual momentum k in the numerator is equal to 4, and therefore the integral diverges logarithmically in the region of large k. In this region $p_1 = p_2 = p_3 = k \gg m$:

$$\begin{aligned} -\frac{e_1^2}{\pi i}\frac{X}{m_1}\int\limits_{-k^2\gg -f^2} &[(k_\mu k_\sigma-\delta_{\mu\sigma}k^2)\,k_\tau k_\nu \\ &+ k_\mu k_\nu(k_\sigma k_\tau-\delta_{\sigma\tau}k^2)+k_\mu k_\sigma(k_\tau k_\nu-\delta_{\tau\nu}k^2) \\ &+ (k_\mu k_\sigma-\delta_{\mu\sigma}k^2)(k_\tau k_\nu-\delta_{\tau\nu}k^2)] \\ &\times[\delta_{\mu\nu}+(k_\mu k_\nu/k^2)(d_l-1)]\,d^4k/(k^2)^4. \end{aligned}$$

The nonzero result gives, in the numerator, the product of the longitudinal part of the photon function by the second term in the square brackets. Averaging over angles and integrating, we find

$$\frac{e_1^2}{16\pi}\frac{3X}{m_1}\delta_{\sigma\tau}\int\limits_{\ln(-f^2/m^2)}^{\ln(\Lambda^2/m^2)}(d_l(z)-1)\,dz$$

in complete agreement with (12) (the expression obtained should be doubled to take account of exchanging the positions of quanta (q_1 and q_2). Therefore for $d_l = 1$ the Compton diagrams are finite.

b) Vertex part with two intersecting photon lines. The vertex diagram with two intersecting photon lines (Fig. 2) can be treated similarly. The matrix element for this diagram is of order e_1^4 and is proportional to the integral

$$\Lambda_\sigma(p, p-l, l) \tag{A1}$$

$$\sim \int \{\beta_\mu G(p-k)\beta_\rho G(p-k_1-k_2)\beta_\sigma$$

$$\times G(p-l-k_1-k_2)\beta_\nu G(p-l-k_2)\beta_\tau\} D_{\mu\nu}(k_1)$$

$$\times D_{\rho\tau}(k_2)\, d^4k_1 d^4k_2.$$

We shall not write out the whole expression in the brackets in the integrand, which is extremely complicated, and shall consider only the denominators

$$(p-k_1)^2(p-k_1-k_2)^2 \tag{A2}$$

$$\times (p-l-k_1-k_2)^2(p-l-k_2)^2 k_1^2 k_2^2.$$

If we exclude integration in those regions of k_1 and k_2 which can give double logarithmic integrals, then it can be seen that there are two possibilities.

1. $k_1 >> k_2$ (or $k_2 >> k_1$). Then the numerator of the integrand should contain terms in the fourth power of k_1. With the choice $d_l = 1$, no such terms appear, as has been shown above.

2. The case in which $k_1 + k_2$ is small in comparison with k_1 (although large in comparison with p and l), which corresponds to a change of variables $k_2 = q - k_1$ or $k_1 = q - k_2$). The denominator of Eq. (A2) is about equal to

$$(k_1^2)^2[(k_1-q)^2]^2(p-l-q)^2(p-q)^2.$$

We must therefore look for terms in the expression for $\Lambda_\sigma(p, p-l, l)$ which can give the power k_1^4 in the numerator. Such terms are easily found. The corresponding double logarithmic integral (for $d_l = d_t$) will be

$$\frac{X}{m_1}\int \{(k_\mu k_\rho - \delta_{\mu\rho}k^2)(k_\mu k_\rho - \delta_{\mu\rho}k^2)(2p-l-2q)_\sigma\}$$

$$\times \frac{d^4k\, d^4q}{(k^2)^4 q^4 (1-2(p,q)/q^2)(1-2(p-l,q)/q^2)}.$$

It thus follows that the logarithmic term gives only integration over k, and integration over q after averaging over angles vanishes.

With respect to the diagram being considered, we must bear in mind the following. In calculating the polarization tensor

$$P_{\mu\nu}(l) = (e_1^2/\pi i)$$

$$\times \int \mathrm{Sp}\,[B_\mu(p-l, p, l)G(p)\beta_\nu G(p-l)]\, d^4p$$

it turns out that the combination of factors $G(p)\beta_\nu G(p-l)$ contains the following powers of p in the numerator: p^2, p^3/m_1. Therefore, in general, in $B_\sigma(p-l, p, l)$ in the region $p >> l$ we must know, in addition to the term proportional to β_σ, also the corrections of order l^2/p^2 and $m_1 l^2/p^3$. Terms proportional to β_σ, as we have seen above, do not occur. Terms $\sim l^2/p^2$ and ml^2/p^3 occur in (A1) from the integration region

$$p \gg k_1' \gg k_1' + k_2 \gg l\ (k_1' = p - k_1).$$

Their total contribution, however, to the polarization tensor vanishes. The same is true about the diagram of Fig. 1, for all corrections having a matrix structure other than expression (20). Consideration of higher order diagrams in the vertex part is complicated by the increasing complexity of the matrix expressions and the integrals. The above consideration of the matrix element of the vertex diagram with two intersecting photon lines allows us, however, to assume that for $d_l = d_t$ the higher approximations also give no contribution to the equation for the vertex part. The validity of this assumption is demonstrated by the final expression for the photon Green's function (24).

APPENDIX II

Gauge transformation of the vertex part. We shall find the vertex part $B_\mu(p, p-l, l)$ for arbitrary d_l on the basis of the relation [10]

$$G(p)\,\delta B_\mu(p, p-l, l)G(p-l) \tag{A3}$$

$$= -\frac{ie_1^2}{\pi}\int \{G(p)B_\mu(p, p-l, l)[G(p-l)$$

$$-G(p-l-k)] + G(p-k)$$

$$\times [B_\mu(p-k, p-l-k, l)G(p-l-k)$$

$$-B_\mu(p, p-l, l)G(p-l)]\}\,\delta d_l(k^2)\, d^4k/(k^2)^2,$$

which gives the form of the infinitesimal gauge transformation of $B_\mu(p, p-l, l)$. Considering only slowly varying $d_l(k^2)$, we see that the integral on the right side of (A3) is logarithmic in the region $|-k^2| \gg |(p-l)^2|$.

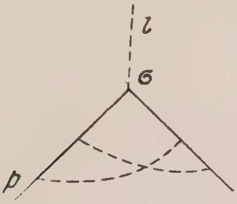

FIG. 2

We note, first of all, that the expressions (38) for the meson Green's function can be written in the matrix form

$$G(p) \approx \beta(p^2)\left\{\hat{p} + m_1(p^2) + \frac{\hat{p}^2 - p^2}{m_1(p^2)} - \frac{Yp^2}{m_1(p^2)}[\varphi(p^2) - 1]\right\}\frac{1}{p^2}, \tag{A4}$$

where $m_1(p^2)$ is given by (36),

$$\beta(p^2)/m_1(p^2) = \lambda(p^2)/m_1, \ \varphi(p^2) = \frac{1}{4\lambda(p^2)}[\lambda(p^2) + 3\mu(p^2)].$$

From (14a) and (A4) it follows that

$$G^{-1}(p) = \left\{\hat{p} - m_1(p^2) + \frac{Xp^2}{m_1(p^2)}[\varphi(p^2) - 1]\right\}\frac{1}{\beta(p^2)\varphi(p^2)}. \tag{A5}$$

In the region $p \gg l$ or $p \sim l$, we shall attempt to find the vertex part in the form

$$B_\mu(p, p-l, l) = \beta_\mu \alpha[(p-l)^2] + (2p-l)_\mu X\rho[(p-l)^2]. \tag{A6}$$

Turning to (A3), we see that the first term in the second square bracket can be dropped, and Eq. (A3) can be written in the form

$$\begin{aligned}\delta B_\mu(p, p-l, l) = -\frac{ie_1^2}{\pi}\Big\{&B_\mu(p, p-l, l)\int\frac{\delta d_l(k^2)\,d^4k}{(k^2)^2} - B_\mu(p, p-l, l)\int G(p-l-k)\\ &\times G^{-1}(p-l)\frac{\delta d_l(k^2)\,d^4k}{(k^2)^2} - G^{-1}(p)\int G(p-k)\\ &\times\frac{\delta d_l(k^2)\,d^4k}{(k^2)^2}B_\mu(p, p-l, l)\Big\}.\end{aligned} \tag{A3a}$$

In order to obtain the logarithmic expressions in the second and third terms, we need consider only the quadratic terms in the numerator

$$(\beta(k^2)/m_1(k^2))\{\hat{k}^2 - k^2 - Yk^2[\varphi(k^2) - 1]\}.$$

After averaging over angles this expression becomes

$$-(3/4m_1)\mu(k^2)Yk^2.$$

Going over to Euclidean space $k_0 \to ik_0$, introducing the new variable $\xi = \ln[(p-l)^2/m^2]$, and comparing corresponding terms in both parts of Equation (A3a), we obtain the following equations for the functions $\alpha(\xi)$ and $\rho(\xi)$:

$$\delta\alpha(\xi) = \frac{e_1^2}{4\pi}\alpha(\xi)\left\{\int_\xi^L \delta d_l(z)\,dz - \frac{3}{\lambda(\xi) + 3\mu(\xi)}\int_\xi^L \mu(z)\,\delta d_l(z)\,dz\right\}; \tag{A7a}$$

$$\delta\rho(\xi) = \frac{e_1^2}{4\pi}\left\{\rho(\xi)\int_\xi^L \delta d_l(z)\,dz + \frac{3\alpha(\xi)}{m_1(\xi)(\lambda(\xi) + 3\mu(\xi))}\int_\xi^L \mu(z)\,\delta d_l(z)\,dz\right\}, \tag{A7b}$$

where $L = \ln(\Lambda^2/m^2)$.

By comparing (A7a) with Eqs. (39a) and (39b), we obtain

$$\delta\alpha(\xi)/\alpha(\xi) = -\delta[\lambda(\xi) + 3\mu(\xi)]/[\lambda(\xi) + 3\mu(\xi)].$$

Using the boundary condition

$$\alpha(\xi)|_{d_l = d_t} = \beta^{-1}(\xi)|_{d_l = d_t}$$

and the fact that the function $m_1(\xi)$ does not depend on d_l, we obtain

$$\alpha(\xi) = [\varphi(\xi)\beta(\xi)]^{-1},$$

which is in agreement with (A5) and the Ward identity. Dividing (A7a) by $m_1(\xi)$ and adding it to (A7b), we find

$$\delta\left[\rho(\xi) + \frac{\alpha(\xi)}{m_1(\xi)}\right] = \frac{e_1^2}{4\pi}\left[\rho(\xi) + \frac{\alpha(\xi)}{m_1(\xi)}\right]\int_\xi^L \delta d_l(z)\,dz.$$

We have $\rho(\xi)|d_l = d_t = 0$. Integrating the previous equation, we obtain the following expression for $\rho(\xi)$:

$$\rho(\xi) = [1 - \alpha(\xi)\beta(\xi)]/m_1(\xi)\beta(\xi), \qquad \text{(A9)}$$

which again is in agreement with (A5).

In the other case, when $l \gg p$, expression (A6) for the vertex part becomes inexact. Instead of this, $B_\mu(p, p-l, l)$ is represented in the following form:

$$\begin{aligned} B_\mu(p, p-l, l) &= \beta_\mu \alpha[(p-l)^2] \qquad \text{(A10)} \\ &+ (2p-l)_\mu X \rho[(p-l)^2] \\ &+ p_\mu X \chi_1(p-l, p) + \beta_\mu X \chi_2(p-l, p). \end{aligned}$$

The logarithmic functions $\chi_1(\xi, \eta)$ and $\chi_2(\xi, \eta)$ vanish for $d_l = 0$ and when $\xi = \eta$. Insertion of (A10) into Eq. (A3a) leads to equations for the functions χ_1 and χ_2, which can be transformed to the following expressions:

$$\begin{aligned} &\delta[\chi_1(\xi, \eta) + \rho(\xi)] \\ &= \frac{e_1^2}{4\pi}\left\{[\chi_1(\xi, \eta) + \rho(\xi)]\int_\xi^L \delta d_l(z)\,dz + \frac{3[\alpha(\xi) + \chi_2(\xi, \eta)]}{[\lambda(\eta) + 3\mu(\eta)]\,m_1(\eta)}\int_\xi^L \mu(z)\,\delta d_l(z)\,dz\right\}; \\ &\delta[\chi_2(\xi, \eta) + \alpha(\xi)] \\ &= \frac{e_1^2}{4\pi}[\chi_2(\xi, \eta) + \alpha(\xi)]\left\{\int_\xi^L \delta d_l(z)\,dz - \frac{3}{\lambda(\eta) + 3\mu(\eta)}\int_\xi^L \mu(z)\,\delta d_l(z)\,dz\right\}. \end{aligned}$$

The solutions of these equations cannot be simply expressed in terms of the functions $\lambda(\xi)$, $\mu(\xi)$, and $m_1(\xi)$. We note only that the following relation holds:

$$m_1(\eta)\chi_1(\xi, \eta) + \chi_2(\xi, \eta) = [m_1(\xi) - m_1(\eta)]\,\rho(\xi).$$

The expressions we have obtained for the vertex part show again that for arbitrary d_l the functions entering into this expression do not satisfy the renormalizability condition.

---

[1] Landau, Abrikosov and Khalatnikov, Dokl. Akad. Nauk SSSR **95**, 497, 773, 1177 (1954).

[2] M. Gell-Mann and F. Low, Phys. Rev. **95**, 1300 (1954)

[3] R. Feynman, Phys. Rev. **76**, 749, 769 (1949).

[4] D. Peasly, Phys. Rev. **81**, 94 (1951)

[5] P. Matthews and A. Salam, Rev. Mod. Phys. **23**, 311 (1951).

[6] A. Salam, Proc. Roy. Soc. (London) **211A**, 276 (1952).

[7] F. Dyson, Phys. Rev. **75**, 1736 (1949).

[8] I. Ia. Pomeranchuk, Dokl. Akad. Nauk SSSR **103**, 1005 (1955).

[9] J. Schwinger, Proc. Nat. Acad. Sci. **37**, 452 (1951).

[10] L. D. Landau and I. M. Khalatnikov, J. Exptl. Theoret. Phys. (U.S.S.R.) **29**, 89 (1955); Soviet Phys. JETP **2**, 69, (1956).

Translated by E. J. Saletan
221

SOVIET PHYSICS JETP VOLUME 4, NUMBER 6 JULY, 1957

Heavy Nuclear Fragments from Disintegration Produced by Fast Protons in Nuclear Emulsions*

O. V. LOZHKIN AND N. A. PERFILOV
Radium Institute of the Academy of Science, USSR

(Submitted to JETP editor, June 26,1956)
J. Exptl. Theoret. Phys. (U.S.S.R.) 31, 913–922 (December,1956)

Fine-grain type P–9 nuclear emulsions have been used for the study of that interaction process of 350 to 660 mev protons with the nuclei of the emulsion which leads to the formation of multiple–charge particles with $Z \geq 4$. It has been observed that the production of multiple-charge particles of high energy (E_{kin} per nucleon > 3–4 mev) takes place on the light nuclei of the emulsion (C, N, O) as well as on the heavy ones (Ag, Br). The main characteristics of the nuclear fragment disintegration have been investigated. The analysis shows that–to explain the formation of fragments–one has to assume a series of specific properties of primary interactions of fast protons with nuclei

1. INTRODUCTION

IT has been noted long ago[1–7] in the study of the stars produced by cosmic rays in nuclear emulsions that, in addition to hydrogen and helium isotopes, heavy nuclear fragments with $Z \geq 3$ are also emitted by the disintegration of the nucleus. Similar multiple–charge fragments have been observed[8–14] in the disintegration produced by fast protons, neutrons and α-particles with energy in the hundreds of mev. The study of their formation mechanism has indicated a series of peculiarities which have not been explained until now. The experimental data[15–17] show that the emission of the fragments cannot be explained by the usual model of evaporation of the highly excited nucleus or highly asymmetric fission. There is also a series of arguments against the assumption of a spallation mechanism of their formation.

A study of nuclear disintegration with emission of particles with $Z \geq 4$ has been carried out in our laboratory since 1955. We are reporting below the main results of our experiments.

2. EXPERIMENTAL METHOD

The experiment has been carried out on fine grain nuclear emulsions of type P–9, irradiated by protons with energy of 350, 460, 560 and 660 mev, from the synchrocyclotron of the Institute of Nuclear Problems of the USSR Academy of Science.

The use of fine grain emulsions, sensitive to protons with energy of about 30 mev, permitted visual discrimination between particles with multiple charge and α-particles or protons. This is possible because of the good differentiating capacity of the fine grain emulsion, and because of the well known fact that the tracks of the particles with multiple charge have a characterisitc thin-down toward their end.

It has been shown, by means of photometric measurements on the track of multiple-charge particles of known nature, that a reliable visual identification of such particles is possible only for $Z \geq 4$. The latter may be seen in Fig. 1, which shows the darkening $(I_{\varphi}-I_C)/I_{\varphi}$ as a function of the residual path length for the ions N^{14}, B^8 and Li^8 in a P–9 emulsion. The darkening along the path can be appreciated visually in a reliable fashion only if it is not less than 15% for 25 μ of the path; a reliable visual discrimination between particles with multiple charge and α-particles is therefore possible only for $Z \geq 4$. The tracks of particles with $Z = 3$ can hardly be differentiated visually from the tracks of α-particles.

The experimental data described below correspond therefore to the events of radiation of particles with $Z \geq 4$ in nuclear fissions. Also included in the statistics are events of radiation of Li^8–nuclei (because of their reliable identification), and events of radiation of pairs of α-particles of approximately equal energies that are emitted in directions forming small angle (≈ 1 to $3°$); these particles are apparently[15] the decay products of $Be_4{}^8$ nuclei.

Figure 2 shows some examples of nuclear disintegration where the emission of one or several particles with multiple charge has been observed. The microphotographs show well the main characteristics of the tracks of the particles with multiple charges: high grain density and presence of darkening which enables us to differentiate them from α-particles.

---

*The main results of this work have been reported at the All Union Conference on High Energy Particles Physics (May, 1955), and at the International Conference on Nuclear Reactions at Amsterdam (June, 1956).

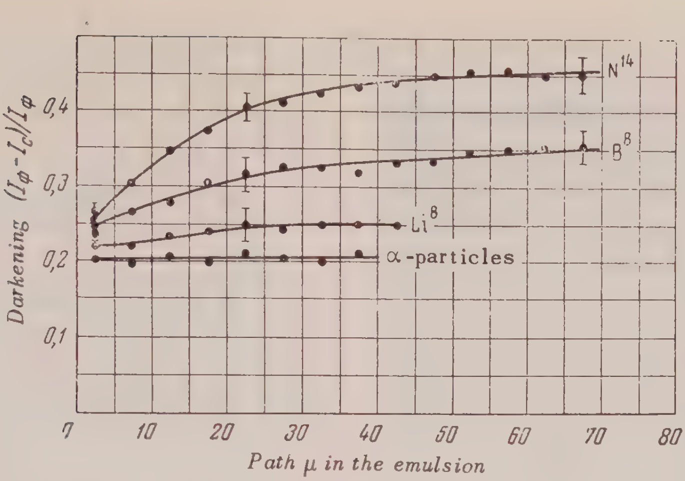

FIG. 1. Dependence of the darkening $(I_\varphi - I_c)/I_\varphi$ on residual path for ions N^{14}, B^8 and Li^8 in the P–9 emulsion.

The nuclear disintegrations which were observed to yield particles with multiple charge have been subjected to measurements with an ocular goniometer and an ocular scale. Furthermore, the multiple-charge fragments found in the plate irradiated by 660 mev protons have been investigated photometrically to determine their charge. The photometry has been performed with a "wide" slit the(width of the slit was larger than the width of the track) of dimensions $5 \times 0.8\ \mu^2$. The dependence ofthe total darkening on the residual path $(I_\varphi - I_C)/I_\varphi = P(R_{\mathrm{resid}})$ was obtained. The charge was determined by a method described in Ref. 18, with the use of the slope ofthe curve $P(R_{\mathrm{resid}})$ characterized by a certain average of the change $\overline{\Delta P}$ on the first 25 μ of the track from the end of the track, and a scaling curve which relates $\overline{\Delta P}$ to Z. The scaling curve was obtained from the experiment in the emulsion P–9 of the known particles N^{14}, B^8 and Li^8.

A few words should be said about the means of differentiating between the stars on light nuclei of the emulsion (C, N, O) and the stars on heavy ones (Ag, Br).

The following criteria were used: the presence or the absence of a recoil nucleus track and the total charge of the fission fragments which should not exceed 8 for a light nucleus. The accuracy of such a differentiation was checked by the amount of angular anisotropy forthe fragments formed on the light nuclei, and by the results of the measurements ofthe fragments' charge: if the number of the tracks radiated from the star is ≤ 4, and there is no recoil nucleus track, the measurements do not give a value > 8 for the charge of the fragment.

3. EXPERIMENTAL RESULTS

In this section a description will be given of the experimental data for 660 mev protons; the characteristics of the fragments emission process are quite similar at other proton energies in the range which was studied.

1) *Yield of nuclear disintegrations with multiple charge particles*

The interaction of fast protons with the nuclei of the elements of the emulsion leading to the formation of stars with fragments is a very rare event for the proton energy range considered here. An important property of the process of fragments radiation is the fast rise of the yield when the proton energy is increased. Figure 3 shows the dependence on the energy of the inducing protons of the relative number of stars with fragments. The total number of such stars which was observed in the emulsion is 2500. The relative number of stars with fragments increases more than twice when the proton energy varies from 350 to 660 mev.

The relative yield of fragment disintegration of heavy nuclei has been determined with respect to the total number of stars with fragments at the proton energies of 350, 460 and 660 mev. A total of about 1000 stars with fragments has been analyzed at the proton energy of 660 mev, and about 250 stars with fragments have been analyzed for

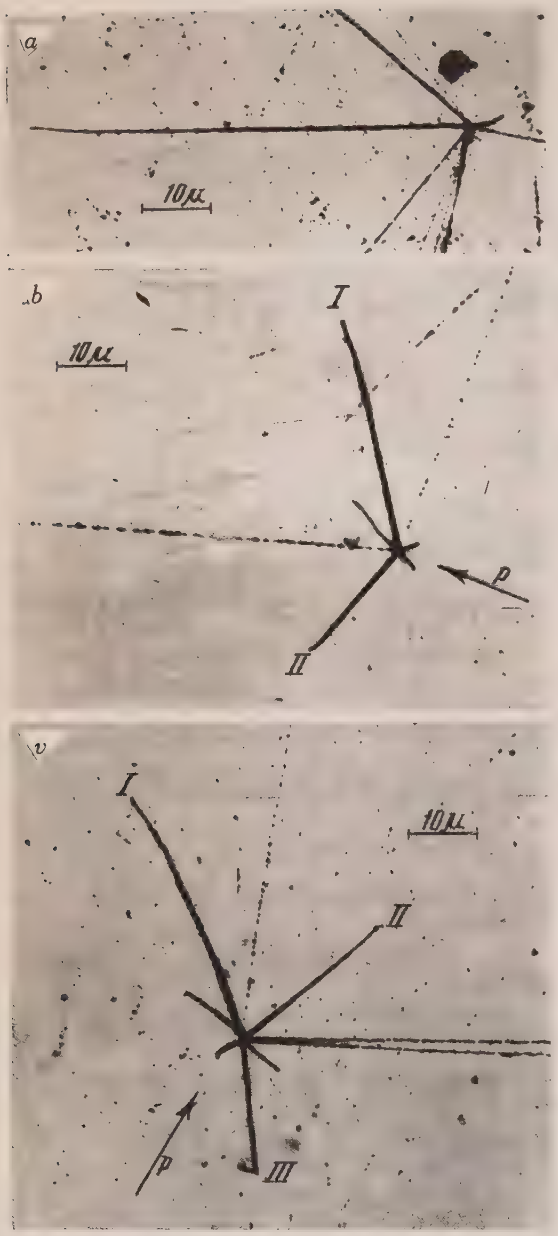

FIG. 2. Microphotographs of stars with fragments due to the disintegration of Ag and Br nuclei induced by 660 mev protons: *a*—disintegration with a single particle with multiple-charge ($Z = 7 \pm 1$), *b*—disintegration with two particles with mutliple charge ($Z_I=7\pm1$. $Z_{II}= 8\pm1$), *v*—disintegration with three particles with multiple charge and with a recoil nucleus ($Z_I=7\pm1.5$, $Z_{II}=6\pm1$, $Z_{III}=4\pm1$).

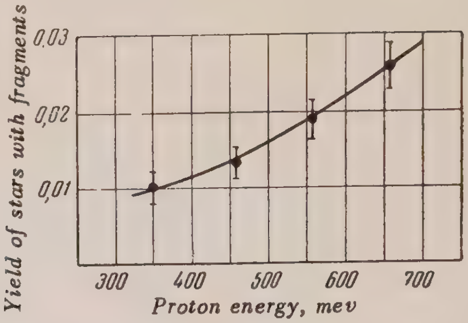

FIG. 3. Dependence of the relative yield of stars with fragments on the proton energy.

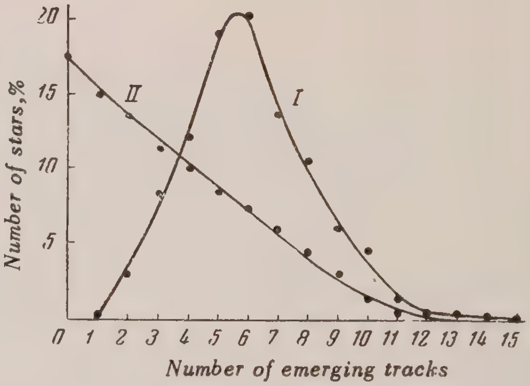

FIG. 4. Distribution of stars according to the number of rays: *I*—stars with fragments; *II*—stars without fragments, according to ref. 21.

each one of the 350 and 460 mev energies.

A lower limit to the number of fragment disintegrations produced on Ag and Br nuclei is about 80, 70 and 65% for the proton energies of 660, 460 and 350 mev respectively. From these data, and from the value of the total inelastic cross section of fast protons on Ag and Br nuclei, it is possible to estimate an approximate value of the absolute cross section of the interaction leading to disintegration with fragments. This cross section turns out to be of the order of 10^{-26} cm^2—which is appreciably larger than the value of the cross section obtained by the radiochemical method[14, 17, 19, 20]. This discrepancy could be due to a relatively large contribution of the stable isotopes of the particles with multiple charge being considered.

The process of fragment formation on heavy nuclei of the emulsion has another important property. As one can see in Fig. 4 (which shows the distribution of the stars with fragments on Ag and Br nuclei according to the number of rays), the particles with multiple charge are mainly related to multiple-ray stars. From the comparison of the distribution of stars with fragments according to the number of rays with the analogous distribution of stars without fragments (obtained from the work of Ostroumov[21]), the following conclusion can be drawn: the probability of formation of stars with fragments rises with the increase of the number of the rays in the star. The mean number of α-particles and of protons in the stars with fragments produced on Ag and Br nuclei is close to 5 for a proton energy of 660 mev; the number of α-particles and protons is approximately 3.5 in the case of the usual disintegrations.

In addition to single-fragment stars, the interaction of fast protons with heavy nuclei can produce disintegration with two or more multiple-charge particles for which $Z \geq 4$. Examples of such disintegrations are shown on the microphotographs of Fig. 2. It should be noted that in these cases there is, in addition to the multiple-charge particle tracks, a recoil nucleus track. For a proton energy of 660 mev, the disintegrations with two particles having $Z \geq 4$ is approximately equal to 0.04 relative to the total number of single-fragment stars; the yield of stars with three multiple-charge particles is approximately 0.009 relative to the single-fragment stars. It should be emphasized that the cases of radiation of two multiple-charge particles in a single disintegration considered here are such that their characteristics do not allow their interpretation by the process of fission. The number of cases which can be interpreted as a fission of Ag or Br nuclei into fragments of comparable masses is about 3% of the total number of stars with fragments. In the further analysis such cases were not considered.

As far as the distribution of the stars with two fragments according to the number of rays is concerned, it should be noted that they have a somewhat larger mean value of α-particles and protons (5,6) than the stars with single fragments (5).

2) *Charge distribution of fragments due to disintegration of Ag and Br nuclei*

For the determination of the distribution mentioned, 142 fragments from the stars formed on Ag and Br nuclei were subjected to photometric measurements. The distribution of the quantity ΔP for the measured tracks is shown in Fig. 5; this gives a feeling of the degree of differentiability between particles of neighboring charges by the method described. Figure 6 shows the charge distribution of the fragments. In this case, events of emission of Be_4^8 forming pairs of α-particles have been added to the events of particles of charge 4. Two kinds of corrections should be made in this distribution: a) correction for the number of tracks for which the charge could not be measured, because of the short path in the emulsion (< 20 μ) and, b) correction for the number of fragments which left the emulsion (geometry correction). The following could be said about these two corrections: the mean path of the fragment is decreasing with the increase of the charge; therefore the geometry correction will be important for small Z, whereas the first correction is important only for large Z. If one assumes that all the fragments with a path < 20 μ (approximately 10% of all the fragments) have a charge > 9, and if one takes into account the distribution of these fragments according to the path, then one can expect a charge distribution which will be approximately uniform up to $Z = 15-16$; for each charge there will be from one to two fragments. The geometry correction does not play a substantial role for particles with smaller charge, because only such fragments which made an angle < 14° with the

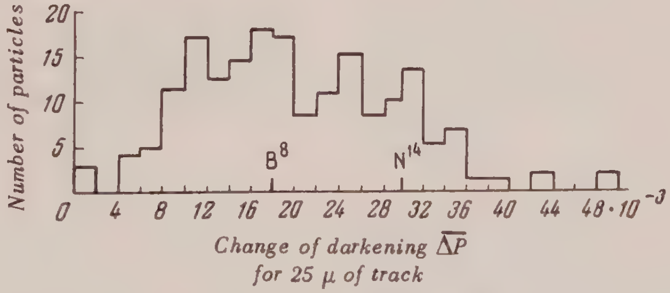

FIG. 5. Distribution of the measured quantities $\overline{\Delta P}$ for mutliple charge particles in disintegration($\overline{\Delta P}$ average change of darkening over the first 25 μ of track, starting from the end of the track).

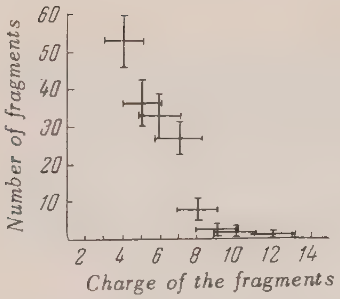

FIG. 6. Distribution of multiple-charge particles from Ag and Br nuclei, vs. charge.

plane of the emulsion were chosen for the photometric analysis.

The character of the charge distribution of the fragments as well as the absolute value of their yield, differs appreciably from what could be expected from the theory of evaporation of a highly excited nucleus. This can be illustrated by the data plotted in Fig. 7; Figure 7 shows, on one hand, the dependence of the probability of emission of multiple-charge particles on the charge of the particles as calculated by the evaporation theory,[22] and on the other hand, the experimental data. In both cases, the probability is given relative to the probability of proton emission. In the calculation by the evaporation theory, it was assumed that, for nuclei with $A = 80$, the mean excitation energy for fragment disintegration is equal to 150 mev.

3) *Angular distribution of charged particles in stars with fragments*

The angular distribution of the α-particles, of the protons and of the fragments (with respect to the proton beam) was investigated in the cases where a disintegration of Ag and Br nuclei (with emission of a fragment with $Z \geq 4$ produced by a proton bombarding energy of 660 mev) was found.

The amount of anisotropy in the angular distribution of the α-particles and of the protons turned out to be quite close to that which is observed for the usual disintegrations of Ag and Br nuclei by 660 mev protons. The ratio of the number of particles in the forward and backward hemispheres (with respect to the proton beam) is equal to 1.37 ± 0.17 and 1.26 ± 0.1 for the α-particles and the protons respectively. The angular distribution of the fragments, relative to the proton beam, shown in Fig. 8, is substantially anisotropic. The ratio of the number of particles in the forward and backward hemispheres is equal to 2.8 ± 0.3. For the 460 and 350 mev protons, the amount of anisotropy is about the same (3.0 and 3.1 respectively). If the center of mass motion is taken into account, these amounts change on the average by no more than 10 –15%.

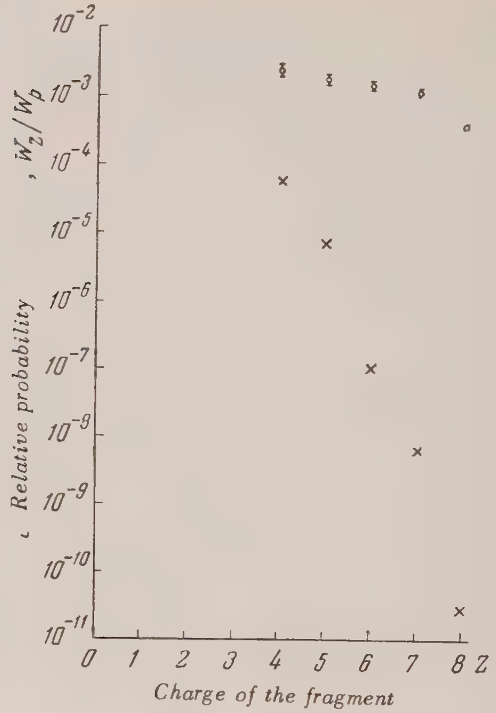

FIG. 7. Dependence of the relative probability (W_z/W_p) of the emission of a fragment on the charge. O—experimental data, × — theoretical calculation of W_z/W_p for the isotopes Be^9, B^{11}, C^{12}, N^{14} and O^{16}.

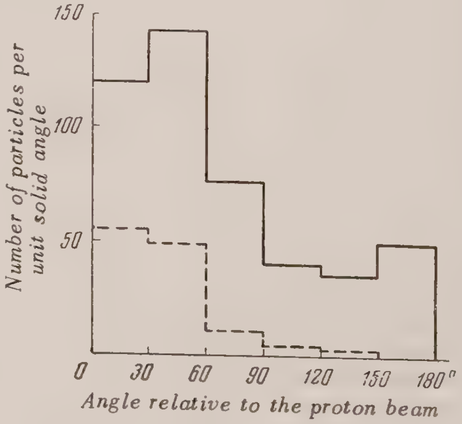

FIG. 8. Angular distribution for the fragments formed on heavy and light nuclei of the emulsion. ———— fragments in stars on Ag and Br, – – – – – –fragments in stars on C, N and O.

The angular correlation between the fragments and the residual (recoil) nucleus is a problem which presents a substantial interest. It follows from the distributions shown on Fig. 9 that the direction of the recoil nucleus motion in most of the cases is determined by the direction of the fragment's motion; the fragment and the recoil nucleus separate preferentially in opposite directions. In the case of disintegration of Ag and Br nuclei accompanied by the emission of two multiple-charge particles, a definite correlation between the fragments is also observed: in most of the cases the angle between the fragments is close to 180°. Among 32 fissions with two fragments, there are only three cases where the angle between the fragments is somewhat smaller than 90°.

The multiple-charge particles from the interaction with the light nuclei of the emulsion are characterized by a strong forward peaking (cf. Fig. 8). The ratio of the number of particles in the forward and backward hemispheres is about 15 for proton energies of 660 mev. The amount of anisotropy is about the same for 460 and 350 mev proton energies.

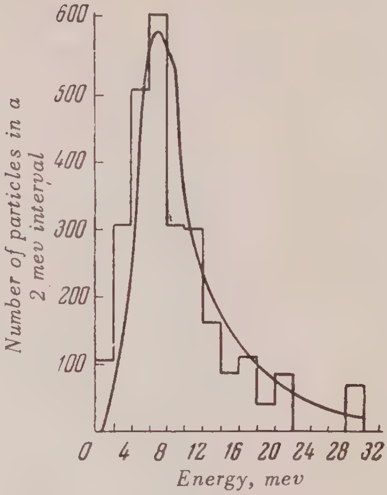

FIG. 10. Energy distribution of protons from fragment disintegration of Ag and Br. The energy of the inducing protons is 660 mev. The curve for stars without fragments was obtained from the data of Ref. 21.

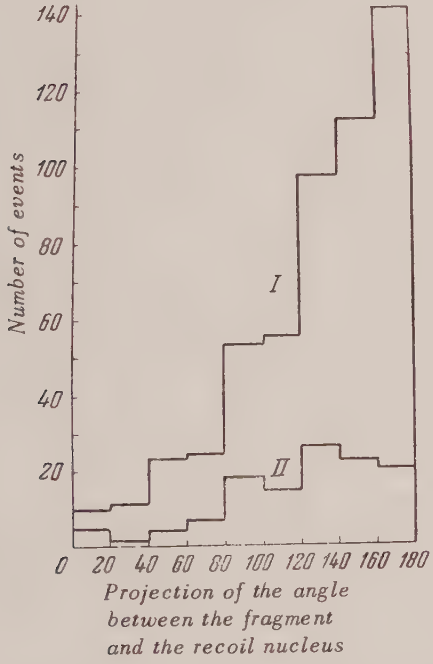

FIG. 9. Angular correlation of the fragment and of the recoil nucleus: I—all the stars, II—stars with a number of rays ≥ 8.

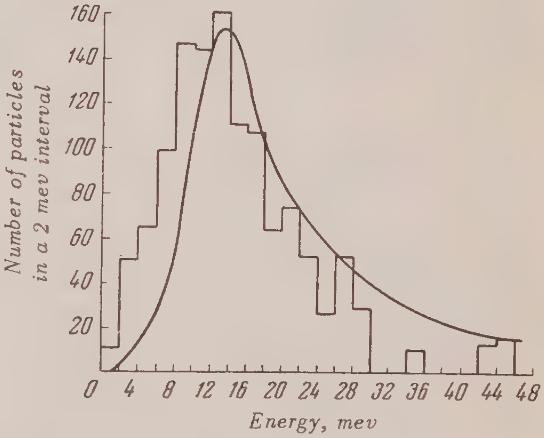

FIG. 11. Energy distribution of α-particles from fragment disintegration of Ag and Br. The energy of the inducing protons is 660 mev. The curve for stars without fragments was obtained from the data of Ref. 21.

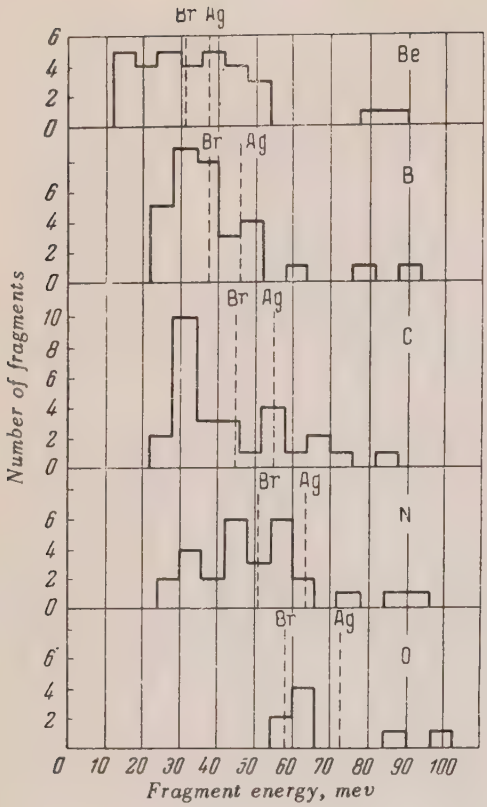

FIG. 12. Energy distribution of multiple-charge particles. The nominal value of the Coulomb repulsion energy for a given Z of the remaining nucleus is represented by a dotted line.

4) *Energy distribution of the α-particles, protons and fragments*

An interesting property of the fragment disintegration of Ag and Br nuclei is a certain difference between the energy spectra of the protons and of the α-particles, and the distribution obtained for the usual disintegrations of the same nuclei by 660 mev protons.[21] The spectra of the α-particles and protons obtained from the particles which have stopped inside the emulsion are shown in Figs. 10 and 11; they have been corrected for geometry. The data of Ostroumov[21] —spectra of α-particles and protons from the usual disintegration of Ag and Br nuclei—is also shown on the graphs. As it can be seen from the graphs, α-particles and protons dominate in the small-energy region of the spectra.

The energy distribution of multiple-charge particles could not be obtained with good statistics because of the small number of photometered tracks. Figure 12 shows the energy distribution of the fragments for $Z = 4, 5, 6, 7$ and 8. From the shape of the distribution, it can be said that, irrespective of the charge, the energy of the particles is in most cases close to the value determined by the Coulomb repulsion between the fragments and the recoil nucleus. The energy distribution for multiple-charge fragments from light nuclei was not investigated. Only the dependence of the mean path of the fragments on the energy of the inducing protons was obtained. As the energy of the protons is increased, the mean path of the fragments from light nuclei increases appreciably. It is approximately 76, 50 and 34 μ for energies of 660, 460 and 350 mev, respectively. The mean path of the fragments from Ag and Br nuclei remains constant for the different proton energies.

An important property of the energy distribution of the fragments radiated by Ag and Br nuclei is that the number of fragments with energies substantially higher than the Coulomb repulsion energy is small.

4. DISCUSSION OF RESULTS AND CONCLUSIONS

The process of formation of fragments with $Z \geq 3$ in the interaction of high energy protons with the nuclei of the emulsion was observed to have the following characteristics.

1. The formation of multiple-charge particles with high energy (kinetic energy per nucleon > 3–4 mev) occurs in the interaction of high energy protons with heavy nuclei of the emulsion as well as in the interaction with the light ones.

2. The probability of fragment radiation rises rapidly with the increase in the energy transferred to the nucleus in the collision with the proton.

3. The particles with $Z \leq 8$ constitute the majority of the fragments observed in the fission of heavy nuclei. The remaining charge distribution is approximately uniform, up to Z = 15–16.

4. The angular distribution of the fragments is highly anisotropic; in the case of heavy nuclei (Ag, Br) this anisotropy barely changes when the energy of the inducing particles is increased from 350 to 660 mev (the "forward-to-backward" ratio is approximately 3 to 1). The angular anisotropy in the distribution of the fragments formed from light nuclei (C, N, O) is appreciably larger than for the stars on the heavy nuclei of the emulsion (the "forward-to-backward" ratio is 15 to 1 for 660 mev protons).

5. The energy distributions of particles with different charges have one common characteristic. The multiple-charge particles are distributed in energy principally around the value determined by the Coulomb charge repulsion. In a small number of cases, the energy of the multiple-charge particles exceeds the Coulomb repulsion energy by an appreciable amount.

6. There is a noticeable probability of radiation of two or more multiple-charge particles in a single disintegration of a heavy nucleus. In the case of the radiation of two multiple-charge particles, there is a definite angular correlation between them: in most of the observed cases the angle between the fragments is close to 180°.

7. The energy spectra of the α-particles and of the protons from the disintegration of the Ag and Br nuclei with multiple-charge particles differs somewhat from the spectra of the α-particles and of the protons from the usual fissions; namely they are enriched by particles of small energy.

8. There is a definite angular correlation between the fragment and the recoil nucleus: the fragment and the recoil nucleus separate preferentially in opposite directions.

The process of the interaction of a proton, with an energy of a few hundreds mev, with a heavy nucleus, is nowadays viewed as presenting two stages. In the first stage, the collision of the incoming particle with the nucleons in the nucleus produces a nuclear cascade process, as a result of which a certain number of protons, neutrons and possibly α-particles are knocked out from the nucleus; the remaining energy is statistically distributed among the nucleons of the nucleus. The phenomena which occur in the second stage of the process are described either by the evaporation model, or by a fission process which would be a result of the vibration of the nucleus (drops if the conditions are adequate). Each of these processes is characterized by a particular angular and energy distribution of the radiated particles.

The angular distribution of the nuclear fragments strongly disagrees with the assumption that a substantial part of these fragments could appear in the processes of usual evporation or fission of a highly excited nucleus. The high probability of fragment radiation, the shape of the charge distribution of the fragments and the formation of two or more fragments in a single fission are also facts which are hard to fit by the evaporation model. This does not exclude the possibility that a small part of the fragments could have an evaporation origin (mainly the fragments with small charge). The latter two situations disagree also with a fission mechanism for the formation of the fragments.** In addition, it is necessary to bear in mind that, in the considered process, we have to deal with fragments which are apparently stable isotopes in most of the cases. This deduction, which was made from comparison of the cross sections of the fragments (see above), is checked also by the investigation of the properties of the residual nucleus in the range of mass numbers which corresponds to the radiation of fragments.[17]. It can be expected, however, that the usual fission mechanism yields principally unstable particles with neutron excess.

Hence, the major part of the fragments observed in the fission of heavy nuclei can be explained neither by the evaporation, nor by the fission process, i.e., by the processes which take place after the energy released has been statistically distributed among the nucleons of the nucleus.

Let us now consider the possibility of the formation of the considered multiple-charge particles in the primary process of the interaction of a fast proton with heavy nuclei. The possibility of the formation of energetic particles with multiple-charge in the process of the collision of the primary proton with a group of nucleons in a heavy nucleus can be assumed, considering the fact that similar multiple-charge particles are formed in the interaction of protons with light nuclei of the emulsion. In the latter case, the observation of multiple -charge particles with high energy (energy per nucleon ≥ 4 mev) cannot be explained without the assumption of a direct transfer of the energy and momentum of the primary proton to the whole light nucleus or to one of its parts, but without the breaking of the nucleons' binding. The elastic scattering of fast protons by light nuclei at large angles could be such a process. If it is assumed that in the case of heavy nuclei (Ag, Br) the multiple-charge particles are also related to a similar process, then one has to make a series of assumptions to explain the observed characteristics of the fragment disintegration; for instance, 1) one has to assume a substantial, although maybe short lived, existence of strongly bound clusters of nucleons in the nucleus, 2) one has to assume a high probability for the scattering of a fast fragment inside the nucleus, to explain the cases of radiation of fragments on the backward hemisphere and, 3) one has to assume that in addition to the knocking out of the fragment, the residual nucleus is left with a high excitation energy.

In addition to the mentioned assumptions, each one of which can raise objections, there is a series of experimental data, which show the difficulties of the considered effect as a spallation process: for instance, the appearance of two or more multiple-charge particles in a single disintegration with the lack of the expected dependence of the fragment's energy on the energy of the primary particles and on the angle with respect to the direction of the primary particle. Indeed, the comparison of the

---

**As discussed in Sec. 3, about 3% of all the stars with fragments can be interpreted by a fission process where Ag and Br nuclei split in fragments of comparable mass. Such cases are not considered here.

observed energy distribution of the fragments for a proton energy of 660 mev with the data from the work of Perkins[15] shows that the mean fragment energy changes only slightly when one switches to disintegration due to cosmic rays, whereas the energy of the primary particles changes drastically. If the spallation interaction is assumed, a substantial dependence of the secondary particles on the energy of the primary ones should be expected. There would also be no dependence of the fragment energy on the direction of the primary proton. This dependence of fragments formed in the disintegration of Ag and Br nuclei by 660 mev protons and whose $Z = 5$ and 6 is plotted on Fig. 13. The dependence calculated from the elastic scattering theory can also be found there.

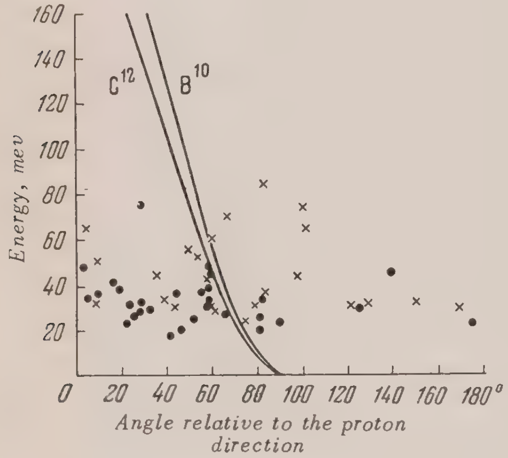

FIG. 13. Dependence of the energy of the fragment with $Z = 5$ and 6 on the angle with the direction of the proton beam: ●—fragments with $Z = 5$, ×—fragments with $Z = 6$. The curves are calculated from the formula for inelastic scattering for a proton energy of 660 mev.

To explain the fragment formation in the interaction of fast protons with heavy nuclei by a spallation process requires the assumption of very specific properties of the collision process. However, one could look for the reason for the multiple -charge particles formation in the primary interaction process of fast particles with nuclei, because it determines all the subsequent behavior of the nucleus.

A series of hypotheses has been made recently in the attempt to explain the effect of fragment formation in the disintegration induced by cosmic rays: the hypothesis of long range nuclear forces; the hypothesis that the fragment radiation is required to lower the high angular momentum of the excited nucleus;[15] the Heisenberg "turbulent effect" hypothesis; and the hypothesis that the fragment radiation is a result of pure surface oscillations.[24] The above hypotheses cannot explain all of the observed data for the disintegration induced by cosmic rays nor do they explain the observations made in the present work. For a more satisfactory explanation, further investigations are required.

---

1 Heitler, Powell and Fertel, Nature **144**, 283 (1939).

2 G. Occhialini and C. Powell, Nature **159**, 93 (1947).

3 C. Franzinetti and R. Payne, Nature **161**, 735 (1948).

4 G. Lowera, Ric. Sci. Ricostruz, **17**, 118 (1947).

5 E. Schopper, Naturwiss **34**, 118 (1947).

6 P. E. Hodgson and D. H. Perkins, Nature **163**, 439 (1949).

7 A. Bonetti and C. Dilworth, Phil. Mag. **40**, 585 (1949).

8 S. C. Wright, Phys. Rev. **79**, 838 (1950).

9 E. W. Titterton, Phil. Mag. **42**, 113 (1951).

10 L. Marquez and I. Perlman, Phys. Rev. **81**, 953 (1951).

11 D. H. Greenberg and J. M. Miller, Phys. Rev. **84**, 845 (1951).

12 R. Batzel and G. Seaborg, Phys. Rev. **82**, 607 (1951).

13 W. H. Barkas and J. K. Bowker, Phys. Rev. **87**, 207 (1952).

14 L. Marquez, Phys. Rev. **86**, 405 (1952).

15 D. H. Perkins, Proc. Roy Soc. (London) **203**, 399 (1950).

16 S. O. Sorenson, Phil. Mag. **42**, 207 (1951).

17 P. Kruger and N. Sugarman, Phys. Rev. **99**, 1459 (1955).

18 O. V. Lozhkin, J. Exptl. Theoret. Phys. (U.S.S.R.) (in print).

19 A. P. Vinogradov et al., in Session of the Academy of Science, USSR, July, 1955. Conference of the Chemical Sciences Division, p. 132.

20 B. V. Kurtchatov et al., same as above, p. 178.

21 V. I. Ostroumov, J. Exptl. Theoret. Phys. (U.S.S.R.) (in print).

22 R. Hagedorn and W. Macke, *Kosmische Strahlung*, Berlin, (1953). p. 201.

23 W. Heisenberg, Z. Physik **126**, 569 (1949).

24 Y. Fujimoto and Y. Yamaguchi, Progr. Theor. Phys. **5**, 76 (1950).

Translated by E. S. Troubetzkoy
202

SOVIET PHYSCIS JETP VOLUME 4, NUMBER 6 JULY, 1957

Spatial Distribution of the Particles of Extensive Air Showers Produced by Primary Cosmic Rays of Various Energies

S. P. DOBROVOL'SKII, S. I. NIKOL'SKII, E. I. TUKISH
AND V. I. IAKOVLEV
P. N. Lebedev Physical Institute, Academy of Sciences, USSR

(Submitted to JETP editor July 16, 1956)
J. Exptl. Theoret. Phys. (U.S.S.R.) 31, 939-942 (December, 1956)

The spatial distribution of charged particles in the central region of extensive air showers produced by primary cosmic ray particles of various energies was experimentally investigated. It has been found that, within the limits of experimental error, the spatial distribution is independent of the energy of the primary particle producing the shower in the energy region of $10^{13}-6\times10^{15}$ ev.

EARLIER experiments[1] have determined the spatial distribution of charged particles near the core of extensive air showers for primary energies between 6×10^{13} ev and 10^{15} ev. In the summer of 1954, we carried out experiments which had the purpose of widening the energy interval of the investigated extensive air showers. The spatial distribution of particles in showers of primary energy lower than 6×10^{13} and higher than 10^{15} ev was studied at 3860 m above sea-level.

The experimental arrangement described in Ref. 1 was used for the investigation of the spatial distribution of the flux of charged particles in showers produced by primaries with energy $> 10^{15}$ ev. Groups of hodoscoped counters, each 16 cm^2 in area, were used to ensure accurate measurements of high density particle flux. The methods of particle flux density determination, of core selection, and of the counting of the number of particles, used in each case of an air shower detection, were identical with those described in Ref. 1. The resulting average spatial distribution of particles in showers consisting of 1.2×10^6 particles is shown in Fig. 1 (curve 1). The x-axis represents the distance from the core in meters, the y-axis the flux density of shower particles, expressed in number of particles per square meter.

A difficulty connected with the small number of particles in showers arises in the investigation of showers with less than 10^4 particles. We studied showers which discharged 4–7 counters out of the 456 counters, with the area of each equal to 100 cm^2, present in our arrangement (Fig. 2). The cores of such showers were selected by groups of hodoscoped counters shielded with 2 cm and, in some of the measurements, with 4 cm of lead. The cascade multiplication of the electron-photon component in lead increases with the proximity of the core to the shielded group of counters. The determination of the core location

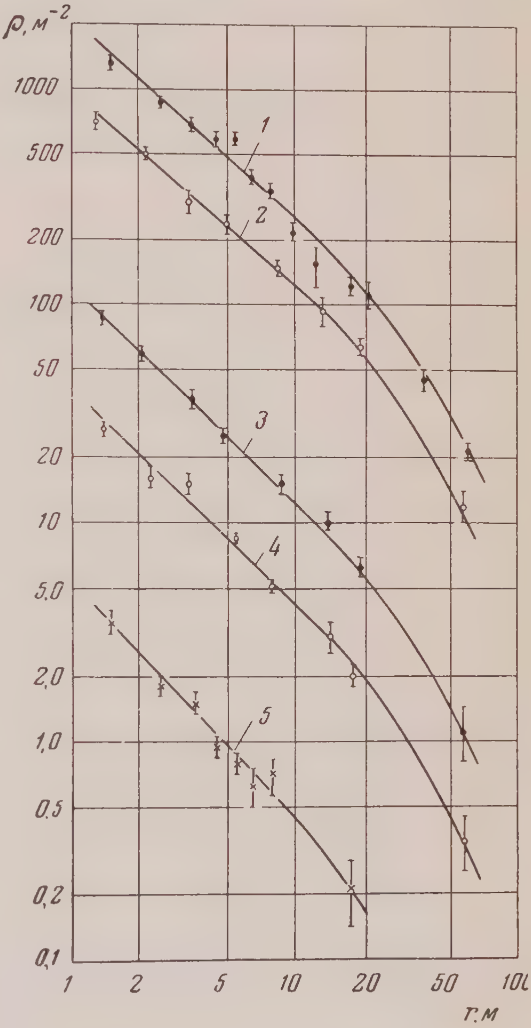

FIG. 1. Spatial distribution of the flux density of charged particles in extensive air showers with different numbers of particles: curve 1—1.25×10^6; 2—5.7×10^5 3—6.3×10^4; 4—2.1×10^4; 5—2.5×10^3.

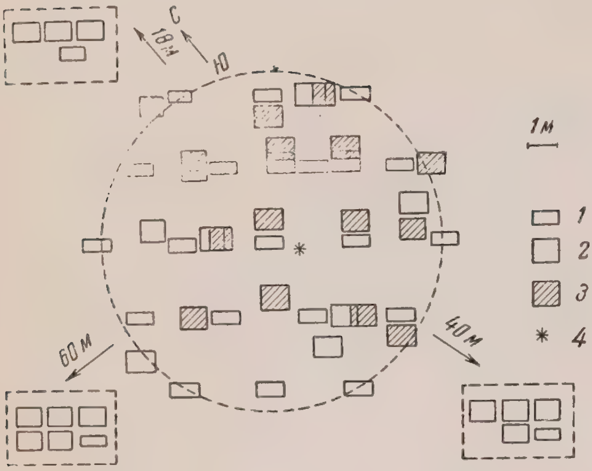

FIG. 2. Position diagram of hodoscope counters: *1*—nonshielded counters: 100 × 24 = 2400 cm^2; *2*—nonshielded counters: 330 × 12 = 3960 cm^2. *3*—shielded counters: 330 × 12 = 3960 cm^2; *4*—group of master counters.

by means of the shielded hodoscoped counters was effected without any difficulty.*

For the showers with total number of particles between 10^3 and 4×10^3 ($\bar{N} = 2.5 \times 10^3$), the difference between the actual number of particles in individual showers was disregarded, since the error of the determination of the number of particles in an individual shower amounted to 50% in each case. We measured the ratio of the total number of counters to the number of counters recording the passage of a shower particle, at a given distance from the core, for all the investigated showers. The margin of each measured distance from the core amounted to one meter, which was similar to the error of the determination of the core position for an individual shower. The resulting spatial distribution of particles is shown in Fig. 1 (curve 5). The results of Ref. 1 are included for comparison in the same figure (curves 2,3 and 4). The slopes of the linear portions of the curves were analyzed by means of least-square method. The values of the exponent n of the spatial distribution function $\rho(r) \sim 1/r^n$ corresponding to a straight line in a log-log plot, for showers with different numbers of particles and, consequently, of various primary energies are given in the Table. It can be seen both from Fig. 1 and the Table that the experimental results of Ref. 1 are in good agreement with the present work.

The normalized spatial distribution of particles in showers produced by primaries of different energies is shown in Fig. 3.

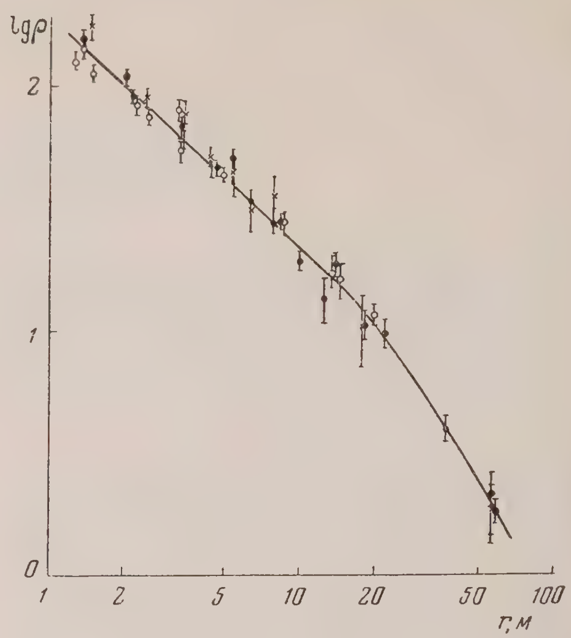

FIG. 3. Normalized spatial distribution of the flux density of charged particles in extensive air showers of different primary energies. The densities are normalized at the distance of 10 m.

Total number of particles $\bar{N}$	Energy of the primary particle $E_0 = 5 \times 10^9\ N$	n
$1.25 \cdot 10^6$	$6.2 \cdot 10^{15}$	0.93 ± 0.06
$5.7 \cdot 10^5$	$2.9 \cdot 10^{15}$	0.90 ± 0.02
$6.3 \cdot 10^4$	$3.2 \cdot 10^{14}$	1.03 ± 0.03
$2.1 \cdot 10^4$	$1.0 \cdot 10^{14}$	1.00 ± 0.06
$2.5 \cdot 10^3$	$1.2 \cdot 10^{13}$	1.11 ± 0.08

It should be noted that, in order to determine the total number of particles in a shower, it is necessary to make use of the distribution function up to distances of the order of several hundred meters from the core. We used the results of Ref. 2, assuming the independence of the spatial distribution from the primary energy, which, as it can be seen from the Table, is fully ascertained for the central part of the shower.

Theoretical considerations, based on the electron-photon cascade theory[3] as well as on the nuclear cascade theory of shower development with an account of the angular distribution of particles produced in the elementary processes of nuclear interaction[4] show that, with the decrease of the primary energy, one should expect a steeper slope of the spatial distribution function near the core of an extensive air shower. It can be seen from the Table that the expected change in the spatial distribution function is not observed experimentally.**

---

*This method was proposed by G. T. Zatsepin.

The experimental results obtained can be explained under the assumption of the presence of a single, energetically distinct nuclear-active particle in the core of the extensive air shower having a primary energy less than 10^{15} ev. This particle produces then the high-energy electron-photon component in the depth of the atmosphere.[6]

This conclusion can be illustrated by the comparison of our results on the spatial distribution with the angular distribution of particles in the nucleon-nucleon interaction processes observed in photographic emulsions. Under the assumption that the extensive air showers, recorded by us, which are produced by primary nucleons of 1.2×10^{13} ev, are formed at ~ 15 km, it follows from the experimentally observed spatial distribution that the greater part of the energy released in the primary interaction is carried away by particles within a solid angle equal to $\sim 10^{-4}$ sterad. In Ref. 7, only one particle was found within the angle of 10^{-4} sterad in a nucleon–nucleon interaction at $\sim 10^{13}$ ev primary energy, the single particle evidently carrying away the greater part of the energy of the primary particle.

The authors wish to express their deep gratitude to Prof. N. A. Dobrotin and G. T. Zatsepin for their interest in the present work. O. I. Dovzhenko, Iu. I. Vavilov, V. V. Batov, Iu. F. Evstigneev, M. S. Tuliakina, N. S. Il'ina and other collaborators took part in the measurements. The authors wish to express to all of them their sincere appreciation.

**The tendency of the spectral distribution function for showers of 10^{15} ev to be steeper, which may possibly be connected with the change of the nature of the primary nuclear interaction process for particles of 10^{15} ev[5] needs an additional investigation.

[1] Vavilov, Nikol'skii and Tukish, Dokl. Akad. Nauk SSSR 93, 233 (1953).

[2] Zatsepin, Rozental', Sarycheva, Khristiansen and Eidus, Izv. Akad. Nauk SSSR Ser. Fiz. 17, 39 (1953).

[3] S. Z. Belenkii, *Cascade Processes in Cosmic Rays*, GITTL, Moscow, 1948.

[4] I. L. Rozental' and D. S. Chernavskii, Uspekhi Fiz. Nauk 52, 185 (1954).

[5] Nikol'skii, Batov and Vavilov, Dokl. Akad. Nauk SSSR 111, 1 (1956).

[6] Dobrotin, Zatsepin, Nikolskii, Sarycheva and Khristiansen, Izv. Akad. Nauk SSSR, Ser. Fiz. 19, 666 (1955).

[7] Schein, Glasser and Haskin, Nuovo Cimento 2, 647 (1955).

Translated by H. Kasha
205

SOVIET PHYSICS JETP VOLUME 4, NUMBER 6 JULY, 1957

Nuclear Disintegrations Produced by 660 mev Protons in Photographic Emulsions

E. L. GRIGOR'EV AND L. F. SOLOV'EVA
Institute for Nuclear Problems, Academy of Sciences, USSR

(Submitted to JETP editor July 18, 1956)
J. Exptl. Theoret. Phys. (U.S.S.R.) 31, 932-938 (December, 1956)

We present experimental material from an investigation of nuclear disintegrations produced in photographic emulsion by 660 mev protons. The general features of the disintegration, the magnitude of the cross section for inelastic processes, and the distributions in energy and angle of secondary protons and alpha particles are presented. The yield of charged π-mesons per disintegration is obtained, and an approximate value is suggested for the lower limit of the cross section for emission of two charged π-mesons in a disintegration.

AT the present time there has been accumulated a large amount of experimental material from investigation of nuclear disintegrations occurring through the action of particles with energies of some hundreds of mev.

Experiments on stars in photographic emulsion, radiochemical investigations of reaction products, and experiments on scattering and absorption of particles have enabled us to establish the quantitative features of some aspects of the process of interaction of high energy particles with nuclei, and to compare the experimental data with various pictures of the nuclear model and the mechanism of interaction. However, a detailed analysis of the experimental data is made difficult by the great variety of the processes which occur, and also by the lack of a complete theory of the nucleus and of nuclear interactions. Despite this situation, any new factual material makes a definite contribution to the program of studying the properties of nuclear matter, especially if the experimental conditions under which it was obtained extend the scope of previous investigations. This situation has prompted us to carry out some measurements on disintegrations produced in photographic emulsion by 660 mev protons. The fundamental questions which were investigated were the general features of the disintegration, the interaction cross section, and the distribution in angle and energy of charged particles in disintegrations.

TABLE I

Number of prongs	2	3	4	5	6	7	8	9	10	11	12	Total number of stars	Average number of prongs
All stars, %	8	17	22	18	13	9	7	3	2	1	—	1333	4.9
Stars with black tracks, %	21	24	21	15	9	4	3	1.5	1.0	0.5	—	463	4.0

DISTRIBUTION OF STARS ACCORDING TO NUMBER OF PRONGS

The distribution of stars according to number of prongs, as measured in electron-sensitive plates, is given in Table I. The distribution confirms the familiar fact that the average number of prongs per star changes very little with the energy of the incident particle; with increasing energy, the number of many-pronged stars increases somewhat.

The tracks of fast particles, mainly protons, with energy greater than 50 mev are usually called grey tracks; these tracks are produced by protons knocked out of nuclei by the primary particle. The average number of such tracks per disintegration is 0.98 ± 0.20. The frequency of occurrence of such tracks is shown in Table II.

The grey tracks are highly collimated along the direction of the incident protons (Figure 1), with a half-width in angle of about 20°. Earlier we found[1] that the average number of prongs in distributions from 460 mev protons was 4.2. The closeness of the numbers of prongs in disintegrations produced by protons with such different energies is a reflection of the fact that the nuclear excitation changes very little with increasing energy of the primary particle. This is also evidence of the fact that the major part of the energy imparted to the nucleus by the particle is carried off in the primary interaction.

CROSS SECTION FOR INELASTIC INTERACTIONS

A count of cases of interactions of protons with nuclei was made by scanning along the tracks of the initial protons. This method eliminates the possibility of missing such events as no-pronged stars, small-angle scattering, and one-prong stars. The results of the measurement, including the necessary corrections for elastic scattering, are presented in Table III.

In computing the total free path for light nuclei, Λ_l, and heavy nuclei, Λ_h, it was considered that 83% of the collisions occur on nuclei of silver and bromine.[2] The experimental ratios of the interaction cross section to the geometrical cross section of the nucleus were 0.46 ± 0.18 and 0.87 ± 0.12 for the light and the heavy nuclei respectively. Such ratios, as calculated from the semi-transparent nucleus theory, give 0.70 for light nuclei and 0.86 for heavy nuclei. Thus for the heavy component of the emulsion we find within the limits of error of the measurement agreement with the computed cross section, while for the light nuclei the respective values differ by about a factor of two: $\sigma_{\text{theor.}} \approx 2\sigma_{\text{exp.}}$

This result indicates that light nuclei are much more transparent than the theory predicts.

TABLE II

Number of grey prongs	0	1	2	3	Total no. of stars
% of stars . . .	29	46	21	4	1333

SLOW CHARGED PARTICLES

Slow charged particles (protons with energy less than 50 mev, and α-particles), were studied by constructing angular and energy distributions. For this purpose, tracks of singly and doubly charged particles were measured in plates of relatively low sensitivity, which had good charge discrimination. All the singly charged particles were identified as protons, all the doubly charged particles as alpha particles. In order to consider interactions only with heavy nuclei (Ag or Br), to which the evaporation theory is reasonably applicable, we selected disintegrations containing 6 or more tracks, and with excitations above a certain limiting value. The selection was made so that the average number of black prongs per star was 7.4.

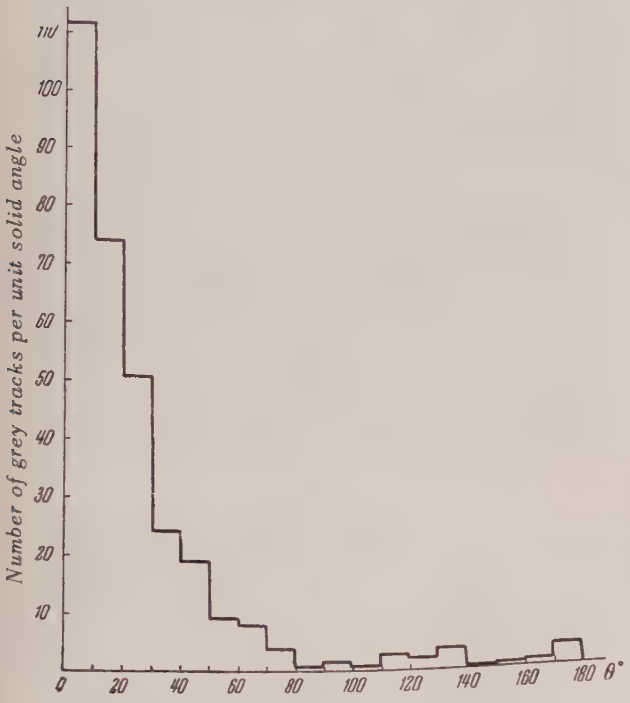

FIG. 1. Angular distribution of grey tracks. Total number of tracks = 946.

Table IV gives the ratio α/P of the number of doubly charged particles to the number of singly charged particles for stars with 6 to 8 prongs. The values for stars with a greater number of prongs are not given because of insufficient experimental material.

The results given in the Table are in agreement with the data of other work[3,4] on stars with the same prong number, and also, as in Ref. 4, indicate a negligible change in the ratio with increase of number of particles emitted. Later it will be shown that the average number of black tracks, which was 7.4, corresponds to an excitation energy of $U = 230$ mev. The calculated[5] value of α/P for this energy should be 0.45. If we now take account of the cascade particles (about 30% of the protons and 20% of the α-particles, cf. below), then our average ratio α/P becomes 0.42, which is not too different from the computed value.

The charged particles are not emitted isotropically, as is demonstrated by the distributions in Figures 2 and 3. If we assume that in the evaporation process the protons and α-particles are distributed isotropically, we can roughly estimate from the graphs the number of particles emitted in the cascade process. Both for the α-particles and the protons, the distributions become isotropic beyond about 100°. It then follows from the graphs that about 30% of the protons and approximately 20% of the α-particles are emitted in the cascade process. These estimates apparently give somewhat low values, since the many-pronged stars correspond to large nucleon cascades, in which the preference for the initial direction of the particle is lost as the result of the large number of collisions in the nucleus, and the recoil particles can emerge from the nucleus in various directions.

The proton energies were determined by measuring track lengths or, if the track did not end in the emulsion, by measuring the grain density. In order to make this latter method possible, we constructed a calibration curve of grain density vs. energy by measuring numbers of grains along tracks of particles stopping in the emulsion. This method made possible the determination of energy to an accuracy of only about 20%.

TABLE III

Total length of tracks, in meters	26, 10	Λ, см	39 ± 5
Number of stars	58	Λ_l, см	237 ± 74
Number of scatterings by nuclei	50	Λ_h, см	47 ± 7
Number of p–p scatterings	3	σ_l, 10^{-24} см^2	$0{,}16 \pm 0{,}06$
Number of disappearances of tracks	2	σ_h, 10^{-24} см^2	$1{,}06 \pm 0{,}15$
Corrected number of all inelastic collisions	67	—	—

For the purpose of obtaining at least partial separation of evaporation protons from recoil protons, two particle distributions were constructed, one for those emitted into the forward hemisphere and another for the backward hemisphere. The corresponding distributions are shown in Figure 4. The spectra differ from one another only in the somewhat longer tail on the high energy side for the protons emitted into the forward hemisphere. If we omit the long-range protons with energies greater than 30 mev, the spectra are characterized by the quantities given in Table V.

TABLE IV

Number of prongs	α/P
6	0.35 ± 0.04
7	0.37 ± 0.05
8	0.36 ± 0.05
Average	0.36 ± 0.05

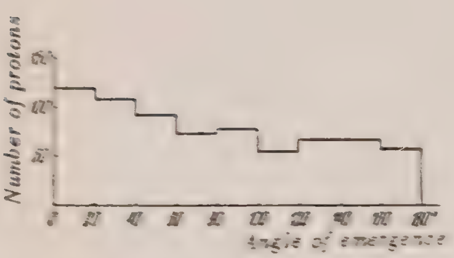

FIG. 2. Angular distribution of slow protons.

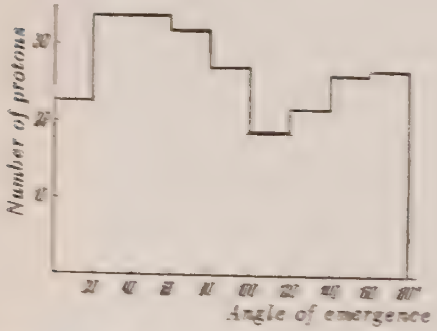

FIG. 3. Angular distribution of α-particles.

The probable energy is the same for both spectra, and agrees with the value predicted by the evaporation theory.[5] The energy distribution of the protons emitted into the backward hemisphere is satisfactorily described by the expression

$$P(T)\,dT = (\bar{T} - V')\,\tau^{-2} \exp\{-(\bar{T} - V')\} \quad (1)$$

with $\bar{T} = 9$ mev, $V' = 2$ mev and $\tau = 4$ mev.

The energies of the α-particles were determined from their range. In constructing the spectrum (Figure 5), corrections were made for particles not stopping in the emulsion. The principle characteristics of the spectra are given in Table VI.

The difference between the average energies for the "forward" and "backward" spectra may be caused by the participation of the α-particles in the nuclear cascade. However, this fact in combination with the observed considerable number of low-energy α-particles (far greater than the number of slow protons), may also support the assumption of preferential emission of α-particles during the initial stage of the evaporation when the nucleus is still highly excited and is moving in the direction of impact of the primary particle. In some papers[4] it is indicated that, with increasing excitation energy, the number of slow particles increases simultaneously with the increase in number of long-range α-particles. At the same time, the value of the probable energy decreases. At the present time, the only explanation for the presence in the spectrum of slow α-particles is the assumption that the nuclear barrier is decreased. If we accept this point of view, the experimental facts presented do not contradict the assumption that the emission of α-particles occurs before the emission of protons.

TABLE V

	Average energy, mev	Probable energy, mev
Particles emitted forward .	10.2	7
Particles emitted backward .	9	7

EXCITATION ENERGY

The experimental determination of the excitation energy of the nuclei undergoing disintegration in the photoemulsion is greatly hampered by the impossibility of observing neutrons. In addition it is difficult to take account of those cascade particles which have energies in the region of energy of the evaporated particles. An estimate of the number of neutrons emitted can be made on the assumption that the final nucleus has maximum stability. This assumption can be supported experimentally from observations of decay electrons at the center of stars. Among 303 stars with prong number $n \geq 6$, we found only 21 stars in which an electron was emitted; these represent only 7% of the total number of disintegrations. Thus the observations show that most of the nuclear mass is left in the final stable state.

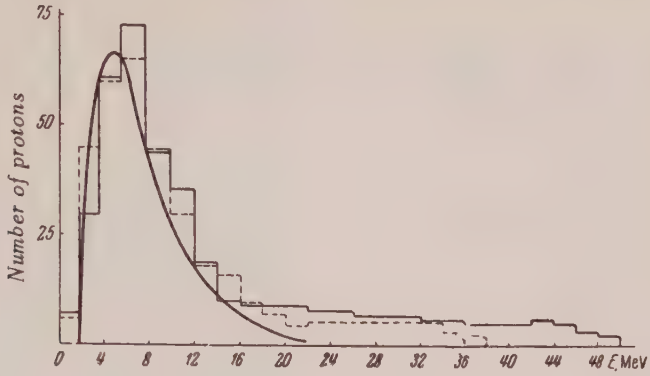

FIG. 4. Energy distribution of slow protons emitted forward (———) and backward (– – – –). The solid curve is computed from formula (1) with $V' = 2$ mev and $T = 4$ mev.

Since we are here observing disintegrations of only Ag and Br, the initial values of A and Z, averaged over the two types of nuclei, are 94 and 41, respectively. Using the numbers found for emerging α-particles and protons, we find that on the average about 10 neutrons are emitted in each star. Knowing the average energies in the spectra of protons and α-particles, and also taking account of the recoil particles, we can make an estimate of the the average excitation energy imparted by the protons. It turns out to be close to 230 mev. In this computation it was assumed that the number and average energy of the recoil neutrons are the same as the corresponding values for recoil protons.

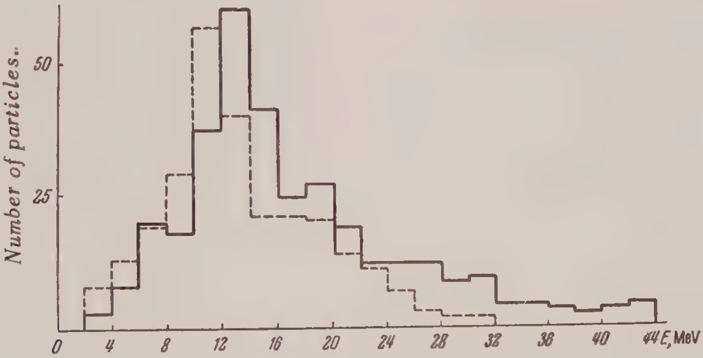

FIG. 5. Energy distribution of α-particles emitted forward (———) and backward (– – – –).

Computations according to the evaporation theory[5] predict 5.5 charged particles for an excitation energy of 230 mev. Our measurements gvee 5.4 particles. Thus our measurements, including the determination of the ratio α/P, the number of charged particles, and the investigation of the shape of the proton spectrum are in agreement with the corresponding data as calculated according to the evaporation theory.

The quantitaive data which we have obtained, such as the fraction of cascade particles and the energy of excitation, are not sufficiently accurate to be used safely in comparing with theoretical calculations. One can only say that the material presented is compatible with general crude ideas about the interaction of fast particles with complex nuclei.

EMISSION OF MESONS

Among the singly charged particles emitted in disintegrations, there are also π-mesons, whose production intensity increases markedly with the energy of the incident particles.

TABLE VI

	Average energy, mev	Probable energy, mev
Particles emitted forward .	16	13
Particles emitted backward .	13.7	12

In order to determine the number of charged mesons occurring in a disintegration, all grey tracks in stars formed in an electron-sensitive emulsion of thickness 400-600 μ were measured in order to identify the particles. For this purpose we constructed a calibration curve of grain density versus meson energy from measurements of the number of grains in tracks of π-mesons stopped in the emulsion and in proton tracks. 530 grey tracks in 507 stars were measured by this method, and it was found that 20 of them belonged to π-mesons. Thus, on the average, in one out of 25 disintegrations a single charged π-meson is emitted. Of especial interest is the frequency of emission of two mesons, formed in a single collision of a proton with a nucleus. The threshold energy for formation of two mesons in the collision of free nucleons is about 600 mev. For collisions of particles with nucleons in the interior of a nucleus the threshold is reduced to ~ 450 mev. In view of this last fact, we undertook a search for cases of production of two mesons, selecting for measurement those disintegrations which contained two or more grey tracks. These tracks had a length greater than 1 mm, and their grain density corresponded to that for tracks of mesons having an energy greater than 10 mev. Among the 3000 disintegrations, two stars were found which each had two π-meson tracks. The characteristics of these tracks are given in Table VII.

TABLE VII

Case number	Track no.	$\bar{\alpha}^\circ_{100\,\mu}$	Grain density dN/dR	Energy				Angle of emergence in °	Angle between tracks in °.
				π-meson		proton			
				from $\bar{\alpha}^\circ$	from dN/dR	from $\bar{\alpha}^\circ$	from dN/dR		
1	1	0.30	52	50 ± 12	30 ± 6	49 ± 12	195 ± 40	21	7
	2	0.237	40	65 ± 16	56 ± 13	59 ± 15	360 ± 100	28	
2	1	0.184	32	88 ± 14	76 ± 10	79 ± 13	500 ± 100	63	14
	2	0.354	62	39 ± 7	20 ± 4	40 ± 7	140 ± 25	49	

Columns 5–8 show the energy values found both from scattering measurements and from grain density measurements, for the two kinds of particles assumed. There is satisfactory agreement between the energy values determined separately by the two methods only if the particles are π-mesons. Using the value of the cross section for star formation, we can assign an approximate lower limit for the cross section for emission of two charged mesons. This estimate gives a value ~ 10^{-28} cm^2.

---

[1] E. L. Grigor'ev, Reports of Institute for Nuclear Problems, Academy of Sciences USSR, 1955.

[2] M. Blau, A. R. Oliver, Bull. Am. Phys. Soc. 27, 6 (1952).

[3] N. Page, Proc. Phys Soc. (London) 63A, 250 (1950).

[4] D. H. Perkins, Phil. Mag. 41, 138 (1950).

[5] K. J. LeCouteur, Proc. Phys. Soc. (London) 65A, 718 (1952).

Translated by M. Hamermesh
204

SOVIET PHYSICS JETP VOLUME 4, NUMBER 6 JULY,1957

Galvanomagnetic Properties of Gold

N. E. ALEKSEEVSKII AND IU. P. GAIDUKOV
Institute for Physics Problems, Academy of Sciences, USSR

(Submitted to JETP editor August 13,1956)
J. Exptl. Theoret. Phys. (U.S.S.R.) 31, 947-950 (December,1956)

The dependence of the electrical conductivity on temperature of four samples of gold of various purities has been investigated in the temperature range 0.05°–20.4°K. In this temperature range observations were also made of the dependence of the electrical conductivity on the magnetic field.

THE present communication is concerned with a study of the anomalous behavior of the resistivity of gold at low and very low temperatures. In spite of the fact, that a considerable amount of work has been devoted to this problem, there still remain many aspects of this phenomenon which have not been explained.

We have conducted experiments on the dependence of the resistivity of gold on temperature in the range 20.4° to 0.05°K. We have also observed the dependence of the resistivity on the magnetic field in this same temperature interval. Temperatures above 4.2°K were obtained by means of the method proposed by Keesom[1]. Temperatures below 1.4°K were attained by the adiabatic demagnetization of iron-ammonium alum. Figure 1 shows the apparatus, adapted by us for the observation of the relation between electrical resistance and magnetic field in the region of very low temperatures. A glass ampoule contained a block of alum, 1, into which strips of copper were pressed. A copper "cold conductor" was soldered to these strips. The "cold conductor" was terminated by a wider portion, 3, onto which the samples to be investigated, 4, were attached by means of BF–2 cement. During demagnetization, the "exchange gas" is absorbed on the alum block and the "dessicating" salt, 5, thus breaking thermal contact between the helium bath and the internal parts of the ampoule. At this point the apparatus was transposed in such a way, that the alum was inserted into a magnetic screen 6, made of Armco iron, while the sample of gold found itself in a homogeneous magnetic field.

The samples attained the same temperatures as the alum block. The validity of this assumption was proven in separate experiments.

Four samples of gold were investigated. Some of the characteristics of the samples are shown in the accompanying Table.

The potential leads were either cut out of the sample itself (for the case of flat samples) or (for the case of wires) they were prepared from the same material as the sample and were brazed to the samples with an oxygen torch.

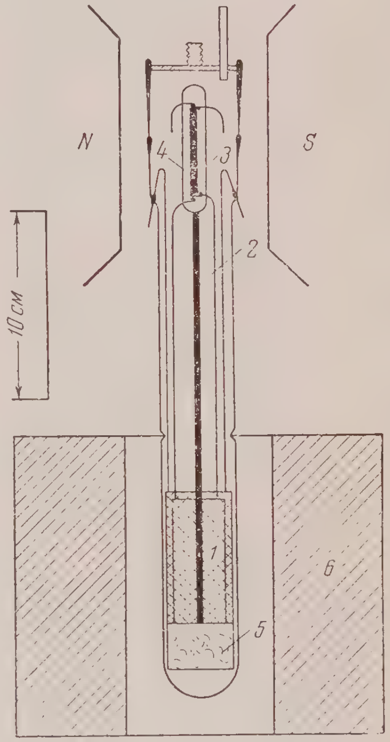

FIG. 1.

Figure 2 presents the results of the measurement of the resistance, at various temperatures of four samples, plotted on semilogarithmic coordinates. The resistance of three samples showed an anomalous behavior. It follows that for the samples which have a minimum in the $r(T)$ curve, the resistance is independent of the temperature in the region 0.05°–0.3° K, and at higher temperatures the resistance becomes a linear function of lg T.*

---

*This portion of the $r(T)$ curve can be represented satisfactorily by the equation $r = A \lg(T/T_{\min})/(1+B \lg(T/T_{\min})$ where A and B are constants and $T_{\min}$ is the temperature of the resistance minimum.

TABLE

№	purity rating in %	$\frac{r_{295°\,K}}{r_{\min}}$	Fe impurity in %	Temperature Curve	$\frac{r_0 - r_{\min}}{r_{\min}}$ in %
Au-1	99.99	92	—	Anomalous	13.2
Au-2	99.999 Hilger	159	0.0001	Anomalous	11.3
Au-3	99.99	9.8	0.001	Anomalous	7.2
Au-4	99.99	172	—	Normal	0

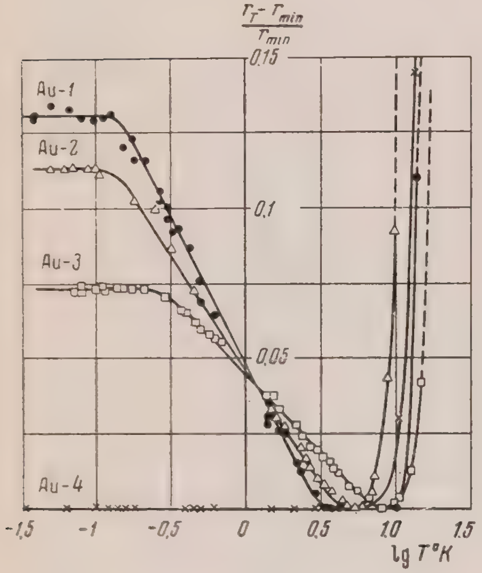

FIG. 2.

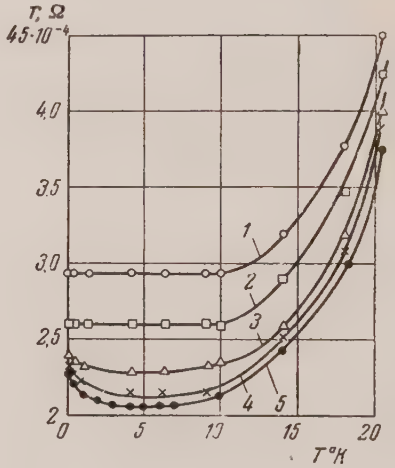

FIG. 3. Au–2; 1–H= 14 Koe; 2–H = 10 Koe; 3–H = 6 Koe; 4–H = 3 Koe, and 5–H = 0.

If, analogously, the dependence of the resistance on temperature in a magnetic field is determined, it is found that as the intensity of the field is increased, the depth of the resistance minimum decreases and for a certain value of the field the minimum disappears completely. Figure 3 illustrates this situation. The results shown are for sample Au–2; similar results were, however, found for samples Au–1 and Au–3.

If we observe the dependence on the magnetic field of the quantity

$$\Delta r = \frac{(r_0 - r_{\min})}{r_{\min}},$$

where r_0 is the resistance in the saturation region at very low temperatures and $r_{\min}$ is the minimum resistance of the sample, it is found, that for all three samples (Au–1, Au–2, and Au–3) this quantity approaches zero for $H \approx 8$ K oe (Fig. 4). Preliminary measurements of the Hall constant for Au–1 have shown that for this field intensity the Hall constant increases almost discontinuously, where the magnitude of the increase depends on the temperature.

In Figs. 5–8, we show the dependence of the resistance on the magnetic field for various temperatures. From these drawings it is evident, that, while for Au–4 and curves of $r(H)$, taken at various temperatures can be practically superimposed on each other, this is not true for Au–1, Au–2 and Au–3. Thus for Au–3, a decrease of resistance is observed in a magnetic field up to the same high fields intensities, i.e., $H \approx 23$Koe. On the other hand, for Au–1 the resistance decreases for small fields but increases for larger fields.

We must admit that it is hard to believe the hypothesis which has been suggested by a number of authors, namely, that the inclusion of very small amounts of ferromagnetic impurities in gold brings about a decrease in the overall resistance of the samples. We are inclined to reject this hypothesis on the grounds that the spectroscopic analysis which was described above, showed that even in Au–3 (which had the highest Fe content) the Fe concentration does not exceed 0.001 percent. Furthermore magnetic measurements which were conducted on sample Au–1 showed that the sample remains diamagnetic even at liquid He temperatures. It can be safely said, however, that the anomalous behavior of gold in the low temperature region is

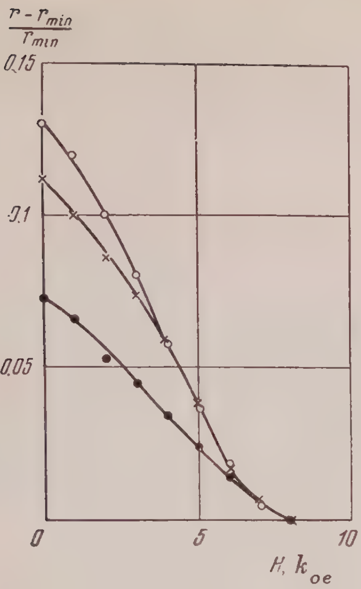

FIG. 4. O–Au–1:X–Au–2 and ●–Au3.

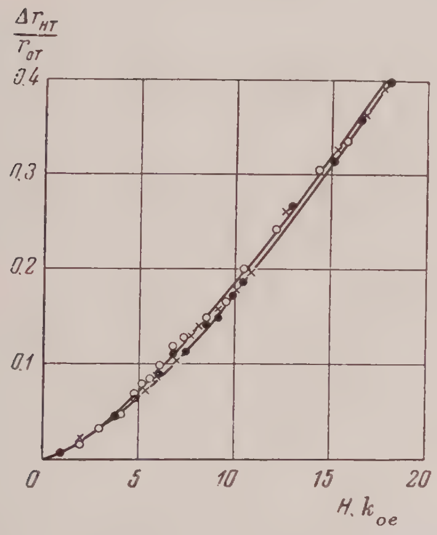

FIG. 5. SampleAu–4:O–T=4.2°K; X–T=1.4 K; ●–T= 0.05° K.

caused, apparently, by extremely small concentrations of impurities, in the presence of which the dependence of the magnitude of the effect on the impurity concentration can be visualized from the curves which have maxima. We do not exclude the possibility that the impurities which are responsible for the anomalous behavior of the resistivity of gols are metals with unfilled d–shells.

Although for a final explanation of the cause of the anomalous behavior of the resistivity of gold further experimental investigation of the effect are necessary, on the basis of the experiments which have been performed it is possible to say that the magnitude of the increase of the resistance when

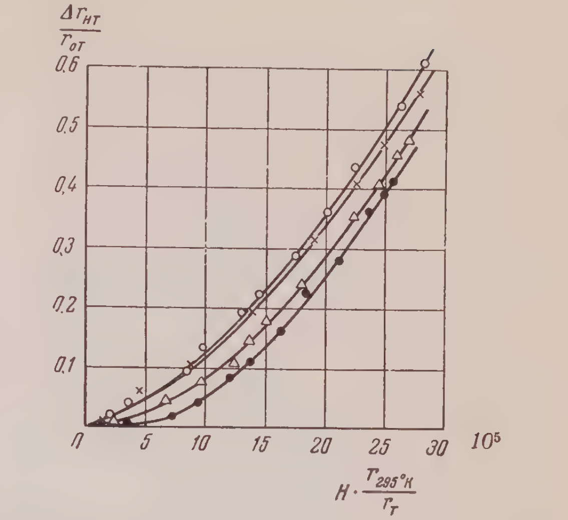

FIG. 6. SampleAu–2:O–T=4.2° K; X–T=1.4°K; Δ–T= 0.46°K; ●–T= 0.1° K.

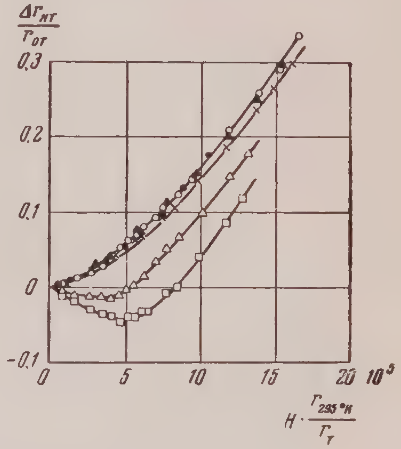

FIG. 7. SampleAu–1:O–T=4.2°K; X–T=1.69°K; Δ–T=0.25°K; □ –T=0.05°K; ●–T=20.4° K and ▲–T= 10.5° K.

the temperature is lowered, turns out to be a function of the magnetic field and approaches zero for certain critical values of field intensity. The existence of such a critical field, as well as a comparison of the behavior of r (T) and r (H) permit one to conclude, that the resistivity increase accompanying a temperature decrease and the decrease of the resistivity in a magnetic field should be attributed to a single cause and do not appear to be independent effects.** It should also be noted that the existence of a saturation in the curves of r (T) and the linear relation between resistivity

---

**It has not been determined whether the disappearance of "antiferromagnetism" in gold should be attributed to this same cause.

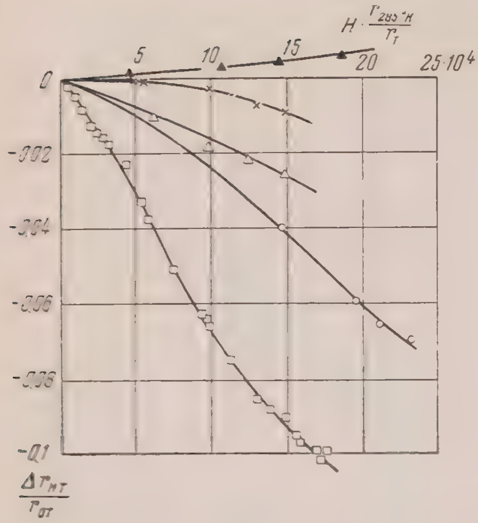

FIG. 8. Sample Au–3: ▲–T=8 °K; X–T= 4.2 °K; Δ–T=1.61 °K; O–T= 1.36 °K and ◻ –T=0.14 °K.

and lg T seem to be associated with different laws from those which govern the effect described in the preceding sentence. Similar observations have been made by other authors.[2,3,4]

---

[1] B. Keesom, *Helium*, IIL, Moscow (1949) p. 201 (Russian translation).

[2] A. I. Croft, Phil. Mag. **44**, 289 (1953).

[3] E. Mendoza and I. G. Thomas, Proceedings of the International Conference on Low Temperature Physics (1951) p. 39.

[4] Guy K. White, Canad. J. Phys. **33**, 119 (1955).

Translated by J. J. Loferski
207

SOVIET PHYSICS JETP VOLUME 4, NUMBER 6 JULY, 1956

Critical Currents in Superconducting Tin Films

N. E. ALEKSEEVSKI AND M. N. MIKHEEVA
Institute for Physical Problems, Academy of Sciences, USSR

(Submitted to JETP editor August 4, 1956)
J. Exptl. Theoret. Phys. (U.S.S.R.) 31, 951–954 (December, 1956)

Measurements of critical currents in tin films were performed, using a pulse method with specimens in the shape of a disk. These measurements were made in the temperature region $\Delta T = T_c - T = 0.5$ °K for a range in thickness between 6.9×10^{-6} and 6.4×10^{-5} cm. For four of the specimens the external critical magnetic fields parallel to the film surface were also measured. For one film, in the form of a flat ring 2×10^{-5} cm in thickness, critical currents were measured over the temperature interval from 3.7 to 1.6 °K from the damping of a current induced in the ring.

THE problem of investigating critical currents in films has been taken as the subject of a comparatively small number of papers. The first results, obtained by Shal'nikov[1], showed Silsbee's rule to be completely disobeyed in thin films. This result was seen to be in qualitative agreement with the results of the theoretical work of London, in which it was concluded that as the external magnetic field parallel to the film increases, a decrease in the magnitude of the critical currents for the film should be observed. Quantitative verification of the experimental data was, however, impeded by the fact that in investigating critical currents in thin superconductors it was usually found difficult to determine the magnetic field at the surface of the superconductor due to the current. In addition, it was possible to assume that some of the experimental results would show reduced values for the critical currents due to the influence of heating and boundary effects. It seemed, therefore, of interest to conduct an investigation of critical currents in films under somewhat more favorable experimental conditions.

An attempt has been made by authors to obtain values of the critical current for a plane film in the form of a disk. The current was introduced through a lead perpendicular to the plane of the disk and was taken out at its periphery. For this case the field at the surface of the disk due to the current has a configuration analogous to that of the field surrounding a cylindrical conductor; i.e., $H = 2I/R$, where r is the distance from the center to the point at which the field at the surface of the disk due to the current is measured.

The films were prepared by sputtering tin in the

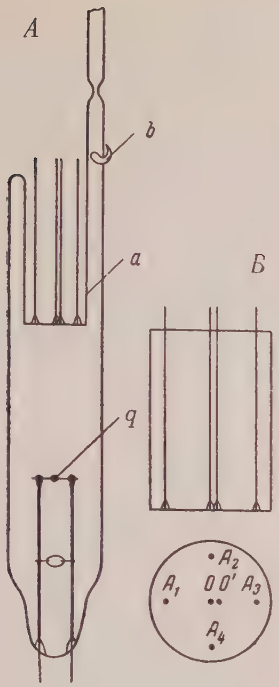

FIG. 1. Apparatus for measuring critical currents by the pulse method. *A*—general layout of the apparatus: *q*—sputtering source, *a*—glass vessel onto which film was sputtered, *b*—glass spur for admission of liquid helium to the system; *B*—glass vessel and distribution of leads on its surface: *O*—central current lead, A_1, A_2, A_3, A_4—peripheral current leads, O'—potential lead. Potential difference measured between O' and one of peripheral leads.

glass system shown in Fig. 1. The tin film was deposited from a point source under high vacuum. The sputtering was done at the temperature of liquid nitrogen under the vacuum produced by a diffusion pump; the system was then warmed up to room temperature, sealed off, and placed in the Dewar flask.

In view of the possibility that the accuracy of the results might be affected by heating in the connecting wires, we made use of specially-prepared superconducting leads and of a pulse method; the film, moreover, was placed in direct contact with liquid helium during the measurements.

To establish direct contact between the film and the liquid helium, the thin-walled glass "spur" *b* shown in Fig. 1 was broken off with the aid of a rod passing through a sliding seal in the Dewar cap and the system was filled with liquid helium.

The superconducting leads were prepared by drawing through a die a 0.3 × 0.9 mm platinum capillary through which was run a tantalum wire 0.3 mm in diameter. After drawing, the wire was baked out under vacuum and then sealed into the apparatus.

The current pulses through the specimen were generated by applying a voltage source across a circuit consisting principally of a circuit-breaking relay, a choke, a variable resistance, and the specimen under study. The current and voltage pulses were recorded on a Shleifov oscillograph. The circuit was driven by a 220 V laboratory battery. By varying the circuit parameters it was possible to obtain pulses of various durations and amplitudes (the usual pulse length was about 0.1 sec).

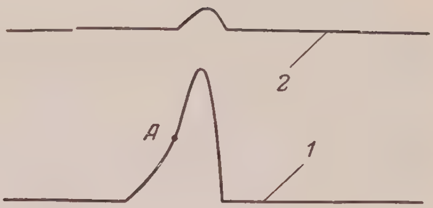

FIG. 2. Oscillograms: *1*—current pulse flowing through film, and *2*—potential difference between O' and A_3.

Figure 2 shows an oscillograph recording of the voltage and current pulses. It is evident from these oscillograms that the voltage pulse begins at some definite value for the current flowing through the specimen (point *A* in Fig. 2). This value is that of the critical current for the given experimental conditions.

To verify the radial character of the distribution of current over the film, the critical currents were measured with an apparatus incorporating three potential leads placed at different distances from the center lead. The linear dependence obtained for $I_c(r)$ testifies to the nearly radial current distribution and to the small effect of heating during the pulse within that part of the film lying between the central and potential leads.

Measurements of critical currents in the films were conducted over the temperature interval $\Delta T \approx 0.5°$ K. The films thus investigated ranged in thickness from 6.9×10^{-6} to 6.4×10^{-5} cm; more than 20 films were studied. For four of the films, in addition to the fields H_{cl} of the critical currents, measurements were made on the external magnetic fields parallel to the film surface. These results for H_c agree satisfactorily with the data obtained by other authors.

Figure 3 shows the dependence of H_{cl} and H_c upon temperature for a film of thickness d=3.27 × 10^{-5} cm. In Fig. 4 the variation of H_{cl} with ΔT is shown on a logarithmic scale, for films of various thicknesses. Figure 5 shows the dependence, also on a logarithmic scale, of H_{cl} upon the thickness d, for two values of the temperature.

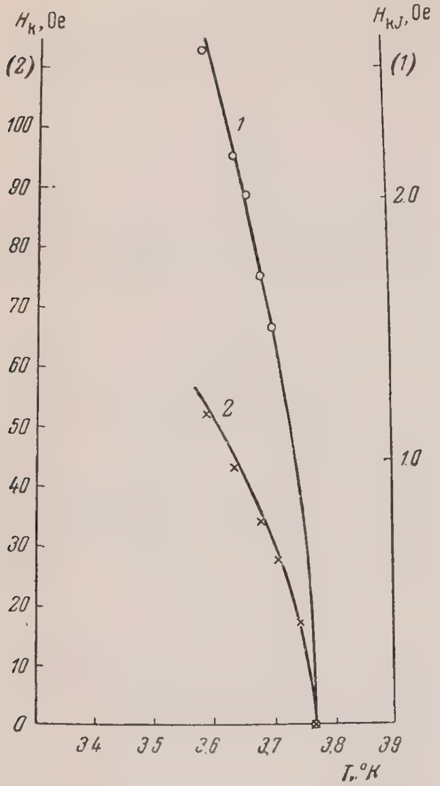

FIG. 3. Dependence of the critical current field and the external magnetic field parallel to the film upon temperature. Film thickness d=3.27 × 10^{-6} cm. 1—curve for critical current field, 2—curve for critical field parallel to film surface.

The observed dependence $H_{cJ}(\Delta T)$ can be represented in the form $H_{cJ} \sim \Delta T^n$, where $n < 1$ (approximate evaluation yields $n \approx 0.6$). The dependence of H_c upon d may be approximately described as linear.

In order to verify the results obtained with pulses a study of the critical current in tin films was made using a different method. A film in the form of a flat ring of width $2a$= 1.5 mm was deposited under vacuum from a point source onto a flat, polished glass surface without leads. At the lowest helium temperature which could be reached an undamped current was induced in the film by means of a magnetic field. The magnitude of the critical current was determined by measuring the magnetic field of the current flowing in the plane ring. Measurements were continued as the film warmed up, using a ballistic method whose sensitivity was improved by a factor of about 100 through the use of a photo-relay. The temperature was measured with a phosphor-bronze thermometer, contact being made with the helium inside the apparatus through a thick (diameter 1mm.) platinum rod. The galvanometer deflection, proportional to the change in magnetic flux $\Delta\Phi$ through the flat measuring coil, was subsequently calibrated in a separate experiment, in which current from an external source was passed through an open copper ring of the same dimensions as the ring of superconducting film. The advantage of this method lies in the absence of contacts and the heating they cause in the film. Substantial difficulties are encountered, however, in obtaining numerical values for the fields due to the critical currents determined in this manner.

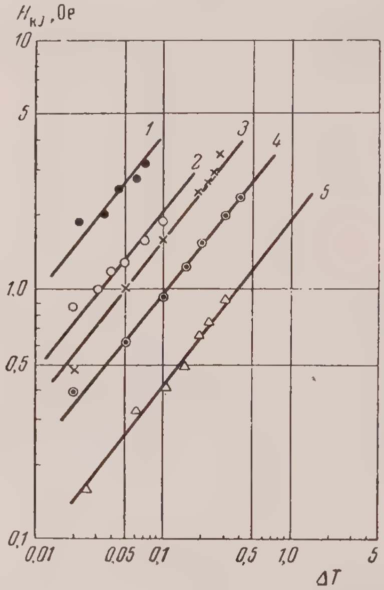

FIG. 4. Dependence of critical current fields upon temperature for tin films of varying thickness. 1—d=6.4×10^{-5}, 2—d=3.3×10^{-5}, 3—d=2.29×10^{-5}, 4—d=9.85×10^{-6}, 5—d=6.9×10^{-6} cm.

This method made it possible to carry out measurements of the critical current for a film 2×10^{-5} cm in thickness over the temperature interval from 1.6 to 3.7° K. The curve obtained for $I_c(T)$ has a break at $T \approx 3$°K. Near T_c the behavior of the $I_c(T)$ curve obtained in this manner is in approximate accordance with the results of our pulse measurements.*

Consideration of the results of this experiment shows that the fields due to the critical currents obtained by the first method agree** in order of magnitude with the results of the Landau-Ginzberg theory.[2] The temperature dependence of the critical current fields, however, is not in accordance

---

*It should be mentioned that for a film 2×10^{-5} cm in thickness at T=1.6° K the critical current was found to be 10.8 a.

**The agreement is best in the vicinity of T_c.

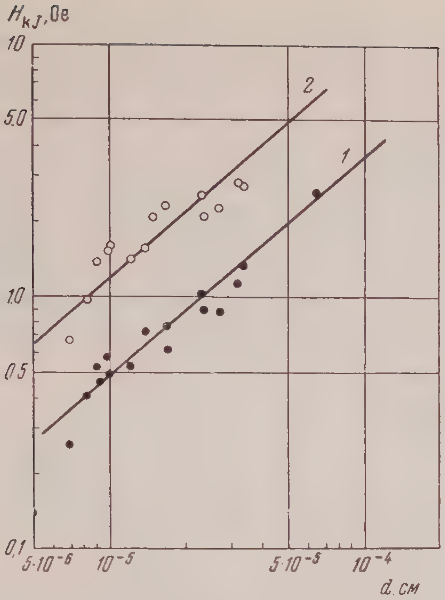

FIG. 5. Dependence of critical current fields upon film thickness for two temperatures. $1-\Delta T = T_c - T = 0.05°$ K, $2-\Delta T = 0.2°$K.

with the theoretical preduction; this may be due to inapplicability of the theoretical formulas derived for thin films to the film thicknesses we have been studying. For the future, a similar investigation of critical currents in films, covering a greater range of thicknesses and temperatures, seems to be in order.

---

[1] A. L. Shal'nikov, J. Exptl. Theoret. Phys. (U.S.S.R.) 10, 630 (1940).

[2] V. L. Ginzburg and L. D. Landau, J. Exptl. Theoret. Phys. (U.S.S.R.) 20, 1064 (1950).

Translated by S. D. Elliott
208

SOVIET PHYSICS JETP VOLUME 4, NUMBER 6 JULY, 1957

Investigation of the Effect of Pressure on the Galvanomagnetic Properties of Tellurium at Low Temperatures

N. E. ALEKSEEVSKII, N. B. BRANDT AND T. I. KOSTINA
Institute of Physical Research, Academy of Sciences, USSR
Moscow State University

(Submitted to JETP editor July 12, 1956)
J. Exptl. Theoret. Phys. (U.S.S.R.) 31, 943-946 (December, 1956)

An investigation has been conducted of the galvanomagnetic properties of tellurium and of the effect of hydrostatic pressure on these properties for samples of tellurium of various purity in the temperature range 1.4°–4.2°K, 14°–20°K and 60°–78° K and in magnetic fields as high as 2.0×10^4 oersteds.

THE existence of a minimum in the curve of the dependence of the electrical resistance on the intensity of the magnetic field at liquid helium temperatures has been confirmed. It was found that the depth of the minimum is a function of the impurity content and that it increases under hydrostatic pressure. The appearance of the minimum in the curves of the dependence of the electrical resistivity on the intensity of the magnetic field is attributed to the Zeeman splitting of impurity levels.

During an investigation of the galvanomagnetic properties of tellurium at the temperatures of liquid helium, Chentsov[1] discovered an anomalous behavior of the dependence of the electrical resistivity of tellurium on the intensity of the applied magnetic field. As the magnetic field was increased, the resistivity of tellurium decreased, passed through a minimum and then increased again. The effect increased as the temperature was lowered; it depended on the orientation of the samples in the field. Because the reason for the existence of the minimum remained unknown, it became interesting to investigate this effect in greater detail in samples of tellurium of varying degrees of purity, and also to investigate the way the effect changes when hydrostatic pressure is applied. Finally our interest was aroused because of our investigation of the effect of pressure on the galvanomagnetic properties of bismuth with added impurities (in particular, tellurium) at low temperatures, which we recently completed.[2]

In order to obtain pressures at low temperatures the method of freezing water in a bomb of constant volume[3] was used. The magnitude of the pressure was determined by the displacement of the critical temperature of a tin wire, enclosed inside the bomb. Low temperatures were attained by using baths of liquid helium, hydrogen and nitrogen. These baths allowed measurements to be made in the temperature intervals 1.4°–4.2°K; 14°–20°K and 60°–77°K in the usual way. The temperature was determined from the pressure of the vapors above the surfaces of the liquids in the dewar vessels. Measurements in the regions between the specified temperature intervals were performed by warming the apparatus. Warming from 4.2 to 300°K required 4–5 hours which guaranteed sufficient time for the measurements. In this case the temperature was determined by means of a copper–constantan thermocouple fastened to the outer wall of the bomb.

Electrical resistance and Hall voltage were measured with the aid of the usual potentiometer scheme, which used standard elements to produce all possible permutations of direction of the current and magnetic field. The instruments used were a high impedance potentiometer of the type P. P. T. V.–1 and a galvanometer of the type M–21 4 which had a sensitivity of 1 × 10⁻⁷ μ V mm.

The samples, on which the measurements were performed, were cut out of different parts of original samples of tellurium.* Current and potential leads and leads for measuring the Hall voltage were made from platinum or copper wires of 0.05 mm dia. which were soldered onto the samples in various ways. The orientation of the samples were determined from the reflection pattern and from a diagram of the variation of the electrical resistivity in a constant magnetic field. In all the samples the direction of the current which was used for measurement was approximately perpendicular to the direction of the principal axis.

A study of the properties of polycrystalline samples of tellurium was made difficult by the unavoidable cracking of the samples whenever the temperature changed. This is a consequence of the strong anisotropy of the temperature coefficients of expansion.[1,4,5] Experimental investigation of the effect of pressure on polycrystalline samples of Te showed that pressure reduced the resistivity of the samples by an extraordinarily large amount. Thus, for example, for the sample Te–1, a pressure of the order of 1700 atmospheres at 4.2° K produced a decrease in the resistivity by a factor of 27 and at 220° K by a factor of 14.** Therefore an interpretation of the results obtained on polycrystalline samples is difficult. In contrast to the polycrystalline samples, the electrical resistivity of single crystals increased with pressure for the temperature region below 170° K and decreased for higher temperatures. (Fig. 1).

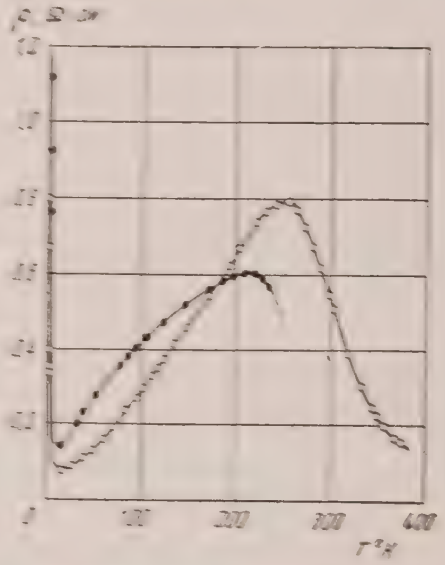

FIG. 1. Dependence of resistivity on temperature for sample Te–3: O–p=0; ●–p= 1700 atmospheres.

For the majority of the samples investigated at helium temperatures, there was observed a minimum in plots of the electrical resistivity vs. the intensity of the magnetic field. Figure 2 shows plots of the change of the electric resistivity in a magnetic field for sample Te–3a for various temperatures and for orientations of the samples in the field which correspond to the largest and smallest values of the effect. The relative depth of the minimum, characterized by the equation

$$(\Delta r_{HT}/r_{0T})_{\min} = [r_{0T} - (r_{HT})_{\min}]/r_{0T},$$

where r_{HT} is the resistivity in field H at temperature T, is greatest for the crystalline direction for which the biggest increase of resistivity is observed at the higher magnetic fields and the minimum is shallowest for the direction perpendicular to this. As is evident from Figure 3, the anisotropy of the depth of the minimum in its dependence on the orientation of the crystals in the field decreases as the temperature is decreased so that for each crystallographic direction there exists a certain temperature T, above which a minimum is not observed.

---

*The original samples were kindly supplied to us by S. S. Shalyt for which the authors wish to express their gratefulness.

**Similar phenomena have been observed by other authors at room temperature.

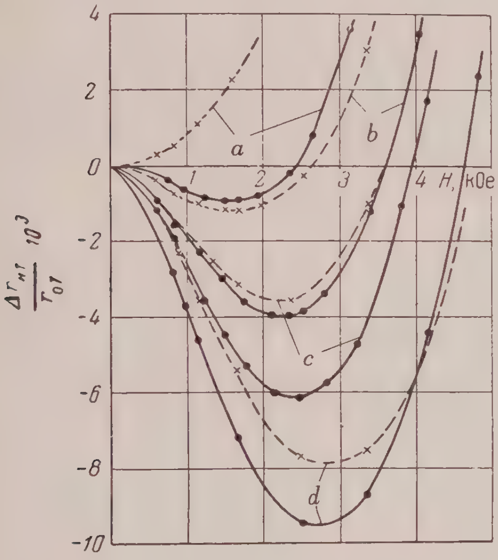

FIG. 2. Change in electrical resistance of sample Te–3a in a magnetic field: ●—for the sample orientation which yields a maximum value of the effect; X—maximum value of the effect; a–T= 4.2°K; b–T= 2.55°K; c–T = 1.95°K and d–T= 1.5°K.

In order to elucidate the cause of the development of the minimum, experiments were performed, (a) on samples of various shapes and dimensions, (b) on the effect of using different methods of attaching the leads and (c) on samples of different purity. In this way it was determined that the value of the minimum does not depend on (a) or (b). In heavily doped Te samples, which had a metallic behavior of r (T) in the helium temperature region, the minimum is absent down to 1.4°K. The minimum appears with purer samples of Te, whose electrical resistance in the absence of the magnetic field increases with decreasing temperature below 4.2°K. In such samples, the value of the minimum increases in proportion to the purity of the samples. However, for the purest samples available to us the magnitude of the effect again decreases. These samples are the basis of the surmise, that the dependence of the magnitude of the effect on the concentration passes through a maximum.

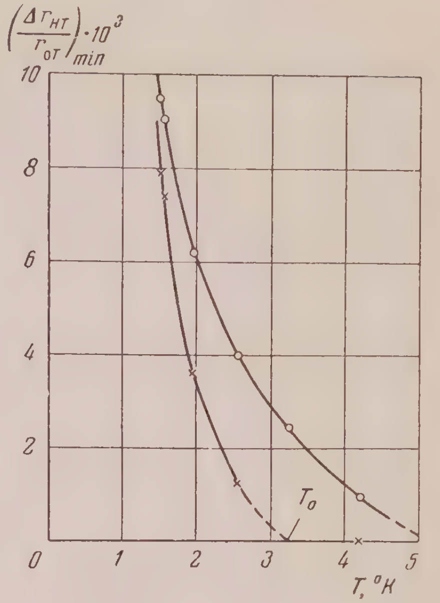

FIG. 3. The dependence of the magnitude of the minimum on the temperature for sample Te–3a, for the orientations which produce the largest (O) and the smallest (X) values of the effect.

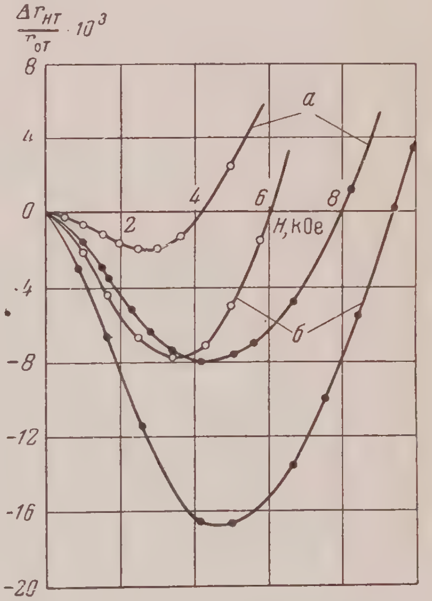

FIG. 4. Change in electiical resistance of sample Te–3b in a magnetic field: O–p=0; ●–p= 1700 atmospheres; a–T= 4.2°K, b–T= 1.77°K.

It was observed, that hydrostatic pressures in the range of 1700 atmosphere provoke a significant change in the galvanomagnetic properties of Te. Figure 4 shows plots of $\Delta r_{HT}/r_{OT}$ (H) in the vicinity of the minimum for sample Te–3b with and without applied pressure at a temperature of 4.2°

and 1.77 °K. As is evident from these curves, pressure in the vicinity of 1700 atmospheres causes an increase in the minimum by a factor somewhat greater than 2. In the region of highest magnetic fields, hydrostatic pressures produce an increase in the function $\Delta r_{HT} / r_{OT}$ (*H*) at temperatures of 77° K and 20.4° K and a decrease in this parameter at helium temperatures (Fig. 5).

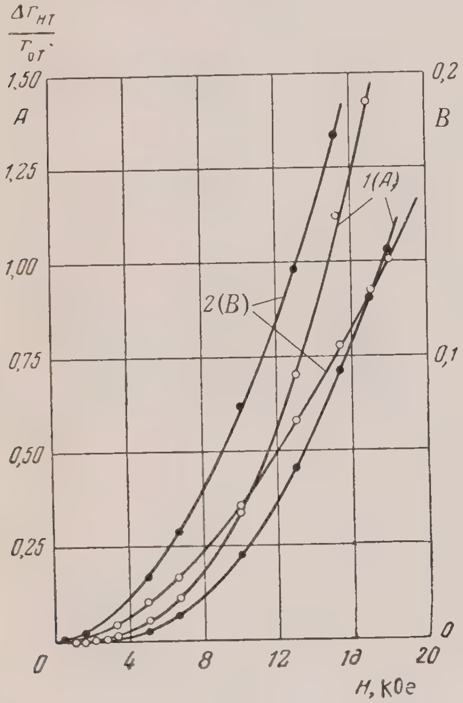

FIG. 5. The effect of pressure on the change of electrical resistance in large magnetic fields for sample Te—3: O—p= 0, ●—p= 1700 atmospheres; 1(*A*)—T = 1.56°K; 2(*b*)—T = 77°K.

It seems possible to attribute the appearance of a minimum in the curves of $\Delta r_{HT} / r_{OT}$ (*H*) to a splitting (similar to the Zeeman effect) of the impurity levels of Te in a magnetic field. The possibility of splitting impurity levels in a magnetic field has been pointed out in the literature.[6] An estimate of the magnitude of the Zeeman splitting in magnetic fields of about 1000 oersted, is obtained from the equation $\Delta E = 1.16 \times 10^{-5}$ ev. On the basis of this picture, the effect will be observable only for low temperatures, where KT is about 10^{-4} ev. Measurement of the temperature dependence of the electrical resistivity of tellurium in the helium temperature region argues, apparently, for the existence of impurity levels with an activation energy of 10^{-4}–10^{-5} ev. in the samples used in these experiments. It should be possible to demonstrate the splitting of an impurity level in a magnetic field by showing that there is an increase in the concentration of carriers in the conduction band. Observations of the dependence of the Hall constant, (which were performed for this reason) on the intensity of the magnetic field confirmed this hypothesis (Fig. 6). For those fields, in which the minimum of the resistivity occurred, there was a region of an observable decrease in the Hall constant. Furthermore, dR/dH had a maximum in this region. At a temperature of 77° K the Hall constant does not change in the magnetic field.

The absence of a minimum in Te samples which have a metallic dependence of resistance on temperature can be explained, supposedly, by a widening of impurity level responsible for the effect into a band, which blends into the valence band of tellurium.

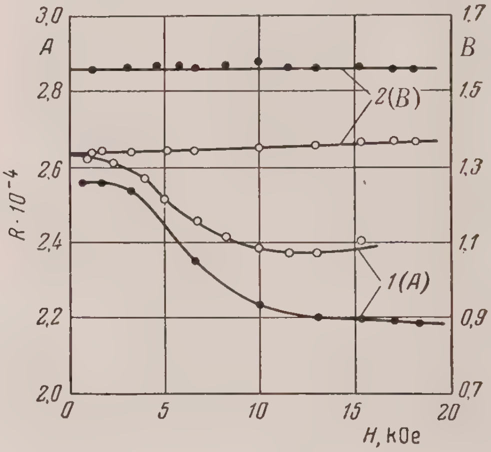

FIG. 6. Dependence of Hall constant on the intensity of the magnetic field for sample Te—3: O—p=0; ●—p = 1700 atmospheres; 1(*A*)—T = 4.2°K; 2(*b*)—T=77°K.

---

[1] R. A. Chentsov, J. Exptl. Theoret. Phys. (U.S.S.R.) 18, 374 (1948).

[2] Alekseevskii, Brandt and Kostina, Dokl. Akad. Nauk SSSR 105, 26 (1955).

[3] B. F. Lazarev and A. S. Kan, J. Exptl. Theoret. Phys. (U.S.S.R.) 14, 470 (1944).

[4] C. Wistrand, Dissertation, Upsala (1916).

[5] B. Beckmann, Ann. Physik 46, 931 (1915).

[6] Egren, Diuga and Ettsel, "Semiconductors" IIL, Moscow, 1954, p. 127.

Translated by J. J. Loferski
206

SOVIET PHYSICS JETP VOLUME 4, NUMBER 6 JULY, 1957

On the Mass Spectrum of Charged Cosmic Ray Particles

A. I. ALIKHANIAN, N. V. SHOSTAKOVICH*, A. T. DADAIAN,
V. N. FEDOROV AND B. N. DERIAGIN
P. N. Lebedev Physical Institute, Academy of Sciences, USSR
Physical Institute, Academy of Sciences, Armenian SSR

(Submitted to JETP editor July 21, 1956)
J. Exptl. Theoret. Phys. (U.S.S.R.) 31, 955–970 (December, 1956)

Results of an investigation of the cosmic ray particles mass spectrum at 3200 m are reported. The measurements were carried out by means of a magnetic spectrometer used in conjunction with two cloud chambers. Protons, deuterons, π-mesons and K-particles were observed among the particles locally generated in stars above the experimental arrangement.

The cases of 11 particles with masses of about 500–600 m_e stopping in the lower chamber are discussed. In all these events, neither a star nor a shower was observed in the upper chamber. It was found that some of these particles entered the apparatus from the outside in a similar manner to the μ-mesons.

1. INTRODUCTION

SYSTEMATIC measurements of the momentum and range of charged cosmic ray particles, dating from 1946, have led us to conclude that unstable particles heavier than the μ-meson exist. Under the assumption that the particles were stopped as a result of ionization losses, it was impossible to explain the experimental data obtained by us by postulating the existence of only one new particle heavier than the μ-meson. It was necessary to assume the existence of three groups of particles with masses intermediate between those of the μ-meson and of the proton, namely of particles with masses equal to 350, 500–600 and 950 electron masses.[1]

Having increased the resolving power of the magnetic spectrometer, we were later able to resolve spectrally the π-mesons and the μ-mesons. The groups of particles with masses 580 and 950 m_e, well resolved from π-mesons and protons, were again found in the mass spectrum, obtained from range and momentum measurements.[2,3] Since the observed particles traversed a path longer than one meter, we concluded that the mean life of the particles of all three groups should be longer than 5×10^{-9} sec.

The mass determination from range and momentum measurements can sometimes be in error, since the π-mesons present in the beam of particles can be stopped in absorbers for any value of momentum, and in this way imitate particles of larger mass. In using this method of mass determination it is therefore necessary to have proof that the particle was stopped due to ionization losses. Alikhanian and Kharitonov[4,5] added proportional counters to the magnetic spectrometer and determined the specific ionization of the particles of intermediate masses, together with their range and momentum. It was shown that the majority of particles of the 950 m_e group possess a larger specific ionization, and only a part is due to relativistic π-mesons stopping in absorbers as the result of nuclear collisions. These measurements made it possible to establish the existence of mesons with mass $\sim 1000\ m_e$.

The observations of many authors, using an extended set-up containing cloud chambers, later confirmed our conclusions as to the relatively long life time of charged particles with mass equal to $\sim 1000\ m_e$ (K-particles).

The existence of charged particles with mass equal to 500–600 m_e has until recently been uncertain. Several authors expressed doubt as to their existence. A few trajectories of particles with mass 500 m_e were observed in experiments of Daniel and others[6,7] without any further confirmation.

In 1952, we carried out a series of observations of heavy particles stopping in a multiple-plate cloud chamber, used in conjunction with a magnetic spectrometer. This set up made it possible to determine, for each particle, whether the stopping was due to ionization losses and, the momentum being known, to find its mass. In the course of a prolonged series of measurements carried out by means of the above set up, we found 32 particles, stopping in the multiple-plate chamber, the masses of which, determined from the momentum and the ionization range, were between 460 and 1100 m_e.

In this series of measurements, another large rectangular cloud chamber containing lead plates was placed above the magnetic spectrometer. Studying (in the upper chamber) the trajectories of the particles which traverse the magnetic spectrometer and are stopped in the lower chamber, it was possible in many instances to determine the mechanism and the place of creation of particles with

---

*Deceased.

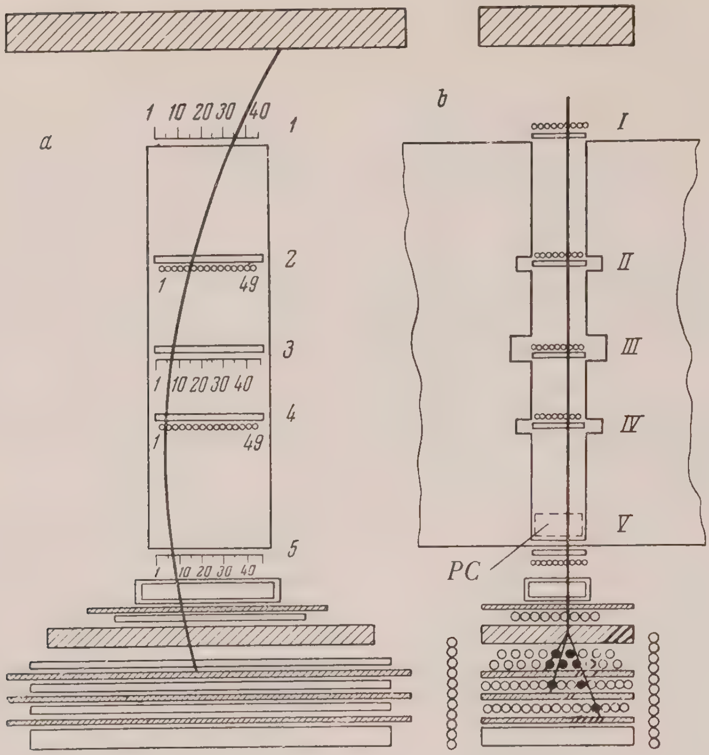

FIG. 1. Schematic diagram of the magnetic spectrometer with a proportional counter and the arrangement of absorbers. *PC*—proportional counter *1*.

different masses. In the majority of cases a star could be found in the upper chamber, from which the π- and K-mesons originated. Not in a single case of stopping particles with the mass 500–600 m_e was it possible to observe a star, or a shower, in the upper chamber.

2. RANGE–MOMENTUM MEASUREMENTS OF THE MASS SPECTRUM

In this Section, we present a brief summary of the basic results of the particle mass measurements carried out in 1950–1952 by means of the magnetic spectrometer. The mass of the particle was determined from the momentum and the amount of matter traversed by the particle in the filter arrangement. Two rectangular proportional counters were placed in the particle trajectory, at the exit from the magnetic spectrometer. This made it possible to determine the specific ionization of the particle.

The magnetic spectrometer of high resolving power, which was placed at 3200 m above sea level[2], is shown in Fig. 1. A large electromagnet weighing 76 tons forms the main part of this instrument. The pole pieces are 100 cm long and 30 cm wide, the distance between them being equal to 12 cm. The maximum field strength in the gap of this electromagnet can attain 1900 Oe. The cross sections of the instrument in two perpendicular planes are shown in Fig. 1. Five trays of thin-walled counters 4.6 mm in diameter are placed in the gap (1–5, view *a*), which make it possible to determine five points of the circular trajectory of the particle. A tray consists of 49 hodoscoped counters.

The counters in trays 2,3 and 4 are constructed of aluminum tubes, with walls about 100 μ thick, to minimize scattering. Five trays of coordinating thin-walled counters (I–V) make it possible to determine simultaneously the straight-line trajectory in the plane parallel to the magnetic field (view *b*). The particle leaving the magnet gap enters the absorber arrangement, consisting of five trays of coordinating counters, separated by graphite slabs 2 or 4 cm thick each.

The accuracy of the mass measurements in the magnetic spectrometer is limited basically by the following three factors: 1) the finite dimensions of counters, 2) scattering in counter walls, and 3) errors in the range determination. For the case of particles stopping only as a result of ionization losses, the errors in the value of the range are caused by the finite thickness of filters. It follows from a calculation that, in a field of 6400 Oe, the

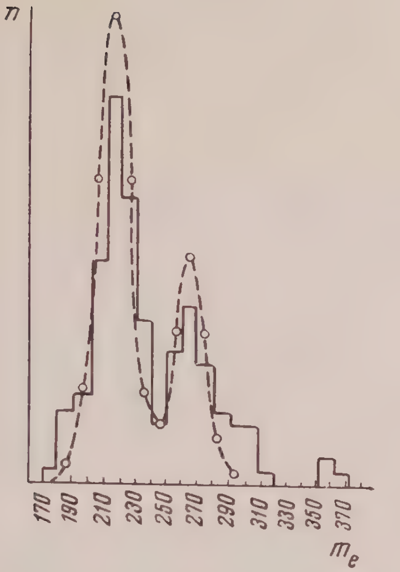

FIG. 2. Mass spectrum of negative particles in the 180–400 m_e interval (without aperture correction)

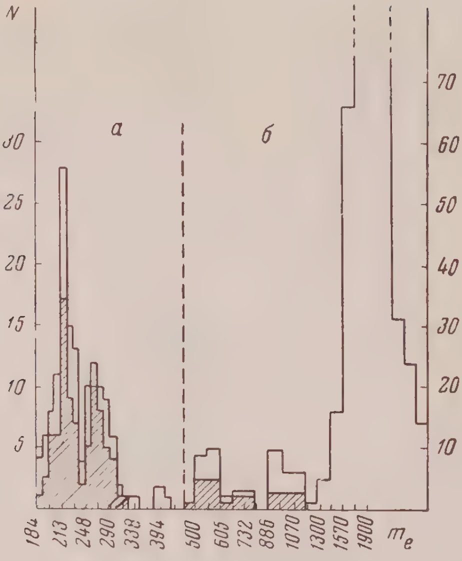

FIG. 3. Mass spectrum (without aperture correction): a) at 6400 Oe, $24 > R > 16$ cm C; b) at 6400, 9200, and 10500 Oe, $24 > R > 12$ cm C.

half width of the μ-meson line amounts to 16 m_e, thus enabling a good resolving of the π- and μ-mesons. The mass spectrum of negative particles in the interval 180–400 m_e is shown in Fig. 2. In these measurements, a lead block 10 cm thick was placed under the set up. It can be seen in Fig. 2 that the μ-meson group shows up distinctly, next to the π-meson group. The broken curve represents the Gaussian distribution curve, calculated for a probable error of 16 m_e, which closely fits the observed distribution. This result is a good illustration of the resolving power of the magnetic mass-spectrometer.

In the course of these measurements in 1950-1951, we obtained the mass spectrum in the total interval between the μ-meson and the proton.[8,9] This spectrum is shown in Fig. 3. Two groups of heavy mesons, concentrated around the values 600 m_e and 1000 m_e, are visible in the mass spectrum.

It followed from the complete data that a considerable part of the particles of masses 600 and 1000 m_e was stopped in the absorbers as the result of ionization energy losses. 1) A sharp grouping of the particles around two mass values was observed, which would have been impossible if the particles were stopped in the absorbers as the result of nuclear collisions. 2) The mean values of the momentum of the particles with intermediate mass values increase with the range of the particles. The average momentum of particles with a range of 4–12 cm in graphite was found to be equal to 2.9×10^8 ev/c, and that of particles with a range of 12–16 and 16–24 cm in graphite to 3.12 and 3.61×10^8 ev/c, respectively. A systematic increase of the average momentum with the range can take place only as the result of ionization stopping. 3) The measurements of the specific ionization of particles, carried out in 1951 by means of proportional counters placed in the magnetic spectrometer, showed that the value of the specific ionizations for the intermediate particles is larger than the minimum ionization by a factor of 1.5–2.

The measurements of the specific ionization of particles in 1951 were carried out by means of two proportional counters, the position of which is shown in Fig. 1. It was necesssary to calibrate the pulses given by each counter in order to obtain the relative specific ionization of different particles. Penetrating particles with a range larger than 14 cm were used for this purpose. The pulse size distribution, obtained with the counter No. 2 shown in Fig. 4, is based on data obtained from 14,829 penetrating particles, the momentum of which was determined from the curvature in the magnetic field (curve 2). Curve 1 in this figure represents the theoretical curve of energy loss fluctuations in the counter gas according to the theory of Landau.[9]

Alikhanian and Kharitonov[5] measured the specific ionization of 87 particles which, from the values of their range and momentum, were classified as particles of intermediate mass. From the total of 87 particles, data were obtained simultaneously, by means of the two counters 1 and 2, for 26 particles only. For all remaining particles, the ionization was determined by means of counter 2 only. The

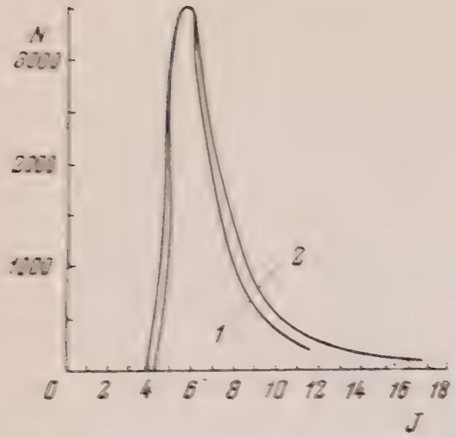

FIG. 4. Distribution of minimum ionization particles. N—number of particles, J—relative ionization.

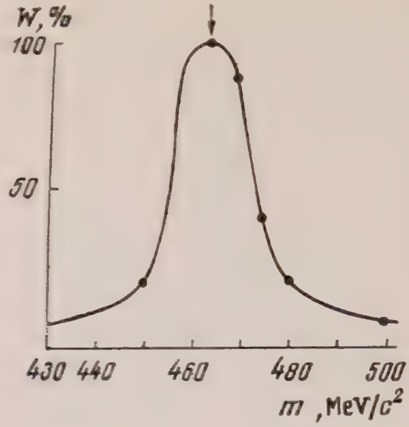

FIG. 5. Probability curve of various mass values in the interval 800–1100 m_e.

results of these measurements are given in Ref. 10. It was shown that the specific ionization of heavy mesons is considerably larger than that of μ-mesons of the same values of momentum ($2.8 - 4.5 \times 10^8$ ev/c). Besides, it is much smaller than the specific ionization of protons having the same range. Distribution curves of the specific ionization were plotted for heavy mesons and protons. In the case of protons, the proportion of cases when the ionization was twice the most probable one was equal to 14 ± 3.5%, while for heavy mesons (of both groups) it amounted to 12 ± 4%. It follows that the increased specific ionization of these particles cannot result from a mixture of a separate group of strongly ionizing particles with particles of minimum ionization. Consequently, the heavy mesons observed by us in the mass spectrum could not have appeared only as a result of nuclear stopping of fast π-mesons.

The data on the specific ionization of the intermediate mass particles were used for an independent determination of the mass of the particles from their momenta and ionization. For this, we used a method suggested by Liubimov.[11] Let a particle with momentum P produce an ionization J in the counter. We shall assume that the mass of the particle equals m. Then, knowing the ratio P/m, it is possible, according to the Landau formula, to find the most probable value J_0 of the specific ionization of the particle, and then, from the experimental curve of the ionization fluctuation, to find the probability that the actual ionization will equal J, and not J_0. We can repeat this procedure for all particles of a given group, and the product of the found probabilities will give us the probability of observation of a given set of the ionization values J, under the assumption that all particles of the group have the mass m and the observed values of momentum.

Assuming another value of the mass m_1, we shall obtain a new value of the probability of observation of a given set of the experimental values of the ionization J, produced by the particles in the working volume of the proportional counter. The sequence of such probabilities, determined for the various values of the particle mass m, and correspondingly normalized, can be regarded as the probabilities of the various values of the mass of the particles, for given sets of observed values of ionization and momentum. The maximum of the curve probability vs. mass will correspond to the most probable value of the mass of the investigated group of particles.

The above procedure was applied to a group of 48 particles, the mass of which, derived from the range and momentum measurements, was found to be between 800 and 1100 m_e. The resulting curve of the probability of the various values of the mass of the particle for the obtained set of experimental values of momentum and ionization is shown in Fig. 5. The curve has a sharp maximum, corresponding to the mass equal to 4.65×10^8 ev/c,^{2} i.e., 910 electron masses. For the values of mass, different from the most probable one by only 10%, the probability curve drops rapidly to zero.

For the sake of comparison, 50 proton trajectories with ranges varying from 4.5 to 5.0 cm were given the same treatment. The results are shown in Fig. 6. The most probable value of the proton mass obtained was equal to 935.5 ev/c^2, i.e., 1830 m_e with a probable error of ± 20 m_e. We tried to apply the same method of evaluation of the momentum and ionization measurements in the case of particles with mass 500–600 m_e. In this case however, the specific ionization of the particles does not exceed the minimum ionization to any extent and the results are therefore less satisfactory than in the case of K-particles and protons.

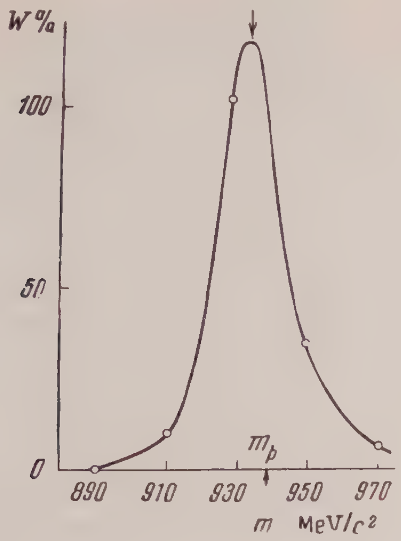

FIG. 6. Probability curve for protons with range between 4.5 and 5.0 cm Pb.

3. MEASUREMENTS OF THE MASS OF THE COSMIC–RAY PARTICLES WITH THE MAGNETIC SPECTROMETER AND A MULTIPLE–PLATE CLOUD CHAMBER

In this Section, we shall report results of observation of charged particles stopping in a multiple plate cloud chamber, used in conjunction with the magnetic spectrometer. This set-up was first used in 1952 by Alikhanian, Kitillov-Ugrimov, Shostakovich and Fedorov at 3250 m altitude (Alagez). Description of the apparatus and details of results can be found in Refs. 12, 13 and 14. A schematic drawing of the apparatus in two perpendicular projections is shown in Fig. 7. A rectangular cloud chamber, containing lead or copper plates of various thicknesses, was placed under the magnetic spectrometer. A tray of counters A, connected to an anti-coincidence circuit, was placed below the bottom of the chamber. The set-up was triggered when a particle, traversing the magnetic spectrometer, discharged counters in trays 2,4 and 5 and failed to discharge a counter in the tray A (series 1). The rectangular cloud chamber 400 × 250 × 120 mm contained in the illuminated space seven filters: one filter consisting of a lead plate 10 mm thick and a copper plate 3 mm thick, and 6 copper plates each 3 mm thick.

In the second series of measurements, the trigger was given by the anti-coincidence 1,3,5–A and a larger chamber, 600 × 280 × 180 mm was used. In this series, seven lead filters, each 7 mm thick, were placed in the illuminated space. Some of the measurements of the second series were carried out with filters placed in the lower chamber in the following order: the first two lead plates were 7 mm thick each: the following three plates were each 4 mm thick, and the sixth lead plate was of 7 mm thickness. The seventh plate was a copper one, 2 mm in thickness.

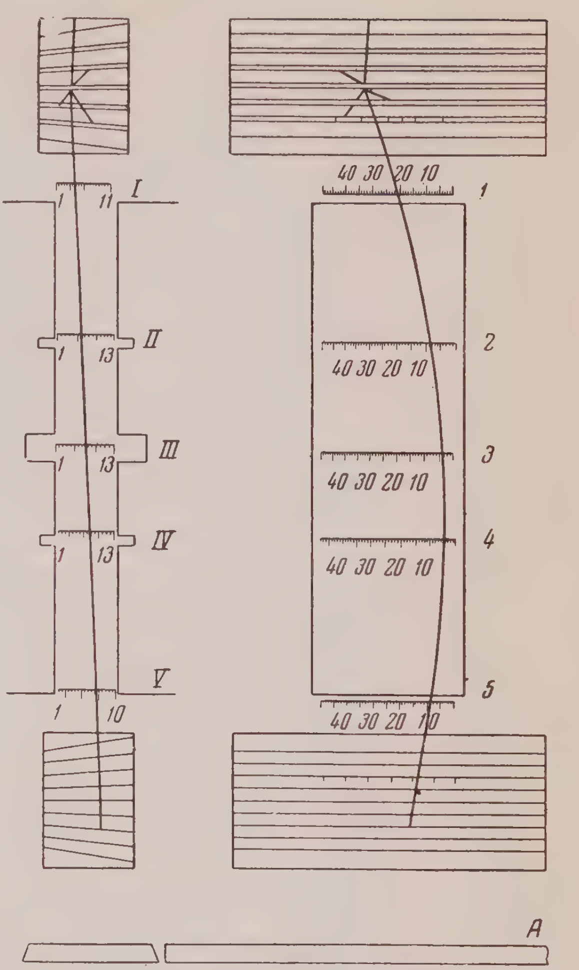

FIG. 7. Schematic diagram of the magnetic spectrometer with two cloud chambers.

A charged particle, before entering the visible space, passed through the top of the chamber, consisting of an aluminum plate 7 mm thick and a copper plate 2 mm thick (a total of 3.7 gm/cm.^{2}). The chamber was illuminated by two pulsed quartz lamps 1PK–600. The tracks in the chamber were photographed with a stereoscopic camera on motion-picture film.

In the second series of measurements, a second cloud chamber, of the same dimensions as the lower one, was placed above the spectrometer instead of the lead block (see Fig. 7). In the illuminated region of the upper chamber, the top and the bottom were 1.2 cm thick (copper) and five lead plates, each 1 cm thick, were placed in the chamber. In this way it was possible to observe the trajectory of the particle before it entered the magnetic spectrometer and stopped in the lower chamber. If the particle recorded by the apparatus left the illuminated region of the upper chamber, either a star in which it originated could be observed, or it could be decided that the particle came from the outside. The efficiency of observation of particles in the upper chamber, which then were recorded in the lower chamber, depends essentially on their momentum. The efficiency is large for protons and heavy mesons, and is very small for slow μ- and π-mesons, the majority of which emerge from the sectional parts of the upper chamber, and in the beginning pass through non-illuminated zones.

4. SELECTION OF TRAJECTORIES, ACCURACY OF MASS MEASUREMENTS, APERTURE.

Range and momentum measurements of a large number of particles stopping in the lower chamber were carried out by means of the apparatus described.

The mass spectrum of particles, which is given below, was derived from trajectories fulfilling the following conditions: a) in the plane of magnetic deviation the trajectories of the particles were determined from at least four points, lying on a circle; b) in the perpendicular plane, the trajectories passed through at least three points lying on a straight line; c) the track of the particle entering the lower cloud chamber was a continuation of the trajectory of the particle in the magnetic spectrometer; the only deviations allowed were in the limits of the angle of multiple scattering in the cover of the chamber; d) the particle stopped in the illuminated region of the lower chamber, the limits of which were determined by special measurements.

From all trajectories fulfilling the above conditions, only those were included in the mass spectrum whose stopping was due to ionization, i.e, when a considerable increase in the track density was observed with decreasing residual range. In the majority of cases, the track density was estimated visually and compared with that of relativistic particles traversing the same region of the chamber. In some of the more interesting cases, the track density was determined from microphotometric measurements. Track density of mesons, protons and minimum ionization particles traversing the same chamber region and photographed on the same film were used as a check.

The method of microphotometric density determination is not accurate enough to measure the specific ionization of particles, and serves only as auxiliary means of objective estimate of the value of ionization and its variation. The sensitivity and accuracy of this method are sufficient, in the majority of cases, to distinguish a sudden stopping of a fast particle from a stopping due to ionization, when a gradual increase in the track density is observed.

One of the cases of a particle stopping in the sixth plate is shown in Fig. 8. The increase of the track density can easily be observed. The same can be deduced from the microphotogram of this case, shown in Fig. 9. The track of a π-meson with momentum 4.0×10^8 ev/c, undergoing a nuclear collision in the fifth plate and producing a two-prong star, is shown in Fig. 10. In this case, the track density remains practically the same along the whole trajectory, which, within the limits of possible fluctuations, is observed in the microphotogram as well (Fig. 11). The range of a particle, the ionization character of the stopping of which was established, was determined from the quantity of traversed matter, the slope of the trajectory being accounted for.

The main source of error of the mass determination is the error of the momentum measurement. For the case of slow particles, these errors are mainly caused by scattering in counter walls and, in part, by the finite dimensions of counters. Experiments on scattering of cosmic ray particles within the telescope of the mass-spectrometer, with magnetic field absent, showed that for penetrating particles, the mean square value of the false curvature is not larger than $0.016\ \text{m.}^{-1}$ For slow particles, stopping in the lower chamber (μ-mesons and protons with ranges from 0.55 to 2.55 cm Pb), the mean square value of the false curvature equalled $0.045\ \text{m.}^{-1}$ The experimental scattering curves, obtained in experiments without the magnetic field, confirmed the correctness of the calculated errors of momentum measurements, in which both the multiple scattering in the walls of the counters and their finite dimensions were taken into account.[15]

In magnetic field of 4800 gauss, in which the measurements were carried out, the total mean square error of the mass determination of an individual particle amounted to 9–10% for particles with mass 1000 m_e and 8% for particles with mass 500 m_e. The error due to the finite size of the counter is not larger than 2–2.5%. The efficiency of particle recording in a magnetic spectrometer (the aperture) decreases with decreasing value

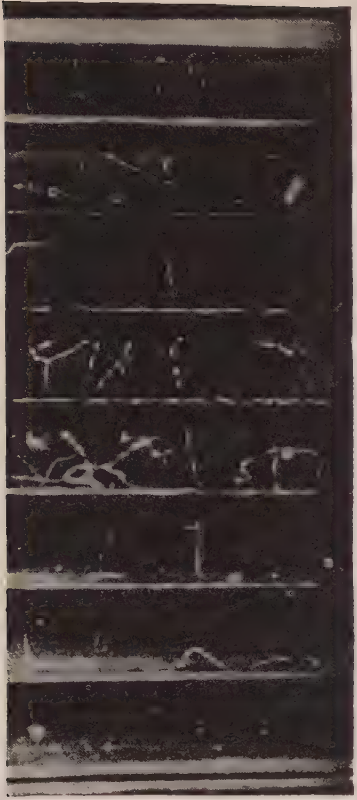

FIG. 8. Stopping of a negative particle. Mass equal to 500 m_e (range–momentum method).

of the momentum of the particle. We calculated the curves of the efficiency of recording of particles of different momenta under the assumption of an isotropic angular distribution of incident particles. With the help of these curves, and taking into account the limits of the illuminated region in the lower chamber and the place of the end of the range of the particle, we constructed a family of curves of the recording efficiency of particles of different momenta, stopping in the illuminated region of the chamber.

5. MASS SPECTRUM

The mass spectrum of particles stopping in the plates of the lower chamber, is shown in Fig. 12. The spectrum is based on the trajectories of particles, selected according to conditions mentioned in Sec. 4. A group of 21 *K*-particles and of particles with masses between 500 and 600 m_e can be seen in the spectrum next to the main peaks due to mesons (μ and π) and protons. The accuracy of the mass measurement of a single *K*-particle lies, for the majority of cases, within the limits of 80–100 m_e, and of a proton, within 180–200 m_e, thus ensuring the spectral resolution of *K*-particles from the large proton peak.

Fifteen of the 17 *K*-particles recorded in the second series of measurements were positive and only two were negative. One of the cases in which a positive *K*-particle stops and decays is shown in Fig. 13. A primary particle with momentum $p = 3.25 \times 10^8$ ev/c is stopped in the fourth plate, so that the total amount of matter traversed after the particle has left the magnetic field equals 2.53 cm Pb. The mass, determined from the range and momentum, equals $910 \pm 75\ m_e$. A fast meson which leaves the chamber after traversing 21.5 g/cm^2 Pb emerges from the end point of the track of the K^+ particle.

Fast decay products were observed in about half of the cases of stopping K^+ particles. In a number of cases, the absence of decay products can be connected with absorption of these in the lead plate (τ-decay or *K*-decay). In other cases, the absence of a visible decay product can be explained by an unfortunate direction of flight of the secondary particle. The frequency of observation of *K*-particles, as compared with π-mesons and protons in the same range interval, can be found from the spectrum in Fig. 12 after a correction is made for different recording efficiencies of particles with various momenta. This correction was determined approximately, on the basis of the isotropic angular distribution of the particles under

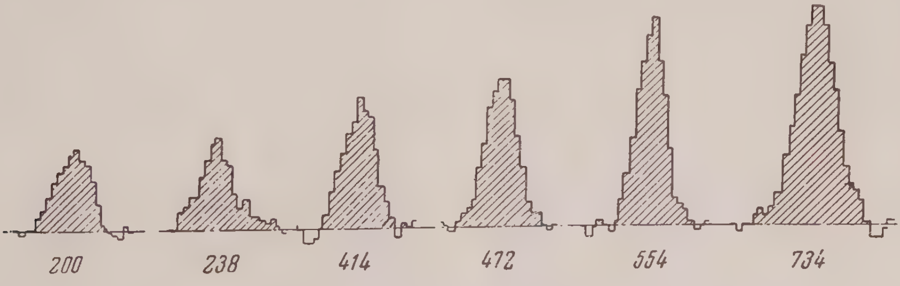

FIG. 9. Microphotogram of the particle track shown in Fig. 8. The numbers express the relative track density.

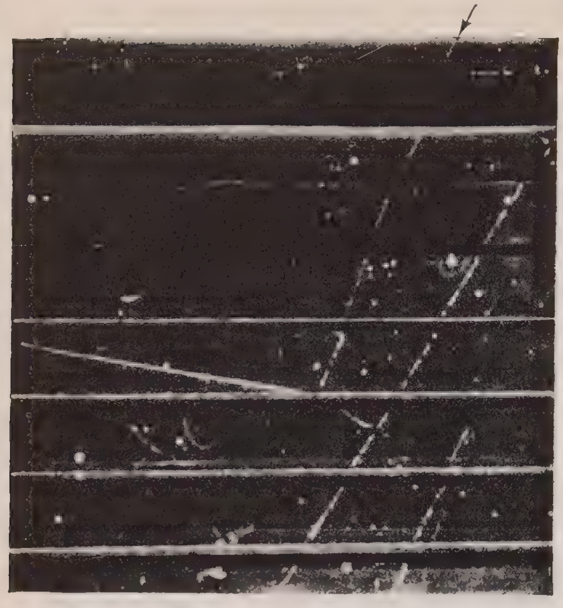

FIG. 10. Sudden stopping of a π-meson of momentum 4×10^8 ev/c accompanied by a production of a star.

consideration. The data given in Table I show that in the same range interval, 20K$^+$ particles are observed, as compared with 240π-mesons stopping as the result of ionization losses, which amounts to about $(8 \pm 2)\%$.

In thesame period of observation, 9 fast π-mesons stopping in absorbers as the result of nuclear interactions were recorded. The mass values of these mesons, determined formally from their range and momentum, were found to lie in the limits $800-1200\ m_e$. The thin tracks of fast π-mesons, imitating heavy mesons, could easily be distinguished from stopping K-particles, for which the track density increases sharply towards the end of the track. Studying the trajectories in the upper chamber it was possible to ascertain that the K-particles and π-mesons originated in stars produced in the matter present in the upper chamber, or emerged from non-illuminated zones. Fast π-mesons and K-particles with values of momentum equal to $2.5-4.5 \times 10^8$ ev/c could be sufficiently well studied in the upper chamber. Thus, for instance, of seventeen K-particles recorded in the lower chamber, thirteen originated in stars occurring in the illuminated part of the chamber, and only four in the non-illuminated part. Eleven out of eighteen π-mesons with momenta in the range of $2-4.5 \times 10^8$ ev/c stopping suddenly in the absorbers of the lower chamber were accompanied by stars in the illuminated part of the upper chamber (Table II).

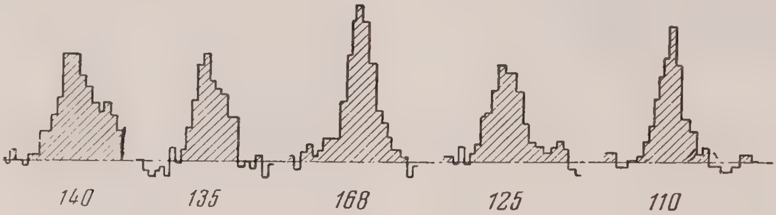

FIG. 11. Microphotogram of the track of the fast π-meson shown in Fig. 10.

The spectrum shown in Fig. 14, is based on particles which originated in stars, all the particles whose origin in the upper chamber is uncertain being excluded. It is found that the mass spectrum of particles locally produced in stars differs basically from the total spectrum. π-mesons, K-particles, protons and deuterons are present in the spectrum of the star–born particles, while particles with the mass $500-600\ m_e$ are completely absent. Evidently the latter type of particles either does not originate in stars at all, or at least the frequency of such events is considerably lower than is the case for K-particles. The spectrum in Fig. 14 is not corrected for the efficiency of recording of particles with different values of momentum, which depends, basically, on the dimensions of the illuminated parts of the upper and lower chambers.

Data on particles whose mass, as measured by the range–momentum method, was found to be intermediate between the masses of the π-meson and of the K-particle, are given in Table III. Eleven such particles were recorded in the course of the second series of measurements, which was the most prolonged, and one was recorded in the first series.

It can be seen from the Table that the mean square error of the mass measurement of a single particle does not exceed $40-50\ m_e$. The grouping of particles around the mass value $550\ m_e$ serves as a serious proof of the existence of particles with this mass.

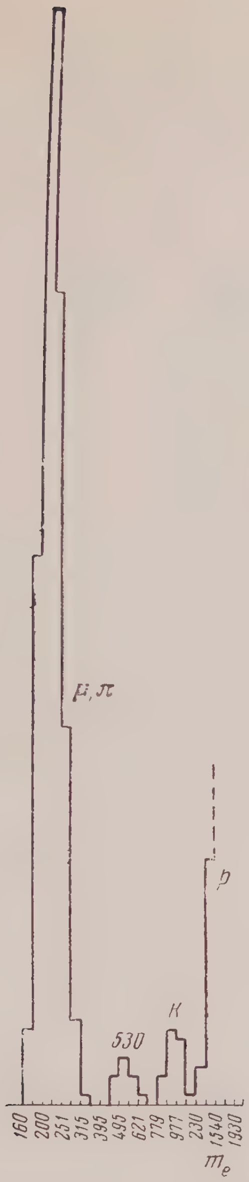

FIG. 12. Total mass spectrum of particles stopping in the lower chamber as the result of ionization loss (without aperture correction)

The results of the tracing of the trajectories of these particles in the upper chamber are given in the last column of Table III. The cases when the particle entered the chamber from above or originated in the thin cover of the chamber are marked by an arrow. In the case where the particle emerged from a dark region of the chamber, its origin was classified as not established. It should be noted that the apparatus was so situated within the building that the amount of matter above the upper chamber was small. This amount was 2gm/cm^2 of wood for two-thirds of the solid angle used, and not more than 10gm/cm^2 for the remaining part of it.

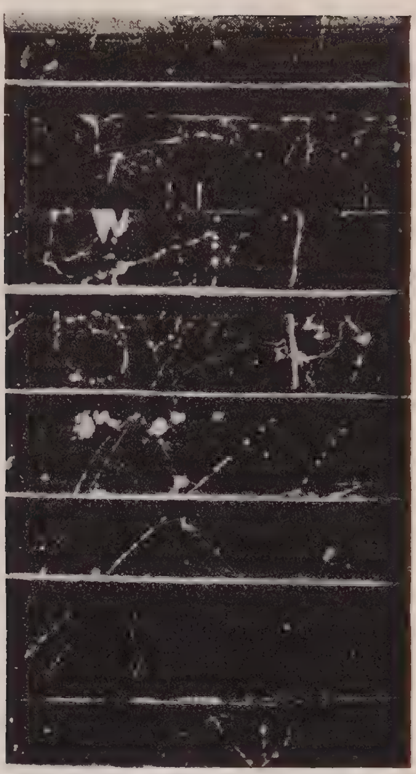

FIG. 13. Stopping and decay of a K^+-particle in the fourth plate.

TABLE I

Range, cm Pb	2—5
Number of π-mesons, n_π	71
Number of π-mesons with aperture correction, N_π	240
Number of K-particles, n_K	15
Number of K-particles with aperture correction, N_K	20
N_K / N_π	0.08±0.02

The detailed analysis has shown that four out of six particles which definitely entered the chamber through the thin cover traversed the thin layer of 2 gm/cm^2 only. Also, no case of production of particles with mass 500–600 m_e was observed in the plates of the upper chamber containing about 65 gm/cm^2 of matter.

In the majority of cases, stopping particles of the 500–600 m_e group were not accompanied by fast secondary particles (decay products). It should be noted that nine out of the eleven particles of this group were of negative sign. It may be possible that this fact made it impossible to detect

TABLE II

Momentum $P \times 10^8$ ev/c	Sign	Range, cm Pb	False mass M	Product	Upper chamber observation
2.09	—	3.04	430 m_e	⊥	*
2.57	+	3.52	520	*	*
2.06	—	2.32	450	⊥	*
2,57	—	2.95	585	*	Non-illuminated region
2.25	+	1.64	640	*	The same
2.77	+	2.50	720	*	"
2.23	+	2.20	560	*	
2.96	+	2.72	750	⊥	Camera did not operate
3.50	+	2.30	1070	*	*
2.92	—	1.60	970	⊥	*
4.00	+	3.83	1000	⊥	↓
2.70	+	1.58	860	*	*
3.65	+	4.00	840	*	*
3.42	—	1.55	1200	*	*
4,43	—	4.40	1080	*	*
3.85	—	3.85	1085	*	Non-illuminated region
4.50	—	4.65	1050	⊥	The same
3.00	—	3.00	730	*	*

Explanation of signs: *—star; ⊥ —stopping of a π-meson without visible star; ↓ —particle incident upon the upper chamber from above.

TABLE III

No. of case	Momentum $P \times 10^8$ ev/c	Sign	Range, cm Pb	Mass m_e	Product	Upper chamber observation
1	2.02	—	2.40	460 ± 40	absent	
2	2.66	—	4.35	505 ± 35	"	Non-illuminated region
3	2.70	—	3.52	590 ± 40	"	Camera did not operate
4	2.35	—	3.90	445 ± 45	"	
5	3.00	+	5.35	550 ± 60	e?	↓
6	2.84	—	3.65	610 ± 55	absent	Non-illuminated region
7	3.14	—	4.80	600 ± 60	"	Part of the track in the non-illuminated region
8	2.33	—	3.15	495 ± 40	"	
9	3.46	—	5.25	630 ± 65	"	↓
10	2.60	+	4.58	475 ± 40	"	Non-illuminated region
11	2.92	—	4.48	550 ± 50	"	↓
12	2.12	+	2.23	540 ± 35	2e	

any fast decay products.

In one case (No. 12, Table III), the stopping of a positive particle in a copper plate 3 mm thick was accompanied by the release of a small electron cascade (Fig. 15). In another case of a stopping positive particle (No. 5, Table III). the release of two electrons is observed. The quality of this picture, however, is poorer, and the particle stopped near the edge of the chamber. The stopping of the negative particles with the mass ~550 m_e resembles rather the stopping of negative μ-mesons and differs greatly from that of K-particles and fast π-mesons (see Fig. 2).

On the basis of our data, it is possible to estimate roughly the intensity of the anomalous particles relative to μ-mesons in the same range interval. 255 μ-mesons with ranges between 2 and 5 cm Pb, and 10 particles with the mass ~ 550 m_e were recorded in the second series of measurements. Under the assumption of an isotopic angular distribution of the investigated particles, 15 particles were found compared to 1600 μ-mesons which is about 1%, the correction for recording efficiency having been applied. The accuracy of this estimate is small, and if we account for the angular distribution of the μ-mesons the above ratio will be

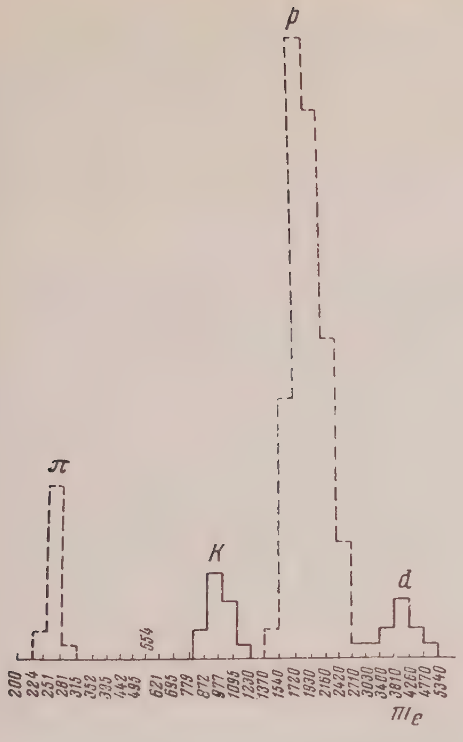

FIG. 14. Mass spectrum of particles produced in stars (without aperture correction)

closer to 0.5%.

Naturally, the question arises whether such a small number of particles with mass $550\, m_e$ can be explained by μ-mesons whose range or momentum were determined with a large error due to random causes. It should be noted first that, for a mean square error of $\sim 50\ m_e$, the appearance in the spectrum of a group of 11 particles with mass between 450 and 650 m_e on account of μ-mesons is completely excluded. Secondly, if the 11 particles of the mass $\sim 550\ m_e$ appeared in the mass spectrum because of the errors of measurements, there would be much greater numbers of particles with measured mass in the range of 300–450 m_e.

TABLE IV

No. of case	Radius of curvature from counter data, cm	Radius of curvature from entrance and exit angles, cm
1	148	161
4	174	158
5	222	200
7	232	240
8	170	174
9	256	244
11	216	192

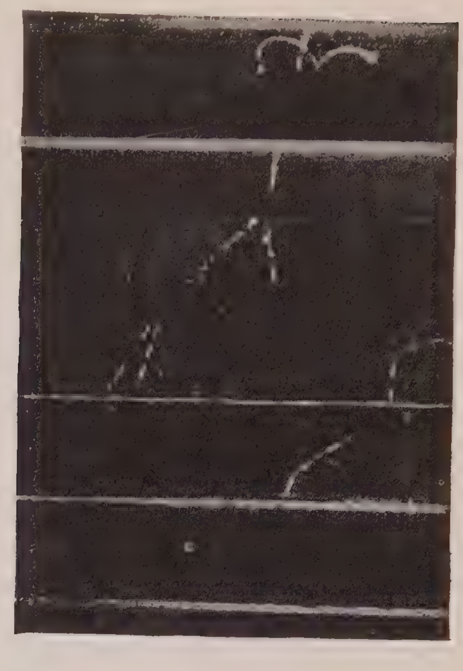

FIG. 15. Stopping of a positive particle accompanied by a small electron cascade. Mass equal to 540 m_e (range–momentum method)

It can be seen from Fig. 12 that not a single particle was found in this interval.

It has been of considerable interest to investigate the spectrum of particles which entered the set-up from the outside, traversing the thin lid of the upper chamber.* This spectrum is shown in Fig. 16. In contrast to the spectrum of particles locally produced in stars, μ-mesons and a group of particles with mass $\sim 550\ m_e$ are observed, while π-mesons and K-particles are completely absent.

The spectrum in Fig. 16 is given without aperture correction, which is very large for μ-mesons with

TABLE V

Type of particle	Mass determined from range and scattering angles, m_e	Number of scattering angles
μ	180 ± 27	100
π	290 ± 47	70
K	1050 ± 200	52
p	1750 ± 190	200
500—600 m_e	525 ± 140	46

---

*A small amount of particles locally produced in the cover may be present in this spectrum.

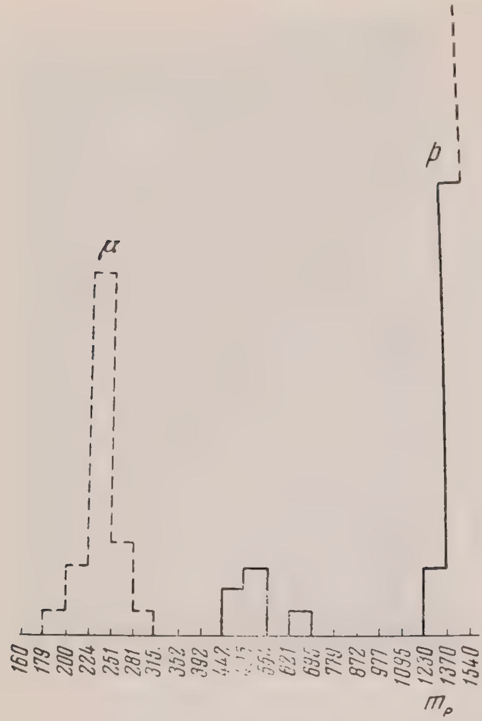

FIG. 16. Mass spectrum of particles entering the apparatus from the outside and traversing the thin cover of the upper chamber (without aperture correction).

momenta in the $1.4–1.7 \times 10^8$ ev/c range. This is connected with the fact that the overwhelming majority of the μ-mesons stopping in the illuminated region of the lower chamber must enter the upper chamber at a large angle to the zenith, thus missing the thin cover. It is difficult to make the exact aperture correction in that case, and the group of μ-mesons actually observed during the experiment is shown in Fig. 16 outlined by the dashed line. Due to the absence of π-mesons, the resolution between μ-mesons and particles with mass 550 m_e is still better. It can be seen in Fig. 16 that there is no particle in the interval of 300–400 m_e.

Since, in our experiments, the mass of particles was determined by the range-momentum method, we undertook an exact analysis of the trajectories of the particles with mass ~ 550 m_e both in the telescope and in the lower chamber. For seven particles it was possible to determine the value of the momentum not only from the coordinates of the telescope counters but also from the angle of entrance of the particle into the magnet gap out of the upper chamber and the angle of exit of the particle from the gap into the lower chamber. The values of the radii of curvature of the trajectories of these particles, measured by the two independent methods, are given in Table IV. It can be seen that both methods yield similar results. This fact indicates that the possibility of large random errors of momentum measurements of the group of particles of interest is excluded. The analysis of the tracks of these particles in the lower chamber ascertained that large errors of range measurements also are improbable.

It was found that:

1. All particles listed in Table III stopped far from the limits of the illuminated region and the glass windows of the chamber.
2. In the majority of cases, it was possible to estimate qualitatively an increase in the track density near its end by means of comparison with the density of proton tracks.
3. The measurements of the angles of multiple scattering in lead plates show that the mean square angle of scattering of particles of the 500–600 m_e group increases towards the end of the track. It equals 12 ± 2° for the residual range of 8.5 gm/cm.^{2}, 9.8 ± 2° for 17 gm/cm^2 and about 6° for 30 gm/cm.^{2} The measured values of the mean square angle for μ-mesons of corresponding ranges were found to be equal to 18°, 13° and 9.9° respectively.
4. The measured value of the mean square scattering angle of μ-mesons with momenta equal to $2.4 – 2.6 \times 10^8$ ev/c at the point of scattering was 4.8°. This value, as well as the angular distribution of the scattering of μ-mesons with these values of momentum, is very different from those observed for the particles of the 500–600 m_e group with similar momenta.

All the data of this section indicate that the particles with mass 500–600 m_e cannot be identified either as π- and μ-mesons or K-particles.

6. DETERMINATION OF THE MASS OF PARTICLES FROM THEIR SCATTERING AND RANGE

We determined the mass of particles independently from the momentum measured in the magnetic spectrometer, by means of measurement of the angle of scattering of the particle in the lead plates and of the residual range in the point of scattering. Experimentally, it is most convenient to measure the projection of the scattering angle on a given plane. Having found the value of $\bar{\varphi}$ or $\bar{\varphi}^2$ for a group of identical particles, and making use of the momentum–range relation, and of the theory of multiple scattering of particles, it is possible to determine their mass. This method of mass determination from the scattering of particles in a multiple–plate cloud chamber was used earlier by Rossi, Annis and others [16], who made use of the theory of scattering by nuclei to finite size, developed by Olbert.[17]

The mass of the particle is given by the following formula:

$$\left[\frac{1}{n}\Sigma\varphi_i^2 R_i^{2\alpha}\right]^{1/2} = k\left(\frac{m_e}{m}\right)^{1-\alpha},$$

where use is made of the mean square value of angle projections, n is the number of scattering angles, R is the residual range, m is the mass to be determined, $\alpha = 0.55$ and k is constant, slowly varying with v/c.

The influence of the finite size of nuclei on the scattering of particles was recently more correctly taken into account by M. L. Ter–Mikaelian, who made use of the experimental data on the scattering of fast electrons in lead. He also determined the coefficients k for finite-size nuclei more accurately.

For each group of homogeneous particles of the spectrum shown in Fig. 12, we carried out a second determination of the mass from the scattering angles and the range. The results are given in Table V. It can be seen that the second method of mass determination gives correct values of the mass of known particles. Making use of ~ 100 scattering angles, we obtain sufficient accuracy of the mass determination for a group of particles.

We estimated the possible fluctuations in the following way: the value of mass was determined for 25 groups of particles, each group consisting of ten randomly chosen μ-mesons. The mean number of scatters for each group was not more than 40–50. For no group did the value of mass amount to 500 m_e. The maximum value of the mass was in each case smaller than the mass of the μ-meson. For particles with mass ~ 550 m_e, the value of mass was determined both from $\bar{\varphi}$ and $\overline{\varphi^2}$. The results of the mass determination for the group of particles with mass 500–600 m_e are given in the end of the Table, and evidently are in good agreement with mass values obtained by means of the range-momentum method. This agreement between values of the mass of particles of this group, obtained by means of various independent methods, constitutes another indication of the existence of particles with the mass ~ 550 m_e.

7. CONCLUSION

A magnetic spectrometer with two cloud chambers was used for the analysis of the masses of charged cosmic ray particles. It is evident from the results of measurements given in Sec. 5 that, as in preliminary experiments, two groups of particles—particles with mass ~ 1000 m_e (K-particles) and particles with mass ~ 550 m_e —are observed in the mass spectrum between the π-mesona and the proton. It has been shown, that when only the particles locally generated in matter above the set-up are considered, the group of particles with mass ~ 550 m_e is completely absent and the mass spectrum consists of π-mesons, K-particles, protons and deuterons. The mass spectrum of particles produced in stars, shown in Fig. 14, is in good agreement with the observations of a number of authors, who used a cloud chamber controlled by a star or shower produced by fast primaries in the matter above the set-up (Leprince–Ringuet, Rossi and others). The frequency of observation of K-particles as compared with π-mesons in the same range interval was in our experiments found to be of the order of 0.08, in accordance with data obtained by several workers who obtained $N_k / N_\pi \approx 0.07$ for cosmic rays.

In the total mass spectrum (Fig. 12), we found a group of 11 particles, whose mass, determined from range–momentum measurement as well as from range–scattering measurements, was found to lie between 500 and 600 m_e. This result sharply contradicts all experiments on the mass of cosmic ray particles carried out by means of cloud chambers and emulsions, in the course of which no mesons with mass ~ 500 m_e were detected. We will now look into this matter more closely. First of all, it is found that in practically all cloud chamber experiments, the mass measurements were carried out for particles locally produced in the matter of the recording apparatus.

It is necessary, therefore, to compare the results of such measurements with the mass spectrum of Fig. 14, with which they are in good agreement, and not with the total mass spectrum. In several cases, we were able to deduce directly that the particles of the anomalous group entered the apparatus from the outside, similarly to μ-mesons.

If the lifetime of such particles is long, it is possible that, through accumulation in a column of air, they can amount to a considerable part of the number of K-particles locally produced above the apparatus. It is possible that this is the cause of the difference between the total mass spectrum and the mass spectrum of locally produced particles.

Our method of mass determination is based on the establishment of the fact that the particles are stopping, which is judged qualitatively from the increase in the track density in the chamber. Together with the mass determination from range, momentum, and scattering measurements, we deem it necessary to determine with good accuracy the specific ionization of the individual particles. This will make it possible to determine the mass of the particle by an independent method—from the ionization and momentum. Only such measurement will help us reach the final conclusion about the existence of particles with mass $\sim 500\, m_e$. We have already started a new series of measurements in which the specific ionization of particles is determined before the particle enters the cloud chamber by means of multiple-layer proportional counters. Systematic and accurate mass measurements of a large number of particles stopping in emulsion stacks, independently of the character of the process at the end of the track, would also be of great importance.

Finally, the authors wish to express their gratitude to M. Daion, G. Merzon, A. Galper, F. Arutiunian and G. Badalian for their part in the measurements and in the evaluation of results, and to B. Dolgosheinyi and A. Shmeleva for the great help in the evaluation of the results of measurements.

---

[1] Alikhanian, Alikhanov, Morozov, Muskhelishvili and Khrimian, Dokl. Akad. Nauk SSSR 58, 1321 (1947).

[2] A. Alikhanian and A. Alikhanov, J. Exptl. Theoret. Phys. (U.S.S.R.) 21, 1029 (1951).

[3] Alikhanian, Dadaian and Shostakovich, Dokl. Akad. Nauk SSSR 82, 693 (1952).

[4] Kharitonov, Marikian and Alikhanian, Dokl. Akad. Nauk SSSR 80, 201 (1952).

[5] A. Alikhanian and V. Kharitonov, Dokl. Akad. Nauk SSSR 85, 295 (1952).

[6] Daniel, Davis, Mulvey and Perkins, Phil. Mag. 43, 753 (1952).

[7] R. Daniel and D. Perkins, Proc. Roy. Soc. (London) 221A, 351 (1954).

[8] A. Alikhanian, J. Exptl. Theoret. Phys. (U.S.S.R.) 21, 1063 (1951).

[9] L. Landau, J. Exptl. Theoret. Phys. (U.S.S.R.) 8, 201 (1944).

[10] A. Alikhanian and V. Kharitonov, Dokl. Akad. Nauk SSSR 92, 6 (1953).

[11] Eliseev, Liubimov and Kosmacherskii, Dokl. Akad. Nauk SSSR 90, 995 (1953).

[12] Alikhanian, Kirillov-Ugriumov, Shostakovich and Fedorov, Dokl. Akad. Nauk SSSR 92, 255 (1953).

[13] Alikhanian, Kirillov—Ugriumov, Shostakovich, Fedorov and Merzon, Dokl. Akad. Nauk SSSR 92, 915 (1953).

[14] Alikhanian, Kirillov—Ugriumov, Shostakovich, Fedorov and Merzon, Dokl. Akad. Nauk SSSR 92, 511 (1953).

[15] Daion, Fedorov, Merzon and Shostakovich, PTE 1, (1957).

[16] Bridge, Peyrou, Rossi and Safford, Phys. Rev. 90, 921 (1953).

[17] Annis, Bridge and Olbert, Phys. Rev. 89, 1216 (1953).

Translated by H. Kasha
209

SOVIET PHYSICS JETP VOLUME 4, NUMBER 6 JULY, 1957

The Theory of Galvanomagnetic Phenomena in Semiconductors

M. I. KLINGER
Chernovitskii State University

(Submitted to JETP editor May 27, 1954)
J. Exptl. Theoret. Phys. (U.S.S.R.) 31, 1055-1061 (1956)

The technique of studying galvano-magnetic phenomena, described previously by the author, using crossed electric and magnetic fields and taking into account the quantization of the energy spectrum of the current carriers, is applied to calculations of the resistivity and the Hall constant in a strong transverse magnetic field in semiconductors in which the electron gas is not degenerate.

1. INTRODUCTION

IN a study of galvano-magnetic phenomena one does not usually take into account the quantization of the energy spectrum of the current carriers in crossed electrical field E and magnetic field H. However, the quantization of the spectrum changes the kinetic relations of the galvano-magnetic phenomenon.

In a previous work[1] an attempt was made to prove the method of calculation used by Titeica[2] to obtain the isothermal hole effect and the resistivity in a transverse magnetic field. This method allowed the inclusion of the quantization of energy spectrum of the current carriers. In the given work[1], this method was applied to the calculation of the resistivity of the semiconductor and the Hall constant in a strong transverse magnetic field.

It should be noted that Titeica made the first attempt to include the quantization of the energy spectrum of the current carriers in the fields $E \perp H$ in a calculation of the resistivity of metal in a magnetic field. However, it seems to us that the physical essence of the method was not sufficiently developed in his work and the meaning of the physical quantities used in it was not given. Furthermore, the derivation of the equations used for the calculation of resistivity ρ in the magnetic field and of the Hall constant R was not given, and therefore the conditions under which they are applicable were not well determined.

The object of study is the current carrier which moves in a solid body in the presence of crossed electrical and magnetic fields and interacts with phonons. As is well known[1,2], the crossed electrical and magnetic fields ($E \perp H$) change the spectrum of the current carrier, so that the energy of the current carrier is determined by an expression (including the spin of the electron)

$$\mathscr{E}_{Q\pm} = P_z^2/2\mu + \hbar\omega_0(n + {}^1/_2) + eEx_0 \pm \mu_B H, \qquad (1)$$
$$n = 0, 1, 2, \ldots; \quad \omega_0 = eH/\mu c;$$
$$x_0 = -P_y/\mu\omega_0 - eE/\mu\omega_0^2,$$

where x_0 is the center of the oscillator, μ_B is Bohr magneton, μ is the effective mass of the appropriate quasi-particle.

Since with the application of the fields the motion of the current carrier becomes anisotropic, one should introduce the conduction tensor $\sigma_{ik}(H)$ ($i, k = 1, 2, 3$) and $\rho_{ik}(H)$, in which $\sigma_{13} = \sigma_{23} = \rho_{13} = \rho_{23} = 0$. In Ref. 1 the equations were developed for the resistivity ρ in a transverse magnetic field H and for the Hall constant R:

$$\rho = j_x E_x/(j_x^2 + j_y^2); \qquad (2)$$
$$R = -j_y E_x/(j_x^2 + j_y^2)H,$$

where j_x, j_y are the total electrical macroscopic currents in an infinite gyrotropic medium. If one is considering an amphoteric semiconductor, then $j_x = j_x^+ + j_x^-$ and $j_y = j_y^+ + j_y^-$ where the plus and minus signs relate to conduction holes and electrons, respectively.

2. THE HALL EFFECT AND THE ELECTRICAL RESISTIVITY IN STRONG TRANSVERSE MAGNETIC FIELDS IN SEMICONDUCTORS

The current j_y in an infinite gyrotropic medium can be determined for the general case in the following way: a) one calculates $\hat{v}_y = [y\hat{\mathscr{H}}]$, where $\mathscr{H}$ is the Hamiltonian of the considered system in crossed fields, b) one determines the current $j_y = |eS_p(\hat{\rho}\hat{v}_y)|$ by means of the density matrix ρ corresponding to $\mathscr{H}$.

As has been shown previously[1], the average value of the operator of the y component of x velocity of a current carrier v_y is in the first approximation equal to

$$\bar{v}_y = (1/\mu)(P_y + \mu_0\omega_0 x_0) = -cE/H \equiv \gamma.$$

Therefore, in the simplest case, when the current carriers are quasi-particles with some effective mass (quadratic dispersion law),

$$j_y = -e\,\mathrm{Sp}(\hat{\rho}\hat{v}_y) = (ecE/H)N(H, T), \qquad (3)$$

where $N(H, T)$ is the number of the current carriers in the semiconductor per cm^3. Since we are at first interested only in the case of electric fields E small enough so that the current j_x and j_y are proportional to E (and nonadequate electron gas),

$$N(H, T) = N_0(H, T)\, e^{\Phi/kT},$$
$$N_0(H, T) = 2\left(\frac{2\pi\mu kT}{h^2}\right)^{3/2} \tag{4}$$
$$\times \quad \frac{\hbar\omega_0}{2kT\sinh(\hbar\omega_0/2kT)} \cosh\left(\frac{\mu_B H}{kT}\right),$$

are the statistical sums of the electron gas in magnetic fields including the spin of the electron (Φ is the chemical potential). It is clear that the current j_y fundamentally lacks the Ohmic character.

In the method of the stationary states, the current j_x is calculated in the following way.

1. In the Hamiltonian $\mathcal{H}$ of the system under study, we separate several main terms $\mathcal{H}_0$ which give the fundamental energy spectrum of the system and small interaction terms V that are considered as perturbations.

2. We solve the problem $\hat{\mathcal{H}}_0\Psi_Q = \varepsilon_Q\Psi_Q$ and calculate the average value of

$$\overline{x}_Q = \int \Psi_Q^* x \Psi_Q \, d\tau,$$

in which the zero approximation is such that $\overline{x}_q$ depends on the quantum number Q of the unperturbed problem.

3. We introduce the operator V, which takes into account the interactions of the quasi-particles of the system that were omitted in the unperturbed problem. This operator is considered as a perturbation which causes transitions between stationary states. Since $\overline{x}_Q$ depends on Q, then the transitions induced by the perturbing operator V change $\overline{x}_Q$, and thus specify displacement of the current carrier to some other point $\overline{x}_{Q'} \neq \overline{x}_Q$.

In the present formulation of the problem, the following difference should be noted compared to the usual formulation. It is usually assumed that the field E accelerates the current carrier, which gains energy from the field and scatters this acquired energy in interactions with phonons. In the point of view adopted here the process takes place as follows: the field E (together with $H \perp E$) participate in the formation of the stationary states of the current carrier, and the part of the energy of the carrier which depends on E, is equal to eEx_0 (cf. Eq. (1)).

The current carrier in displacing from x_0 to any x_0' exchanges energy with phonons $eE(x_0' - x_0) = eE\Delta x_0$. As follows from the probability of the displacement, Δx_0 depends on E and has different magnitudes for $\Delta x_0 > 0$ (displacement of the current carrier along the field E) and for $\Delta x_0 < 0$ (displacement against the field). These conditions specify microscopic current j_x different from zero.

A number of the current carriers passing in one second through a plane $x = 0$ from left to right is equal to

$$N_1 = \sum_{\alpha=1,\,2}\ \sum_{(\overline{x}_Q>0,\ \overline{x}_{Q'}<0)} |V_{QQ'}|^2 \rho_{Q'\alpha},$$

where $\rho_{Q\alpha}$ is the equilibrium distribution function, $\alpha = 1$ corresponds to the spin of the electron parallel to the field H, and $\alpha = 2$ to the antiparallel spin. The number of current carriers passing through the plane $x = 0$ from right to left is equal to

$$N_2 = \sum_{\alpha=1,\,2}\ \sum_{(\overline{x}_Q>0,\ x_{Q'}<0)} |V_{QQ'}|^2 \rho_{Q\alpha}.$$

Therefore the resultant current density j_x is equal to

$$\bar{j}_x = -e(N_1 - N_2) \tag*{(5}$$
$$= -e \sum_{\alpha=1,\,2}\ \sum_{(\overline{x}_Q>0,\ \overline{x}_{Q'}<0)} |V_{QQ'}|^2 (\rho_{Q\alpha'} - \rho_{Q\alpha}).$$

In the approximation used here as previously[1], $\overline{x}_Q = x_0$ is the oscillator center; as perturbation V we use the interaction of the current carrier with the acoustical phonons. We shall limit ourselves to the single phonon scattering. The perturbation operator has the usual form:

$$V(\mathbf{r}) = \sum (\mathbf{e}_f \nabla V_p)\{b_f e^{i(\mathbf{fr})} \tag{6}$$
$$+ b_f^+ e^{-i(\mathbf{fr})}\} \sqrt{\hbar/2Msf},$$

where $\mathbf{e}_f$ is equal to $\mathbf{f}/f$ (the longitudinal waves), s is the sound velocity, b_f^+, b_f are the creation and annihilation operators of the phonon momentum $h\mathbf{f}$; $V_p(\mathbf{r})$ is the periodic lattice potential. As is customary, we impose the periodic conditions by introducing the unit cell of the linear dimensions L, $f \leq f_0$.

Since $V_p(\mathbf{r})$ varies substantially over the distances of the order of the lattice constant, then on calculation of $W_{QQ'} = |V_{QQ'}|^2$ the operator $\mathcal{H}_0$ should be taken in the following form

$$\hat{\mathcal{H}}_0 = \frac{p_x^2}{2m} + \frac{1}{2m}\left(p_y + \frac{e}{c}H_x\right)^2 \tag{7}$$
$$+ \frac{p_z^2}{2m} + eEx + V'(\mathbf{r}) + V_p(\mathbf{r})$$

and the function ψ_Q should be determined from the equation

$$\hat{\mathcal{H}}_0\Psi_Q = \varepsilon_Q\Psi_Q, \quad V'(\mathbf{r})$$

$V'(\mathbf{r})$ is the operator for the interaction energy of the electron with the optical phonons[3].

According to the theorem of Pekar[3], generalized by Luttinger[4], for the case $H \neq 0$, close to the bottom of the conduction band

$$\Psi_Q = \sum_{\mathbf{k}} \alpha_{Qk} = e^{i\mathbf{kr}} u_{\mathbf{k}}(\mathbf{r}); \quad \alpha_{Qk} = \int \varphi_Q e^{-i(\mathbf{kr})} d\tau,$$

where the wave function φ_Q is found from the equation

$$\tilde{\mathscr{H}}_0 \varphi_Q = \varepsilon_Q \varphi_Q; \quad \tilde{\mathscr{H}}_0 = \frac{p_x^2}{2\mu} + \frac{1}{2\mu}\left(p_y + \frac{e}{c} Hx\right)^2 + \frac{p_z^2}{2\mu} + eEx + V'(\mathbf{r}), \tag{8}$$

in which $\mu(H)$ is the effective mass of the current carrier in a magnetic field[5].

Using the result of Pekar[3] in the solution of Eq. (8) we obtain, after several transformations

$$W_{QQ'}^{\pm} = \frac{2fg^2}{9\hbar sM} \delta(\varepsilon_{Q'} - \varepsilon_{Q'} \pm \hbar\omega_f)\, \Delta \times (P_y - P'_y \pm \hbar f_y) \times \Delta(P_z - P'_z \pm \hbar f_z)\, W_{nn'} \begin{cases} N_f \\ N_f + 1 \end{cases} \tag{9}$$

(The upper factor is used in the absorption of phonons, the lower factor in the emission of phonons). Here $\Delta(x) = 0$ for $x \neq 0$, $\Delta x = 1$ with $x = 0$; $g = h^2/2m \times \int (\nabla u_0)^2 d\tau$ is the Bloch constant; N_f is the number of acoustical phonons with the momentum hf;

$$W_{nn'} = \left| \int_{-\infty}^{\infty} \exp\{\pm i f_x x\} H_n(x - x_0) H_{n'}(x - x'_0)\, dx \right|^2, \tag{10}$$

$H_n(x - x_0)$ is the Hermite polynomial, M is the mass of ions per unit volume.

Introducing the expression for $W_{QQ'}$ into Eq. (7), we express P_y in terms of x_0 and use the properties of the symbol $\Delta(x)$ to exclude the summation over f_y, f_z:

$$j_x = \frac{2eg^2}{9M\hbar s(2\pi)^5} \left(\frac{\mu\omega_0}{\hbar}\right)^2 L^2 \sum_{n,n',\alpha} \int\int_{-\hbar f_0}^{+\hbar f_0} dP_z dP'_z \times \int_{(x_0>0)} dx_0 \int_{(x'_0<0)} dx'_0 \sum_{f_x} f W_{nn'} \{[\rho^0_{Q\alpha} N_f - \rho^0_{Q'\alpha}(N_f + 1)]\, \delta(\varepsilon_Q - \varepsilon_{Q'} - \hbar\omega_f) + [\rho^0_{Q\alpha}(N_f + 1) - \rho^0_{Q'\alpha} N_f]\, \delta(\varepsilon_Q - \varepsilon_{Q'} + \hbar\omega_f)\}, \tag{11}$$

Here Q is a function of the quantities n, P_z and P_y, or $x_0(P_y)$; l is the linear dimension of the unit cell; $x_0{}' < 0$; $x_0 > 0$.

Since we are limiting ourselves to the consideration of the phenomena linear in E (Ohm's law), ρ is chosen in the following way

$$\rho_{Q\alpha} = \rho(\mathscr{E}_{Q+}) = \exp\left\{\frac{1}{kT}\left(\Phi - \frac{P_z^2}{2\mu} - \hbar\omega_0\left(n + \frac{1}{2}\right) \pm \mu_B H\right)\right\}. \tag{12}$$

Substituting $\rho_{q\alpha}$ from Eq. (13) into Eq. (11), and assuming that the field of the acoustical phonons is in a thermal equilibrium, we obtain

$$N_f \rightarrow \bar{N}_f = \{e^{\hbar sf/kT} - 1\}^{-1}. \tag{13}$$

Now we make in the Eq. (11) the following changes of variables and the following transformations[2]:

1. $x_0 - x'_0 = r$; $x_0 + x'_0 = s$;

$$0 \leqslant s \leqslant r; \quad 0 \leqslant r \leqslant r_0 = (\hbar/\mu\omega_0) f_0$$

since $x_0 > 0, x'_0 < 0$); $P'_z - P_z = v$;

$$P'_z + P_z = u; -\hbar f_0 \leqslant u \leqslant \hbar f_0, -\hbar f_0 \leqslant v \leqslant \hbar f_0.$$

2. We integrate over s and u, using the properties of the δ-function and pass from a sum over f_x to integral over df_x.

3. Taking into account that according to Eq. (9) $P_{y,z} - P'_{y,z} \pm \hbar f_{y,z} = 0$,

we introduce new variables

$$r \rightarrow f_y = (\mu\omega_0/\hbar)\, r; \quad 0 \leqslant f_y \leqslant f_0;$$

$$v \rightarrow f_z = v/\hbar; \quad -f_0 \leqslant f_z \leqslant f_0,$$

and finally in the plane (f_x, f_y) we introduce the polar coordinates f' and α'. After making all the above described transformations we obtain:

$$j_x = \frac{j_0}{(2\pi)^5} \cosh\frac{\mu_B H}{kT} \times \sum_{n,n'} \int_0^{\pi} \sin\alpha' d\alpha' \int_0^{f_0} df' \int_{-f_0}^{f_0} df_z \frac{f'^2 f}{f_z} \times W_{nn'} \frac{\exp(-\hbar^2 f_z^2/8\mu kT)}{\sinh(\hbar sf/2kT)} \times \sinh\left(\frac{\hbar\gamma f' \sin\alpha'}{2kT}\right) \left\{e^{-(X_0^+ + X_1^+)} + e^{-(X_0^- + X_1^-)}\right\}, \tag{14}$$

$$j_0 = (4e\mu g^2/9M\hbar^2 s)\, e^{\Phi/kT}, \quad X_1^+ \sim \gamma;$$

We shall limit ourselves to those fields E, for which j_x is proportional to E, i.e., we replace in Eq. (14) sinh by its argument and X_1^+ by zero. Then integrating over $\alpha\alpha'$ we obtain

$$j_x = \frac{j_0\gamma}{4kT\omega_0(2\pi)^4}\int\limits_0^{f_0} df'$$

$$\times \int\limits_{-f_0}^{f_0} df_z \frac{f'^3 f}{|f_z|\sinh(\hbar s f/2kT)} e^{-\hbar^2 f_z^2/8\mu kT} P(f', f_z),$$

$$P = \sum_{n,n'} \hbar\omega_0 W_{nn'} \left\{e^{-X_0^{\pm}} + e^{-X_0^{\pm}}\right\}.$$

Introducing the polar coordinates in the plane (f', f_z) and the new variable

$$\xi = \hbar s f/kT \; (0 \leqslant \xi \leqslant \xi_{\max} = T_D/T),$$

for which

$$f_z = (\xi kT/\hbar s)\cos\varphi;\;\; f' = (\xi kT/\hbar s)\sin\varphi,$$

and expressing j_x in the form

$$j_x = \left(\frac{kT}{\hbar s}\right)^5 \frac{j_0\gamma\cosh(\mu_B H/kT)}{4kT\omega_0(2\pi)^4} \int\limits_0^{\pi/2} \frac{\sin^3\varphi}{\cos\varphi} d\varphi \qquad (15)$$

$$\times \int\limits_0^{T_D\,T} \frac{\xi^4 e^{-\nu\xi^2\cos^2\varphi}}{\mathrm{sh}\,(\xi/4)} P(\xi, \varphi)\, d\xi,$$

where T_D is the Debye temperature, $\nu = kT/8\mu s^2$.

According to Rumer[5], P can be expressed in the form of a contour integral which in the case considered above has the following form:

$$P(\xi, \varphi) = \frac{\hbar\omega_0}{i\sinh(\hbar\omega_0/2kT)}$$

$$\times \sqrt{\frac{\alpha_1 kT}{\pi}} \int\limits_{\tau - i\infty}^{\tau + i\infty} \exp\left\{\alpha_1 kT y^2\right. \qquad (16)$$

$$\left. + \hbar\omega_f y + \frac{\beta}{\hbar\omega_0} \frac{\cosh(\hbar\omega_0 y) - \mathrm{ch}\,(\hbar\omega_0/2kT)}{\sinh(\hbar\omega_0/2kT)}\right\} dy,$$

$$\beta = kT\nu\xi^2\sin^2\varphi; \quad \alpha_1 = 4kT\nu\xi^2\cos^2\varphi,$$

in which $\tau < 1/2kT$, and may one set $\tau = 0$. We are interested only in the case of large magnetic fields, when $h\omega_0 \gg kT$, since in the opposite case the quantization of the energies has a small effect and the usual kinetic theory apparently is more satisfactory than the method used in the present work.

For $h\omega_0 \gg kT$, , and setting $\tau = 0$ and retaining only the main term

$$P(\xi, \varphi) \approx \hbar\omega_0 \exp\left\{-\frac{\hbar\omega_0}{2kT} - 1/16\,\nu\cos^2\varphi\right\}. \quad (17)$$

In electronic semiconductor $|j_y| \gg |j_x|$, so that the resistivity ρ is determined from Eqs. (2), (15) and (17) and by the expression

$$\rho \approx \frac{j_x E}{j_y^2} = \rho_0 I \left(\frac{kT}{\hbar s}\right)^5 \frac{\hbar\omega_0}{kT} \exp\left[-\frac{\Phi + \hbar\omega_0/2}{kT}\right], \quad (18)$$

$$\rho_0 = 8\mu^2 g^2/9M\hbar^2 s e^2 N_0^2,$$

$$I = \int\limits_0^{\pi/2} \frac{\sin^3\varphi}{\cos\varphi} d\varphi \qquad (19)$$

$$\times \int\limits_0^{T_D/T} \frac{\xi^4 d\xi}{\sinh(\xi/2)} \exp\left[-\nu\xi^2\cos^2\varphi - 1/16\,\nu\cos^2\varphi\right].$$

Since we are considering low temperatures only, we can replace the limit T_D/T by ∞. Considering that the greatest contribution into the integral is from small ξ and investigating the expression inside the integral in Eq. (19) it is not difficult to see that for $\nu \gg 1$, $I \approx 128\pi$ neglecting the terms of the order of $1/\nu$ etc.

To make a final calculation of $\rho(H,T)$ one must find $\Phi(H, T)$.

In the case of an electronic semiconductor we use the corresponding equation of neutrality and take into account the spin of the admixed electron in the absence of degeneracy of the electron gas:

$$N_0(H, T)\, e^{\Phi^*} + n_{\mathrm{loc}} = n_1, \qquad (20)$$

where n_1 is the concentration of the (univalent)[1] impurity

$$n_{\mathrm{loc}}/n_1 = (1 + {}^1\!/_2$$

$$\times \exp\{-\Delta E^* - \Phi^* - \mu_B^* H\})^{-1} \qquad (21)$$

$$+ (1 + {}^1\!/_2 \exp\{-\Delta E^* + \mu_B^* H - \Phi^*\})^{-1}.$$

In Eqs. (20) and (21) and below, the asterisk denotes the division by kT; ΔE is the energy gap between the impurity level and the bottom of the conductor band. From Eqs. (20) and (21) it follows that for $\hbar\omega_0^* \gg 1$, $\mu_B^* H \gg 1$ approximately

$$e^{\Phi^*} \approx \sqrt{\frac{n_1}{2Z_0\hbar\omega_0^*}} \qquad (22)$$

$$\times \exp\left(\frac{\hbar\omega_0^*}{4} - \mu_B^* H - \frac{\Delta E^*}{2}\right).$$

Substituting Eq. (22) into Eqs. (4), (2) and (18) we obtain, for H large,

$$N(H_1 T) = 2^{-1/2}\sqrt{n_1 Z_0 \hbar\omega_0^*} \qquad (23)$$

$$\times \exp(-\Delta E^*/2 - \hbar\omega_0^*/4),$$

$$R \approx -1/Nec = (-\sqrt{2}/ec)(n_1 Z_0 \hbar\overset{*}{\omega}_0)^{-1/2} \quad (24)$$

$$\times \exp(\Delta E^*/2 + \hbar\overset{*}{\omega}_0/4),$$

$$\rho = \frac{16\,g^2}{9\pi^3 M e^2 \hbar^2 s\sqrt{2n_1}} \left(\frac{kT}{\hbar s}\right)^5 \frac{\exp(\Delta E^*/2 + \hbar\overset{*}{\omega}_0/4)}{e^2 Z_0^{3/2}\sqrt{\hbar\overset{*}{\omega}_0}}. \quad (25)$$

From Eqs. (23) through (25) it is evident that the dependence of ρ and R on H,T is determined by the dependence of $N(H,T)$. However, $N(H,T)$ increases with increasing H because the ground level of the charged oscillator $h\omega_0/2$ (and also all its other levels) increase with the increasing H; at the same time the decrease in the interaction energy between the spin magnetic moments of the current carriers parallel to the field H with the increase in H is approximately compensated by analogous phenomenon for electrons in the ground impurity level. Therefore with increasing H for a given temperature both ρ and R increase very rapidly $(\sim \exp(\hbar\overset{*}{\omega}_0/4))$. We note that in the ordinary kinetic theory, which does not include the quantization of the energy in a magnetic field, both ρ and R approach a saturation value in semiconductors for large H. This result is indeed obtained because the dependence of $N(H, T)$ is not taken into account, and this quantity has an appreciable value for $\hbar\omega_0 \gg kT$.

It should be noted, however, that the character of the change of $N(H,T)$ with an increasing H depends on the type of semiconductor. For example, for an intrinsic semiconductor, the behavior of $N(H,T)$ with the change of H is different from the one described above. In that case, in the effective mass approximation[1] $j_y = j_y^+ + j_y^- = 0$, since $N_+(H,T) = N_-(H,T)$ (the plus and minus signs relate to the holes and the electrons, respectively).

In this case, in the absence of degeneracy, one may use the relationship $(\hbar\overset{*}{\omega}_{0\pm} > 1)$:

$$\sqrt{\mu_+}\exp(-\delta\varepsilon^* - \Phi^* - {}^1/_2\hbar\overset{*}{\omega}_{0+})$$

$$= \sqrt{\mu_-}\exp(\Phi^* - {}^1/_2\hbar\overset{*}{\omega}_{0-}),$$

to evaluate Φ, from which

$$e^{\Phi^*} = (\mu_+/\mu_-)^{1/4} e^{-\delta\varepsilon^*/2}\exp[\overset{*}{\mu}_B H(s_- - s_+)], \quad (26)$$

where $s_\pm = m/\mu_\pm$, $\delta\varepsilon$ is the width of the forbidden zone. We obtain

$$N_+(H,T) = N_-(H,T)$$
$$= {}^1/_2 Z_{0+}\hbar\overset{*}{\omega}_{0+}\exp\{\overset{*}{\mu}_B H(1 - s_+) + \Phi^*\}. \quad (27)$$

Consequently,

$$\rho = \frac{E}{j_x^+ + j_x^-} = \frac{9\pi^3 M\hbar^6 s^6 H}{8g^2 ce(kT)^4}\cdot e^{\delta\varepsilon^*/2} \quad (28)$$

$$\times\left(\frac{\mu_+}{\mu_-}\right)^{-1/4}\frac{\exp[\overset{*}{\mu}_B H(s_+ - 1)]}{\mu_+^{-1}\exp[\overset{*}{\mu}_B H(s_- - s_+)] + \mu_-^{-1}}.$$

In this case, ρ can both increase and decrease with an increase in H, depending on the relationship between n, μ_+ and μ_-. If, for example,

$$\mu_+ > \mu_-, \quad s_+ < s_-, \quad s_+ < 1,$$

then with increasing H ρ will decrease.

In conclusion, the author expresses gratitude to Prof. A. G. Samoilovich, for suggesting this work and for valuable discussions and help in carrying out the present work.

---

[1] M. I. Klinger, J. Exptl. Theoret. Phys. (U.S.S.R.) **29**, 439 (1955); Soviet Phys. JETP **4**, 251 (1957).

[2] S. Titeica, Ann. Physik **22**, 129 (1935).

B. I. Davydov and I. Pomeranchuk, J. Exptl. Theoret. Phys. (U.S.S.R.) **9**, 1294 (1939).

[3] S. I. Pekar, *Investigation of the electron theory of crystals*, GTTI, Moscow-Leningrad, 1952.

[4] R. Peierls, Z. Physik.**80**, 763 (1933); J. Luttinger, Phys. Rev. **84**, 814 (1951)

[5] Iu. B. Rumer, J. Exptl. Theoret. Phys. (U.S.S.R.) **22**, 214 (1952).

[6] M. I. Klinger, J. Exptl. Theoret. Phys. (U.S.S.R.) **26**, 159 (1954).

Translated by M. J. Stevenson
220

SOVIET PHYSICS JETP VOLUME 4, NUMBER 6 JULY,1957

An Analysis of Some Cosmic Ray Meson–Production Events. II.

N. G. BIRGER, V. V. GUSEVA, K. A. KOTEL'NIKOV,
V. M. MAKSIMENKO, S. V. RIABIKOV, S. A. SLAVATINSKII
AND G. M. STASHKOV
P. N. Lebedev Physical Institute, Academy of Sciences, USSR

(Submitted to JETP editor July 21,1956)
J. Exptl. Theoret. Phys. (U.S.S.R.) 31,982–986 (December, 1956)

Three cases of meson production by cosmic rays are described. In each one, the momentum of the primary particle was measured by a magnetic method using two cloud chambers. The analysis confirms the existence of a large spread in the number of secondary particles and in the energy carried away by π-mesons.

BOTH cloud chamber and emulsion techniques have been used to study the interaction between cosmic ray particles and nuclei. Up to now, the energy of the primary particles has been measured indirectly through the angles in which the secondary particles were emitted. This method can lead to appreciable errors, especially for complex nuclei, since the errors increase with increasing mass of the target nucleus. It would be interesting to measure the energy of the primary particle directly. In order to do this, we modified our previously described apparatus[2] * by adding a second cloud chamber as shown in Fig. 1. The work was carried out during the winter of 1955–1956. For the second cloud chamber, d= 30 cm, and the illuminated region was 10 cm deep. After passing through the upper cloud chamber, charged particles are deflected by the field of the electromagnet (whose strength was about 10^4 Oe) and are then detected above the Be slab in the lower cloud chamber. If the particle initiates a shower in the beryllium slab (thickness 9.2 gm/cm^2), then the origin of the shower can be found by projecting the tracks of the secondary particles backwards. The displacement between the point where the shower started and the direction of the primary particle, as found from the track in the upper chamber, determined the momentum and charge of the primary. The relative orientation of the two chambers was adjusted by using mesons of the hard component, which had energies more than 5 bev, The same pictures were used to find the largest momentum we could measure with the two camera method. In our case, $p_{\max}$ turned out to be 50 bev/c.

It should be noted, however, that the use of two cloud chambers decreased the sensitivity of the apparatus considerably. We here able to obtain only four pictures for which the momentum of the primary could be obtained and which showed more than four charged particles. The characteristics of the showers are summarized in the Table. In three of the showers it was possible to both find

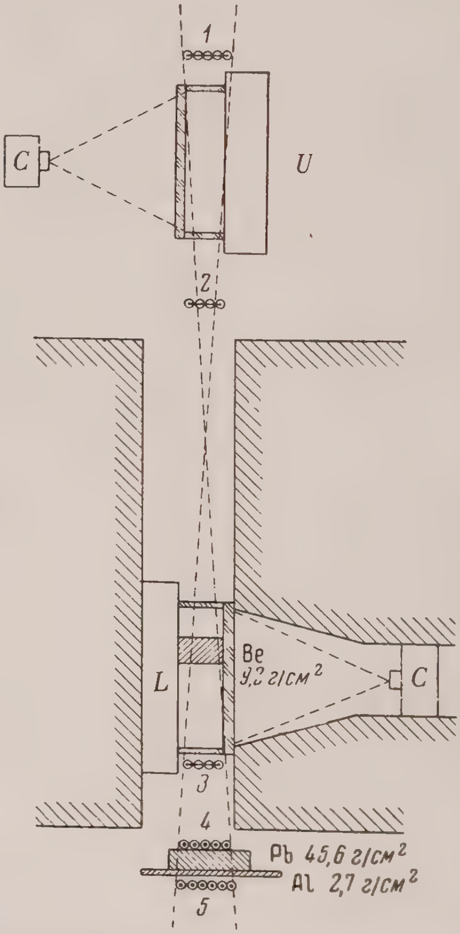

FIG. 1. Schematic drawing of apparatus. U—upper cloud chamber, L—lower cloud chamber, C—picture taking equipment.

---

*Denoted in the following by I.

out how the energy of the primary particle was distributed among the secondary ones, and also the angular distribution of the particles in the center-of-mass system. This assumes that the generating particle interacted with only one nucleon in the beryllium nucleus. Since, for energies up to about 5 bev, the meson production cross section for nucleon-nucleon and nucleon–π–meson collisions is about $1/2\ \sigma_{\text{geometric}}$ of the nucleon[3], this assumption seems to be justified.

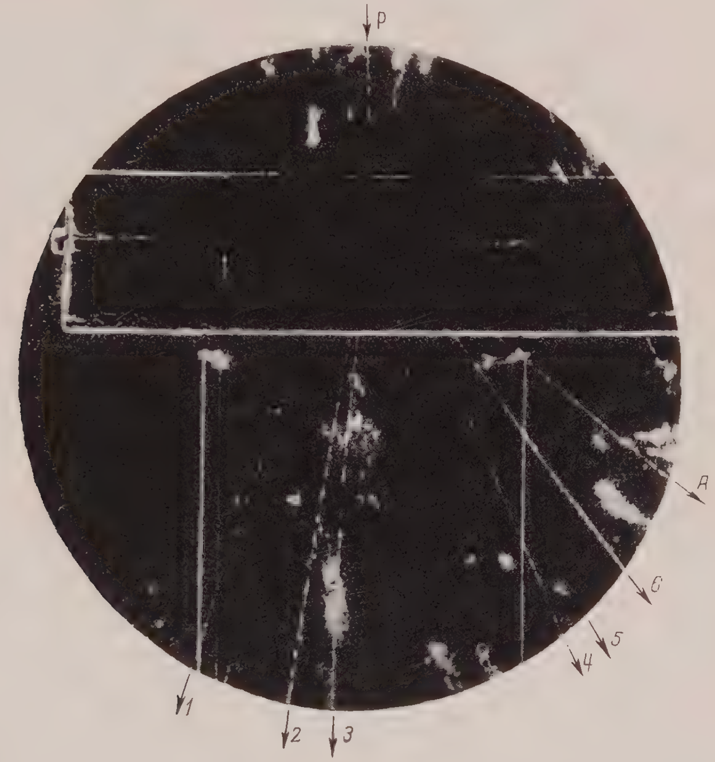

FIG. 2. Shower No. 27.16, initiated by a primary particle which made a track in the upper cloud chamber U, then stopped in the beryllium slab placed in the lower cloud chamber L. Particle A does not go through the origin of the shower.

Shower No. 27.16: This shower is illustrated in Fig. 2. Since there was no more than 8 gm/cm^2 of material above the apparatus, the (positive) incident particle is probably a proton. Energy and momentum are conserved if we assume that a nucleon-nucleon collision occurs, and that a neutron carried away 2.3 bev/c of momentum in some direction making a small angle with the primary direction. The reaction is then $p + p \rightarrow 3\pi^+ + 2\pi^- + p + n$.

Charge conservation eliminates a p–n interaction.

It should be noted that the angle of emission and the momentum of the proton in the laboratory frame, as computed using Eqs. (4) and (5) in I, agree well with experiment.* Thus,

$$\theta_{L\,\text{calc.}} < 38°; \quad \theta_{L\,\text{obs.}} = 23°;$$

$$4\times10^8 < p_{L\,\text{calc.}} < 8\times10^8 \text{ ev}/c;$$

$$p_{L\,\text{obs.}} = 5\times10^8 \text{ ev}/c.$$

The emission angles and momenta, in the center-of-mass system, for the particles in this reaction are given in Table I, while the angular distribution is shown in Fig. 3. From this Figure we see that the particles are emitted almost isotropically in the center-of-mass system. Consideration of the energy balance shows that almost all the kinetic energy of the primary proton was used up in creating π-mesons. The fast nucleons take away only a fairly small fraction (about 43%) of the total primary energy. Reference 4 describes a similar

---

*In the following, a subscript L indicates the laboratory and C the center-of-mass reference frames.

Picture number	Particle number	sign	Ionization	Momentum, in laboratory coordinates $p \times 10^{-8}$ ev/c	Angle of emission relative to the primary. Lab. coord. θ°_{L}	Momentum in the center-of-mass system. $P_c \times 10^{-8}$ ev/c.	Total energy in the center-of-mass system $E_c \times 10^{-8}$ ev/c	Angle of emission relative to the primary.c.o.m.coord. θ°_{c}	Kind of particle
I	II	III	IV	V	VI	VII	VIII	IX	X
27.16	primary	+	~ 1 *min.*	56 ± 6	—	15,4	18	—	proton
	1	+	~ 1 *min.*	$2{,}8^{+0.8}_{-0.4}$	28	1.4	2	104	π-meson
	2	?	~ 1 *min.*	>13	15	4.3	4,5	52	π-meson (from conservation laws)
	3	+	~ 1 *min.*	$2^{+0.3}_{-0.2}$	20	1,0	1,6	111	π-meson
	4	+	~ 1 *min.*	11^{+7}_{-3}	22	4,4	4,5	67	π-meson (from conservation laws)
	5	?	~ 1 *min.*	—	23	—	—	—	(π?)
	6	+	~ 5 *min.*	$3{,}0^{+0.3}_{-0.2}$ taking the range in Be into account $p = 5{,}0 \cdot 10^{8}\ \frac{\text{ev}}{c}$	28	9	13	165	proton

68.18	primary	—	~ 1 *min.*	~65	—	17	17	—	π-meson
	1	—	~ 1 *min.*	—	34	—	—	—	π-meson
	2	—	~ 1 *min.*	$1{,}5\pm0{,}2$	17	1,1	1,8	149	π-meson
	3	?	~ 1 *min.*	>25	11	7	7,1	41	(π?)
	4	+	~ 1 *min.*	$2{,}7^{+0.4}_{-0.3}$	9	0.4	1.5	83	π-meson
	5	+	~ 8 *min.*	$2{,}5^{+0.4}_{-0{,}21}$ taking the range in Be into account $p = 3{,}8\cdot10^{8}\,\frac{\text{ev}}{c}$	22	10	13.7	172	proton
6.116	primary	?	~ 1 *min.*	>540	—	>50	>51	—	(proton?)
	1	+	~ 1 *min.*	11^{+4}_{-2}	10	2	2.4	107	(π?)
	2	+	~ 1 *min.*	$5^{+1}_{-0{,}5}$	2	0,5	1,5	169	π-meson
	3	—	~ 1 *min.*	$9{,}5^{+3}_{-2}$	2	0,6	1.5	39	π-meson
	4	?	~ 1 *min.*	$\geqslant38$	8	$>4{,}5$	4,7	70	(π?)
	5	+	~ 1 *min.*	$5^{+1}_{-0{,}5}$	15	2	2,4	135	π-meson

shower, in which an $n-p$ interaction ($E_0 = 5.6$ bev) produced 5 π-mesons. In this case, the π-mesons carried away 70% of the kinetic energy of the primary nucleon, while $\epsilon < 0.52$.

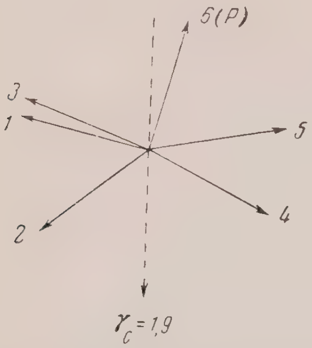

FIG. 3. Angular distribution (in the center-of-mass system) for the particles in shower No. 27.16.

Shower No. 68.18: in this case the primary particle is negative and is presumably a π-meson formed in the graphite layer above the apparatus. Its energy was about 6.5 bev. The analysis of this case is less clear-cut than the previous one because the momenta of the primary and secondary particles are less well known. The shower apparently was produced by the reaction $\pi^- + n \rightarrow 2\pi^+ + 3\pi^- + p + m\pi^0$, where m is the number of neutral π-mesons.

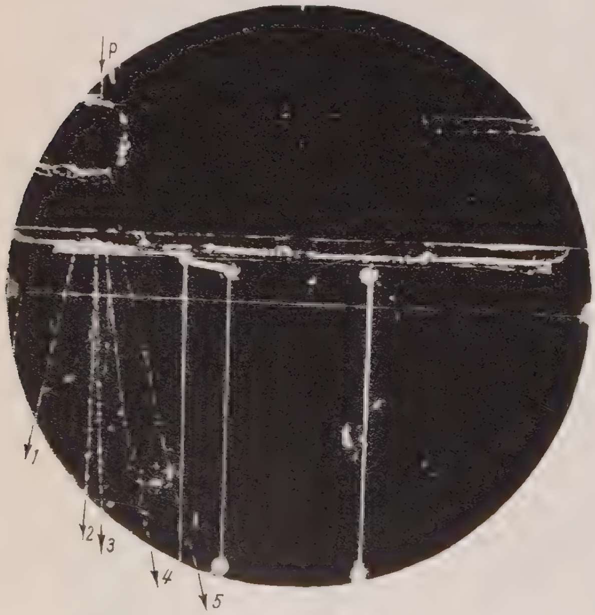

FIG. 4. Shower No. 6.116.

As in the previous case, particles are emitted symmetrically in the center-of-mass system. It is interesting to note that in contrast to the shower first described, a large part of the energy is concentrated not on the nucleons but on particle No.3 (Table I), which appears to be a π-meson. This particle was emitted at 11° to the direction of the primary and carried more than 40% of the primary energy.

Shower No. 6.116 (Fig. 4): The momentum of the primary particle was $\gtrsim 54$ bev/c. Inasmuch as this particle, with such a large momentum, was not accompanied by another charged particle in the upper chamber, it was probably a proton. Calculations based on Eqs. (4) and (5) of I show that neither particle *1* nor particle *4* (Table I) can be protons. Assuming this, either of the following reactions could account for the process:

$$p + n \rightarrow 3\pi^+ + 2\pi^- + n + n + k\pi^0$$

$$p + p \rightarrow 3\pi^+ + 2\pi^- + p + n + k\pi^0.$$

The δ-nucleon must be emitted at an angle $\theta_\delta < 63°$ (in the laboratory system) and cannot have a momentum larger than 4×10^8 ev/c (such a proton has a large chance of stopping in the Be). In the center-of-mass system, the corresponding statement is that the δ-nucleon must be emitted at an angle $\theta_{\delta c} < 175°$. Within experimental error, energy and momentum balance in this case for the charged π-mesons alone. If the π^0-mesons are emitted with the same energies in the center-of-mass system as the π^+-mesons, then the nucleon emitted forward makes an angle of about 5° (in the center-of-mass system) with the direction of the primary and carries away about 80 per cent of the energy of the primary nucleon. Thus, in this shower only a small fraction of the total energy goes into π-mesons. It should be noted that the number of π^+-mesons in this shower is the same as in shower No. 27.16 ($n_s = 5$), although the primary energies differ by a factor of about 10.

The events described indicate that in the interaction of a proton with a light nucleus (Be), relatively many particles may be produced ($n_s = 5$ at $E_0 = 5.7$ bev) with large energy loss, or relatively few particles ($n_s = 5$ at $E_0 > 54$ bev) with small energy loss.

In conclusion, we present shower No. 27.34

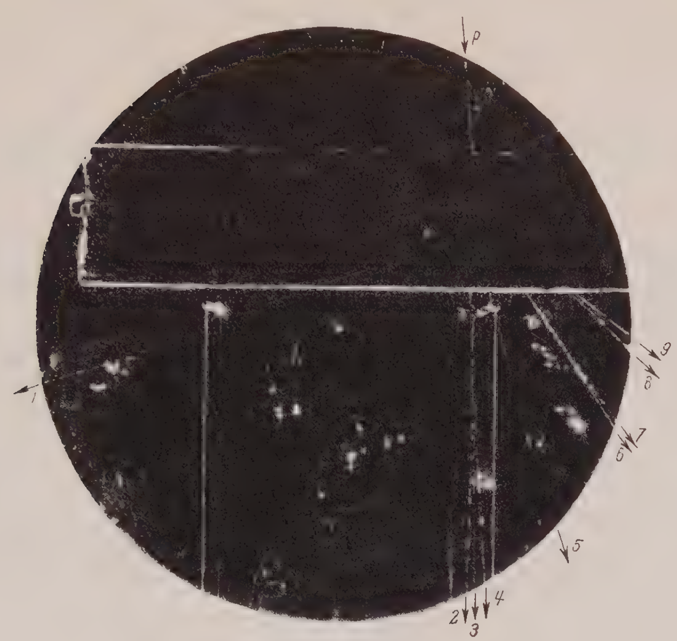

FIG. 5. Shower No. 27.34. Particles 3–4, 6–7 and 8–9 form three narrow pairs, with angles between particles in a pair no larger than 2°.

(Fig. 5), which was initiated by a 6 bev proton. This shower is interesting because of the nine relativistic secondaries, 6 form 3 narrow pairs, the angle in each pair being no larger than 2°. The tracks were distorted by turbulence, so that it was not possible to measure the momenta of the secondary particles.

The authors are grateful to N. A. Dobrotin for discussion of the results.

---

[1] Crussard, Walker and Koshiba, Phys. Rev. 94,736 (1954); Engler, Haber-Shaim and Winkler, Nuovo Cimento 12, 930 (1954); Castagnoli, Cortini, Franzinetti, Manfredini and Moreno, Nuovo Cimento 10, 1539 (1953).

[2] Birger, Grigorov, Guseva, Zhdanov, Slavatinskii and Stashkov, J. Exptl. Theoret. Phys. (U.S.S.R.) 31, 971 (1956); Soviet Phys. JETP 3, 809 (1956).

[3] Rochester Conference, April, 1956; Wright, Saphir, Powell, Maenchen and Fowler, Phys. Rev. 100, 1802 (A) (1955).

[4] Fowler, Maenchen, Powell, Saphir and Wright, Phys. Rev. 101, 911 (1956).

Translated by R. Krotkov
211

SOVIET PHYSICS JETP VOLUME 4, NUMBER 6 JULY, 1957

Production of Postive π-Mesons in Various Nuclei by 660 mev Protons

A. G. MESHKOVSKII, IU. S. PLIGIN,
IA. IA. SHALAMOV AND V. A. SHEBANOV

(Submitted to JETP editor August 15, 1956)
J. Exptl. Theoret. Phys. (U.S.S.R.) 31, 987-992 (December, 1956)

We measured the energy spectrum of π^+-mesons produced at 45° to the incident beam by 660 mev protons incident on Li, Be, C, Al, and Cu. The cross section $d\sigma/d\Omega$ for π^+ formation in these elements is calculated, and conclusions drawn from the fact that all the spectra are similar. The differential cross section $d^2\sigma/d\Omega dE$ for production of π^+-mesons was measured at 158 mev in Ag and Pb. Conclusions are drawn about the dependence of the π^+-mesons production cross section on atomic weight for elements between Li and Pb. For elements between Li and Al the dependence is given by $d\sigma/d\Omega = (1.17 \pm 0.05)\,A^{2/3}$. Considerably fewer π^+-mesons than indicated by this formula are produced in elements after Cu.

1. INTRODUCTION

CHARGED π-mesons are produced when high energy protons are incident on complex nuclei. The relation between the number of π-mesons produced and the number of nucleons in the nucleus has been investigated by several authors[1–6] for proton energies in the range 240–380 mev and for various elements from beryllium to lead. These investigations showed that in the energy range considered, the yield of charged π-mesons does not increase in proportion to A, the number of nucleons, but rises as $A^{2/3}$ or even more slowly.

The production of π^+ and π^--mesons in seven elements from Be to Pb by 240 mev protons has been investigated in Refs. 1,2. It was established that the yield of π^+-mesons emitted at angles of 130–150° and with energies 20–40 mev varies approximately as $A^{2/3}$ for elements from Be to Cu inclusive. The yield of π^+-mesons from heavier elements (Ag, W and Pb) is considerably smaller than indicated by the $A^{2/3}$ law. Similar statements hold for 40 mev π-mesons emitted at angles of 30–50°.[2]

The results with 340 mev protons incident on a series of elements are qualitatively the same for 53 mev π^+-mesons emitted at 0°[3] and for 33 mev π^+-mesons at 90°.[4] The yield of π^+-mesons with energies 52, 88 and 147 mev emitted at 0° from C, Cu, and Pb bombarded by 340 mev protons was also measured.[5] If these latter results are normalized relative to carbon, the π^+-meson yield from Cu and Pb is again less than would be indicated by the $A^{2/3}$ law. π-meson production at 90° by 381 mev protons incident on C, Cu and Pb has been investigated over the whole π^+-meson energy range.[6] Qualitatively, the results were the same as in the above mentioned papers.

Thus, when protons of various energies from 240–380 mev interact with complex nuclei, charged π-mesons are produced essentially by collisions with surface nucleons ($A^{2/3}$ law). Departures from the $A^{2/3}$ law in the direction of fewer π-mesons for elements after Cu is presumably due to a decrease in the transparency of the nucleus with increasing atomic weight.

The purpose of the present work was to investigate the production of π^+-mesons in complex nuclei by protons of considerably higher energy than used by previous authors.

2. PROCEDURE

Our experiments were performed with the external proton beam of the synchrocyclotron of the Institute for Nuclear Problems of the Academy of Sciences, USSR. The π-mesons were detected and their energy measured by a magnetic method we have described previously.[7]

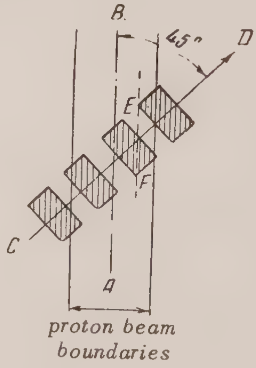

FIG. 1. Construction of the targets.

All measurements were taken at 45° to the incident beam of 660 mev protons. The angular spread in the π-mesons observed was no more than ± 1°. The solid angle defined by the scintillation counter telescope was 2.5×10^{-4} steradian. The momentum resolution varied from 4 percent at $p = 400$ mev/c to 10 percent at $p = 150$ mev/c.

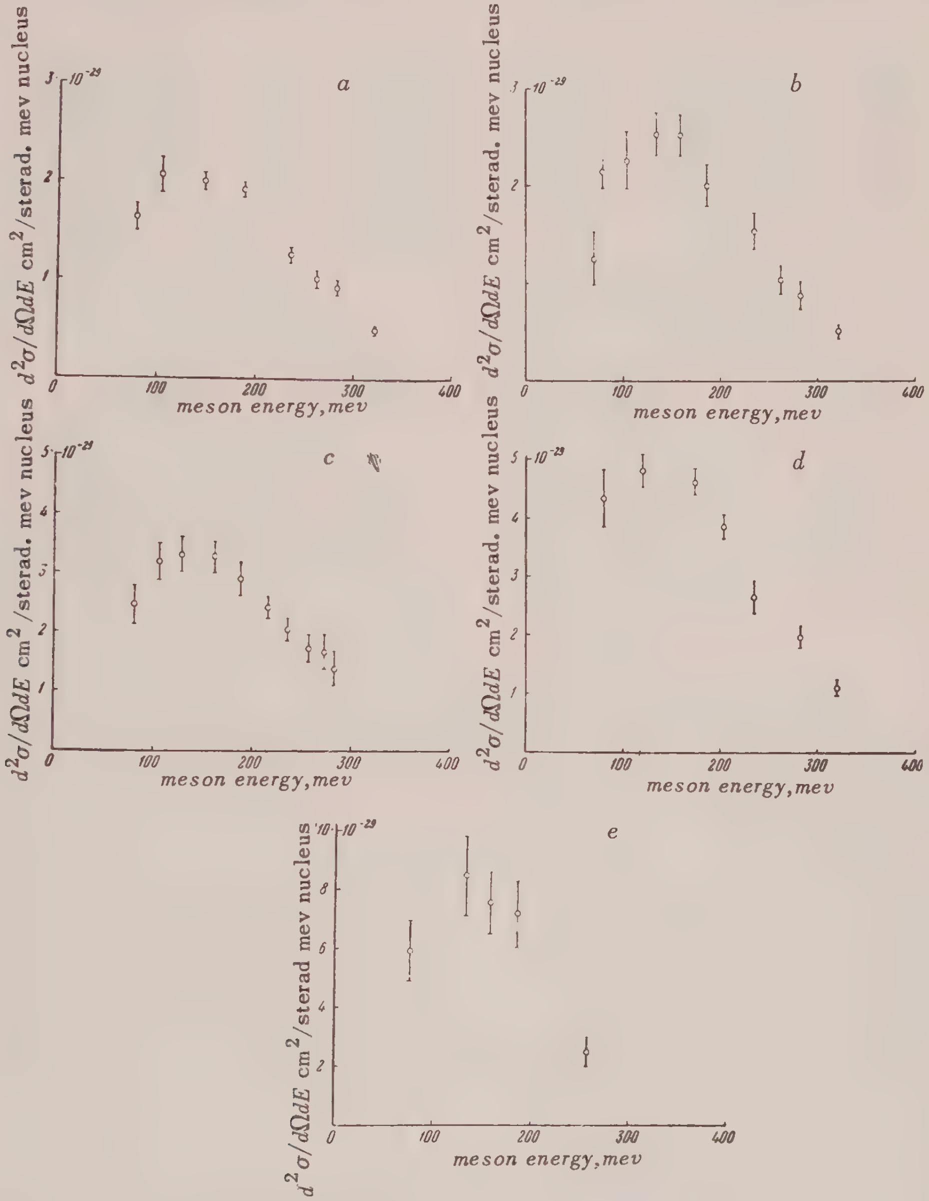

FIG. 2. π^+-meson spectra. a—lithium, b—beryllium, c—carbon, d—aluminum, e—copper.

As indicated in our previous paper[7], some preliminary experiments were necessary to estimate the electron background due to neutral π-mesons produced in the targets. To do this, the magnetic field was adjusted so that negative particles reached the counter telescope, and then a paraffin target compared with a carbon one. The paraffin and carbon targets were of the same length (in atomic units) along the direction in which the π-mesons to be counted would be moving. We concluded that the electron background in our apparatus could not be larger than 2–3%. In order that the electron background be no larger during the actual experiments, the target thicknesses (in atomic units) along the direction in which the π-mesons to be counted were going were made the same as the thickness of the paraffin target in the control experiments.

TABLE I

Lithium		Beryllium		Carbon	
Meson energy,mev	$\frac{d^2\sigma}{d\Omega dE}\cdot 10^{29}$	Meson energy,mev	$\frac{d^2\sigma}{d\Omega dE}\cdot 10^{29}$	Meson energy,mev	$\frac{d^2\sigma}{d\Omega dE}\cdot 10^{29}$
79	1,65 ± 0.13	71	1.25 ± 0,27	80	2,49 ± 0.33
104	2,07 ± 0,18	79	2.15 ± 0.18	105	3,21 ± 0,29
146	2.00 ± 0,09	104	2,26 ± 0,29	128	3,32 ± 0,30
186	1.92 ± 0,07	134	2,53 ± 0.22	161	3.31 ± 0.27
234	1,26 ± 0.08	159	2,52 ± 0.21	187	2.94 ± 0.30
261	1,02 ± 0,09	186	2,01 ± 0.22	215	2,47 ± 0.18
282	0.93 ± 0,08	234	1,54 ± 0.19	235	2.10 ± 0,20
320	0.50 ± 0.04	261	1.04 ± 0.15	257	1.78 ± 0.24
—	—	282	0.88 ± 0.14	272	1,72 ± 0,31
—	—	320	0,51 ± 0,06	283	1.43 ± 0.30

Aluminum		Copper	
Meson energy,mev	$\frac{d^2\sigma}{d\Omega dE}\cdot 10^{29}$	Meson energy,mev	$\frac{d^2\sigma}{d\Omega dE}\cdot 10^{29}$
78	4,34 ± 0,50	77	5,92 ± 1.04
119	4,80 ± 0,28	133	8.47 ± 1.38
172	4.62 ± 0,26	158	7,56 ± 1,13
202	3,84 ± 0.23	185	7,14 ± 1,18
234	2.65 ± 0.29	257	2.49 ± 0.50
282	1.98 ± 0,20	—	—
320	1.02 ± 0.13	—	—
—	—	—	—
—	—	—	—
—	—	—	—

TABLE II

Element	Li	Be	C	Al	Cu
Cross section for production of π^+-mesons $(d\sigma/d\Omega)\times 10^{27}$ in cm^2 sterad^{-1} ,calculated per nucleus	4,24 ± 0,32	4,91 ± 0,45	6,77 ± 0,62	9,79 ± 0,85	14,45 ± 1,86

Seven elements were used as targets: lithium, beryllium, carbon, aluminum, copper, silver and lead. The lithium target was in the form of a solid slab 1 cm. thick. Targets of the other elements were made of several layers, as shown in Fig. 1. *AB* is the direction of the collimated proton beam, *CD* the direction in which π-mesons had to move to be counted in the telescope The plane of the drawing was horizontal and the cross-hatched rectangles represent the cross sections of the layers. The distance between layers was adjusted so that the dotted line *EF* was parallel to *AB*. This arrangement ensured that all protons travelled the same distance in the target, irrespective of where they hit it. The number of layers and the thickness of each was chosen so that the number of radiation lengths in the direction *CD* was the same for targets of each element.

The condition that all targets have the same number of radiation lengths in the direction *CD* limited the amount of matter exposed. As a result for the heavier elements relatively few π-mesons were counted in our apparatus. Hence in the runs with silver and lead, we measured the π^+ -meson yield at only one meson energy. For the other elements, differential spectra were obtained for π^+ -mesons in the energy range 70 to 320 mev.

3. RESULTS

Table I shows our results on the differential cross section for production of π^+ -mesons at 45° in Li, Be, C, Al, and Cu by 660 mev protons. For each π^+ -meson energy, in mev, the Table gives the corresponding differential cross section $d^2\sigma/d\Omega dE$ in cm^2 sterad^{-1} mev^{-1} per nucleus.

The π^+ -meson yield from Ag and Pb was measured at a meson energy of 158 ± 5 mev. $d^2\sigma/d\Omega dE$ (per nucleus) was $(7.90 \pm 1.33) \times 10^{-29}$ cm^{2}sterad mev^{-1} for Ag and $(7.62 \pm 1.43) \times 10^{-29}$ cm^{2}sterad^{-1}

mev^{-1} for Pb.

The data of Table I are plotted in Fig. 2. The errors shown in both figure and Table are only the statistical errors. Systematic errors, amounting to ± 5%, are taken into account in integrating the spectra, i.e., in calculating $d\sigma/d\Omega$.

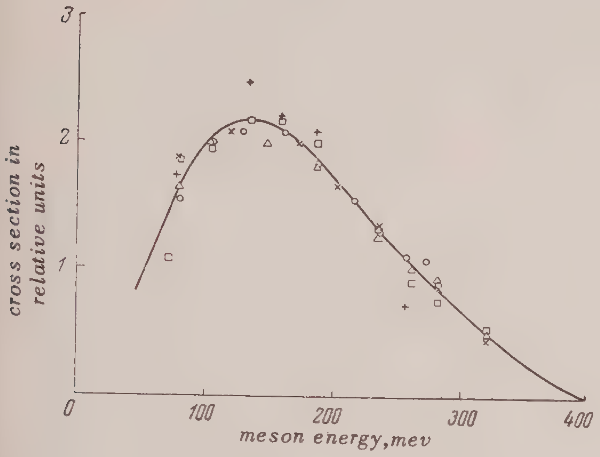

FIG. 3. Results for Li,Be,C,Al and Cu, all drawn to the same scale. Δ–Li, □–Be, O–C, ×–Al, +–Cu.

Table II gives the integrated spectra. In calculating the entries in Table II, the high energy cut off for the spectra was taken to be 390 mev. This was the maximum energy a π-meson could have under our experimental conditions, and was calculated on the assumption that nucleons in a nucleus have an energy of 25 mev.

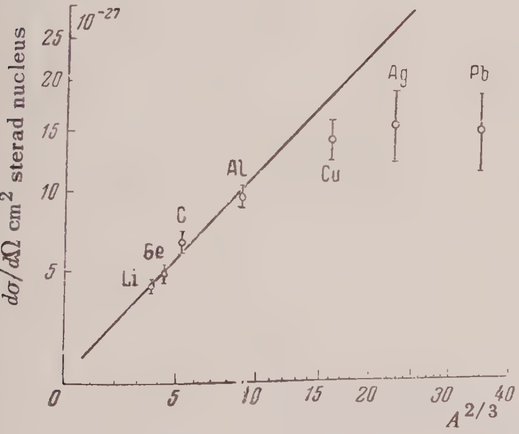

FIG. 4. Cross section for π^+ -meson production as a function of atomic weight.

4. DISCUSSION OF RESULTS

The fundamental point about our spectra is that they are similar, as is evident from Fig. 2. This is particularly clear if the spectra are all plotted on the same scale, as is done in Fig. 3. The curve in Fig. 3 is drawn to fit all the experimental points best. This it does quite well, for no experimental point deviates from the curve by more than the statistical error associated with the point. The latter are not shown on the Figure to avoid confusion.

As mentioned in Sec. 3, the maximum meson energy in our set-up was calculated to be 390 mev. Extrapolation of the curve in Fig . 3 to high energies agrees well with this value.

Figure 3 shows that when the elements we investigated are bombarded by 660 mev protons, the cross section for π^+ -meson production at 45° reaches a maximum at about 140 mev. Under similar experimental conditions the yield of π^+ -mesons from the reaction $p + p \to \pi^+ + p + n$ attains a maximum at about the same energy (in the laboratory system). This was shown by us in a previous paper.[7]

If we assume that the meson spectra are about the same in Ag and Pb as they are for the lighter elements, then we can use our measured values of $d^2\sigma/d\Omega dE$ at 158 mev for Ag and Pb to calculate the cross section at 45° for these elements. The value turns out to be $(16.05 \pm 3.39) \times 10^{-27}$ cm^2 sterad^{-1} for Ag and $(15.48 \pm 3.52) \times 10^{-27}$ cm^2 sterad^{-1} for Pb.

The dependence of the π^+ -meson production cross section on atomic weight is illustrated in Fig. 4. Here the abscissa is $A^{2/3}$, while the ordinate is the cross section $d\sigma/d\Omega$. The relation $d\sigma/d\Omega = kA^{2/3}$ corresponds to the straight line, which was drawn to give a least squares fit to the first four points. The slope of this line is $k = 1.17 \pm 0.05$. Figure 4 also shows the points for Ag and Pb, calculated by the method described above. If the meson spectra for Ag and Pb were not really similar to the other spectra, as we have assumed them to be, then it is possible that our values for $d\sigma/d\Omega$ differ from the true ones. In this case the points for Ag and Pb indicated on the graph give the dependence of the π^+ -meson yield on atomic weight for a definite meson nnergy (158 mev in our case).

From the above discussion it appears that the dependence of π^+ -meson yield on atomic weight is generally the same at 660 mev proton energy as at lower proton energies (240–380) mev. Since the first four points (Fig. 4) lie on the straight line $kA^{2/3}$, we can conclude that in the elements from Li to Al π^+ -mesons are produced on the surface of the nucleus. At larger atomic weights, the π^+ – meson yield is less than that given by the $A^{2/3}$ law (cf. the points for Cu, Ag and Pb). This is presumably due to an increase in the absorption of protons and charged π-mesons by nuclear matter.

---

[1] D. Clark, Phys. Rev. 81, 313 (1951).

[2] D. L. Clark, Phys. Rev. 87, 157 (1952).

[3] Hamlin, Jakobson, Merritt and Schulz, Phys. Rev. 84, 857 (1951).

[4] R. Sagane and W. Dudziak, Phys. Rev. 92, 212(1953).

[5] J. Merritt and D. A. Hamlin, Phys. Rev. 99, 1523 (1955).

[6] Block, Passman and Havens, Phys. Rev. 88, 1239 (1952).

[7] Meshkovskii, Pligin, Shalamov and Shebanov, J. Exptl. Theoret. Phys. (U.S.S.R.) 31, 560 (1950); Soviet Phys. JETP 3, 426 (1956).

Translated by R. Krotkov
212

SOVIET PHYSICS JETP VOLUME 4, NUMBER 6 JULY,1957

On the Theory of Phase Phenomena in Barium Titanate

L. P. KHOLODENKO
Smolensk Pedagogical Institute

(Submitted to JETP editor October 25,1955)
J. Exptl. Theoret. Phys. (U.S.S.R.) 31, 1034-1045 (December,1956)

An explanation is given of "temperature hysteresis" which accompanies phase transitions. The temperature dependence of the dielectric constant in the vicinity of phase transition points has been found. Expressions are found for the coefficients involved in the thermodynamic theory; these are determined in terms of easily measured quantities. The relaxation time has been estimated.

INTRODUCTION

THE thermodynamic theory of piezoelectric phenomena in barium titnate[1-7] is built on a consideration of the thermodynamic potential (or the free energy), and on a search for those conditions under which it takes on minimum values. In this way the presence of four different phases has been established and the transition conditions from one phase to another have been made clear. Here it has been assumed that the transition from one phase to another takes place at that temperature for which the value of the thermodynamic potential becomes identical for both phases under consideration. In essence, this approach implies a neglect of metastable states, which are characterized by a relative, and not an absolute, minimum of the thermodynamic potential. It is known that in a number of cases, the relaxation time is so large that the metastable states are practically stable. Neglect of the metastable states allows us to make clear the chief features of the phenomenon, but it does not allow a satisfactory look at a number of details, including hysteresis phenomena and the piezoelectric properties close to the transition point.

In order to carry out such an analysis, we must (in addition to a consideration of the metastable states) make a definite hypothesis on the temperature dependence of the coefficients in the well-known expression of the thermodynamic potential

$$\Phi = \Phi_0 + \alpha P^2 + {}^1/_2\beta_1 P^4 + \beta_2 (P_x^2 P_y^2 + P_y^2 P_z^2 + P_z^2 P_x^2) + {}^1/_3\gamma_1 P^6 + \gamma_2 [P_x^4 (P_y^2 + P_z^2) + P_y^4 (P_z^2 + P_x^2) + P_z^4 (P_x^2 + P_y^2)] + \gamma_3 P_x^2 P_y^2 P_z^2. \tag{1}$$

In the case of a second order phase transition, we can regard (1) as an expansion in a power series P. It is evident that not only α but also β_1, β_2, γ_1, γ_2, γ_3 are in this case functions of the temperature and pressure. In the case of a first order phase transition, it is no longer possible to regard Eq. (1) as an expansion in a series, but only as a more or less successful approximation. It is evident that in this case also, there is no basis for considering the quantities β_1, β_2, γ_1, γ_2, γ_3 as constants. Moreover, the fact of the temperature dependence of these coefficients is immediately evident from the independence of P (as observed experimentally) of temperature in the orthorhombic and rhombic phases.* While, in the literature (for example, Refs. 2,3, 8), all the enumerated coefficients are regarded as constant. In the present research, the following approximation is used: the quantities γ_1, γ_2, γ_3 are considered constant, but the quantities $\alpha\ {}_1\beta_1$, β_2 are considered as linear functions of the temperature. This approximation permits an explanation of the order of the phase changes observed experimentally, and reduces to a series of relations which are easily tested experimentally.

Unfortunately there is a lack in the literature today of data on a sufficiently complete investigation (if only of a single specimen) which includes the temperature dependence of the polarization and the dielectric constant in both phases, on the consideration of temperature hysteresis, heat capacity, elastic modulus and piezomodulus. Such a complete investigation would permit a quantitative comparison of theory with experiment, which would be the more desirable in that the theory of other piezoelectrics with "perovskite" structure ought to be built in analogy with the theory of barium titanate.

---

*Actually, in the orthorhombic phase, for example, P^2 is given by the relation[4]

$$P^2 = [2\gamma_1 + {}^3/_2\gamma_2]^{-1} [-\beta_1 - {}^1/_2\beta_2) + \sqrt{(\beta_1 + {}^1/_2\beta_2)^2 - 4\alpha(\gamma_1 + {}^3/_4\gamma_2)}\,].$$

For α increasing linearly with the temperature, and for constant $P2$ increases monotonically upon a decrease in temperature, and does not remain constant. (For details, see Sec. 2).

1. CONDITIONS FOR THE STABILITY (METASTABILITY) OF THE DIFFERENT PHASES AND THEIR INTERPRETATION

As is well known, the thermodynamic potential (1) has extrema for the values P_x, P_y, P_z which correspond to I) nonpiezoelectric (cubic), II) tetragonal, III) orthorhombic, IV) rhombic phases,* where the equations that are satsfied by nonzero components, their solutions, and the conditions that the extrema be minima, have the forms:[4]

$$\text{Phase I}\quad P_x = P_y = P_z = 0, \quad \alpha > 0. \tag{2}$$

$$\text{Phase II}\quad \gamma_1 P^4 + \beta_1 P^2 + \alpha = 0, \quad (P = P_z \quad \text{or} \quad P_x \quad \text{or} \quad P_y), \tag{3}$$

$$P^2 = [-\beta_1 + \sqrt{\beta_1^2 - 4\alpha\gamma_1}]/2\gamma_1, \tag{4}$$

$$\beta_1 + 2\gamma_1 P^2 > 0. \tag{5}$$

$$\beta_2 + \gamma_2 P^2 > 0, \tag{6}$$

$$\text{Phase III}\quad (\gamma_1 + {}^3/_4\gamma_2) P^4 + (\beta_1 + {}^1/_2\beta_2) P^2 + \alpha = 0, \tag{7}$$

$$P^2 = {}^1/_2(\gamma_1 + {}^3/_4\gamma_2)^{-1}[-(\beta_1 + {}^1/_2\beta_2) + \sqrt{(\beta_1 + {}^1/_2\beta_2)^2 - 4\alpha(\gamma_1 + {}^3/_4\gamma_2)}]. \tag{8}$$

($P_x^2 = P_y^2$, $P_z = 0$ or similar solutions),

$$(2\beta_1 + \beta_2) + (4\gamma_1 + 3\gamma_2) P^2 > 0, \tag{9}$$

$$2\beta_2 + (\gamma_3 - \gamma_2) P^2 > 0, \tag{10}$$

$$\beta_2 + \gamma_2 P^2 < 0. \tag{11}$$

$$\text{Phase IV}\quad (\gamma_1 + {}^2/_3\gamma_2 + {}^1/_9\gamma_3) P^4 + (\beta_1 + {}^2/_3\beta_2) P^2 + \alpha = 0, \tag{12}$$

$$P^2 = {}^1/_2(\gamma_1 + {}^2/_3\gamma_2 + {}^1/_9\gamma_3)^{-1} \times \left[-(\beta_1 + {}^2/_3\beta_2) + \sqrt{(\beta_1 + {}^2/_3\beta_2)^2 - 4\alpha\left(\gamma_1 + {}^2/_3\gamma_2 + \frac{1}{9}\gamma_3\right)}\right]. \tag{13}$$

$$(P_x^2 = P_y^2 = P_z^2),$$

$$(\beta_1 + {}^2/_3\beta_2) + 2(\gamma_1 + {}^2/_3\gamma_2 + {}^1/_9\gamma_3) P^2 > 0, \tag{14}$$

$$3\beta_2 + \gamma_3 P^2 < 0^{**} \tag{15}$$

In order to give graphic meaning to these general conditions, which characterize the minimum of Φ relative to an arbitrarily small deviation from the equilibrium position, let us consider some concrete deviations. With this aim, we set $P_z = 0$ and introduce polar coordinates in the plane P_x, P_y. Substituting $P_y = P \cos\varphi$ $P_x = P \sin\varphi$ in Eq. (1), we get

$$\Phi = \Phi_0 + \alpha P^2 + {}^1/_2\beta_1 P^4 + {}^1/_3\gamma_1 P^6 + \cos^2\varphi \sin^2\varphi P^4 (\beta_2 + \gamma_2 P^2). \tag{16}$$

The extrema (16) are found from the equations $\partial\Phi/\partial P = 0$, $\partial\Phi/\partial\varphi = 0$, which have the solutions I) $P = 0$, II), $P \neq 0$, $\varphi = 0$, III) $P \neq 0$, $\varphi = \pi/4$, which evidently correspond to phases I, II, III. Calculating the second derivatives of Φ we find that the solutions II ($\varphi = 0$) correspond to a minimum for

$$\beta_2 + \gamma_2 P^2 > 0 \text{ и } \alpha + 3\beta_1 P^2 + 5\gamma_1 P^4 > 0,$$

and the solutions III for

$$\beta_2 + \gamma_2 P^2 < 0, \ \alpha + 3\beta_1 P^2 + 5\gamma_1 P^4 + {}^3/_2\beta_2 P^2 + {}^{15}/_4\gamma_2 P^4 > 0.$$

These conditions, by virtue of Eqs. (3) and (7), coincide with the conditions (9) and (11), which can then be interpreted as the conditions for a minimum in Φ relative to the value of the vector P and the angle φ.

In order to interpret the inequalities (10), (14) and (15), let us consider small departures from equilibrium of another type. To be precise, we set

---

*For brevity, we shall call these phases I,II,III,IV.

**Another minimum condition is given in Ref. 4 for the phase IV; however, it appears as a consequence of Eqs. (14) and (15).

$$P_x = P\cos\theta; \quad P_y = P_z = 2^{-1/2} P\sin\theta,$$

which correspond to the position of the vector P in the plane which passes through the x axis and the diagonal of the yz plane. In this case, Eq. (1) has the form

$$\Phi = \Phi_0 + \alpha P^2 + {}^1/_2\,\beta_1 P^4 + {}^1/_3\,\gamma_1 P^6 \tag{17}$$

$$+ \beta_2 P^4 (\sin^2\theta\cos^2\theta + {}^1/_4 \sin^4\theta)$$

$$+ \gamma_2 P^6 [\cos^4\theta\sin^2\theta + {}^1/_2 \sin^4\theta\,(\cos^2\theta$$

$$+ {}^1/_2 \sin^2\theta)] + {}^1/_4\,\gamma_3 P^6 \cos^2\theta\sin^4\theta.$$

Investigation of this equation leads to the following result. The extrema of Φ occur, for II), at $\theta = 0$, for III) at $\theta=\pi/2$, and for IV) at $\tan\theta=2$. These correspond to the phases II, III, IV. The necessary conditions that these extrema be minimal are the satisfaction of the conditions $\Phi_{\varphi\varphi} > 0$, $\Phi_{\varphi\varphi} > 0$. The first of these, which is applicable to solutions of II and III, as should be expected, again reduce to the equations (5) and (9), while that applicable to the solution of IV reduces to the inequality (14). The second requirement gives, for the solution of II: $\beta_2+\varphi\varphi_2 P^2 > 0$. for the solution of III): $2\beta_2 + (\gamma_3 - \gamma_2) P^2 > 0$, and for the solution of IV): $3\beta_2 + \gamma_3 P^2 > 0$.

Summing up the results we can say that the conditions for a minimum of Φ for each of the phases II, III, IV consist of a single inequality, which expresses the minimum in the quantity P and which contains coefficients both for the isotropic and for the anisotropic terms of Φ, and of one or two inequalities which express the minimum in terms of angles and which contain only the coefficients for the anisotropic terms.

2. TEMPERATURE HYSTERESIS

If we consider that the metastable states are states of virtual equilibrium, which is evidently valid for $BaTiO_3$, the state of the crystal (in the sense of the attachment of it to a certain phase which we denote as phase A) remains unknown so long as this relative minimum of the thermodynamic potential (to which phase A corresponds) does not disappear. Only after this does the transition to another phase B take place. We denote the temperature, at which this occurs, by T_{AB}, The reverse transition from phase B to phase A takes place at the same temperature T_{BA} at which phase B loses stability (it ceases to correspond to a minimum). The temperature T_{BA}, generally speaking, does not coincide with T_{AB}, which indicates the presence of temperature hysteresis.

For a concrete consideration of temperature hysteresis, it is first of all necessary to establish the temperature dependence of β_1 and β_2. Within the framework of the chosen approximation (β_1 and β_2 are linear functions of temperature; γ_1, γ_2 γ_3 are constants) the problem reduces to the sign and value of the derivatives $(\partial\beta_1/\partial T)_p \equiv \beta_1$ and $(\partial\beta_2/\partial T)_p \equiv \beta_2$. To find these quantities, it is convenient to make use of the fact that, as experiment shows,[9] P^2_{III} and P^2_{IV} are practically independent of temperature.* Differentiating Eqs. (7), (12) with respect to temperature, we have for $\partial P^2/\partial T = 0$:

$$(\dot\beta_1 + {}^1/_2\,\dot\beta_2)\, P^2_{III} = -\alpha, \tag{18}$$

$$(\dot\beta_1 + {}^2/_3\,\dot\beta_2)\, P^2_{IV} = -\dot\alpha,$$

where P^2_{III} and P^2_{IV} are the values of P in the phases III and IV, and $\alpha \equiv (\partial\alpha/\partial T)_p$. We find from Eq. (18)

$$\dot\beta_1 = \dot\alpha\,(3/P^2_{IV} - 4/P^2_{III}), \tag{19}$$

$$\dot\beta_2 = 6\dot\alpha\,(P^2_{IV} - P^2_{III})/P^2_{III}P^2_{IV}.$$

In accord with the experimental data,[10] $P^2_{IV} > P^2_{III}$ and $P^2_{IV} - P^2_{III} << P^2_{III}$. It therefore follows that $\dot\beta_1 < 0$ and $\dot\beta_2 > 0$ and is small in comparison with $\dot\beta_1$. Thus β_1 falls off rapidly, while β_2 increases slowly with increase in temperature.

Furthermore, it is not difficult to establish that $\dot\gamma_2 < 0$** Inasmuch as the regions of stability of phases II and III overlap (temperature hysteresis), conditions (6) and (11) are simultaneously satisfied in the region of overlap, for any temperature. Then, by virtue of the fact that $P_{\rm II}^2 < P_{\rm III}^2$ [10], it is true that $\gamma_2 < 0$.

---

*The independence of P of T in phases III and IV probably has an accidental character and cannot be observed in other piezoelectrics of the type of $BaTiO_3$. However, we can also find $\dot\beta_1$ and $\dot\beta_2$ without making use of this independence.

**As a consequence of the uncertainty of the experimental data, the opposite assumption has been made in Ref. 4.

Assembling this information on the coefficients $\beta_1, \beta_2, \gamma_2$, it is easy to determine which of the conditions (5), (6) limits the region of existence of phase II on the high temperature side. This cannot be Eq. (6), since if $\gamma_2 P_{\rm II}^2 + \beta_2 (T_{21}) = 0$ held at the temperature T_{21}, then, for much lower temperatures $T < T_{21}$, it would be necessary that $\gamma_2 P_{\rm II}^2 + \beta_2 < 0$, and phase II could not exist. Consequently, the transition from phase II to phase I proceeds at the temperature T_{21} which satisfies the condition $2\gamma_1 P^4 + \beta_2 P^2 = 0$. The reverse transition from phase I to phase II proceeds at a temperature T_{12} which is determined by the condition $\alpha = 0$, since for $\alpha < 0$, $P = 0$ corresponds to maximum Φ.

Let us proceed to the transition between phases II and III. We first note that condition (9), which is, by Eq. (8), equivalent to

$$[(\beta_1 + {}^1/_2\,\beta_2)^2 - 4\alpha(\gamma_1 + {}^3/_4\,\gamma_2)]^{1/2} > 0,$$

is automatically satisfied if $\alpha < 0$.* Consequently, the region of stability of phase III is determined by the conditions (10), (11). Let the crystal be in phase II and let us carry out a decrease in the temperature. Initially, Eq. (6) is satisfied. With a decrease in the temperature, β_2 decreases and at temperature T_{23} [determined from $\gamma_2 P_{\rm II}^2 + \beta_2(T_{23}) = 0$] phase II loses stability. A transition to phase III occurs. Inasmuch as $P_{\rm III}^2 > P_{\rm II}^2$, condition (11) will be satisfied at the temperature T_{23}. We now trace the reverse transition from phase III to phase II. It takes place at the temperature $T_{32} > T_{23}$, determined by the condition $\gamma_2 P_{\rm III}^2 + \beta_2 (T_{32}) = 0$. At this temperature, phase III loses its stability, since condition (6) will be satisfied.

Now let us consider transitions between phases III and IV. Here the coefficient γ_3 plays an essential role. For the interpretation of the transitions considered, we must regard γ_3 as negative (with the subordinate condition $\gamma_1 + 2/3\,\gamma_2 + 1/9\,\gamma_3 > 0$[4]).

Let the crystal be in phase III and the temperature be lowered. Further, let the condition

$$3\beta_2 + \gamma_3 P_{\rm III}^2 > 0, \tag{20}$$

hold, along with condition (11). Condition (10) then follows from (11) and (20). For a lowered temperature, β_2 decreases and at the temperature T_{34}, which satisfies the condition $3\beta_2 + \gamma_2 P_{\rm III}^2 = \beta_2 + \gamma_2 P_{\rm III}^2 < 0$ or $2\beta_2 (T_{34}) + (\gamma_3 - \gamma_2) P_{\rm III}^2 = 0$, phase III loses its stability and the crystal undergoes a transition to phase IV, the stability condition for which [Eq. (15)] is of course satisfied since $T_{43} < T_{34}$. The reverse transition from phase IV to phase III takes place at a temperature $T_{43} < T_{34}$, at which the quantity $3\beta_2 + \gamma_3 P_{\rm IV}^2$ vanishes and, consequently, phase IV loses its stability. It is easy to see that the conditions for the stability of phase III are satisfied at temperature T_{43}. Condition (14) for $\alpha < 0$, $\gamma_1 + 2/3\,\gamma_2 + 1/9\,\gamma_3 > 0$[4] is also satisfied automatically.

In the picture drawn here of the phase transitions, it is clear that the sequence of phase changes depends sensitively on the size of the coefficients; therefore we can expect that other piezoelectrics of the BaTiO$_3$ type can be found with another sequence of phases or with the absence of some of them.

Operating on the above basis, it is not difficult to calculate the width of the regions of temperature hysteresis.

Region $T_{21} - T_{12} \equiv (\Delta T)_{21}$. It is easily seen that in the case of a second order phase transition, hysteresis is absent, as would be expected.* In the case of a first order transition,

---

*Condition (9), as was pointed out in Ref. 4, only determines the choice of the sign in front of the square root in the solution of (7). So far as the sign of $(\gamma_1 + 3/4\,\gamma_2)$ is concerned, this quantity is positive.[4]

*Phase II loses its stability at a temperature T_{21} determined from $2\gamma, P^4 + \beta_1 P^2 = 0$ or, by virtue of Eq. (3), from $\beta_1 P_{\rm II}^2 + 2\alpha = 0$. Since, for a second order phase transition, P tends to zero at the ransition point, the latter condition means that $\alpha(T_{21}) = 0$, i.e., that $T_{21} = T_{12}$.

$$\alpha(T_{12}) = 0, \quad 2\gamma_1 P^2_{\mathrm{II}} + \beta_1(T_{21}) = 0. \qquad (21)$$

By taking Eq. (4) into account, the latter equation can be written in the form

$$\alpha(T_{21}) = [\beta_1(T_{21})]^2 / 4\gamma_1. \qquad (22)$$

Substituting $(\Delta T)_{21}$ α for α (T_{21}), we get

$$(\Delta T)_{21} = [\beta_1(T_{21})]^2 / 4\gamma_1\alpha. \qquad (23)$$

Region $T_{32} - T_{23} \equiv (\Delta T)_{32}$. The temperatures T_{23} and T_{32} are determined by the equations

$$\gamma_2 P^2_{\mathrm{II}}(T_{23}) + \beta_2(T_{23}) = 0, \qquad (24)$$

$$\gamma_2 P^2_{\mathrm{III}}(T_{32}) + \beta_2(T_{32}) = 0.$$

Replacing β_2 (T_{32}) by β_2 $(T_{23}) + \beta_2$ $(\Delta T)_{32}$, we findfrom these equations,

$$(\Delta T)_{32} = (\gamma_2/\dot{\beta}_2)\,[P^2_{\mathrm{II}}(T_{23}) - P^2_{\mathrm{III}}(T_{32})]. \qquad (25)$$

Region $T_{43} - T_{34} \equiv (\Delta T)_{43}$. Here the temperatures T_{34} and T_{43} are determined by the equations

$$2\beta_2(T_{34}) + (\gamma_3 - \gamma_2) P^2_{\mathrm{III}} = 0, \qquad (26)$$

$$\beta_2(T_{43}) + \gamma_3 P^2_{\mathrm{IV}} = 0.$$

Setting β_2 $(T_{43}) = \beta_2$ $(T_{34}) + (\Delta T)_{43}$ β_2, we find

$$(\Delta T)_{43} = [\gamma_3(P^2_{\mathrm{III}} - 2P^2_{\mathrm{IV}}) - \gamma_2 P^2_{\mathrm{III}}]/2\dot{\beta}_2. \qquad (27)$$

To conclude this Section, we note that Eqs. (23), (25), (27) are approximately true even if the dependence of the coefficients β_1 and β_2 on the temperature is more complicated than is assumed in this work.

3. BEHAVIOR OF THE DIELECTRIC CONSTANT NEAR THE POINTS OF PHASE TRANSITIONS

Having Eqs. (21), (24), (26) for the temperatures of the phase transitions, and making use of the general expressions for the dielectric constant in each of the phases [that were obtained in Ref. 4], we can make explicit the temperature dependence of the dielectric constant near the transition points.

Boundaries of phases I, II. Here we need to distinguish between the cases of phase transitions of the first and second kind. In the latter case the well known "pair law" holds.[1] We pause only on the first order phase transition. Near T_{12}, for $T > T_{12}$, we have

$$\varepsilon = 2\pi/\alpha = c_{12}/(T - T_{12}), \text{ где } c_{12} = 2\pi/\dot{\alpha}. \qquad (28)$$

If the crystal is in phase II near $(T < T_{21})$ we have

$$\varepsilon_{\parallel} = -\pi / (\beta_1 P^2 + 2\alpha) = \pi / (2\gamma_1 P^4 + \beta_1 P^2); \qquad (29)$$

$$\varepsilon_{\perp} = 2\pi / (\beta_2 P^2 + \gamma_2 P^4),$$

where T_{21} satisfies Eq. (21). From Eqs. (4) and (21) it follows that

$$[\beta_1(T_{21})]^2 = 4\gamma_1\alpha(T_{21}), \quad P^2(T_{21}) = -\beta_1 / 2\gamma_1.$$

Making use of these expressions, and limiting ourselves to terms of lowest order, we obtain the small quantity

$$2\gamma_1 P^4 + \beta_1 P^2 = -(\beta_1 / 2\gamma_1)\,[-2\dot{\beta}_1\beta_1(T_{21}) \qquad (30)$$

$$+ 4\dot{\alpha}\gamma_1]^{1/2}(T - T_{21})^{1/2}.$$

From Eqs. (29)–(30) we get

$$\varepsilon_{\parallel} = c_{21} / (T_{21} - T)^{1/2}, \text{ where } c_{21} \qquad (31)$$

$$= -[2\pi\gamma_1 / \beta_1 (4\dot{\alpha}\gamma_1 - 2\beta_1\dot{\beta}_1)]_{T=T_{21}}.$$

$\epsilon_{\perp}$ has no singularity at $T = T_{21}$.

Boundaries of phases II and III. The temperature T_{23} is determined from Eq. (24). It is evident from (29) that $\epsilon_{||}$ has no singularity at this temperature, whereas $\epsilon_{\perp}$ obeys the Curie-Weiss law. Actually, expanding the denominator of Eq. (29) in powers of $T-T_{23}$ and considering that P^2 changes slowly in the neighborhood of T_{23} (so that we can neglect the terms dP^2/dT), we get*

$$\varepsilon_{\perp} \approx c_{23} / (T - T_{23}), \tag{32}$$

$$c_{23} = (-2\pi\gamma_2 / \beta_2\dot{\beta}_2)_{T=T_{23}}.$$

The temperature T_{32} is obtained foom Eq. (24). In phase III, if we choose the coordinate axes so that $P_x = 0$, $P_y{}^2 = P_z{}^2$, the following components are different from zero:

$$\varepsilon_{ik} : \varepsilon_{xx}, \quad \varepsilon_{yy} = \varepsilon_{zz} \text{ И } \varepsilon_{yz} = \varepsilon_{zy}.$$

They are expressed by the equations (3), (7) from the work of Ref. 4. It is immediately clear from these equations that the component ϵ_{xx} has no singularity at the temperature T_{32}, while the remaining non-zero components obey the Curie-Weiss law. Because of insufficient space, we shall not deduce the expressions for the corresponding constants, and limit ourselves only to a consideration of the principal values of the tensor ϵ_{ik}. These will be the components ε'_{xx}, ε'_{yy}, ε'_{zz}, where the axes z', x', y' are directed respectively along the vector P, the original x-axis and the direction perpendicular to the first two.

The components ϵ'_{xx}, ϵ'_{yy}, ϵ'_{zz} have the form:[4]

$$\varepsilon'_{xx} = 8\pi / [2\beta_2 P^2 + (\gamma_3 - \gamma_2) P^4]; \tag{33}$$

$$\varepsilon'_{yy} = -2\pi / (\beta_2 P^2 + \gamma_2 P^4);$$

$$\varepsilon'_{zz} = -2\pi / (4\alpha + (2\beta_1 + \beta_2) P^2).$$

It is evident from these formulas that the longitudinal component ϵ'_{zz} and the one of the transverse components (ϵ'_{xx}), which corresponds to the direction of the crystallographic axis of a fourth order cubic crystal, have no singularities at the transition point. Conversely, the transverse component ϵ'_{yy}, which corresponds to the direction of the diagonal of the cubic crystal, obeys the Curie-Weiss law.

Repeating the calculations used in deriving Eq. (32), we obtain for T close to T_{32} ($T < T_{32}$),

$$\varepsilon_{yy} = c_{32} / (T_{32} - T); \tag{34}$$

$$c_{32} = (-2\pi\gamma_2 / \beta_2\dot{\beta}_2)_{T=T_{32}}.$$

Boundaries of regions III and IV. The temperatures T_{34} and T_{43} are determined by Eqs. (26). Let the crystal be in phase III and T close to T_{34} ($T < T_{34}$). As is evident from Eq. (2.7),[4] the components $\epsilon_{yy} = \epsilon_{zz}$ and $\epsilon_{yz} = \epsilon_{zy}$ have no singularities at thepoint T_{32}. However, the component $\epsilon_{xy} = \epsilon'_{xx}$ follows the Curie-Weiss law. Close to T_{34}, the denminator of the first of Eqs. (33) can be written in the form $2\dot{\beta}_2 P^2_{\text{III}} (T - T_{34})$, and consequently,

$$\varepsilon_{xx} = \varepsilon'_{xx} = c_{34} / (T - T_{34}); \tag{35}$$

$$c_{34} = 4\pi / \dot{\beta}_2 P^2_{\text{III}} = -4\pi (\gamma_3 - \gamma_2) / 2\beta_2 \dot{\beta}_2.$$

The remaining components ϵ'_{yy} and ϵ'_{zz} have no singularities for $T = T_{34}$. Thus, even in the case of a transition to the second phase, one of the transverse dielectric constants tends to infinity, but not that one which has a singularity at the point T_{32}.

Now let the crystal be in phase IV, close to the point T_{43} ($T < T_{43}$). As is evident from Eq. (3.8) of Ref. 4, all the components ϵ_{ik} in this case ($\epsilon_{xx} = \epsilon_{yy} = \epsilon_{zz}$ and $\epsilon_{xy} = \epsilon_{yz} = \epsilon_{zx}$) satisfy the Curie-Weiss law. Not computing the corresponding constants, we return to the principal values. They are expressed by the equations*

$$\varepsilon'_{zz} = -3\pi / [6\alpha + (3\beta_1 + 2\beta_2) P^2]; \tag{36}$$

$$\varepsilon'_{xx} = \varepsilon'_{yy} = -3\pi / (\beta_2 + {}^1/_3\gamma_3 P^2) P^2.$$

It follows from these equations that the longitudinal component ϵ'_{zz} has no singularity for

---

*In order to obtain the more accurate expression for c_{23}, we must consider that

$$dP^2/dT = -(\beta_1 P^2 + \alpha) / (2\gamma_1 P^2 + \beta_1),$$

which is obtained upon differentiation of Eq. (3) with respect to the temperature.

*As the z'-axis, we chose the direction of the vector P, and for x', y', any mutually perpencicular directions that are also perpendicular to P.

$T = T_{43}$, but the transverse components ϵ'_{xx} $\epsilon'_{yy} = \epsilon_\perp$ obey the Curie-Weiss law:

$$\varepsilon_\perp = c_{43} / (T_{43} - T);$$

$$c_{43} = 3\pi / \dot{\beta}_2 P^2_{\mathrm{IV}} = -\pi\gamma_3 / \dot{\beta}_2\beta_2. \tag{37}$$

Are the temperature dependences obtained here validated by experiment? Unfortunately, it is difficult to give a complete answer to this question in the absence of accurate measurements.

4. EXPRESSION OF THE CONSTANTS IN TERMS OF EASILY MEASURABLE QUANTITIES

The problem of the experimental determination of the constants on which the theory is constructed is undoubtedly of practical interest. In Ref. 4 formulas were proposed for the calculation of the theoretical coefficients. However, in the first place, these formulas contain quantities whose accurate measurement is very difficult, and, in the second place, which is more important, these formulas were introduced without consideration of metastable states. It is appropriate therefore to turn our attention to the problem of the coefficients.

The quantities which we need to find are, first, the constants $\gamma_1, \gamma_2, \gamma_3$. Further, as a consequence of the assumed linear dependence for each of the quantities α, β_1, β_2, it suffices to point out one value for some temperature and the value of the derivative at that temperature.

Finding of α . Inasmuch as one value of α is known from $\alpha(T_{12}) = 0$, we need only to find This quantity has repeatedly been found from the temperature dependence of ϵ in phase I:

$$\dot{\alpha} = 2\pi / \varepsilon (T - T_{12}). \tag{38}$$

Finding of $\gamma_1, \beta_1(T_{21}), \dot{\beta}_1$. Here we need to distinguish the cases of phase transitions of first and second order. Let the transition between the phases I and II be of second order. Then we can find $\beta_1(T_{21})$ from the initial slope of the curve $P(T)$ in phase II. From $P^2 = -\alpha/\beta$,[1] near $T = T_{12}$, it follows that

$$\dot{\beta}_1 = -\dot{\alpha} / (dP^2/dT)_{T=T_{21}}. \tag{39}$$

The value of $\dot{\beta}_1$ was found in Sec. 2. The value of γ_1 can be found from Eq. (3):

$$\gamma_1 = -\alpha(T) P^{-4} - \beta_1(T_{21}) P^{-2} - \dot{\beta}_1 P^{-2}(T - T_{21}), \tag{40}$$

where T is an arbitrary temperature $T_{21} < T < T_{23}$, and P is the corresponding polarization.

In the case of a first order phase transition, Eq. (39) does not occur. To find the desired quantities, we have

$$[\beta_1(T_{21})]^2 = 4\gamma_1\alpha(T_{21}), \quad (P^2)_{T_{21}} = -\beta_1(T_{21}) / 2\gamma_1; \quad \alpha(T_{21}) = (\Delta T)_{21}\dot{\alpha}.$$

From these equations, we find that

$$\beta_1(T_{21}) = -2\frac{(\Delta T)_{21}\dot{\alpha}}{(P^2)_{T_{21}}}; \quad \gamma_1 = \frac{(\Delta T)_{21}\dot{\alpha}}{(P^4)_{T_{21}}}. \tag{41}$$

Finding of $\beta_2(T_{32})$ and γ_2. Solving the second of Eqs. (24) and (7), we obtain

$$\gamma_2 = -4[\alpha(T_{32}) / P^4_{\mathrm{III}} + \beta_1(T_{32}) / P^2_{\mathrm{III}} + \gamma_1]; \tag{42}$$

$$\beta_2(T_{32}) = 4P^2_{\mathrm{III}}[\alpha(T_{32}) / P^4_{\mathrm{III}} + \beta_1(T_{32}) / P^2_{\mathrm{III}} + \gamma_1],$$

$$\alpha(T_{32}) = \dot{\alpha}(T_{32} - T_{12});$$

$$\beta_1(T_{32}) = \beta_1 T_{21}) + \dot{\beta}_1(T_{32} - T_{31}).$$

Finding of $\dot{\beta}_2$. The qunntity β_2 was found in Sec. 2. For a control, and in the vanishing of the small distances $P^2_{\mathrm{IV}} - P^2_{\mathrm{III}}$ entering in Eq. (19), we can find $\dot{\beta}_2(T_{23})$ from the first Eq. (24) and compute $\dot{\beta}_2$ from

$$\beta_2(T_{32}) - \beta(T_{23}) = \dot{\beta}_2(T_{32} - T_{23}). \tag{43}$$

Finding of γ_3. We have, from Eq. (26),

$$\gamma_3 = -P^{-2}_{\mathrm{IV}}\beta_2(T_{43}) = -P^{-2}_{\mathrm{IV}}[\beta_2(T_{32}) + \dot{\beta}_2(T_{43} - T_{32})]. \tag{44}$$

In addition to the expressions obtained for the coefficients $\alpha, \beta_1, \beta_2, \gamma_1, \gamma_2, \gamma_3$, it is evidently possible to put together many others to which, in the case of sufficiency of the approximation assumed, we can give approximate values.

5. LATENT HEAT. HEAT CAPACITY. ADIABATIC DIELECTRIC CONSTANT

Based on the derived temperature dependence of the coefficients, it is not difficult to write down the expressions for the latent heat and the heat capacity. If we limit ourselves to phase transitions between the first and second phases, we have for the latent heat

$$\lambda_{12} = T(S - S_0) = -T[\dot{\alpha}P^2 + {}^1\!/_2\dot{\beta}_1 P^4] \quad (45)$$

[here it is taken into account that for thermodynamic equilibrium, $(\partial\Phi/\partial p) = 0$]. In the case of a second order phase transition, $\lambda_{12} = 0$.

The first order transition from phase I to phase II occurs at a temperature T_{12}, we should therefore substitute $P_{\mathrm{II}}^2(T_{12}) = -\beta_1(T_{12})/\gamma_1$ in Eq. (45). For the reverse transition from phase II to phase I, Eq. (45) must be written in the form $\lambda_{21} = T_{21}(\dot{\alpha}P^2 + 1/2\,\dot{\beta}_1 P^4)$, where now $P^2 = P_{\mathrm{II}}^2 \times (T_{21}) = -\beta_1(T_{21})/2\gamma_1$.

For determining the heat capacity, we have

$$(C_p)_{\mathrm{II}} - (C_p)_{\mathrm{I}} = -T\left[\left(\frac{\partial S}{\partial T}\right)_{\mathrm{II}} - \left(\frac{\partial S}{\partial T}\right)_{\mathrm{I}}\right] \quad (46)$$

$$= -T(\dot{\alpha} + \dot{\beta}P^2)\frac{dP^2}{dT},$$

where, in accord with Eq. (4), P^2 is expressed by the formula

$$\frac{dP^2}{dT} = \frac{1}{2\gamma_1}\left[-\dot{\beta}_1 + \frac{\beta_1\dot{\beta}_1 - 2\dot{\alpha}\gamma_1}{\sqrt{\beta_1^2 - 4\alpha\gamma_1}}\right]. \quad (47)$$

In the case of a second order phase transition, the transition point is determined from $\alpha = 0$, where $\beta_1 > 0$, and the square root entering into Eq. (47) must be set equal to $+\beta_1$ at the transition point. We then obtain the usual expression

$$(C_p)_{\mathrm{II}} - (C_p)_{\mathrm{I}} = T_{12}\dot{\alpha}^2/\beta_1. \quad (48)$$

from Eqs. (46), (47).

In the case of a first order transition, $\beta_1 < 0$ and the heat capacities at the two transition points T_{12} and T_{21} are equal. For $T = T_{12}$, the square root entering inoo Eq. (53) is equal to $-\beta_1$ and

$$(C_p)_{\mathrm{II}} - (C_p)_{\mathrm{I}} = -\frac{T_{12}}{\beta_1(T_{12})}\left(\dot{\alpha} - \dot{\beta}_1\frac{\beta_1 T_{12})}{\gamma_1}\right)^2. \quad (49).$$

For $T = T_{21}$, dP^2/dT, and consequently $(C_p)_{\mathrm{II}}$ also, go to infinity. Near R_{21}, for $T < T_{21}$, we get from Eqs. (30), (46), (47),

$$(C_p)_{\mathrm{II}} - (C_p)_{\mathrm{I}} \to T_{21}(4\dot{\alpha}\gamma_1 \quad (50)$$

$$- 2\beta_1\dot{\beta}_1)^{3/2}/8\gamma_1^2(T_{21} - T)^{1/2}.$$

We now turn to the calculation of the adiabatic dielectric constant. It is essential for the following reason. The measurements of the initial dielectric constant are usually carried out on a variable current of sonic frequency. Inasmuch as thermal exchange at these frequencies is practically negligible, we can consider that the measured values of ϵ are closer to the adiabatic than to the isothermal dielectric constants.

The connection between the adiabatic and the isothermal dielectric constants is given by the expression

$$\varepsilon_S = (C_P/C_E)\,\varepsilon_T, \quad (51)$$

where C_P is the heat capacity at constant polarization, and C_E is the heat capacity at constant field. Applying Eq. (51) to the case of a transition between phases I and II, and using Eq. (46) [where now we write $(C_p)_{\mathrm{II}} = C_E$; $(C_P)_{\mathrm{I}} = C_P$], we can obtain the following equations:

for a second order phase transition,

$$\varepsilon_S = \varepsilon_T C_P/(C_P + T_{12}\dot{\alpha}^2/\beta_1(T_{12})); \quad (52)$$

for a first order phase transition, close to T_{12},

$$\varepsilon_S = \varepsilon_T C_P/[C_P \quad (53)$$

$$- (T_{12}/\beta_1(T_{12}))(\dot{\alpha} - \dot{\beta}_1\beta_1(T_{12})/\gamma_1)^2].$$

Near the point T_{21},

$$\varepsilon_S = -8\varepsilon_T C_p \gamma_1^2 (T_{21} - T)^{1/2} / T_{21} \times (4\dot{\alpha}\gamma_1 - 2\beta_1\dot{\beta}_1)^{3/2}_{T=T_{21}}. \tag{54}$$

Substituting ϵ_T [from Eq. (31)] in Eq. (54) we find

$$\varepsilon_S = (16C_p\gamma_1^3 / T_{21}\beta_1(T_{21})) \times (4\dot{\alpha}\gamma_1 - 2\beta_1\dot{\beta}_1)^{-2}_{T=T_{21}}. \tag{55}$$

Thus ϵ_S, in contrast to ϵ_T, has no singularities at the point T_{21}.

In view of the fact that P is almost independent of temperature near the points of transition between phases II and III, and III and IV, the difference between ϵ_s and ϵ_T here is not large.

6. ESTIMATE OF THE RELAXATION TIME

In the theory outlined above, it was assumed that the transition from one phase to another occurs only when the first phase loses stability.

Such an assumption amounts to a neglect of fluctuations. The system can be found for a suitably long time in the metastable state and, consequently, the relaxation time will be infinite.

In order to correct the validity of such a consideration, it is necessary to estimate the relaxation time τ. We limit ourselves to an estimate of for the transition from phase I to phase II. The thermodynamic potential for this case can be written in the form

$$\Phi = \Phi_0 + \alpha P^2 + {}^1/_2\beta_1 P^4 + {}^1/_3\gamma_1 P^6. \tag{56}$$

The dependence of $\Phi(P)$ for $0 < \alpha < 3\beta_1^2/16\gamma_1$ has the form* sketched in the Figure, where P_2 and P_1 are the values of P corresponding to the minimum and maximum, equal to

$$P_2^2 = (-\beta_1^2 + \sqrt{\beta_1^2 - 4\alpha\gamma_1}) / 2\gamma_1;$$

$$P_1^2 = (-\beta_1 - \sqrt{\beta_1^2 - 4\alpha\gamma_1}) / 2\gamma_1,$$

where, close to $\alpha = 0$,

$$P_1^2 \approx -\alpha / \beta_1.$$

Let the crystal be found in phase I ($P = 0$) and let the temperature decrease. In this case the height of the barrier separating the minimum corresponding to the values $P = 0$ and $P = P_2$ decreases. Neglecting fluctuations, we should expect that the transition from phase I to phase II takes place at that temperature T_{12} for which this barrier disappears, i.e., when

$$\Phi(0) - \Phi(P_1) = 0. \tag{58}$$

Then, substituting P_1 from Eq. (57), and solving the the resultant equation for α, we find $\alpha(T_{12}) = 0$ in accord with Sec. 2.

Taking into consideration the fluctuations, it should be observed that the phase transition I →II takes place for $\alpha > 0$ also, but satisfies the condition

$$\alpha < 3\beta_1^2/16\gamma_1,$$

where the relaxation time τ depends on α. For an estimate of $\tau(\alpha)$, we assume that the phase transition in each specimen is guaranteed upon the formation of a nucleus of phase II in a small macroscopic volume $\Delta\nu$. For the probability of formation of such a nucleus, we must consider the probability of the origin in the volume $\Delta\nu$ of a polarization which exceeds the "barrier" value P_1. The latter proabbility is equal to [11]

$$q = C\int_{P_1}^{\infty} \exp\{-[\Phi(P) - \Phi(0)]\,\Delta v / kT\}\, dP. \tag{59}$$

In view of the fact that large fluctuations do not make significant contribution to the integral in (59), we can limit ourselves to the square term in $\Phi(P)$, and determine C from the normalization condition

$$C\int_0^{\infty} e^{-\alpha P^2 \Delta v / kT}\, dP = 1. \tag{60}$$

We further assume that the fluctuations are recorded at the moments Δt, $2\Delta t$, $3\Delta t$, . . . , where Δt is so chosen that, on the one hand, it is small enough that in a time Δt there takes place only a small number of fluctuations, and, on the other hand, large enough that the recorded fluctuations can be regarded as statistically independent.

---

*For $0 < \alpha < \dfrac{3\beta_1^2}{16\gamma_1}$, phase I is metastable.[7]

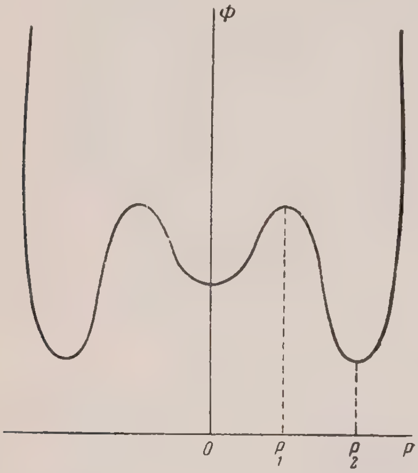

We introduce the probability p that in the time interval Δt, in the volume $\Delta \nu$, there does not take place a fluctuation exceeding the "barrier" value P_1. We can regard the quantity q in Eq. (59) as a fraction of theinterval Δt during which the system is in microstates corresponding to $P > P_1$ (in the volume $\Delta \nu$), and $(1-q)$ as the fraction of this interval which corresponds to $P < P_1$. Therefore, we can take for the probability $p=1-q$. Then we can estimate the mean relaxation time in the following way:

$$\bar{\tau} \sim pq\Delta t + 2p^2q\Delta t + 3p^3q\Delta t + \cdots \qquad (61)$$

Actually, pq is the probability that the value P_1 is achieved at the instant t lying between Δt and $2\,\Delta t$; $p^2 q$ is the probability that it occurs at a time lying between $2\,\Delta t$ and $3\,\Delta t$, etc. Summing the right side of Eq. (61),* we get

$$\bar{\tau} \sim q\Delta t p/(1-p)^2 = \Delta t p/(1-p). \qquad (62)$$

In order to establish the dependence of τ on the parameters ofthe system, let us find p from Eqs. (59), (60):

$$p = \sqrt{2/\pi}\int_0^{x_1} e^{-x^2/2}\,dx, \qquad (63)$$

$$x_1 = \alpha\sqrt{-2\Delta v/\beta_1 kT}$$

$$= (T - T_{12})\,\dot{\alpha}\sqrt{-2\Delta v/\beta_1 kT},$$

For an estimate of x_1, we take $\Delta \nu \sim 10^{-4}$ and take the values

$$\alpha \approx 4\cdot 10^{-5}, \qquad \beta_1 \approx 3\cdot 10^{-13}$$

from Ref. 8 (all quantities in the cgs. system). Then we get

$$x_1 \sim 10^6 (T - T_{12}).$$

We can simplify Eq. (63) for large values of x_1 by making use of the asymptotic value of the integral in it[12]

$$p \approx 1 - \sqrt{2/\pi}\, e^{-x_1^2/2}/x_1. \qquad (64)$$

From Eqs. (62) and (64), we get

$$\bar{\tau}(\alpha) \sim x_1 e^{x_1^2/2}\,\Delta t. \qquad (65)$$

There remains in Eq. (65) theundetermined quantity Δt, equal (in order of magnitude) to the mean time interval between two successive fluctuations. An estimate of Δt without a detailed knowledge of the fluctuation mechanism is very difficult. Fortunately, the strucuure of Eq. (65) is such that any accurate estimate of Δt is unnecessary in practice. Inasmuch as the fluctuations of the quantity P are determined by the thermal motion of the atoms of the crystal, we can estimate the minimum value of Δt by assuming

$$\Delta t \sim a/c \sim 10^{-8}/10^5 \sim 10^{-13}\ \text{sec.}$$

We further set $T - T_{12} = 10^{-3}$ degrees, which corresponds to $x_1 \sim 10^5$. We then get from Eq. (65) $\ln\bar{\tau} \sim 10^5$. It is clear that the order of magnitude of τ would not be changed for any other

---

*For this we must write Eq. (61) in the form

$$\tau = q\Delta t(p + p^2 + \ldots) + q\Delta t(p^2 + p^3 + \ldots) + \ldots,$$

sum the series in parantheses and the series obtained from a summation of the paranthetical expressions.

assumptions on the value of Δt.

Thus, even at a temperature very close to T_{12} (from the viewpoint of experimental possibilities), the relaxation time can be considered as practically infinitely large, which supports the basic assumption made in the research.

In conclusion, I am pleased to thank V. L. Ginzburg for supervising the research and for several suggestions made during the final editing.

1 V. L. Ginzburg, J. Exptl. Theoret. Phys. (U.S.S.R.) 19, 36 (1949).
2 A. F. Devonshire, Phil. Mag. 40, 1040 (1949).
3 A. F. Devonshire, Phil. Mag. 42, 1065 (1951).
4 M. Ia. Shirobokov and L. P. Kholodenko, J. Exptl. Theoret. Phys. (U.S.S.R.) 21, 1239 (1951).
5 L. P. Kholodenko and M. Ia. Shirobokov, J. Exptl. Theoret. Phys. (U.S.S.R.) 21, 1250 (1951).
6 G. A. Smoleiskii and R. E. Pasynkov, J. Exptl. Theoret. Phys. (U.S.S.R.) 24, 69 (1953).
7 L. P. Kholodenko , J. Exptl. Theoret. Phys. (U.S.S.R.) 31, 244 (1956); Soviet Phys. JETP **4**, 188 (1957).
8 W. J. Merz, Phys. Rev. 91, 513 (1953).
9 W. J. Merz, Phys. Rev. 76, 1221 (1949).
10 H. F. Kay and P. Vousden, Phil. Mag. 40, 1019 (1949).
11 V. L. Ginzburg, Uspekhi Fiz. Nauk 46, 348 (1952).
12 G. B. Dwight, *Tables of Integrals* IIL, 1949 (Russian translation)

Translated by Robert T. Beyer
218

SOVIET PHYSICS JETP VOLUME 4, NUMBER 6 JULY, 1957

The Method of Envelopes for Investigating Free Oscillations in Accelerators*

A. M. BALDIN, V. V. MIKHAILOV,* M. S. RABINOVICH
P. N. Lebedev Physical Institute, Academy of Sciences, USSR

(Submitted to JETP editor July 18, 1956)
J. Exptl. Theoret. Phys. (U.S.S.R.) 31, 993-1001 (December, 1956)

We present a derivation of the equation for free oscillations in accelerators with an arbitrary magnetic field having a plane of symmetry. To solve the basic problems of the theory of free oscillations, which arise in the design of accelerators, an envelope method has been developed in which the study of individual orbits is replaced by consideration of the envelope of the trajectory of the particles over a large number of revolutions. The application of the method is illustrated for accelerators with a sector magnet and for strong-focusing accelerators.

1. INTRODUCTION

In cyclic accelerators, the displacement of a particle from some average position is called a free oscillation. This average position of the particle is usually called the instantaneous orbit. The term "free" means that these oscillations are not directly connected with the process of acceleration. We can therefore consider the free oscillations in a constant magnetic field and for constant energy of the particle.

The fact that the free oscillations are independent of the acceleration process was demonstrated in the very first papers on the theory of cyclic accelerators. It was shown that with increasing magnetic field H (for a given configuration) the oscillation amplitude is damped like $H^{-1/4}$

The separation of the particle motion into a motion along the instantaneous orbit and free oscillations can be done uniquely in the absence of resonances. At resonance, the frequency of the free oscillations is integrally related to the frequency of revolution, so that the particle orbit is always closed. In this case the trajectory of the particle over a large number of revolutions does not fill an area, but merely traces out a line. (The plane area filled out by the orbit will be the subject of our investigation .) For practical purposes, because of the presence of all sorts of perturbations in the magnetic field, the acceleration process cannot proceed at resonance, since the amplitude of the free oscillations increases sharply. We shall exclude the resonance case from our further considerations

Free oscillations develop during the process of injection of particles, and also from scattering of particles by the residual gas in the accelerator chamber. One of the most difficult problems in constructing present-day ring accelerators (synchrotron, synchrophasotron) is the problem of achieving effective injection of particles, i.e., admission of particles into the chamber without colliding with the injector (inflector plates) and the walls of the vacuum chamber.

---

*The present paper is based on work$^{1-5}$ completed during the period 1950–1953.

*Deceased.

The essential point is that the efficiency of injection determines the intensity of the accelerated beam, since the loss of particles during the acceleration process is usually small. The geometrical dimensions of the accelerator. magnet gap determine all the other geometrical dimensions and the stability of the accelerator. The choice of dimensions is determined to a large extent by the need for achieving conditions for effective injection.

In recent years, various designs have been worked out for strong focusing accelerators. It is of interest to evaluate the efficiency of various types of strong-focusing accelerators. One comparison criterion might be the character of the free oscillation; other well-known criteria are the tolerances in magnet construction and field configuration.

The envelope method developed by us makes it possible, from a unified point of view, to describe the effect of free oscillations on the process of injection and acceleration in cyclic accelerators of any type.

2. EQUATIONS OF FREE OSCILLATIONS

We consider the free oscillations in an arbitrary magnetic field H having a plane of symmetry.

The motion of the particle in the magnetic field is described by the relativistic equation

$$\frac{d}{dt}\left(\frac{m\mathrm{v}}{\sqrt{1-v^2/c^2}}\right)=\frac{e}{c}\,[\mathrm{v}\times\mathrm{H}] \qquad (1)$$

If H does not depend on the time (as we can always assume in considering free oscillations), then |v|= const. From now on we shall express the velocity in the form v=vn, where n is a unit vector. Replacing differentiation with respect to the time t by derivatives with respect to σ, the distance along the trajectory, we get

$$\frac{mv}{\sqrt{1-v^2/c^2}}\,\frac{d\mathrm{n}}{d\sigma}=\frac{e}{c}\,[\mathrm{n}\times\mathrm{H}] \qquad (2)$$

We shall assume from now on that the field lines cut some plane at a constant angle. If the upper and lower poles of the magnet are mirror images, the median plane of the magnet will be such a plane. Of all the possible orbits, we select a closed (but otherwise, entirely arbitrary) orbit, lying in this plane. We call this orbit the equilibrium orbit. Of course, a more general formulation of the problem is possible with an arbitrary space curve as equilibrium orbit, but the simplification made above is sufficient for the purposes of accelerator technology. In this case Eq. (2) becomes very simple:

$$RH=\mathrm{const}, \qquad (3)$$

where R is the radius of curvature at a particular point where the magnetic field is H. We shall denote the curvature and magnetic field at each point of the equilibrium orbit by the subscript zero.

To study the deviation of the particular from the equilibrium orbit, we introduce curvilinear (in general, nonorthogonal) coordinates: σ is the length measured along the equilibrium trajectory, ρ is the distance along the normal to this trajectory. In these coordinates, the radius of curvature is:

$$\begin{aligned}\frac{1}{R}=\Big[-\rho''\left(1+\frac{\rho}{R_0}\right) & \qquad (4)\\ +2\rho'^2\frac{1}{R_0}-\rho' R_0'\frac{\rho}{R_0^2} & \\ +\frac{1}{R_0}\left(1+\frac{\rho}{R_0}\right)^2\Big] & \\ \times\left[\left(1+\frac{\rho}{R_0}\right)^2+\rho'^2\right]^{-3/2}, &\end{aligned}$$

where the primes denote differentiation with respect to σ.

Since the deviations of the particle from the equilibrium orbit are small, we can use a linear approximation for Eq. (4) and for the field strength $H(\sigma,\rho)$ as a function of ρ:

$$\frac{1}{R}=\frac{1}{R_0}-\rho''-\frac{\rho}{R_0}\,; \qquad (5)$$

$$H(\sigma,\rho)=H(\sigma,0)+\frac{\partial H}{\partial\rho}\,\rho.$$

After substitution of (5), Eq. (3) takes the form

$$\frac{1}{R_0}-\rho''-\frac{\rho}{R_0}=\mathrm{const}\left[H(\sigma,0)+\frac{\partial H}{\partial\rho}\,\rho\right].$$

By its definition, $1/R_0\,(\sigma)$ = const. $H(\sigma,0)$ along the equilibrium orbit, so that the equation for the free oscillations takes the following simple form:

$$\rho''+q(\sigma)\rho=0,\quad q(\sigma)=R_0^{-2}(\sigma)\,[1-n(\sigma)], \qquad (6)$$

where $n(\sigma)$ is the field index

$$n(\sigma) = -(R_0(\sigma) / H(\sigma, 0)) \qquad (7)$$

$$(\partial H(\sigma, \rho) / \partial \rho)_{\rho=0}.$$

3. SOLUTION OF THE EQUATIONS OF FREE OSCILLATIONS

The function $q(\sigma)$ is a periodic function of σ. In weak-focusing accelerators the period is equal to the perimeter Π of the orbit: $q(\sigma + \Pi) = q(\sigma)$. In strong-focusing accelerators and in accelerators with a sector magnet, the period of the function $q(\sigma)$ is $\Pi/N = L$, where N is the number of periodicity elements in the system. The general theory of equations with periodic coefficients can be applied to Eq. (6).

We write the solution of Eq. (6) in the stable region in the following form:

$$\rho(\sigma) = \operatorname{Re} D e^{i\mu\sigma/L} \varphi(\sigma), \qquad (8)$$

where $\varphi(\sigma)$ is a periodic function of σ with period L.

The characteristic exponent μ and the complex Floquet function $\varphi(\sigma)$ can be found for each specific case by an analytic method or by numerical integration over one of the sections of length L.* In addition, we note that the Wronskian of the complex solutions of Eq. (6):

$\Psi = e^{i\mu\sigma/L} \varphi(\sigma)$ and Ψ^*

$= e^{-i\mu\sigma/L} \varphi^*(\sigma)$ is $-2i$.

The solution of Eq. (8) can also be written in another more convenient form:

$$\rho(\sigma) = F(\sigma) \cos[\mu\sigma / L + \alpha(\sigma)], \qquad (9)$$

$$F(\sigma) = |D\varphi(\sigma)|; \; \alpha(\sigma) = \arg(D\varphi(\sigma)). \qquad (10)$$

Obviously $F(\sigma)$ and $\alpha(\sigma)$ are periodic functions with period L.

Thus the free oscillations can always be represented as sinusoidal, with variable amplitude $F(\sigma)$, phase $\alpha(\sigma)$ and frequency μ/L. However, this interpretation gives nothing new, since in most cases the frequency of variation of $F(\sigma)$ and $\alpha(\sigma)$ is greater than or of the same order as μ/L. It is therefore meaningless to regard the free oscillations as modulated harmonic oscillations, as has been done by some authors.[6]

In accelerator theory, when we investigate free oscillations we consider two problems: a) collisions of particles with the injector plates, and b) collision of particles with the walls of the vacuum chamber.

We consider a particle which leaves the injector at an angle γ to the instantaneous orbit and at a distance ρ_0 from it. If the displacement ρ at the injector azimuth σ_i on succeeding turns is greater than $\rho_0 - \Delta$, then the particle will collide with the injector plates. Here Δ is the distance from the point of emergence of the particle to the front plate of the injector (Figure 1).

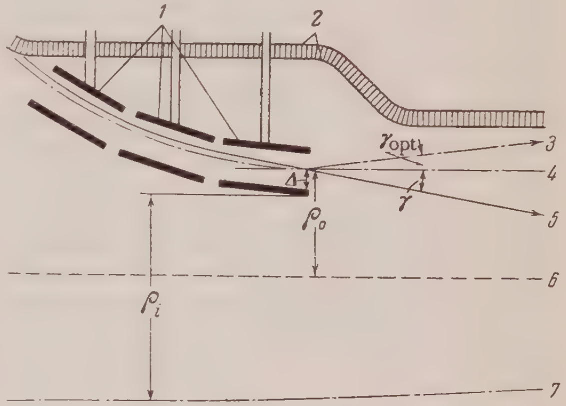

FIG. 1. Diagram of entry of particles into the acclerator. 1—injector plates, 2—chamber walls, 3—optimum direction, 4—direction tangent to the instantaneous orbit, 6—instantaneous equilibrium orbit, 7—mean orbit in the chamber.

For the solution of the problems formulated here, we need only know the deviation of the particle at some definite azimuth σ, in particular at the azimuth of the injector. Obviously the coordinates σ and $\sigma + \Pi k$ correspond to the same azimuth (Π is the perimeter of the orbit, and k is an integer). In this case, (9) can be rewritten as

$$\rho(\sigma) = F(\sigma) \cos(\mu N k + \alpha(\sigma)). \qquad (11)$$

Here σ is a fixed number, and k is the number of revolutions carried out by the particle; $\rho(\sigma)$ is the position of the particle at azimuth σ after the kth revolution. If k were a continuous variable, we could say that the oscillation of the particles at a given azimuth is always harmonic with a constant amplitude. When we change from one azimuth to another, only the amplitude and phase of the oscillation changes. Thus we have a situation analogous to that of standing waves, although, in our case, not only the amplitude but also the phase changes in space.

---

*For example, if we set $\Psi(0) = 1 + 1 \times 0$, then $\cos \mu = \operatorname{Re} \Psi(L)$.

Actually k can only take on integer values. If, for example, $N\mu$ were equal to $2\pi l/g$, where l and g are integers, then the displacement would take on g values at each azimuth. In practice, g must be sufficiently large so that no dangerous resonances arise; we may then assume that at any azimuth ρ takes on practically all values from $-F(\sigma)$ to $+F(\sigma)$.

We have been regarding $F(\sigma)$ as the amplitude of quasi-harmonic vibrations at azimuth σ. We can also consider the curve $\rho = \pm F(\sigma)$ to be the envelope of the particle trajectory. In fact, if $\rho(\sigma) = F(\sigma)$, then according to (9), $d\rho/d\sigma = dF/d\sigma$; i.e., the tangents to the particle trajectory (9) and to the curve $\rho = F(\sigma)$ coincide at azimuths where ρ is a maximum. From now on we shall call the curves $\rho = \pm F(\sigma)$ envelopes.

The trajectory of the particles is contained between the curves $\rho = \pm F(\sigma)$ and, in cases of practical interest, will fill the whole region between the envelopes after a large number of revolutions. Finding the envelope is much simpler than calculating the particle trajectories. At the same time, all the basic problems of accelerator theory which are related to the free oscillations can be solved if the envelope is known.

4. THE ENVELOPE

We shall find the expression for the square modulus of the function $F(\sigma)$ as a function of the initial conditions:

$$\sigma = \sigma_i; \quad \rho(\sigma_i) = \rho_0; \quad (d\rho/d\sigma)_{\sigma_i} = \gamma; \quad k = 0,$$

where σ_i is the azimuth of the injector, ρ_0 is the initial deviation of the particle from the orbit, and γ is the angle between the direction of emergence of the particle and the tangent to the instantaneous orbit (cf. Fig. 1). Substituting the initial conditions in (8), we get the value of the constant D

$$D^* = i\,[\gamma\Psi(\sigma_i) - \rho_0\Psi'(\sigma_i)]. \tag{12}$$

Here the prime denotes differentiation with respect to σ, and the asterisk denotes the complex conjugate:

$$F^2(\sigma) = DD^*\varphi(\sigma)\varphi^*(\sigma) = DD^*\Phi(\sigma), \tag{13}$$

where $\Phi(\sigma)$ is the square modulus of the Floquet function.

Substituting (12) in (13) and simplifying, we get

$$F^2(\sigma) = \frac{\Phi(\sigma)}{\Phi(\sigma_i)}\Big[\rho_0^2 + \Phi^2(\sigma_i)\Big(\gamma - \frac{\rho_0\Phi'(\sigma_i)}{2\Phi(\sigma_i)}\Big)^2\Big]. \tag{14}$$

In the usual weak–focusing accelerator, $\Phi(\sigma)$ has the constant value $R_0/\sqrt{1-n}$, where R_0 is the radius of curvature of the orbit and n is the field index. In this case,

$$F^2(\sigma) = \rho_0^2 + \frac{R_0^2\gamma^2}{1-n}. \tag{15}$$

If we are interested in the collisions with the injector plates, then it is essential to know by how much $F(\sigma)$ exceeds ρ_0 for a given angle of inclination γ; the smaller this excess, the less probable is a collision of the particles with the injector. Thus, the smaller $\Phi(\sigma_i)$ the greater the permissible deviation from the optimal angle [$\gamma = 0$, for equation (15)]; the stronger the focusing, the smaller $\Phi(\sigma)$.

The function $\Phi(\sigma)$ has the dimensions of a length, so that we may call the maximum value of $\Phi(\sigma)$ the effective radius of the accelerator

$$\max\Phi(\sigma) = R_{\text{eff}}. \tag{16}$$

We know that the gap dimensions determine the weight of the magnet, which is of prime importance for ultra–high energy accelerators. When comparing accelerators of different types, the ratio of the linear dimensions of the magnet gap to R_{eff} is a parameter which characterizes the maximum value of the focusing forces and the required accuracy of injection of particles into the accelerator chamber, whereas the ratio of these quantities to the radius of curvature R has no physical significance.

The minimum value of the oscillation amplitude at the azimuth of the injector is ρ_0, and occurs when the particle is injected at the optimum angle

$$\gamma = \gamma_{\mathrm{opt.}} = (\rho_0 / 2)\,(d \ln \Phi(\sigma) / d\sigma)_{\sigma_i}. \tag{17}$$

The direction of optimum entry of particles into the chamber of the accelerator coincides with the direction of the tangent to the envelope. An essential feature is that the optimum entrance angle depends on ρ_0. When injecting into a synchrophasotron, ρ_0 usually varies from zero to some maximum value, so that the optimum angle also varies. If the angular width of the injected beam is less than $\gamma_{\mathrm{opt.}}$, the number of particles captured for acceleration decreases markedly. It is true that one can find an azimuth at which $\Phi'(\sigma_i)=0$, but it is not always convenient for reasons of construction to place the injector plates at this azimuth.

To solve the problem of collision with the chamber walls, we have to study the function $f(\sigma)=\Phi(\sigma)/\Phi(\sigma_i)$ which gives the ratio of the oscillation amplitudes at an arbitrary azimuth σ and at the injector azimuth. The way this is done in practice will be shown in Secs. 5 and 6.

Up to now we have considered the radial oscillations. The vertical oscillations are treated similarly. We need only remember that in this case the quantity $q(\sigma)$ has the value

$$q(\sigma) = n(\sigma)\, R_0^{-2}(\sigma). \tag{18}$$

5. ACCELERATOR WITH SECTOR MAGNET

Synchrophasotrons with weak focusing are usually built with four straight sections. For example, in the 10 bev synchrophasotron of the Academy of Sciences of the USSR, there are four 8-meter straight sections. The average radius of the four magnet sectors is 28 meters. In Eq. (6), we can in first approximation set

$$q(\sigma) = \begin{cases} 0 & \text{in the straight sections of length } l, \\ \varkappa^2 = (\quad - n) / R_0^2 & \text{in the magnet sectors of length } \nu. \end{cases}$$

To find the envelope, it is sufficient to know the solution over a single periodicity element of length L

$$\Psi(\sigma) = \begin{cases} D(\sin \varkappa\sigma + d \cos \varkappa\sigma) & \text{in the magnet sectors} \\ D(e^{i\mu} \varkappa\sigma + s + dc_i) & \text{in the straight sections} \end{cases}$$

Here we have used the following abbreviations:

$$s = \sin \varkappa\nu; \quad c = \cos \varkappa\nu; \quad d = (c - e^{i\mu}) / s; \tag{19}$$
$$\cos \mu = c - \varkappa l s / 2.$$

In the formulas given above, the length σ is measured from the beginning of the sector, and from the beginning of the straight section, respectively.

As already noted, the constant D must be chosen* so that the Wronskian of the functions Ψ and Ψ^* is equal to $-2i$, so we require

$$DD^* = s / \varkappa \sin \mu. \tag{20}$$

From this it is easy to find the expression for the envelope

$$\Phi(\sigma) = \begin{cases} [s + \varkappa l \cos \varkappa\sigma \cdot \cos \varkappa(\nu - \sigma)] / \varkappa \sin \mu & \text{for magnet sectors} \\ [s + \varkappa l c + s\varkappa^2 (\sigma - l)\, \sigma] / \varkappa \sin \mu & \text{for straight sections} \end{cases} \tag{21}$$

For the data of the synchrophasotron of the Academy of Sciences of the USSR, the envelope is shown in Fig. 2. The function $\Phi(\sigma)$ is a maximum in the middle of the sectors and a minimum in the middle of the straight sections. From (21), it is easy to find the optimum angle of emergence of the particles from the acclerator chamber. For the parameters of the Soviet synchrophasotron, γ_{opt} is shown in Fig. 3.

For small lengths of straight sections, $\varkappa\Phi(\sigma)$ is of course not very different from unity, but this difference already affects the computation of the beam intensity[3] and the scattering by residual gas. The envelope is extremely important in the design of strong-focussing accelerators.

6. STRONG–FOCUSING ACCELERATORS

As an example, we consider a standard type of strong–focusing accelerators. To simplify the formulas, we shall treat an acclerator without straight sections. Of course, the general theory developed here can be applied to any type of accelerator with a constant or variable magnetic field.

Suppose that the accelerator consists of $2N$ magnets with the same lengths ν of arc with radius R_0 and with field index $n_1 < 0$ in the even sectors and $n_2 > 0$ in the odd sectors. At the end of the sectors, n changes abruptly from n_1 to n_2. If we are not designing a specific accelerator, but are interested in the characteristics of the motion, this assumption is not important. There is no difficulty in including straight sections or the transition region between n_1 and n_2. In our case,

---

*If $D = 1/d$, then $\Psi(0)=1$ and $\mathrm{Re}\,\Psi(L) = \cos\mu$ (cf. footnote on p.).

$$q(\sigma) = \begin{cases} \varkappa_1^2 = (1 - n_1)/R_0^2 & \text{for even sectors,} \\ -\varkappa_2^2 = (n_2 - 1)/R_0^2 & \text{for odd sectors.} \end{cases}$$

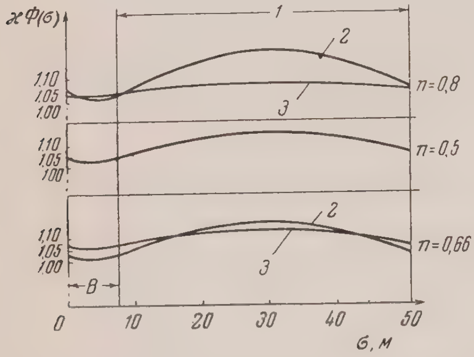

FIG. 2. Modulus of the Floquet function of the equation of free (vertical and radial) oscillations for the data of the synchrophasotron of the Academy of Sciences, USSR. *1*—circular sector, *2*—vertical oscillations, *3*—radial oscillations, straight section.

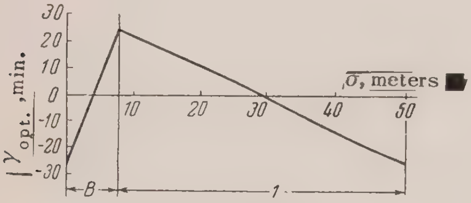

FIG. 3. Optimum angle γ_{opt} for the data of the synchrophasotron of the Academy of Sciences, USSR. $\rho_0/R = 1/56$; $l/R = 2/7$; *1*—circular sector, *B*—straight section.

Solving Eq. (1) by matching solutions, we find the complex solutions over a periodicity element of length $L=2\nu$:

$$\Psi(\sigma) = \sqrt{\frac{2}{\varkappa_1 (f - f^*)}}$$

$$\times \begin{cases} \sin \varkappa_1 \sigma + f \cos \varkappa_1 \sigma & \text{for even sectors.} \\ p(c - fs) \operatorname{sh} \varkappa_2 (\sigma - \nu) + (s + fc) \operatorname{ch} \varkappa_2 (\sigma - \nu) & \\ & \text{for odd sectors.} \end{cases}$$

The lengths are measured from the beginning of the focusing sector. Here we have used the following notation:

$$p = \varkappa_1 / \varkappa_2; \; s_1 = \sin \varkappa_1 \nu; \; c_1 = \cos \varkappa_1 \nu;$$

$$c_2 = \operatorname{ch} \varkappa_2 \nu; \; s_2 = \operatorname{sh} \varkappa_2 \nu,$$

while the function f is

$$f = f_1 - f_2 e^{i\mu}, \; f_1 = (s_1 s_2 + p c_1 c_2) / (p s_1 c_2 - c_1 s_2);$$

$$f_2 = p / (p s_1 c_2 - c_1 s_2).$$

It is easily verified that $\Psi(\sigma)$ satisfies Eq. (1) and the conditions given above if

$$\cos \mu = c_1 c_2 + (1 - p^2) s_1 s_2 / 2p.$$

We first find the expression for $\Phi(\sigma)$ in a focusing (even) sector

$$\Phi_1(\sigma) = \Phi(0) + [(1 + p^2) s_2 / 2\varkappa_1 p \sin \mu] \times [\cos \varkappa_1 (\nu - 2\sigma) - c_1], \tag{22}$$

$$\Phi(0) = (s_1 c_2 + p c_1 s_2) / \varkappa_1 \sin \mu. \tag{23}$$

The function $\Phi_1(\sigma)$ is a maximum in the middle of the focusing sector

$$\Phi_1(\nu/2) = \Phi(0) + (1 - c_1) \times (1 + p^2) s_2 / 2\varkappa_1 p \sin \mu. \tag{24}$$

We note that the function $\Phi(\sigma)$ is symmetric with respect to the point $\sigma = \nu/2$. For the defocusing sector

$$\Phi_2(\sigma) = \Phi(0) - [s_1 (1 + p^2) / 2\varkappa_1 \sin \mu] \times [c_2 - \operatorname{ch} \varkappa_2 (3\nu - 2\sigma)]. \tag{25}$$

As we see from this formula, $\Phi_2(\sigma)$ is a minimum at the middle of the defocusing sector.

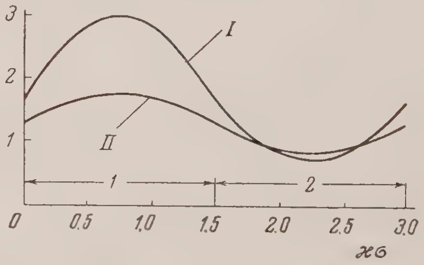

FIG. 4. Modulus of the Floquet function of the equation of free oscillations for a strong-focusing accelerator, at the center of the stability region ($\varkappa\nu = 1/5$; $n_1 + n_2 = 0$). *1* – focusing sector, *2* – defocusing sector; $\varkappa\sigma$ is the length along the orbit in dimensionless units. $\varkappa\nu = 1.5$; I – $\Phi(\sigma)/\nu$; II – $\sqrt{\Phi(\sigma)/\nu}$.

A graph of the dimensionless quantity $\Phi(\sigma)/\nu$ as a function of $\varkappa\sigma$ is shown in Fig. 4 for the case when $n_1 + n_2 = 0$ and $\varkappa\nu = 1.5$. With these parameters, the stability of the motion is a maximum. As abscissa in Fig. 4, we have used the dimensionless quantity $\varkappa\sigma$ in place of the length σ. The choice of such a scale enables one to use the graphs for different values of $\varkappa$.

In order to get a picture of the function $\Phi(\sigma)$ for values of $\varkappa\nu$ other than those corresponding to the center of the stability region, we show in Fig. 5 the dependence of the function $\Phi(\sigma)/\nu$ on $\varkappa^2\nu^2$ for three azimuths: the function $\Phi_1(\nu/2)/\nu$ at the middle of the focusing sector, the function $\Phi_2(3\nu/2)/\nu$ at the middle of the defocusing sector, and the function $\Phi(0)/\nu$ at the junction of the two sectors. As we see from Fig. 5, the stability remains practically constant over a wide range of variation of $\varkappa\nu$. As is well-known, rigid limits of tolerance on the value of $\varkappa\nu$ are not determined by the problem of stability in a given magnetic field, but rather by the presence of a large number of resonances with imperfections in the magnetic field. Obviously, for a strong-focusing accelerator

$$R_{\rm eff} = \Phi_1(\nu/2).$$

For example, for $n_1 + n_2 = 0$,

$$R_{\rm eff} = \nu 2\sqrt{3}\left(1+\frac{\varkappa^2\nu^2}{4}-\frac{\varkappa^4\nu^4}{80}+\dots\right) \qquad (26)$$

$$\div\ \varkappa^2\nu^2\sqrt{1-\varkappa^4\nu^4/12+\dots}\,.$$

The minimum value of $\Phi_1(\nu/2)/\nu$ (as a function of $\varkappa\nu$) can be found from Fig. 5 or Eq. (26). It is equal to 3.026 (for $\varkappa\nu \approx 1.5$). Thus the optimum value $R_{\rm eff}^{\rm opt}$ is

$$R_{\rm eff}^{\rm opt} \approx 3\nu = 3R_0\,\delta, \qquad (27)$$

where δ is the length of a sector in radians.

The two figures (6 and 7) are constructed similarly to Figs. 4 and 5, for the logarithmic derivative of $\Phi(\sigma)$, which is proportional to $\gamma_{\rm opt.}$, the optimum angle of emergence of the particle from the injector.

Figure 6 shows a graph of the function

$$(R/\varkappa\nu)\, d\ln\Phi(\sigma)/d\sigma = 2R\gamma_{\rm opt.}/\varkappa\nu\rho_0$$

for $\varkappa\nu = 1.5$, as a function of $\varkappa\sigma$. (ρ_0 is the distance from the injector to the instantaneous orbit.)

In Fig. 7 the same function is shown plotted against $\varkappa^2\nu^2$ for a fixed value of $\varkappa\sigma$ (at the junction of focusing and defocusing **sectors**, where $\gamma_{\rm opt}$ takes on its maximum value). At the center of the stability region, $\gamma_{\rm opt} \approx 0.6\,\rho_0/R$. The change of the optimum angle with time (which accompanies the change of ρ_0) leads to additional difficulties for multi-turn injection into strong-focusing accelerators.

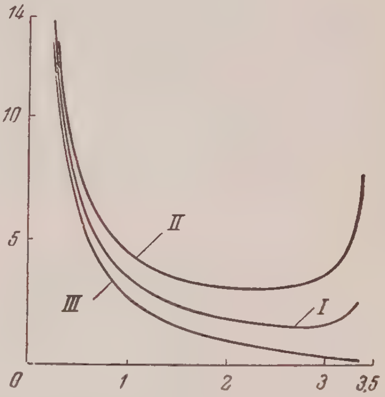

FIG. 5. Values of the modulus of the Floquet function at the centers of focusing and defocusing sectors ($\Phi_1(\nu/2)$ and $\Phi_2(3\nu/2)$, and between sectors ($\Phi(0)$, as a function of the parameter of focusing strength $\varkappa^2\nu^2$. ($n_1 + n_1 = 0$). The ordinates are I–$\Phi(0)/\nu$; II–$\Phi_1(\nu/2)/\nu$; III–$\Phi_2(3\nu/2)/\nu$. The abscissa is $\varkappa^2\nu^2$.

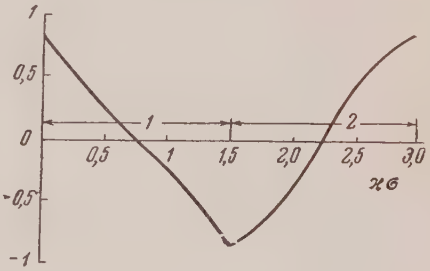

FIG. 6. Dependence of optimum angle on azimuth for strong-focusing accelerators, at the center of the stability region ($\varkappa\nu = 1.5$, $n_1 + n_2 = 0$). 1–focusing sector, 2–defocusing sector, $\varkappa\sigma$ is the length along the orbit in dimensionless units. The solid curve is $(R/\varkappa\nu)\, d \times \ln\Phi(\sigma)/d\sigma = (2R/\varkappa\nu\rho_0)\gamma_{\rm opt}$.

The general theory developed here and the examples considered show that the method of envelopes is entirely adequate for the problems arising in the computation and design of different types of

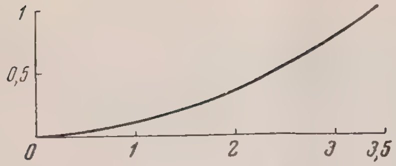

FIG. 7. Dependence of optimum angle on accelerator parameter $\varkappa^2 \nu^2$ ($n_1 + n_2 = 0$) for injector located between sectors. The ordinates are $(2R/\varkappa\nu\rho_0)\,\gamma_{\rm opt}$. The abscissa is $\varkappa^2 \nu^2$.

accelerators. By means of this method one can easily compare the focusing of different types of accelerators and solve the problems associated with the achievement of maximum efficiency of injection.

1 Baldin, Mikhailov and Rabinovich, *Investigation of particle motion in a synchrophasotron with straight sections;* Reports of Phys. Inst. Acad. Sci. USSR, 1949.

2 Baldin, Mikhailov and Rabinovich, *On the theory of free oscillations;* Reports of Phys. Inst. Acad. Sci. USSR, 1950.

3 M. S. Rabinovich, *Fundamentals of the theory of the synchrophasotron;* Dissertation, Phys. Inst. Acad. Sci. USSR 1952.

4 A. M. Baldin and V. V. Mikhailov. *Almost-periodic motion of charged particles in an arbitrary constant magnetic field;* Reports of Phys. Inst. Acad. Sci. USSR, 1952.

5 M. S. Rabinovich, *Theoretical Investigation of accelerators with variable field index;* Reports of Phys. Inst. Acad. Sci. USSR, 1953.

6 D. M. Dennison and T. H. Berlin, Phys. Rev. 70, 764 (1946).

Translated by M. Hamermesh
213

SOVIET PHYSICS JETP VOLUME 4, NUMBER 6 JULY, 1957

Interaction of 230–250 mev Negative π-Mesons with Carbon and Lead Nuclei

V. P. DZHELEPOV, V. G. IVANOV, M. S. KOZODAEV,
V. T. OSIPENKOV, N. I. PETROV AND V. A. RUSAKOV
Institute for Nuclear Problems, Academy of Science, USSR

(Submitted to JETP editor, July 17, 1956)
J. Exptl. Theoret. Phys. (U.S.S.R.) 31, 923-931 (December, 1956)

The interaction of 230–250 mev negative pions with carbon and lead nuclei was investigated by the method of the Wilson chamber in a magnetic field. The total and differential cross sections for both elastic and inelastic scattering were determined, as well as the total cross section for all the inelastic scattering processes. Within the experimental errors, the elastic scattering is in agreement with the diffraction pattern of an opaque nucleus. The energy spectrum of the scattered pions shows that the major part of the inelastic scattering between 60° and 180° is due to the collisions of the incoming pions with single nucleons in the nucleus.

THE most complete data on the different interaction processes of pions with complex nuclei have been obtained in experiments with thick layer photo-emulsions and Wilson chambers. Most data correspond to an energy range from 30 to 150 mev; there have been only a few experiments done for nuclei in emulsion[1–3] at higher energies, and a single experiment for the helium nucleus[4] at higher energy.

The present work has been carried out on the synchrocyclotron of the Institute of Nuclear Problems of the USSR Academy of Sciences. The interaction of 230–250 mev pions with carbon and lead nuclei was investigated by the method of a Wilson chamber in a magnetic field.

EXPERIMENTAL ARRANGEMENT AND METHOD OF PROCESSING THE PHOTOGRAPHS*

The experimental arrangement is shown schematically on Fig. 1. The source of negative pions was a graphite target placed inside the accelerator in the circulating beam of 670 mev protons. The 230–250 mev pions ejected from the target in the forward direction were directed by a four meter collimator and by a deflecting magnet on the Wilson chamber; the Wilson chamber had a diameter of 400 mm and was placed behind a concrete shield.** The sample plate was placed in the center of the chamber, at an angle of 90° with the incoming pion beam. In the case of graphite, the thickness of the plate was 4.29 gm/cm^2, in the case of lead it was 4.6 gm/cm^2.

---

*A detailed description of the experimental arrangement is given in Ref. 5.

The chamber was placed in the 10^4 uniform magnetic field produced by the electromagnet-solenoid. The amount of non-uniform field did not exceed 3%. The chamber was synchronized with the acclerator in the so-called "single-burst" state. During the working cycle of the chamber, which lasted for 1.5 min, the accelerator emitted only a single burst at the moment when the widening was concluded in the chamber. The magnetic field was increased to its nominal value only forthe time necessary for the action ofthe chamber.

The photograph ofthe tracks was taken by a stereocamara from a distance of 1,000 mm on a negative panchromatic film of 800–1,000 GOST units. The stereocamera had a base of 120 mm and a diameter of 24 mm. The photographs were processed on a reprojector and a stereocomparator designed for the stereocamera used.

In the computing ofthe total flux of impinging pions, only such tracks were taken into account a) which intersected the plate at a point not less than 10 mm away from its edges, b) which entered the plate at an angle of 90 ± 10°, and c) which were bright enough to enable one to measure them on a projector and on the stereocomparator. All the tracks chosen according to the above criteria were subjected to the following measurements: measurement of the magnetic curvature, and measurement of the height-with respect to a small rod in the plate- and of the coordinates of the point in the plate where a nuclear interaction took place. In the case of nuclear interactions, the curvatures and the emission angles of the scattered pions and secondary particles were also measured. The average error in the angular measurements was 1–2°. The error in the measurement of the radius of curvature of the incoming pions (taking into account the curvature due to multiple Coulomb scattering of the particles in the chamber gas and to the motion of the gas) was of 6–7%. The usual classification of nuclear interactions was used: star (stop), elastic scattering, inelastic scattering and radiative absorption (exchange scattering). The cases of elastic and inelastic scattering were differentiated according to the magnitude of the energy release: if the energy release in the scattering was less than 45 mev, the scattering was considered elastic; if the energy release in the scattering was greater or equal to 45 mev. the scattering was considered inelastic. The magnitude of this limiting release was determined by the average error in the determination of the meson energy difference before and after scattering.

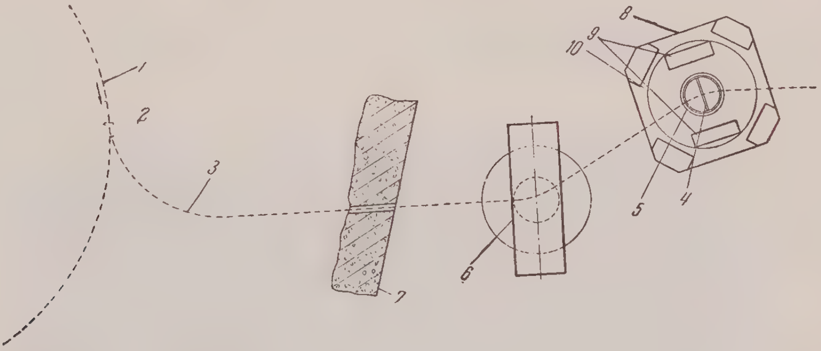

FIG. 1. Experimental arrangement: *1*—circulating proton beam; *2*—target; *3*—π-—meson beam; *4*—target; *5*—Wilson chamber; *6*—deflecting magnet; *7*—shield; *8*—magnet.sollenoid; *9*—scintillators; *10*—sollenoid coil.

Geometry corrections were made on all the measurements of elastic and inelastic scattering. The scanning of the photoplates, the measurements of the tracks and the identification of the nuclear interaction events were performed independently by two observers. The value of the total flux of particles impinging on the plate was obtained by taking the average of the results ofthe two independent calculations. In the calculation of the cross sections, the errors on the determination of the total meson flux and on the differentiation between cases of elastic and inelastic scattering were taken into account, in addition to the statistical deviations.

**The number of μ-mesons and electrons mixed to the beam was 12.5 ±3% ofthe total number of particles.

EXPERIMENTAL RESULTS

During the exposure time of the camera to the negative pion beam, a total of 6,000 photographs were taken; they recorded 760 events of pion interaction with carbon and 629 events of interaction with lead. A few examples of nuclear interactions are given in Figs. 2 and 3.

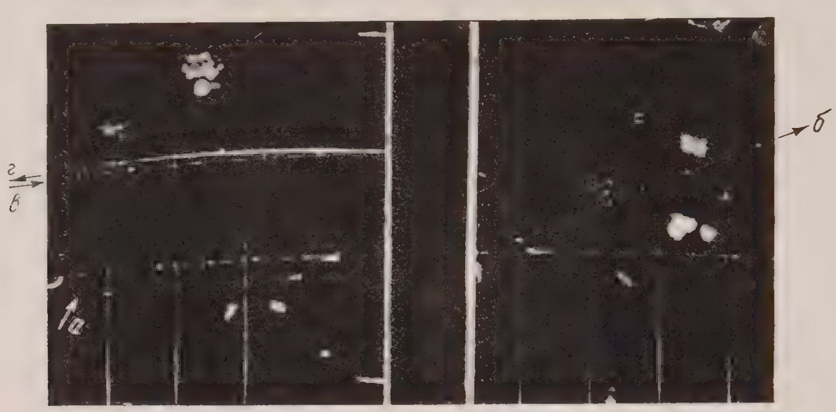

FIG. 2. Elastic scattering of the π^--meson: *a*—incident π^--meson, *b*—scattered π^--meson; 2—star: *c*—incident π^--meson, *d*—proton

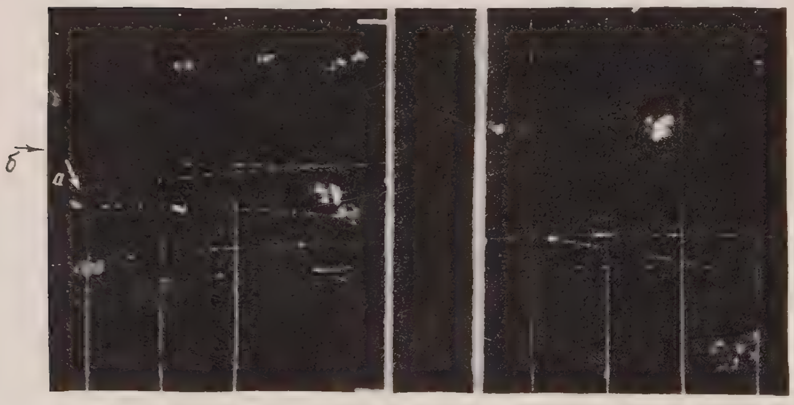

FIG. 3. Inelastic scattering of the π-meson: *a*—incident π^--meson; *b*—scattered π^--meson.

The analysis of these data gives, for carbon and lead nuclei, a) the total and differential cross sections for elastic scattering at angles between 10 and 180° ; b) the total and differential cross sections for inelastic scattering; c) the total cross section for all the inelastic interaction processes. All the measured cross sections for carbon nuclei refer to the energy of 230 ± 30 mev; for lead nuclei— to the energy of 250 ± 30 mev.

A. ELASTIC SCATTERING

Under the conditions of the present experiment, the elastic scattering of pions by C and Pb nuclei at small angles is determined mainly by the multiple and single Coulomb scattering; it is only for angles greater than 10–15° that the scattering has practically a nuclear character. The total elastic scattering of pions by C and Pb nuclei measured in the indicated angular interval (from 10 to 180°) is given in Tabel I.

The measured angular distribution for elastic scattering is shown in Fig. 4. For the carbon nuclei, the graph also shows a plot of the angular distribution computed for the optical model with a uniform distribution of the nuclear matter inside a

TABLE I.

Total cross section (in units of 10^{-27}cm^2)

Element	Elastic scattering at $\theta > 10°$	Inelastic scattering $\Delta E \geq 45$ mev	Stars and Stops	Total inelastic interaction cross section	Geometric cross section
C	200 ± 32	90 ± 15	217 ± 26	307 ± 37	325
Pb	329 ± 53	555 ± 83	1600 ± 160	2153 ± 194	2150

sphere of radius $R = 1.4\,A^{1/3} \times 10^{13} = 3.2 \times 10^{-13}$ cm and with the following values of the coefficient K of pion absorption in the matter and of the real part of the potential:

Curve	K (in units of 10^{-13} cm)	V (in mev)
A	∞	0
B	0.79	+32[3]
C	0.79	0

In the cases B and C, the value of the absorption coefficient is determined (as in Ref. 6) from the value of the total cross section for 230 mev pion interaction with free neutrons and protons, according to the formula $K = 1/2\,(\sigma_{\pi,p} + \sigma_{\pi,n})\,A/4/3\,\pi R^3$, where R is the radius of the carbon nucleus. The comparison of the experimental and theoretical distribution shows that the inelastic scattering of 230 mev pions by carbon nuclei is described satisfactorily by the optical model. However, the experimental cross sections are determined with a large error and the shape of the angular distribution for a large pion absorption in the nucleus depends only weakly on the magnitude of the real part of the complex potential, and the experimental data fit the diffraction scattering by an opaque nucleus as well as the elastic scattering described by the curves B and C.

The total cross section at the angles $\theta > 10°$ is equal to 219×10^{-27} cm^2 and to 193×10^{-27} cm^2 for the cases B and C, respectively. The total inelastic cross section is 300×10^{-27} cm^2 in these cases.

As Table I shows, the experimental total cross sections are in agreement with the total cross sections computed for the optical model. It can be concluded that, for an absorption coefficient $K = 0.79 \times 10^{13}$ cm^{-1}, the real part of the complex potential is bound by the limits 0 and 30–40 mev.

B. INELASTIC SCATTERING

The experimental data on inelastic scattering are obtained in the entire interval of scattering angles, excluding the range from 0 to 10° for lead, in which region the inelastic scattering cases cannot be identified reliably because of the large number of single electrons. The total experimental cross sections for inelastic scattering are listed in Tabel I, and the angular distributions of inelastic scattering are plotted on Fig. 5. The anisotropy of the scattering with a prevailing forward and backward peaking is a characteristic property of these angular distributions; the same is also observed in the scattering of pions by free nucleons at the same energy.

The authors of a series of papers[1-4, 7-11] conclude (from the measured energy release in inelastic scattering, and from the investigations of the energetic dependence of the total cross section for pion nucleus interaction)—that the interaction of pions with complex nuclei is a result of their quasi-elastic scattering by single nucleons in the nucleus. The data from the present work confirm this conclusion.

As Fig. 6 shows, the mean energy loss of pions in inelastic scatterings by carbon and lead nuclei are 135 and 150 mev respectively, which is 60% of the original pion energy. Such large values for the energy transferred in inelastic scattering cannot be explained on the basis of a mechanism where pions transfer energy to several nucleons in a single collision event. Another experimental fact— the equality of the mean energy of pions scattered inelastically by carbon and lead nuclei, which nuclei

---

*This value is equal to the one computed[6] from the scattering amplitudes in the forward direction of 230 mev pions by free nucleons.

differ in size—forces the assumption that the observed inelastic scattering is, apparently, the result of a small number of pion collisions with single nucleons in the nucleus. This assumption is confirmed by the existence of a correlation between the scattering angle and the energy release, in the scattering angle range between 60 and 180°.

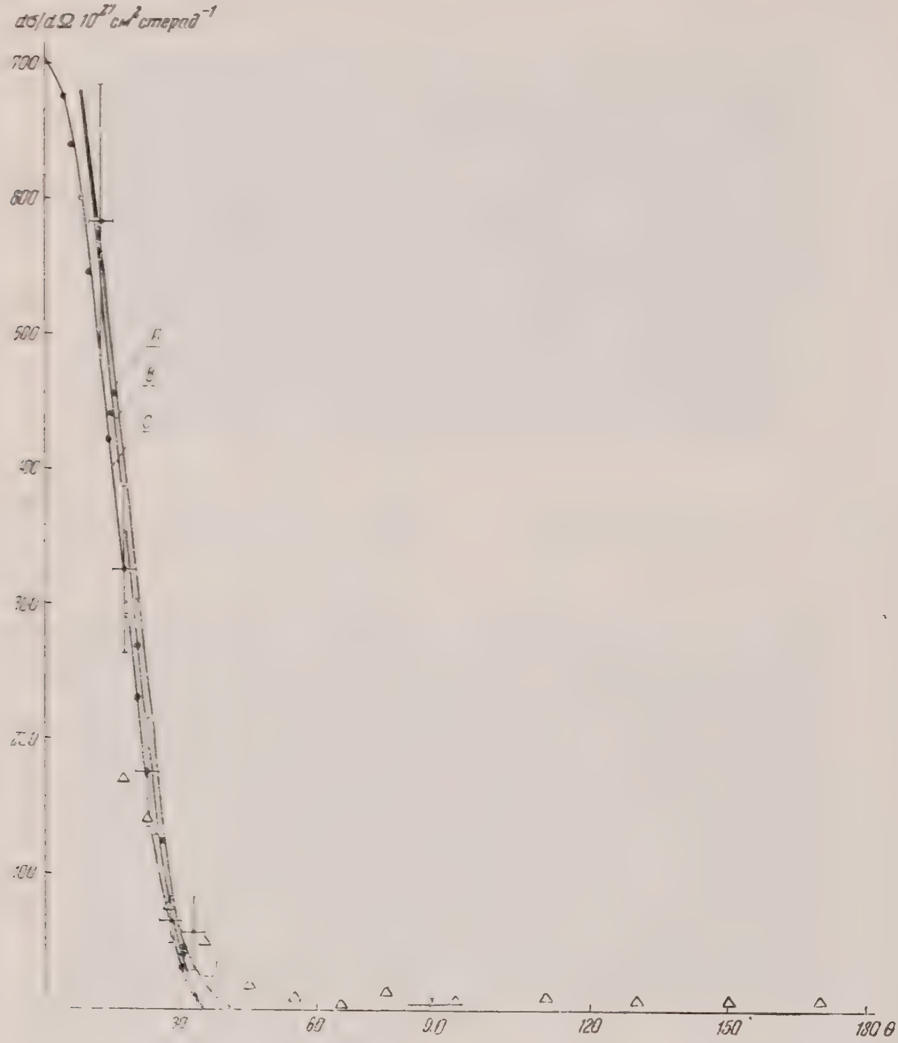

FIG. 4a. Angular distribution of the cross section for π⁻-meson elastic scattering by carbon nuclei; Δ—elastic scattering of 125 mev π⁻-mesons according to Ref. 2.

Table II shows the ratio of the calculated energy release (for a single pion scattering by a free nucleon, averaged over three angular intervals) to the observed energy release. It can be seen from the Table that, in the cases of carbon and lead, these ratios for the angular intervals of 120–180° and 60–120° are close to unity and are 3 to 4 times larger than the corresponding ratio for the angular interval of 0 to 60°. Such a large difference cannot be explained by the experimental errors and by the unsufficient statistics of the number of cases of pion inelastic scatterings used in the determination of these ratios. On the other hand, the mentioned ratios could not have been substantially overestimated because, in their calculation, the relatively small contribution of such scattering cases in which the slowly scattering mesons were stopped in the plate due to ionization were not taken into account.*

---

*It was found in Ref. 3—which reports on the interaction of 210 mev pions with nuclei in emulsion—that the relative number of scattered pions with energies between 0 and 40 mev is 6%.

TABLE II.

Element	π-meson energy mev	Angular interval, in degrees	Ratio of calculated to observed energy releases	Number of scattering events
C	230	0—60 60—120 120—180	23 77 99	20 14 35
Pb	250	0—60 60—120 120—180	22 85 87	16 10 28
Emulsion nuclei	500	0—60 60—120 120—180	61* 63 —	37 42 —

*The data for the emulsion nuclei is taken from Ref. 1.

The mean free path of pions with a mean energy of 230–250 mev for interaction with nuclear matter being of 1.2×10^{-13} cm, the nucleons mostly responsible for the inelastic scattering of pions are in the surface layer of the nucleus. This conclusion is confirmed by the proportionality between the experimental inelastic scattering total cross sections and the geometrical nuclear cross secrions (cf. Table I, columns 3 and 6, and Table III).

TABLE III.

Element	Meson energy mev	Ratio of total inelastic scattering cross section to geometric cross section, in %
C	230	30
Emulsion nuclei	250 210	26 25—31*

*The data is taken from Ref. 3

It should be noted that this agreement between the cross sections for C and Pb nuclei improves if one computes the data relative to the scattering angles interval between 60 and 180°. It is easy to understand that such a picture for the inelastic scattering of pions by complex nuclei will be observed only for the energy range for which the pion mean free path for the second collision inside the nucleus is considerably larger than the mean free path for the first collision, i.e, for the energy range corresponding to the position of the maximum of the curve of the cross section of pions by free nucleons vs. energy. Indeed, (see Table II), the ratios of calculated to measured energy releases for all three angular intervals are already equal. when pions have an energy of 500 mev.

The observed angular distribution of inelastically scattered pions are apparently conditioned by two facts: the shape of the angular distribution of pions scattered by free nucleons and by the character of the absorption process of pions by the nuclear matter. In particular, it follows from the experimental data that about 70–75% of the pions scattered in the backward hemisphere in the first collision are absorbed by the nuclear nucleons. The absorption probability will apparently rise with the distance between the collision point and the nuclear surface. As it has been shown[8], this distance increases on the average, as the trajectory of the scattered pions deflects form the backward direction. Therefore, the observed decrease of the cross section in the angular interval between 180 and 90° can be explained qualitatively by the following two reasons: decrease of the pion scattering by nucleons as the scattering angle is changed from 180 to 90° and increase of the pion absorption effect after the first collision, for this scattering angle range.

C. TOTAL CROSS SECTION FOR INELASTIC INTERACTION PROCESSES

The main process of 230–250 mev inelastic interaction with complex nuclei is the absorption process, which finally leads to star formation (and stops). For carbon nuclei, the ratio between the number of stars and the number of stops (corrected for ionization absorption of protons in the plate) is one to one. If one assumes that the observed stops correspond to events of pion absorption by (p–n) pairs and if one takes into consideration that the number of stops decreases because of nucleon cascades from pion-nucleon collisions prior to the absorption and from pion capture, than one can conclude that the mentioned ratio is not in disagreement with the assumption that such a mechanism is predominantly responsible for pion absorption by nuclear matter at 230–250 mev, as well as at lower energies. The total cross sections for all inelastic interaction processes of pions with C and Pb nuclei (cf. Table I) are, within experimental errors, equal to the geometrical nuclear cross sections and the cross sections[7] for 125 mev pions. This is in agreement with the data from Ref. 9 and 12; it is shown in these papers that the total cross section for inelastic interaction of pions with complex nuclei does not practically change with energy in the energy range from 100 to 240 mev.

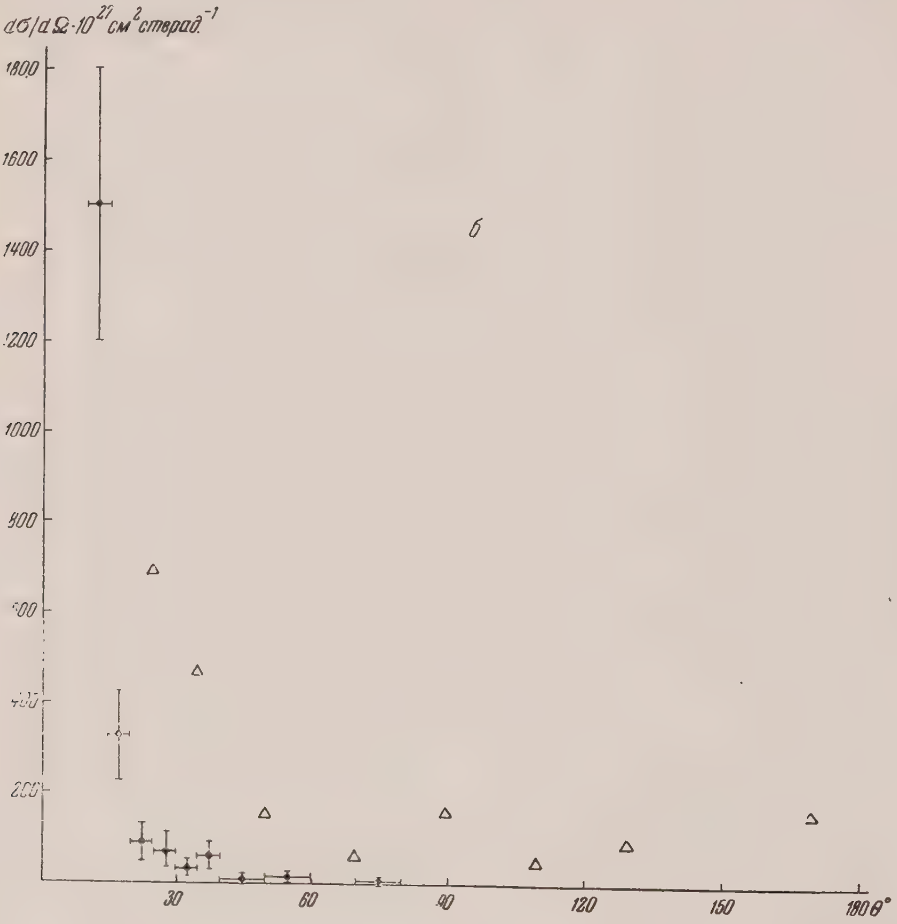

FIG. 4b. Angular distribution of the cross section for π^-—meson elastic scattering by lead nuclei, Δ—elastic scattering of 225 mev π^-—mesons according to Ref. 2.

CONCLUSION

The investigation of the different interaction processes of 230–250 mev negative pions with carbon and lead nuclei gave the following results:

1. The observed distributions and total elastic cross sections for pions at $\theta > 10^\circ$ as well as the total inelastic interaction cross section can be described on the basis of an optical model for the interaction of pions with complex nuclei. For an absorption coefficient $K = 0.79 \times 10^{13}$ cm^{-1}, the real part of the complex potential is bound by the limits 0 and 30–40 mev.

2. The inelastic scattering in the scattering angle interval between 10 and 180° is mostly produced as a result of single collisions between the impinging pions with single nuclear nucleons. One can think that the situation can be taken advantage of in the future for the investigation of the momentum distribution of the nuclear nucleons.

3. The pion absorption in the nuclear matter is

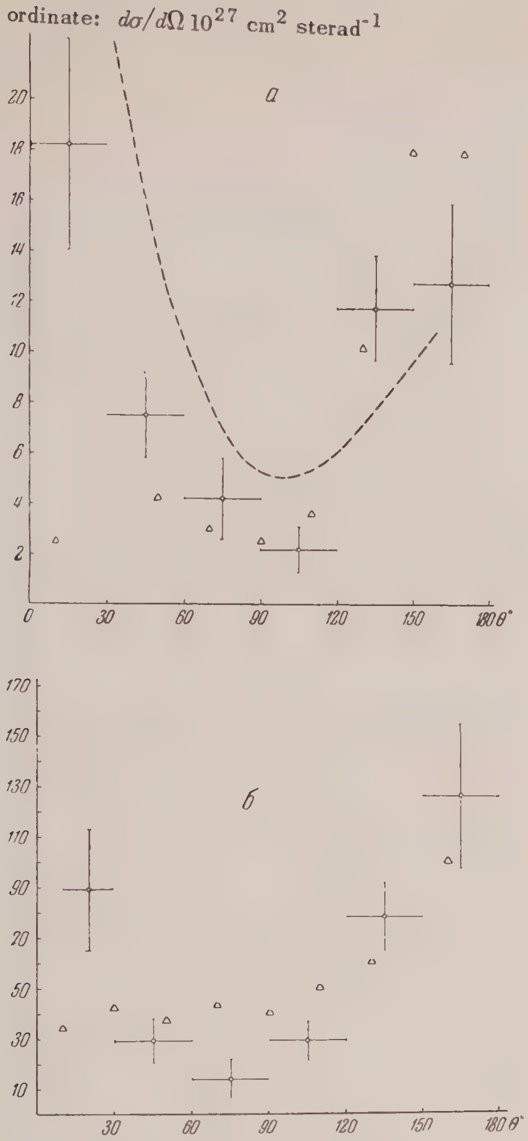

FIG. 5(a,b). π^-—meson inelastic scattering angular distribution: a—by carbon nuclei, b—by lead nuclei. Dotted line—angular distribution of the π^+—meson—proton elastic scattering at 240 mev; Δ—inelastic π^-—meson scattering at 125 mev.[2]

apparently primarily due to their capture by p—n pairs of nuclear nucleons (as in the case of lower energy).

5. The total pion cross sections for inelastic interaction processes are equal to the geometric cross sections.

The authors express their gratitude to Iu. A. Budagov for his help in the data processing and to L. A. Kuliuna, I. V. Popova and G. N. Tertukova who took part in some of the calulations.

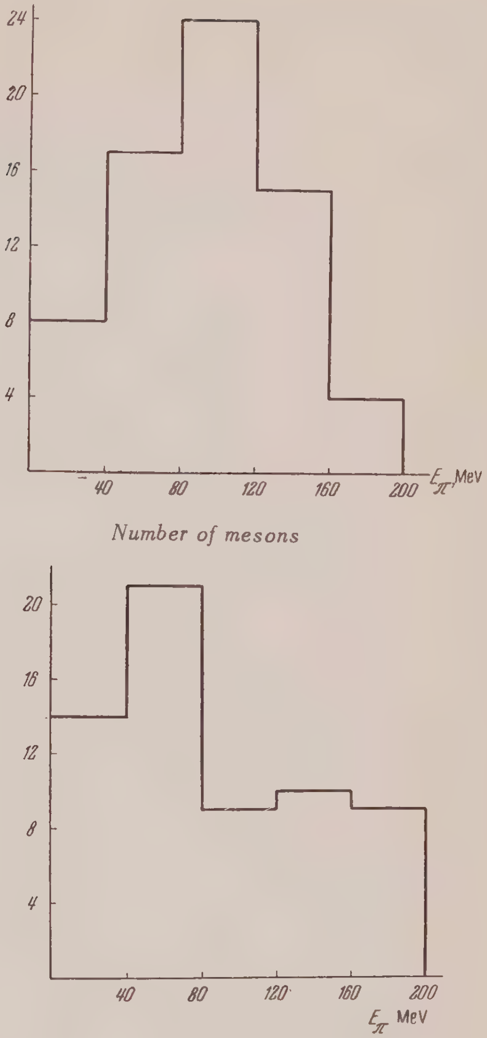

FIG. 6(a,b). π^-—meson inelastic scattering energy distribution: a—on carbon nuclei, $E_{cp} = 95$ mev; b—on lead nuclei, $E_{cp} = 101$ mev.

---

[1] M. Blau and M. Caulton, Phys. Rev. 96, 150 (1954).

[2] W. F. Fray, Phys. Rev. 93, 845 (1954).

[3] A. Morrish, Phil. Mag 45, 47 (1954).

[4] Kozodaev, Suliaev, Filippov and Shcherbakov, J. Exptl. Theoret. Phys. (U.S.S.R.) 31, 701 (1956); Soviet Phys. JETP 4, 580 (1957).

[5] Dzhelepov, Kozodaev, Osipenkov, Petrov and Rusakov PTE 3, 3 (1956).

[6] R. M. Sternheimer, Phys. Rev. 101, 384 (1956).

[7] J. O. Kessler and L. M. Lederman, Phys. Rev. 94, 689 (1954).

[8] G. Takeda, Phys. Rev. 93,848 (1954).

[9] Ignatenko, Mukhin, Ozerov and Pontecorvo, Report of the Institute for Nuclear Problems, Acad. of Sciences USSR (1955).

[10] N. A. Mitin and E. L. Grigoriev, Dokl. Akad. Nauk SSSR 103, 219 (1955).

[11] Bernardini, Booth and Lederman, Phys. Rev. 83, 1075 (1951). G. Bernardini and I. Levy, Phys. Rev. 84, 610 (1951).

[12] Grigoriev, Osipenkov, Petrov and Rusakov, J. Exptl. Theoret. Phys. (U.S.S.R.) 31, 1097 (1956); Soviet Phys. JETP 4, 922 (1957).

Translated by E. S. Troubetzkoy
203

SOVIET PHYSICS JETP VOLUME 4, NUMBER 6 JULY,1957

Interaction of 5–50 bev Cosmic Ray Particles with Be Nuclei. I

N. G. Birger, N. L. Grigorov, V. V. Guseva, G. B. Zhdanov,
S. A. Slavatinskii and G. M. Stashkov
P. N. Lebedev Physical Institute, Academy of Sciences, USSR

(Submitted to JETP editor July 21, 1956)
J. Exptl. Theoret. Phys. (U.S.S.R.) 31, 971–981 (December, 1956)

Meson production by cosmic ray particles with energy 5–50 bev was investigated in a cloud chamber containing a 9.8 gm/cm^2 Be plate under conditions closely approximating nucleon-nucleon interaction. Eleven interactions involving formation of four or more secondary charged particles are analyzed in detail. The angular distribution of pions and nucleons in the center-of-mass system of the two colliding nucleons was obtained, as well as the energy distribution of the energy of the primary particle among the various secondary particles.

THE character of nucleon–nucleon interactions can be conveniently studied today up to energies ~ 5 bev[1] by means of artificially accelerated particles. For the study of the interaction at higher energies, we must make use of cosmic ray particles. Here, however, the situation is complicated by the low intensity of cosmic radiation and by indefiniteness in the energy determination. The low intensity does not permit us to obtain direct evidence on nucleon–nucleon interaction by irradiating hydrogen with cosmic ray particles. The analysis of large experimental material, obtained in the irradiation of nuclei of heavy atoms (photoplates) by cosmic rays, can give only indirect evidence on the nucleon–nucleon interactions of high energy.

1. APPARATUS

The purpose of our research was the investigation of meson generation by cosmic ray particles with energies in excess of 5 bev under conditions that are close to nucleon–nucleon collisions. We used a Wilson cloud chamber, which contained a plate of Be of thickness 9.8 gm/cm^2 (for 100 hours of the research, a graphite plate was used inside the chamber in place of the beryllium). The Wilson chamber, of diameter 30 cm and depth of irradiated region 8 cm, was placed in the magnetic field of an electromagnet of average magnetic field 8500 Oe. Control of the chamber was maintained by a system of counters located as shown in Fig. 1. Coincidence discharges were recorded in the counters of groups 1,2,3 (combined in parallel) and in any two counters of the groups 4 and 5 in the absence of discharges in the counters of group *A*. A lead filter was placed over the entire apparatus, to diminish the background of the electron component. The work was carried out at an altitude of 3860 m above sea level (Pamir Scientific Station). The total research time with the apparatus, after deduction of the dead time of the chamber (2 min) was equal to 950 hours. In this time about 5300 photographs were obtained.

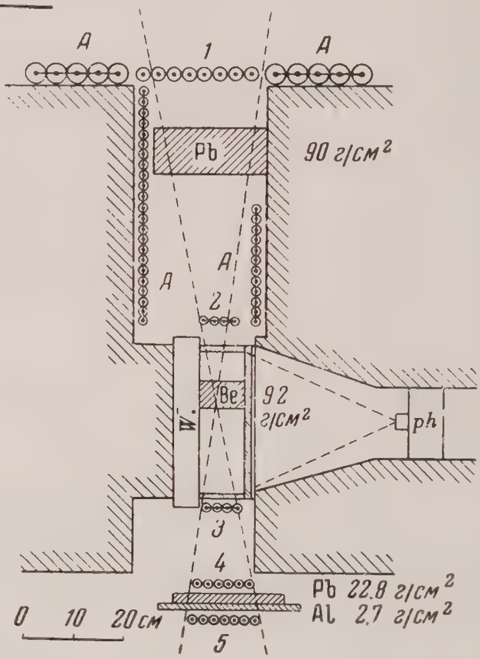

FIG. 1. Experimental scheme: *ph*—photographic apparatus; *W*—Wilson chamber.

In 31 photographs there were electron–nuclear showers of four and more particles, formed in Be or C inside the chamber. Showers with a smaller number of particles (2,3 secondary particles) were observed in about 10 cases. The discrimination of showers of a small number of particles was determined by a system of control counters. Comparison of the number of observed showers, formed in Be, with the number of expected showers which ought to be produced by nucleons with energies $\geq$ 5 bev (minimum value of the energy of nucleons which form the observed shower, see Table III, below), shows that the events which are separated by the apparatus amount to about 10% of all cases of interaction with atomic nuclei of nucleons having energies $\geq$5 bev. This points to the fact that showers of a small number of particles are formed in a large number of interactions at these energies.

Below we shall consider the characteristics of such interactions which lead to the emission of not less than four secondary particles. Here we selected only those showers for which it proved possible to measure the momenta of the majority of secondary particles. In such showers, we measured the spatial angles which are formed by secondary particles with the direction of motion of the primary particle, and the momenta of the secondary particles. The error in the measurement of the three-dimensional angles did not exceed 1.5°; the maximum measured momentum for tracks of particles with track length ~8 cm was 3.7 bev/c.

2. SHOWERS FROM $n_s \geq 4$ SECONDARY PARTICLES

Data are given in Table I for showers with an equal number of secondary particles, formed in beryllium and graphite plates in the chamber during the entire time of operation of the apparatus.

The numbers in parentheses denote the number of showers for which quantitative measurements of momenta and angles of most of the secondary particles was impossible, either because of their position inside the chamber, or because of the poor quality of the photographs. Data on the angles of emission of the particles relative to the direction of motion of the generating particle, θ, momenta p and ionization I of the secondary particles in the case of "excellent" showers are given in Table II. As a footnote, we mark the presence in the volume of the chamber of other rapid charged particles, in addition to the shower particles. These arrive in the chamber simultaneously with the shower-forming particles. In Figs. 2 and 3 (inset), there are shown two showers as examples, Nos. 43.27 and 95.87.

3. THE ENERGY OF THE SHOWER GENERATING PARTICLES

The experimental characteristics of the observed showers permit us to make an estimate of the energy of the generating particles under the assumption that in the center-of-mass system of the colliding particles there takes place a symmetric scattering of the secondary particles that are formed. Such an assumption is natural if the shower arises in the interaction of two nucleons. However, in our case, the interaction cannot be a nucleon-nucleon interaction for two reasons:

1. The presence of the lead filter over the entire apparatus can lead to the fact that the showers inside the chamber will be produced by particles which are formed in the lead filter overhead. In such a case, the shower-generating particles can be nucleons as well as pions. Below we shall therefore consider only the case of the passage of the generating particle through the chamber without the accompaniment of other fast charged particles, not connected with the shower.

2. The formation of the shower on a compound nucleus, even as light as Be or C, can occur in the interaction of the primary nucleon with certain nucleons inside the nucleus. We can point out a criterion, non-fulfillment of which means that the observed shower is not the result of nucleon-nucleon interaction.

TABLE I

Plate in chamber	No. of hours of research	Total no. of frames	Generating particle	n_s											Total showers
				4	5	6	7	8	9	10	11	12	13	14	
Be	824	4650	Charged	2 (3)	2 (4)	1 (1)	3 (1)	1 (1)	2 (1)	— —	— —	— —	1 —	— —	12 (11)
Be			Neutral	1 —	— —	— —	— —	— —	— —	— —	— —	— —	1 —	— —	2 - -
C	131	667	Charged	2 (1)	— —	— —	1 (1)	— —	— —	— —	— —	— —	— —	1 —	4 2)
C			Neutral	—	—	—	—	—	—	—	—	—	—	—	- -

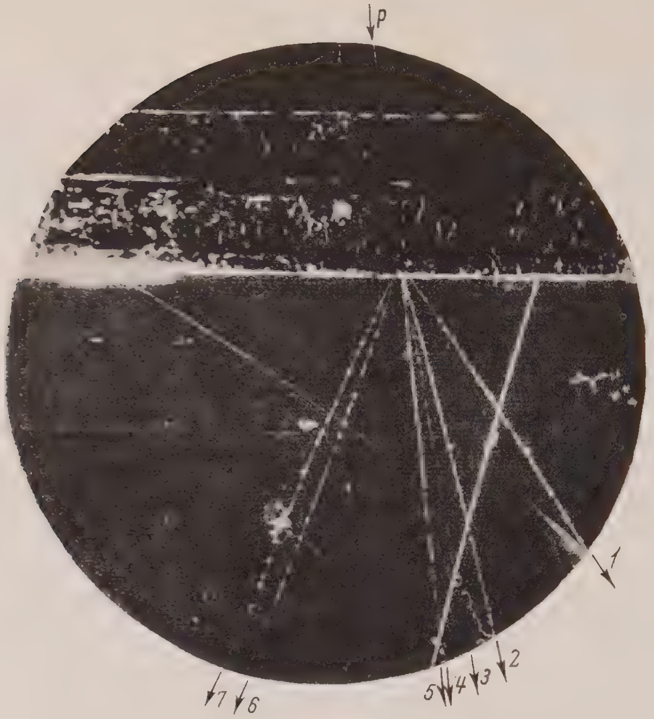

FIG. 2. Shower No. 43.27. Shower particle No. 1 (pion) creates a star in the gas of the chamber.

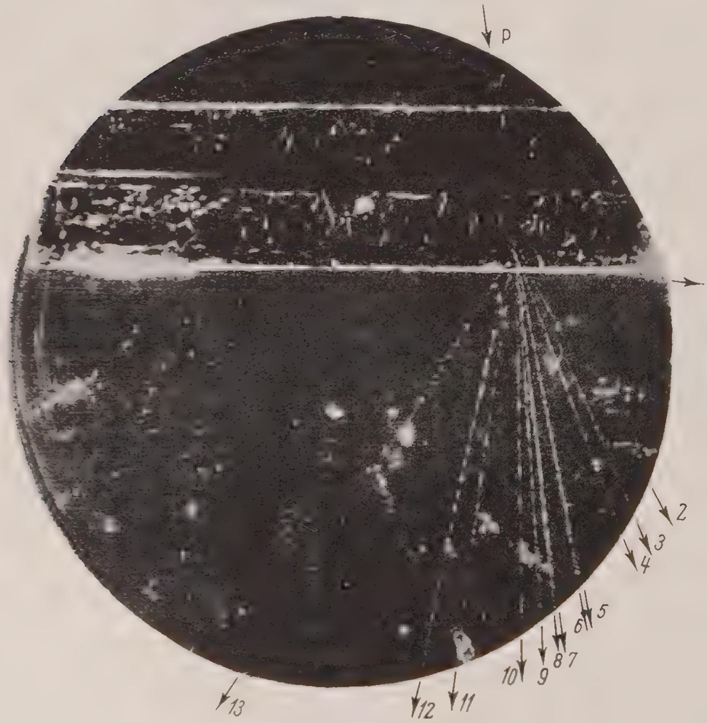

FIG. 3. Shower No. 95.87.

Let us consider the interaction of two nucleons with the formation of pions. Making use of the laws of conservation of energy and momentum, we can write

$$(E_0 - p_0 c) + Mc^2 = \Sigma (E_i - p_i c \cos \theta_i) + E_\delta - p_\delta c \cos \theta_i, \qquad (1)$$

where E'_p, p_0 are the total energy and momentum of the emergent nucleon in the laboratory system, E_i, p_i θ_i are the energy, momentum and angle of emergence of the shower particles; E_δ, p_δ and θ_δ are the corresponding quantities for the nucleon at a distance; M is the mass of the nucleon.

The energy of the generating nucleon for all the observed showers exceeds 5 bev; therefore, we can neglect the difference $E_0 - p_0 c$ in comparison with Mc^2. Then, for charged shower particles, assuming that all the particles are pions, the following condition must be satisfied:

$$Mc^2 > \Sigma (E_i - p_i c \cos \theta_i). \qquad (2)$$

If $Mc^2 < \Sigma (E_i - p_i c \cos \theta_i)$, then the generation of the shower occurs without nucleon–nucleon interaction. Applying the condition (2) to the showers of Table II, we can show that the shower from graphite No. 14.20 is formed in the interaction of the incident particle with several nucleons inside the nucleus. Actually, in this case, $\Sigma (E_i - p_i c \cos \theta_i) = 13 \times 10^8$ ev. For the remaining showers of Table II, which are formed by a single generating particle, condition (2) is satisfied (for shower No. 95.87, this condition is satisfied on the boundary). This does not mean, naturally, that interaction in all such cases takes place only between two nucleons. However, in what follows we shall depart from the assumption that for all showers of Table II, which are generated by a single particle and which satisfy condition (2), the scattering of the secondary particles in the center-of-mass system (c.o.m.) of two colliding nucleons takes place symmetrically with respect to the plane perpendicular to the direction of motion of the primary particle. Making use of such an assumption, we can obtain an estimate of the energy of the primary particle in the following way.

According to the equation

$$\operatorname{tg} \theta_{iC} = \sin \theta_i / \gamma_C [\cos \theta_i - (\beta_C / \beta_i)]$$

we find the angles θ_{ic} which are formed (in the c. o. m. system) by the shower particles with the direction of motion of the emergent nucleon for different values of the velocity of the c. o. m. system β_c in the laboratory system of coordinates (l.s.). (β_i is the velocity of the secondary particles in the laboratory system of coordinates). We consider that the real value of the velocity β_c corresponds to that value for which the angular scattering of charged particles in the c. o. m. system is very close to symmetric. Determination of

$$\gamma_C = 1 / \sqrt{1 - \beta_C^2}$$

in this fashion is the more accurate the greater the number of particles in the shower. For example, the angular distribution of the charged particles in shower No. 95.87 for $\gamma_C = 3$, $\gamma_C = 4$, $\gamma_C = 5$ is plotted in Fig. 4.* The value $\gamma_C = 4$ corresponds best to the symmetry condition.

By the method just described, we have determined γ_C for all showers. The results are shown in Table III (third column). The scatter of the angular distribution of the charged particles in the c.o.m. system and the number of neutral π°–mesons do not permit us to calculate the errors in the values of γ_C in each individual case. However, analysis of diagrams similar to those in Fig. 4 allow us to think that the errors in γ_C do not exceed 50% in showers of 4–6 particles, and 30% in showers with the number of particles ≥ 7.

It should be noted that the determination of the energy by this method gives results which differ from those obtained by the method of finding γ_C with the aid of the angular distribution of secondary particles under the supposition that $\beta_C = \beta_{ic}$, where β_{ic} is the velocity of the secondary particles in the c.o.m. system. For primary energies $\sim 10^{10}$ ev, the latter assumption leads to a noticeable increase in the value of γ_C in certain cases. Thus, for example, for the shower 60.89, γ_C, determined under the assumption that $\beta_C = \beta_{ic}$, is equal to 5.3 instead of 3.5 (see Table III).

4. DISTRIBUTION OF THE ENERGY AMONG THE SECONDARY PARTICLES

For the characteristics of the interaction process of the nucleons, the energy distribution among the different secondary particles is essential. In particular, we need to know the distribution between nucleons and pions. Direct determination of the amount of energy retained by a fast nucleon is impossible, inasmuch as it is not possible in the showers that we have studied to intensify the fast particles which emerge (in the c.o.m. system) in the direction of motion of the primary nucleon. The situation is different with shower particles that emerge in the reverse direction in the c.o.m. system. For most of these particles, we can determine their nature by their momentum and by the ionization they produce in the gas of the chamber, and consequently separate the pions from the

---

*Here and below, we shall denote, in the indices, the quantities which relate to the c.o.m. system by the letter C and those pertaining to the l.s. by the letter L.

TABLE II

Momenta and emission angle of slower particles, formed in Be by charged particles

No. of photograph	No. of particles	Sign	Momentum, $10^8 \frac{eV}{c}$	Angle in l.s. θ_L degrees	Ionization	Nature of particle	Comment
1	2	3	4	5	6	7	8
43.27 Shower without accompaniment	1	+	7 ± 2	25	~ min.	π	Creates a star in the gas of the chamber
	2	+	$11^{+4.5}_{-2.5}$	13	»	?	
	3	?	—	22	»	?	
	4	+	24^{-9}_{+36}	2	»	?	
	5	?	>38	6	»	?	
	6	+	5.5 ± 1	28	»	π	
	7	—	2.9 ± 0.3	34	»	π	
47.14 Shower with accompaniment	1	—	$7^{+1.4}_{-1.0}$	27	~ min.	π	
	2	+	$8.5^{+2.5}_{-1{,}5}$	10	»	?	
	3	—	11^{+4}_{-2}	7	»	π	
	4	?	>38	5	»	?	
	5	—	$16^{+17}_{-5.5}$	9	»	π	
	6	—	$7^{+2.5}_{-1\ 5}$	3	»	π	
	7	?	—	13	»	?	short track
	8	?	>24	14	»	?	
	9	—	$0{,}57\pm0.01$	9	»	δ-electron	
50.38 Shower without accompaniment	1	?	>40	6	~ min.	?	
	2	—	19^{+18}_{-6}	3	»	π	
	3	?	>40	3	»	?	
	4	?	>30	4	»	?	
70.52 Shower without accompaniment	1	—	$2+0.1$	41	~ min.	π	
	2	?	—	40	~ 5 min.	proton	
	3	+	$10^{+4.5}_{-1.5}$	2	~ min.	?	
	4	+	9^{+4}_{-1}	14	»	?	
	5	?	>9	48	»	?	
74.39 Shower without accompaniment	1	—	$4.5^{+1.2}_{-0.9}$	30	~ min.	π	
	2	+	10^{+12}_{-3}	16	~ min.	?	
	3	+	$8.5^{+3}_{-1.5}$	25	~ min.	?	
	4	+	$3{,}9\pm0.4$	10	~ min.	π	
87.52 Shower without accompaniment	1	—	2.3 ± 0.2	6	~ min.	π	
	2	?	>29	5	»	?	
	3	+	15^{+15}_{-5}	6	»	?	
	4	?	>25	13	»	?	
	5	?	—	11	»	?	short track

TABLE II (continued)

No. of photograph	No. of particles	Sign	Momentum, $10^8 \frac{eV}{c}$	Angle in l.s. θ_L degrees	Ionization	Nature of particle	Comment
1	2	3	4	5	6	7	8
89.51 Shower without accompaniment	1	—	$4\ 5^{+2}_{-1}$	77	~ min.	π	
	2	?	>14	16	"	?	
	3	?	—	21	"	?	tracks 3—7 almost run together
	4	?	—	2	"	?	
	5	?	—	2	"	?	
	6	?	—	2	"	?	
	7	?	—	2	"	?	
	8	+	$10^{+5}_{-2.5}$	2	"	?	
	9	+	$18^{+14}_{-4.5}$	5	"	?	
60.89 Shower without accompaniment	1	?	>13	48	~ min.	?	
	2	+	$3\ 7^{+0.8}_{-0.6}$	31	"	π	
	3	—	$6^{+4}_{-1.5}$	14	"	π	
	4	+	11.5^{+16}_{-3}	2	"	?	
	5	—	25^{+80}_{-11}	2	"	π	
	6	?	>38	6	"	?	
	7	?	—	11	"	?	short track
	8	?	> 9	25	"	?	
93.46 Shower without accompaniment	1	?	> 7	22	~ min.	(π?)	
	2	?	>39	7	"	?	
	3	—	23^{+34}_{-8}	8	"	π	
	4	+	$13^{+5.5}_{-2.5}$	20	"	?	
	5	—	5,2±0.5	4	"	π	
	6	+	10^{+6}_{-2}	13	"	?	
	7	+	12^{+6}_{-3}	32	"	?	
95.87	1	?	—	71	~ min.	?	short tracks
	2	?	—	32	"	?	
	3	+	$8^{+1.3}_{-3}$	26	"	(π?)	
	4	+	12^{+38}_{-5}	16	"	?	
	5	?	>26	13	"	?	
	6	?	>25	4	"	?	
	7	?	>29	2	"	?	
	8	?	>27	3	"	?	
	9	+	$13.5^{+12}_{-4.5}$	5	"	?	
	10	+	11^{+6}_{-3}	6	"	?	
	11	—	$7,8^{+1.9}_{-1.1}$	18	"	π	
	12	—	$5\ 7^{+1.1}_{-0,7}$	24	"	π	
	13	+	8^{+5}_{-2}	45	"	(π?)	

TABLE II (continued)

No. of photograph	No. of particles	Sign	Momentum, $10^8\ \frac{\text{eV}}{c}$	Angle in l.s. θ_L degrees	Ionization	Nature of particle	Comment
1	2	3	4	5	6	7	8
98.80	1	?	—	14	~ min.	?	short track
Shower without	2	?	>17	8	"	?	
accompaniment	3	—	1.2 ± 0.05	8	"	π	
	4	—	10^{+3}_{-2}	16	"	π	
	5	?	>38	4	"	?	
	6	+	17^{+13}_{-5}	14	"	?	
	7	?	—	45	"	?	short track
98.87	1	?	>3	37	min.	(π?)	
Shower without	2	—	1.0 ± 0.3	5	"	π	
accompaniment	3	+	>37	9	"	?	
	4	+	$10.5^{+4.5}_{-2.5}$	12	"	?	
	5	+	13^{+6}_{-3}	10	"	?	
	6	?	>3	55	"	(π?)	
44.55	1	—	$2.0\pm0{,}2$	5*	min.	π	
Shower is formed	2	+	13^{+32}_{-5}	4	"	?	
by a neutral particle	3	+	$6.5^{+3.5}_{-1.5}$	5	"	π	
	4	?	—	2	"	?	tracks of particles 4–9 almost run together
	5	?	—	2	"	?	
	6	?	—	2	"	?	
	7	?	—	2	"	?	
	8	?	—	2	"	?	
	9	?	—	2	"	?	
	10	+	$11.5^{+8.5}_{-3.5}$	2	"	?	
	11	?	>27	3	"	?	
	12	+	$15^{+9.5}_{-4.5}$	4	"	?	
	13	?	>27	6	"	?	
Showers formed in graphite by charged particles							
16.X.53 No. 9	1	—	$5^{+1.5}_{-1.0}$	25	~ min.	π	
Shower without	2	?	>23	10	"	?	
accompaniment	3	+	12^{+36}_{-5}	6	"	?	
	4	?	>14	15	"	?	
14.20	1	+	7^{+4}_{-2}	50	~ 2 min.	proton	
	2	?	—	25	min.	?	
	3	+	$6.5^{+3}_{-2.5}$	18	"	π	
	4	+	20^{+20}_{-9}	11	"	?	
	5	?	>23	2	"	?	

*From the direction of the motion of the neutral generating particle we get the direction of the total momentum of the charged particles.

TABLE II (continued)

No. of photograph	No. of particles	Sign	Momentum, $10^8 \frac{eV}{c}$	Angle in l.s. θ_L degrees	Ionization	Nature of particle	Comment
1	2	3	4	5	6	7	8
14.20 .	6	—	$13^{+16}_{-4.5}$	2	min.	π	
	7	—	12^{+12}_{-4}	2	„	π	
	8	—	12^{+11}_{-4}	6	„	π	
	9	?	>23	13	„	?	
	10	—	4^{+2}_{-1}	28	„	π	
	11	+	12^{+22}_{-45}	19	„	?	
	12	?	—	32	„	?	short track
	13	+	14^{+20}_{-7}	30	„	?	
	14	—	$12^{+2.1}_{-4.5}$	31	„	π	
22.44-a Shower without accompaniment	1	+	$3.8^{+0.8}_{-0.6}$	33	min.	π	
	2	?	>22	14	„	?	
	3	+	$5.5^{+4.5}_{-2}$	5	„	π	
	4	+	8.5^{+6}_{-3}	4	„	?	
	5	?	>22	6	„	?	
	6	?	>7	8	„	(π?)	
	7	?	>6	9	„	(π?)	

protons.* We can then find the amount of energy transferred to pions in the backward cone in the c.o.m. system: therefore, if the emission of the secondary particles is symmetric we can also obtain the amount of energy α_C transferred to all mesons,

$$\alpha_C = 1{,}5\,\Sigma E_{iC}^{\pi +} / \gamma_C M c^2. \tag{3}$$

We consider that the neutral pions make up one third of all mesons. The amount of energy retained by each nucleon will be

$$\varepsilon_C = E_{NC} / \gamma_C M c^2 = 1 - 1{,}5 \Sigma E_{iC}^{\pi\pm} / \gamma_C M c^2.$$

Transforming to the laboratory system of coordinates, under the assumption of nucleon-nucleon interaction, we find that the fraction of energy retained by a fast nucleon is equal to

$$\varepsilon = \frac{E_N}{E_0} = \frac{\gamma_C}{2\gamma_C^2 - 1}[\varepsilon_C \gamma_C \tag{4}$$

$$+ \beta_C \sqrt{\varepsilon_C^2 \gamma_C^2 - 1} \cos \theta_{NC}],$$

where E_N is the total energy of the nucleon in the l.s. after the interaction, E_0 is the initial total energy of the nucleon in the l.s., θ_{NC} is the emergence angle of the nucleon in the c.o.m. system. Making use of Eq. (4), we can find the limits, for a shower with known γ_C , within which the quantity ϵ will lie in its dependence on the angle θ_{NC} . Table IV gives the estimates of the amount of energy ϵ retained, obtained by this method. Analyzing Table IV, we see that for all cases, the energy of a fast nucleon is less than 60% of the energy of the primary nucleon.

It should be noted that the data we have obtained bear an approximate character, inasmuch as in showers with a small number of particles, an appreciable scatter is possible both in the values of the energy transferred to the pions in the backward cone , and in the values of the energy possessed by the π°–mesons.

---

*In certain cases when relativistic particles, emerging at large angles in the l.s., possess a momentum $p > 8 \times 10^8$ ev/c, we consider them to be protons. As will be evident in what follows, this leads to an increased amount of energy concentrated on a single nucleon.

5. ANGULAR DISTRIBUTION OF PARTICLES IN THE CENTER-OF-MASS SYSTEM

For showers whose energy is determined by the method just described, we can obtain the angular distribution of all shower particles in the center-of-mass system. Such a distribution for 68 particles which gave tracks with minimum ionization is presented in Fig. 5. The broken curve corresponds to the isotropic distribution of the particles. In the limits of statistical errors, the angular distribution that we obtained coincides with the isotropic.

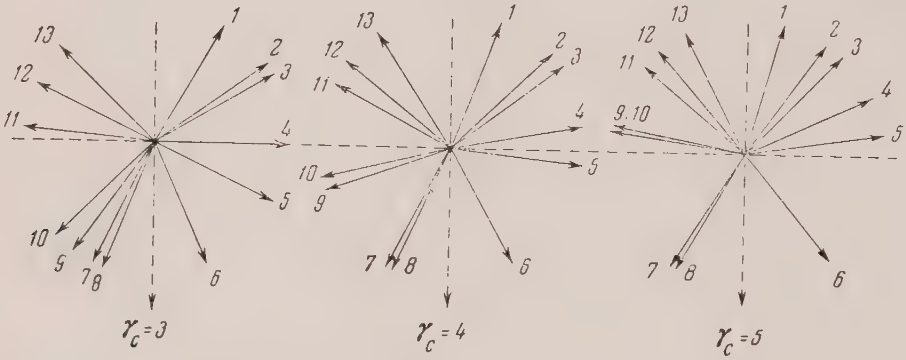

FIG. 4. Angular distribution of the shower particles in the c.o.m. system for shower No. 95.87. In finding the angles for particles 1 and 2, it is assumed that the momentum of these particles is equal to 5 bev/c.

TABLE III

No. of shower	Total no. of particles in shower	γ_C	$E_0'\,10^{-9}$ ev for $N+N$ collisions
43.27	7	2.5	10.8
60.89	8	3.5	22
70.52	5	2	6.6
89.51	9	5	49
93.46	7	3.5	22
98.80	7	3	16
95.87	13	4	29*
98.87	6	2	6.6
44.55	13	6	66
22.44-a	7	4	29
74.39	4	1.5	3.5

*It is possible that this is not a nucleon-nucleon interaction.

In one shower (No. 70.52) a slow δ-proton was registered; in the others, δ-protons were not seen. However, it is possible, making use of Eq. (1), to attempt to determine the angles and momenta in the l.s. of those nucleons which emerge in the forward direction in the c.o.m. system. Actually,

$$E_\delta - p_\delta c \cos\theta_\delta = Mc^2 - \Sigma\,(E_i - pc\cos\theta_i).$$

As before, we neglect π°–mesons, and consider all secondary charged particles which produce minimum ionization in the gas of the chamber to be π–mesons (the presence in the medium of fast charged particles of one proton has slight effect on the result).* We denote

$$Mc^2 - \Sigma\,(E_i - p_i c\cos\theta_i)$$

by B. Then,

$$p_\delta c = [B\cos\theta_\delta \tag{5}$$

$$\pm\sqrt{\cos^2\theta_\delta B^2 - \sin^2\theta_\delta\,(M^2c^4 - B^2)}]\,/\sin^2\theta_\delta.$$

It therefore follows that

$$\operatorname{ctg}\theta_\delta \geqslant \sqrt{M^2c^4 - B^2}\,/\,B. \tag{6}$$

Equation (6) determines the maximum angle for which δ-nucleons can emerge in the laboratory system. Here

$$(M^2c^4 - B^2)\,/\,2B < p_\delta c \tag{7}$$

$$< \sqrt{(E_0 + Mc^2 - \varepsilon E_0 - 1{,}5\,\Sigma E_i)^4 - M^2c^4}.$$

---

*Consideration of π°–mesons and of a fast nucleon leads to some diminution of the limit angle θ_δ.

TABLE IV

No. of shower	γ_C	without consideration of π^0-mesons			with consideration of π^0-mesons		
		α_C	$\varepsilon(\theta_{NC}=0)$	$\varepsilon(\theta_{NC}=90°)$	α_C	$\varepsilon(\theta_{NC}=0)$	$\varepsilon(\theta_{NC}=90°)$
43.27	2,5	0,35	0.58	0,35	0,5	0,43	0.27
60.89	3.5	0,34	0,65	0,35	0.5	0,46	0,26
70.52	2	0,5	0,29	0,29	—	—	—
89.51	5	0.4	0.6	0.3	0,6	0,37	0.2
93.46	3,5	0.27	0,7	0.36	0,4	0,57	0.31
95.87	4	0.5	0,48	0.26	0,75	0.13	—
98.87	2	0.3	0,65	0,35	0.45	0 43	0.31
22.44-a	4	0,27	0.70	0,4	0,4	0.6	0,3

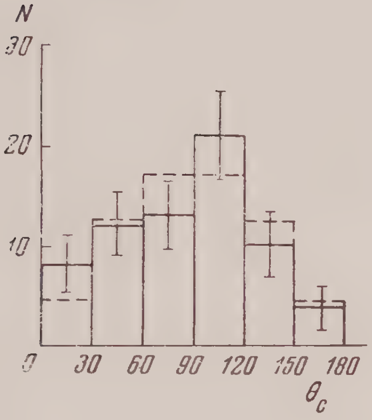

FIG. 5. Angular distribution in the c.o.m. system of shower particles which produce relativistic ionization in the gas of the chamber.

The upper limit for p_δ is determined from the law of conservation of energy, in which we take for ϵ the minimum values from Table IV, and in the composition of ΣE_i , we do not include the value of the energy of the fastest particle of the shower. Here we obtain a reduced value of p_δ . Equations (6) and (7) allow us to determine the minimum angle at which a δ-nucleon emerges in the c.o.m. system. The limiting angles of emergence of δ-nucleons in the l.s., and c.o.m. system, $\theta_{\delta L}$ and $\theta_{\delta C}$, for showers with known γ_C are given in Table V.

The values of the limiting angles $\theta_{\delta C}$ of Table V are significantly reduced , inasmuch as in their determination we have made use of the reduced values of momenta of the δ-nucleons in the l.s. This applied particularly to the showers 44.55 and 89.51 in which about half of the particles possess unmeasured momenta.

TABLE V

No. of shower	$\theta^\circ_{\delta L}$	$p_\delta \cdot 10^{-8}$ eV/c	$\theta^\circ_{\delta C}$
43.27	$\leqslant 37$	5—18	> 130
70.52	$\leqslant 34$	6—15	> 125
89.51	$\leqslant 26$	9—220	> 90
93.46	$\leqslant 30$	11—50	> 120
98.80	$\leqslant 40$	4—18	> 140
98.87	$\leqslant 34$	6—25	> 120
44.55	$\leqslant 62$	1,5—270	> 115
22.44-a	$\leqslant 48$	6—105	> 125

It then follows from Table V that the emergence of δ-nucleons in the c.o.m. system takes place anisotropically.

6. CONCLUSIONS

We can now make some conclusions relative to the character of the interactions isolated by our apparatus.

1. The angular distribution of the shower particles (pions) in the c.o.m. system of two colliding nucleons is close to isotropic.

2. The scattering of nucleons in the c.o.m. system occurs anisotropically, principally in the direction of motion of the primary nucleon.

3. The fraction of energy retained by the fastest nucleon does not exceed 60%. It should be noted that these conclusions cannot be extended to all interactions of nucleons with $E_0 \geq 5$ bev with Be nuclei, inasmuch as the cases that we have analyzed, which differ in the comparatively large number of secondary particles, form an insignificant fraction of the total number of interactions. Comparison of the value of the amount of energy transferred to the pion, which is obtained for the cases analyzed, with the significantly smaller value of this same quantity which follows from analysis of processes of passage of cosmic ray nucleons through the atmosphere,[2] points up the presence of large fluctuations in the characteristics of nuclear interactions.

In conclusion, the authors consider it their pleasant duty to thank A. G. Novikov and D. V. Emel'ianov for assistance in the development and assembling of the apparatus.

The authors also thank N. A. Dobrotin, I. L. Rosental' and Iu. A. Smorodin for discussion of the results obtained, and K. A. Kotel'nikov, V. M. Maksimenko and S. V. Riabikov for their help in the measurements.

---

[1] Wright, Saphir, Powell, Maenchen and Fowler, Phys. Rev. 100, 1802 (1955); Fowler, Maenchen, Powell, Saphir and Wright, Phys. Rev. 101, 911 (1956); Materials of the Rochester Conference, April, 1956.

[2] N. L. Grigorov, Uspekhi Fiz. Nauk 58, 599 (1956).

Translated by R. T. Beyer
210

SOVIET PHYSICS JETP VOLUME 4, NUMBER 6 JULY, 1957

Many Electron Treatment of Motion of an Electron (Hole) in a Deformed Crystal. II.

T. I. KUCHER AND K. B. TOLPYGO
Kiev State University and Zhitomir Pedagogical Institute

(Submitted to JETP editor September 26, 1956)
J. Exptl. Theoret. Phys. (U.S.S.R.) 31, 1002–1011 (1956)

A many electron treatment of the motion of an electron (hole) is given for an ionic crystal for the case of unfixed nuclei and the presence of vacancies of any ion. The theory is developed in the close coupling approximation using antisymmetrized wave functions and can be used also for the states of small radius. A method of calculation of the deformation of crystal and the energy of local self consistent state are described.

IN a previous work[1] we described a technique of calculation of the local state of an electron (hole) in a perturbed crystal on the assumption that the external field does not lead to displacements of the nuclei while deforming the electron shells of the ions. This means that only the polarization of the lattice by the field of the electron (hole) was considered. Since the Hartree approximation was used, it was not possible to describe correctly the motion of the hole and to take into account the exchange forces between ions which provide for the equilibrium of the lattice together with the Coulomb forces.

For a step-by-step calculation of the deformation of the lattice, which certainly exists near the local level of the electron and substantially influences its energy, a many electron formulation of the problem should allow calculation of the exchange forces. Therefore such a formulation should be based on an antisymmetrized lattice function, i.e., the Fock approximation. The present work is devoted to this generalized problem.

1. BASIC SIMPLIFYING ASSUMPTIONS

We shall consider a binary cubic ionic lattice with one vacancy at the origin of the coordinates. Let us assume that an extra electron (hole) is present in the lattice if a negatively charged (positively charged) ion is removed from the lattice. We shall denote by $\mathbf{r}_s^l$ and $\mathbf{R}_s^l = \mathbf{r}_s^l + \mathbf{u}_s^l$ the equilibrium and the displaced positions of the nucleus of the s th ion in the lth cell (s=1, 2 for + and – ion). By $\rho_s^{l\lambda}$ we shall denote the totality of the $3N_s$ coordinates of the N_s electrons of the ion s, l (λ is an index of the permutation of the electrons of the lattice), and by $\rho_{sn_s}^l$ we shall denote the radius vector of the n_s electron ($n_s = 1, 2, \ldots, N_s$).

The lattice function is taken in the form of a linear combination of antisymmetrized products Ψ_s^l of the wave functions of individual ions. Let $\psi_s^l(\rho_s^{l\lambda})$ denote a wave function of the normal ion and $\varphi_s^l(\rho_s^{l\lambda})$ the wave function of an anomalous ion on which an electron (s = 1) or a hole (s=2) is localized. We shall consider an electron to be moving about the positively charged ions and a hole about the negatively charged ions. Then

$$\Psi_s^l = (N!)^{-1/2}\sum_{\lambda}(-1)^{\lambda}\varphi_s^l(\boldsymbol{\rho}_s^{l\lambda})\prod_{s'l'}{}'\psi_{s'}^{l'}(\boldsymbol{\rho}_{s'}^{l'\lambda}). \quad (1)$$

The wave functions of the individual ions will be considered to be orthogonal in the sense that

$$\int\varphi_s^{*l}(\rho_s^{l\lambda})\prod{}'\psi_{s''}^{l''}(\boldsymbol{\rho}_{s''}^{l''\lambda})\varphi_{s'}^{l'}(\boldsymbol{\rho}_{s'}^{l'\lambda'})\prod{}'\psi_{s''}^{l''}(\boldsymbol{\rho}_{s''}^{l''\lambda'})\,d\tau = \delta_{\lambda\lambda'}; \quad (2)$$

where $\delta_{\lambda\lambda'} = 0$ if λ and λ' differ by an interchange of only one pair of electrons between different ions or by an interchange of only one electron between ions s, l and s', l' so that

$$\int\Psi_s^{l*}\Psi_{s'}^{l'}\,d\tau = \delta_{ss'}. \quad (3)$$

It is evident that the wave functions of ions may always be orthogonalized without a change in the antisymmetrized product. In doing so we shall neglect the interchange of ψ_s^l and φ_s^l in displacing ions by $\mathbf{u}_s^l$.

In distinction to the works of Pekar[2] and Heisenberg[3] we shall include the effect of the electron (hole) on the wave function of the remaining ions. For a freely moving electron this effect is apparent mainly in polarization of the environment; it causes a slight change in the periodic potential and consequently a lowering of the depth of the conduction band.[4] The interaction of the electron with the dipoles introduced by the same defect results in a change in the potential of the defect (in the macroscopic approximation it decreases it by n_0^2 times, where n_0 is the optical index of refraction). We shall include this effect only as polarization of the surrounding ions, neglecting the non-uniformity of the field of the electron and the defect within the boundaries of each ion, and we shall assume that the polarization follows adiabatically the motion of the electron from one lattice point s, l to another. This is true if the kinetic energy of the electron (hole) is small compared to the lattice excitation energy.

2. THE WAVE FUNCTION OF THE SYSTEM IN THE ADIABATIC APPROXIMATION

The Hamiltonian of the lattice, $\hat{H}$, is equal to the sum of the Hamiltonians of the individual ions $\hat{H}_s^l$, of the interaction energy of the different ions $\hat{H}_{ss}^{ll'}$ and the energy of all ions in the external field $\mathbf{E}^0$ with the potential v (r):

$$\hat{H}^0 = \sum_{s,l} H_s^{0l} = \sum_{s,l} e\left[z_s v(\mathbf{R}_s^l) - \sum_{n_s=1}^{N_s} v(\rho_{sn_s}^l)\right], \tag{4}$$

where z_s is the nuclear charge of the sth ion.

Following the adiabatic approximation, we shall determine the wave function of all ions for an arbitrary position of the anomalous site s,l. One can use the variation principal by minimizing the average Hamiltonian, $\hat{H}$, constructed from the trial functions Ψ_s^l:

$$H\binom{ll}{ss} = \int \Psi_s^{l*} \hat{H} \Psi_s^l \, d\tau \tag{5}$$

$$= \sum_{s'l'} \Big\{ \int \psi_{s'}^{l'*} [\hat{H}_{s'}^l + \hat{H}_{s'}^{0l'}] \psi_{s'}^{l'} \, d\tau_{s'}'$$

$$+ {}^1/_2 \sum_{s''l''}' \iint \psi_{s'}^{l'*} \psi_{s''}^{l''*} H_{s's''}^{l'l''} \psi_{s''}^{l''} \psi_{s'}^{l'} \, d\tau_{s'}^{l'} \, d\tau_{s''}^{l''}$$

$$- \frac{e^2}{4} \sum_{s''l''}^{(n)}{}' N_{s'} N_{s''} \iint \psi_{s'}^{l'*} (\ldots\boldsymbol{\rho}'\ldots)$$

$$\times \psi_{s''}^{l''*} (\ldots\boldsymbol{\rho}''\ldots) \frac{1}{|\boldsymbol{\rho}' - \boldsymbol{\rho}''|} \psi_{s''}^{l''} (\ldots\boldsymbol{\rho}''\ldots) \psi_{s'}^{l'} (\ldots\boldsymbol{\rho}''\ldots) d\tau' \, d\tau'' \Big\}.$$

In view of the orthogonality condition of Eq. (2), it is sufficient to retain in the product $\Psi_s^{l*} \, \Psi_s^l$ only the identical rearrangments and rearrangements which differ by one transposition. In the latter case it is necessary to retain only those terms of the Hamiltonian which contain the coordinates of the transposed electrons ρ' and ρ''. The exchange integrals will be retained only for the closest neighbors, whose number we shall denote by n. The sums denoted by primes are carried out over all terms except those where s', $l' = s''$, l''. For s', $l' = l, s$ or $s'' l'' = s, l$ it is necessary to change ψ_s^l by φ_s^l.

We shall assume that the difference between $\psi_s^{l'}$ and the wave function of the ground state of the isolated ions $\underline{\psi}_{s0}^{l'}$ is small. In the expansion

$$\psi_{s'}^{l'} = \sum_{i=0}^{\infty} c_{s'i}^{l'} \psi_{s'i}^{l'}, \quad \sum_{i=0}^{\infty} |c_{s'i}^{l'}|^2 = 1, \tag{6}$$

where $\psi_{si}^{l'}$ are the wave functions of the excited states, we shall assume that the first term $c_{s'0}^{l'} \approx 1$ plays the most important role. The coefficients $c_{si}^{l'}$, $i \geq 1$ will also serve as parameters of the approximation. Inserting the expansion of Eq. (6) into Eq. (5) we shall retain only the terms to the second order in $c_{si}^{l'}$ in the integrals for $\hat{H}_s^{l'}$ and in the Coulomb integrals. For those states which give a contribution for the dipole moment of the ions

$$P_{s'x}^{l'} = -eN_{s'} \times \sum_{i=1}^{\infty} [(0|x|i) c_{s'i}^{l'} + (0|x|i)^* c_{s'i}^{l'*}], \tag{7}$$

where

$$(0|x|i) = \int \psi_{s'0}^{l'*} \rho \psi_{s'i}^{l'} \, d\tau_{s'}^{l'}.$$

Thus the dipole-dipole interaction between ions is taken into account. In the exchange integrals and in the integrals of $\hat{H}_s^{0l'}$, we shall retain only the first order terms. In Eq. (7) it is sufficient to retain the terms linear in $c_{si}^{l'}$ since only the product of $\mathrm{P}_s^{l'}$ and vacancy fields of the excess electron and E^0 (all considered small) enter into the energy. If this condition of small fields is not met it is not possible to consider the difference between ${}_s^{l'}$ and $\psi_{s0}^{l'}$ small. Then Eq. (5) takes the form

$$H\binom{ll}{ss} = (M-1)(E_{10}+E_{20}) + \overline{E}_{s0} \qquad (8)$$
$$+ \sum_{s'l'} \Big\{ \sum_{i=1}^{\infty} |c_{s'i}^{l'}|^2 (E_{s'i} - E_{s'0})$$
$$+ {}^1/_2 \sum_{s''l''}{}' [e_{s'} e_{s''}/R - 2e_{s''} \mathbf{P}_{s'}^{l'} \mathbf{R}/R^3$$
$$+ \mathbf{P}_{s'}^{l'} \mathbf{P}_{s''}^{l''}/R^3 - 3(\mathbf{P}_{s'}^{l'}\mathbf{R})(\mathbf{P}_{s''}^{l''}\mathbf{R})/R^5]$$
$$+ e_{s'} v(\mathbf{R}_{s'}^{l'}) - \mathbf{P}_{s'}^{l'} \mathbf{E}^0(\mathbf{R}_{s'}^{l'}) - \sum_{s''l''}^{(n)}{}' [\omega_{s'0}(\mathbf{R})$$
$$+ \sum_{i=1}^{\infty}{}' (c_{s'i}^{l'} \omega_{s'i}(\mathbf{R}) + c_{s'i}^{l'*} \overset{*}{\omega}_{s'i}(\mathbf{R}))] \Big\}$$

where for thesake of brevity we write the radius vector $\mathrm{R}_{s's''}^{l'l''}$ simply as R. $E_{s'i}$ is the *i*th energy level of the s'th ion, $e_{s'} = e(z_{s'} - N_{s'})$ is its charge, M is the numberof cells in thelattice, E_{s0} is the energy of the anomalous ion in its ground state;

$$\omega_{s'i} = \frac{e^2}{2} N_{s'} N_{s''} \iint \psi_{s'0}^{l'*}(\ldots\boldsymbol{\rho}'\ldots)\, \psi_{s''0}^{*l''}(\ldots\boldsymbol{\rho}''\ldots) \qquad (9)$$
$$\frac{1}{|\boldsymbol{\rho}' - \boldsymbol{\rho}''|} \psi_{s'i}^{l'}(\ldots\boldsymbol{\rho}''\ldots) \psi_{s''0}^{l''}(\ldots\rho'\ldots) d\tau' d\tau''.$$

and $\omega_{s'0}$ has an analogous value but contains only the zero order functions and is multiplied by a factor of 1/2. In particular, the sums over s', l', s'', l'' contain terms for the anomalous ion for which the charge e_s, the dipole moment, and the coefficients ω_{s0}, ω_{si} have different values:

$$\overline{e}_s,\ \overline{\mathbf{P}}_s^l,\ \overline{\omega}_{s0},\ \overline{\omega}_{si}.$$

It is convenient to find the minimum of Eq. (8) in $c_{s'i}^{l'}$, by the method described by one of the authors,[5] in two steps: first, one finds therelative minimum of $H\binom{ll}{ss}$ for arbitrary fixed $\mathrm{P}_{s'}^{l'}$, i.e., under the conditions of Eq. (7), and then one minimizes $H\binom{ll}{ss}$ over $\mathrm{P}_{s'}^{l'}$. In the first step,

$$H_{ss}^{ll} = \sum_{s'l'} \Big\{ \frac{1}{2\alpha_{s'}} (\mathbf{P}_{s'}^{l'})^2 \qquad (10)$$
$$+ \sum_{s''l''}^{(n)}{}' \mathbf{P}_{s'}^{l'} \beta_{s's''}^{l'l''}(\mathbf{R}) + U(\ldots \mathbf{R} \ldots) \Big\}$$
$$+ (M-1)(E_{10}+E_{20}) + \overline{E}_{s0} + \sum_{s'l'}{}' \{ e_{s'} v(\mathbf{R}_{s'}^{l'})$$
$$- \mathbf{P}_{s'}^{l'} [\mathbf{E}^0(R_{s'}^{l'}) + {}^1/_2 \mathbf{E}'(R_{s'}^{l'})]$$
$$+ {}^1/_2 \sum_{s''l''}{}' [e_{s'} e_{s''}/R - 2e_{s''} \mathbf{P}_{s'}^{l'} \mathbf{R}/R^3] \},$$

where

$$\alpha_{s'} = 2e^2 N_{s'}^2 \,\mathrm{Re} \sum_{i=1}^{\infty} |(0|x|i)|^2 / (E_{s'i} - E_{s'0})$$

where the coefficient of polarizability of the s'th ion

$$\beta_{s's''x} = \frac{2e}{\alpha_{s'}} \mathrm{Re} \sum_{i=1}^{\infty} (0|x|i)\, \omega_{s'i}(\mathbf{R}) / (E_{s'i} - E_{s'0});$$

where $U(\ldots \mathrm{R} \ldots)$ is a function depending on the separation R of the ion s', l' from its n closest neighbors and is approximately equal to the sum of the central pair interactions $U \approx \sum_{s''l''}^{(n)} u(R)$. Since normal ions have spherical symmetry, then $\alpha_{s'}$ is a scalar and $\beta_{s's''}$ has the direction of R and depends only on its modulus, while β_{12} and β_{21} are different (for anomalous ions $\overline{\beta}_{12}$ and $\overline{\beta}_{21}$).

$$\mathbf{E}'(\mathbf{R}_{s'}^{l'}) = \sum_{s''l''}{}' [3(\mathbf{P}_{s''}^{l''}\mathbf{R})\mathbf{R}/R^5 - \mathbf{P}_{s''}^{l''}/R^3] \qquad (11)$$

determines the field of all dipoles $\mathrm{P}_{s''}^{l''}$ at the point $\mathrm{R}_{s'}^{l'}$.

Thus the problemof finding the function $\psi_{s'}^{l'}$ results in theproblem of determining the dipole moment $\mathrm{P}_{s'}^{l'}$, which may be solved by a method pointed out previously [1] and already carried out in the work of one of the authors[6] for the particular case of the absence of vacancies and displacements.

3. EVALUATION OF THE IONIC DIPOLE MOMENTS

We shall expand $H\binom{ll}{ss}$ in orders of the displacements of the ions $\mathrm{u}_{s'}^{l'}$, retaining the quadratic form relative to the dipole moments of the displacements $\mathrm{p}_{s'}^{l'} = e_{s'} \mathrm{u}_{s'}^{l'}$ and the electron shells $\mathrm{P}_{s'}^{l'}$. Completing Eq. (7) for the energy of an ideal crystal, and taking into account that

$$\sum_{s''l''}{}' \mathbf{r}/r^3 = 0, \qquad (12)$$
$$\sum_{s''l''}{}' [3(\mathbf{r}, \mathbf{u}_{s'}^{l'})\mathbf{r}/r^5 - \mathbf{u}_{s'}^{l'}/r^3] = 0,$$
$$\sum_{s''l''}^{(n)}{}' \boldsymbol{\beta}_{s's''}(\mathbf{r}) = \sum_{s''l''}^{(n)}{}' \beta_{s's''} \mathbf{r}/r = 0, \quad \mathbf{r} \equiv \mathbf{r}_{s's''}^{l'l''},$$

we introduce a displacement field E″ expressed by means of $p_s^{l''}$ analogously to the formula of Eq. (11) for E′. Then using the condition $\partial H\binom{ll}{ss}/\delta P_s^{l'} = 0$ we obtain

$$\mathbf{P}_{s'}^{l'} = \alpha_{s'}\{(\mathbf{E}' + \mathbf{E}'')_{\mathbf{R}_{s'}^{l'}} - \sum_{s''l''}^{(n)} (\mathbf{u}_{s'}^{l'} - \mathbf{u}_{s''}^{l''}) \nabla\beta_{s's''}|_{\mathbf{r}} + \mathbf{G}_{s'}^{l'}\}, \tag{13}$$

where

$$\mathbf{G}_{s'}^{l'} = \mathbf{E}^0(\mathbf{r}_{s'}^{l'}) + (\bar{e}_s - e_s)\,\mathbf{r}_{s's}' / - |\mathbf{r}_{s's}^{l'l}|^3 \tag{14}$$

$$- e_\sigma \mathbf{r}_{s'}^{l'} / |\mathbf{r}_{s'}^{l'}|^3 + \beta_{s'\sigma'}\gamma_{s'\sigma'}^{l'0} - (\bar{\beta}_{\sigma s} - \beta_{\sigma s})\,\gamma_{s's}^{l'l}.$$

Here we neglect the small change of the field $G_s^{l'}$ which is due to the displacement of the ion s', l' by $u_s^{l'}$. The type of ionic vacancy is designated by σ and the symbols $\gamma_{s\,s}^{l'l}$ and $\gamma_{s\,\sigma}^{l'0}$ are equal to unity if the ion $s'l'$ is the nearest neighbor of the corresponding ion s, l and of a vacant lattice site, and equal to zero in the opposite case.

For an ideal lattice, where $G_s^{l'} = 0$, Eqs. (13) are solved by expanding the quantities $P_s^{l'}$ and $p_s^{l'}$ and the fields E′, E″ in plane waves. The presence of a vacant lattice site and also of ion s, l with a different polarizability and a different $\beta_{ss'}$ disturbs the translation symmetry. It is evident that in the first approximation one may write the system of Eqs. (13) in the same way for all lattice sites, express it in the form of a Fourier expansion $G_s^{l'}$ and find all $P_s^{l'}$, then specify P_s^l and set $P_\sigma^0 = 0$. It is convenient to transform to new variables $q_{\alpha\mathbf{k}}$, $R_s^{\mathbf{k}}$ instead of $p_s^{l'}$ and $P_s^{l'}$:

$$\mathbf{p}_{s'}^{l'} = \frac{ea}{M}\sum_{\mathbf{k},\alpha} \mathbf{p}_{s'}^{\alpha,\mathbf{k}} q_{\alpha\mathbf{k}} \exp\{i\mathbf{k}\mathbf{r}_{s'}^{l'}\}; \tag{15}$$

$$\mathbf{P}_{s'}^{l'} = \frac{ea}{M}\sum_{\mathbf{k}}\Big[\sum_{\alpha} \mathbf{P}_{s'}^{\alpha,\mathbf{k}} q_{\alpha\mathbf{k}} + \mathbf{R}_{s'}^{\mathbf{k}}\Big] \exp\{i\mathbf{k}\mathbf{r}_{s'}^{l'}\},$$

where $q_{\alpha\mathbf{k}}$ are the normal coordinates of crystal, $p_{s'}^{\alpha,\mathbf{k}}$, $P_{s'}^{\alpha,\mathbf{k}}$ are the amplitudes of the lattice vibration of an ideal lattice normalized so that

$$\sum_s \mu_s \mathbf{p}_s^{\alpha,\mathbf{k}} \mathbf{p}_s^{\alpha',-\mathbf{k}} = \delta_{\alpha,\alpha'},$$

where $\mu_s = m_s/\mu$; $\mu = m_1 m_2/(m_1 + m_2)$ is the reduced mass of an ion pair, α is the index of the branch of oscillations. Similarly the fields acting on the dipole $P_s^{l'}$ are expanded in Fourier series:

$$\mathbf{E}^0(\mathbf{r}_{s'}^{l'}) = -\frac{2ie}{Ma^2}\sum_{\mathbf{k}} \mathbf{E}_{s'}^{0\mathbf{k}} \exp\{i\mathbf{k}\mathbf{r}_{s'}^{l'}\};\ \mathbf{r}_{s's}^{l'l}/|\mathbf{r}_{s's}^{l'l}|^3$$

$$= -\frac{2ie}{Ma^3}\sum_{\mathbf{k}} \vec{\Psi}_{m\mathbf{k}} \exp\{i\mathbf{k}\mathbf{r}_{s's}^{l'l}\}; \tag{16}$$

$m = 1$ for $s' = s$

and $m = 2$ for $s' \neq s$:

$$\beta_{s'\sigma}\gamma_{s'\sigma}^{l'0} = -\frac{2ie}{Ma^2} h_{s'\sigma} \sum_{\mathbf{k}} \mathbf{A}_{\mathbf{k}} \exp\{i\mathbf{k}\mathbf{r}_{s'}^{l'}\};$$

$$(\bar{\beta}_{\sigma s} - \beta_{\sigma s})\,\gamma_{s's}^{l'l} = -\frac{2ie}{Ma^2}\Delta h_{\sigma s}\sum_{\mathbf{k}} \mathbf{A}_{\mathbf{k}} \exp\{i\mathbf{k}\mathbf{r}_{s'}^{l'}\}.$$

Here

$$\mathbf{G}_{s'}^{l'} = -\frac{2ie}{Ma^2}\sum_{\mathbf{k}} \mathbf{G}_{s'}^{\mathbf{k}} \exp\{i\mathbf{k}\mathbf{r}_{s'}^{l'}\}; \quad h_{s'\sigma} = \frac{a^2}{e}\beta_{s'\sigma}|_{r=a},$$

$$\mathbf{G}_{s'}^{\mathbf{k}} = \mathbf{E}_s^{0\mathbf{k}} + \frac{\bar{e}_s - e_s}{e}\vec{\Psi}_{m\mathbf{k}} \exp\{-i\mathbf{k}\mathbf{r}_s^l\} \tag{17}$$

$$-\frac{e_\sigma}{e}\vec{\Psi}_{m\mathbf{k}} + h_{s'\sigma}\mathbf{A}_{\mathbf{k}} - \Delta h_{\sigma s}\exp\{-i\mathbf{k}\mathbf{r}_s^l\}\,\mathbf{A}_{\mathbf{k}}.$$

$$(E_x' + E_x'')_{\mathbf{r}_{s'}^{l'}} = \frac{e}{Ma^2}\sum_{\mathbf{k}} \exp\{i\mathbf{k}\mathbf{r}_{s'}^{l'}\} \tag{18}$$

$$\times\sum_{s''y}\varphi_{s's''xy}^{\mathbf{k}}\Big[\sum_{\alpha}(p_{s''y}^{\alpha,\mathbf{k}} + P_{s''y}^{\alpha,\mathbf{k}})\,q_{\alpha\mathbf{k}} + R_{s''y}^{\mathbf{k}}\Big],$$

$$\sum_{s''l''}^{(n)} (\mathbf{u}_{s'}^{l'} - \mathbf{u}_{s''}^{l''})\,\nabla\beta_{s's''x}$$

$$= \frac{e}{Ma^2}\sum_{\alpha\mathbf{k}x}(p_{s'x}^{\alpha\mathbf{k}} g_{s'1x}^{\mathbf{k}} + p_{s''x}^{\alpha,\mathbf{k}} g_{s'2x}^{\mathbf{k}})\,q_{\alpha\mathbf{k}} \exp\{i\mathbf{k}\mathbf{r}_{s'}^{l'}\}.$$

For a lattice of the NaCl type the quantities $\Psi_{m\mathbf{k}}$ and $\varphi_{ss'xy}$ were calculated by us previously[6,8] over 1/8 of the reciprocal lattice cell for all oblique-angled components of the wave vector k.

For this lattice a direct calculation yields

$$\mathbf{A}_{\mathbf{k}} = \mathbf{e}_x \sin ak_x + \mathbf{e}_y \sin ak_y + \mathbf{e}_z \sin ak_z;$$

$$g_{s'1x}^{\mathbf{k}} = \frac{e}{e_{s'}}\Big[4h_{s's''} + \frac{2a^3}{e}\frac{d\beta_{s's''}}{\partial r}\Big]; \tag{19}$$

$$g_{s'2x}^{\mathbf{k}} = \frac{e}{e_{s'}} 2h_{s's''}(\cos ak_x + \cos ak_y + \cos ak_z)$$

$$+ \frac{e}{e_{s'}}\Big[-2h_{s's''} + \frac{2a^3}{e}\frac{d\beta_{s's''}}{\partial r}\Big]\cos ak_x$$

As was shown previously,[5] a fairly good agreement with experiment may be obtained for a series of alkali halide crystals if one neglects the quantity β_{12} compared with β_{21}. Then

$$g^{\mathbf{k}}_{11x} = 0; \tag{19'}$$

$$g^{\mathbf{k}}_{21x} = g = -4h_{21} - (2a^3 / e)\, d\beta_{21} / dr;$$

$$g^{\mathbf{k}}_{12x} = 0;$$

$$g^{\mathbf{k}}_{22x} = [-2h_{21}(\cos ak_x + \cos ak_y + \cos ak_z) + (g + 6h_{21}) \cos ak_x].$$

In the notation of Eqs. (17) and (18), the expressions for the dipole moments in the Fourier components can be written in the form:

$$\sum_{\alpha} P^{\alpha,\,\mathbf{k}}_{s'x} q_{\alpha\mathbf{k}} + R^{\mathbf{k}}_{s'x} = A_{s'} \Big\{ \sum_{s''y} \varphi^{\mathbf{k}}_{s's''xy} \Big[\sum_{\alpha} (p^{\alpha,\,\mathbf{k}}_{s'y} + P^{\alpha,\,\mathbf{k}}_{s'y})\, q_{\alpha\mathbf{k}} + R^{\mathbf{k}}_{s''y} \Big] - (p^{\alpha,\,\mathbf{k}}_{s'x} g^{\mathbf{k}}_{s'1x} + p^{\alpha,\,\mathbf{k}}_{sx} g^{\mathbf{k}}_{s'2x})\, q_{\alpha\mathbf{k}} - 2iG^{\mathbf{k}}_{s'x} \Big\}; \tag{20}$$

$$A_{s'} = \alpha_{s'} / a^3.$$

In the absence of the field $G^{\mathbf{k}}_{s'}$ Eqs. (20) give the expressions for dipole moments of electron shells for free lattice vibrations and are satisfied exactly for any $q_{\alpha\mathbf{k}}$. The solution of the remaining equations for the ionic polarizability component

$$\sum_{s''y} C^{\mathbf{k}}_{s's''xy} R_{s''y} = -2iG^{\mathbf{k}}_{s'x},$$

$$\text{where } C^{\mathbf{k}}_{s's''xy} = \delta_{xy}\delta_{s's''} / A_{s'} - \varphi^{\mathbf{k}}_{s's''xy}$$

has the form

$$R^{\mathbf{k}}_{s'x} = -2i \sum_{s''y} C^{-1\mathbf{k}}_{s's''xy} G^{\mathbf{k}}_{s''y}. \tag{21}$$

In the same way in the dipole approximation, the effect of the position of the anomalous lattice site on the form of the ψ wave function of the remaining ions istaken into account.

4. EVALUATION OF THEPOTENTIAL AND KINETIC ENERGY OF THE EXCESS CHARGE

If we add the expression for the mean Hamiltonian of Eq. (10) taken for the wave functions Ψ^{l}_{s} to the energy of ideal lattice we obtain

$$H\binom{ll}{ss} = \overline{H}_{\mathrm{id}} - \sum_{s'l'} (\mathbf{P}^{l'}_{s'}\mathbf{G}^{l'}_{s'} + \mathbf{p}^{l'}_{s'}\mathbf{F}^{l'}_{s'}) + V\binom{l}{s} + H_1, \tag{22}$$

$$\mathbf{F}^{l'}_{s'} = \mathbf{E}^0(r^{l'}_{s'}) + \frac{\overline{e}_s - e_s}{|\mathbf{r}^{l'l}_{s's}|^3}\mathbf{r}^{l'l}_{s's} - \frac{e_\sigma}{|\mathbf{r}^{l'}_{s'}|^3}\mathbf{r}^{l'}_{s'} - \frac{1}{e_{s'}r}\frac{\partial \Delta u(r)}{\partial r}\bigg|_{r=a}\mathbf{r}^{l'l}_{s's} + \frac{1}{e_{s'}r}\frac{\partial u(r)}{\partial r}\bigg|_{r=a}\mathbf{r}^{l'}_{s'} + \frac{\delta_{s's}\delta_{l'l}}{e_{s'}}\Big[(\overline{e}_s - e_s)\,\mathbf{E}^0(\mathbf{r}^l_s) + \overline{e}_\sigma(e_s - e_s)\frac{\mathbf{r}^l_s}{|\mathbf{r}^l_s|^3} + \frac{1}{a}\frac{\partial \Delta u}{\partial r}\bigg|_{r=a}\mathbf{r}^l_s\Big]. \tag{23}$$

$$V\binom{l}{s} = -E_{\sigma 0} + \Delta E_{s0} + \frac{e^2_\sigma \alpha_m}{a} - \frac{(\overline{e}_s - e_s)\ {}_s\alpha_m}{a} - nu(a) + n\Delta u(a) - \frac{e_\sigma(\overline{e}_s - e_s)}{r^l_s} + (\overline{e}_s - e_s)\, v(\mathbf{r}^l_s) - e_\sigma v(0) + \Delta u \gamma^{l0}_{s\sigma'}. \tag{24}$$

where H_1 denotes all terms of the second order in $\mathbf{p}^{l'}_{s}$, $\mathbf{P}^{l'}_{s}$ which are due to the formation of a defect and an anomalous ion and which will be neglected in the further calculation. The presence of these terms destroys the translation symmetry and makes a solution of the problem very difficult.

Substituting Eq. (15), and using the fact that the amplitudes of $\mathbf{p}^{\alpha,\mathbf{k}}_{s}$, $\mathbf{P}^{\alpha,\mathbf{k}}_{s}$ are the solutions of the system

$$-(m_s / e^2_s)\, \omega^2_{\alpha\mathbf{k}} p^{\alpha,\,\mathbf{k}}_s = -\partial\overline{H}_{\mathrm{id}} / \partial \mathbf{p}^{\alpha,\,\mathbf{k}}_s;$$

$$0 = -\partial\overline{H}_{\mathrm{id}} / \partial \mathbf{P}^{\alpha,\,\mathbf{k}}_{s'};$$

Eq. (22) can be written in the form

$$H\binom{ll}{ss} = \frac{e^2}{2aM}\sum_{k}\Big\{\sum_{\alpha}[\Omega^2_{\alpha,\mathbf{k}} q_{\alpha,\,\mathbf{k}} q_{\alpha,\,-\mathbf{k}} + 4i(\mathbf{p}^{\alpha,\,\mathbf{k}}_{s'}\mathbf{F}^{-\mathbf{k}}_{s'} + \mathbf{P}^{\alpha,\mathbf{k}}_{s'}\mathbf{G}^{-\mathbf{k}}_{s'})\, q_{\alpha\mathbf{k}}] + 4i\sum_{s'}\mathbf{R}^{\mathbf{k}}_{s'}\mathbf{G}^{-\mathbf{k}}_{s'}\Big\} + V\binom{l}{s} + H_1 + \text{const}, \tag{25}$$

where $\mathbf{F}^{\mathbf{k}'}_{s}$ is the Fouriercomponentof theexpansion of $\mathbf{F}^{l'}_{s}$

$$\mathbf{F}_{s'}^{l'} = -\frac{2ie}{Ma^2}\sum_{\mathbf{k}} \mathbf{F}_{s'}^{\mathbf{k}} \exp\{i\mathbf{k}\mathbf{r}_{s'}^{l'}\}, \tag{26}$$

$$\mathbf{F}_{s'}^{\mathbf{k}} = \mathbf{E}_{s'}^{0k} + \frac{\bar{e}_s - e_s}{e}\Psi_{m\mathbf{k}}\exp\{-i\mathbf{k}\mathbf{r}_s^l\} - \frac{e_\sigma}{e}\Psi_{m\mathbf{k}}$$
$$+\left[\frac{e_{s'}}{e}(1-\delta_{ss'})\,\Delta H\exp\{-i\,\mathbf{k}\mathbf{r}_s^l\} - H\frac{e_{s'}}{e}(1-\delta_{\sigma s'})\right]\mathbf{A}_\mathbf{k}$$
$$-\frac{\delta_{ss'}}{2ie}\left[a^2\frac{\bar{e}_s - e_s}{e_s}e_\sigma\frac{\mathbf{r}_s^l}{|r_s^l|^3}\exp\{-i\mathbf{k}\mathbf{r}_s^l\} + \frac{e_s}{a}\Delta H\mathbf{r}_s^l\exp\{-i\mathbf{k}\mathbf{r}_s^l\}\right.$$
$$\left.+\frac{a^2(\bar{e}_s - e_s)}{e_s}\mathbf{E}^0(\mathbf{r}_s^l)\exp\{-i\mathbf{k}\mathbf{r}_s^l\}\right]; \quad H = -\frac{a^2}{e^2}\frac{\partial u(r)}{\partial r}\bigg|_{r=a};$$

where ΔH denotes the change in H if only one ion is anomalous.

The expression (25) plays the role of the potential energy of the excess charge which is present at the lattice site s,l.

The wave function of the moving charge is sought in the form of the linear combination

$$\Psi_s = \sum b_s^l \Psi_s^l, \tag{27}$$

where the coefficients $b_s{}^l$ will be evaluated from the variational principle—the minimum of $\bar{H}$:

$$\bar{H} = \int \Psi_s^* \hat{H}\Psi_s d\tau = \sum_{ll'} b^{l*} b_s^{l'} H\left(\begin{smallmatrix} ll' \\ ss \end{smallmatrix}\right), \tag{28}$$
$$H\left(\begin{smallmatrix} ll' \\ ss \end{smallmatrix}\right) = \int \Psi_s^{l*}\hat{H}\Psi_s^{l'} d\tau, \qquad \sum_l |b_s^l|^2 = 1.$$

The matrix elements $H\left(\begin{smallmatrix} ll \\ ss \end{smallmatrix}\right)$ $l' \neq l$ play the role of the kinetic energy since they depend on two positions of the charge near the lattice sites s, l and s,l' analogously to the operator $\Delta\psi$. In view of the orthogonality condition of Eq. (3) and the small overlaps of the wave functions of the remote ions, it is sufficient to retain only the subdiagonal matrix elements $H\left(\begin{smallmatrix} ll \\ ss \end{smallmatrix}\right)$ when the sites s, l and s,l' are the nearest neighbors of the same kind. Furthermore, we neglect in them the dependence of the wave function of ions ψ on the position of the anomalous site and we shall consider them equal to $\psi_{s\,0}{}'$ and retain in the integrals of Eq. (20) only those terms in which the permutation in $\Psi_s{}^{l'}$ differs from the permutation in Ψ_s^l by the transposition of one electron from the anomalous site s,l' to the site s,l (or conversely in the case of a hole). Then the Hamiltonian $\hat{H}$ retains only those terms which contain the coordinates of the transposed electron $\boldsymbol{\rho}$. This is the kinetic energy $-(\hbar^2/2m)\Delta\rho$ and the energy of its interaction with all electrons and charges of the surrounding ions. The potential of the external field can be neglected in view of its uniformity and the condition of Eq. (3). Integration over the coordinates of electrons of the remaining ions gives the sum of their potentials at the point ρ:

$$\sum_{s''\,l''}{}'' V_{s''}(\boldsymbol{\rho} - \mathbf{R}_{s''}^{l''}).$$

The result is

$$H\left(\begin{smallmatrix} li' \\ ss \end{smallmatrix}\right) = \int \psi_s^{l'^*}\varphi_s^{l*}\left\{-\frac{\hbar^2}{2m}\Delta_\rho\right.$$
$$-e\sum_{s''l''}{}'' V_{s''}(\boldsymbol{\rho} - \mathbf{R}_{s''}^{l''}) + \sum_{n_s}\frac{e^2}{|\boldsymbol{\rho} - \boldsymbol{\rho}_{sn_s}^l|} \tag{29}$$
$$+\sum_{n_{s'}}\frac{e^2}{|\boldsymbol{\rho} - \boldsymbol{\rho}_{sn_s}^{l'}|} - \frac{e^2 z_s}{|\boldsymbol{\rho} - \mathbf{R}_s^l|}$$
$$\left. - \frac{e^2 z_{s'}}{|\boldsymbol{\rho} - \mathbf{R}_s^{l'}|}\right\}\psi_s^l\varphi_s^{l'} d\tau.$$

For the case of an extra electron in a lattice constructed of ions with closed shells (for example, NaCl), one may set $\varphi_s^l = \psi_s^l \chi_s(\rho - R_s^l)$. Then the integration over the coordinates $\rho_{sn_s}^l$, $\rho_{sn_s}^{l'}$ gives the sum of potentials of these ions

$$V_s(\boldsymbol{\rho} - \mathbf{R}_s^l) + V_s(\boldsymbol{\rho} - \mathbf{R}_s^{l'}).$$

Since in the integrals over ρ the main role is played by the terms with $\rho \approx 1/2\,(\mathrm{R}_s^l + \mathrm{R}_s^{l'})$, i.e., members sufficiently remote from the remaining ions, one may set

$$\sum_{s''l''}{}'' V_{s''}(\boldsymbol{\rho} - \mathbf{R}_{s''}^{l''}) \approx \sum{}'' - ee_{s''}/|\boldsymbol{\rho} - \mathbf{R}_{s''}^{l''}|.$$

We shall add this sum to the potential of all ions. If one neglects its weak dependence on the displacement of ions, then one may neglect it entirely in view of the fact that this potential has a plateau near

$$\boldsymbol{\rho} = {}^1\!/_2(\mathbf{r}_s^l + \mathbf{r}_s^{l'})$$

and is equal to zero at its center because of the symmetry of the lattice. Then

$$H\binom{ll'}{ss} = \int \chi_s^*(\boldsymbol{\rho} - \mathbf{R}_s^l)\Big\{-\frac{h^2}{2m}\Delta_\rho - eV_s(\boldsymbol{\rho} - \mathbf{R}_s^l) - eV_s(\boldsymbol{\rho} - \mathbf{R}_s^{l'}) + \frac{ee_s}{|\boldsymbol{\rho} - \mathbf{r}_s^l|} + \frac{ee_\sigma}{|\boldsymbol{\rho}|} + \frac{ee_s}{|\boldsymbol{\rho} - \mathbf{r}_s^{l'}|}\Big\}\chi_s(\boldsymbol{\rho} - \mathbf{R}_s^{l'})\,d\tau. \tag{30}$$

For the case of a hole one uses Eq. (29). As a rough approximation one may suppose that

$$\psi_s^l = \varphi_s^l \chi_s^l(\boldsymbol{\rho} - \mathbf{R}_s^l).$$

Then an expression similar to Eq. (30) is obtained, only it is necessary to move the star from

$$\chi_s(\boldsymbol{\rho} - \mathbf{R}_s^l) \quad \text{to} \quad \chi_s(\boldsymbol{\rho} - \mathbf{R}_s^{l'}),$$

and the potential V_s replaced by the potential of ions deficient in electrons:

$$\overline{V}_s(\boldsymbol{\rho} - \mathbf{R}_s^l) = V_s(\boldsymbol{\rho} - \mathbf{R}_s^l) + e\int \frac{|\chi_s(\boldsymbol{\rho}' - \mathbf{R}_s^l)|^2}{|\boldsymbol{\rho} - \boldsymbol{\rho}'|}\,d\tau'. \tag{31}$$

Since the product

$$\chi^*(\boldsymbol{\rho} - \mathbf{R}_s^l)\,\chi(\boldsymbol{\rho} - \mathbf{R}_s^{l'}),$$

is sensitive to the change in the separation between the ions R_{ss}^{ll}, we shall expand $H\binom{ll'}{ss}$ in the powers of the displacements of these ions. Transforming to normal coordinates we obtain, using Eq. (15) in a linear approximation [sufficiently good in view of the small value of $H\binom{ll'}{ss}$]:

$$H\binom{ll'}{ss} = I_{ss}^{ll'} + \frac{2ie^2}{aM}\sum_{\alpha,\mathbf{k}} I_{ss\alpha\mathbf{k}}^{ll'} q_{\alpha\mathbf{k}};$$
$$I_{ss\alpha\mathbf{k}}^{ll'} = \frac{a^2}{2iee_s|\mathbf{r}_{ss}^{ll'}|}\frac{dH\binom{ll'}{ss}}{dR_{ss}^{ll'}} \tag{32}$$
$$\times\, \mathbf{p}_s^{\alpha\mathbf{k}}\mathbf{r}_{ss}^{ll'}(\exp\{i\mathbf{k}\mathbf{r}_s^l\} - \exp\{i\mathbf{k}\mathbf{r}_s^{l'}\}),$$

$$I_{ss}^{ll'} = H\binom{ll'}{ss}_{\mathbf{R}_{ss}^{ll'} = \mathbf{r}_{ss}^{ll'}}. \tag{33}$$

5. EVALUATION OF THE SELF CONSISTENT ELECTRON (HOLE) STATES

In evaluation of the energy of the local state we shall assume with Pekar[4] that the displacement of ions corresponds to the minimum of the average energy $\overline{H}$, i.e., we shall seek the self-consistent state. For states of small radius, it is not sufficient to limit oneself to the calculation of the interaction only with the longitudinal optical branch of vibrations and neglect the dispersion, as was done by Pekar.[4] Our expressions allow us to calculate the states of any arbitrary radius. We must minimize the average energy $\overline{H}$ of Eq. (28) both over b_s^l and over $q_{\alpha\mathbf{k}}$. The latter may be carried out in a general way. Substituting Eqs. (25) and (32) into Eq. (28) we obtain the equilibrium displacement from the condition $\partial\overline{H}/\partial q_{\alpha,-\mathbf{k}} = 0$:

$$q_{\alpha,\mathbf{k}} = q_{\alpha,\mathbf{k}}^0 = -2i\Omega_{\alpha,\mathbf{k}}^{-2}\Big[\sum_l |b_s^l|^2(\mathbf{p}_{s'}^{\alpha,-\mathbf{k}}\mathbf{F}_{s'}^{\mathbf{k}} + \mathbf{P}_{s'}^{\alpha,-\mathbf{k}}\mathbf{G}_{s'}^{\mathbf{k}}) + \sum_{ll'} b_s^{l*}b_s^{l'}I_{ss\alpha,-\mathbf{k}}^{ll'}\Big]. \tag{34}$$

It is necessary to keep in mind that $q^\circ_{\alpha,\mathbf{k}}$ is determined not by the instantaneous but the quantum-mechanical average of the position of the anomalous site l,s and thus the quantity

$$\Omega_{\alpha\mathbf{k}}^2 q_{\alpha\mathbf{k}} q_{\alpha,-\mathbf{k}}$$

in Eq. (28) may be taken out of the summation over l. Using Eqs. (34), (25) and (32) we obtain from Eq. (28):

$$\overline{H} = (2e^2/aM) \tag{35}$$
$$\times \sum_{\mathbf{k},\alpha}\Omega_{\alpha\mathbf{k}}^{-2}\Big\{\sum_l |b_s^l|^2(\mathbf{p}_{s'}^{\alpha,-\mathbf{k}}\mathbf{F}_{s'}^{\mathbf{k}} + \mathbf{P}_{s'}^{\alpha,-\mathbf{k}}\mathbf{G}_{s'}^{\mathbf{k}})$$
$$+ \sum_{ll'}{}' b_s^{l*}b_s^{l'}I_{ss'\alpha,-\mathbf{k}}^{ll'}\Big\}\Big\{\sum_l |b_s^l|^2(\mathbf{p}_{s'}^{\alpha,\mathbf{k}}\mathbf{F}_{s'}^{-\mathbf{k}}$$
$$+ \mathbf{P}_{s'}^{\alpha,\mathbf{k}}\mathbf{G}_{s'}^{-\mathbf{k}}) + \sum{}' b_s^{l*}b_s^{l'}I_{ss\alpha\mathbf{k}}^{ll'}\Big\}$$
$$+ \sum_l |b_s^l|^2\Big\{\frac{4e^2}{aM}\sum_{\substack{hs's''\\xy}} G_{s'x}^{-\mathbf{k}}C_{s's''xy}^{-1\mathbf{k}}G_{x''y}^{\mathbf{k}} + V\binom{l}{s}\Big\}$$
$$+ \sum_{ll'}{}' b_s^{l*}b_s^{l'}I_{ss}^{ll'}.$$

Minimizing Eq. (35) over b_s^1, it is not possible to obtain the minimum of Eq. (35) over b_s^l for a general case. It is necessary to carry out minimizing for each particular case by numerical method since $\partial\overline{H}/\partial b_s^l = 0$ gives a system of cubical equations for b_s^l. In order to solve these equations one must know all

$$\Omega_{\alpha,\mathbf{k}},\ \mathbf{p}_s^{\alpha,\mathbf{k}},\ \mathbf{P}_s^{\alpha,\mathbf{k}},\ I_{ss}^{ll'},\ I_{ss\alpha,\mathbf{k}}^{ll'},$$

and also the parameters

$$h_{s's},\ \Delta h,\ H,\ \Delta H.$$

The problem may be simplified by making use of the symmetry of the lattice and thus reducing the number of independent coefficients b_s^l. For example, for the ground state of an F–center b_s^l are identical for all ions equidistant from the vacant site σ and it is sufficient to limit b_s^l to the first and the third configuration spheres. Thanks to the normalization condition

$$\sum_l |b_s^l|^2 = 1$$

only one approximation parameter remains.

The proposed method is useful also for the calculation of hole states of small radii for which a theory is lacking at present.

---

[1] T. I. Liberberg and K. B. Tolpygo, J. Exptl. Theoret. Phys. (U.S.S.R.) 26, 35 (1954). Scient. Progress Reports of Shevihenko Kiev State University 14; Phys. Series, 7, 21 (1955).

[2] S. I. Pekar, J. Exptl. Theoret. Phys. (U.S.S.R.) 18, 525 (1948).

[3] W. Heisenberg, Ann. Physik 10,888 (1931).

[4] S. I. Pekar, *Investigation of the electron theory of crystals*, GTTI, Moscow-Leningrad 1951.

[5] K. B. Tolpygo, J. Exptl. Theoret. Phys. (U.S.S.R.) 20, 497 (1950).

[6] T. I. Kucher, J. Exptl. Theoret. Phys. (U.S.S.R.) 30, 724 (1956); Soviet Phys. JETP 3,580 (1956).

[7] K. B. Tolpygo, Mathem. symp. of Kiev State University 5, 99(1951).

[8] K. B. Tolpygo and I. G. Zaslavskaia, Ukrain. Fiz. Zh. 1, 226 (1956).

Translated by M. J. Stevenson
214

SOVIET PHYSICS JETP VOLUME 4, NUMBER 6 JULY, 1957

On Distributions in Representation Space

R. L. STRATONOVICH
Moscow State University

(Submitted to JETP editor September 29, 1955)
J. Exptl. Theoret. Phys. (U.S.S.R.) 31, 1012-1020 (December, 1956)

The concept of representation distributions is introduced for quantum systems. The quantum generalization is found for certain relations in the theory of correlated random points. The general formulas are illustrated in a concrete way for the cases of distribution of spin orientation.

THE statistical nature of quantum theory is manifested in the process of physical "measurement." From this it follows that the "pre-observation" state of a quantum system, which exists before the "measurement" and is independent of it (one can speak of such a state, to be understood in a definite sense), is a statistical state.

In the classical theory the "pre-observation" state of a statistical system is described by distribution functions in a certain space (we denote this space by M). We assume that in the quantum theory such a "pre-observation" state is described by distribution functions in this same "representation" space M, which accordingly has a classical meaning. But owing to the fact that a quantum "measurement" is more complicated than a macroscopic measurement, and is inevitably associated with an integral operation in the representation space, in contrast to the classical situation, negative values of the distribution function are possible at particular points of this space. The "representation distributions" of course do not give an entirely classical interpretation of quantum theory, but they provide a basis for that interpretation of the quantum theory which has maximum closeness to classical ideas and thus has the greatest physical-intuitive meaning.

1. We define the "representation distribution" by the following requirements.

1) The space in which it is defined has a classical meaning, for example, phase space or the space of directions.

2) The distribution can be expressed linearly in terms of the density matrix ρ. This requirement is directly related to the linearity of the whole apparatus of quantum theory, i.e., it is connected with the statistical interpretation of the theory. The density matrix, like any other operator A, has associated wtih it a function in the representation space

$$\rho(M) = \operatorname{Tr} \rho L(M); \quad A(M) = \operatorname{Tr} AL(M) \qquad (1)$$

by means of the kernel $L(M)$, which is an operator depending on the point M as a parameter.

3) The distribution must be a real function; in general, to a Hermitian operator there must correspond a real function $A(M)$. This requirement amounts to the condition of Hermiticity of the operators $L(M)$ for all points M.

4) Statistical averaging of the classical functions $A(M)$ must give the same results as the rule for averaging of operators

$$\int A(M)\rho(M)\,dM = \operatorname{Tr} A\rho. \qquad (2)$$

From Eqs. (1) and (2) there follows the formula

$$A = \int A(M) L(M)\,dM. \qquad (3)$$

Thus the condition (4) is equivalent to the requirement that the direct and inverse transformations are accomplished by means of the same kernel.

Regarding the operators $A, B, \ldots$ as elements of a complex Euclidean space with scalar product—the trace $(A,B) = \operatorname{Tr} AB^*$ (B^* is the Hermitian adjoint to B)—we introduce an orthonormal basis $A_1, A_2, \ldots$ ($\operatorname{Tr} A_i A_j^* = \delta_{ij}$). The kernel $L(M)$ is represented by the expansion

$$L(M) = \sum_i A_i^* A_i(M), \quad (A_i(M) = \operatorname{Tr} A_i L(M)). \qquad (4)$$

It is readily proved that the requirement (4) is equivalent to the condition

$$\int A_i(M) A_j^*(M)\,dM = \delta_{ij}. \qquad (5)$$

According to Eq. (2) the normalization condition $\operatorname{Tr}\rho = 1$ takes the form

$$\int \rho(M)\lambda(M)\,dM = 1; \quad (\lambda(M) = \mathrm{Tr} L(M)). \tag{6}$$

Consequently, as the normalized density of the distribution we must take

$$w(M) = \rho(M)\lambda(M) \tag{7}$$

and the rule for averaging must be written in the form

$$\overline{A} = \int A(M)\lambda^{-1}(M)\,w(M)\,dM = \overline{A(M)\lambda^{-1}(M)}. \tag{8}$$

The definition presented above, together with simple transformation principles that give the connection with the specific physical case, can be applied to derive concrete distributions.

An important special case is the Wigner distribution in phase space

$$w(p, q) = h^{-n}\int e^{ivp/\hbar}\,\rho_{q+v/2,\ q-v/2}\,d^n v \tag{9}$$

(n is the number of degrees of freedom), which is frequently considered in connection with the statistical interpretation of quantum mechanics.[1] For this case $L(M)$ has the form

$$L_{x'x''} = \pm h^{-n/2} e^{i(x'-x'')p/\hbar}\,\delta\left(q - \frac{x'+x''}{2}\right). \tag{10}$$

The Wigner distribution can be derived from the definition of the "representation" distribution by applying the principles of homogeneity and equivalence of directions (invariance under translations and reflection).

2. Another example of a "representation" distribution is the peculiar distribution in the space of orientations of the spin, which corresponds to the spin degrees of freedom. We deal first with the nonrelativistic case of spin $s = 1/2$, with the spin variable taking two values and the corresponding operators being two-rowed matrices. For simplicity we shall not at once take into account the dependence of the elements of these matrices on other variables.

First of all we note the failure of Moyal's attempt[1] to generalize the Wigner distribution to cases of the spin-variable type. In this case it is natural to take as the noncommuting operators r and s two components of the spin, for example s_y and s_z. Since the "possible values" of these operators comprise only the values $s_{yj} = \pm 1/2, s_{zh} = \pm 1/2$, the characteristic function

$$\sum_{j,k} F(s_{yj}, s_{zk}) \exp\{i(\tau s_{yj} + \theta s_{zk})\}$$

[$F(\pm 1/2, \pm 1/2)$ are probabilities] defined by Moyal must be periodic in τ and θ. On theother hand, the function

$$\mathrm{Tr} \exp\{i(\tau s_y + \theta s_z)\}\rho$$

is in general not periodic, and consequently these functions cannot be equated.

The cause for the failure of Moyal's approach consists in the fact that with a discrete set of characteristic values of the "basis" operators one must not restrict the distribution to these discrete values only, but must include the continuous spectrum in the treatment. Therefore, unlike Moyal, we shall consider a continuous manifold of possible values, taken two-dimensional as before. Moreover, we choose this manifold symmetrically with respect to the three coordinate axes. The direct physical meaning of the concept "spin" suggests that as such a manifold one should take the manifold on points of a sphere

$$s_x = {}^1/_2 \cos\varphi \sin\vartheta;$$

$$s_y = {}^1/_2 \sin\varphi \sin\vartheta; \quad s_z = {}^1/_2 \cos\vartheta,$$

or the manifold of directions of the spin, i.e., a manifold invariant under space rotations. Thus by a point M of the representation space we shall mean a point of the sphere, so that $M = (\varphi, \theta)$.

The Euclidean space of two-rowed matrices is four-dimensional. As basis elements we can take the orthonormal matrices

$$A_i = \sigma_i / \sqrt{2} \quad (i = 0, 1, 2, 3), \tag{11}$$

where $\sigma_1, \sigma_2, \sigma_3$ are the Pauli matrices and σ_0 is the unit matrix.

In consequence of Eq. (4) the choice of L is equivalent to the choice of the functions $A_i(M)$. In order to have a representation distribution, it is sufficient to choose them orthonormal, real, and with $A_0 = 0$. But there will be no room left for multiple values if we take account of the transformation principle, i.e., require that the correspondence of matrix to function be of a character invariant under rotations. Using Eqs. (1), (4), and (11), we have

$$\sqrt{2}\,\rho(M) = (\rho, \sigma_0)A_0(M) + \sum_{j=1}^{3}(\rho, \sigma_j)A_j(M). \tag{12}$$

Taking note of the fact that $\rho\,(M)$, like $w\,(M)$ must be a scalar function, we examine the transformation properties of the terms appearing in Eq. (12). According to the normalization condition $(\rho\,,\sigma_0\,)$ is an invariant; consequently, $A_0\,(M)$ must also remain unchanged by rotations, i.e., must be constant over the whole sphere. Furthermore, as is well known, $(\rho\,,\sigma_j\,)$, like $\psi^*\,\sigma_j\,\psi$, are the components of a three-dimensional vector (that it is axial is immaterial). From this it follows that the functions $A_j\,(M)$ also transform on rotations like the components of a vector. This means that they must be proportional to the functions

$$n_1(\varphi,\ \vartheta) = \cos\varphi\sin\vartheta;$$
$$n_2(\varphi,\ \vartheta) = \sin\varphi\sin\vartheta;\quad n_3(\varphi,\ \vartheta) = \cos\vartheta. \tag{13}$$

Taking into account the normalization condition, we have

$$A_0(M) = \pm 1/\sqrt{4\pi};$$
$$\mathbf{A}(M) = \pm\sqrt{3/4\pi}\,\mathbf{n}(\varphi,\ \vartheta). \tag{14}$$

These functions satisfy all of the conditions: they are orthonormal and real, and $\lambda = \pm A_0$ tr $\sigma_0/2^{1/2} = \pm 1/(2\pi)^{1/2} \neq 0$. With this choice the desired functions have, according to Eqs. (4) and (7), the form

$$L(\varphi,\ \vartheta) = \pm(8\pi)^{-1/2}[\sigma_0 + \sqrt{3}\ \sigma\mathbf{n}(\varphi,\ \vartheta)]; \tag{15}$$

$$w(\varphi,\ \vartheta) = (1/4\pi)\,[1 + \sqrt{3}\,\mathbf{n}(\varphi,\ \vartheta)\ \mathrm{tr}\,(\sigma\rho)]. \tag{16}$$

Let us consider the special case of a diagonal density matrix in the z-representation:

$$\rho = \|\, c_k\delta_{kl}\,\| = {}^1/_2\sigma_0 + {}^1/_2\,(c_1 - c_2)\,\sigma_3.$$

In this case, by Eq. (16),

$$w(\varphi, \vartheta) = (1/4\pi)\,[1 + \sqrt{3}\,(c_1 - c_2)\cos\vartheta]. \tag{17}$$

In the other special case of a "pure" state $\rho = \psi\psi^*$ we have

$$w(\varphi,\ \vartheta) = (1/4\pi)\,[1 + \sqrt{3}\,\mathbf{n}(\varphi,\ \vartheta)\,\psi^*\sigma\psi]$$
$$= (1/4\pi)\,[1 + \sqrt{3}\cos\alpha], \tag{18}$$

where α is the angle between the direction considered and the average, most probable, direction of the spin.

3. An analogous method for the derivation of the representation distribution can be applied in the case of an arbitrary spin s. The wave function consists of a column of the $2s+1$ components ψ^i $(i = -s\,,\ldots,s\,)$, which are the components of a contravariant irreducible s-tensor; the complex conjugate quantities are the components of the covariant tensor. The products $^{i*}\,\psi^j = \psi^*\,B^j_i\,\psi\,(i,j = -s,\ldots,s\,)$ are therefore the components of a reducible tensor of the second rank, covariant in the index i and contravariant in j. Here B^j_i denotes the matrix with the elements

$$(B^j_i)_{kr} = \delta_{ki}\delta_{jr}. \tag{19}$$

According to the definition of the density matrix its elements $\rho^j_i = (B^j_i\,,\rho) = B^j_i$ have the same transformation properties. We go over from ρ^j_i to the set of irreducible l-tensors $(l = 0,\ldots, 2s\,)$. This is done by the formula

$$\bar{A}_{lm} = \sum_{i,\,j} b^{si}_{lm;sj}\rho^j_i \quad (l = 0,\ldots,2s;\quad m = -l,\ldots,l). \tag{20}$$

Here $b^{si}_{lm;sj} = \rho_l\ c^{si}_{lm;sj}$; $c^{si}_{lm;sj}$ are any appropriate tabulated values, and ρ_l are numbers chosen not only from considerations of the unitary property of the entire transformation (20), but also in such a way that the $\bar{A}_{lm}$ form an l-tensor in the strict sense, i.e., transform covariantly with the spherical functions

$$Y_{lm}(\varphi,\ \vartheta)$$
$$= (-1)^{\beta_m}\left(\frac{(2l+1)\,(l-|\,m\,|)}{4\pi\,(l+|\,m\,|)}\right)^{1/2} P^{|m|}_l(\cos\vartheta)\,e^{im\varphi};$$
$$(\beta_{2\mu} = 0;\quad \beta_{2\mu+1} = \mu).$$

Then the sums $\sum\limits_{m=-l}^{l} Y_{lm}\,\bar{A}^*_{lm}$ $(l = 0,\ldots, 2s)$ are scalars. The scalar function $\rho\,(M)$, which by Eq. (4) is given by the expansion

$$\rho(M) = \sum_{l,m} A_{lm}(M)\,\bar{A}^*_{lm}, \tag{21}$$

must be the sum of the scalars in question.

From the orthonormal property of the matrices (19) and the unitary nature of the transformation (20) there follows the orthonormal property of the basis

$$A_{lm} = \sum_{i,j} b_{lm,\, sj}^{si} B_i^j \quad (l = 0, \ldots, 2s; \; m = -l, \ldots, l). \qquad (22)$$

Since together with this the relations (5) must be satisfied, the functions $A_{lm}(M)$ must be taken in the form

$$A_{lm}(M) = \pm Y_{lm}(\varphi, \vartheta), \qquad (23)$$

where for a particular value of l the sign must be the same for all values $m = -l, \ldots, l$. Consequently

$$L(M) = \sum_{l=0}^{2s} (\pm 1) \sum_{m=-l}^{l} Y_{lm}(\varphi, \vartheta) A_{lm}^*; \qquad (24)$$

$$(\lambda = \pm Y_{00} \operatorname{tr} A_{00}^* = \pm \sqrt{(2s+1)/4\pi}).$$

The expression (24) satisfies all of the requirements, since it is Hermitian in virtue of the relations

$$Y_{lm}^* = Y^{lm} = (-1)^m Y_{l,\,-m};$$

$$A_{lm}^* = A^{lm} = (-1)^m A_{l,\,-m}. \qquad (25)$$

One can convince oneself of the last of these relations by obtaining

$$b_{lm,\, sj}^{*si} = (-1)^m b_{l,\,-m;\, si}^{sj} \equiv b_{si}^{lm;\, sj}$$

from Eq. (20), taking account of the facts that $\overline{A}_{lm}^* = \overline{A}^{lm}$ and $\rho_i^{j*} = \rho_j^i$. Thus by means of Eq. (24) we indeed obtain the representation distribution

$$w(\varphi, \vartheta) = \sqrt{\frac{2s+1}{4\pi}} \sum_{l=0}^{2s} (\pm 1) \times \sum_{m=-l}^{l} \sum_{i,j=-s}^{s} Y_{lm}(\varphi, \vartheta)\, b_{si}^{lm;\, sj} \rho_j^i. \qquad (26)$$

The signs + and – in Eqs. (24) and (26) are readily determined from the physical meaning. For this it suffices to consider special forms of distributions, for example those having axial symmetry, i.e., not depending on φ.

In the particular case when $s = 1$, for axial symmetry we have from the general formula

$$w(\varphi, \vartheta) = \sqrt{3/4\pi}\,[\pm Y_{00}(A_{00}, \rho) \pm Y_{10}(A_{10}, \rho) \pm Y_{20}(A_{20}, \rho)]$$
$$= (1/4\pi)\Big[1 \pm (3/\sqrt{2})(\rho_1^1 - \rho_{-1}^{-1}) \times \cos\vartheta \pm \frac{\sqrt{10}}{8}(\rho_1^1 + \rho_{-1}^{-1} - 2\rho_0^0)(3\cos 2\vartheta + 1)\Big]. \qquad (27)$$

According to the physical meaning, in the case of the z-representation an increase of ρ_1^1 at the expense of ρ_{-1}^{-1} must lead to an increase of the probability of the positive z-orientation of the spin. Analogously, an increase of ρ_0^0 at the expense of $\rho_1^1 + \rho_{-1}^{-1}$ must lead to an increase of the probability of the equatorial orientation. From this we find that in both terms of the last equation we must take the sign +. For the "pure" state with positive z-orientation of the spin ($\rho_1^1 = 1$; $\rho_0^0 = \rho_{-1}^{-1} = 0$) we accordingly have

$$w(\varphi, \vartheta) = (1/4\pi)\,[1 + (3/\sqrt{2})\cos\vartheta + (\sqrt{10}/8)(3\cos 2\vartheta + 1)]. \qquad (28)$$

This last formula gives a sharper maximum than Eq. (18). With increase of the spin it is natural to expect a tendency of the corresponding expressions toward a δ-like distribution.

4. Up to now we have considered the distribution in dynamical and spin variables separately. No difficulty is presented by the generalization to the case when the elements of the density matrix $\rho_{x,x'}$ depend on both types of variables: $x = (q, \sigma)$ (for conveneince we shall use a form of writing as if all variables were continuous).

As the basic operators of the extended operator space we may take the products $A_i A_{lm}$ of basis operators of the original bases. In the space of representation functions the products $A_i(p, q)$ $A_{lm}(\varphi, \theta)$ of the original basis functions will form an orthonormal system. The fulfillment of the other requirements for the extended system also follows from their fulfillment for the original systems. Therefore the combined representation distribution can be found by means of the kernel

$$L(p, q; \varphi, \vartheta) = L_1(p, q)\, L_2(\varphi, \vartheta);$$
$$\lambda = \lambda_1 \lambda_2 = \pm h^{-n/2} \sqrt{(2s+1)/4\pi}. \qquad (29)$$

For the same reason the same multiplicative law holds in the case of N particles:

$$L(M_1, \ldots, M_N) = L_1(M_1) \ldots L_N(M_N); \qquad \operatorname{Tr} L(M_1, \ldots, M_N) = \lambda^N. \tag{30}$$

Here M_i are the "representation" variables of the ith particle, for example $p_i, q_i, \varphi_i, \theta_i$, and $L_i(M_i) = [L(M_i)]_{x_i, x'_i}$.

The corresponding "distribution density"

$$w_N(M_1, \ldots, M_N) = \lambda^N (L_1(M_1) \ldots L_N(M_N), \rho_N) \tag{31}$$

can be understood in two ways. On one hand, (31) is the distribution in the N-fold representation space. On the other hand, $w_N(M_1, \ldots, M_N)$ can be understood as an N-fold "distribution density" in a one-fold space, while $M_1, \ldots, M_N$ are different points of this space. The second point of view has a great advantage over the first in the case of an unspecified (chance) number of particles.

5. In the case of a chance number of particles it is convenient to make use of the apparatus of second quantization. For simplicity we shall restrict ourselves as before to the nonrelativistic case, for which the operator wave functions satisfy the commutation relations

$$\Psi(x)\Psi^*(x') - \Psi^*(x')\Psi(x) = \delta(x - x') \tag{32}$$

(for definiteness we shall confine ourselves to bosons). The state of the system is described by an operator for state $R = \mathrm{M}\,\Phi\Phi^*$. The vacuum state operator R_0 is defined by the equations

$$\Psi(x) R_0 \equiv 0; \qquad R_0 \Psi^*(x) \equiv 0. \tag{33}$$

We consider the operators

$$(F_r)_{x_1 \ldots x_r;\, x'_1 \ldots x'_r} = \Psi^*(x'_r) \ldots \Psi^*(x'_1)\Psi(x_1) \ldots \Psi(x_r), \tag{34}$$

which, using the concept of an "ordered" N-product introduced by Wick,[2], we can write

$$F_r = N(F_1 \ldots F_1). \tag{35}$$

Expanding them in terms of an orthonormal basis,

$$(r!\,s!)^{-1/2}\Psi^*(x'_s) \ldots \Psi^*(x'_1) R_0 \Psi(x_1) \ldots \Psi(x_r) = (r!\,s!)^{-1/2} E_{rs}(x_1 \ldots x_r; x'_1 \ldots x'_s) \qquad 36)$$

by interchanges using Eq. (32) we find

$$(F_r)_{x_1 \ldots x_r;\, x'_1 \ldots x'_r} = \sum_{k=0}^{\infty} \frac{1}{k!} \times \int \ldots \int (E_{r+k})_{x_1 \ldots x_r y_1 \ldots y_k;\, x'_1 \ldots x'_r y_1 \ldots y_k}\, dy_1 \ldots dy_k \qquad (E_m \equiv E_{mm}). \tag{37}$$

From this, going over to the M-representation and writing

$$\lambda^r \bar{F}_r(M_1, \ldots, M_r) = f_r(M_1, \ldots, M_r); \tag{38}$$
$$\lambda^r \bar{E}_r(M_1, \ldots, M_r) = e_r(M_1, \ldots, M_r),$$

we obtain

$$f_r(M_1, \ldots, M_r) = \sum_{k=0}^{\infty} \frac{1}{k!} \int \ldots \int e_{r+k}(M_1, \ldots, M_{r+k}) \times dM_{r+1} \ldots dM_{r+k}. \tag{39}$$

The identical relation occurs in the theory of correlated random points,[3] if by f_r we understand the distribution functions defining the probability

$$dP = f_r(M_1, \ldots, M_r)\, dM_1 \ldots dM_r \tag{40}$$

for the occurrence of at least one particle (point) in each of the elementary regions (of volumes dM_i) near the points $M_1, \ldots, M_r$, and by e_r we understand the conditional probability functions giving the probability of the analogous event under the supplementary conditions that no further point falls in any other place ($e_N = N! w_N$ when the number N of particles is not a matter of chance). In the quantum case, to be sure, "probability" is not to be understood literally. But in some sense one can preserve the "probability" interpretation: in this connection the equation

$$\operatorname{Tr} R = \sum \frac{1}{N!} \int \cdots \int e_N (M_1, \ldots, M_N) \times dM_1 \ldots dM_N = 1 \qquad (41)$$

will play the part of the normalization condition of the "probability" in the summation over the whole set of mutually exclusive events. The operator function in the representation space $\xi(M) = \lambda F_1(M)$ is the quantum analogue of the "stochastic density function" $\sum_i \delta(M - M_i)$.

The generating functional is

$$L[u(M)] = \langle \prod_j (1 + u(M_j)) \rangle \qquad (42)$$

$$= \sum_{r=0}^{\infty} \frac{1}{r!} \int \cdots \int f_r(M_1, \ldots, M_r)\, u(M_1) \ldots u(M_r) \times dM_1 \ldots dM_r$$

and the characteristic functional of the function $\xi(M)$ can be regarded as the average ϑ of the operator functionals

$$\mathbf{L}[u] = N(e^{(F_1 U)}); \quad \theta[u] = e^{i(F_1 U)}; \qquad (43)$$
$$\left((F_1 U) = \operatorname{Tr} F_1 U = \int \xi(M)\, u(M)\, dM\right).$$

In contrast with the classical case, the functionals (43) are defined only over the class of functions $u(M)$ that can be represented in the form $\lambda^{-1} \operatorname{Tr} UL(M)$ by means of the operator U. The formula relating these functionals,

$$\mathbf{L}[u] = N(\theta[-iu]) \qquad (44)$$

is the quantum analogue of the formula

$$L[u] = \theta[-i \ln(1 + u)]. \qquad (45)$$

By means of the symbol N the relations (37) and their inverses can be written in the form

$$F_r = N(E_r e^{\operatorname{Tr} F_1}); \quad E_r = N(F_r e^{-\operatorname{Tr} F_1}), \qquad (46)$$
$$\left(\operatorname{Tr} F_1 = \int \xi(M)\, dM\right).$$

If we compare Eq. (46) with the definition (36) of the operators E_r, we can obtain the following expression for the vacuum state operator:

$$R_0 = N(e^{-\operatorname{Tr} F_1}) = \mathbf{L}[-1]. \qquad (47)$$

This result is connected with the formula of the theory of random points, according to which $L[-1]$ is equal to the probability that not a single point (particle) occurs.

6. The operator moments $\xi(M_1) \ldots \xi(M_r)$ of the operator density function $\xi(M)$ are expressible in terms of the operator distribution function. In contrast with the classical case, all that need be done to obtain these formulas is to carry out the "ordering" of the wave functions, using Eq. (32). As the result we obtain the following formula:

$$\lambda^r F_1(M_1) \ldots F_1(M_r) \qquad (48)$$
$$= \sum \mathrm{S} \int Q_2^{(\alpha_1)} Q_3^{(\alpha_2)} \ldots \lambda^s F_s(M_1'', \ldots, M_s'') \times dM_1'' \ldots dM_s''$$
$$(s = \alpha_1 + \alpha_2 + \ldots).$$

Here the first summation Σ is taken over all possible ways of separating r into summands, $r = 1\alpha_1 + 2\alpha_2 + \ldots$ (α_1 are positive integers). In the second summation S the numbers $\alpha_1, \alpha_2, \ldots$ are fixed, and the sum is taken over all ways of distributing the arguments $M_1, \ldots, M_r$ into s groups ($s = \alpha_1 + \alpha_2 + \ldots$), there being α_1 groups with one argument, α_2 groups of two arguments, etc. The number of terms in the latter sum is $r! / \alpha_1! (1!)^{\alpha_1} \alpha_2! (2!)^{\alpha_2} \ldots$, and each term is of the form

$$\int Q_2(M_1', M_1'') \ldots Q_2(M_{\alpha_1}', M_{\alpha_1}'')\, Q_3(M_{\alpha_1+1}', M_{\alpha_1+2}', M_{\alpha_1+1}'') \ldots$$
$$\ldots Q_3(M_{\alpha_1+2\alpha_2-1}', M_{\alpha_1+2\alpha_2}', M_{\alpha_1+\alpha_2}'') \ldots F_s(M_1'', \ldots, M_s'')\, dM_1'' \ldots dM_s'',$$

where $M_1', \ldots, M_r'$ is some rearrangment of the arguments $M_1, \ldots, M_r$ and

$$Q_m(M_1, \ldots, M_m) \qquad (49)$$
$$= \lambda^{m-2} \operatorname{Tr}(L(M_1) \ldots L(M_m))$$

(the quantity whose trace is taken is a product in the sense of matrix multiplication; do not confuse with the case of Eq. (30), where $L_1(M_1)\dots L_N(M_N)$ denotes an operator of a greater number of dimensions than $L(M)$]. Formulas of analogous structure are encountered in the theory of random functions and random points. The formulas (48) (for averages) go over into the formulas of the classical theory if we set the quantities $Q_m(M_1,\dots M_m)$ equal to δ-functions,

$$Q_m(M_1,\dots,M_m)=\delta(M_1,\dots,M_m) \tag{50}$$

$$\equiv\delta(M_2-M_1)\dots\delta(M_m-M_1).$$

Although each function $Q_m(M_1,\dots,M_m)$ is cyclically symmetrical, nevertheless in the general case it does not possess complete symmetry. This manifests itself in the fact that the operator moments (48), unlike the F_r, are not completely symmetrical. If from all the moments $<\xi(M_1)\dots(M_r)>$ we form the symmetrized moment, according to Eq. (48) it will be equal to

$$m^s_{(r)\xi}(M_1,\dots,M_r) \tag{51}$$

$$=\sum S\int\dots Q^{s(\alpha_i)}_{i+1}\dots f_k(M''_1,\dots,M''_k)$$

$$\times dM''_1\dots dM''_k,$$

where $\overset{s}{Q}_{i+1}$ is the function Q_{i+1} symmetrized in i arguments, and thus also fully symmetrized (because of the previously existing cyclic symmetry).

The difference between the $Q_m(M_1,\dots,M_m)$ and δ-functions is equivalent to the presence of specifically quantum correlations. Generally speaking, in the quantum case f_k cannot be equal to every function. Thus, the function

$$f_k(M_1,\dots,M_k) \tag{52}$$

$$=\delta(M_1-M^*)\dots\delta(M_k-M^*),$$

corresponding to a Poisson distribution concentrated in the limit at a single point, cannot be among the possible ones. But if as a trial procedure we admit (52) and substitute it into (51), then $m^s_{(r)\xi}$ will be expressible in terms of $Q_{i+1}(M_1,\dots,M^*)$ in just the way that the moments of an ordinary random function are expressible in terms of its correlation functions $k_{(r)\xi}(M_1,\dots,M_r)$. Consequently, instead of the classical formula $k_{(r)\xi}=\delta(M_1,\dots,M_2,M^*)$ the formula

$$k^s_{(r)\xi}(M_1,\dots,M_r) \tag{53}$$

$$=Q^s_{r+1}(M_1,\dots,M_r,M^*),$$

will hold, from which it follows that $Q^s_{r+1}(M_1,\dots M_{r+1})$ describes the effects of the quantum correlation of the $(r+1)$st order between the points $M_1,\dots,M_r,M_{r+1}$. It can be maintained that the difference between quantum theory and classical theory is comprised in the difference between the functions Q_m and δ-functions.*

If the functions $a(M)=[(A,L,(M)]/\lambda$ and $b(M)=[B,L(M)]/\lambda$ are given in the representation space, then according to the rule for multiplication of operators one must take as the product of these functions in the quantum case not $a(M)\,b(M)$ but

$$(AB,L(M))/\lambda$$

$$=\int Q_3(M,M_1,M_2)\,a(M_1)\,b(M_2)\,dM_1\,dM_2.$$

The difference between this expression and the ordinary product again reduces to the difference between Q_3 and a δ-function.

In view of the special part played by the functions Q_m, we shall calculate them for the special cases considered above. For spinless particles, using the kernel (10) and taking the sign + to make it a definite case, we find.

$$Q_{2m+1} \tag{54}$$

$$=(\pi\hbar)^{-2mn}\exp\left\{\frac{2i}{\hbar}\sum_{k>l}(-1)^{k+l}(p_kq_l-p_lq_k)\right\};$$

$$Q_{2m+2}=\delta(q_1-q_2+\dots-q_{2m+2})\,\delta(p_1-p_2$$

$$+\dots-p_{2m+2})\,Q_{2m+1}.$$

---

*The possibility of negative values of the distribution functions is due to this same feature.

In particular, along with the previously known equation

$$Q_2 = \delta(q_1 - q_2)\,\delta(p_1 - p_2),$$

we have

$$Q_3 = (\pi\hbar)^{-2n} e^{2i\Delta/\hbar}; \qquad (55)$$

$$Q_3^s = (\pi\hbar)^{-2n} \cos(2\Delta/\hbar),$$

$$\Delta = \begin{vmatrix} 1 & 1 & 1 \\ q_1 & q_2 & q_3 \\ p_1 & p_2 & p_3 \end{vmatrix}.$$

For the spin kernel (15) ($s = ½$) we find

$$Q_2 = (1/4\pi)(1 + 3\mathbf{n}_1\mathbf{n}_2); \qquad (56)$$

$$Q_3 = {}^1/_4\,(2\pi)^{-3/2}(1 + 3\mathbf{n}_1\mathbf{n}_2 + 3\mathbf{n}_2\mathbf{n}_3 + 3\mathbf{n}_3\mathbf{n}_1 + 3\sqrt{3}\,i\mathbf{n}_1[\mathbf{n}_2\mathbf{n}_3]);$$

$$Q_3^s = {}^1/_4\,(2\pi)^{-3/2}(1 + 3\mathbf{n}_1\mathbf{n}_2 + 3\mathbf{n}_2\mathbf{n}_3 + 3\mathbf{n}_3\mathbf{n}_1).$$

Equations (54) and (55) are characterized by a lesser degree of quantum degeneracy (correlation) than Eq. (56), since Q_2, and also the reduced functions $\int Q_{r+1}\, dq_1 \ldots dq_r$ and $\int Q_{r+1}\, dp_1 \ldots dp_r$, have the "classical" form (are equal to δ-functions), which is not true of the functions with spin.

---

[1] J. Moyal, *Quantum mechanics as a statistical theory*, in the collection *Questions of Causality in Quantum Mechanics*, edited by Ia. P. Terletskii and A. A. Gusev, Foreign Lit. Press, Moscow, 1955.

[2] G. Wick, *Calculation of the collision matrix*, in the collection *Newest Developments of Quantum Electrodynamics*, edited by D. D. Ivanenko, Foreign Lit. Press, Moscow, 1954.

[3] P. I. Kuznetsov and R. L. Stratonovich, Izv. Akad. Nauk SSSR, Ser. Mat. 20, 167 (1956).

Translated by W. H. Furry
215

SOVIET PHYSICS JETP VOLUME 4, NUMBER 6 JULY,1957

On the Derivation of the Fokker-Planck Equation for a Plasma

S. V. Temko

(Submitted to JETP editor October 6,1955)
J. Exptl. Theoret. Phys. (U.S.S.R.) 31, 1021-1026 (December,1956)

The Fokker-Planck equation for a many-component plasma is derived by the method of N. N. Bogoliubov, and the coefficients are calculated in explicit form.

THE Fokker-Planck equation is usually derived from Smoluchowski's equation for stochastic processes,[1] and thus the dependence of the coefficients in the Fokker-Planck equation on the law of interaction between the particles is left undetermined. For a plasma the Fokker-Planck equation can be obtained from a known kinetic equation of a form given by Landau.[2] In this case divergences appear for large and small distances, owing to the long-range nature of the Coulomb forces, so that in Ref. 2 the integrals are cut off at the limits of small and large distances.

The method of Bogoliubov[3] makes it possible to derive the Fokker-Planck equation on the basis of the mechanics of an assembly of molecules and to calculate the coefficients in explicit form for a given interaction law. In the case of a plasma the divergence of the Fokker-Planck coefficients at large distances is disposed of by cutting off at the Debye radius, which is not introduced from outside, as in Ref. 2, but follows automatically from Bogoliubov's method. In the present paper we give a derivation of the Fokker-Planck equation for a many-component plasma with uniform spatial distribution, and study the asymptotic cases of the behavior of plasma particles at large and small energies of motion.

We consider the plasma in a state of statistical equilibrium and investigate the behavior of a certain individual particle belonging to the plasma (or a foreign charged particle projected into the plasma). In the derivation of the equation for the distribution function of such a particle we assume that its interaction with the plasma does not disturb the statistical equilibrium of the plasma. Let the plasma, contained in the volume V, consist of N charged particles, which ϑ belong to $M \geq 2$ different kinds. Let N_a be the number of particles with charge e_a and mass μ_a, $a = 1, 2, \ldots, M$. The Hamiltonian of such a system has the form[3]

$$H = \sum_{\left(\substack{1\leqslant a\leqslant M\\ 1\leqslant i\leqslant N_a}\right)} H_a(x_i) \qquad (1)$$

$$+ \sum_{\left(\substack{1\leqslant a,b\leqslant M\\ 1\leqslant i<j\leqslant N_a}\right)} \Phi_{ab}(|q_i - q_j|),$$

$$H_a(x_i) = \sum_{(1\leqslant\alpha\leqslant 3)} \frac{(p_i^\alpha)^2}{2\mu_a};$$

$$\Phi_{ab}(|q_i - q_j|) = \frac{e_a e_b}{|q_i - q_j|},$$

$x_i = (q_i, p_i)$ are the coordinates and momenta of the ith particle of the plasma.

Now let

$$F_{a,b,\ldots,b_s}(X, x, \ldots, x_s;$$
$$F_a(X,t), F_b(x,t), \ldots, F_{b_s}(x_s,t))$$

be the distribution functions of ϑ systems of particles composed of the chosen particle of kind a and s other particles of the plasma of kinds $b_\vartheta, \ldots b_s$. These functions at an arbitrary instant of time $t > 0$ are assumed to depend on the single particle distribution functions for the kinds of particles in question, $F_a, F_b, \ldots$, at the same instant. Here $X = (Q, P)$ are the coordinates and momenta of the chosen particle (or of the charged particle projected into the plasma).

The equation for the distribution function of any single particle of the plasma has the form[3]

$$\frac{\partial F_a}{\partial t} = \Big[\sum_\alpha \frac{(P^\alpha)^2}{2\mu_a} + U_a(F_a; Q); F_a\Big] \qquad (2)$$

$$+ \sum_b n_b \int_\Omega [\Phi_{ab}(|Q - q|); g_{ab}]\, dx.$$

Moreover, for the correlation functions g_{ab} we have (cf. Ref. 3)

$$D_0 g_{ab} = \Big[\sum_\alpha (P^\alpha)^2/2\mu_\alpha + \sum_\alpha (P^\alpha)^2/2\mu_b \qquad (3)$$

$$+ U_a(F_a; Q) + U_b(F_b; q); g_{ab}\Big]$$

$$+ \sum_c (n_c/v) \int [\Phi_{ac}(|Q - q'|); \quad g_{bc} F_a]\, dx'$$

$$+ \sum_c (n_c/v) \int [\Phi_{bc}(|q - q'|);$$

$$g_{ac} F_b]\, dx' + (1/v)[\Phi_{ab}(|Q - q'|); F_a F_b].$$

Here the integration is taken over the entire phase space Ω; U_a and U_b are self-consistent potentials, $v = V/N$ is the mean volume per particle, and $n_c = N_c/N$ are the concentrations of particles of kind c, $c = 1, 2, \ldots, M$. By substituting into Eq. (2) the solutions of the equations (3), one can obtain the equation of motion of charged particles in the plasma

In the special case of a spatially homogeneous distribution of the plasma Bogoliubov's equation has the form:[3]

$$\frac{\partial w_a(t,P)}{\partial t} \qquad (4)$$

$$= \sum_{b,\alpha} n_b \frac{\partial}{\partial P^\alpha} \int \frac{\partial \Phi_{ab}(|\zeta|)}{\partial \zeta^\alpha} h_{ab}(\zeta, P; w_a(t,P))\, d\zeta,$$

$$h_{ab}(\zeta, P; w_a) = \int g_{ab}(\zeta, P, p; w_a, w_b)\, dp \qquad (5)$$

$$= -\sum_{c,\alpha} n_c \frac{1}{v} \int\int_0^\infty\int \frac{\partial w_b(p)}{\partial p^\alpha}$$

$$\times \frac{\partial \Phi_{bc}(|\zeta - q' - (P/\mu_a - p/\mu_b)\tau|)}{\partial \zeta^\alpha}$$

$$\times h_{ac}(q', P, w_a)\, dp\, d\tau\, dq'$$

$$- \sum_{c,\alpha} n_c \frac{\partial w_a(t,P)}{\partial P^\alpha}$$

$$\times \frac{1}{v} \int\int_0^\infty\int \frac{\partial \Phi_{ac}(|\zeta - q' - (P/\mu_a - p/\mu_b)\tau|)}{\partial \zeta^\alpha}$$

$$\times h_{bc}(-q', p; w_b)\, dp\, d\tau\, dq'$$

$$- \sum_\alpha \frac{1}{v} \int_0^\infty\int \frac{\partial \Phi_{ab}(|\zeta - (P/\mu_a - p/\mu_b)\tau|)}{\partial \zeta^\alpha}$$

$$\times \Big\{\frac{\partial w_a(t,P)}{\partial P^\alpha} w_b(p) - \frac{\partial w_b(p)}{\partial p^\alpha} w_a(t,P)\Big\}\, dp\, d\tau.$$

Here $\zeta = Q - q$, and $w_a(t; P)$ and $w_b(p)$ are the distribution functions of the chosen particle of kind a and of any other particle in the plasma for a uniform distribution in space. The first two integral forms in the equations (5) produce the effect of the Debye screening, which cuts off the correlation functions h_{ab} at large distances.[3]

To simplify the calculations we apply to the correlation functions h_{cb} an approximation of the form:[3]

$$h_{bc}(-q', p; w_b) = g^0_{bc}(-q')\, w_b(p), \tag{6}$$

where g^0_{bc} are the Debye functions:

$$g^0_{bc}(-q') = -(\lambda_b \lambda_c / r_D^2) \exp\{-\varkappa |q'|\} / |q'|;$$

$$\lambda_b = e_b / \sqrt{4\pi \Sigma n_s e_s^2};$$

$$1 / r_D^2 = 4\pi \Sigma n_s e_s^2 / \Theta v; \quad \varkappa = 1 / r_D.$$

For the solution of the problem we employ the Fourier integral[3]

$$h_{ab}(\zeta, P; w_a) = \int e^{i(\nu\zeta)} H_{ab}(\nu, P; w_a)\, d\nu;$$

$$\Phi_{ab}(|\zeta|) = \frac{v}{4\pi} \int e^{i(\nu\zeta)} Y_{ab}(|\nu|)\, d\nu;$$

$$g_{bc}(q, q_1) = \int e^{i(\nu(q-q_1))} K_{bc}(|\nu|)\, d\nu,$$

$$Y_{ab}(|\nu|) = \Theta 2\lambda_a \lambda_b / \pi r_D^2 \nu^2;$$

$$K_{bc}(|\nu|) = -(\lambda_b \lambda_c / 2\pi^2)/(\nu^2 r_D^2 + 1).$$

Applying the inverse transformation to the equations (5), we find, in virtue of Eq. (6):

$$\begin{aligned} &H_{ab}(\nu, P; w_a) \\ &+ 2\pi^2 \sum n_c Y_{bc}(|\nu|)\, B_b(\nu, P)\, H_{ac}(\nu, P; w_a) \\ &\qquad = L_{ab}(\nu, P; w_a); \end{aligned} \tag{7}$$

$$\begin{aligned} L_{ab} = &-\frac{i}{4\pi} Y_{ab} A_b(\nu, P; w_a) \\ &- \frac{i}{4\pi} \sum_{c,\alpha} \frac{\partial w_a(t, P)}{\partial P^\alpha} \nu^\alpha n_c B_b Y_{ac} K_{bc}; \end{aligned}$$

$$\begin{aligned} A_b(\nu, P; w_a) = &\sum_c \frac{\partial w_a(t, P)}{c P^\alpha} \lambda^\alpha B'_b(\nu, P) \\ &- w_a(t, P)\, B_b(\nu, P); \end{aligned}$$

$$\begin{aligned} B_b(\nu, P) = &\sum_\alpha \gamma^\alpha \int_0^\infty \!\! \int \frac{\partial w_b(p)}{\partial p^\alpha} \\ &\times \exp\left\{ i\tau \left(\nu \left(\frac{p}{\mu_b} - \frac{P}{\mu_a} \right) \right) \right\} dp\, d\tau, \end{aligned} \tag{8}$$

$$\begin{aligned} B'_b(\nu, P) = &\int_0^\infty \!\! \int w_b(p) \\ &\times \exp\left\{ i\tau \left(\nu \left(\frac{p}{\mu_b} - \frac{P}{\mu_a} \right) \right) \right\} dp\, d\tau. \end{aligned}$$

The solution of the system (7) for fixed a and b taking all possible values from l to M is given by the ratio

$$H_{ab} = D_{ab} / \Delta,$$

where Δ is the determinant of the system

$$\Delta = 1 + 2\pi^2 i \sum_c n_c Y_{cc}(|\nu|)\, B_b(\nu, P)$$

and D_{ab} is the determinant in which the bth column has been replaced by the right members of the equations of the system

$$D_{ab} = L_{ab}\left(1 + 2\pi^2 i \sum_c n_c Y_{cc} B_b\right) - 2\pi^2 i \sum_c n_c Y_{bc} B_b L_{ac}.$$

The solution of the system (7) can now be written in the form

$$H_{ab}(\nu, P; w_a) = H^0_{ab}(\nu, P; w_a) + \delta H_{ab}(\nu, P; w_a), \tag{9}$$

where H^0_{ab} describes the influence of the whole assembly of charged particles of the plasma on the behavior of the chosen particle of kind a:

$$H_{ab} = -(i/4\pi)\, Y_{ab} A_b \Big/ \left(1 + 2\pi^2 i \sum_c n_c Y_{cc} B_c\right)$$

and δH_{ab} describes the influence of the plasma particles on each other:

$$\delta H_{ab} = -\frac{i}{4\pi} \sum_{b',d} \frac{\partial w_a(t, P)}{\partial P^\alpha} \nu^\alpha n^{b'} Y_{ab'} K_{bb'} B'_b / \Delta.$$

Applying the inverse transformation to Eq. (4), we find

$$\frac{\partial w_a(t, P)}{\partial t}$$

$$= i\frac{v}{4\pi}\sum_{b,\alpha} n_b \frac{\partial}{\partial P^\alpha}\int_{(\nu)} \nu^\alpha Y_{ab}(|\nu|)\, H_{ab}(\nu, P; w_a)\, d\nu,$$

from which there follows the Fokker-Planck equation for a multicomponent plasma

$$\frac{\partial w_a(t, P)}{\partial t} = \sum_{\alpha,\beta=1}^{3} \frac{\partial}{\partial P^\alpha} B^{\alpha\beta}(P) \frac{\partial}{\partial P^\beta} w_a(t, P) \quad (10)$$

$$-\sum_{\alpha=1}^{3} \frac{\partial}{\partial P^\alpha} A^\alpha(P)\, w_a(t, P).$$

Here $A^\alpha(P)$ and $B^{\alpha\beta}(P)$, the coefficients in the Fokker-Planck equation, are given by

$$A^\alpha(P) = -\frac{v}{16\pi^2}\sum_b n_b \int_{(\nu)} \frac{\nu^\alpha}{\Delta} Y^2_{ab}(|\nu|)\, B_b(\nu, P)\, d\nu;$$

$$B^{\alpha\beta}(P)$$

$$= \frac{v}{16\pi^2}\sum_b n_b \int_{(\nu)} \frac{\nu^\alpha \nu^\beta}{\Delta} Y^2_{ab}(|\nu|)\, B'_b(\nu, P)\, d\nu$$

$$+ \frac{v}{16\pi^2}\sum_{b,\, b'} n_b n_{b'}$$

$$\times \int_{(\nu)} \frac{\nu^\alpha \nu^\beta}{\Delta} Y_{ab}(|\nu|)\, Y_{ab'}(|\nu|)\, K_{bb'}(|\nu|)\, B'_b(\nu, P)\, d\nu.$$

For the determination of these coefficients it is necessary to calculate $B_b(\nu, P)$ and $B'_b(\nu, P)$. In statistical equilibrium of the plasma the distribution function for each of its particles, with the exception of the chosen particle, whose motion is assumed nonstationary, can be taken to be a Maxwell distribution

$$w_b(p) = (2\pi\mu_b\theta)^{-3/2} \exp\left\{-\sum_\alpha (p^\alpha)^2 / 2\mu_b\Theta\right\}.$$

Substituting this into Eq. (8) and integrating over p, we find

$$B_b(\nu, P) = -i\frac{\nu^2}{\mu_b}\int_0^\infty \tau \exp\left\{-\frac{\Theta\nu^2}{2\mu_b}\tau^2 - i\,\frac{\tau}{\mu_a}(\nu P)\right\} d\tau,$$

$$B'_b(\nu, P) = \int_0^\infty \exp\left\{-\frac{\Theta\nu^2}{2\mu_b}\tau^2 - i\,\frac{\tau}{\mu_a}(\nu P)\right\} d\tau.$$

Here it is convenient to make a change of the variable of integration

$$\tau' = \nu\tau(\Theta/\mu_b)^{1/2}$$

and introduce the notation

$$u_{ab}(\nu, P) = (\mu_b/\mu_a)^{1/2}(\boldsymbol{\nu}\mathbf{P}/\nu\sqrt{\mu_a\Theta}).$$

It is now easy to calculate* B_b and B_b', and the resulting expressions for A^α and $B^{\alpha\beta}$ are

$$A^\alpha(P) = -v\frac{(\mu_a\Theta)^{1/2}}{16\pi^2 r_D^3 t_0 \Theta^2}\sum_b n_b \quad (12)$$

$$\times \int_{(\mathbf{k})} \frac{k^\alpha}{f} Y^2_{ab}(|k|)\, u_{ab}(k, P)$$

$$\times \exp\{-{}^1/_2\, u^2_{ab}(k, P)\}\, dk;$$

$$B^{\alpha\beta}(P) = v\frac{\mu_a}{16\pi^2 r_D^3 t_0 \Theta}\sum_b n_b \left(\frac{\mu_b}{\mu_a}\right)^{1/2} \quad (13)$$

$$\times \int_{(\mathbf{k})} \frac{k^\alpha}{f}\frac{k^\beta}{k} Y^2_{ab}(|k|) \exp\{-{}^1/_2 u^2_{ab}(k, P)\}\, dk$$

$$- v\frac{\mu_a}{16\pi^2 r_D^3 t_0 \Theta}\sum_{b,\, b'} n_b n_{b'}\left(\frac{\mu_b}{\mu_a}\right)^{1/2}$$

$$\times \int_{(\mathbf{k})} \frac{k^\alpha k^\beta}{fk} Y_{ab}(|k|)\, Y_{ab'}(|k|)\, K_{bb'}(|k|)$$

$$\times \exp\{-{}^1/_2 u^2_{ab}(k, P)\}\, dk.$$

Here

$$f = 1 + 2\pi^2 \sum_c n_c(1 + \eta_{ac})\, Y_{cc}(|k|)/\Theta,$$

$$\eta_{ac}(k, P) = u_{ac}(k, P)\int_0^\infty e^{-\tau^2/2} \sin u_{ac}(k, P)\, \tau\, d\tau,$$

We have taken as the unit of time $t_0 = r_D(2\mu_a/\pi\Theta^{1/2}$; k is a dimensionless wave-number: $k = \nu r_D$.

Let us examine the coefficients of the Fokker-Planck equation for a plasma. We note than $B^{\alpha\beta} = 0$ for $\alpha \neq \beta$. If the energy of the selected particle is small, much smaller than the average energy of the thermal motion of the plasma particles, i.e., for

$$P^2/2\mu_a \ll \Theta,$$

expansion of A^α and $B^{\alpha\beta}$ in series gives (since here $\eta_{ac}(k, P) \ll 1$)

---

*B and B', respectively, are given by the absolute values of the real parts of the expressions (11).

$$A^{\alpha}(P) = -{}^{1}/_{3}\,\rho\,(P/\mu_a\Theta)\,B + o\,(1/\Theta^2); \qquad (14)$$

$$B^{\alpha\beta}(P) = {}^{1}/_{3}\,\rho B - (1/48\pi^3)\,\rho\,BL^{-1} + o\,(1/\Theta), \qquad (15)$$

$$B = 4\pi \sum_{c} (n_c e_c^2 e_a^2/u_c)\,L,$$

u_c is the reduced speed of particles of kind c in the plasma,

$$u_c = 2\pi^4\,(2\Theta/\pi\mu_c)^{1/2},$$

ρ is the mean density of the plasma, $\rho = N/V$, and L is a logarithmic factor:

$$L = \int_0^{k_{\max}} \frac{k\,dk}{k^2+1}. \qquad (16)$$

The upper limit of the integration, $k_{\max} = r_D/r_1$, is introduced because of the divergence of L at small distances $r < r_1$, which correspond to large wave-numbers. At large distances and at small wave-numbers the Debye screening, which follows naturally from Bogoliubov's method, assures the good convergence of the coefficients A^{α} and $B^{\alpha\beta}$. Indeed, choosing r_1 in the form[2] $r_1 = e^2/\Theta$, we find

$$L = \ln\sqrt{1 + (r_D^2\Theta^2/e^4)}.$$

Expanding the integral (16) in series, we find a formula agreeing with that of Landau[2]

$$L = \ln\,(k_{\max}/k_0), \qquad (17)$$

where the lower integration limit $k_0 = r_D/r_2$ is introduced because of the logarithmic divergence of L at large distances $r > r_2$ and small wave-numbers.

From a comparison of Eqs. (16) and (17), we find k_0:

$$k_0 = (1 + k_{\max}^{-2})^{-1/2}.$$

If the temperature Θ of the plasma is sufficiently high the screening radius r_2 is equal to the Debye radius r_D:

$$r_2 \doteq r_D/k_0 = r_D\sqrt{1 + e^4/r_D^2\Theta^2}$$

$$= r_D\,(1 + e^4/2r_D^2\Theta^2 - \cdots) \approx r_D.$$

The factor L can now be expressed by theordinary Landau formula. At high plasma temperature the second term in Eq. (15), which takes account of the mutual influences of the plasma particles, can be neglected.

For the very slow particles of the plasma we have from Eqs. (14) and (15)

$$|A^{\alpha}(P)| \ll |B^{\alpha\beta}(P)|,$$

so that the equation for the asymptotic behavior of the distribution function of such particles can be taken in the form

$$\frac{\partial w_a(t,P)}{dt} = \sum_{\alpha,\beta} \frac{\partial}{\partial P^{\alpha}}\,B^{\alpha\beta}(P)\,\frac{\partial}{\partial P^{\beta}}\,w_a(t,\ P).$$

For large energy of the selected particle of the plasma, i.e., for

$$P^2/2\mu_a \gg (\mu_a/\mu)\,\Theta,$$

we find from Eqs. (12) and (13), since $\eta_{ac}(k,P) \approx 1$,

$$A^{\alpha}(P) = -\sqrt{2\pi}\,\frac{(\mu_a\Theta)^{1/2}}{P^2}\left(\frac{\mu_a}{\mu}\right)^{3/2} B;$$

$$B^{\alpha\beta}(P) = \sqrt{2\pi}\,\frac{(\mu_a\Theta)^{3/2}}{P^3}\left(\frac{\mu_a}{\mu}\right)^{3/2} B,$$

where μ is the average mass of the plasma particles.

For the very fast particles of theplasma

$$|B^{\alpha\beta}(P)| \ll |A^{\alpha}(P)|,$$

in consequence of which the equation for the asymptotic behavior of the distribution function of the high-energy charged particles takes the following form:

$$\frac{\partial w_a(t,\ P)}{\partial t} = -\sum_{\alpha,\beta} \frac{\partial}{\partial P^{\beta}}\,A^{\alpha}(P)\,w_a(t,\ P).$$

For the stationary motion of the selected particle of the plasma we get the Maxwell distribution in each of the cases considered.

In conclusion I express my deep gratitude to

Academician N. N. Bogoliubov for suggesting the problem and directing the work, and to D. N. Zubarev for a discussion of the work.

---

[1] A. N. Kolmogorov, Uspekhi Matem. Nauk 5, 5 (1938).
[2] L. D. Landau, Phys. Z. Sowjetunion 10, 154 (1936).
[3] N. N. Bogoliubov, *Problems of Dynamical Theory in Statistical Physics*, State Tech. Press, 1946.

Translated by W. H. Furry
216

SOVIET PHYSICS JETP VOLUME 4, NUMBER 6 JULY, 1957

On the Equations of Motion of Finite Masses in the General Theory of Relativity*

M. F. Shirokov and V. B. Brodovskii
Moscow State University

(Submitted to JETP editor October 8, 1955)
J. Exptl. Theoret. Phys. (U.S.S.R.) 31, 1027-1033 (December, 1956)

On the basis of the theorem of the center of mass in the general theory of relativity and the principle of equivalence, there is proved for systems of bodies of astronomical type an approximate theorem (with neglect of gravitational radiation, etc.) on the motion of the center of mass of each body along geodesic lines in the gravitational fields of the other bodies, which are regarded as point sources. This theorem gives the laws of motion of finite masses in the general theory of relativity. It provides the basis for a rather simple derivation of the relativistic equations of motion of n-body systems, by substitution into the equation for geodesic lines of the second-order solutions of the Einstein gravitational equations. The resulting equations agree with the equations of motion found in a more complicated way as the conditions for solubility of the gravitational equations in third approximation.

The theorem reveals the cause of the agreement between the work of Einstein and that of Fock and his coworkers based on different conceptions of the bodies of the system as finite or point masses, and shows the fundamental and practical insignificance of the principle of equivalence in the Einstein theory of gravitation.

1. INTRODUCTION

ONE of the most important problems of the general theory of relativity is the problem of the motion of n-bodies interacting by gravitational forces only. Under certain conditions, of which the most important is the smallness of the velocity v of their motion in comparison with the speed of light c, such bodies form systems of astronomical type, such as, for example, our planetary system.

Einstein and his co-workers[1-3] considered such systems as sets of point masses giving rise to gravitational fields surrounding them, determined by the well-known gravitational equations of the general theory of relativity,

$$R_{\mu\nu} - {}^1\!/_2 g_{\mu\nu} R = -kT_{\mu\nu}, \qquad (1.1)$$

where $R_{\mu\nu}$ is Einstein's curvature tensor; $T_{\mu\nu}$ is the energy momentum tensor, which is taken to be unequal to zero only at singular points of the field; $g_{\mu\nu}$ is the metric tensor; and $k = 8\pi\gamma/c^2$, where γ is the gravitational constant of Newton's theory of gravitation. Here also

$$(T^{\mu\nu})_\nu = 0. \qquad (1.2)$$

It was found that the equation of motion of such masses are contained in Eq. (1.1) as the conditions for solubility in one approximation or another; a result, by the way, which cannot be accepted as altogether natural, since Eq. (1.2) follows entirely from Eq. (1.1), and the structure of the tensor $T_{\mu\nu}$ as point singularities is not fixed by any supplementary equations.

Fock and his co-workers[4-6] approached the solution of the same problem, starting from more realistic assumptions about the bodies of the system, which they regarded as certain finite masses with their distribution and motion given by a tensor $T_{\mu\nu}$ different from zero in a certain spatial region of spherical shape. A special feature of Fock's method was the imposition of coordinate conditions

$$\partial(\sqrt{-g}\, g^{\mu\nu}) / \partial x^\nu = \partial G^{\mu\nu} / \partial x^\nu = 0, \qquad (1.3)$$

fixing the choice of special coordinates, called by Fock "harmonic" coordinates. Despite the great difference in the statement of the problem and the methods of solution, the equations of motion with inclusion of relativistic corrections, as found by Petrova[5] by Fock's method, agree completely with the equations of Einstein and his co-workers[3], being obtained in both cases as conditions of solubility of the gravitational equations (1.1) in third approximation.

In Fock's opinion[4,7], the coordinates defined by Eq. (1.3) are preferred coordinates, which is of course in contradiction with the general principle of relativity. In opposition to this, Infeld[8] showed by direct calculation that the coordinate condition (1.3) is not essential for the derivation of the equations of motion. Infeld's point of view can be supported by a number of other considerations of a fundamental character.[9]

At the same time Infeld continues to treat the bodies of the system as point masses. It still remains unclear, however, why the treatment ot the bodies as masses of finite spatial dimensions gives the same equations of motion as for point masses. We give below a new derivation of the equations of motion of a system of bodies of the astronomical type, providing an explanation of this fact and showing the deep organic connection of the gravitational equations with the general principle of relativity. Moreover, the new derivation is distinguished by great simplicity in the calculations, since it leads to the equations of motion including relativistic corrections on the basis of the solution of the gravitational equations (1.1) in only the second approximation, while in the methods of Einstein and of Fock and co-workers the equations of motion are obtained as conditions of solubility of the system (1.1) only in the third approximation.

---

*Presented at the Lomonosov Jubilee Symposium, Moscow State University, May, 1955.

2. ON THE LAW OF MOTION OF RELATIVISTIC CENTERS OF MASS OF BODIES IN AN ISOLATED SYSTEM OF ASTRONOMICAL TYPE

In classical mechanics this law states: the centers of mass of the bodies of the system move as if they had applied to them all the external forces that act on each body from the other bodies of the system. Since the concept of center of mass exists also in the general theory of relativity and the theorem of the center of mass is strictly valid,[10] it can be supposed that according to this theorem the centers of mass of the bodies move according to a quite definite law, containing in itself as a special case the law of classical mechanics stated above. We confine our consideration to systems of astronomical type, which we take to satisfy the following conditions[4]

$$a \ll L, \quad v \ll c, \; R \ll L,$$

$a = \gamma m/c^2$ is the gravitational radius of a body of mass m; L is a length characterizing its linear dimensions; v is the speed of the body or of its parts; and R is the distance of the body from any other body of the system.

We note also that according to the virial theorem

$$\overline{\sum_a m_a v_a^2} = \overline{\sum_{(a \neq b)} \frac{\gamma m_a m_b}{2 | r_a - r_b |}}. \tag{2.2}$$

Here a and b are indices numbering the bodies of the system.

The total energy-momentum tensor, including also the tensor $(-g t^{\mu\nu})$ of the gravitational field,

$$S^{\mu\nu} = -g \left(T^{\mu\nu} + t^{\mu\nu}\right) \tag{2.3}$$

and the corresponding angular momentum tensor

$$M^{\mu\nu\sigma} = x^\mu S^{\nu\sigma} - x^\nu S^{\mu\sigma} \tag{2.4}$$

satisfy the conservation laws

$$\partial S^{\mu\nu}/\partial x^\nu = 0, \quad \partial M^{\mu\nu\sigma}/\partial x^\sigma = 0. \tag{2.5}$$

Integration of the relations (2.5) over the surface of the volume ω of a body, with account taken of the fact that $T^{\mu\nu} \neq 0$ only inside it, gives

$$\frac{\partial}{\partial t}\left\{\int_\omega (-g)\left(T^{i0} + t^{i0}\right) d\omega\right\} + \oint_f (-g)\, t^{ik} df_k = 0; \tag{2.6}$$

$$\frac{\partial}{\partial t}\left[\int_\omega (-g)\left(T^{00} + t^{00}\right) d\omega\right] + \oint_f (-g)\, t^{0k} df_k = 0; \tag{2.7}$$

$$\frac{\partial}{\partial t}\left[\int_\omega M^{ik0}\, d\omega\right] + \oint_f (-g)\left(x^i t^{kl} - x^k t^{il}\right) df_l = 0; \tag{2.8}$$

$$\frac{\partial}{\partial t}\left(\int_\omega M^{i00} d\omega\right) + \oint_f (-g)\left(x^i t^{0l} - x^0 t^{il}\right) df_l = 0. \tag{2.9}$$

The second of the conditions (2.1) allows us to neglect the change of the gravitational energy, i.e., to take $t^{i0} \approx 0$. In virtue of the third of the conditions (2.1), inside a given body, the change of the gravitational field due to the other bodies can be neglected, and therefore we can choose a system of reference such that inside the body the gravitational field is produced only by itself. In such a system of reference

$$\oint_f g t^{ik} df_k \approx 0. \tag{2.10}$$

Consequently, in this system, in virtue of Eqs. (2.6)–(2.10)

$$\begin{aligned} P^\mu &= \int_\omega S^{\mu 0} d\omega = \text{const}, \\ M^{\mu\nu} &= \int_\omega M^{\mu\nu 0} d\omega = \text{const}. \end{aligned} \tag{2.11}$$

But then, by the theorem of the center of mass,[10] in this system of reference there will exist a four-vector of the center of mass of this body

$$Y^{\mu} = M^{\mu\nu} P_{\nu} / P_{\alpha} P^{\alpha}, \tag{2.12}$$

satisfying the relation

$$d^2 Y^{\mu} / ds^2 = 0. \tag{2.13}$$

Making a transformation now to a system of reference connected with the center of mass of the system as a whole, we get instead of Eq. (2.13)

$$(d^2 Y^{\mu} / ds^2) + \Gamma^{\mu}_{\alpha\beta} (dx^{\alpha} / ds)(dx^{\beta} / ds) = 0. \tag{2.14}$$

As is well known, the quantity $\Gamma^{\mu}_{\beta\alpha}$ transforms in the following way when we go from one system of reference to another:

$$\Gamma^{\mu}_{\alpha\beta} = \frac{\partial x^{\mu}}{\partial x'^{\sigma}} \left(\frac{\partial x'^{\tau}}{\partial x^{\alpha}} \frac{\partial x'^{\varepsilon}}{\partial x^{\beta}} \Gamma'^{\sigma}_{\tau\varepsilon} + \frac{\partial^2 x'^{\sigma}}{\partial x^{\alpha} \partial x^{\beta}} \right). \tag{2.15}$$

Taking the coordinates x'_{σ} to refer to the system of reference of the center of mass of our body, in which by Eq. (2.13) $\Gamma'^{\sigma}_{\tau\epsilon} = 0$, we get instead of Eq. (2.15) the simple relation

$$\Gamma^{\mu}_{\alpha\beta} = (\partial x^{\mu} / \partial x'^{\sigma})(\partial^2 x'^{\sigma} / \partial x^{\alpha} \partial x^{\beta}). \tag{2.16}$$

This shows that the symbols $\Gamma^{\mu}_{\alpha\beta}$ occurring in Eq. (2.14) owe their existence only to the transformation of coordinates leading to the appearance of the gravitational field at the center of mass of the body, produced by all the bodies of the system except the given one. Therefore, in using Eq. (2.14) in what follows, we shall substitute into it the $\Gamma^{\mu}_{\alpha\beta}$ calculated for the center of mass of the given body from the quantities $g_{\mu\nu}$ corresponding to the external gravitational field of the other bodies of the system.

The relations (2.14) also express the law of motion of the relativistic center of mass of the given body in a reference system connected to the center of mass of the system as a whole, providing a generalization of the law formulated above for the motion of the center of mass in the external force field of classical mechanics.

The new relativistic law can be formulated in the following way: the center of mass of any body of the system moves along a geodesic line in the gravitational field of the other bodies. This proposition can be used for the direct derivation of the equations of motion of finite masses from Eq. (2.14), as will be done below. For this purpose it is first of all necessary to transform Eq. (2.14) into a form closer to the usual one.

The expression for the square of the interval between two infinitely close points has the well-known form

$$ds^2 = g_{\mu\nu} dx^{\mu} dx^{\nu}. \tag{2.17}$$

We shall suppose that in the Galilean approximation

$$ds^2 = c^2 dx_0^2 - dx_1^2 - dx_2^2 - dx_3^2, \tag{2.18}$$

where $x_0 = t$ is the time coordinate.

According to Eq. (2.17) we have, along the geodesic line followed by the center of mass of the body

$$ds = dt \sqrt{g_{ik} \dot{x}_i \dot{x}_k + 2 g_{i0} \dot{x}_i + g_{00}} = dt A, \tag{2.19}$$

where $x_i = dx_i / dt$ and A will be functions of the time. Then after eliminating A we can write Eq. (2.14) in the form

$$\begin{gathered} \ddot{x}_i + (\Gamma^{i}_{lk} - \dot{x}_i \Gamma^{0}_{lk}) \dot{x}_l \dot{x}_k \\ + 2 (\Gamma^{i}_{l0} - \Gamma^{0}_{l0} \dot{x}_i) \dot{x}_l + \Gamma^{i}_{00} - \Gamma^{0}_{00} \dot{x}_i = 0. \end{gathered} \tag{2.20}$$

3. DERIVATION OF THE RELATIVISTIC EQUATIONS OF MOTION FROM THE SOLUTION OF THE GRAVITATIONAL EQUATIONS IN SECOND APPROXIMATION, FOLLOWING FOCK[4]

For convenience in the calculations and in comparing Fock's results with ours, we shall use the notation of his paper.[4] There, in the second approximation, proceeding in terms of an expansion in powers of $1/c$, the solutions of Eq. (1.1) are

$$\begin{gathered} G^{00} = \frac{1}{c} + \frac{4U}{c^3} + \frac{7U^2}{c^5} + \ldots, \\ G^{0i} = \frac{4U_i}{c^3} + \frac{4S_i}{c^5} + \ldots, \\ G^{ik} = -c\delta_{ik} + \frac{4S_{ik}}{c^3} + \ldots \end{gathered} \tag{3.1}$$

The quantities appearing in these relations satisfy the equations:

$$\begin{gathered} \Box U = -4\pi\gamma (c^2 + {}^1/{}_2 U) T^{00}, \\ \Box U_i = 4\pi\gamma g T^{0i} = 4\pi\gamma (c^2 + 4U) T^{0i}, \end{gathered} \tag{3.2}$$

$$\begin{gathered} \Box S_i = -3 (\partial U / \partial t)(\partial U / \partial x_i) \\ + 4 (\partial U_i / \partial x_j - \partial U_j / \partial x_i) \partial U / \partial x_j, \end{gathered} \tag{3.3}$$

$$\Delta U_{ik} = -4\pi\gamma c^2 T^{ik}, \tag{3.4}$$

$$\Delta V_{ik} = {}^1/{}_2 \delta_{ik} (\operatorname{grad} U)^2 - \frac{\partial U}{\partial x_i} \frac{\partial U}{\partial x_k},$$

$$S_{ik} = U_{ik} + V_{ik}. \tag{3.5}$$

Here use has been made of the value of the determinant g, which is given in second approximation by the relation

$$g = -c^2 - 4U - (7u^2/c^2) + 4S/c^2, \tag{3.6}$$

where

$$S = S_{11} + S_{22} + S_{33}.$$

We note that the $G^{\mu\nu}$ still have to satisfy the condition for harmonic coordinates, Eq. (1.3).

By means of Eqs. (3.1) and (3.6) and the use of the formula

$$G_{\mu\nu} = \sqrt{-g}\, g_{\mu\nu} = -\text{ min. } G^{\mu\nu} \tag{3.7}$$

we can find the covariant components of the metric tensor with accuracy to and including the order $1/c^2$:

$$g_{00} = c^2 + 2U + (5U^2/2c^2) - 2S/c^2; \tag{3.8}$$
$$g_{0i} = 4U_i/c^2, \quad g_{ik} = -(1 + 2U/c^2)\,\delta_{ik}.$$

We note that, to the required degree of accuracy

$$\sqrt{-g} = (c + 2U/c) + (3U^2/2c^3) - 2S/c^3. \tag{3.9}$$

By means of Eqs. (3.1), (3.8), and (3.9) we find the Christoffel symbols of the second kind that are nonvanishing in our approximation; substitution of these into Eq. (2.20) gives

$$\ddot{x}_i - \frac{\partial U}{\partial x_i} \tag{3.10}$$
$$= \frac{1}{C^2}\left(-\frac{9}{2}U\frac{\partial U}{\partial x_i} + \frac{\partial S}{\partial x_i} + 4\frac{\partial U_i}{\partial t}\right.$$
$$+ 4\frac{\partial U_i}{\partial x_l}\dot{x}_l - 4\frac{\partial U_l}{\partial x_i}\dot{x}_l - 3\frac{\partial U}{\partial t}\dot{x}_l.$$
$$\left. + \frac{\partial U}{\partial x_i}v^2 - 4\frac{\partial U}{\partial x_l}\dot{x}_l\dot{x}_i\right),$$

where $v^2 = \dot{x}_1^2 + \dot{x}_2^2 + \dot{x}_3^2$. The quantities U, S, and U_i are determined by the solutions of Eqs. (3.2) –– (3.8) for the point coinciding with the center of mass of the given body a, with coordinates a_1.

The energy-momentum tensor in second approximation has the form:

$$T^{ik} = (1/c^2)\,\rho_a(r)\,\dot{a}_i\dot{a}_k + (1/_3 c^2)\,\psi_a(r)\,\delta_{ik}, \tag{3.11}$$
$$T^{00} = (1/c^2)(1 - U/c^2)\,\rho_a(r)$$
$$\times\{1 + (1/_2 c^2)(v_a^2 - U^a(r))\},$$
$$T^{0i} = (1/c^2)(1 - 2U/c^2)\,\rho_a(r)$$
$$\times\{1 + (1/_2 c^2)(v_a^2 - U^a(r))\}\,\dot{a}_i + (1/_3 c^4)\,\psi_a(r)\,\dot{a}_i.$$

Outside the body a its components are, of course, equal to zero.

The potentials $U^a(a)$ and $U_i^a(a)$ from the other bodies at the center of mass of the given body are, in virtue of Eqs. (3.2) and (3.11), given by the expressions

$$U^a(a) = \sum_b{}' \frac{\gamma m_b}{|a-b|}\left\{1 + \frac{1}{2c^2}(v_b^2 - U^b(b)\right\} \tag{3.12}$$
$$+ \frac{1}{2c^2}\frac{\partial^2}{\partial t^2}\left[\sum_b{}' \gamma m_b|a-b|\right],$$
$$U_i^a(a) = \sum_b{}' \frac{\gamma m_b b_i}{|a-b|}\left\{1 + \frac{1}{2c^2}(v_b^2 + 6U^b(b)\right\}$$
$$+ \frac{1}{2c^2}\frac{\partial^2}{\partial t^2}\sum_b{}' \gamma m_b \dot{b}_i|a-b| + \frac{22}{3c^2}\sum_b{}' \frac{\gamma\varepsilon_b\dot{b}_i}{|a-b|},$$

where

$$\varepsilon_b = \int_0^\infty \psi_b(r)\,d\omega \tag{3.13}$$

is the absolute value of the potential energy of the Newtonian gravitational field of the mass of body b. The symbol Σ' denotes a sum not including the term with the index $b = a$.

The solutions of the equations (3.4) outside the masses are given by the relations

$$U_{ii} = \sum_a\left(\frac{\gamma m_a v_a^2}{|r-a|} + \frac{\gamma\varepsilon_a}{|r-a|}\right), \tag{3.14}$$

$$V_{ii} = \sum_a\left(\frac{\gamma^2 m_a^2}{4|r-a|^2}\right. \tag{3.15}$$
$$\left. + \sum_{b\neq a}\frac{\gamma^2 m_a m_b}{2}\frac{\partial^2 \ln S}{\partial a_j \partial b_j} - \frac{\gamma\varepsilon_a}{|r-a|}\right),$$

in which ϵ_a is defined by Eq. (3.13) and

$$S = |r-a| + |r-b| + |a-b|. \tag{3.16}$$

It must be noted that at distances large in comparison with the linear dimensions of the body

$$U \approx \gamma m_a/|r-a|. \tag{3.17}$$

It is essential that, in accordance with Eqs. (3.14) and (3.15), the quantity $S = U_{ii} + V_{ii}$ defined by Eq. (3.5) does not contain terms involving ϵ_a, while at the center of mass of the given body

$$S(x) = \sum_b \left(\frac{2\gamma m_b v_b^2}{|x-b|} - \frac{\gamma m_b \dot{v}_b}{4|x-b|^2} \right) \quad (3.18)$$

$$-\sum_b \sum_{c \neq b} \frac{\gamma^2 m_b m_c}{2} \frac{\partial^2 |x-b|}{\partial x_i \partial x_i}.$$

We now introduce the potential energy of interaction of the bodies of the system.

$$\Phi = -\frac{1}{2} \sum_a \sum_b{}' \frac{\gamma m_a m_b}{|a-b|}. \quad (3.19)$$

Multiplying Eq. (3.10) by m_a and substituting into it the quantities defined by the relations (3.12), (3.18), and (3.19), we obtain the equations of motion with relativistic corrections:

$$m_a \ddot{a}_i + \frac{\partial \Phi}{\partial a_i} \quad (3.20)$$

$$-\frac{1}{c^2}\left\{ \dot{v}_a^2 - 4U^{(a)}(a)\frac{\partial \Phi}{\partial a_i} - 4\dot{a}_i \dot{a}_k \frac{\partial \Phi}{\partial a_k} \right.$$

$$-\gamma m_a \sum_b{}' \left(\frac{7}{2|a-b|} \frac{\partial \Phi}{\partial b_i} \right.$$

$$\left. + \frac{(a_i-b_i)(a_k-b_k)}{2|a-b|^3} \frac{\partial \Phi}{\partial b_k} \right)$$

$$-\gamma m_a \sum_b{}' m_b \left[-\frac{1}{2}\dot{b}_k \dot{b}_l \frac{\partial^3 |a-b|}{\partial a_i \partial a_k \partial a_l} + \frac{a_i-b_i}{|a-b|^3} \right.$$

$$\times \left(\frac{3}{2} v_b^2 - 4\dot{a}_k \dot{b}_k - U^{(b)}(b) \right)$$

$$\left.\left. + \frac{a_k-b_k}{|a-b|^3}\left(4\dot{a}_k \dot{b}_i - 4\dot{b}_k \dot{a}_i + 3\dot{b}_k \dot{b}_i\right) \right] \right\} = 0.$$

They are in complete agreement with the equations obtained by Petrova[2] by Fock's method as the condition of solubility of the gravitational equations (1.1) in the third approximation. It is appropriate here to emphasize once again that Eq. (3.20) has been found on the basis of Eq. (1.1) in only the second approximation.

The new derivation of Eq. (3.20) shows that in the method of Fock there is essentially a replacement of extended bodies by masses located at their centers of mass. We also get an understanding of why the relativistic equations of motion turn out the same when obtained from different hypotheses about the bodies, either as finitely extended masses[4,5] or as point masses,[3] since in both cases it is a question of the centers of mass of the bodies, in which their masses are, as it were, concentrated. The correctness of what has been said can also be verified by direct calculation.

4. THE RELATIVISTIC EQUATIONS OF MOTION AS A CONSEQUENCE OF THE SOLUTION OF THE GRAVITATIONAL EQUATIONS IN SECOND APPROXIMATION BY THE METHOD OF EINSTEIN AND HIS COWORKERS[3]

In this work the bodies are treated as point masses, for which the tensor $g_{\mu\nu}$ of the external field is to be found in the form

$$g_{\mu\nu} = \eta_{\mu\nu} + h_{\mu\nu}, \quad (4.1)$$

where $\eta_{\mu\nu}$ are the elements of the matrix

$$\eta^{\mu\nu} = \begin{pmatrix} 1 & 0 & 0 & 0 \\ 0 & -1 & 0 & 0 \\ 0 & 0 & -1 & 0 \\ 0 & 0 & 0 & -1 \end{pmatrix}. \quad (4.2)$$

Here we have set $x_0 = ct$; the $h_{\mu\nu}$ are expanded in series

$$h_{00} = c^{-2}\underset{2}{h}_{00} + c^{-4}\underset{4}{h}_{00} + \dots;$$

$$h_{0m} = c^{-3}\underset{3}{h}_{0m} + c^{-5}\underset{5}{h}_{0m} + \dots, \quad (4.3)$$

$$h_{mn} = c^{-2}\underset{2}{h}_{mn} + c^{-4}\underset{4}{h}_{mn} + \dots$$

Use is also made of the quantities

$$\gamma_{\mu\nu} = h_{\mu\nu} - \tfrac{1}{2}\eta_{\mu\nu}\eta^{\alpha\beta}h_{\alpha\beta}, \quad (4.4)$$

which are also expanded in series analogous to Eq. (4.3).

For the case of two bodies values of $h_{\mu\nu}$ and $\gamma_{\mu\nu}$ have been found in second approximation that made it possible to obtain the value of the metric tensor $g'_{\mu\nu}$, with, as before, $x_0 = t$. At the location of the particle with mass m_a, or, with our approach, at the center of mass of the body with mass m_a, these values $g'_{\mu\nu}$ have the form

$$g'_{00} = c^2 - \frac{2\gamma m_b}{|a-b|} - \frac{3\gamma m_b v_b^2}{c^2 |a-b|}$$

$$+ \frac{4\gamma^2 m_b^2}{c^2 |a-b|^2} - \frac{\gamma m_b}{c^2}\frac{\partial^2}{\partial t^2}|a-b|, \quad (4.5)$$

$$g'_{0m} = \frac{4\gamma m_b \dot{b}_m}{c^2 |a-b|}; \quad g'_{mn} = -\delta_{mn}\left(1 + \frac{2\gamma m_b}{c^2 |a-b|}\right).$$

It is not hard to verify that the relations (4.5) agree precisely with (3.8), if in these latter relations the values of U, U_i and S are substituted and the system is taken to consist of only two bodies. It is obvious that substitution of (4.5) into the equation of motion (2.20) and replacement of x_i by a_i lead to the relations written for a system of two bodies.

---

[1] A. Einstein and J. Grommer, Sitzber. Berl. Acad., p. 2, 1927.

[2] A. Einstein, Sitzber. Berl. Acad. p. 235, 1927.

[3] Einstein, Infeld, and Hoffman, Annals of Math. 39, 55 (1938).

[4] V. A. Fock, J. Exptl. Theoret. Phys. (U.S.S.R.) 9, 375 (1939).

[5] N. M. Petrova, J. Exptl. Theoret. Phys. (U.S.S.R.) 19, 989 (1949).

[6] I. G. Fikhtengol'ts, J. Exptl. Theoret. Phys. (U.S.S.R.) 20, 233 (1953).

[7] V. A. Fock, Priroda 12, 1953.

[8] L. Infeld, Bull. Pol. Acad. Sci., Sect. III, 2, 4 (1954).

[9] M. F. Shirokov, J. Exptl. Theoret. Phys. (U.S.S.R.) 30, 180 (1956); Soviet Phys. JETP 3, 197 (1956).

[10] M. F. Shirokov, J. Exptl. Theoret. Phys. (U.S.S.R.) 27, 251 (1954).

Translated by W. H. Furry
217

SOVIET PHYSICS JETP VOLUME 4, NUMBER 6 JULY, 1957

The Three Body Problem for Short Range Forces II

G. V. SKORNIAKOV

Leningrad Physico-Technical Institute, Acad. Sci. USSR

(Submitted to JETP editor October 31, 1955)
J. Exptl. Theoret. Phys. (USSR) **31**, 1046-1054 (December, 1956)

An iteration method is proposed for finding the wave function and binding energy of a three body system for the case of short range forces. The method is applied to the ground state of H^3.

---

1. METHOD

IN Ref. 1, an integral equation was obtained for the Fourier-transformed wave function of three identical particles

$$F(\mathbf{k}_1, \mathbf{r}_{23}) = \int e^{-i\mathbf{k}_1\mathbf{s}_1}\Psi(\mathbf{s}_1, \mathbf{r}_{23})\, d\mathbf{s}_1,$$

which, for the case of a bound state, can be written in the form

$$F(\mathbf{k}_1, \mathbf{r}_{23}) = \int \frac{\exp\{-\sqrt{\alpha^2 + 3k_1^2/4}\,|\mathbf{r}_{23} - \mathbf{r}|\}}{|\mathbf{r}_{23} - \mathbf{r}|} V(r) F(\mathbf{k}_1\mathbf{r})\, d\mathbf{r} + 8\pi \int \frac{\cos(\mathbf{r}_{23}, \mathbf{k}_1/2 + \mathbf{k})}{\alpha^2 + k_1^2 + k^2 + \mathbf{k}_1\mathbf{k}} V(r) \times \cos(\mathbf{r}, \mathbf{k}_1 + \mathbf{k}/2) F(\mathbf{k}, \mathbf{r})\, d\mathbf{r} \frac{d\mathbf{k}}{(2\pi)^3}. \qquad (1)$$

Here

$$\mathbf{s}_1 = \mathbf{r}_1 - \tfrac{1}{2}(\mathbf{r}_2 + \mathbf{r}_3); \quad \mathbf{r}_{23} = \mathbf{r}_2 - \mathbf{r}_3$$

are the variables describing the relative motion;

$$V(r) = -MU(r)/4\pi\hbar^2;$$

$U(r)$ is the interaction potential between any pair of particles; $\alpha^2 = -ME/\hbar^2$, E is the energy of the system.

From Eq. (1) it follows that if the potential $V(r)$ has a finite range r_0, then to determine the wave function over all space it is sufficient to know $F(\mathbf{k}, \mathbf{r})$ for $r < r_0$. This makes possible the development of an iteration method for finding the eigenfunction F and the eigenvalue α for the case where the characteristic dimensions of the system far exceed the force range r_0.

We shall assume that $V(r)$ is practically zero for $r > r_0$, while for $r < r_0$, $V(r) >> \alpha^2$, where $\alpha r_0 << 1$. The quantity $1/\alpha$ determines the effective linear dimensions of the system.

In addition, we shall assume that there is a single bound state for two particles with small binding energy ϵ (as for the deuteron). The wave function φ_0 of such a system satisfies the integral equation

$$\varphi_0(r) = \int \frac{\exp\{-\gamma|\mathbf{r} - \mathbf{r}'|\}}{|\mathbf{r} - \mathbf{r}'|} V(r')\varphi_0(r')\, d\mathbf{r}', \qquad (2)$$

where $\gamma = \sqrt{M\varepsilon}/\hbar$,

where $\gamma r_0 \ll 1$.

It is not hard to see that with these assumptions concerning the structure of Eq. (1), the second term on the right is smaller than the first by a factor of order αr_0 when $r_{23} < r_0$. This enables us to apply to the solution of Eq. (1) a method of successive approximations analogous to the usual perturbation theory.

In fact, let us rewrite Eq. (1) in the following form:

$$F(\mathbf{k}_1, \mathbf{r}_{23}) = \int \frac{\exp\{-\gamma|\mathbf{r}_{23} - \mathbf{r}|\}}{|\mathbf{r}_{23} - \mathbf{r}|} V(r) F(\mathbf{k}_1, \mathbf{r})\, d\mathbf{r} + \int \frac{\exp\{-\sqrt{\alpha^2 + 3k_1^2/4}\,|\mathbf{r}_{23} - \mathbf{r}|\} - \exp\{-\gamma|\mathbf{r}_{23} - \mathbf{r}|\}}{|\mathbf{r}_{23} - \mathbf{r}|} \times V(r) F(\mathbf{k}_1, \mathbf{r})\, d\mathbf{r} + 8\pi \int \frac{\cos(\mathbf{r}_{23}, \mathbf{k}_1/2 + \mathbf{k})}{\alpha^2 + k_1^2 + k^2 + \mathbf{k}_1\mathbf{k}} \times V(r) \cos(\mathbf{r}, \mathbf{k}_1 + \mathbf{k}/2) F(\mathbf{k}, \mathbf{r})\, d\mathbf{r} \frac{d\mathbf{k}}{(2\pi)^3}. \qquad (3)$$

From this expression it is clear that for $r_{23} < r_0$ the last two terms on the right are smaller than the first by a factor of order αr_0, since

$$\int V(r)\, d\mathbf{r} \sim r_0,$$ [1,3]

and the last two terms unlike the first do not contain a denominator of order r_0. In addition we must take into account the fact that in the integral over $\mathbf{k}$ the essential region of integration should be the region $k \lesssim \alpha$, since for large k the function $F(\mathbf{k}, \mathbf{r})$, $(r < r_0)$ decreases rapidly.

Therefore the solution of Eq. (1) when $r_{23} < r_0$ must coincide, to terms of order αr_0, with the solution of the equation

$$F^0(\mathbf{k}_1, \mathbf{r}_{23}) = \int \frac{\exp\{-\gamma \,|\mathbf{r}_{23} - \mathbf{r}|\}}{|\mathbf{r}_{23} - \mathbf{r}|} V(r) F^0(\mathbf{k}_1, \mathbf{r})\, d\mathbf{r}. \tag{4}$$

The solution of this equation, corresponding to an S-state of the system, will be

$$F^0(\mathbf{k}_1, \mathbf{r}_{23}) = \chi(k_1)\varphi_0(r_{23}), \tag{5}$$

where χ is an as yet unknown function and φ_0 is determined by Eq. (2).

Thus the wave function in zeroth approximation has the form (5) in the region $r_{23} < r_0$. Using this function, we can determine the zeroth approximation wave function $F_0(\mathbf{k}_1, \mathbf{r}_{23})$ over all space by substituting (5) into the right side of Eq. (1):

$$\begin{aligned} F_0(\mathbf{k}_1, \mathbf{r}_{23}) &= \chi(k_1) \\ &\times \int \frac{\exp\{-\sqrt{\alpha_0^2 + 3k_1^2/4}\,|\mathbf{r}_{23} - \mathbf{r}|\}}{|\mathbf{r}_{23} - \mathbf{r}|} V(r)\varphi_0(r)\, d\mathbf{r} \\ &+ 8\pi \int \frac{\cos(\mathbf{r}_{23}, \mathbf{k}_1/2 + \mathbf{k})}{\alpha_0^2 + k_1^2 + k^2 + \mathbf{k}_1\mathbf{k}} \\ &\times V(r)\cos(\mathbf{r}_1, \mathbf{k}_1 + \mathbf{k}/2)\varphi_0(r)\, d\mathbf{r}\, \frac{d\mathbf{k}}{(2\pi)^3}. \end{aligned} \tag{6}$$

For $r_{23} < r_0$, the function $F_0(\mathbf{k}_1, \mathbf{r}_{23})$ thus determined must reduce (up to terms of order $\alpha_0 r_0$) to the product $\chi(k_1)\varphi_0(r_{23})$.

It is easy to show that the difference

$$\begin{aligned} F_0(\mathbf{k}_1, \mathbf{r}_{23}) - \chi(k_1)\varphi_0(r_{23})\big|_{r_{23}<r_0} &= \Delta(\mathbf{k}_1, \mathbf{r}_{23}) \\ &= \chi(k_1) \\ \times \int \frac{\exp\{-\sqrt{\alpha_0^2 + 3k_1^2/4}\,|\mathbf{r}_{23} - \mathbf{r}|\} - \exp\{-\gamma\,|\mathbf{r}_{23} - \mathbf{r}|\}}{|\mathbf{r}_{23} - \mathbf{r}|} \\ &\times V(r)\varphi_0(r)\, d\mathbf{r} \\ &+ 8\pi \int \frac{\cos(\mathbf{r}_{23}, \mathbf{k}_1/2 + \mathbf{k})}{\alpha_0^2 + k_1^2 + k^2 + \mathbf{k}_1\mathbf{k}} \\ &\times V(r)\cos(\mathbf{r}, \mathbf{k}_1 + \mathbf{k}/2)\varphi_0(r)\, d\mathbf{r}\, \frac{d\mathbf{k}}{(2\pi)^3} \end{aligned} \tag{7}$$

when expanded in powers of $(\alpha_0 r_0)$, contains a term proportional to $(\alpha_0 r_0)$

$$\begin{aligned} &\Big\{(\gamma - \sqrt{\alpha_0^2 + 3k_1^2/4})\,\chi(k_1) \\ &+ 8\pi \int \frac{\chi(k)}{\alpha_0^2 + k_1^2 + k^2 + \mathbf{k}_1\mathbf{k}} \frac{d\mathbf{k}}{(2\pi)^3}\Big\} \int V(r)\varphi_0(r)\, d\mathbf{r}, \end{aligned} \tag{7a}$$

which does not depend on r_{23}, and also terms proportional to higher powers of $(\alpha_0 r_0)$. $\chi(k_1)$ and α_0 (the eigenvalue in zeroth approximation) are as yet undetermined. To determine them we demand that, for $r_{23} < r_0$, the difference

$$\Delta(\mathbf{k}_1, \mathbf{r}_{23}) = F_0(\mathbf{k}_1, \mathbf{r}_{23}) - \chi(k_1)\varphi_0(r_{23})$$

shall vanish on the average:

$$\int V(r_{23})\varphi_0(r_{23})\Delta(\mathbf{k}_1, \mathbf{r}_{23})\, d\mathbf{r}_{23} = 0. \tag{8}$$

Since for $r_{23} < r_0$ the term in $\Delta(\mathbf{k}_1, \mathbf{r}_{23})$ proportional to $(\alpha_0 r_0)$ does not depend on $\mathbf{r}_{23}$, and can be taken out from under the integral sign, this requirement means that when $r_{23} < r_0$ the function $F_0(\mathbf{k}_1, \mathbf{r}_{23})$ reproduces itself up to terms of order $(\alpha_0 r_0)$ inclusive. Since the function $F(\mathbf{k}_1, \mathbf{r}_{23})$ is determined over all space by $F(\mathbf{k}_1, \mathbf{r}_{23})$ for $r_{23} < r_0$, the function $F_0(\mathbf{k}_1, \mathbf{r}_{23})$ determined in this way will satisfy the integral Eq. (1) to this same degree of accuracy.

However, we cannot simply equate to zero the term (7a) in the difference $\Delta(\mathbf{k}_1, \mathbf{r}_{23})$, which is proportional to $(\alpha_0 r_0)$, since such a requirement leads to the equation for $\chi(k_1)$ which was obtained[1] on the assumption of zero range of the forces, in which case it is known[2] that a bound state of three particles cannot exist.

It is therefore necessary even when we determine the zeroth approximation to the eigenfunction and eigenvalue, to treat the force range r_0 as finite; we then effectively include higher terms of the expansion of $\Delta(\mathbf{k}_1, \mathbf{r}_{23})$ in powers of r_0.

The condition (8) gives an integral equation for determining $\chi(k_1)$ and α_0:

$$\begin{aligned} &\chi(k_1) \\ &\times \int \frac{\exp\{-\sqrt{\alpha_0^2 + 3k_1^2/4}\,|\mathbf{r}_{23} - \mathbf{r}| - \exp\{-\gamma\,|\mathbf{r}_{23} - \mathbf{r}|\}}{|\mathbf{r}_{23} - \mathbf{r}|} \\ &\times V(r_{23})V(r)\varphi_0(r_{23})\varphi_0(r)\, d\mathbf{r}d\mathbf{r}_{23} \\ &+ 8\pi \int \frac{\cos(\mathbf{r}_{23}, \mathbf{k}_1/2 + \mathbf{k})\,\chi(k)}{\alpha_0^2 + k_1^2 + k^2 + \mathbf{k}_1\mathbf{k}} \\ &\times \cos(\mathbf{r}, \mathbf{k}_1 \\ &+ \mathbf{k}/2)V(r_{23})V(r)\varphi_0(r_{23})\varphi_0(r)\, d\mathbf{r}d\mathbf{r}_{23}\, \frac{d\mathbf{k}}{(2\pi)^3} = 0. \end{aligned} \tag{9}$$

We note that for k_1, k small the kernel of the integral equation (9) does not depend on the specific form of the potential, while for large k_1, k, because of the cosines in the integral, the kernel decreases rapidly. The manner in which the kernel decreases also depends very little on the specific form of the potential and is determined only by the effective range of the forces.

According to formula (6), the determination of the eigenfunction $\chi(k_1)$ and eigenvalue α_0 of Eq. (9) gives us the zeroth approximation to the eigenfunction $F(\mathbf{k}_1, \mathbf{r}_{23})$. α_0 is the zeroth approximation to the eigenvalue α. Thus the solution of the multidimensional Eq. (1) reduces in zeroth approximation to the solution of the one-dimensional integral Eq. (9) and the quadriture in (6).

In finding the higher approximations, we can make use of the following iteration method. The higher approximations to the eigenvalue α will be determined from the equation

$$\int |F_{n-1}(\mathbf{k}_1, \mathbf{r}_{23})|^2 \, d\mathbf{k}_1 d\mathbf{r}_{23} \qquad (10)$$

$$= \int F^*_{n-1}(\mathbf{k}_1, \mathbf{r}_{23}) \left\{ \int \frac{\exp\left\{-\sqrt{\alpha_n^2 + 3k_1^2/4}\,|\mathbf{r}_{23} - \mathbf{r}|\right\}}{|\mathbf{r}_{23} - \mathbf{r}|} \times V(r) F_{n-1}(\mathbf{k}_1, \mathbf{r}) \, d\mathbf{r} \right.$$

$$+ 8\pi \int \frac{\cos(\mathbf{r}_{23}, \mathbf{k}_1/2 + \mathbf{k})}{\alpha_n^2 + k_1^2 + k^2 + \mathbf{k}_1\mathbf{k}} \cos(\mathbf{r}, \mathbf{k}_1 + \mathbf{k}/2) V(r)$$

$$\left. \times F_{n-1}(\mathbf{k}, \mathbf{r}) \, d\mathbf{r} \, \frac{d\mathbf{k}}{(2\pi)^3} \right\} d\mathbf{k}_1 d\mathbf{r}_{23},$$

where α_n is the nth approximation to the eigenvalue, and F_{n-1} is the $(n-1)$st approximation to the eigenfunction.

It is easy to see that this determination of α_n (and consequently of the energy of the system in nth approximation) is equivalent to computing the matrix element of the Hamiltonian using the wave function of the $(n-1)$st approximation.*

After having determined the nth approximation to the eigenvalue α, by substituting the $(n-1)$st approximation to the eigenfunctiom and the nth approximation to the eigenvalue on the right of Eq. (1), we get the nth approximation to the eigenfunction

$$F_n(\mathbf{k}_1, \mathbf{r}_{23}) = \int \frac{\exp\left\{-\sqrt{\alpha_n^2 + 3k_1^2/4}\,|\mathbf{r}_{23} - \mathbf{r}|\right\}}{|\mathbf{r}_{23} - \mathbf{r}|} \qquad (11)$$

$$\times V(r) F_{n-1}(\mathbf{k}_1, \mathbf{r}) \, d\mathbf{r}$$

$$+ 8\pi \int \frac{\cos(\mathbf{r}_{23}, \mathbf{k}_1/2 + \mathbf{k})}{\alpha_n^2 + k_1^2 + k^2 + \mathbf{k}_1\mathbf{k}}$$

$$\times \cos(\mathbf{r}, \mathbf{k}_1 + \mathbf{k}/2) V(r) F_{n-1}(\mathbf{k}, \mathbf{r}) \, d\mathbf{r} \frac{d\mathbf{k}}{(2\pi)^3}.$$

Thus each successive approximation is obtained from the preceding one by a multiple integration. If $\alpha_0 r_0 \ll 1$, we can limit ourselves to the zeroth approximation for a practical solution of the problem.

2. APPLICATION TO H^3

The method we have presented is easily generalized to the case of a system of three nucleons (H^3). The operator for the interaction of the nucleons in the H^3 nucleus will be assumed to be a sum of interaction potentials between pairs of nucleons.

In addition we shall assume that the interaction potential between a pair of nucleons is central and that the nuclear forces are charge independent. The most general expression for such a potential is

$$\hat{U}_{ik} = U_1(|\mathbf{r}_i - \mathbf{r}_k|) + (\boldsymbol{\sigma}_i\boldsymbol{\sigma}_k) U_2(|\mathbf{r}_i - \mathbf{r}_k|) \qquad (12)$$

$$+ (\boldsymbol{\tau}_i\boldsymbol{\tau}_k) U_3(|\mathbf{r}_i - \mathbf{r}_k|)$$

$$+ (\boldsymbol{\sigma}_i\boldsymbol{\sigma}_k)(\boldsymbol{\tau}_i\boldsymbol{\tau}_k) U_4(|\mathbf{r}_i - \mathbf{r}_k|).$$

Under these assumptions concerning the nuclear forces, the spin S and isotopic spin T of the three-nucleon system are conserved. In the ground state of H^3, $S = T = \frac{1}{2}$. The wave function of such a state can be written as[1,4]

$$\Psi_{1/2,\,1/2} = \Psi_a \Phi_c - \Psi_s \Phi_a + \Psi_1 \Phi_2 - \Psi_2 \Phi_1.$$

The spin functions Φ were determined in Ref. 1, which also gives a detailed description of the transformation properties of the space functions Ψ under permutations.

Using the Green's function[1]

---

* It can be shown that the difference between the binding energies ϵ_0 and ϵ_1, calculated in zeroth and first approximations, respectively, is a quantity of order $\epsilon_0(\alpha_0 r_0)^2$.

$$G = \int \frac{\exp\{-\sqrt{\alpha^2 + 3k^2/4}\ |\mathbf{r} - \mathbf{r}'|\}}{|\mathbf{r} - \mathbf{r}'|}\, e^{i\mathbf{k}(\mathbf{s}-\mathbf{s}')}\, \frac{d\mathbf{k}}{(2\pi)^3} \tag{13}$$

we write the Schrodinger equation in integral form:

$$\Psi_{1/2,\,1/2} = \int G\,\{\hat{V}_{12} + \hat{V}_{13} + \hat{V}_{23}\}\,\Psi_{1/2,\,1/2}\,d\tau, \tag{14}$$

$$\hat{V}_{ik} = -\,(M/4\pi\hbar^2)\,\hat{U}_{ik}.$$

If we multiply Eq. (14) by $\Phi^*_\alpha(\alpha = s,\ a,\ 1,\ 2)$ and sum over the spin variables, then by making use of the transformation properties of the space wave function under permutations we find as the result of very messy but (in principle) simple calculations, the following system of integral equations for the Fourier transforms

$$f_\alpha(\mathbf{k}_1, \mathbf{r}_{23}) = \int e^{-i\mathbf{k}_1\mathbf{s}_1}\,\Psi_\alpha(\mathbf{s}_1,\ \mathbf{r}_{23})\,d\mathbf{s}_1,$$

of the space functions:

$$\begin{aligned}
f_s(\mathbf{k}_1, \mathbf{r}_{23}) = \int & \frac{\exp\left\{-\sqrt{\alpha^2 + 3k_1^2/4}\,|\mathbf{r}_{23} - \mathbf{r}|\right\}}{|\mathbf{r}_{23} - \mathbf{r}|} \left\{\frac{1}{2}[V_t(r) + V_s(r)]\,f_s(\mathbf{k}_1, \mathbf{r})\right.\\
& \left. + \frac{1}{2}[V_s(r) - V_t(r)]\,f_2(\mathbf{k}_1, \mathbf{r})\right\} d\mathbf{r} + 8\pi \int \frac{\cos(\mathbf{r}_{23}, \mathbf{k}_1/2 + \mathbf{k})}{\alpha^2 + k_1^2 + k^2 + \mathbf{k}_1\mathbf{k}} \cos(\mathbf{r}, \mathbf{k}_1 + \mathbf{k}/2)\\
& \times \left\{\frac{1}{2}[V_t(r) + V_s(r)]\,f_s(\mathbf{k}, \mathbf{r}) + \frac{1}{2}[V_s(r) - V_t(r)]\,f_2(\mathbf{k}, \mathbf{r})\right\} d\mathbf{r}\,\frac{d\mathbf{k}}{(2\pi)^3};\\
f_a(\mathbf{k}_1, \mathbf{r}_{23}) = \int & \frac{\exp\left\{-\sqrt{\alpha^2 + 3k_1^2/4}\,|\mathbf{r}_{23} - \mathbf{r}|\right\}}{|\mathbf{r}_{23} - \mathbf{r}|} \left\{\frac{1}{2}[V_q(r) + V_r(r)]\,f_a(\mathbf{k}_1, \mathbf{r})\right.\\
& \left. + \frac{1}{2}[V_q(r) - V_r(r)]\,f_1(\mathbf{k}_1, \mathbf{r})\right\} d\mathbf{r} - 8\pi \int \frac{\sin(\mathbf{r}_{23}, \mathbf{k}_1/2 + \mathbf{k})}{\alpha^2 + k_1^2 + k^2 + \mathbf{k}_1\mathbf{k}} \sin(\mathbf{r}, \mathbf{k}_1 + \mathbf{k}/2)\\
& \times \left\{\frac{1}{2}[V_q(r) + V_r(r)]\,f_a(\mathbf{k}, \mathbf{r}) + \frac{1}{2}[V_q(r) - V_r(r)]\,f_1(\mathbf{k}, \mathbf{r})\right\} d\mathbf{r}\,\frac{d\mathbf{k}}{(2\pi)^3};\\
f_2(\mathbf{k}_1, \mathbf{r}_{23}) = \int & \frac{\exp\left\{-\sqrt{\alpha^2 + 3k_1^2/4}\,|\mathbf{r}_{23} - \mathbf{r}|\right\}}{|\mathbf{r}_{23} - \mathbf{r}|} \left\{\frac{1}{2}[V_s(r) - V_t(r)]\,f_s(\mathbf{k}_1, \mathbf{r})\right.\\
& \left. + \frac{1}{2}[V_t(r) + V_s(r)]\,f_2(\mathbf{k}_1, \mathbf{r})\right\} d\mathbf{r} + 8\pi \int \frac{\cos(\mathbf{r}_{23}, \mathbf{k}_1/2 + \mathbf{k})}{\alpha^2 + k_1^2 + k^2 + \mathbf{k}_1\mathbf{k}} \left\{\cos(\mathbf{r}, \mathbf{k}_1 + \mathbf{k}/2)\right.\\
& \times \left[\frac{1}{4}(V_t(r) - V_s(r))\,f_s(\mathbf{k}, \mathbf{r}) - \frac{1}{4}(V_t(r) + V_s(r))\,f_2(\mathbf{k}, \mathbf{r})\right]\\
& - i\sin(\mathbf{r}, \mathbf{k}_1 + \mathbf{k}/2)\left[\frac{\sqrt{3}}{4}(V_r(r) - V_q(r))\,f_a(\mathbf{k}, \mathbf{r}) - \frac{\sqrt{3}}{4}(V_r(r) + V_q(r))\right.\\
& \left.\left. \times f_1(\mathbf{k}, \mathbf{r})\right]\right\} d\mathbf{r}\,\frac{d\mathbf{k}}{(2\pi)^3};\\
f_1(\mathbf{k}_1, \mathbf{r}_{23}) = \int & \frac{\exp\{-\sqrt{\alpha^2 + 3k^2{}_1/4}\,|\mathbf{r}_{23} - \mathbf{r}|\}}{|\mathbf{r}_{23} - \mathbf{r}|} \left\{\frac{1}{2}[V_q(r) - V_r(r)]\,f_a(\mathbf{k}_1, \mathbf{r})\right.\\
& \left. + \frac{1}{2}[V_q(r) + V_r(r)]\,f_1(\mathbf{k}_1, \mathbf{r})\right\} d\mathbf{r} + 8\pi i \int \frac{\sin(\mathbf{r}_{23}, \mathbf{k}_1/2 + \mathbf{k})}{\alpha^2 + k_1^2 + k^2 + \mathbf{k}_1\mathbf{k}} \left\{\cos(\mathbf{r}, \mathbf{k}_1 + \mathbf{k}/2)\right.\\
& \times \left[\frac{\sqrt{3}}{4}(V_t(r) - V_s(r))\,f_s(\mathbf{k}, \mathbf{r}) - \frac{\sqrt{3}}{4}(V_t(r) + V_s(r))\,f_2(\mathbf{k}, \mathbf{r})\right]\\
& - i\sin(\mathbf{r}, \mathbf{k}_1 + \mathbf{k}/2)\left[\frac{1}{4}(V_q(r) - V_r(r))\,f_a(\mathbf{k}, \mathbf{r})\right.\\
& \left.\left. + \frac{1}{4}(V_q(r) + V_r(r))\,f_1(\mathbf{k}, \mathbf{r})\right]\right\} d\mathbf{r}\,\frac{d\mathbf{k}}{(2\pi)^3}.
\end{aligned} \tag{15}$$

Equation (15) is the generalization of Eq. (1) to the case of three nucleons. The potentials V_t, V_s, V_r, and V_q are directly related to processes occurring in the two-nucleon system: the potential V_t is responsible for the existence of the deuteron as well as for the scattering of two nucleons in a state of spin 1 and even orbital angular momentum; the potential V_s causes the scattering of nucleons with spin 0 and even orbital angular momentum, and V_q the scattering for spin 0 and odd orbital angular momentum.

3. METHOD OF APPROXIMATE SOLUTION OF THE EQUATION

For an approximate solution of the system (15), we shall make use of the fact that the potentials V_t, V_s, V_r and V_q are short-range, and that the range of the nuclear forces, r_0, can be regarded as approximately the same for all four potentials in making rough estimates. From the transformation properties of the wave functions in coordinate representation it follows that $\Psi_s(\mathbf{s}_1, \mathbf{r}_{23})$ and $\Psi_2(\mathbf{s}_1 \mathbf{r}_{23})$ are symmetric with respect to the permutation P_{23}, while $\Psi_a(\mathbf{s}_1, \mathbf{r}_{23})$ and $\psi_1(\mathbf{s}_1, \mathbf{r}_{23})$ are antisymmetric with respect to this permutation.[1] Since the Fourier transformation of the wave function does not affect the variable $\mathbf{r}_{23}$, the functions f_α have these same properties.

Using the antisymmetry of the functions $f_a(\mathbf{k}_1, \mathbf{r}_{23})$ and $f_1(\mathbf{k}_1, \mathbf{r}_{23})$ with respect to a change in sign of $\mathbf{r}_{23}$, it is not difficult to show that, to terms of order $(\alpha r_0)^3$, the system of integral equations (15) reduces to the following:

$$f_s(\mathbf{k}_1, \mathbf{r}_{23}) = \int \frac{\exp\left\{-\sqrt{\alpha^2 + 3k_1^2/4}\,|\mathbf{r}_{23} - \mathbf{r}|\right\}}{|\mathbf{r}_{23} - \mathbf{r}|} \left\{\frac{1}{2}[V_t(r) + V_s(r)]\, f_s(\mathbf{k}_1, \mathbf{r})\right.$$
$$\left. + \frac{1}{2}[V_s(r) - V_t(r)]\, f_2(\mathbf{k}_1, \mathbf{r})\right\} d\mathbf{r} + 8\pi \int \frac{\cos(\mathbf{r}_{23}, \mathbf{k}_1/2 + \mathbf{k})}{\alpha^2 + k_1^2 + k^2 + \mathbf{k}_1\mathbf{k}} \cos(\mathbf{r}, \mathbf{k}_1 + \mathbf{k}/2)$$
$$\times \left\{\frac{1}{2}[V_t(r) + V_s(r)]\, f_s(\mathbf{k}, \mathbf{r}) + \frac{1}{2}[V_s(r) - V_t(r)]\, f_2(\mathbf{k}, \mathbf{r})\right\} d\mathbf{r}\, \frac{d\mathbf{k}}{(2\pi)^3}; \quad f_a(\mathbf{k}_1, \mathbf{r}_{23}) \equiv 0; \tag{16}$$

$$f_2(\mathbf{k}_1, \mathbf{r}_{23}) = \int \frac{\exp\left\{-\sqrt{\alpha^2 + 3k_1^2/4}\,|\mathbf{r}_{23} - \mathbf{r}|\right\}}{|\mathbf{r}_{23} - \mathbf{r}|} \left\{\frac{1}{2}[V_s(r) - V_t(r)]\, f_s(\mathbf{k}_1, \mathbf{r})\right.$$
$$\left. + \frac{1}{2}[V_t(r) + V_s(r)]\, f_2(\mathbf{k}_1, \mathbf{r})\right\} d\mathbf{r} + 8\pi \int \frac{\cos(\mathbf{r}_{23}, \mathbf{k}_1/2 + \mathbf{k})}{\alpha^2 + k_1^2 + k^2 + \mathbf{k}_1\mathbf{k}} \cos(\mathbf{r}, \mathbf{k}_1 + \mathbf{k}/2)$$
$$\times \left\{\frac{1}{4}[V_t(r) - V_s(r)]\, f_s(\mathbf{k}, \mathbf{r}) - \frac{1}{4}[V_t(r) + V_s(r)]\, f_2(\mathbf{k}, \mathbf{r})\right\} d\mathbf{r}\, \frac{d\mathbf{k}}{(2\pi)^3};$$

$$f_1(\mathbf{k}_1, \mathbf{r}_{23}) = 8\pi i \int \frac{\sin(\mathbf{r}_{23}, \mathbf{k}_1/2 + \mathbf{k})}{\alpha^2 + k_1^2 + k^2 + \mathbf{k}_1\mathbf{k}} \cos(\mathbf{r}, \mathbf{k}_1 + \mathbf{k}/2) \left\{\frac{\sqrt{3}}{4}[V_t(r) - V_s(r)]\right.$$
$$\left. \times f_s(\mathbf{k}, \mathbf{r}) - \frac{\sqrt{3}}{4}[V_t(r) + V_s(r)]\, f_2(\mathbf{k}, \mathbf{r})\right\} d\mathbf{r}\, \frac{d\mathbf{k}}{(2\pi)^3}.$$

Thus in this approximation we have obtained a system of two integral equations for determining the functions f_s and f_2, while f_1 is determined from f_s and f_2 by integration. It is an essential point that only the two potentials $V_t(r)$ and $V_s(r)$ appear in (16), while it is precisely these potentials which determine all processes in a two-nucleon system for low energies of relative motion.

It is convenient to introduce in place of the functions f_s and f_2 the functions

$$\eta_1 = f_s + f_2; \quad \eta_2 = f_s - f_2, \tag{17}$$

for whose determination we obtain the following systems of integral equations:

$$\eta_1(\mathbf{k}_1, \mathbf{r}_{23}) = \int \frac{\exp\left\{-\sqrt{\alpha^2 + 3k_1^2/4}\,|\mathbf{r}_{23} - \mathbf{r}|\right\}}{|\mathbf{r}_{23} - \mathbf{r}|} \tag{18}$$
$$\times V_s(r)\, \eta_1(\mathbf{k}_1, \mathbf{r})\, d\mathbf{r} + 8\pi \int \frac{\cos(\mathbf{r}_{23}, \mathbf{k}_1/2 + \mathbf{k})}{\alpha^2 + k_1^2 + k^2 + \mathbf{k}_1\mathbf{k}}$$
$$\times \cos(\mathbf{r}, \mathbf{k}_1 + \mathbf{k}/2) \left\{\frac{1}{4} V_s(r)\, \eta_1(\mathbf{k}, \mathbf{r})\right.$$
$$\left. + \frac{3}{4} V_t(r)\, \eta_2(\mathbf{k}, \mathbf{r})\right\} d\mathbf{r}\, \frac{d\mathbf{k}}{(2\pi)^3}; \qquad \eta_2(\mathbf{k}_1, \mathbf{r}_{23})$$
$$= \int \frac{\exp\left\{-\sqrt{\alpha^2 + 3k_1^2/4}\,|\mathbf{r}_{23} - \mathbf{r}|\right\}}{|\mathbf{r}_{23} - \mathbf{r}|} V_t(r)\, \eta_2(\mathbf{k}_1, \mathbf{r})\, d\mathbf{r}$$
$$+ 8\pi \int \frac{\cos(\mathbf{r}_{23}, \mathbf{k}_1/2 + \mathbf{k})}{\alpha^2 + k_1^2 + k^2 + \mathbf{k}_1\mathbf{k}} \cos(\mathbf{r}, \mathbf{k}_1 + \mathbf{k}/2)$$
$$\times \left\{\frac{3}{4} V_s(r)\, \eta_1(\mathbf{k}, \mathbf{r}) + \frac{1}{4} V_t(r)\, \eta_2(\mathbf{k}, \mathbf{r})\right\} d\mathbf{r}\, \frac{d\mathbf{k}}{(2\pi)^3}.$$

To solve the equation system (18) it is necessary to know the functions only within the range of the nuclear forces. In complete analogy to the case of three identical particles, we may assume approximately that, within the range of action of the nuclear forces, the wave functions η_1 and η_2 can be represented in the form of products

$$\eta_1(\mathbf{k}_1, \mathbf{r}_{23}) \approx \chi_1(k_1)\,\varphi_1(r_{23}); \tag{19}$$

$$\eta_2(\mathbf{k}_1, \mathbf{r}_{23}) \approx \chi_2(k_1)\,\varphi_2(r_{23})$$

for $r_{23} < r_s$ and $r_{23} < r_t$, respectively; φ_1 and φ_2 are the wave functions within the range of nuclear forces for two nucleons in singlet and triplet states.

The wave functions φ_1 and φ_2 satisfy the following integral equations:

$$\varphi_1(r_{23}) = \int \frac{\exp\{-\alpha_s\,|\mathbf{r}_{23}-\mathbf{r}|\}}{|\mathbf{r}_{23}-\mathbf{r}|}\,V_s(r)\,\varphi_1(r)\,d\mathbf{r}, \tag{20a}$$

$$\varphi_2(r_{23}) = \int \frac{\exp\{-\alpha_t\,|\mathbf{r}_{23}-\mathbf{r}|\}}{|\mathbf{r}_{23}-\mathbf{r}|}\,V_t(r)\,\varphi_2(r)\,d\mathbf{r}, \tag{20b}$$

where α_s and α_t are defined in terms of the logarithmic derivatives at the interaction radius[*]:

$$\alpha_s = -\frac{d}{dr}\ln\{r\varphi_1(r)\}_{r=r_s}; \tag{21}$$

$$\alpha_t = -\frac{d}{dr}\ln\{r\varphi_2(r)\}_{r=r_t}.$$

From here on the procedure is completely analogous to the case of three identical particles.

Using the approximate expressions (19) for the wave functions within the range of the nuclear forces, we construct the zeroth approximation wave function:

$$\begin{aligned}
\eta_1^0(\mathbf{k}_1, \mathbf{r}_{23}) &= \chi_1(k_1)\int \frac{\exp\left\{-\sqrt{\alpha_0^2 + 3k_1^2/4}\,|\mathbf{r}_{23}-\mathbf{r}|\right\}}{|\mathbf{r}_{23}-\mathbf{r}|}\,V_s(r)\,\varphi_1(r)\,d\mathbf{r} \\
&+ 2\pi\int \frac{\cos(\mathbf{r}_{23}, \mathbf{k}_1/2 + \mathbf{k})}{\alpha^2 + k_1^2 + k^2 + \mathbf{k}_1\mathbf{k}}\cos(\mathbf{r}, \mathbf{k}_1 + \mathbf{k}/2)\,\{\chi_1(k)\,V_s(r)\,\varphi_1(r) \\
&+ 3\chi_2(k)\,V_t(r)\,\varphi_2(r)\}\,d\mathbf{r}\,\frac{d\mathbf{k}}{(2\pi)^3}; \\
\eta_2^0(\mathbf{k}_1, \mathbf{r}_{23}) &= \chi_2(k_1)\int \frac{\exp\left\{-\sqrt{\alpha_0^2 + 3k_1^2/4}\,|\mathbf{r}_{23}-\mathbf{r}|\right\}}{|\mathbf{r}_{23}-\mathbf{r}|}\,V_t(r)\,\varphi_2(r)\,d\mathbf{r} \\
&+ 2\pi\int \frac{\cos(\mathbf{r}_{23}, \mathbf{k}_1/2 + \mathbf{k})}{\alpha^2 + k_1^2 + k^2 + \mathbf{k}_1\mathbf{k}}\cos(\mathbf{r}, \mathbf{k}_1 + \mathbf{k}/2)\,\{3\chi_1(k)\,V_s(r)\,\varphi_1(r) \\
&+ \chi_2(k)\,V_t(r)\,\varphi_2(r)\}\,d\mathbf{r}\,\frac{d\mathbf{k}}{(2\pi)^3}.
\end{aligned} \tag{22}$$

As before, we determine χ_1, χ_2, and α_0 so that the differences $\eta_1^0(\mathbf{k}_1, \mathbf{r}_{23}) - \chi_1(k_1)\,\varphi_1(r_{23})$ and $\eta_2^0(\mathbf{k}_1, \mathbf{r}_{23}) - \chi_2(k_1)\,\varphi_2(r_{23})$ vanish on the average within the range of the forces:

$$\begin{aligned}
&\int V_s(r_{23})\,\varphi_1(r_{23})\,\{\eta_1^0(\mathbf{k}_1, \mathbf{r}_{23}) - \chi_1(k_1)\,\varphi_1(r_{23})\}\,d\mathbf{r}_{23} = 0, \\
&\int V_t(r_{23})\,\varphi_2(r_{23})\,\{\eta_2^0(\mathbf{k}_1, \mathbf{r}_{23}) - \chi_2(k_1)\,\varphi_2(r_{23})\}\,d\mathbf{r}_{23} = 0.
\end{aligned} \tag{23}$$

These conditions give a system of two integral equations for the determination of χ_1, χ_2, and α_0:

---

[*] From experiments on neutron scattering in ortho- and parahydrogen, we know that α_s is negative. Therefore for $r_{23} \to \infty$, equation (20a) has no physical meaning, since the wave function $\varphi_1(r_{23})$ then tends to infinity. However, it is not difficult to show that for small $r_{23} < r_s$, the function satisfying Eq. (20a) coincides with the wave function for two nucleons which are in a singlet state with low energy of relative motion.

$$
\begin{aligned}
&\chi_1(k_1)\int\frac{\exp\left\{-\sqrt{\alpha_0^2+3k_1^2/4}\,|\mathbf{r}_{23}-\mathbf{r}|\right\}-\exp\{-\alpha_s\,|\mathbf{r}_{23}-\mathbf{r}|\}}{|\mathbf{r}_{23}-\mathbf{r}|}\\
&\qquad\times V_s(r_{23})\,V_s(r)\,\varphi_1(r_{23})\,\varphi_1(r)\,d\mathbf{r}_{23}d\mathbf{r}\\
&+2\pi\int\frac{\cos(\mathbf{r}_{23},\,\mathbf{k}_1/2+\mathbf{k})}{\alpha_0^2+k_1^2+k^2+\mathbf{k}_1\mathbf{k}}V_s(r_{23})\,\varphi_1(r_{23})\cos(r,\,\mathbf{k}_1+\mathbf{k}/2)\,\{\chi_1(k)\,V_s(r)\,\varphi_1(r)\\
&\qquad+3\chi_2(k)\,V_t(r)\,\varphi_2(r)\}\,d\mathbf{r}d\mathbf{r}_{23}\frac{d\mathbf{k}}{(2\pi)^3}=0\,;\\
&\chi_2(k_1)\int\frac{\exp\left\{-\sqrt{\alpha_0^2+3k_1^2/4}\,|\mathbf{r}_{23}-\mathbf{r}|\right\}-\exp\{-\alpha_t|\mathbf{r}_{23}-\mathbf{r}|\}}{|\mathbf{r}_{23}-\mathbf{r}|}\\
&\qquad\times V_t(r_{23})\,V_t(r)\,\varphi_2(r_{23})\,\varphi_2(r)\,d\mathbf{r}_{23}d\mathbf{r}\\
&+2\pi\int\frac{\cos(\mathbf{r}_{23},\,\mathbf{k}_1/2+\mathbf{k})}{\alpha_0^2+k_1^2+k^2+\mathbf{k}_1\mathbf{k}}V_t(r_{23})\,\varphi_2(r_{23})\cos(\mathbf{r},\,\mathbf{k}_1+\mathbf{k}/2)\,\{3\chi_1(k)\,V_s(r)\,\varphi_1(r)\\
&\qquad+\chi_2(k)\,V_t(r)\,\varphi_2(r)\}\,d\mathbf{r}d\mathbf{r}_{23}\,d\mathbf{k}\,|\,(2\pi)^3=0\,.
\end{aligned}
\tag{24}
$$

Thus in this case we obtain in zero approximation a system of two integral equations for two functions which depend on a single variable. The wave functions $f_{\propto}{}^{0}$ of the zeroth approximation are determined, according to Eqs. (16) and (17), from the eigenvalue α_0 and the eigenfunctions χ_1 and χ_2 of Eq. (24), in the following form:

$$
\begin{aligned}
&f_s^0(\mathbf{k}_1,\mathbf{r}_{23})=\int\frac{\exp\left\{-\sqrt{\alpha_0^2+3k_1^2/4}\,|\mathbf{r}_{23}-\mathbf{r}|\right\}}{|\mathbf{r}_{23}-\mathbf{r}|}\left\{\frac{1}{2}V_s(r)\,\varphi_1(r)\,\chi_1(k_1)\right.\\
&\left.+\frac{1}{2}V_t(r)\,\varphi_2(r)\,\chi_2(k_1)\right\}d\mathbf{r}+8\pi\int\frac{\cos(\mathbf{r}_{23},\,\mathbf{k}_1/2+\mathbf{k})}{\alpha_0^2+k_1^2+k^2+\mathbf{k}_1\mathbf{k}}\cos(\mathbf{r},\,\mathbf{k}_1+\mathbf{k}/2)\\
&\times\left\{\frac{1}{2}V_s(r)\,\varphi_1(r)\,\chi_1(k)+\frac{1}{2}V_t(r)\,\varphi_2(r)\,\chi_2(k)\right\}d\mathbf{r}\,\frac{d\mathbf{k}}{(2\pi)^3}\,;\quad f_a^0(\mathbf{k}_1,\mathbf{r}_{23})\equiv0;\\
&f_2^0(\mathbf{k}_1,\mathbf{r}_{23})=\int\frac{\exp\left\{-\sqrt{\alpha_0^2+3k_1^2/4}\,|\mathbf{r}_{23}-\mathbf{r}|\right\}}{|\mathbf{r}_{23}-\mathbf{r}|}\left\{\frac{1}{2}V_s(r)\,\varphi_1(r)\,\chi_1(k_1)\right.\\
&\left.-\frac{1}{2}V_t(r)\,\varphi_2(r)\,\chi_2(k_1)\right\}d\mathbf{r}+8\pi\int\frac{\cos(\mathbf{r}_{23},\,\mathbf{k}_1/2+\mathbf{k})}{\alpha_0^2+k_1^2+k^2+\mathbf{k}_1\mathbf{k}}\cos(\mathbf{r},\,\mathbf{k}_1+\mathbf{k}/2)\\
&\qquad\times\left\{\frac{1}{4}V_t(r)\,\varphi_2(r)\,\chi_2(k)-\frac{1}{4}V_s(r)\,\varphi_1(r)\,\chi_1(k)\right\}d\mathbf{r}\,\frac{d\mathbf{k}}{(2\pi)^3}\,;\\
&f_1^0(\mathbf{k}_1,\,\mathbf{r}_{23})=8\pi i\int\frac{\sin(\mathbf{r}_{23},\,\mathbf{k}_1/2+\mathbf{k})}{\alpha_0^2+k_1^2+k^2+\mathbf{k}_1\mathbf{k}}\cos(\mathbf{r},\mathbf{k}_1+\mathbf{k}/2)\\
&\qquad\times\left\{\frac{\sqrt{3}}{4}V_t(r)\,\varphi_2(r)\,\chi_2(k)-\frac{\sqrt{3}}{4}V_s(r)\,\varphi_1(r)\,\chi_1(k)\right\}d\mathbf{r}\,\frac{d\mathbf{k}}{(2\pi)^3}\,.
\end{aligned}
\tag{25}
$$

To find the successive approximations, one can use a procedure which is completely analogous to that which was presented for finding higher approximations for the eigenvalue and the wave function in the case of three identical particles.

In conclusion I express my deep gratitude to K. A. Ter-Martirosian for his direction and constant interest in the work. I also sincerely thank Academician L. D. Landau, O. B. Firsov and I. M. Shmushkevich for helpful discussions.

---

[1] G. V. Skorniakov and K. A. Ter-Martirosian, Dokl. Akad. Nauk SSSR **106**, 425 (1956); J. Exptl. Theoret. Phys. (USSR) **31**, 775 (1956); Soviet Phys. JETP **4**, 648 (1957).

[2] L. H. Thomas, Phys. Rev. **47**, 903 (1935).

[3] A. Akhiezer and I. Pomeranchuk, *Some Problems of Nuclear Theory*, Moscow, 1950.

[4] M. Verde, Helv. Phys. Acta. **22**, 339 (1949).

Translated by M. Hamermesh
219

Letters to the Editor

Paramagnetic Relaxation in Monocrystals of Some Salts of the Iron Group Elements

T. I. VOLOKHOVA

(Submitted to JETP editor May 7, 1956)
J. Exptl. Theoret. Phys. (U.S.S.R.) **31**, 889-890
(November, 1956)

Studies of paramagnetic absorption in parallel fields at room temperature have so far been conducted only in powders of paramagnetic salts. Meanwhile, it follows from the theory of paramagnetic relaxation[1] that anisotropy of the constant of magnetic heat capacity b/c and the spin-lattice relaxation time ρ should be observed in monocrystals of paramagnetic salts.

Presented herein are the results of measurements of the coefficient of absorption χ in the monocrystalline salts $Cu(SO_4) \cdot 5H_2 9$, $Mn(SO_4) \cdot 4H_2O$ and $Fe(NH_4) \cdot (SO_4)_2 \cdot 12H_2O$ as a function of the direction of the static magnetic field with respect to the crystallographic axes. The measurements were carried out using Zavoiskii's method.[2,3] Monocrystals fresh from the mother solution were used in the investigation; this has essential significance for the results.

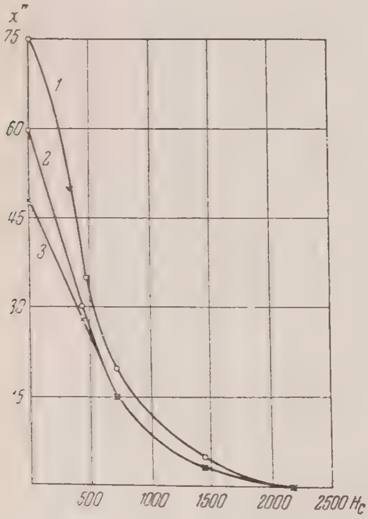

FIG. 1

A generator of the Esau type at a frequency of 6×10^8 cps was assembled for the measurement of the constant of magnetic heat capacity b/c. The monocrystal under study was formed into a sphere of 8 mm diameter. The direction of the magnetic axis was determined[4]. (In the monocrystal $Cu(SO_4) \cdot 5H_2O$, the magnetic axis coincides with the bisector between the tetragonal axes of symmetry). The sample was placed in the coil of the generator.

Measurement of the coefficient χ'' was carried out for three mutually perpendicular orientations of the crystal along the magnetic axis and in two directions perpendicular to the magnetic axis. The results of measurement of χ'' in the monocrystal $Cu(SO_4) \cdot 5H_2O$ as a function of H_c and the direction of the axis is shown in Fig. 1. It is clear from the figure that along the magnetic axis the null absorption (curve 1) is greater than in the direction perpendicular to it (curve 3). The dependence of χ'' on H_c in powdered $Cu(SO_4) \cdot 5H_2O$ is shown on the same Figure (curve 2). The constant of magnetic heat capacity is determined by the formula

$$b/c = \delta^2/0.41, \tag{1}$$

where δ is the halfwidth of the experimental curve in oersteds[5]. Formula (1) results from Shaposhnikov's theory[6]. The results of measurements of b/c for a monocrystal along and perpendicular to the magnetic axis are:

$$(b/c)_{\parallel} = 0.4 \cdot 10^6\,(\mathrm{Oe})^2, \quad (b/c)_{\perp} = 0.6 \cdot 10^6\,(\mathrm{Oe})^2.$$

The magnetic heat capacity along the magnetic axis in the monocrystal $Cu(SO_4) \cdot 5H_2O$ is less than in the perpendicular direction by about 33%, i.e., to the same extent that the static susceptibility is greater. These results agree with the data of Krishnan and Mookherji[4] who found $\chi_{\parallel} = 1922 \times 10^{-6}$, $\chi_{\perp} = 1371 \times 10^{-6}$, and in powder $\chi_0 = 1555 \times 10^{-6}$.

For powdered $Cu(SO_4) \cdot 5H_2O$ our measurements yield $b/c = 0.47 \times 10^6\,(\mathrm{Oe})^2$ which agrees with data obtained earlier by Sitnikov[7].

Studies of paramagnetic relaxation in the monocrystals $Mn(SO_4) \cdot 4H_2O$ and $Fe(NH_4) \cdot (SO_4)_2 \cdot 12H_2O$ yield $b/c = 6.3 \times 10^6\,\mathrm{Oe})^2$ and $0.28 \times 10^6\,(\mathrm{Oe})^2$, respectively for the value of the constants of magnetic heat capacity, which agree with Gorter's data[8]. Here, no dependence of absorption on the orientation of the crystal in the magnetic field was observed.

A generator of the Esau type at a frequency of 10.5×10^6 cps was used for measurements of spin lattice relaxation times. The results of measurements of χ'' as a function H_c and the direction of the crystallographic axes are shown in Fig. 2. It is clear from the Figure that the coefficient of absorption along the magnetic axis

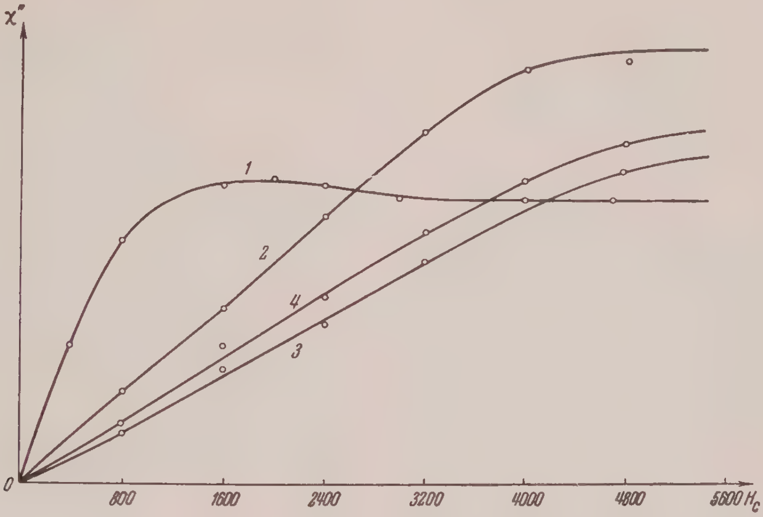

FIG. 2

$\chi''_{||}$ is smaller than in the perpendicular direction $\chi''_{\perp}$ by about 36%. Here, $\chi''_{\perp}$ differed by 10-12% for two mutually perpendicular orientations with respect to the magnetic axis. The mean of these values was used for $\chi''_{\perp}$ in Fig. 2. The measurements were carried out by comparison with a standard[7], for which the substance $Mn(NH_4)_2(SO_4)_2 \cdot 6H_2O$. was used. In addition, a verification was carried out by means of a comparison of the effect on the substance $Mn(SO_4) \cdot 4H_2O$.

Curve 1, Fig. 2, refers to the substance $Mn(NH_4)_2(SO_4) \cdot 6H_2O$, curves 2 and 3 refers to a monocrystal of $Cu(SO_4) \cdot 5H_2O$, the magnetic axis of which was located respectively parallel to and perpendicular to the field H. Curve 4 was obtained for powdered $Cu(SO_4) \cdot 5H_2O$.

The spin-lattice relaxation time ρ was calculated according to the formula of Kazimir and du-Pre[8]

$$\chi'' = \chi_0 Fm\, \rho\nu / (1 + \rho^2\nu^2). \qquad (2)$$

Results of the measurement of spin-lattice relaxation time in the monocrystal $Cu(SO_4) \cdot 5H_2O$ are given in the Table. The relaxation times are denoted by ρ for the powder, and by $\rho_{||}$ and $\rho_{\perp}$ for the monocrystal. The magnitude ρ for powdered $Cu(SO_4) \cdot 5H_2O$ is approximately equal to the arithmetic mean of the relaxation times along the magnetic axis and perpendicular to it.

The measurement of ρ for the monocrystals $Mn(SO_4) \cdot 4H_2O$ and $Fe(NH_4)(SO_4)_2 \; 12H_2O$ also showed no dependence on the orientation of the crystals in the magnetic field.

TABLE

H_c (Oe)	$\rho \cdot 10^8$ sec	$\rho_{\perp} \cdot 10^8$ sec	$\rho_{11} \cdot 10^8$ sec
800	0.8	1.0	0.5
1600	1.1	1.4	0.9
2400	1.6	2,1	1.1
3200	2.1	2.9	1.3
4000	2.4	3.2	1.6
4800	2.8	3.3	1.8
5600	3.0	4.0	2.0

---

[1] J. H. Van Vleck, Phys. Rev. 57, 426 (1940)

[2] Al'tshuler, Zavoiskii and Kozyrev, J. Exptl. Theoret. Phys. (U.S.S.R.) 14,407 (1944)

[3] E. K. Zavoiskii, Dissertation, Phys. Inst. Acad. Sci USSR (1944).

[4] K. S. Krishnan and A. Mookherji, Phys. Rev. 50, 860 (1936). 54, 533, 841 (1938).

[5] N. S. Garif'ianov, Dissertation, Kazan, 1953.

[6] I. G. Shaposhnikov, Dissertation, Molotov State University 1949.

[7] K. P. Sitnikov, Dissertation, Kazan State University, 1954.

[8] K. Gorter, *Paramagnetic Relaxation*, 1949.

Translated by D. Lieberman
185

Interaction between a Moving Current-Carrying Wire and a Conducting Wall

A. I. MOROZOV
Moscow State University

(Submitted to JETP editor July 2,1956)
J. Exptl. Theoret. Phys. (U.S.S.R.) 31, 1079–1080 (December, 1956)

IF a current-carrying wire moves in the vicinity of any object, then a displacement current and a conduction current are induced in this object. The field of these currents will, in turn, act on the wire, causing it to be attracted to or repelled from the surface. To a large degree this is similar to what happens when a moving charge passes close to a dielectric.[1] We shall here consider the simplest case of this phenomenon, namely when a straight wire with current J moves uniformly ($v << c$) in empty space parallel to the plane surface of a conducting medium. Let l be the distance between the wire and the conductor, and σ, ϵ, and μ be the conductivity, complex dielectric constant, and magnetic permeability of the medium, so that $\epsilon = \epsilon_0 + i 4\pi\sigma/\omega$; we shall neglect the dispersion ϵ_0 σ, and μ.

The x axis shall be chosen along the current, and the z axis in the direction of motion of the wire. The origin shall be located on the conductor surface. Then[1]

$$F_y = -(J/c)^2 \operatorname{Re} P;\ F_z = -(J/c)^2 \operatorname{Im} P, \tag{1}$$

$$P = 2\int_0^\infty \frac{1-\alpha}{1+\alpha} e^{-2kl} dk,\ k = \omega/v, \tag{2}$$

$$\alpha = (1/\mu)[1 - (\mu\varepsilon_0 + i4\pi\sigma\mu/kv)\beta^2]^{1/2},\ \operatorname{Re}\alpha > 0. \tag{3}$$

As can be seen from (2) and (3), in this case the well known analog of the critical velocity for Cerenkov radiation $v = c/n$ is the quantity

$$U_1 = c^2/4\pi\mu\sigma l \tag{4}$$

(assuming that $\mu\epsilon_0 \beta^2 << 1$), which we shall call the first characteristic velocity. For instance, for copper, this is $\approx 10^2/l$ cm/sec. To find the force (F_z, F_y), we need only calculate P, which we shall do for the two limiting cases $\mu = 1$ and $\mu >> 1$.

In the first case, for the condition

$$\varepsilon_0 \ll \pi^2\sigma^2 l^2/c^2,$$

which is in fact always satisfied, the wire will be repelled from the wall for any velocity, and

$$P = -\frac{1}{l} - \frac{i}{l\nu} - (e^{-i\nu}/2l)\pi H_1^{(1)}(\nu), \tag{5}$$

where $\nu = v/U_1$, and $H_1^{(1)}$ is the Hankel function. If $\nu << 1$, then

$$F_y = (J/c)^2 \nu\pi/2l,\ F_z = (J/c)^2 (\nu/2l)[\ln(\nu/2) + C - {}^1/_2],$$

and if $\nu >> 1$, then

$$F_y = (J^2/c^2 l)(1 - {}^1/_2\sqrt{\pi/\nu}), \tag{6}$$

$$F_z = -(J^2/c^2 l)({}^1/_2\sqrt{\pi/\nu} - 1/\nu).$$

It can be shown that for $\nu \approx 1.9$, the force F_z is a maximum, physically, this is related to the fact that an increase in v leads to a change in the relation between the ohmic and inductive impedences to the current induced in the conducting wall by the moving wire, The $\nu^{-1/2}$ dependence of F_z is explained by the skin effect.

Let us now consider the other limiting case, in which $\mu >> 1$. The case $v \lesssim U_1$ is of no particular interest, since U_1 is small, and in this case the image forces, proportional to $(\mu-1)/(\mu+1)$, are of most importance. Therefore we shall assume that $v >> U_1$. It can be shown that in this case

$$P = \frac{1}{l}\Big[1 + 2\sqrt{\pi}z + 4z^2\Big(-\frac{1}{2}e^{-z^2}\operatorname{Ei}(z^2) - \sqrt{\pi}e^{-z^2}\int_0^z e^{\alpha^2}d\alpha + \frac{i\pi}{2}e^{-z^2}\Big)\Big], \tag{7}$$

$$z = -e^{-i\pi/4}(v/U_2)^{1/2}\sqrt{2},$$

where $U_2 = \mu^2 U_1$ is the second characteristic velocity, and Ei is an integral exponential function.

In view of the complexity of Eq. (7), we shall write out the components of the force for two limiting cases. In the case $U_1 << v << U_2$,

$$F_y = (J^2 / c^2 l)\,[1 - 2\,(v / U_2)^{1/2}],$$

$$F_z = -\,(2J^2 / c^2 l)\,(v / U_2)^{1/2},$$

and in the case $v >> U_2$

$$F_y = (J^2 / c^2 l)\,[1 - {}^1/_2 \sqrt{\pi}\,(U_2 / v)^{1/2}];$$

$$F_z = -\,(J^2 \sqrt{\pi} / c^2 l 2)\,(U_2 / v)^{1/2}.$$

From these equations it is seen that for $v \sim U_2$, the component F_y changes sign and F_z changes from an increasing function of velocity to a decreasing one.

In conclusion I would like to express my gratitude to Professor A. A. Sokolov for his attention to the work.

---

[1] A. I. Morozov, Vestn. Moscow State University (to be published).

Translated by E. J. Saletan
222

On the Damping Theory of Particle Scattering by a Fixed Center

A. A. SOKOLOV AND B. K. KERIMOV
Moscow State University

(Submitted to JETP editor January 23,1956;
revision submitted September 22,1956)
J. Exptl. Theoret. Phys. (U.S.S.R.) 31,
1080-1081 (December, 1956)

DAMPING theory, which is a stage beyond perturbation theory, enables us to calculate a cross section σ not only for long de Broglie waves ($\sigma < \lambda^2$) but also for small wave lengths ($\sigma >> \lambda^2$).

Damping theory was developed in Refs. 1–3 in the investigation of meson scattering by nucleons; Sokolov[1] established the relation

$$C^+C + \sum_{\mathbf{k}'} C'^+C' = 1, \qquad (1)$$

which states that the sum of incident and scattered particles at any instant of time remains unchanged. Subsequently we applied damping theory to an investigation of particle scattering by a fixed center.[4–5]

It is well known that the exact formula for the cross section of elastic scattering of particles with momentum hk ($k = 2\pi/\lambda$) is

$$\sigma = \frac{4\pi}{k^2} \sum_{l=0}^{\infty} (2l+1) \sin^2 \eta_l.$$

Perturbation theory enables us to determine the phase η_l when $\eta_l << 1$. Damping theory gives the following more exact approximation for the phase shift[5]

$$\mathrm{tg}\,\eta_l = -\frac{\pi K}{c\hbar} \int_0^{\infty} r V(r)\, J^2_{l+1/2}(kr)\, dr, \qquad (2)$$

(hk is the momentum and chK is the energy of the particle), which for $\eta_l << 1$ becomes the expression established for the phase by perturbation theory.

For the elastic scattering differential cross section , damping theory gives the following expression:

$$\frac{d\sigma}{d\Omega'} = \frac{1}{k^2} \sum_{l,l'} \frac{\mathrm{tg}\,\eta_l\,\mathrm{tg}\,\eta_{l'}\,(1 + \mathrm{tg}\,\eta_l\,\mathrm{tg}\,\eta_{l'})\,(2l+1)\,(2l'+1)\,P_l(\cos\theta')\,P_{l'}(\cos\theta')}{(1 + \mathrm{tg}^2\,\eta_l)\,(1 + \mathrm{tg}^2\,\eta_{l'})} \qquad (3)$$

These formulas enable us to investigate the scattering of spinless particles acted on by short-range forces. In particular, we made a detailed study [5] of particle scattering by Yukawa forces. We have been able to extend our results to Dirac particles (i.e., with spin) only for a δ-function interaction.[4]

We shall now investigate particle scattering by damping theory when the interaction potential is of the form

$$V(r) = \begin{cases} B = 3V_0/4\pi a^3, & r < a, \\ 0 & , \quad r > a. \end{cases}$$

Then according to (2) we have for the phase η_l

$$\mathrm{tg}\,\eta_l = -\frac{\pi B K}{c\hbar k^2} \int_0^{ka} J^2_{l+1/2}(y)\, y\, dy.$$

In the one limit $ka >> 1$ scattering is practically determined by the s phase:

$$\sigma = \frac{4\pi}{k^2} \begin{cases} 4B^2K^2a^6k^2/9c^2\hbar^2 & \text{for} \quad 2BKa^3k/3c\hbar \ll 1, \\ 1 & \text{for} \quad 2BKa^3k/3c\hbar \gg 1, \end{cases}$$

i.e., damping will play a decisive part only for

$2bK \gg 1$. In the other limiting case $ka \gg 1$ the high energy region), we obtain for σ

$$\sigma = \frac{4\pi}{k^2}\int_0^\infty \frac{2l\,dl}{1+\operatorname{ctg}^2\eta_l}$$

$$\approx 4\pi a^2 \begin{cases} {}^1/_6\gamma^2 & \text{for } {}^2/_3\gamma^2/_3 BaK/c\hbar k \ll 1, \\ 1 & \text{for } {}^2/_3\gamma \gg 1. \end{cases}$$

Thus the cross section will be four times greater than its classical value. As has been shown by Massey and Mohr[8], the discrepancy between the classical and quantum values is associated with diffraction. Let us compare our results with those given by Mott and Massey[9] (p. 56) for an analogous problem using the smooth joining of wave functions:

$$\sigma = \begin{cases} 4\pi a^2 & \text{for } ka \ll 1, \\ 2\pi a^2 & \text{for } ka \gg 1, \end{cases}$$

i.e., the theories will agree exactly except for numerical coefficients when $ka \gg 1$.

For scattering from a δ-center we were recently able to compare damping theory and other theories. In the nonrelativistic case, the wave equation is (hk_0/c is the mass of a particle)

$$(\nabla^2 + k^2)\Psi = (2k_0/c\hbar)V_0\delta(\mathbf{r})\Psi.$$

The solution of this equation which satisfies the radiation condition for $r \to \infty$ is

$$\Psi = Ae^{ikz} + A'\left(\frac{1}{8\pi^3}\int\frac{\exp\{i\varkappa\mathbf{r}\}}{k^2-\varkappa^2}d^3\varkappa - \frac{i}{4\pi}\frac{\sin kr}{r}\right).$$

Keeping in mind the value of the integral

$$\frac{1}{8\pi^3}\int\frac{\exp\{i\varkappa\mathbf{r}\}}{k^2-\varkappa^2}d^3\varkappa = \begin{cases} -(1/4\pi r)\cos kr, & r>0, \\ -(\alpha/\pi^2) & , \quad r=0, \end{cases}$$

where α defines the range in which the wave vector of the scattered particle changes $(k-\alpha \leqslant \varkappa \leqslant k+\alpha)$, we obtain for the cross section

$$\sigma = \frac{|A'|^2}{4\pi|A|^2}$$

$$= k_0^2V_0^2/\pi c^2\hbar^2\left[\left(1+\frac{2k_0V_0\alpha}{c\hbar\pi^2}\right)^2 + \frac{k_0^2k^2V_0^2}{4\pi^2c^2\hbar^2}\right]^{-1}$$

In solving the problem by perturbation theory, we had to drop terms depending on V_0 in the denominator of (6). In damping theory we had to set α equal to zero in the denominator of (6). This represents the fact that we shall take only resonance terms into account for the scattering ($K \sim K$). Finally, solution by joining of wave functions corresponds to $\alpha \to \infty$. In this case, on complete agreement with (5), we find that for a δ-function interaction scattering should not occur at all.

---

*Particle scattering with account taken of damping has also been discussed in Ref. 6 (p. 212).

1 A. A. Sokolov, Phys. USSR 5, 231 (1941).

2 W. Heitler, Proc. Cambr. Phil. Soc. 37, 291 (1941).

3 A. H. Wilson, Proc. Cambr. Phil. Soc. 37, 301 (1941).

4 A. A. Sokolov and B. K. Kerimov, Dokl. Akad. Nauk SSSR 105, 951 (1955).

5 A. A. Sokolov and B. K. Kerimov, Dokl. Akad. Nauk SSSR 108, 611 (1956); see also abstracts of the All-Union Conference on the Physics of High-Energy Particles of the Academy of Sciences USSR, Moscow, May, 1956, p. 229.

6 H. A. Bethe and F. Hoffman, *Mesons and Fields*, Vol. II, New York, 1955.

6 A. A. Sokolov, Vest. Moscow State University 4, 77 (1947).

8 G. Massey and S. Mohr, Proc. Roy. Soc. (London) A141, 434 (1953).

9 N. Mott and G. Massey, *Theory of Atomic Collisions* (Russian translation IIL, Moscow, 1951).

Translated by I. Emin
223

Total Inelastic Interaction Cross Sections of 225 ± 10 mev Negative π-mesons with C, Al, Cu, Sn, and Pb nuclei

V. G. Ivanov, V. T. Osipenkov,
N. I. Petrov, V. A. Rusakov

(Submitted to JETP editor September 3, 1956)
J. Exptl. Theoret. Phys. (U.S.S.R.) 31,
1097 (December, 1956)

In experiments carried out with the synchrocyclotron of the Laboratory of Nuclear Problems we have determined total cross-sections for the inelastic interaction of π-mesons with nuclei of carbon, aluminum, copper, tin and lead.

For these measurements we used the method of recording the events which result in the removal of the particle from the beam in passing through a scatterer made of the substance under investigation. The mean angle into which the particle was removed was 30°. A telescope consisting of three scintillation counters was used as the meson recording apparatus. In the first and second counters, toluene crystals $30 \times 30 \times 5$ mm in size were used as scintillators; a liquid scintillator (a solution of terphenyl in toluol) 100 mm in diameter was used for the third counter. The first two counters recorded π-mesons incident on the scatterer; the third counter recorded particles which had passed through the scatterer which was in the form of a disc 60 mm in diameter placed in the beam immediately after the second counter. In front of the third counter a lead filter of thickness $5.85\ \mathrm{g/cm}^2$ was placed in order to absorb heavy charged particles formed as a result of the interaction of π-mesons with the nuclei of the scatterer. In order to determine the number of events resulting in the removal of π-mesons from the beam a simultaneous count of double and triple coincidences was made. The efficiency of the last counter was tested in a proton beam of $1\ \mathrm{cm}^2$ cross-section; it turned out to be equal to 96% and practically did not depend on the place at which the particles struck the scintillator.

Element	Cross section in units of $10^{-27}\ \mathrm{cm}^2$	
	Measured	geometric*
C	346 ± 21	325
Al	596 ± 30	553
Cu	1058 ± 45	977
Sn	1550 ± 70	1480
Pb	2290 ± 90	2150

The energy of the π-mesons incident on the scatterer, and also the total content of μ-mesons and electrons in the beam were determined separately by measuring the absorption curve for π-mesons in copper using the same geometry as in the experiment being described. These measurements showed that the energy of π-mesons in the beam is equal to 230 ± 6 mev, while the content of μ-mesons and electrons in the beam amounts to $12.5 \pm 3\%$. The scatterer thickness was on the average equal to 5–6 $\mathrm{g/cm}^2$, so that the mean energy of the π-mesons to which the measured cross sections correspond was equal to 225 ± 10 mev.

Corrections were made to the measured cross sections using the data of reference 1 in which the Wilson cloud chamber was used to study the interaction of negative π-mesons with carbon and lead nuclei at an energy of 230–350 mev; these corrections took into account: a) inelastic scattering of π-mesons into the angular interval from 0 to 30°; b) elastic scattering of π-mesons into the angular interval from 30 to 180° and c) fast secondary protons recorded by the third counter. The total cross sections for the inelastic interaction of π-mesons with nuclei obtained by the method described above are given in the Table. It may be easily seen that at an energy of 225 mev these cross sections are equal to the geometric cross sections of the corresponding nuclei. Within the experimental error these results agree with the results of similar measurements carried out in reference 2 at π-meson energies of 216 and 250 mev.

---

*For the calculation of geometric cross sections the nuclear radius was taken equal to $R = 1.4\ A^{1/3}\ 10^{-13}$ cm.

1 Dzhelepov, Ivanov, Kozodaev, Osipenkov, Petrov and Rusakov, J. Exptl. Theoret. Phys. (U.S.S.R.) 31, 923 (1956).

2 Ignatenko, Mukhin, Ozerov and Pontecorvo, Dokl. Akad. Nauk SSSR 103, 209 (1955).

Translated by G. M. Volkoff
233

Nuclear Interactions with 220-mev Deuterons

L. P. SOLOV'EVA

(Submitted to JETP editor July 18, 1956)
J. Exptl. Theoret. Phys. (U.S.S.R.) 31, 1086-1088
(December, 1956)

IT is characteristic of the interactions between high-energy deuterons and nuclei that fast protons are emitted. At least three processes exist by which fast protons can be produced in inelastic collisions of high-energy deuterons. As has been shown by Serber[1] and confirmed experimentally by Chupp, Gardner and Taylor[2], when a target is bombarded by fast deuterons there occurs a process wherein a deuteron is split on a nucleus with the neutron being captured by the nucleus and the proton proceeding past with energy which is about half of the deuteron energy. The cross section for this "stripping" process is quite high and is only slightly dependent on the atomic number, varying from $0.1 \times 10^{-24}\ \mathrm{cm}^2$ for Be to 0.3×10^{-24} cm for U. Another source of fast protons when various nuclei are bombarded by deuterons is the deuteron disintegration caused by the Coulomb field of the nucleus[3]. This process has a small cross section and is comparable with the cross section for "stripping" only in the case of the heaviest nuclei. Finally, a high-energy proton can be formed by the direct collision of one of the deuteron particles with a nuclear particle. The total number of emitted protons can be approximately equal to the proton yield from "stripping".

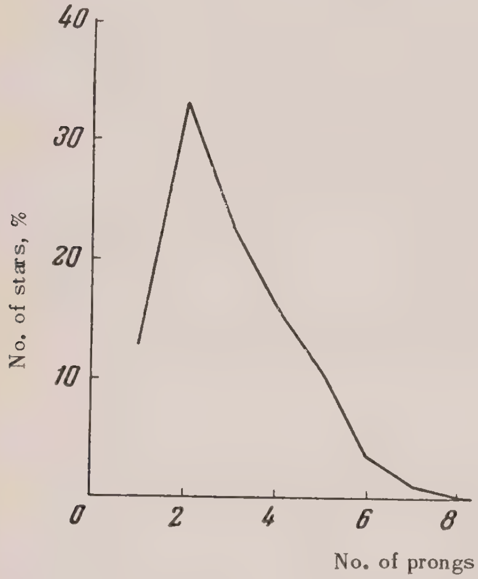

FIG. 1. Star distribution by number of prongs.

The present note presents the results of investigations of an interaction between fast deuterons and the elements contained in nuclear emulsions. We determined the mean free path for star production, the star distribution according to the number of prongs and the angular and energy distributions of the secondary protons.

Electron-sensitive plates covered with a 200μ emulsion were irradiated by a beam of 220-mev deuterons inside a synchrocyclotron. By area scanning, 1570 stars were found, of which number 698 contained one or two gray tracks that were assumed to be proton tracks. The gray tracks were all whose grain density was less than 1350 grains per mm, corresponding to proton energy $\geq$ 50 mev. The star distribution according to the number of prongs for 1570 disintegrations is given in Fig. 1, from which we see that the average number of prongs per star is 3.

The mean free path for nuclear interactions of 220-mev deuterons was determined by on-track scanning. In combined tracks of 994.6 cm we detected 53 inelastic collisions. Hence the mean free path for nuclear interactions of 220-mev deuterons in the emulsion was 18.8 ± 2.6 cm. The mean free path as calculated from the geometric cross sections of the nuclei of the emulsion (excluding hydrogen atoms) was 23.0 cm. Thus the mean free path for 220-mev deuterons in this work was very close to the value which corresponds to the geometric cross section.

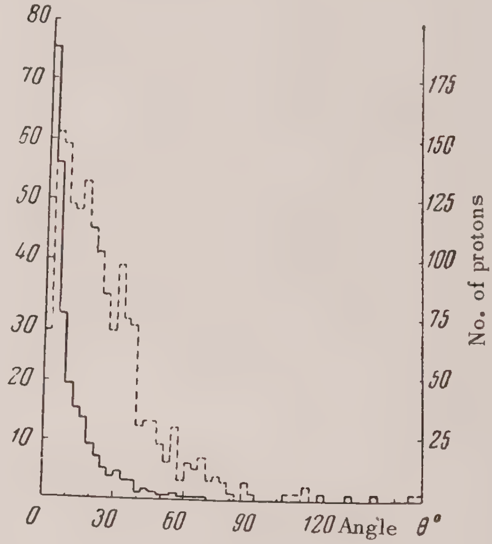

FIG. 2. Angular distribution of fast protons. Per unit solid angle (right-hand scale) - the solid line; per annular zone (left-hand scale) - the dashed line.

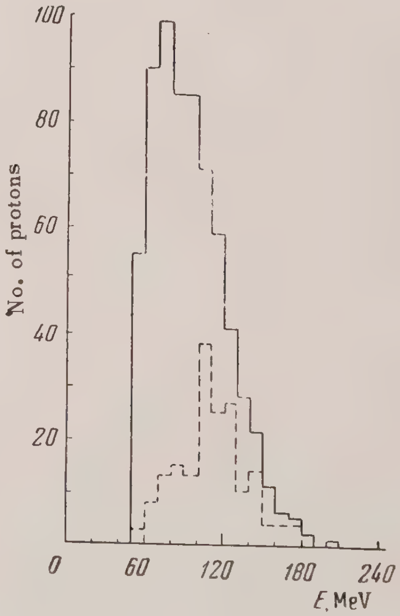

FIG. 3. Energy distribution of fast protons. Solid line - 655 protons; dashed line - 179 protons; $\theta \leq 10°$

Figure 2 gives the angular distribution of secondary protons. It can be seen that a considerable fraction of the particles are emitted in directions close to the line of motion of the deuteron. About 90% of the fast protons are emitted in the forward hemisphere; 30% of these are in a narrow cone of 30° apex angle. The half width of the angular distribution is 18°, which exceeds the calculated half width (9.5°) for the angular distribution of protons resulting from "stripping". The gray tracks are distributed symmetrically to the right and left of the direction of the incident deuteron.

The energy distribution of the protons (Fig. 3) was obtained by counting the grains in the tracks. The energy spectrum covers the range from 50 to 210 mev and possesses a sharp maximum at 80-90 mev. The half width of the energy distribution of all protons is 70 mev.

The dashed line in Fig. 3 is a histogram which represents the energy distribution of protons whose emission angle was not greater than 10°. The peak of this distribution is at about 110 mev, which is half of the initial deuteron energy . The half width of the distribution is 40-50 mev, which agrees with the calculation of $\Delta E_{1/2} = 2(\epsilon_d/E_d) = 45$ mev for the transparent nucleus model and with $\Delta E_{1/2} = 34$ mev for an opaque nucleus. A comparison of the theoretical and experimental results shows good agreement. Therefore the protons included in the above energy distribution resulted predominantly from the disintegration of deuterons by nuclei.

Our analysis of the angular and energy distributions of the protons enables us to state that two processes are mainly responsible for the emission of fast protons; these are "stripping" and a cascade process.

---

[1] R. Server, Phys. Rev. 72, 1008 (1947).

[2] Chupp, Gardner and Taylor, Phys. Rev. 73, 742 (1948).

[3] S. M. Dancoff, Phys. Rev. 72, 1016 (1947).

Translated by I. Emin
227

A Static Solution of the Nonlinear Meson Equation

V. G. IAICHNITSYN
Dniepropetrovsk State University

(Submitted to JETP editor Jan. 25, 1956)
J. Exptl. Theoret. Phys. (U.S.S.R.) 31, 1082-1083
(December, 1956)

IN order to explain the phenomenon of saturation of nuclear forces and to provide a basis for a nuclear shell model Schiff proposed the simplest nonlinear generalization of the Klein-Gordon equation for meson theory[1]

$$\Box \varphi - k_0^2 - \lambda \varphi^3 = 0, \qquad (1)$$

where k_0 and λ are constants. The renormalized equation of the pseudoscalar theory with pseudoscalar coupling has the same form in the case of weak interaction.[2]

If we restrict ourselves to the static approximation we shall obtain for the spherically symmetrical case the equation

$$d^2u / dx^2 - (u^3/x^2) - u = 0, \qquad (2)$$

in which the variables $x = k_0 r$, $u = \sqrt{\lambda r}$ have been introduced.

This equation has been discussed by many authors largely in connection with the phenomenon of nuclear saturation, and in such cases the equation was discussed for the case of a certain given nucleon source density.[3-8] In the present note we shall obtain asymptotic solutions of Eq. (2), and shall also integrate the equation numerically.

According to a theorem due to Hardy,[9-10] every rational function $R(x, u, u')$ is necessarily monotonic along the solution $u(x)$ of the differential equation of the form

$$u'' = P(x, u) / Q(x, u),$$

where Q, P are polynomials in u, x. The application of this statement to the ratio of any two arbitrary terms of equations $Qu' - P = 0$ allows one to find asymptotic solutions of the differential equation for $x \to \infty$. The limit of such a ratio may be equal to $\pm\infty$, 0, or to a constant different from zero, and it is guaranteed that there must exist at least one ratio which tends to a constant different from zero. A similar result may be shown to hold for an equation of the type

$$u'' = P(u, x) / Q(u, x).$$

That solution of Eq. (2) is of physical interest which diminishes as $x \to \infty$. The asymptotic behavior of such a solution for large values of x may be represented in the form

$$u = -g\sqrt{\lambda}\, e^{-x}, \qquad (3)$$

where g is an arbitrary constant.

For small distances, Eq. (2) can be replaced by the asymptotic souation

$$d^2u / dx^2 - u^3 / x^2 = 0. \qquad (4)$$

Equation (4) is an analog of the Emden-Fowler equation, and it can be reduced to an equation of the first order.[10] Indeed, as a result of making the substitution $x = e^{-5}$ and of the introduction of $y = du/dt$, we shall obtain

$$dy / du = u^3 / y - 1. \qquad (5)$$

A qualitative investigation of the behavior of phase trajectories in the (y, u) plane shows that a characteristic feature of all the solutions of Eq. (4) is the existence of a singular point whose position is not fixed, but depends on the constant of integration.

Applying Hardy's theorem to Eq. (5), we obtain for the asymptotic solution (for small distances)

$$u = -\sqrt{2} / \ln (x / x_k), \qquad (6)$$

where x_k is an arbitrary constant.

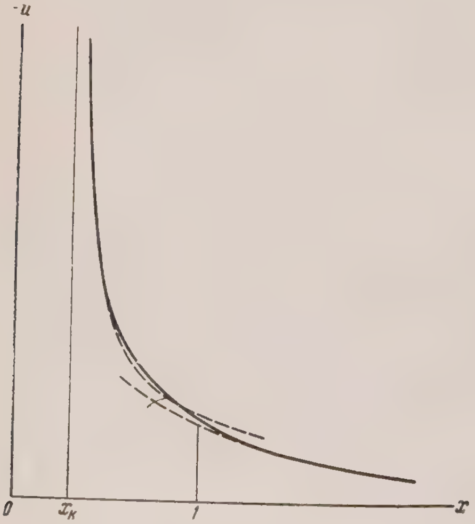

In addition, Eq. (2), was integrated numerically. The integration was carried out by starting with the asymptotic solution at large distances. To each value of the quantity g corresponds a definite value of the quantity x_k.

As may be seen from the diagram the solution obtained by numerical integration (solid curve) may be roughly approximated by the functions (3) and (6) matched at the point $x = 1$ (dotted curves).

The author hopes to give the interpretation of the result obtained above and its application to the description of the properties of a system of two nucleons at low energies in a subsequent article.

The author wishes to express his gratitude to A. A. Borgardt for his interest and assistance in the present work.

---

1 L. I. Schiff, Phys. Rev. 84, 1 (1951).
2 P. T. Matthews and A. Salam. Rev. Mod. Phys. 23, 311 (1951).
3 Ivanenko, Kurdgelaidze and Larin, Dokl. Akad. Nauk USSR 88, 245, 1953.
4 W. Thirring, Z. Naturforsch, 7a, 63, 1952.
5 B. I. Malenka, Phys. Rev. 85, 686 (1951); 86, 68 (1952).
6 P. Mittelstaedt, Z. Physik 137, 545 (1954).
7 R. O. Fornaguera, Nuovo Cimento 1, 132 (1955).
8 N. V. Mitskevich, J. Exptl. Theoret. Phys. (U.S.S.R.) 29, 354 (1955); Soviet Phys. JETP 2, 197 (1956).
9 R. Bellman, *Theory of the stability of solutions of differential equations* (Russian translation) I. I. L., 1954.
10 S. Chandrasekhor, *Introduction to the theory of stellar structure* (Russian translation) I. I. L. 1950.

Translated by G. M. Volkoff
224

On the Hydrodynamic Description of Plasma Oscillations

B. B. KADOMTSEV

(Submitted to JETP editor February 12, 1956)
J. Exptl. Theoret. Phys. (U.S.S.R.) 31, 1083–1084 (December, 1956)

SOMETIMES for the theoretical study of plasma one uses in place of the kinetic equation for the distribution function of the particles the simpler "transport" equations for the moments of this function (see, for example, Refs. 1,2). In so doing, in order to obtain a closed system of equations, one usually assumes that the distribution function is Maxwellian. Such an approximation cannot be applied to the description of high frequency plasma oscillations since in this case the electron distribution deviates appreciably from the Maxwellian distribution. However, in this case also, one can obtain a closed system of transport equations by using the fact that the only reason for the deviation of the distribution from the equilibrium distribution is the presence of a high frequency electrical field.

By restricting ourselves to the investigation of electron oscillations only we regard the ions and the molecules as infinitely heavy. Moreover, we assume that the amplitude of oscillations is small, and that consequently the electron distribution function deviates but little from the Maxwellian distribution $f_0(v)$. As a result of being acted on by the electric field, the electrons acquire a velocity increment $d\mathbf{v} = -(eE/m)\,dt$, as a result of which the distribution function changes at the initial instant by an amount $df' = (\partial f_0/\partial \mathbf{v}) = (e\mathbf{E}/m\,dt.)$ At later times, the distribution df' will vary in accordance with Boltzmann's equation, and during the first stages, this variation will be determined by the free acceleration of the electrons accompanied by their removal from the beam as a result of collisions. By denoting the frequency of collisions of a given electron with other electrons by α, and the frequency of collisions with ions (and molecules) by β and by assuming that α and β do not depend on the velocity, we shall obtain the following expression for the distribution of those electrons which have experienced no collision at all:

$$f'(\mathbf{r}, \mathbf{v}, t) \qquad (1)$$

$$= -\int_{-\infty}^{t}\int \frac{f_0 e\mathbf{v}\mathbf{E}(r', t')}{\varkappa T_0}\, e^{-(\alpha+\beta)(t-t')} \times \delta(\mathbf{r} - \mathbf{r}' - \mathbf{v}(t-t'))\, d\mathbf{r}'dt'$$

($\varkappa$ is the Boltzman constant).

Electrons which have been removed from the initial beam, i.e., which have experienced at least one collision, also lead to a certain change in the equilibrium distribution function. By assuming that one collision is already sufficient to establish a Maxwellian distribution, we represent the above change as a change in the parameters of the Maxwellian distribution—density, velocity and temperature. This process can be described hydrodynamically. If we denote by n, T the deviations of the electron density and temperature from their equilibrium values n_0, T_0, and by u their macroscopic velocity, we can write the hydrodynamic equations in the form

$$\partial n/\partial t + n_0 \operatorname{div} \mathbf{u} = (\alpha+\beta)\, n_0 I_1; \qquad (2)$$

$$\partial \mathbf{u}/\partial t + \beta\mathbf{u} + (\varkappa T_0/mn_0)\nabla n + (\varkappa/m)\nabla T = \alpha \mathbf{I}_2,$$

$$\partial T/\partial t + {}^2/_3 T_0 \operatorname{div} \mathbf{u} - \chi\Delta T = (\alpha+\beta)(m/3\varkappa)\, I_3.$$

Here the term $\beta\, u$ takes into account the slowing down of electrons by the heavy particles, χ is the coefficient of thermal conductivity, and the expressions on the righthand side arise as a result of the removal of electrons from the distribution (1).

In accordance with (1),

$$I_1 = \frac{1}{n_0}\int f'd\mathbf{v}$$

$$= -\frac{e}{\varkappa T_0}\left(\frac{m}{2\pi\varkappa T_0}\right)^{3/2}\int_{-\infty}^{t}\int \frac{(\mathbf{r}-\mathbf{r}')\,\mathbf{E}(\mathbf{r}', \mathbf{t}')}{(t-t')^4}$$

$$\times \exp\left\{-(\alpha+\beta)(t-t') - \frac{m(\mathbf{r}-\mathbf{r}')^2}{2\varkappa T_0 (t-t')^2}\right\} dr'\, dt',$$

while I_2 and I_3 differ from I_1 only by the additional appearance in the integrand of the factors

$$(\mathbf{r}-\mathbf{r}')/(t-t')$$

and

$$(\mathbf{r}-\mathbf{r}')^2/(t-t')^2.$$

respectively. One must also add to the system (2) the equation for the electric field

$$\operatorname{div} \mathbf{E} = -4\pi e(n+n'), \qquad (3)$$

where

$$n' = n_0 I_1.$$

Equations (2), (3) are the desired transport equations. For $\alpha \to \infty$ they reduce to the usual hydrodynamic equations, while for $\alpha = \beta = 0$ Eq. (3) coincides with the dispersion equation obtained from the linearized Vlasov equation.[2] A characteristic feature of the system (2), (3) is the fact that it takes into account roughly, but consistently, the effect of electron collisions.

If one assumes that all the quantities vary in accordance with $e^{i\omega t + ikr}$ then it is not difficult to obtain from (2), (3) the dispersion equation. In the general case it has a rather complicated appearance, but if one restricts the discussion to small k, then an expansion in powers of k can be carried out in the integrals I_i and a simpler equation can be obtained. Up to terms in k^3 it has the form

$$k\left\{\omega\left[\omega_0^2-\omega^2+i\omega\beta+\frac{5}{3}\frac{\varkappa T_0}{m}k^2+\chi k^2(i\omega+\beta)\right]+k^2\omega_0^2\frac{\varkappa T_0}{m}\frac{3i(\alpha+\beta)-4\omega}{(\alpha+\beta+i\omega)^2}-i\omega_0^2\chi k^2\right\}=0, \tag{4}$$

where $\omega_0=\sqrt{4\pi e^2 n_0/m}$.

This equation has the following solutions:

1. $k = 0$,

With

$$n=T=0,\ (i\omega+\beta)u=-e\alpha E/m(\alpha+\beta+i\omega).$$

For $i\omega \neq -\beta$ this gives the current under the influence of the external field

$$j=-en_0u-en_0I_2=n_0e^2E/m(i\omega+\beta).$$

2. $\omega^2\approx\omega_0^2+i\omega_0\beta+\frac{3\varkappa T_0}{m}k^2$

(taking into account that α, $\beta \ll \omega_0$); this is the usual expression for the frequency of plasma oscillations with "friction" taken into account.

3. $i\omega\approx-[\chi-\varkappa T_0/m(\alpha+\beta)]k^2,\ u=eE/m(\alpha+\beta)$,

$$T=-\Gamma_0 n/n_0+i(e/\varkappa k)E,\ n=-(ik/4\pi e)\left[1+\omega_0^2(\alpha+\beta)^{-2}\right]E.$$

This solution can be referred to as the electro-entropy wave. For $e \to 0$ it reduces to the usual entropy wave.[3].

---

[1] E. P. Gross, Phys. Rev. 82, 232 (1954).

[2] A. A. Vlasov, *Theory of many particles*, GITTL, 1950.

[3] L. D. Landau and E. M. Lifshitz, *Mechanics of continuous media*, GITTL, Moscow, 1954 , p. 410.

Translated by G. M. Volkoff
225

The Variational Principle and the Virial Theorem for the Continuous Dirac Spectrum

IU. V. NOVOZHILOV

(Submitted to JETP editor July 9,1956)
J. Exptl. Theoret. Phys. (U.S.S.R.) 31, 1084-1086 (December,1956)

THE variational principle for the phase shifts and scattering amplitudes has been investigated for the nonrelativistic case in several works.[1,2] Parzen[3] has formulated the variational principle for the phase shifts in the relativistic case. The present note gives a generalization of the variational principle for all scattering amplitudes to the case of the Dirac equation, and a derivation of the virial theorem for the continuous Dirac spectrum. The results can be applied to the theory of high-energy electron scattering by nuclei.

Let us consider the functional

$$I\{\Psi_1,\ \Psi_2\}=\int\Psi_2^{+}(\mathbf{r})\left[\alpha\mathbf{p}+\beta m+V(\mathbf{r})-E\right]\Psi_1(\mathbf{r})\,d\mathbf{r}, \tag{1}$$

where the functions Ψ_i are not in general solutions ψ_i of the Dirac equation

$$[\alpha\mathbf{p}+\beta m+V(\mathbf{r})-E]\,\psi_i=0.$$

For the exact solutions, $I\{\psi_1,\psi_2\}=0$. Let us restrict ourselves initially to potentials V which decrease faster than $1/r$ as $r\to\infty$. Then, in order that the functional (1) converge at the upper limit, the asymptotic form of the trial functions ψ_1 and ψ_2 should be

$$\Psi_i=u_i\exp[ip\boldsymbol{\nu}_i\mathbf{r}]+G(\boldsymbol{\nu}_i,\ \mathbf{n})(pr)^{-1}\exp[\pm ipr], \tag{2}$$

where u_i is a unit spinor, $G(\nu, \mathbf{n})$ is a single-valued function of direction, and $\mathbf{n}=\mathbf{r}/r$; the upper sign in the second term of Eq. (2) refers to ψ_1 and the lower one to ψ_2. The function ψ_1 contains a plane wave propagating in the direction ν_1 and an outgoing wave; the function ψ_2, on the otherhand, is seen from Eq. (2) to contain, in addition to a plane wave with propagation direction ν_2, an incoming wave. The asymptotic forms of the exact solutions ψ_1 and ψ_2 are similar to Equation (2), but instead of the function $G(\nu, \mathbf{n})$, they contain scattering amplitudes $G^{\circ}(\nu, \mathbf{n})$. Thus in the asymptotic form, variations $\delta\psi_1$ are due to variations $\delta G(\nu_1, \mathbf{n})$.

The first variation of the functional (1), caused by variations $\delta\psi_1=\psi_i-\psi_i$ of the functions ψ_i about the exact solutions ψ_i, is given by

$$\delta I=\int\psi_2^{+}\{\alpha\mathbf{p}+\beta m+V-E\}\,\delta\Psi_1 d\mathbf{r}=-i\int\psi_2^{+}\alpha\mathbf{n}\,\delta\Psi_1 dS, \tag{3}$$

where the integration is taken over the surface of an infinite sphere, $r \to \infty$, $\mathbf{n} = \mathbf{r}/r$. Here

$$\delta\Psi_1 = \delta G(\boldsymbol{\nu}_1, \mathbf{n})(pr)^{-1}\exp(ipr).$$

Let us write the spinors u and G in the form

$$u = N\begin{pmatrix} v \\ w \end{pmatrix}, \; G = N\begin{pmatrix} F \\ F' \end{pmatrix}, \; N^2 = \frac{1}{2}\left[1 + \frac{m}{E}\right] \qquad (4)$$

and eliminate the two-component spinors w and F' with the aid of the formulas

$$w_2 = p\boldsymbol{\sigma}\boldsymbol{\nu}_2 v_2 / (E+m), \; F' = p\boldsymbol{\sigma}\mathbf{n}F / (E+m).$$

Then, writing $d\omega$ for the element of solid angle, we have from (3)

$$\delta I = -i\frac{r}{p}\int e^{ipr(1-\boldsymbol{\nu}_2\mathbf{n})} u_2^{+}\boldsymbol{\alpha}n\delta G(\boldsymbol{\nu}_1, \mathbf{n})\,d\omega \qquad (5)$$

$$= \frac{2\pi}{pE}\delta(v_2^{+}F(\boldsymbol{\nu}_1, \boldsymbol{\nu}_2)).$$

This Eq. (5) is the variational principle for the scattering amplitude $F^{\circ}(\nu_1, \nu_2)$. From this it follows that the correct scattering amplitude is the stationary value of the quantity

$$\{(v_2^{+}F(\boldsymbol{\nu}_1, \boldsymbol{\nu}_2)) - pEI / 2\pi\}.$$

When V is the potential of a central field, the variational principle for the phase shifts is easy to obtain from Eq. (5). In this case we choose trial functions which differ from the exact solutions in their radial parts. Then the functional (1) will converge if the asymptotic forms of the radial parts, which are the same for both trial functions ψ_1 and ψ_2 differ from the asymptotic form of the exact solutions only in the phase $\tilde{\eta}$ and the amplitude $\tilde{A}$. For $r \to \infty$ we thus obtain the radial parts of the trial functions in the form

$$rg_l(r) = \tilde{A}\sqrt{\frac{E}{m}+1}\cos(pr + \tilde{\eta}_{jl});$$

$$rf_l(r) = -\tilde{A}\sqrt{\frac{E}{m}-1}\sin(pr + \tilde{\eta}_{jl}).$$

Then the variational principle for the phase shifts is of the form

$$\delta I = A^2(p/m)\,\delta\eta_{jl}. \qquad (6)$$

The virial theorem for the continuous Dirac spectrum can be derived by variation of the length scale, as it has been previously derived for other cases by Fock[4] and later by Demkov.[2] Let us set

$$\Psi_i(\mathbf{r}) = \psi_i(\mathbf{r} + \varepsilon\mathbf{r}),$$

where ψ_i is an exact solution. Since the variation of the length scale changes the asymptotic behavior of ψ_i, we must investigate not Equation (1), to assure the convergence of I, but the functional

$$I'\{\psi(\mathbf{r}+\varepsilon\mathbf{r})\} = \int\psi_2^{+}(\mathbf{r}+\varepsilon\mathbf{r})\,[\alpha\mathbf{p}$$

$$+ (1+\varepsilon)(\beta m - E) + V]\,\psi_1(\mathbf{r}+\varepsilon\mathbf{r})\,d\mathbf{r}.$$

For $\epsilon \ll 1$ this functional is given up to terms in ϵ^2 by

$$I'\{\psi(\mathbf{r}+\varepsilon\mathbf{r})\} = -\varepsilon\int\psi_2^{+}(\mathbf{r})\,[V(\mathbf{r}) + \mathbf{r}\nabla V]\,\psi_1(\mathbf{r})\,d\mathbf{r}.$$

On the other hand $I'\{\psi(\mathbf{r}+\epsilon\mathbf{r})\}$ is a functional of the trial function $\psi(\mathbf{r}+\epsilon\mathbf{r}) = \delta\psi + \psi'(\mathbf{r})$ which is hardly different from the function $\psi'(\mathbf{r})$, for which $I\{\psi'(\mathbf{r})\} = 0$. Therefore in order to calculate $I'\{\psi(\mathbf{r}+\epsilon\mathbf{r})\}$ we may also make use of the variational principle (5). The asymptotic form of $\psi'(\mathbf{r})$ differs from that of $\psi(\mathbf{r}+\epsilon\mathbf{r})$ only in the scattering amplitude: the scattering amplitude in $\psi'(\mathbf{r})$ depends on the mass $m(l+\epsilon)$ and the energy $E(l+\epsilon)$, whereas that of $\psi(\mathbf{r}+\epsilon\mathbf{r})$ depends on m and E. Therefore in variation (5) we have the scattering

$$\delta F = -\varepsilon[m\partial/\partial m + E\partial/\partial E]\,F.$$

This means that there exists a relation

$$\left[m\frac{\partial}{\partial m} + E\frac{\partial}{\partial E}\right](v_2^{+}F(\boldsymbol{\nu}_1, \boldsymbol{\nu}_2)) \qquad (7)$$

$$= \frac{pE}{2\pi}\int\psi_2^{+}[V + \mathbf{r}\nabla V]\,\varphi_1\,d\mathbf{r},$$

which is the virial theorem for the continuous Dirac spectrum. The virial theorem is convenient to use at high energies $E \gg m$, when the derivative with respect to mass can be neglected.

For the central field case, the virial theorem is of the form

$$A^2\frac{p}{m}\left[E\frac{\partial\eta}{\partial E} + m\frac{\partial\eta}{\partial m}\right] \qquad (8)$$

$$= \int_0^\infty\left[V(r) + r\frac{dV}{dr}\right][g_l^2 + f_l^2]\,r^2dr.$$

From the variation (5) it is easy to obtain an expression for the change in the scattering amplitude caused by a variation of the potential V (r, λ) $\rightarrow V$ (r, $\lambda + \epsilon\lambda$), where λ is some parameter. From Equation (5) we have

$$\partial (v_2^+ F(\mathbf{v}_1, \mathbf{v}_2))/\partial\lambda = -\frac{pE}{2\pi}\int \psi_2^+ \frac{\partial V}{\partial\lambda}\psi_1 d\mathbf{r}. \tag{9}$$

Variational principles (5) and (6) and the virial theorem (7), (8) are also valid for a Coulomb field for r →∞, if we take account of the fact that in this case the asymptotic form of the wave functions should include terms in ln (pr).

---

[1] J. Schwinger, Phys. Rev. 72, 742 (1947). L. Hulthen, Arkiv Mat. Astron. Fys. 35A, 251 (1948). W. Kohn, Phys. Rev. 74, 1763 (1948).

[2] Iu. N. Demkov, Dokl. Akad. Nauk SSSR **89**, 249 (1953); 97, 1003 (1954).

[3] G. Parzen, Phys. Rev. 80, 2 (1950).

[4] V. A. Fock, Z. Physik 63, 855 (1940).

Translated by E. J. Saletan
226

The Internal Compton Effect

E. G. Melikian
Moscow State University

(Submitted to JETP editor July 26, 1956)
J. Exptl. Theoret. Phys. (U.S.S.R.) 31, 1088-1090 (December, 1956)

Spruch and Goertzel[1] have calculated the relative probability of the internal Compton effect for magnetic 22-pole transitions and Iakobson[2] has obtained an approximate relativistic formula for electric 2^j-pole transitions, but only for small gamma-ray energies. In the present work a general formula is derived for the relative probability of this effect for both magnetic and electric transitions in the Born approximation and numerical calculations are carried through for some specific cases.

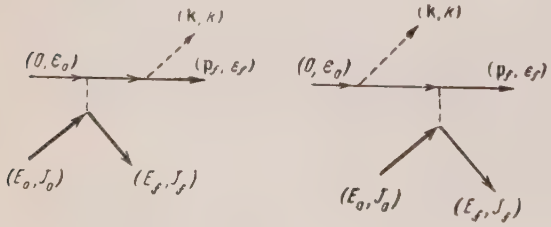

Figure 1.

The process under consideration is characterized by the Feynman diagrams in Fig. 1, where the heavy lines correspond to a nucleus and the thin dashed lines correspond to an electron and photon. In the initial state we have an excited nucleus with charge Z, energy E and angular momentum J_0, and an electron in the K shell with energy ϵ_0. In the final state, the energy and angular momentum of the nucleus are designated by E_f and J_f, and the energy and momentum of the electron and photon by ϵ_f, $\mathbf{p}_f$ and k, $\mathbf{k}$, respectively. Hereinafter, we shall use the system of units in which $h = c = 1$.

Using the general methods of quantum electrodynamics in our calculations (see Ref. 3) we obtain the relative probability of the internal Compton effect (the ratio of the absolute probability of the effect to the probability of a radiation transition of the nucleus) which for the magnetic $2j$-pole transition is expressed by

$$\beta_j^{(0)} = \frac{2\pi\alpha^2 (Zm\alpha)^3 (2j+1)\, p_f}{pk} |L|^2 \left\{\left[1 + \frac{k}{m} + \frac{\Delta E}{mp'}\right] \frac{p_f k}{p^2}(x^2 - 1) - \frac{2\varepsilon_f(\Delta Em + kp')}{mp'} - \left[\frac{1}{m^2} + \frac{1}{p'^2}\right][\Delta Em^2 + k(m+k)\,p'] \sin\vartheta\, d\vartheta\, dk, \tag{1}$$

$$L = (2/\pi)(p/\Delta E)^{j+1/2}(p^2 - \Delta E^2 - 2iZm\alpha\Delta E)^{-1},$$

$$p' = p_f x - \varepsilon_f,\ x = \cos\vartheta,\ \Delta E = E_0 - E_f,\ \varepsilon_0 \sim m,$$

$$p = |\mathbf{p}_f + \mathbf{k}|,\ j = |I_0 - I_f|,$$

where ϑ is the angle between the vectors $\mathbf{p}_f$ and $\mathbf{k}$.

This formula is in agreement with the results of Spruch and Goertzel[1] if we neglect the width of

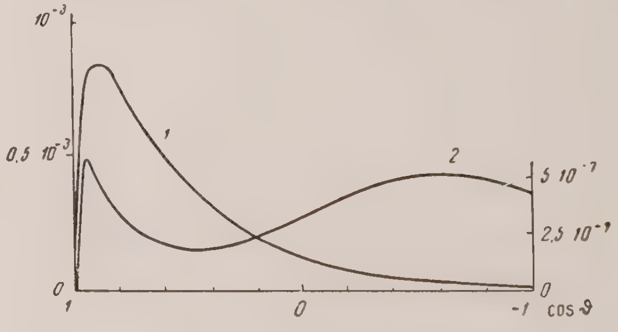

FIG. 2

the nuclear energy level in the latter. It should be noted that in the present problem the width of the nuclear energy level is of no importance.

In the case of an electric transition, the relative probability of the internal Compton effect is given by the following:

$$\begin{aligned}\beta_j^{(1)} = {} & \frac{2\pi (Zm\alpha)^3 (2j+1)\, p_f \alpha^2}{(j+1)\, pk} \mid L \mid^2 \left\{ \left(\frac{1}{m^2} + \frac{1}{p'^2} \right) [\Delta E m^2 + k(m+k)\, p'] \right. \\ & \times \left[j - (2j+1) \frac{\Delta E^2}{p^2} \right] - \frac{2jm^3}{p'^2} + \left(\frac{\Delta E}{mp'} + \frac{m+k}{m^2} \right) \frac{k \Delta E^2}{p^2}\, p_f [(j+1) \cos \vartheta \\ & + (j-1) \cos (\hat{p}p_f) \cos (p\hat{k})] + \frac{1}{mp'} [2j\varepsilon_f [k(\Delta E - m) - 2m^2] \\ & - (2j+1) \frac{m \Delta E^3 \varepsilon_f}{p^2} - \frac{2k\Delta E}{p}\, j\, [m\Delta E + \varepsilon_f (\Delta E + m)] \cos (p\hat{k}) \\ & + \frac{2\Delta E m}{p}\, j p_f [(\Delta E + m) \cos (\hat{p}p_f)] + \frac{1}{m^2} \left[2j [k (\varepsilon_f - m)(k - 2m) - m^2 \varepsilon_f \right] \\ & - (2j+1)\, mk\varepsilon_f \frac{\Delta E^2}{p^2} - \frac{2\Delta E k}{p}\, j \left[k\varepsilon_f + m (\Delta E + m) \cos (p\hat{k}) \right. \\ & \left. \left. - \frac{2\Delta E j}{p}\, p_f\, [k(k+m) - m^2] \cos (\hat{p}p_f) \right] \right\} \sin \vartheta\, d\vartheta\, dk. \end{aligned} \tag{2}$$

Figure 2 presents curves of the angular distribution of gamma rays emitted as a result of the internal Compton effect; these were obtained by numerical integration from (1) and (2) with the photon energy k in the range from 0.05 to 0.4 mev for curve 1 and up to 0.7 mev for curve *2*. Curve *1* refers to a transition in Ba^{137m} ($M4$ transition, $\Delta E = 0.662$ mev), while curve *2* refers to a transition in Mg^{24} ($E2$ transition, $\Delta E = 1.38$ mev).

In conclusion, the author wishes to thank Doctor of Physical and Mathematical Sciences I. S. Shapiro for valuable advice and assistance.

---

[1] L. Spruch and G. Goertzel, Phys. Rev. **94**, 1671 (1954).

[2] A. Iakobson , J. Exptl. Theoret. Phys. (U.S.S.R.) **29**, 703 (1955); Soviet Phys. JETP **2**, 751 (1956).

[3] A. Akhiezer and V. Berestetskii, *Quantum Electrodynamics*, GITTL, Moscow, 1953.

Translated by I. Emin
228

On the Magnetization Mechanism of Some NiZn Ferrites in Very Weak Fields

L. A. Fomenko
Central Laboratory for the Combatting of Industrial Radio Noise

(Submitted to JETP editor August 14, 1956)
J. Exptl. Theoret. Phys. (U.S.S.R.) **31**, 1092-1093
(December, 1956)

RATHENAU and Fast recently published the results[1] of their investigation of the initial permeability σ_a of two types of NiZn ferrites: $Ni_{0.5}Zn_{0.5}Fe_2O_4$ and $Ni_{0.36}Zn_{0.64}Fe_2O_4$ under different external stresses σ_a. The experimental data were interpreted in terms of rotations of the direction of magnetization of ferromagnetic domains. This interpretation has in particular been used by Smit and Wijn[2] as one proof that Snoek[3] was right in attributing the magnetic radio-frequency spectra of NiZn ferrites to gyromagnetic resonance.

As a basis for this view Rathenau and Fast took the agreement between the experimental data and the theoretical formula which they derived for the rotation; this formula (1) establishes a relation between $\Delta\mu_a$ and σ_a:

$$\Delta\mu_a = (9/40\pi)(\lambda_s \sigma_a \mu_a \,/\, I_s^2)\, \mu_a, \tag{1}$$

where I_s is the saturation magnetization and λ_s is the saturation magnetostriction.

Formula (1) was obtained (neglecting the correction for porosity of the sample) by inserting in

$$\Delta\mu_a = {}^1\!/_5 \left({}^3\!/_2\, \lambda_s \sigma_a \mu_a / {}^2\!/_3\, K \right) = (9\lambda_s \sigma_a / 20K\mu_a), \tag{2}$$

the value of K from the equation

$$\mu_{a\,\mathrm{rot}} - 1 = 2\pi I_s^2 \,/\, K, \tag{3}$$

which was given by Wijn[2] and which follows from the theory of pure rotation processes that was first developed by Akulov[4].

Rathenau and Fast[1] arbitrarily assumed

$\mu_{a\,rot} = \mu_a$, which apparently predetermined their result since in actuality μ_a can be written as the sum of the initial permeabilities $\mu_a = \mu_{a\,dis} + \mu_{a\,rot} - 1$ which result from boundary displacements and magnetization rotation, respectively.

Experimental values of the anisotropy constant K_1 and the effective internal fields H_i of some NiZn ferrites have been given by Miles[5]; for example, for $Ni_{0.55}Zn_{0.45}Fe_2O_4$, which is nearly the same in composition as one of the samples investigated in Ref. 1, he gave $K_1 = 105\, I_s$ and $H_i = 190$ oersteds, whence, according to Kittel[6], we obtain the effective anisotropy constant $K = {}^1/_2 H_i I_s = 95 I_s$, which is in good agreement with K_1.

Substitution of this value of the anisotropy with $I_s = 335$ gauss and $\lambda_s = 10 \times 10^{-6}$ in (2) gives for the first sample $\Delta\mu_a = 0.013\ \mu_a$ kg/mm^2 as compared with the experimental value $0.15\mu_a =$ kg/mm^2 which was calculated by Rathenau and Fast using an excessively high estimate of $\mu_{a\,rot} = \mu_a = 240$ gauss/oersted instead of the more probable value $\mu_{a\,rot} \sim 2\pi\,(335/105) + 1 = 20$ gauss/oersted (or, according to Kittel's formula, $\mu_{a\,rot} \sim (4\pi/3) \times (335/105) + 1 = 15$ gauss/oersted).

For boundary displacements, as noted in Ref. 1, the coefficient 1/5 of (2) must be considerably increased. On the basis of the experimental information in Ref. 1 and the values of the anisotropy constant in Ref. 5 it is easily shown that this coefficient must be ~ 2 for the first sample of a NiZn ferrite and ~ 3 for the second sample, i.e., it is of the order of the values obtained by Bozorth and Williams[7] for 45% permalloy.

For boundary displacements, the magnetization process in very weak fields can be attributed, according to Kondorskii's general theory of reversible displacement (Ref. 8, Sec. 53) to impurities and internal stresses σ_i. Since Ref. 1 does not contain information concerning impurities in NiZn ferrites we shall attempt to estimate $\mu_{\alpha\,dis}$ for these ferrites according to Kondorskii's theory of stresses (Ref. 8) p. 359), especially since experimental data definitely indicate the importance of magnetoelastic energy $\lambda_s\sigma_i$ in some ferrites. For this purpose we shall use the graphs of $\mu_a(\sigma_a)$ given in Figs. 1 and 2 of Ref. 1, from which, according to Vonsovskii's theory (Ref. 8, pp. 408 and 767) we can estimate the mean value of the internal stresses, obtaining $\sigma_i \sim 1$ kg/mm^2 for the first sample and $\sigma_i \sim 0.2$ kg/mm^2 for the second sample. Assuming in zero approximation that the stress distribution in the material is sinusoidal, we obtain the values of the internal stress amplitudes $\sigma_{0i} \sim 2$ kg/mm^2 and $\sigma_{0i} \sim 0.4$ kg/mm^2, respectively, whence from

$$\mu_{a\,dis} - 1 \approx 4\pi I_s^2 / 3\lambda_s\sigma_{0i}, \tag{4}$$

we obtain for the first sample $\mu_{a\,dis} = 235$ gauss/oersted and for the second ($I_s = 2966$, $\lambda_s = 5 \times 10^{-6}$ $\times\ \mu_{a\,dis} = 1820$ gauss/oersted. The first of these values is in extremely good agreement with Rathenau and Fast[1]($\mu_a = 240$ gauss/oersted); the second value is in much poorer agreement with these data ($\mu_a = 700$ gauss/oersted), which probably indicates the large role of impurities in the second sample, which was apparently sintered at a relatively low temperature. It is interesting to note that the composition of the second sample is close to the optimum for NiZn ferrites, which is usually used at quite high sintering temperature ~ 1350° in order to obtain cores of high initial permeability $\mu_a \approx 2000$ gauss/oersted. The possibility of obtaining such values of μ_a for the given composition when the effect of impurities is eliminated follows directly from the calculations.

We note in conclusion that the predominant role of displacements in NiZn ferrites sintered at not too low temperatures also follows from our investigations[9] of the magnetic spectra of ferrites with zero and residual magnetization. The foregoing considerations can therefore be regarded as an additional confirmation of our deduction.

---

[1] G. W. Rathenau and J. F. Fast, Physica **21**, 964 (1955).

[2] J. Smit and H. P. J. Wijn, *Advances in Electronics and Electronic Physics*, **6**, 70 (1954) Academic Press, N.Y.

[3] J. L. Snoek, *New Developments in Ferromagnetic Materials*, Elsevier, Amsterdam (Russian translation, IIL, Moscow, 1949).

[4] N. S. Akulov, *Ferromagnetism*, ONTI, Moscow, 1939.

[5] P. A. Miles, Nature, **174**, 177 (1954).

[6] C. Kittel, Symposium, *Ferromagnetic Resonance*, IIL, Moscow, 1952, p. 17

[7] R. M. Bozorth and H. J. Williams, Rev. Mod. Phys. **17**, 72 (1945).

[8] S. V. Vonsovskii and Ia. S. Shur, *Ferromagnetism*, Gostekhizdat, Moscow, 1948.

[9] L. A. Fomenko, J. Exptl. Theoret. Phys. (U.S.S.R.) **30**, 18 (1956); Soviet Phys. JETP 3, 19 (1956). Fiz. Metal. Metallov. 2, 22 (1956).

Translated by I. Emin
230

μ-Pair Production in Nuclei by Gamma Rays

L. M. AFRIKIAN
Physics Institute, Academy of Sciences,
Armenian, SSR

(Submitted to JETP editor August 25, 1956)
J. Exptl. Theoret. Phys. (U.S.S.R.) **31**, 1094-1095
(December, 1956)

IN a recent article by Masek and Panofsky[1], data were given on the electromagnetic production of muon pairs, which had been observed for the first time. It is appropriate to note that in the interaction of high-energy gamma rays ($h\omega > 200$ mev) with nuclei, in addition to the "ordinary" production of free muon pairs, there is another effect which consists of the direct production of the μ-meson of a pair in the K shell of a mesic atom.

A distinguishing characteristic of the problem of μ-pair production in nuclei by gamma rays is the necessity for taking into account the finite size of the nucleus*. In the production of free muon pairs this fact leads, first, to a departure from the Coulomb law because the electrical charge of the nucleus is considerably smeared out at small distances[2] and, second, to the total or partial destruction of coherence in the nuclear process.

With regard to the direct production of the μ-meson of a pair in the K shell of a mesic atom, the necessity for taking into account the finite size of the nucleus follows from the closeness in size of the K-shell "radius" of the mesic atom a and the nuclear "radius" R_0. However, in this case, as will be seen from the following, the question of coherence does not appear in the formulation of the problem. Therefore, consideration of nuclear size reduces to taking into account the weakining of the electrical interaction and can be accomplished approximately by replacing the atomic number Z in the ordinary hydrogen-like wave functions with an effective atomic number $Z_{\text{eff}} (Z_{\text{eff}} < Z)$.

Such an approximation is clearly suitable only when $a > R_0$, i.e., for not too heavy nuclei, since the employment of hydrogen-like wave functions is otherwise meaningless. The transition matrix element for the production of a μ-mesic atom and a μ^+-meson by a gamma ray on a nucleus can be represented (assuming $\hbar = c = 1$) as:

$$S_{if} = -e\left(\frac{2\pi}{\omega}\right)^{1/2}\int\limits_0^\infty \Psi^*_K(\alpha\varepsilon)\, e^{-i\omega\mathbf{r}}\Psi^*_p d^3\mathbf{r}. \qquad (1)$$

In the relativistic Born approximation for the differential cross section of the effect we have

$$d\sigma_K = 2\pi Z^5_{\text{eff}}\, \alpha^4 r_0^2 \frac{\mu^5}{\omega^{7/2}} (\omega - 2\mu)^{3/2} \qquad (2)$$

$$\frac{\sin^2\theta d(-\cos\theta)}{[\omega - \mu - \sqrt{\omega(\omega - 2\mu)}\cos\theta]^4},$$

where θ is the angle between the momenta of the gamma ray and the positive muon; ω is the gamma frequency: $r_0 = e^2/u$, $\alpha = 1/137$. Thus at the threshold, the emitted μ^+-mesons must be emitted mainly at the angle $\pi/2$ to the incident gamma-ray beam.

The total cross section is

$$\sigma_K = (8\pi/3)\, r_0^2 Z^5_{\text{eff}}\, \alpha^4\mu^2\omega^{-7/2}(\omega - 2\mu)^{3/2}. \qquad (3)$$

At the threshold for $\omega \to 2\mu$

$$\sigma_K = (\pi r_0^2/3\sqrt{2})\, Z^5{}_{\text{eff}}\, x^4\, [(\omega - 2\mu)/\mu]^{3/2}. \qquad (4)$$

Departure from the Born approximation is taken into account by inserting in (3) and (4) the factor $f(\zeta)$:

$$\sigma'_K = f(\zeta)\,\sigma_K, \quad f(\zeta) = 2\pi\zeta/(e^{2\pi\zeta} - 1), \qquad (5)$$
$$\zeta = \alpha Z'_{\text{eff}}\,[1 + \mu^2/\omega(\omega - 2\mu)]^{-1/2}.$$

A more general expression than (3) can be obtained in the Born approximation by using the relativistic functions Ψ_k and Ψ_p. In this case

$$\sigma_K = {}^3/_4\, \sigma_0 \alpha^4 Z^5_{\text{eff}}\, (\eta^2 - 1)^{3/2}(\eta + 1)^{-5} \qquad (6)$$
$$\times\left\{\frac{4}{3} + \frac{\eta(\eta - 2)}{\eta + 1}\left[1 - \frac{1}{2\eta\sqrt{\eta^2 - 1}}\ln\frac{\eta + \sqrt{\eta^2 - 1}}{\eta - \sqrt{\eta^2 - 1}}\right]\right\},$$
$$\sigma_0 = 8\pi r_0^2/3, \qquad \eta = (\omega - \mu)/\mu.$$

When $\omega \to 2\mu$ (6) goes over into (3) and (4).

In the other limiting case where $\omega \gg \mu$:

$$\sigma_K = {}^3/_4 \sigma_0 \alpha^4 Z^5_{\text{эфф}}\, \mu/\omega. \qquad (7)$$

The maximum of (6) corresponds to $\omega \approx 7.5 \approx 770$ mev.

The values of Z_{eff} can be obtained by using Wheeler's semi-empirical formula[3] for the lifetime of a muon in a K shell with respect to capture by the nucleus:

$$\tau_{\rm cap} = \tau_{\rm dec}{}'(Z_{\rm eff}/Z_0)^{-4}. \qquad (8)$$

According to Wheeler,

$$Z_{\rm eff} = Z[1 + (Z/37.2)^{1.54}]^{-1/1.54}, \qquad (9)$$

whence it follows in particular that

	Al	Fe	Zn	Ag
$Z =$	13	26	30	47
$Z_{\rm eff} =$	11.58	19.4	21.1	26.4

For these values of $Z_{\rm eff}$ the cross section of the effect under consideration does not exceed $\approx 10^{-34}$ cm^2. The relative role of pair plus mesic-atom production is significant near the threshold for the production of μ pairs. At the threshold, the cross section for the production of a pair of free muons is

$$\sigma \leqslant (^1/_3)\, r_0^2 \alpha Z\, [(\omega - 2\mu)/\mu]^3. \qquad (10)$$

The linear dependence of (10) on Z results from the destruction of coherence of the nuclear effect because of the transfer of large momenta q ($q \approx 2u \gg 1/R_0$). As follows from a comparison of (4) and (10), for $Z_{\rm eff}$ not extremely small, the production of a pair plus a μ-mesic atom can predominate over the production of free muon pairs.

However, the smallness of the cross sections at the threshold makes the experimental investigation of pair production very difficult. It must be emphasized that the present estimates are approximate and give cross sections which are too small. A rigorous theory based on exact wave functions in the field of a finite nucleus will yield results which are more favorable to experiment and will be published hereafter.

In conclusion I wish to express my sincere thanks to Professor A. I. Alikhanian and to G. M. Garibian for very valuable discussions of a number of questions involved in the present note.

---

* Excluding the case for $h\omega/\mu c^2 \gg 1$, where the main contribution to the cross section for the production of free pairs comes from collisions at distances such that the size of the nucleus can be neglected by comparison.

1 G. Masek and W.K.H. Panofsky, Phys. Rev. **101**, 1094 (1956).

2 G. H. Rawitscher, Phys. Rev. **101**, 423 (1956).

3 J. A. Wheeler, Rev. Mod. Phys. **21**, 133 (1949)

Translated by I. Emin
231

Showers in Lead Produced by 360 ± 30 mev Electrons

V. G. Ivanov, N. I. Petrov,
V. A. Rusakov Iu. A. Budagov,
V. T. Osipenkov
United Institute for Nuclear Research

(Submitted to JETP editor February 12, 1956)
J. Exptl. Theoret. Phys. (U.S.S.R.) 31, 1095-1096 (December, 1956)

THE data on electron showers communicated in this note have been obtained in the course of analyzing results of experiments in which the interaction of negative π-mesons with lead nuclei was studied. The experiments were carried out using the synchrocyclotron of the Laboratory of Nuclear Problems with the aid of a Wilson cloud chamber of 400 mm diameter in a magnetic field of intensity 10^4 oersted.

The beam of π-mesons which passed through a lead plate of thickness 4.6 g. cm^{-2} situated inside the cloud chamber contained (2 ± 1)% of electrons. Therefore in addition to the events produced by the interaction of π-mesons with nuclei, the photographs also recorded cases of the formation of electron showers in lead. In the course of the analysis of the photographs, 159 showers were recorded which were produced by electrons whose energy lies in the interval from 330 to 390 mev. An example of one such shower is shown in Fig. 1. This number does not include a few cases in which the primary electron was stopped in the lead plate, since it is practically impossible to distinguish them from the large number of cases of stopping of π-mesons. In counting up the number of particles in the showers only secondary electrons of energy $E \leq 8$ mev were taken into account. By means of this criterion of selection of secondary electrons, we excluded errors related to the presence inside the chamber of a background of low energy electrons.

The experimentally obtained distribution of showers with respect to the number of particles is given in the Table. For comparison the last column of this Table gives the distribution of showers with respect to the number of electrons according to Poisson's law. The average number of electrons per shower in accordance with the data given in the Table is equal to 1.77.

The energy distribution of the secondary electrons is shown graphically in Fig. 2. The value for the average number of secondary electrons in the shower obtained as a result of our measurements agrees within experimental error both with

FIG. 1. Electron-positron shower of 6 particles initiated in the lead plate by an electron of momentum 360 mev/c.

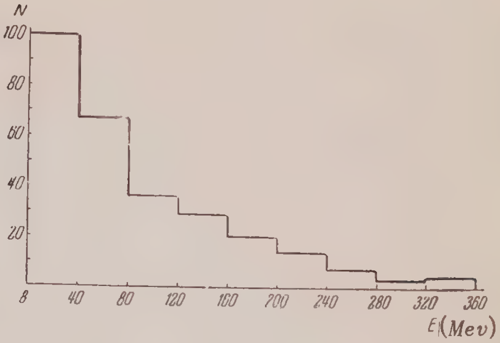

FIG. 2. Energy distribution of the secondary electrons N (E).

the corresponding experimental results of reference 2, and with the theoretical value for this quantity obtained in Ref. 3 by means of a Monte-Carlo calculation of an electron cascade in lead.

Number of electrons per shower	Observed no. of showers with a given number of particles.	Observed no. of particles expressed as % of the total	Number of showers with a given no. of particles corresponding to Poisson's law, expressed in %
0	—	2—3*	17
1	88	53.6	30
2	34	20.7	26.6
3	30	18.3	15.7
4	3	1.8	6.9
5	1	0,6	2,5
6	2	1,2	0.7
7	1	0.6	0,1
8	0	0	0,01

*These data for the relative number of stoppages of primary electrons are taken from Ref. 2.

---

[1] Dzhelepov, Ivanov, Kozodaev, Osipenkov, Petrov and Rusakov, J. Exptl. Theoret. Phys. (U.S.S.R.) 31, 923 (1956). Soviet Phys. JETP **4**, 864 (1957).

[2] Ch. A. O' Andlau, Nuovo Cimento 12, 859 (1954).

[3] R. B. Wilson, Phys. Rev. 86, 261 (1952).

Translated by G. M. Volkoff
232

Generalized Nonsingular Solutions for the Scalar Meson Field of a Point Charge in General Relativity Theory

DUAN'-I-SHI
Moscow State University

(Submitted to JETP editor September 15, 1956)
J. Exptl. Theoret. Phys. (U.S.S.R.) **31**, 1098-1099 (December, 1956)

IT has been shown that in investigating the electromagnetic and meson fields of elementary particles, the effects of gravitational interaction cannot be neglected[1-5]. The present note is an attempt to find solutions to the equations of the general relativistic gravitational and scalar meson fields of a point nuclear charge. The solution is nonsingular at all points of the gravitational and meson fields. Although it contains several functions whose form is not given, this solution can be used to obtain the potential of the scalar meson field, which is a generalization of the Yukawa potential; furthermore, it makes it possible to calculate the mass and self-energy of the nucleon, which turn out to be finite.

We take the general centrally symmetric expression for the interval in the usual form

$$ds^2 = -e^{\lambda}dr^2 - e^{\mu}r^2\{d\theta^2 + \sin^2\theta\, d\Phi^2\} + e^{\nu}dt^2,$$

where λ, μ, and ν are functions of r. The energy-momentum tensor of the scalar meson field is

$$T_i^k = \left(\frac{1}{8\pi}\right)\left\{2g^{ik}\frac{\partial U}{\partial x^i}\frac{\partial U}{\partial x^k} - \delta_i^k\left(g^{lm}\frac{\partial U}{dx^l}\frac{dU}{dx^m} - \chi^2U^2\right)\right\}.$$

We shall consider the field static and set $U = U(r)$. Then

$$T_1^1 = (1/8\pi)(-e^{-\lambda}U'^2 + \chi^2U^2); \tag{1}$$

$$T_2^2 = T_3^3 = T_4^4 = (1/8\pi)(e^{-\lambda}U'^2 + \chi^2U^2).$$

It is easy to show, on the basis of the invariance of the Einstein equations under the transformation $r \to \sigma r$, $\chi \to \chi/\sigma$, where σ is a constant, that the solutions to these equations is of the form

$$U = U_0V(\chi r);\quad e^{\nu} = e^{\nu_0}\Phi(\chi r); \tag{2}$$

$$e^{\lambda} = e^{\lambda_0}\Psi(\chi r);\quad e^{\mu} = e^{\mu_0}X(\chi r),$$

where U_0, e^{ν_0}, e^{λ_0} and e^{μ_0} are solutions for the case $\chi = 0$, and V, Φ, Ψ, and ψ are functions of the one argument χr.

As $\chi r \to 0$, each of these four functions approaches unity; i.e., for $r \to 0$, the solutions for the cases $\chi \neq 0$ and $\chi = 0$ are identical.

Let us set[4]

$$\mu = -2\ln f(r),$$

where $f(r)$ is an arbitrary function with no singularities in the region $0 \leq r \leq +\infty$ and satisfying the following conditions:

$$|f(r)| \leqslant 1;\quad [f(r)]_{r=0} = 0;\quad [f(r)]_{r=\infty} = 1; \tag{3}$$

$$[f'(r)]_{r=0} = \alpha;\quad [f'(r)]_{r=\infty} = 0;$$

$$[f''(r)]_{r=0} = \beta;\quad [f''(r)]_{r=\infty} = 0.$$

Solving the Einstein equation for $\chi = 0$ and inserting the solutions for U_0, e^{ν_0}, e^{λ_0}, and e^{μ_0} into Eq. (2), we arrive at the general solution in the form

$$U_r = \frac{G}{\sqrt{A^2 + 4(kG^2/c^4)}} \tag{4}$$

$$\times\ln\left[\frac{X + (A/2q)(1+q)}{X - (A/2q)(1-q)}\right]V(\chi r);$$

$$e^{\nu} = \left[\frac{X - (A/2q)(1-q)}{X + (A/2q)(1+q)}\right]^q \Phi(\chi r);$$

$$e^{\lambda} = \frac{r^2}{f^4}\left[1 - \frac{rf'(r)}{f(r)}\right]^q \frac{1}{X}\left[\frac{X - (A/2q)(1-q)}{X + (A/2q)(1+q)}\right]^q \Psi(\chi r);$$

$$e^{\mu} = X(\chi r)/f^2(r),$$

where X is the solution to the algebraic equation

$$[X - (A/2q)(1-q)]^{1-q}[X + (A/2q) \tag{5}$$

$$\times(1+q)]^{1+q} = r^2/f^2(r),$$

$$q = A[A^2 + 4(kG^2/c^4)]^{-1/2} < 1,$$

and A is a constant of integration which can be determined from the conditions (3). From Eq. (4) and conditions (3) it is easy to prove that all the components of the metric tensor g_{ik} and of the potential U are nonsingular as $r \to 0$.

The self-energy of a particle is calculated using Tolman's formula[6]

$$W = \int(T_1^1 + T_2^2 + T_3^3 - T_4^4)\sqrt{-g}\,dV \tag{6}$$

$$= G^2\int_0^\infty \text{[illegible]} = \delta.$$

It can be shown that with conditions (3), the integral in Eq. (6) is finite. Then the self-mass of of the nucleon will be $m = G^2\delta/c^2$, and its classical radius is $r_0 = 1/\delta$. If we neglect small quantities of the order of $kG^2/c^4 = 10^{-68}$, then the constant $q \approx 1$.

In this case the potential of the scalar meson is of the form

$$U(r) = -\frac{G}{A}\ln\left[1 - A\frac{f(r)}{r}\right]e^{-\chi r}. \tag{7}$$

In view of the condition $|f(r)| \leq 1$, we can expand the potential $U(r)$ in a series for $r > A$:

$$U(r) = \frac{G}{r}f(r)e^{-\chi r}\left[1 + \frac{1}{2}\left(\frac{A}{r}\right)f(r) + \frac{1}{3}\left(\frac{A}{r}\right)^2 f^2(r) + \ldots\right] \tag{8}$$

For $r >> A$, the function $f(r) \approx 1$, and we obtain the Yukawa potential

$$U(r) = Ge^{-\chi r}/r.$$

Equation (7) is a generalization of the Yukawa potential. When $r \sim A$, the gravitational field greatly alters the potential of the meson field. From (7) and (3) we obtain

$$U(0) = (G/A)\ln[1/(1-A\alpha)].$$

Thus the theory we have here developed is in a position to give not only a finite nucleon mass, but also a finite potential well depth for nuclear forces. In this lies its attractiveness.

In conclusion I express my gratitude to Professor M. F. Shirokov for valuable advice and suggestions during the performance of this work.

---

1 M. F. Shirokov, Vest. Moscow State University 4, 67 (1947).

2 I. Z. Fisher, J. Exptl. Theoret. Phys.(U.S.S.R.) 18, 636 (1948); 19, 271 (1949).

3 M. F. Shirokov, J. Exptl. Theoret. Phys. (U.S.S.R.) 18, 236 (1948)

4 Duan'-I-Shi, J. Exptl. Theoret. Phys. (U.S.S.R.) 17, 756 (1954).

5 A. Einstein and Rosen, Phys. Rev. 48, 73 (1935).

6 R. Tolman, Proc. Roy. Soc. (London) A67, 148 (1938).

Translated by E. J. Saletan
234

The Optical Theorem and Elastic Scattering Through Small Angles

L. I. LAPIDUS
The United Institute of Nuclear Research

(Submitted to JETP editor August 27, 1956)
J. Exptl. Theoret. Phys. (U.S.S.R.) 31, 1099-1101
(December, 1956)

1. AS is known, the total interaction cross section is proportional to the imaginary part of the forward elastic scattering amplitude[1]. This general relation, which is sometimes called the optical theorem, is the result of the unitary character of the S-matrix and holds true for particles with no arbitrary spin. It may be represented thus

$$\sigma_t = (4\pi/k)\,\mathrm{Im\,Tr}\,M(0^\circ)/(2s_1+1)/(2s_2+1), \tag{1}$$

if one introduces the matrix $M(\theta)$, which connects the wave scattered through angle θ with the incident wave, and designates the spins of the colliding particles by s_1 and s_2.

When a spinless particle collides with a particle whose spin is 1/2, the matrix M may be represented as

$$M(\theta) = a(\theta) + b(\theta)(\sigma\mathbf{n}), \tag{2}$$

where a and b are functions of invariants $(\mathbf{k}\mathbf{k}_0)$ and $k_0^2 = k^2$, σ in the spin operator (nucleon), and $\mathbf{n} = [\mathbf{k}_0\mathbf{k}]/|[\mathbf{k}_0\mathbf{k}]|$ is the normal to the scattering surface.

When spin $s_1 = 1$ and $s_2 = 0$, M has the form

$$M(\theta) = X(\theta) + Y(\theta)(\mathbf{S}\mathbf{n}) + Z(\theta)(\mathbf{S}\mathbf{n})^2 + W(\theta)[(\mathbf{S}\mathbf{k}_0)(\mathbf{S}\mathbf{k}) + (\mathbf{S}\mathbf{k})(\mathbf{S}\mathbf{k}_0)], \tag{3}$$

where $\mathbf{s}$ is the spin-operator (deuteron) and the quantities X, Y, Z, and W play the same role as functions a and b in Eq. (2).

For the scattering of particles with a spin of $s_1 = 1/2$ on a target with an arbitrary spin of s_2, we have

$$M(0) = A + \sigma_1\mathbf{H} = A + B(\sigma_1\mathbf{n}) + C(\sigma_1\mathbf{m}) + D(\sigma_1\mathbf{l}); \tag{4}$$

and, for $s_1 = 1$ and an arbitrary s

$$s_2\ [(\mathbf{S},\mathbf{k}\mathbf{k}_0) = (\mathbf{S}\mathbf{k})(\mathbf{S}\mathbf{k}_0) + (\mathbf{S}\mathbf{k}_0)(\mathbf{S}\mathbf{k})\ \mathrm{e.\,t.\,c.}],$$

$$M(\theta) = K + L(\mathbf{S}\mathbf{n}) + M(\mathbf{S}\mathbf{l}) + N(\mathbf{S}\mathbf{m}) + R(\mathbf{S}\mathbf{n})^2 + T(\mathbf{S},\mathbf{k}\mathbf{k}_0) + F(\mathbf{S},\mathbf{n}\mathbf{l}) + V(\mathbf{S},\mathbf{n}\mathbf{m}) + Q(\mathbf{S},\mathbf{m}\mathbf{l}), \tag{5}$$

where $\mathbf{m} = (\mathbf{k}_0 - \mathbf{k})/|\mathbf{k}_0 - \mathbf{k}|$, $\mathbf{l} = (\mathbf{k}_0 + \mathbf{k})/|\mathbf{k}_0 + \mathbf{k}|$, and the quantities A, B, C, ..., K, L, M, ... are linear combinations of the total assembly $(2s_2 + 1)^2$ of the operators in the spin space of a particle with a spin of s_2. When $s_2 = 1/2$ we have

$$A = \alpha + \gamma(\boldsymbol{\sigma}_2\mathbf{n}), \quad B = \gamma' + \beta(\boldsymbol{\sigma}_2\mathbf{n}), \tag{6}$$

$$C = \delta(\boldsymbol{\sigma}_2\mathbf{m}), \quad D = \varepsilon(\boldsymbol{\sigma}_2\mathbf{l})$$

and analogous expressions for the quantities $K, L, M, \ldots$

2. Differential elastic scattering cross sections are expressed[2] by $M(\theta)$ in the following manner:

$$\sigma(\theta) = \mathrm{Tr}\, M^+(\theta) M(\theta) / (2s_1 + 1)(2s_2 + 1), \tag{7}$$

which, in case of an arbitrary s_2, becomes

$$\sigma(\theta) = \mathrm{Tr}\,(AA^+ + HH^+) / 2(2s_2 + 1) \tag{8}$$

when $s_1 = 1/2$ and an analogous equation when $s_1 = 1$.

The equations presented above indicate quite convincingly that when particles with arbitrary spins collide, a simple inequality is applicable

$$\sigma(0^\circ) \geqslant k^2\sigma_t^2 / 16\pi^2. \tag{9}$$

When the collision involves a spinless particle and a particle with a spin of $s_2 = 1/2$, the function $b(\theta)$ in Eq. (2) becomes zero for $\theta = 0^\circ$, and then, just as in the case of a collision of spinless particles, it is easy to arrive directly at proof of the validity of Eq. (9), viz.,

$$\sigma(0^\circ) = [\mathrm{Im}\, a(0^\circ)]^2 + [\mathrm{Re}\, a(0^\circ)]^2 \geqslant [\mathrm{Im}\, a(0^\circ)]^2 = k^2\sigma_t^2 / 16\pi^2.$$

Proof of the validity of Eq. (9) for the case of a collision of two fermions with spins of $s_1 = s_2 = 1/2$ can be provided in the following manner. From Eqs. (1), (4) and (6) we have $k\sigma_t = 4\pi\, \mathrm{Im}\, \alpha(0^\circ)$. On the other hand, $(\gamma(0^\circ) = \gamma'(0^\circ) = 0)$

$$\sigma(0^\circ) = |\alpha(0^\circ)|^2 + |\beta(0^\circ)|^2 + |\delta(0^\circ)|^2 + |\varepsilon(0^\circ)|^2 \geqslant |\alpha(0^\circ)|^2,$$

and therefore,

$$\sigma(0^\circ) \geqslant |\alpha(0^\circ)|^2 \geqslant [\mathrm{Im}\, \alpha(0^\circ)]^2 = k^2\sigma_t^2 / 16\pi^2.$$

When $s_2 = 0$, $s_1 = 1$, the expression for the total cross section and for $\sigma(0^\circ)$ $(Y(0^\circ) = Z(0^\circ) = 0)$ can be represented as

$$k\sigma_t = 4\pi\, \mathrm{Im}\, [X(0^\circ) + {}^2/_3\, W(0^\circ)];$$

$$\sigma(0^\circ) = |X(0^\circ) + {}^2/_3\, W(0^\circ)|^2 + {}^2/_9\, |W(0^\circ)|^2,$$

whence the validity of Eq. (9) follows directly.

For the more general case where the spin of one of the particles is 1/2 or 1 and the other is arbitrary, a similar argument can be applied.

3. In the exceptional case, as in (π-N) scattering as observed by Karplus and Ruderman[3], if $\sigma_t(E)$ is known over a wide energy interval, the dispersion relation can be used to calculate the forward elastic scattering cross section. In other cases, for example, that of ($n - \alpha$) scattering, one can thus far, specify only the lower limit of the value of this cross section.

Inequality (9) represents a useful restriction that may be applied in the treatment of experimental data on elastic particle scattering. For the most part, the region of small angles is not very accessible in experimental research on the angular distribution of scattered particles. In view of this fact, the presence of a lower limit for a cross section is useful; often one can, within the limits of error, pass several curves through the experimental points in the region of large angles which curves can be differentiated only at small angles. As numerical evaluation shows, the lower limit of the magnitude of forward elastic cross sections can in certain cases be rather high. Let us give a few examples. When the neutron energy is 400 mev, the cross section of neutron scattering by protons is, according to Eq. (9), $\sigma_{pn}(0^\circ) \geq 3.4 \times 10^{-27}$ cm^2/ster, and the value of the cross section $\sigma_{np}(13^\circ)$ amounts[4] to about 4×10^{-27} cm^2/ster. Correspondingly, for neutrons with energies of 590 and 630 mev, $\sigma_{np}(0^\circ)$ is not less than 5.8×10^{-27} and 6.6×10^{-27} cm^2/ster. respectively. This shows that in the 400-600 mev energy region one should expect an increase of the cross section in the small-angle region in addition to a further tendency toward an increase with a rise in the energy of the colliding particles (total cross sections of ($n - p$) interaction remain almost constant or even increase in the energy interval from 300 to 2500 mev.

Another example of the use of the restriction of the optical theorem may be afforded by the case of meson scattering in nuclei. The angular distribution of 300 mev π^--mesons elastically scattered by helium nuclei[5] decreases (in comparison with the large-angle region) perceptibly in the region of angles of 10° - 15°, where not a single case of scattering was found. At 15°, one finds $\sigma_{\pi\alpha}(15°) \approx 50 \times 10^{-27}$ cm^2/ster. From Eq. (12) and the known value of the total cross section, which is equal to 150×10^{-27} cm^2, we obtain $\sigma_{\pi\alpha}(0°) \geqslant 75 \times 10^{-27}$ cm^2/ster, which means that there is a minimum in the angular distribution of mesons scattered by helium nuclei. The presence of a minimum in the cross section is indicative of a different sign for the amplitudes of nuclear and Coulomb scattering, and this reveals a change in the sign of the nuclear amplitude in a $(\pi - \alpha)$ interaction in comparison with what took place at energies below 200 mev. This may be connected with the change in the sign of the amplitude for $(\pi - N)$ scattering in the same energy region. The inequality (9) is near equality at high energies. For the region of solid angles $\Delta\omega$, where the differential cross section increases, it is possible to obtain the value $\Delta\omega \leqslant (4\pi / k)^2 \sigma_s / \sigma_t^2$, where σ_s is the elastic cross section.

The author acknowledges his obligation to B. M. Golovin, V. P. Dzhelepov, L. M. Soroko and R. M. Sulaev for their interest in this investigation and for discussing it with him.

---

[1] L. Schiff, Progr. Theor. Phys. **11**, 288 (1954)

[2] L. Wolfenstein and J. Ashkin, Phys. Rev. **85**, 947 (1952).

[3] R. Karplus and M. Ruderman, Phys. Rev. **98**, 771 (1955).

[4] Hartzler, Siegel and Opitz, Phys. Rev. **95**, 591 (1954).

[5] Kozodaev, Suliaev, Filippov and Sherbakov, J. Exptl. Theoret. Phys. (U.S.S.R.) (in press).

Translated by A. Skumanich
235

On Light Emission by a Shock Wave Front

IU. P. LUN'KIN AND G. I. MISHIN
Physico-Technical Institute of the Academy of Sciences USSR

(Submitted to JETP editor May 18, 1956)
J. Exptl. Theoret. Phys. (U.S.S.R.) **31**, 1105 (December, 1956)

IN experiments using a ballistic type of apparatus, emission of light by the leading front of a shock wave in various gases was observed[1] although the temperature behind the shock wave in a polyatomic gas was insufficient in these cases to cause light emission. The following hypothesis may be advanced to explain this phenomenon.

As a result of molecular collisions at the front of a shock wave the energy of directed motion is converted into random heat energy. Zener's calculations[2] have shown that after approximately ten collisions Maxwellian velocity distribution of the molecules is established, while the rotational and vibrational degrees of freedom remain practically unexcited ("frozen"). In the above process all the energy is transferred only to the translational degrees of freedom, and the local gas temperature becomes much higher than the temperature corresponding to thermodynamic equilibrium which is established later.

Electronic energy levels and rotational degrees of freedom are excited only subsequently to the excitation of the translational degrees of freedom. Depending on the individual properties of the molecules the electronic levels may be excited before the rotational levels, or the two may be excited simultaneously. In both cases the local temperature remains higher than the equilibrium value. It is just this nonequilibrium distribution of energy that may be used to explain the observed emission of light, particularly since the light is emitted by the front of the shock wave where the vibrational degrees of freedom have not yet been excited; for their excitation $10^4 - 10^5$ collisions are needed[3].

The subsequent excitation of rotational and vibrational degrees of freedom leads to a lowering of the gas temperature which tends to the equilibrium value, and consequently leads to the cessation of light emission. A more rapid rate of excitation of the internal degrees of freedom will lead to a narrower zone of light emission; therefore in gases with polyatomic molecules the region of light emission will be narrower than in monatomic gases in which the temperature decreases only as a result of light emission.

---

[1] J. Eckerman and R. Schwartz, Phys. Rev. **87**, 912 (1952).

[2] C. Zener, Phys. Rev. **37**, 556 (1931).

[3] E. Senger, Weltraumfahrt, **1**, 4 (1954).

Translated by G. M. Volkoff
238

Surface Electrical Conductivity of Germanium

V. I. Liashenko and T. N. Sitenko
Institute of Physics, Academy of Sciences, Ukrainian SSR

(Submitted to JETP editor, July 20, 1956)
J. Exptl. Theoret. Phys. (USSR) 31, 905-907 (November, 1956)

In a previous work[1] it was shown that in cuprous oxide, the mobility as determined by the Hall effect is greater with molecular adsorption than in vacuum. This may be explained either by a surface zone conductivity, or by scattering of electrons by surface charges. A conclusive answer was not obtained in Ref. 1.

With molecular adsorption, as is well known, the surface charge changes not only as a consequence of changes in the filling of existing surface levels, but also as a consequence of the formation of new ones. Cleaner conditions for experimentation with change of surface charge may be obtained if the latter is changed by means of an external electric field. In this case, only a change in the filling of existing surface levels occurs, no new surface levels being created. Therefore, the present work was carried out using an external electric field as a means for the reversible change of surface change.

The investigation was made on germanium. A monocrystalline plate of germanium with soldered contacts for the measurement of the Hall effect and conductivity was cemented with polystyrene lacquer to a thin sheet of mica (50-30μ). A metallic plate was cemented to the rear side of the mica sheet (opposite the surface of the sample) with a guard ring around it. The Hall effect and conductivity were measured both with and without an external electric field (+V and $-V$ on the metal plate). Based on the results obtained, the effected value of mobility u_e was calculated by the usual formula. In view of the fact that the samples had bipolar conductivity, the real value of mobility could have been obtained by Peierls' formula, but because of the lack of appropriate data, we could not use it. Therefore, for such samples, the calculated values of u_e are somewhat low. The calculated results for some of the samples are given in Table I which contains values of the resistance R , its changes ΔR, evoked by the external electric field, the Hall emf V_x and its change ΔV_x, and also calculated values of u_e and Δu_e. The specific resistances of the samples ρ are also indicated. The measurements were repeated many times and were fully reproducible.

Sample No	V, kV	R, Ω	ΔR, Ω	V_x, mV	ΔV_x, mV	u_ρ, cm^2/V-sec	Δu_e, cm^2/V-sec	ρ, Ω·см
24	0	997	+18	1.65	+0.21	2340	+240	12.0
	−2	1015		1.86		2580		12.2
	0	1008	−65	1.67	−0.23	2340	−192	12.0
	+2	943		1.44		2148		11.3
27	0	4537	+245	1.02	+0.41	653	+197	47.6
	−2	4882		1.43		850		51.3
	0	4556	−1000.	1.04	−0 68	661	−367	47.9
	+2	3556		0.36		294		37.3

Under the action of an external electric field, the resistances of the samples with electronic and proper conductivity increased with +V and decreased with $-V$ on the metal plate. This corresponds with the results observed by us[2] as well as by other authors[3,4]. The Hall emf V_x and the mobility u_e also changed; with $-V$ on the metal plate they increased, and with +V they decreased.

The change of mobility under the influence of an external electric field may be treated as was done by us in a previous work[1], where the surface charge was changed by molecular adsorption, namely: either by the existence of surface zone conductivity, or by scattering of electron waves by surface charges. If surface zone electronic conductivity exists, then the mobility of electrons on the surface is less than in the volume.

Sample No	ρ, $\Omega\cdot$см	u_ρ, cm^2/V-sec	$\Delta\rho_\perp$, $\Omega\cdot$см	$\Delta\rho_\perp/\rho$, %	$\Delta\rho_\parallel$, $\Omega\cdot$см	$\Delta\rho_\parallel/\rho$, %	d, μ
40 (1)	41	1350	0.9	2,2	0.7	1.7	1390
40 (2)	41	1520	1.0	2,4	0.75	1.8	1570
40 (4)	37.1	1350	1,0	3,0	0,6	1.7	160
40 (5)	34.6	1240	0.9	2.6	0.7	2.0	210
41 (1)	6.26	1470	0.21	3.3	0.15	2.4	210
41 (2)	7.46	1030	0,29	3.9	0,20	2.7	200

We also performed measurements of the Hall effect and the specific resistance ρ on 6 samples without the action of an external electric field for various thicknesses of the samples d. It was observed that with a decrease of d, the quantities u_e and ρ decreased. Thus, for example, with sample 38, with a decrease of d from 1880 to 210μ, ρ decreased from 8.9 to 8.2 Ω cm, and u_e decreased from 1480 to 845 cm^2/V sec., and with sample 37, with a decrease of d from 1800 to 200μ, ρ decreased from 8.5 to 4.9Ω cm, and u_e decreased from 1760 to 921 cm^2/Vsec. If the decrease of mobility were due to the scattering of electrons by surface traps, it could be expected that with a decrease of d, ρ would increase. However, it is observed to decrease; u_e decreased in all cases. These results strongly testify to the existence of surface zone conductivity, although scattering by surface charges also exists.

In order to clarify this question finally, we performed experiments on the change of resistance of samples in a magnetic field in two positions; in the first, when the sample was set perpendicular to the magnetic field, $\Delta\rho\perp$, and in the second, when it was set along the field, $\Delta\rho_{||}$. In the first position of the sample, the magnetic field acts on both the volume and the surface conductivity, but in the second position, it acts only on the volume. Measurements were performed on ten samples. It was observed that $\Delta\rho\perp > \Delta\rho_{||}$. In order to remove doubt as to whether the observed $\Delta\rho\perp > \Delta\rho_{||}$ might be due to anisotropy of the magnetic properties of germanium or to inhomogeniety of the sample, we cut two samples out of a monocrystal, the samples having been at right angles to one another in the monocrystal. Furthermore, the homogeneity of the samples was verified by the absence of a volume photo-emf. Two such pairs of samples were cut from one bar, and one pair from another bar. The results of measurement showed that $\Delta\rho\perp > \Delta\rho_{||}$; part of the results are presented in Table II.

It appears to us that the material presented here gives a basis for the assertion that surface zone conductivity exists in the samples of germanium investigated by us. We see no other explanation at present.

The authors express thanks to academician V. E. Lashkarev for discussions on this work.

---

[1] V. E. Lashkarev and V. I. Liashenko, Dokl. Akad. Nauk SSSR 106, 243 (1956).

[2] V. I. Liashenko and R. O. Litvinov, Ukrain. fiz. zh. 1, 78 (1956).

[3] G.G.E.Low, Proc. Phys. Soc. (London) 68, 10 (1955).

[4] S. G. Kalashnikov and A. E. Iunovich, J. Tech.. Phys. (U.S.S.R.) 25, 952 (1955).

Translated by D. Lieberman
196

Perturbation Theory for the One Dimensional Quantum Mechanical Problem and the Lagrange Method

IA. B. ZEL'DOVICH
Institute of Chemical Physics,
Academy of Sciences, USSR

(Submitted to JETP editor September 18,1956)
J. Exptl. Theoret. Phys. (U.S.S.R.) 31,
1101-1103 (December,1956)

IN this note the unknown regular solution is represented as the sum, Eq. (1), of two solutions (regular and irregular) with variable coefficients of the unperturbed problem. This representation is unique, and simple equations are obtained for the coefficients by the application of the well-known auxiliary Lagrange condition, Eq. (2) :

$$\varphi_a(r) = c_a(r)\,\varphi_{0a}(r) + c_b(r)\,\varphi_{0b}(r), \tag{1}$$

$$\dot{\varphi} = c_a\,\dot{\varphi}_{0a} + c_b\,\dot{\varphi}_{0b}, \tag{2}$$

where $\dot{\varphi} = d \quad /dr$. All the functions, including $c_a(r)$ and $c_b(r)$, depend only on the one independent variable r. The proposed method yields unknown expressions for the energy change in the discrete spectrum in a first approximation and for the scattering phase change in the continuous spectrum. The method provides extremely descriptive equations for the change in the wave function itself due to the perturbation. In the case of the discrete spectrum, moreover, a curious equation in the form of a double integral is obtained for the energy change in second order. Let us examine the spherically symmetrical problem of the quantum mechanics of a single particle; after separating the angular variables and introducing $\varphi = r\psi$, where ψ is the wave function, the problem for a definite value for the momentum l is reduced to an equation having the form

$$-(\hbar^2/2m)\,\ddot{\varphi} + V(r)\varphi - E\varphi = (H-E)\,\varphi = 0. \tag{3}$$

Here $V(r)$ also includes, besides the potential, the centrifugal potential $\hbar^2 l(l+1)/2mr^2$.
Equations of second order have two linearly independent solutions. One of them can be selected in such a way that when r is small, then $\varphi_a \sim r^{l+1}$ (regular solution). The second solution φ_b behaves (for small r) as $\varphi_b \sim r^{-l}$. When $E > 0$, φ_a and φ_b behave (at large r) as $\cos(r\sqrt{2mE/\hbar+\alpha})$, and it is possible to select $\alpha_b = \varphi_b + \pi/2$. Actually the second solution satisifes the equation everywhere, except at $r = 0$. The solution of any physical problem is subject to the condition of regularity, i.e., it must be composed of regular functions of the same type as φ_a.

A problem posed in the perturbation theory is to find a φ_a type of solution for a potential $V(r)$ such that $V(r) = V_0(r) + v(r)$, where $v(r)$ is small and the equation for $V_0(r)$ is solved.

Let us substitute Eq. (1) and (2) in Eq. (3). We first examine the case of the continuous spectrum. Since all the functions of φ_{aE}, φ_{oaE}, φ_{obE} apply to the same value for E, we omit the index for E. We bear in mind that c_a and c_b are functions of r. In an elementary way, we obtain

$$\dot{c}_a = -(2v/D)\,(c_a\,\varphi_{0a}\,\varphi_{0b} + c_b\,\varphi_{0b}^2); \tag{4}$$

$$\dot{c}_b = (2v/D)\,(c_a\,\varphi_{0a}^2 + c_b\,\varphi_{0a}\,\varphi_{0b}),$$

$$D = (\hbar^2/m)\,(\varphi_{0a}\,\dot{\varphi}_{0b} - \varphi_{0b}\,\dot{\varphi}_{0a}). \tag{5}$$

Inasmuch as φ_{oa} and φ_{ob} satisfy the same type of equation as Eq. (3), D does not depend on r.

In order to arrive at the regular solution of the perturbation problem we assume $c_b(0) = 0$ and (correct to the last normalization change) $c_a(0)=1$. In the first order in v we obtain

$$c_a(r) = 1 - \frac{2}{D}\int_0^r v\varphi_{0a}\,\varphi_{0b}\,dr; \tag{6}$$

$$c_b(r) = \frac{2}{D}\int_0^r v\varphi_{0a}^2\,dr.$$

Equations (4) are exact. In order for succeeding approximations to differ only slightly from the first approximation, Eq. (6), the well-known condition $\int vr\,dr \ll \hbar^2/2m$ must be satisfied, the smallness of v is not restrictive and the smallness of $\int vr^2\,dr$ is not sufficient. [This condition is obtained by requiring that the second term in expression $c(r)$ in Eq. (6) be small].

When $r < R$, let $v =$ const and let the asymptotic expressions φ_{oa} and φ_{ob} still be valid. Then we have

$$c_a = 1 - k_1 v r^2; \quad c_b = k_2 v r^{2l+3};$$

$$c_b \varphi_{0b} = k_3 v r^{l+3} \ll \varphi_{0a}$$

for small r, k_1, k_2 and k_3 are constants.

In the assumed solution, the function φ_{ob}, which has an inadmissible singularity at $r = 0$, entered with coefficient c_b, which approaches zero sufficiently rapidly as $r \to 0$, so that a solution of the form of Eq. (1) is valid everywhere, including the point $r = 0$, where the correct limiting conditions must be imposed on $c_b(0)$.

In the region where v approaches zero, c_a and c_b are constant, and the stucture of the solution is vastly simpler than in the conventional perturbation theory in which the solution of the perturbation problem for a given E is presented as a sum of regular nonperturbed solutions related to all the possible proper values E', with constant (independent of r) coefficients. As is known, these coefficients even become infinite (when E' approaches E) in the conventional first approximation perturbation theory of the continuous specturm.

In particle scattering theory the cross section and phases of scattering may be expressed by the logarithmic derivative $d \ln \varphi_a / dr$. Employing Eq. (1) and Eq. (2), we find

$$d \ln \varphi_a / dr = (c_a \dot{\varphi}_{0a} + c_b \dot{\varphi}_{0b}) / (c_a \varphi_{0a} + c_b \varphi_{0b}).$$

In the perturbation theory, when $|c_b| << 1$, $|1 - c_a| << 1$ then

$$\frac{d \ln \varphi_a}{dr} = \frac{d \ln \varphi_{0a}}{dr} + \frac{D c_b}{\varphi_{0d}^2} \tag{7}$$

$$= \frac{d \ln \varphi_{0a}}{dr} + \frac{2}{\varphi_{0a}^2} \int v \varphi_{0a}^2 \, dr.$$

This familiar relation is usually obtained by considering $\int (\varphi_{0a} H \varphi_a - \varphi_a H_0 \varphi_{0a}) \, dr$.

Let us examine the discrete spectrum. In this case we apply, simultaneously with a perturbation of the potential $V = V_0 + v$, a small (constant) perturbation to the proper value of energy $E = E_0 + \Delta$. If in the non-perturbed problem $(H_0 - E_0)\, \varphi_0 = 0$ then we must consider

$$(H - E)\, \varphi = (H_0 + v - E_0 - \Delta)\, \varphi = 0.$$

In Eq. (4)–(6) let us substitute $v - \Delta$ for v. The proper function of the non-perturbed problem φ_{0a}, which corresponds to E_0, is not only regular when $r = 0$ but falls exponentially when $r \to \infty$. The second linearly independent solution for the non-perturbed problem φ_{0b} grows exponentially as $r \to \infty$. In order to obtain a proper function in the perturbed problem with the correct behavior as $r \to 0$ and $r \to \infty$, it is necessary that $c_b(0) = c_b(\infty) = 0$. In first order approximation theory we obtain

$$\int_0^\infty [v(r) - \Delta]\, \varphi_{0a}^2 \, dr = \int_0^\infty [v(r) - \Delta]\, \psi_0^2 \, r^2 \, dr = 0;$$

$$\int v \psi_0^2 \, d\omega = \Delta \int \psi_0^2 d\omega,$$

where $d\omega$ is the volume element. In this fashion we obtain the well known equation for the energy change to first order,

$$\Delta_{\mathrm{I}} = \int v(r)\, \psi_0^2 \, d\omega. \tag{8}$$

Substituting Eq. (6), which was obtained to first order, in the right component of Eq. (4) we find c_b to second order. From the condition that $c_b(\infty) = 0$ we find that the energy change to second order is

$$\Delta_{\mathrm{II}} = \Delta_{\mathrm{I}} - 4/D \iint [v(r) - \Delta_{\mathrm{I}}] \tag{9}$$

$$[v(\rho) - \Delta_{\mathrm{I}}]\, \varphi_{0a}^2(r)\, \varphi_{0a}(\rho)\, \varphi_{0b}(\rho)\, d\rho \, dr;$$

where the integral over ρ is from 0 to r, the integral over r is from 0 to ∞, and the normalization is

$$\int \varphi^2_{0a} \, dr = 1.$$

Equation (5), in which D = const, permits one to express φ_{0b} by φ_{0a}, thus

$$\varphi_{0b}(\tau) = -D \varphi_{0a}(\tau) \int^\tau [\varphi_{0a}(x)]^{-2} \, dx.$$

The results in Eq. (7) and Eq. (8), in which φ_{0b} does not enter, obviously are not specific to the Lagrange method and can be easily obtained by other means. The same cannot be said of Eq. (9), where φ_{ob} has entered in a clear fashion.

Translated by A. Skumanich
236

Internal Bremsstrahlung in Electric Monopole $0^+ \rightarrow 0^+$ Nuclear Transitions

Iu. V. Orlov
Moscow State University

(Submitted to JETP editor September 19, 1956)
J. Exptl. Theoret. Phys. (U.S.S.R.) 31, 1103-1105 (December, 1956)

An electric monopole transition from an excited 0^+ nuclear state to a ground state which also has a zero spin and positive parity will in all probability be accompanied by the formation of conversion electrons or electron-positron pairs. At the same time, both the conversion electron and the components of the pair may emit γ quanta of a continuous spectrum with an upper boundary equal respectively to $E - I$ and $E - 2\mu c^2$ (E is the total energy of the nuclear transition, I the ionization energy, and μ the rest mass of the electron). This investigation presents the results of calculations of the relative probability of internal bremsstrahlung emitted by the components of a pair in a $0^+ \rightarrow 0^+$ nuclear transition. As in Ref. 1*, where the same effect is examined in the case of ordinary conversion, the calculation is done in the Born approximation and is therefore applicable only to light nuclei.

The differential probability of internal bremsstrahlung by the emitted pair in an electric monopole transition is ($\hbar = c = 1$)

$$dw = \frac{e^6 Q_0^2}{72(2\pi)^8}\frac{d\omega}{\omega} B\delta(\varepsilon_- + \varepsilon_+ + \omega - E)\, p_- d\varepsilon_- p_+ d\varepsilon_+ d\Omega_{\mathbf{p}_-} d\Omega_{\mathbf{p}_+} d\Omega_{\mathbf{k}}, \tag{1}$$

$$\begin{aligned} B = &-\mu^2(\varepsilon_- - p_- x_-)^{-2}(\varepsilon_+\varepsilon_- + \mathbf{p}_+\mathbf{p}_- + \varepsilon_+\omega + \mathbf{k}\mathbf{p}_+ - \mu^2)\\ &-\mu^2(\varepsilon_+ - p_+ x_+)^{-2}(\varepsilon_-\varepsilon_+ + \mathbf{p}_-\mathbf{p}_+ + \varepsilon_-\omega + \mathbf{k}\mathbf{p}_- - \mu^2)\\ &+\omega(\varepsilon_+\omega + \mathbf{k}\mathbf{p}_+ + \mu^2)/(\varepsilon_- - p_- x_-) + \omega(\varepsilon_-\omega + \mathbf{k}\mathbf{p}_- + \mu^2)/(\varepsilon_+ - p_+ x_+)\\ &+2[\varepsilon_+^2\varepsilon_-^2 + \varepsilon_-^2\mathbf{k}\mathbf{p}_+ + \varepsilon_+^2\mathbf{k}\mathbf{p}_- - \mathbf{p}_+\mathbf{p}_-(\mathbf{p}_+\mathbf{p}_- + \mathbf{k}\mathbf{p}_+ + \mathbf{k}\mathbf{p}_-)\\ &+\mu^2(\mathbf{p}_+\mathbf{p}_- - \varepsilon_+\varepsilon_- - \omega^2)]/(\varepsilon_- - p_-(x_-)(\varepsilon_+ - p_+ x_+), \end{aligned}$$

where $Q_0 = \int \Psi_f^*(\mathbf{r})\Psi_i(\mathbf{r}) r^2 d\mathbf{r}$ is the matrix element of the electric monopole operator (Ψ_i and Ψ_f are the initial and final wave functions of the nucleus); $\varepsilon_-, \mathbf{p}_-; \varepsilon_+, \mathbf{p}_+, \omega, \mathbf{k}$ are the energy and momentum respectively of the electron positron, and photon; and

$$x_- = \mathbf{k}\mathbf{p}_- / \omega p_-, \quad x_+ = \mathbf{k}\mathbf{p}_+ / \omega p_+.$$

After integrating over the directions of emergence of all the particles (the nucleus is considered infinitely heavy) and over the energy of one of the components of the pair (the probability equation is symmetrical with regard to the electron and positron) we obtain

$$dw_{\pi,\gamma} = \frac{e^6 Q_0^2}{9(2\pi)^5} F(E;\ W,\ \omega)\, dW\, d\omega, \tag{2}$$

$$\begin{aligned} F(E;\ W,\ \omega) = (1/\omega)\{&[5W^2 + 5W\omega + 3\omega^2 - 5(E-2)W - (3E-5)\omega - 5E + 9]\\ &\times\sqrt{(W+1)^2 - 1}\sqrt{(E-1-W-\omega)^2 - 1} + \sqrt{(W+1)^2-1}\,[2W^3 + 2W^2\omega + W\omega^2\\ &-2(2E-3)W^2 - 2(E-2)W\omega + \omega^2 + (2E^2 - 8E + 9)W - (2E-5)\omega\\ &+2E^2 - 6E + 5]\ln(E - 1 - W - \omega + \sqrt{(E-1-W-\omega)^2 - 1})\\ &+\sqrt{(E-1-W-\omega)^2-1}\,[-2W^3 - 4W^2\omega - 3W\omega^2 - \omega^3 + 2(E-3)W^2\\ &+2(E-4)W\omega + (E-3)\omega^2 + (4E-9)W + 2(E-2)\omega\\ &+3E - 5]\ln(W + 1 + \sqrt{(W+1)^2 - 1})\\ &-(1 + 2\omega^2)\ln(W + 1 + \sqrt{(W+1)^2-1})\cdot\ln(E - 1 - W - \omega + \sqrt{(E-1-W-\omega)^2 - 1})\}, \end{aligned}$$

where W is the kinetic energy of the electron or positron (the energy is expressed in units of μc^2).

The obtained equation is applicable to the presently known electric monopole transitions between a 7.68 mev state and the ground state in C^{12} and between a 6.06 mev state and the ground state in O^{16} [2]. In both cases the transition is in the main accompanied by the emission of electron-positron pairs. The Born approximation used in the calculation should be correct, because C^{12} and O^{16} are light nuclei, and the transition energy is considerable. The relative probability of bremsstrahlung will be

$$dW^{(0)}_{\pi,\gamma} = \frac{e^2\cdot 10^{-3}}{(2\pi)^2 I(E)} F(E;\ W,\ \omega)\, dW\, d\omega, \qquad (3)$$

$$I(E) = \int_0^{E-2} [E-2+(E-2)x$$

$$-x^2]\sqrt{(E-1-x)^2-1}\sqrt{(x+1)^2-1}\,dx$$

$(e^4 Q_0^2 I(E)/9(2\pi)^3$ is the known[3] expression for the total probability of the formation of an electron-positron pair in an electric monopole transition).

Numerical integration of Eq. (3) permits one to obtain the energy spectrum of the γ rays and a total relative probability of the process. For O^{16} these are

$$N_1(\omega) = 2.64\cdot 10^{-8} \int_0^{9.86-\omega} F(E=11.86;\ W,\ \omega)\, dW,\ N_1$$

$$= \int_{\varepsilon}^{9.86} N_1(\omega)\, d\omega = 3.30\cdot 10^{-3}$$

and for C^{12}

$$N_2(\omega) = 0.79\cdot 10^{-8} \int_0^{13.03-\omega} F(E=15.03;\ W;\ \omega)\, dW;$$

$$N_2 = \int_{\varepsilon}^{13.03} N_2(\omega)\, d\omega = 3.96\cdot 10^{-3},$$

where ϵ is a small constant.

The graphs show functions $\omega N_1(\omega)$ and $\omega N_2(\omega)$ (in units of μc^2). The values N_1 and N_2 present the ratio of the number of γ quanta emitted simultaneously with electron-positron pairs to the number of pairs not accompanied by bremsstrahlung in unit time. They are equal in order of magnitude (10^{-3}) to the integral relative probability of bremmstrahlung in an ordinary conversion for an electric monopole nuclear transition. We also evaluated the contribution to the continuous spectrum of γ rays by a process in which the energy of the $0^+ \to 0^+$ transition goes into the formation of a conversion electron and a γ quantum, with the γ quantum being emitted by the nucleus itself. As might have been expected, the role played by this process is insignificantly small, especially in the region of small γ ray energies. Its total contribution is about 10^4 times less than those made by the process examined here and the one dealt with in the investigation conducted by I. S. Shapiro and this author[1].

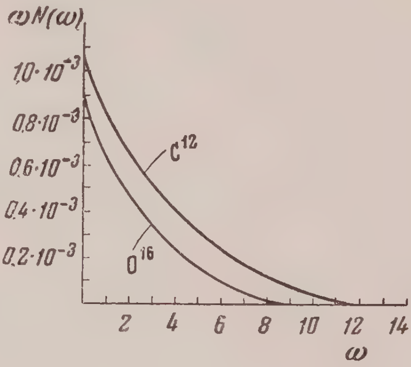

In conclusion I express my sincere gratitude to I. S. Shapiro for the interest he has shown in this investigation and to V. V. Turevtsev, who called my attention to this effect.

---

[*] In this paper a factor 1/2 must be introduced in the equation for the matrix element and correspondingly, a factor 1/4 in the probability equations. Then the order of magnitude of the integral relative probability must be 10^{-3}.

[1] I. S. Shapiro and I u. V. Orlov, Dokl. Akad. Nauk SSSR **101**, 1047 (1955).

[2] L. I. Shiff, Phys. Rev. **98**, 1281 (1955).

[3] A. I. Akhiezer and V. B. Berestetskii, *Quantum Electrodynamics*, Moscow (1953).

Translated by A. S. Skumanich
237

The Numerical Calculation of Path Integrals

I. M. GEL'FAND AND N. N. CHENTSOV

(Submitted to JETP editor August 2, 1956)
J. Exptl. Theoret. Phys. (U.S.S.R.) 31, 1106-1107
(December, 1956)

IT is known that we can write down the answers to many physical problems in the form of so-called paths integrals — integrals in function spaces. However, the actual calculation of a path integral produces a number of difficulties; only rarely can the analytic contributions be found numerically. Therefore the opinion that these are useless in practice is given repeatedly.

However, we should expect that as soon as methods of numerical path integration are worked out, the solutions of problems by such means will provide practical interest. In the present work, the following course of calculations is proposed. The path integral, described as an integral over a certain measure, is approximated by a finite measure Stieltjes integral of sufficiently high multiplicity, which is then calculated in ordinary fashion. This course of action is shown to be entirely acceptable, since the calculation of multiple integrals with the aid of modern computing machine techniques does not present any great difficulties.

By way of an example of such a calculation, we determine in the present note thevalue E_0 of the lowest energy level of the polaron — a slow electron in an ionic crystal. The theory of polarons has been treated by Pekar^1, who, in particular, calculated the value of E_0 in the adiabatic approximation. Feynman^2 has shown that the determination of E_0 can be put in the form of the calculation of the asymptotic form of the path integral

$$K = \int \exp S\, D\mathrm{x}(t), \tag{1}$$

where the functional S depends on the coupling parameter α:

$$S = -\frac{1}{2}\int_0^T \left(\frac{d\mathrm{x}}{dt}\right)^2 dt + \frac{\alpha}{2\sqrt{2}}\int_0^T\!\!\int_0^T |\mathrm{x}(t)-\mathrm{x}(s)|^{-1} e^{-|t-s|}\, dt\, ds, \tag{2}$$

$$\alpha = {}^1\!/_2\,(1/\varepsilon_\infty - 1/\varepsilon)\,(e^2/\hbar\omega)\,(2m\omega/\hbar)^{1/2}.$$

here ϵ and ϵ_∞ are the static and high frequency values of the dielectric constant. Then for $T \to \infty$, $K(T) \sim \exp\{-E_0 T\}$. For the numerical determination of the value of E_0 as a function of α, Feynman made use of variational methods. The approximated expansion of E_0 as a function of α that he obtained are plotted in Ref. 2. For large α, the adiabatic approximation of Pekar^1 is very satisfactory.

For our purposes, Eq. (1) has been transformed. The exponential factor $\exp\left\{-{}^1\!/_2\int_0^T (d\mathrm{x}/dt)^2\, dt\right\}$ is put under the differential sign, and then the integral is described in the form of the mean value of a certain functional in Wiener measure:

$$K(T) = \int \exp\left\{\frac{\alpha}{2\sqrt{2}} \times \int_0^T\!\!\int_0^T |\mathrm{x}(t)-\mathrm{x}(s)|^{-1} e^{-|t-s|}\, dt\,ds\right\} d_W \mathrm{x}(t) \tag{3}$$

$$= \mathfrak{M}_W\left[\exp\left\{\frac{\alpha}{2\sqrt{2}} \times \int_0^T\!\!\int_0^T |\mathrm{x}(t)-\mathrm{x}(s)|^{-1} e^{-|t-s|}\, dt\, ds\right\}\right],$$

$$E_0(\alpha) = -\lim_{T\to\infty}\frac{1}{T}\ln K(T) \tag{4}$$

It is not difficult to see that the limit

$$-\lim_{T\to\infty}\frac{1}{T}\mathfrak{M}_W[\exp\{\alpha I\}], \tag{5}$$

where

$$I = \frac{1}{\sqrt{2}}\int_0^T d\eta \int_0^{\Xi} \sqrt{\xi}\, e^{-\xi}\, |\mathrm{x}(t)-\mathrm{x}(s)|^{-1} d\sqrt{\xi}, \tag{6}$$

$(\xi = t - s,\ \eta = t + s)$, , differs from $E_0(\alpha)$ by a sufficiently small amount provided that Ξ is large enough. At the same time the order of the remaining term in (5) is smaller than in (4). Since $\sqrt{\xi}\, e^{-\xi}$ falls off rapidly with increase in ξ, it suffices in approximate calculations to carry out the integration over ξ up to $\Xi \sim 5$-7. The mean value of the functional $e^{\alpha I}$ was calculated by the Monte Carlo method. Two variants were considered, with $T = 4.5$ and $T = 9.0$. In both variants, $\Xi = 5.0$, which gives an error in integral I of about 0.3% in the lower direction. With a step of $\tau = 0.05$ from $t = 0$ to $t = T + \Xi$, we determined the random positions of the three dimensional Brownian trajectory. The region of integration was divided into rectangles, the double integral over each rectangle being calculated according to a simple difference scheme, in which only the value of the function under the integral at the center of the rectangle enters. Then, for the set of values of α, $e^{\alpha I}$ was computed, as was its arithmetic mean over all N trajectories. Thus we calculated (by the Monte

T N	4.5 300	4.5 600	9.0 300	9.0 400
α	$-E_0$ (α)			
0.5	0.5051	0.5048	0.5047	0.5043
1.0	1.0208	1.0195	1.0195	1.0192
2.0	2.0880	2.0819	2.0839	2.0851
4.0	4.3900	4.3[illegible]87	4.3469	4.3538
5.0	5.6271	5.5787	5.5205	5.5305

Carlo approximation) 190- and 280-fold integrals in place of the path integral. The results, after the production of statistical corrections, are given in Tables 1 and 2.

As a control, we computed the mean value of random quantities and their chief moments, according to which we found the coefficients of expansion of the function $E_0(\alpha)$ in the series $E_0(\alpha) = (\varkappa_1 / 1!)\, \alpha + (\varkappa_2 / 2!)\, \alpha^2 + \ldots$

T	4.5	4.5	9.0	9.0	exact value according to Ref. 3
N	300	600	300	400	
$-\varkappa_1$	1.0063	0.9999	0.9912	0.9940	1.0000
$-\varkappa_2$	0.0397	0.0370	0.0354	0.0370	0.0252

Both A. S. Frolov and V. Iu. Krylov took part in this research. V. N. Toroptseva and T. I. Frolova programmed the problem. The authors express their gratitude to M. R. Shura-Bura for valued advice on the problems of programming the problem.

---

[1] S. I. Pekar, *Investigation of the electron theory of crystals*. Gostekhizdat, Moscow,

[2] R. P. Feynman, Phys. Rev. 97, 660 (1955). E. Haga, Prog. Theor. Phys. 11, 449 (1954).

Translated by R. T. Beyer
239

On Quantities with Anomalous Parity and on a Possible Explanation of Parity Degeneracy of K-Mesons

I. M. GEL'FAND AND M. L. TSETLIN

(Submitted to JETP editor Sept. 21, 1956)
J. Exptl. Theoret. Phys. (U.S.S.R.) 31, 1107-1109
(December, 1956)

IT is well known that K-particles may decay into two or three π-mesons. The corresponding functions must have different parity with respect to the transformation of spatial reflection (i.e., the transformation $x_i \to - x_i$, $i = 1, 2, 3$, $t \to t$), in particular: the function corresponding to the θ-decay must be even, while the function corresponding to the τ-decay must be odd. At the same time it has been established that within experimental error the rest-masses of the θ- and τ-mesons coincide. This coincidence of masses is referred to as the parity-degeneracy of K-mesons. Since the situation in connection with this problem is not at all clear, it seems to be useful to investigate the behavior of quantities with respect to reflections (we use here the word quantity to denote a representation of the complete Lorentz group including reflections of both the space and the time coordinates). Such an investigation has a certain intrinsic interest of its own. It turns out that in addition to the well known possible parities with respect to reflections of the space or the time coordinates there exists also one additional possibility which we shall here refer to as anomalous parity.

In quantum mechanics wave functions are determined up to a factor. It is therefore natural to define transformations of quantities with respect to some given group also up to a factor. Well known examples of the appearance of such factors are provided by spinors which change sign as a result of a rotation by 360°, or wave functions of a system of particles obeying Fermi statistics which change sign as a result of an interchange of particles. The corresponding mathematical concepts are well known – they are the so-called projective representations of the group. We say that a projective representation of the group G is given if to each element $g \epsilon G$ there corresponds a linear transformation T_g such that $T_{g_1 g_2} = \alpha(g_1, g_2)\, T_{g_1} T_{g_2}$, where $\alpha(g_1, g_2)$ is a scalar. It may be shown that the quantities $\alpha(g_1, g_2)$ satisfy the following functional equation:

$$\alpha(g_1 g_2, g_3)\, \alpha(g_1, g_2) = \alpha(g_1, g_2 g_3)\, \alpha(g_2, g_3).$$

We shall consider the representations of a group of reflections which consist of four elements – the unit element and the operators of space, time, and space-time reflections, which we shall respectively denote by 1, t_{10}, t_{01}, t_{11}. The elements t are commutative and satisfy the following relations:

$$t_{10}t_{01} = t_{11}; \quad t_{01}t_{11} = t_{10}; \quad t_{10}t_{11} = t_{01}. \qquad (1)$$

We denote by T_t the operator of a certain projective representation $t \to T_t$ of the group of reflections. Then the operators T_t should satisfy the equation

$$T_{tt'} = \alpha(t, t')\, T_t T_{t'}.^{*} \qquad (2)$$

In the case that the operators T_t commute, i.e., if $\alpha(t, t') = \alpha(t', t)$, we can assume that $\alpha(t, t') = 1$ for all t, t'. Then the quantities which are transformed by the operators of the representation have with respect to the group of reflections the usual parity properties, giving rise to the four possibilities: (1, 1, 1), (1, –1, –1), (–1, 1, –1) (–1, –1, 1), where in brackets we have given the coefficient by which the quantities are multiplied as a result of being acted upon respectively by the operators T_{01}, T_{10}, T_{11}. The only additional possibility arises if we drop the requirement of the commutativity of the operators, i.e., when $\alpha(t, t') \neq \alpha(t', t)$. In this case relations (2) for the operators may be reduced to the following table:

$$\begin{array}{c|cccc}
 & 1 & T_{01} & T_{10} & T_{11} \\
\hline
1 & 1 & T_{01} & T_{10} & T_{11} \\
T_{01} & T_{01} & 1 & -T_{11} & -T_{10} \\
T_{10} & T_{10} & T_{11} & 1 & T_{01} \\
T_{11} & T_{11} & T_{10} & -T_{01} & -1
\end{array} \qquad (3)$$

in which the operator which corresponds to the product may be found at the intersection of the appropriate row and column. We shall refer to quantities transformed by the operators of such a representation as quantities with anomalous parity.

In the simplest case when the quantities being transformed are scalars the operators may be written out in the form of three anticommuting matrices of the second rank analogous to the well known Pauli matrices

$$T_{01} = \begin{pmatrix} 1 & 0 \\ 0 & -1 \end{pmatrix}; \quad T_{10} = \begin{pmatrix} 0 & 1 \\ 1 & 0 \end{pmatrix}; \quad T_{11} = \begin{pmatrix} 0 & -1 \\ 1 & 0 \end{pmatrix}, \qquad (4)$$

while the transformed quantities themselves ("scalars of anomalous parity") are pairs of numbers (ξ_1, ξ_2), which are unchanged by proper Lorentz transformations and which are transformed in accordance with the matrices (4) under reflections.

The representations of the Lorentz group are described in detail, for example, by Gel'fand and Iaglom' whose notation we shall employ in the following. From the commutation relations between the reflections and the Lorentz transformations we may obtain the following description. The irreducible representation of the Lorentz group together with the reflections nay be decomposed into two representations of the proper Lorentz group determined by the numbers (k_0, k_1) and ($-k_0$, k_1)*. If $k_0 \neq 0$ and ξ_p^k are basis vectors in the first representation ($k = |k_0|, |k_0| + 1, \ldots, k_1 - 1$) while η_p^k are basis vectors of the second representation, then the operators T_{10}, T_{01}, T_{11} are given by formulas (5), (6), (7), (7'), of which (5) and (6) correspond to normal parity, while (7) and (7') correspond to anomalous parity:**

$$T_{01} = \begin{pmatrix} 0 & (-1)^k \\ (-1)^k & 0 \end{pmatrix}; \quad T_{10} = \begin{pmatrix} 0 & (-1)^k \\ (-1)^k & 0 \end{pmatrix}; \qquad (5)$$

$$T_{11} = \begin{pmatrix} 1 & 0 \\ 0 & 1 \end{pmatrix},$$

$$T_{01} = \begin{pmatrix} 0 & (-1)^k \\ (-1)^k & 0 \end{pmatrix}; \qquad (6)$$

$$T_{10} = \begin{pmatrix} 0 & (-1)^{k+1} \\ (-1)^{k+1} & 0 \end{pmatrix}; \quad T_{11} = \begin{pmatrix} -1 & 0 \\ 0 & -1 \end{pmatrix},$$

$$T_{01} = \begin{pmatrix} 0 & (-1)^k \\ (-1)^k & 0 \end{pmatrix}; \qquad (7)$$

$$T_{10} = \begin{pmatrix} 0 & i(-1)^k \\ -i(-1)^k & 0 \end{pmatrix}; \quad T_{11} = \begin{pmatrix} i & 0 \\ 0 & -i \end{pmatrix},$$

$$T_{01} = \begin{pmatrix} 0 & (-1)^k \\ (-1)^k & 0 \end{pmatrix}; \qquad (7')$$

$$T_{10} = \begin{pmatrix} 0 & -i(-1)^k \\ i(-1)^k & 0 \end{pmatrix}; \quad T_{11} = \begin{pmatrix} -i & 0 \\ 0 & i \end{pmatrix}.$$

In the above, for example, the first of formulas (5) should be interpreted as follows:

$$T_{01}\,\xi_p^k = (-1)^k\,\eta_p^k; \quad T_{01}\,\eta_p^k = (-1)^k\,\xi_p^k.$$

Similar formulas also hold for the case $k_0 = 0$. In this case four normal and one anomalous possibilities arise.

It may be shown that the product of two quantities of anomalous parity is a normal quantity which decomposes into four quantities corresponding to the four possibilities with respect to space and time reflections. In the case of a product of a normal and an anomalous representation the corresponding quantities have anomalous parity.

Since the interaction Lagrangian must be a scalar (i.e., it must be invariant with respect to the transformations T_{01}, T_{10}, T_{11}), each term of the interaction operator must contain an even number of wave functions of particles with anomalous parity. Therefore in the case of invariance under space and time reflections the following statement must hold: if in a reaction only particles with normal parity occur then conservation of parity must hold; however, if particles with anomalous parity also take part in the reaction then conservation of normality must hold, i.e., the left and the right hand parts of the reaction equation must both contain either an even or an odd number of anomalous particles.

This argument enables us to divide particles into classes with normal and anomalous parities. If we ascribe anomalous parity to K-mesons and normal parity to π-mesons we may conclude that the Λ, Σ particles have the same normality, and so do the particles n, Ξ. For this it is sufficient for example, to consider the strong interaction reaction

$$\pi^- + p \rightarrow \Lambda^0 + \theta^0; \; K^- + p \rightarrow \Sigma^+ + \pi^-; \; \Xi^- \rightarrow K^- + \Lambda^0.$$

We have ascribed anomalous parity to the K-meson. The operator for the spatial reflection is given by the matrix T_{10} [Eq. (4)], and consequently the K-meson may exist in two states differing in their spatial parity. The masses corresponding to these two states must be the same.

From the fact that K-mesons which have anomalous parity decay into π-mesons it follows that normality is not conserved in slow reactions. Within the framework of the above explanation this is possible only in the case that the Lagrangian is not invariant under time reflections. The hypothesis proposed by Feynman with respect to the lack of invariance under spatial reflections appears to us to be improbable. On the other hand, sufficient foundations do not exist to assume that the Lagrangian is invariant under time reflections in the case of weak interactions. Such an explanation may also be related to the work of Lee and Yang[2].

We express our thanks to Ia. B. Zel'dovich and V. V. Sudakov for valuable discussions.

---

* The first representation contains $|k_0 + k_1|$ undotted and $|k_0 - k_1|$ dotted indices, while the second representation has these numbers reversed (in spinor notation).

** These formulas hold for integral values of k. For half-integral k in the above formulas k should be replaced by $k + ½$.

[1] I. M. Gel'fand and A. M. Iaglom, J. Exptl. Theoret. Phys. (U.S.S.R.) **18**, 703 (1948).

[2] T. D. Lee and C. N. Yang, Phys. Rev. **102**, 290 (1956).

Translated by G. M. Volkoff
240

$\gamma - \gamma$ Angular Correlation in Transitions of Mesic Atoms

V. A. DZHRBASHIAN
Physics Institute, Academy of Sciences,
Armenian SSR

(Submitted to JETP editor August 3, 1956)
J. Exptl. Theoret. Phys. (U.S.S.R.) **31**, 1090-1092
(December, 1956)

PODGORETSKII[1] has pointed out that it would be possible to determine the spin of a muon by using data on the angular correlation between gamma rays emitted in successive transitions of mesic atoms. We wish to examine this problem in the present note and also to propose a method of verifying the spins of nuclei[2] for which $l = 0$ is doubtful or has been obtained only from theoretical considerations unsupported by experiment; the formulas which are derived will be used to determine the spins of all types of mesons.

We know[3] that for light mesic atoms ($Z < 15$), the probabilities of radiation transitions are small compared with the probabilities of conversion transitions. For heavier mesic atoms with small quantum numbers (n, l), the probabilities of conversion transitions can be neglected. The following is an expression for the correlation function $W(\vartheta)$ which is suitable for not very large Z ($15 < Z < 50$)*:

$$W(\vartheta) = \sum_{k=0}^{N} A'_{2k} P_{2k}(\cos\vartheta); \quad A'_{2k} = A_{2k} b_{2k}; \tag{1}$$

$$A_{2k} = A_{2k}(L_1 L_2 j_A j_B j_C) = (-1)^{j_A - j_B} (2L_1 + 1) \tag{1a}$$

$$(2L_2 + 1)(2j_B + 1) C^{2k\,0}_{L_1 1;\, L_1 -1} C^{2k\,0}_{L_2 1;\, L_2 -1} W(j_B j_B L_1 L_1; \times 2k j_A) W(j_B j_B L_2 L_2;\, 2k j_C);$$

$$b_{2k} = \sum_{F_B} (2F_B+1)^2 W^2 (j_B I\, 2kF_B;\ F_B j_B) / 2I+1. \qquad \text{(1b)}$$

Here L_1 and L_2 are the angular momenta of the light quanta; j_A, j_B and j_C are the total (orbital plus spin) angular momenta of the meson in the initial, intermediate and final states; and F is the sum of the mesic (j) and nuclear (I) angular momenta. In (1b), it was considered that for these mesic atoms the ratio of the hyperfine structure to the level width of the intermediate state is $\gamma_{FF'}/2\gamma_B \gg 1$. (For example, for Al, $\gamma_{FF'}/2\gamma_B \sim 10$ ev$/10^{-5}$ ev $= 10^6$.)

Formula (1), which was derived on the assumption that the nuclear spin does not change in mesic-atom transitions, agrees in form with the function obtained by Alder[5] for the angular correlation of gamma rays emitted by a nucleus. This expression can be used to verify the spins of nuclei (such as $_{16}S^{34}$, $_{20}Ca^{40}$ and $_{34}S^{74}$) for which $I = 0$ has not been confirmed experimentally.

As an example, we note that the anisotropy is $A = 0.43$ and 0.25 for the transitions 1/2(D)3/2(D)1/2 with $I = 0$ and 1/2, respectively.

For heavy mesic atoms, finiteness of the nucleus requires the calculation of the correlation function in transitions of the type $l_A(L_1)l_B(L_2)l_C$ where l_A, l_B and l_C are the orbital angular momenta of the meson in the initial intermediate and final states, respectively. In this case the fine structure must be taken into account, as well as the hyperfine structure. Their contribution results from the fact that, because of the spin-orbit interaction, after emission of the first quantum, the direction of the orbital angular momentum is changed in the intermediate state, while interaction with the nucleus results in a change of direction of the total angular momentum j. These effects are important because the lifetime of the intermediate state exceeds the precessional periods of the angular momenta. (For example, for lead $\nu_{jj'} \sim 200$ kev, $\nu_{FF'} \sim 3$ kev, $2\gamma \sim 1$ kev.)

Thus for heavy mesic atoms, confining ourselves to electric transitions (which are the most important) we obtain

$$W(\vartheta) = \sum_{k=0}^{N} A'_{2k} P_{2k} (\cos\vartheta), \qquad \text{(2)}$$

$$A'_{2k} = A_{2k} (L_1 L_2 l_A l_B l_C)\, b_{2k}; \qquad \text{(2a)**}$$

$$b_{2k} = \sum_{F_B \cdot F'_B j_\beta j'_\beta} \frac{(2F_B+1)(2F'_B+1) W^2 (j_\beta I 2kF'_B;\ F_B j'_\beta)}{(2I+1)(2s+1)[1+(\nu_{FF'}/2\gamma_B)^2]} \qquad \text{(2b)}$$

$$\times (2j_\beta+1)(2j'_\beta+1) W^2 (l_B s\, 2kj'_\beta;\ j_\beta l_B),$$

with both the fine structure and the hyperfine structure entering into $\nu_{FF'}$.

For a hyperfine structure which is small compared with $2\gamma_B$, Eq. (2) will reduce to Alder's function (as occurs for $I = 0$).

Any additional interaction can be taken into account by an analogous change in b_{2k}. In particular, for the mesic atoms under consideration, there arises the question of taking into account the interaction with the electron shells. However, because of the small splitting with $2\gamma_B$ the resulting b_{2k} reduces to (2b).

Since for the mesic atoms under consideration $\nu_{jj'}/2\gamma_B \gg 1$.

$$b_{2k} = \sum_{F_B F'_B j_\beta} \frac{(2F_B+1)(2F'_B+1) W^2 (j_B I 2kF'_B;\ F_B j_\beta)(2j_\beta+1)^2 W^2 (l_B s\, 2kj_\beta;\ j_\beta l_B)}{(2I+1)(2s+1)[1+(\nu_{FF'}/2\gamma_B)^2]}, \qquad \text{(3)}$$

where $\nu_{FF'}$ is the sum of the splittings induced by the interactions of the nuclear magnetic dipole and electric quadrupole moments with the meson.

Denoting b_{2k} by means of $b^{sl}_{2k}(l_B)$, we have;

$$b^{sl}_0 (l_B) = 1, \qquad \text{(3a)}$$

$$b^{00}_{2k} (l_B) = 1, \qquad \text{(3b)}$$

$$b^{s0}_{2k} (l_B) = \sum_{j_\beta} \frac{(2j_\beta+1)^2 W^2 (l_B s\, 2kj_\beta;\ j_\beta l_B)}{2s+1}; \qquad \text{(3c)}$$

$$b^{s\,1/2}_{2k} (l_B) = \frac{1}{1+(\nu/2\gamma_B)^2} \sum_{F_B j_\beta} \left[1 + \frac{1}{2}\left(\frac{\nu}{2\gamma_B}\right)^2 \right. \qquad \text{(3d)}$$

$$\left. \times (2F_B+1)^2 W^2\left(j_\beta \tfrac{1}{2}\ 2kF_B;\ F_B j_\beta\right)\right]$$

$$\times \frac{(2j_\beta+1)^2 W^2 (l_B s\, 2kj_\beta;\ j_\beta l_B)}{2s+1};$$

$$b_{2k}^{s>{}^1/_2\, I>{}^1/_2}(l_B) = \sum_{F_B j_\beta} \frac{(2F_B+1)^2 W^2(j_\beta I 2k F_B;\ F_B j_\beta)(2j_\beta+1)^2 W^2(l_B s 2k j_\beta;\ j_\beta l_B)}{(2I+1)(2s+1)}. \tag{3e}$$

We see from (3a) that the renormalization $\int W(\vartheta)\, do/4\pi = 1$ is insured. In the absence of interactions, the "reduction factor" b_{2k} has its maximum value (= 1) (3*b*). The special case $I = 0$ (3c) was examined by Podgoretskii[1], who did not, however, take the fine structure into account. His criterion for deciding whether the spin of a μ meson is 1/2 or 3/2 in the transition $3p \to 2s \to 2p$ is incorrect, since it follows from (2) that in both instances the distribution is isotropic.

In (3d), ν is the hyperfine structure of a mesic atom which results from the interaction of the nuclear and mesic magnetic moments. In (3e), it is considered that the splitting which results from the electric quadrupole interaction is of the order of magnitude of the spin-orbit coupling[6], i.e., $\nu_{FF'}/2\gamma_B \gg 1$.

Following are the values of the anisotropy A for the radiative transition $2s \to 2p \to 1s$ for different μ-meson spins (with $I = 0$):

$$s = 0 \qquad {}^1/_2 \qquad 1 \qquad {}^3/_2$$

$$A = 1 \qquad 0.273 \quad 0.225 \quad 0.197$$

Substituting for lead $(\nu/2\gamma)^2 \doteq 9$, we get

$$I = {}^1/_2 \qquad s = {}^1/_2 \qquad A = 0.175$$

$$s = {}^3/_2 \qquad A = 0.150.$$

Thus, measurement of the anisotropy A with an accuracy which makes it possible to distinguish a difference of 0.08 is sufficient to determine the spin of the μ meson when the nuclear spin is zero with mesic spin 1/2; then it is also sufficient to determine whether the nucleus has zero spin (for example, ${}_{74}W^{182}$, ${}_{78}Pt^{194}$ and ${}_{82}Pb^{204}$).

I am deeply grateful to Professor I. Ia. Pomeranchuk for suggesting the problem and to K. A. Ter-Martirosian and L. M. Afrikian for their interest.

---

* In deriving this as well as the following expression we used the well-known contraction relation of Clebsch-Gordon coefficients and also the contraction relation of Racah coefficients[4]:

$$\sum_\lambda (2\lambda+1)\, W(a'\lambda\alpha c;\ ac')\, W(b\lambda\beta c';\ b'c)\, W(a'\lambda\gamma b;$$

$$ab') = W(a\alpha b\beta;\ c\gamma)\, W(a'\alpha b'\beta;\ c'\gamma).$$

** See (1a).

[1] M. I. Podgoretskii, J. Exptl. Theoret. Phys. (U.S.S.R.) **29**, 374 (1955); Soviet Phys. JETP 1, 379 (1955).

[2] *Experimental Nuclear Physics*, Ed. Segre (Russian translation IIL, 1955).

[3] J. A. Wheeler, Rev. Mod. Phys. **21**, 133 (1949).

[4] Biedenharn, Blatt and Rose, Rev. Mod. Phys. **24**, 249 (1952).

[5] K. Alder, Helv. Phys. Acta. **25**, 235 (1952).

[6] L. N. Cooper and E. M. Henley, Phys. Rev. **92**, 801 (1953).

Translated by I. Emin
229

Dielectric Properties of Alkali-Halide Single Crystals

B. N. MATSONASHVILI
P. N. Lebedev Physical Institute,
Academy of Sciences, USSR

(Submitted to JETP editor September 24, 1956)
J. Exptl. Theoret. Phys. (U.S.S.R.) **31**, 1110-1111
(December, 1956)

SOME time ago, it was established[1] that the dielectric losses (tan δ) of alkali-halide crystals are determined by conductivity losses. Breckenridge[2], studying the properties of certain alkali-halide crystals and the silver halides, was the first to find that after preliminary heat treatment of these crystals, small maxima of relaxation losses of the Debye type were observed in the value of tan δ. Many authors have attempted to reproduce these results. Some of them[3-6] succeeded in observing relaxation losses in these crystals; however, the results of the observations of different authors were contradictory. We have undertaken a careful study of the dielectric properties of alkali-halide crystals, especially the nature of losses in them.

In contrast to the investigations of previous authors, we have carried out a study of both temperature and frequency dependencies of the dielectric constant and tan δ, not only under atmospheric conditions, but also in a vacuum, over a wide range of temperatures and frequencies (from −170° to 330° and from 10^2 to 10^7 cps under atmospheric conditions, and from −140° to 550° and from 10^2 to 10^6 cps in a vacuum). We studied single crystals of LiF, NaCl, KCl, KBr, CsBr, KJ, KPC-5 and KCl-KBr, both pure and with impurities of Ag, Cu, Tl, Cd, Pb, In, introduced in

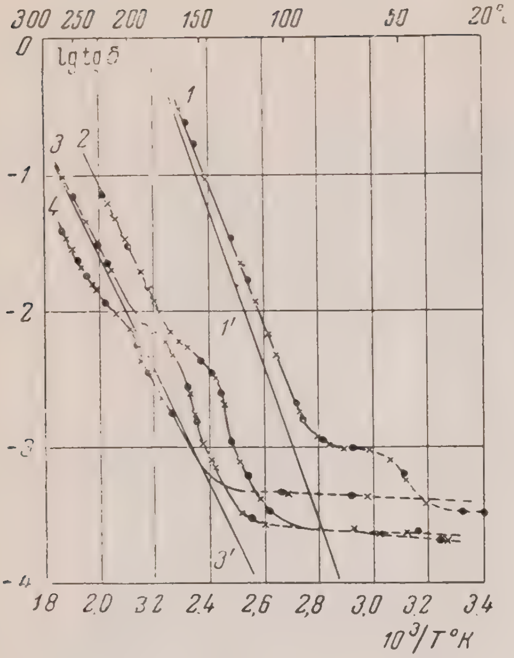

Frequency: *1* = 1 kc, *2* = 300 kc, *3* = 1 mc, *4* = 4.75 mc; *points* – direct process, *circles* – reverse process *Upper scale* – °C.

various concentrations. Growth of crystals was carried out in various crucibles; porcelain, enamel, corundum, fire clay, quartz. The crystals of LiF and KPC-5 were not grown by us). Prepared plane-parallel specimens (ground or polished to within 1-2μ) had areas of 15-20 cm^2 and thickness 0.26-1 mm, the capacity of the specimens amounting to 70-200 mmfd.

Various methods of coating the electrodes were used: silver and platinum platings compressed into pastes, glued foils, aquadag coating, vacuum evaporation of Al, Ag, Au. However, it appeared that the method of "optical trimming" appeared to be most suitable (in this method, the specimen was not subjected to thermal treatment and was not contaminated, while hygroscopic specimens could always be measured also). The specimens were tightly compressed onto flat (machined with an accuracy to within 2μ) electrodes of chemically pure iron which does not react with the alkali-halides at elevated temperatures.

In the temperature and frequency curves of tan δ, there were discovered relaxation maxima in all specimens, which were not subjected to additional thermal treatment. In "pure" monocrystals, as a rule, there was a single maximum; in crystals with impurities, up to four maxima. (By way of illustration, curves are given in the Figure for LiF at atmospheric pressure). After heat working at high temperatures, these maxima were leveled down. The majority of the relaxation maxima at high frequencies were observed in a temperature region where the absolute value of tan δ was of the order of 10^{-3}-10^{-1}. (In this region, the loss measurements on a Q-meter were reliable.)

We also investigated the electric conductivity of crystals γ in a vacuum at constant pressure. For some crystals with impurities, an additional "break" in ln γ was established near 200°, with a temperature dependence. In the case of thermal working of the crystals near the melting point, the values of tan δ and γ declined somewhat.

From a comparison of tan δ, computed from γ (the straight lines 1′ and 3′ in the Figure), with the experimental values of tan δ, it follows that the losses of conductivity are fundamental down to 40-50° at low frequencies, but only to 150-200° at higher frequencies; at the lowest temperatures, significant departures from this rule were noted.

The low temperature "tails" (dashed lines in the Figure) of the curves for tan δ are located in a region of very small losses, and the sensitivity of the Q-meter is insufficient for the investigation of these losses. With the aid of sensitive apparatus (at $f \sim 10^7$ cps) we measured tan δ for 20° for CsBr, LiF and NaCl. The losses were of the order of $(3\text{-}5) \times 10^{-5}$.

The magnitudes of the activation energy U were calculated by the usual method from various pairs of temperature and frequency curves of tan δ. It turns out that the values of U coincide with accuracy to within ± 0.1 ev. The values of U for different crystals are equal to 0.7-1 ev.

As optical and polarographic investigations have shown, the amount of impurities in the crystal resulting from the fusion amount to 6-10%. Here it is characteristic that there are impurities entering into the crystal which are not specially introduced in the fusion. In view of the significant effect on its properties of the previous history of the specimen the whole cycle of measurement of γ, ϵ and tan δ was carried out on the same specimen as a rule.

The relaxation losses that we have observed in the crystals studied can be explained by the reorientation of complex pairs: bivalent impurity ion + cation vacancy[2], cation vacancy + anion vacancy[2,7], and also by the interaction of the vacancy with a dislocation (in particular, with point dislocations). The theoretically computed values of U of the "complexes", as is well known, are of the order of 0.4-0.6 ev, which is somewhat lower than our experimental values.

---

[1] N. P. Bogoroditskii and V. N. Malyshev, J. Tech. Phys. (U.S.S.R.) **4**, 1306 (1934).

[2] R. G. Breckenridge, J. Chem. Phys. **16**, 959 (1948); **18**, 913 (1950).

[3] Y. Haven, J. Chem. Phys. **21**, 171 (1953).

[4] G. Jacobs, Naturwiss, **42**, 575 (1955).

[5] Burstein, Davisson and Sclar, Phys. Rev. **96**, 819 (1954).

[6] J. Teltow and K. Wilke, Naturwiss **41**, 423 (1954).

[7] T. B. Grimbey, J. Chem. Phys. **17**, 496 (1949).

Translated by R. T. Beyer
241

SOVIET PHYSICS JETP VOLUME 4, NUMBER 6 JULY, 1957

Author Index to Volume 4

References with L are Letters to the Editor

Abashidze, K. A. (see Shakhulov, O. A.) – 281L

Abrikosova, I. I. and B. V. Deriagin. Direct Measurement of Molecular Attraction of Solid Bodies. II. Method for Measuring the Gap. Results of Experiments – 2.

Adirovich, E. I., G. M. Guro and V. F. Kuleshov. Dependence of the Life Time of Nonequilibrium Charge Carriers in Germanium on Temperature and Composition – 202

Ado, Iu. M. A Method of Investigation of Radial-Phase Oscillations of Electrons in a Synchrotron – 437L.

Afrikian, L. M. Level Shifts in μ-Mesic Hydrogen and the Structure of the Proton – 770L.

— μ-Pair Production in Nuclei by Gamma Rays – 933L.

— Selection Rules for Antiproton Annihilation into π-Mesons – 135L.

Akulov, N. S. and A. Cheremushkina. On the Theory of the Hall Effect in Ferromagnetics – 150L.

Aleksandrov, Iu. A. and I. I. Bondarenko. Scattering of Fast Neutrons by a Nuclear Coulomb Field – 612L.

Alekseev, A. I. Parapositronium Annihilation Probability, with Account of the First Radiative Corrections – 261L

— The Photoproduction Cross Section for Positronium in an External Field Taking into Account Radiative Corrections – 771L.

Alekseevskii, N. E., N. B. Brandt, and T. I. Kostina. Investigation of the Effect of Pressure on the Galvanomagnetic Properties of Tellurium at Low Temperatures – 813.

— **and Iu. P. Gaidukov.** Galvanomagnetic Properties of Gold – 807

— **and M. N. Mikheeva.** Critical Currents in Superconducting Tin Films – 810

Alikhanian, A. I., N. V. Shostakovich, A. T. Dadaian, V. N. Fedorov, and B. N. Deriagin. On the Mass Spectrum of Charged Cosmic Ray Particles – 817

Alikhanov, S. G. A New Impulse Technique for Ion Mass Measurements – 452L.

Alpers, V. V. and A. P. Mishakova. Decay of a τ-Meson 768L.

Andronikashvilli, E. A. (see Shakhulov, O. A.) – 281L.

Askarian, G. A. On the Mechanism of Initiation of Boiling of Liquid Metastable Systems by Ionizing Radiation – 761L.

Azbel', M. Ia., V. I. Gerasimenko, and I. M. Lifshitz. Paramagnetic Resonance and the Polarization of Nuclei in Thick Metal Foils – 296L.

— (see Lifshitz, I. M.) – 41

Azimov, S. A., U. G. Guliamov, E. A. Zamchalova, M. Nizametdinova, M. I. Podgoretskii, and A. Iuldashev. Investigation of α-stars Induced by Negative π-Mesons 632.

Balashova, B. M. and Iu. V. Sharvin. Structure of the Intermediate State of Superconductors – 54.

Balats, M. Ia., P. I. Lebedev, and Iu. V. Obukhov. Measurement of the Lifetimes of K-Mesons – 436L.

Baldin, A. M., V. V. Mikhailov and M. S. Rabinovich. The Method of Envelopes for Investigating Free Oscillations in Accelerators* – 213

Band, I. M. (see Sliv, L. A.) – 133L.

Barashenkov, V. S. Compton Effect in the Extended Electron – 599L.

— Theory of Nonlocal Interaction – 709.

Bass, F. G. and I. M. Tsidil'kovskii. Theory of Isothermal Galvanomagnetic and Thermomagnetic Effects in Semiconductors – 565.

Baz', A. I. Expansion of Single Particle Wave Functions in Functions of the Relative Motion of the Nucleons – 704.

— Polarization of Neutrons Scattered by Lead – 259L.

Berestetskii, V. B., and B. V. Geshkenbein. Ionizational Slowing Down of High-Energy Electron Positron Pairs – 609L.

— **and E. V. Kuznetsov.** Diffraction Scattering of High-Energy Photons by Nuclei – 610L.

— **and I. Ia. Pomeranchuk.** Correlative Phenomena in K-Meson Capture – 289L.

Berezniak, N. G. and B. N. Eselson. Density of the Normal Component for Solutions of the Isotopes of Helium – 766L.

Biberman, L. M. and B. A. Veklenko. Application of the theory of Random Processes to Radiation Transfer Phenomena – 440L.

Birger, N. G., N. L. Grigorov, V. V. Guseva, G. B. Zhdanov, S. A. Slavatinskii and G. M. Stashkov. Interaction of $5 \times 10^4 - 5 \times 10^{10}$ ev Cosmic Ray Particles with Be Nuclei – 872

— **V. V. Guseva, K. A. Kotel'nikov, V. M. Maksimenko, S. V. Riabikov, S. A. Slavatinskii, and G. M. Stashkov.** An Analysis of Some Cosmic Ray Meson Production Events. II – 836

Blinov, G. A., Iu. S. Krestnikov, and M. F. Lomanov. Measurement of the Ionizing Power of Particles in a Bubble Chamber – 661.

— (see **Kuznetsov, E. V.**) – 773L.

Bogdankevich, O. V., L. E. Lazareva, and F. A. Nikolaev. Inelastic Scattering of Photons by Indium-115 Nuclei – 320.

Bonch-Bruevich, V. L. Spectral Representation of Green's Function in the Nonrelativistic Many-Body

Problem – 456L.
— Statistics of Electrons and Holes in a Homopolar Semiconductor Taking into account their Interaction with the Lattice Vibrations – 196.
Bondarenko, I. I., (see **Aleksandrov, Iu. A.**) – 612L.
Bondarenko, V. V. (see **Kvartskhava, I. F.**) – 623, 637.
Borovik-Romanov, A. S., V. R. Karasik, and N. M. Kreines. Antiferromagnetism of Anhydrous Sulphates of Ni^{++}, Fe^{++}, Co^{++}, Cu^{++} – 109.
— **and M. P. Orlova.** Magnetic Properties of Cobalt and Manganese Carbonates – 531.
Brandt, N. B. (see **Alekseevskii, N. E.**) – 813
Brodovskii, V. B. (see **Shirkov, M. F.**) – 904
Budagov, Iu. A. (see **Ivanov, V. G.**) – 934L
Bulatova, R. F. (see **Kogan, V. S.**) – 593L.
Bydin, Iu. F. and V. M. Dukel'skii. Electron Detachment from Negative Halogen Ions in Collisions with Inert-Gas Atoms and Hydrogen Molecules – 474.
Chentsov, N. N. (see **Gel'fand, I. M.**) – 945L
Cheremushkina, A. (see **Akulov, N. S.**) – 150.
Chernov, A. A. On the Motion of Inclusions in a Solid – 585L.
— (see **Kvartskhava, I. F.**) – 623.
Dadaian, A. T. (see **Alikhanian, A. I.**) – 817
Davidov, A. S. and F. G. Filippov. Scattering Lengths of Slow Neutrons on Deuterons – 267L.
Deigen, M. F. Theory of Localized Electron States in an Isotropic Homopolar Crystal – 424.
Demeshina, A. I. (see **Skanavi, G. I.**) – 524.
Denisov, N. G. On a Singularity of the Field of an Electromagnetic Wave Propagated in an Inhomogeneous Plasma – 544.
Deriagin, B. N. (see **Alikhanian, A. I.**) – 817
Deriagin, B. V. (see **Abrikosova, I. I.**) – 2
Dmitrenko, I. M. (see **Verkin, B. I.**) – 432L.
Dobrovol'skii, S. P., S. I. Nikol'skii, E. I. Tukish, and V. I. Iakovlev. Spatial Distribution of the Particles of Extensive Air Showers Produced by Primary Cosmic Rays of Various Energies – 799
Drukarev, G. F. The Theory of Collisions of Electrons with Atoms – 309.
Duan'-I-Shi. Generalized Nonsingular Solutions for the Scalar Meson Field of a Point Charge in General Relativity Theory – 935L
Dukel'skii, V. M. (see **Bydin, Iu. F.**) – 474.
Dushin, N. V. Photoproduction of π-Meson Pairs in Hydrogen and Deuterium Near Threshold and Isotopic Invariance – 274L.
Dzhelepov, V. P., V. G. Ivanov, M. S. Kozodaev, V. T. Osipenkov, N. I. Petrov, and V. A. Rusakov. Interaction of 230-250 mev Negative π-Mesons with Carbon and Lead Nuclei – 864
— (see **Golovin, B. M.**) – 303.
Dzhrbashian, V. A. γ-γ-Angular Correlation in Transitions of Mesic Atoms – 949L
Esel'son, B. N., B. G. Lazarev, K. D. Sinel'nikov, and A. D. Shvets. Some Properties of Rotating He II – 774L.
— (see **Berezniak, N. G.**) – 766L.
Estulin, I. V., L. F. Kalinkin, and A. S. Melioranskii. Gamma Quanta Emitted by I, Rh, and Co Nuclei in Thermal Neutron Capture – 752L.
Evseev, Z. Ia. The Effect of a Tranverse Magnetic Field on the Thermal Conductivity of Metals – 440L.
Fedorchenko, A. M. (see **Tolpygo, K. B.**) – 713.
Fedorov, F. I. Reduction of Wave Equations for Spin 0 and 1 to the Hamiltonain Form – 139L.
Fedorov, V. N. (see **Alikhanian, A. I.**) – 817
Filippov, A. I. (see **Kozodaev, M. S.**) – 580L.
Filippov, G. F. (see **Davidov, A. S.**) – 267L.
Fogel, Ia. M., R. V. Mitin, and A. G. Koval'. Investigation of Two-Electron Capture in Collisions between Positive Carbon or Oxygen Ions and Gas Molecules – 359.
Fomenko, L. A. On the Magnetization Mechanism of Some NiZn Ferrites in Very Weak Fields – 931L
Fradkin, E. S. A Dispersion Relation for all Scattering Angles – 450L.
Fradkin, M. I. (see **Ginzburg, V. L.**) 462L.
Frankl', F. I. Isentropic Relativistic Gas Flows – 401.
Gaek, Iu. V. and B. L. Timan. Effect of Multiple Thermal Ionization on the Specific Heat of Gases – 578L.
Gaidukov, Iu. P. (see **Alekseevskii, N. E.**) – 807
Galanin, A. D. and L. I. Lapidus. A Note on Mixed Meson Theory – 290L.
Galperin, F. M. Atomic Magnetic Moments of Ferromagnetic Metals and Alloys – 147L.
— **and M. L. Tsetlin.** On Quantities with Anomalous Parity and on a Possible Explanation of Parity Degeneracy of K-Mesons – 947L
Gel'fand, I. M. and N. N. Chentsov. The Numerical Calculation of Path Integrals,– 945L
Gerasimenko, V. I. and L. N. Rosentsveig. Two Electron Charge Exchange of α-Particles in Helium – 509.
— (see **Azbel', M. Ia.**) – 276L.
Gershman, B. N. Note on Waves in a Homogeneous Magnetoactive Plasma – 582.
Geshkenbein, B. V. (see **Berestetskii, V. B.**) – 609L.
Ginzburg, V. L. An Experimental Manifestation of Instability of the Normal Phase in Superconductors – 594L.
— Ferromagnetic Superconductors – 153.
— **and M. I. Fradkin.** On the Composition of Primary Cosmic Rays – 462L.
Glauberman, A. E. Theory of Classical Systems of Interacting Particles Obeying a Noncentral Interaction Law. I. – 169.
Gol'danskii, V. I. On Molecular Neutronoscopy – 604L.

Gol'din, L. L. and D. G. Koshkarev. Synchrotron Oscillations in Strong Focussing Accelerators. I. Linear Theory – 681.
— (see Kondrat'ev, L. N.) – 645.
Gol'fand, Iu. A. Generalized Phase Analysis as a Corollary of the Unitary Property of the *S*-Matrix – 103.
— Transformation Properties of the Electron-Positron Field Amplitudes – 446L.
Golovin, B. M. and V. P. Dzhelepov. An Investigation of the Elastic Scattering of 590 Mev Neutrons – 303.
Golubenkov, V. N. and Ia. A. Smordinskii. The Lagrangian Function for a System of Identically Charged Particles – 442L.
Gor'kov, L. P. and I. M. Khalatnikov. Electrodynamics of Charged Scalar Particles – 777
Gornyi, N. B. Discrete Energy Losses of Electrons Reflected from a MoO$_2$ Surface – 131L.
— Investigation of the Angular and Energy Distributions of Secondary Electrons from Cuprous Oxide – 346.
Gramenitskii, I . M. Investigation of High-Energy Electron Showers by the "Emulsion Chamber" Technique – 586L
Grechukhin, D. P. Spin-Orbit Interaction in Nuclear Magnetic Multipole Radiation – 448L.
— The Effect of Finiteness of Target-Nucleus Mass on Angular Distribution in (d,p) and (d,n) Reactions – 759L.
Gribov, V. N. and L. E. Gurevich. On the Theory of the Stability of a Layer Located at a Superadiabatic Temperature Gradiant in a Gravitational Field – 720.
Grigorev, E. L. and N. A. Mitin. Elastic Scattering of 310 Mev π^+-Mesons from Protons – 10.
— and L. P. Solov'eva. Nuclear Disintegrations Produced by 660 Mev protons in Photographic Emulsions – 801
Grigorov, N. L. (see Birger, N. G.) – 872
Gubanov, A. I. Electron Scattering from Thermal Vibrations in a Liquid – 465.
Guliamov, U. G. (see Azimov, S. A.) – 632.
Guliev, N. A. Polarization of Neutrons Scattered by Carbon Taking Nuclear Volume into Account – 142L.
Gurevich, I. I. and M. I. Pevzner. "Repulsion" of Nuclear Levels – 278L.
Gurevich, L. E. (see Gribov, V. N.) – 720.
Guro, G. M. (see Adirovich, E. I.) – 202.
Guseva, V. V. (see Birger, N. G.) – 836, 872.
Guzhavin, V. V. (see Guzhavina, O. A.) – 690.
Guzhavina, O. A., V. V. Guzhavin, and G. T. Zatsepin. A Comparison of the Fermi-Landau Theory with Some Experimental Data on Cosmic Rays – 690.
Iaichnitsyn, V. G. A Static Solution of the Nonlinear Meson Equation – 925L.
Iakovlev, L. G. On Theories of Multiple Meson Production – 141L.
Iakovlev, V. I. (see Dobrovol'skii, S.) – 799.
Iavor, I. P. (see Komar, A. P.) – 432L.
Ignatenko, A. E., A. I. Mukhin, E. B. Ozerov, and B. M. Pontecorvo. Interaction of π-Mesons with Lead, Copper, Oxygen, and Beryllium Nuclei – 351.
Inopin, E. V. Excitation of Nuclear Vibrational Levels by Scattering of Fast Neutrons – 764L.
Ioffe, B. L. Dispersion Relations for Scattering and Photoproduction – 534.
— I. Ia. Pomeranchuk, and A. P. Rudik. Dispersion Relations for Pions Scattered by Deuterons – 588L.
Isaev, P. S. and V. S. Murzin. On a Certain Regularity of Decaying Unstable Particles – 591L.
Iuldashev, A. (see Azimov, S. A.) – 632.
Ivanenko, D. D. and B. K. Kerimov. Two-Nucleon Potential of Intermolecular Type and Nuclear Saturation – 417.
Ivanenko, I. P. Cascade Showers Produced by Electrons and Photons in Light and Heavy Elements – 115.
Ivanov, V. G., V. T. Osipenkov, N. I. Petrov, and V. A. Rusakov. Total Inelastic Interaction Cross Sections of 225^*-10 Mev Negative π-Mesons with C, Al, Cu. Sn, and Pb Nuclei – 922L.
— N. I. Petrov, V. A. Rusakov, Iu. A. Budagov, and V. T. Osipenkov. Showers in Lead Produced by 360 ± 30 Mev Electrons – 934L.
— (see Dzhelepov, V. P.) – 864
Ivanova, N. S. Mean Excitation Energy of Fissioning Uranium Nuclei on Absorption of Slow π-Mesons – 597L.
— The Cross Section for the Fission of Uranium by High-Energy Protons – 365.
— and I. I. P'ianov. Uranium Fission Induced by High-Energy Protons – 367.
Kachinskii, V. N. (see Peshkov, V. P.) – 607L.
Kadomtsev, B. B. On the Hydrodynamic Description of Plasma Oscillations – 926L.
Kaganov, M. I., I. M. Lifshitz, and L. V. Tanatarov. Relaxation between Electrons and the Crystalline Lattice* – 173.
— (see Kaner, E. A.) – 393.
— (see Lifshitz, I. M.) – 41.
Kalinkin, L. F. (see Estulin, I. V.) – 752L.
Kaner, E. A. and M. I. Kaganov. On the Possibility of Introducing an Effective Dielectric Constant at High Frequencies – 393.
Karasik, V. R. (see Borovik-Romanov, A. S.) – 109.
Kazarinov, Iu. M. and Iu. N. Simonov. Elastic Scattering of Neutrons by 580 Mev Protons – 161.
Kazarnovskii, M. V. Relation between Neutron Scattering in Polycrystals and Specific Heat – 600L.
Kebuladze, N. A. (see Shakhulov, O. A.) – 281L.
Kerimov, B. K. (see Ivanenko, D. D.) – 417.
— (see Sokolov, A. A.) – 396

Khalatnikov, I. M. (see Gor'kov, L. P.) – 777

Kholodenko, L. P. Contribution to the Theory of Phase Phenomena in Barium Titanate. 847

— Contribution to the Thermodynamical Theory of the Ferroelectric Properties of Barium Titanate – 188.

Khoziainov, V. T. Remarks on the Theory of Scattering of Particles with a Given Total Angular Momentum – 137L.

Khutsishvili, G. R. Nuclear Magnetic Relaxation in Ionic Crystals – 382.

Kizel', V. A. and A. F. Stepanov. Concerning the Existence of a Transition Layer on a Liquid Surface – 458L.

Klinger, M. I. The Theory of Galvanomagnetic Phenomena in Semiconductors – 831

Kogan, A. V. and I. A. Sokolov. On the Total Energy of the β-Transition RaC-RaC′ – 767L.

Kogan, V. S., B. G. Lazarev, and R. F. Bulatova. The Crystalline Structure of Hydrogen and Deuterium – 593L

Komar, A. P. and I. P. Iavor. Photoprotons from A^{40} – 432L.

Kompaneets, A. S. The Establishment of Thermal Equilibrium between Quanta and Electrons – 730.

— and E. S. Pavlovskii. The Self-Consistent Field Equations in an Atom – 328.

Kondratenko, V. N. (see Samoilovich, A. G.) – 481.

Kondrat'ev, L. N., G. I. Novikov, Iu. P. Sobolev, and L. L. Gol'din. Alpha Decay of Pu^{240} – 645.

Kornilov, S. G. A Polarization Method for Measuring the Velocities of Particles with Intrinsic Magnetic Moment – 444L.

Korolev, A. M. The Dynamical Magnetic Moment of the Deuteron – 73.

Koshkarev,D. G. (see Gol'din, L. L.) – 681.

Kostina, T. I. (see Alekseevskii, N. E.) – 813

Kotel'nikov, K. A. (see Birger, N. G.) – 836

Koval', A. G. (see Fogel', Ia. M.) – 359.

Kozodaev, M. S., R. M. Sulaev, A. I. Filippov, andIu. A. Shcherbakov, Interaction between Negative Pions and Helium Nuclei at 330 Mev Energy – 580L.

— (see Dzhelepov, V. P.) – 864

Kreines, N. M. (see Borovik-Romanov, A. S.) – 109.

Krestnikov. Iu. S. (see Blinov, G. A.) – 661.

Krivoglaz, M. A. Theory of Diffuse Scattering of X-rays by Solid Solutions. I.– 293.

— and S. I. Pekar. Relation between the Parameters of Longitudinal and Transverse Optical Vibrations of Ions in Crystals – 286L.

Kucher, T. I. and K. B. Tolpygo. Many Electron Treatment of Motion of an Electron (Hole) in a Deformed Crystal. II. – 883

Kudriavtsev, V. S. On Quasi-Classical Quantization – 527.

Kuleshov, V. E. (see Adirovich, E. I.) – 202.

Kuznetsov, E. V., M. F. Lomanov, G. A. Blinov, and Chaun Chen-Niang (Kuan Shen-nian). A Bubble Chamber for the Study of Cosmic Rays – 773L.

— (see Berestetskii, V. B.) – 610L.

Kvartskhava, I. F., V. V. Bondarenko, R. D. Meladze and K. V. Suladze. Electrical Explosion of Wires in Vacuum – 637.

— V. V. Bondarenko, A. A. Pliutto, and A. A. Chernov. Oscillographic Determination of Energy of Electric Explosion of Wires – 623.

Lapidus, L. I. Determination of the Spins of *K*-Particles and Hyperons – 447L.

Isotopic Invariance and the Creation of Particles – 742

— The Optical Theorem and Elastic Scattering Through Small Angles – 937L

— (see Galanin, A. D.) – 290L.

Lazarev, B. G. (see Eselson, B. N.) – 771L.

— (see Kogan, V. S.) – 593L.

— (see Verkin, B. I.) – 432L.

Lazareva, L. E. (see Bogdankevich, O. V.) – 320.

Lazukin, V. N. A Possible Application of Cyclotron Resonance to Mass Spectrometry – 266L.

Lebedev, P. I. (see Balats, M. Ia.) – 436L.

Levin, M. L. Thermal Radiation of Good Conductors – 225.

Levkovskii, V. N. Relative Cross Sections for n-p Reactions Involving Nuclei with Several Stable Isotopes – 291L.

Liashenko, V. I. and T. N. Sitenko. Surface Electrical Conductivity of Germanium – 940L

Lifshitz, I. M., M. Ia. Azbel', and M. I. Kaganov. The Theory of Galvanomagnetic Effects in Metals – 41.

— and G. I. Stepanova. The Effect of Ordering on the Energy Spectrum of Phonons – 151L.

— (see Azbel', M. Ia.) – 276L.

— (see Kaganov, M. I.) – 173.

Likhter, Ia. I. On the Relation between the Distribution of a Quasi-Monochromatic Stationary Process and the Distribution of its Envelope – 146L.

Litvin, V. F. (see Nemilov, Iu. A.) – 606L.

Livshits, M. S. The Application of Nonself-Adjoint Operators to Scattering Theory – 91.

Lomanov, M. F. (see Blinov, G. A.) – 661.

— (see Kuznetsov, E. V.) – 773L.

Lomsadze, Iu. M. Concerning a Certain Possibility in Quantum Field Theory – 754L.

Lozhkin, O. V. and N. A. Perfilov. Heavy Nuclear Fragments from Disintegrations Produced by Fast Protons in Nuclear Emusions* – 790

Lun'kin, Iu. P. and G. I. Mishin. On Light Emission by a Shock Wave Front – 939L

Maksimenko, V. M. and A. I. Nikishov. Multiple Formation of Particles in 5.3 Bev Nucleon-Nucleon Collisions – 614L.

— (see Birger, N. G.) –

Mamasakhlisov, V. I. Investigation of the $Be^9(dn)B^{10}$

Nuclear Reaction — 527.

Manenkov, A. A. and A. M. Prokhorov. Hyperfine Structure of the paramagnetic Resonance Spectrum of $^{53}Cr^{3+}$ in Al_2O_3 — [illegible]L.

Matinian, S. G. On $K_{\mu 2}$-Decay — 434L.

— On the Absorption of K-Mesons by Helium Nuclei — [illegible]L.

Matsonashvili, B. N. Dielectric Properties of Alkali Halide Single Crystals — 951L

Matveev, A. N. The Role of Spin in the Radiation from a "Radiating" Electron — 409.

Medvedev, B. V. On the Construction of the Scattering Matrix. I. Integral Causality Condition in Bogoliubov's Method — 671.

Meladze, R. D. (see **Kvartskhava, I. F.**) — 637.

Melikian, E. G. The Internal Compton Effect — 930L

Melioranskii, A. S. (see **Estulin, I. V.**) — 752L.

Mescheriakov, M. G., S. B. Nurushev, and G. D. Stoletov. Polarization of 660 Mev Protons Scattered by Nuclei — 337.

— **I. K. Vzorov, V. P. Zrelov, B. S. Neganov, and A. F. Shabudin.** The Production of Charged Mesons by the Bombardment of Beryllium and Carbon with 660 Mev Protons — 79.

— **V. P. Zrelov, B. S. Neganov, I. K. Vzorov, and A. F. Shabudin.** π^--Meson Energy Spectrum for pp→np π^+-Reaction at 556 and 657 Mev — 60.

Meshkovskii, A. G., Iu. S. Pliagin, Ia. Ia. Shalamov and V. A. Shebanov. Production of Positive π-Mesons in Hydrogen by 660 Mev Protons — 404.

— **Iu. S. Pligin, Ia. Ia. Shalamov, and V. A. Shebanov.** Production of Positive π-Mesons in Various Nuclei by 660 Mev Protons — 842

— **and L. I. Sokolov.** The Ionization Spectrum of Cosmic Rays 3250 m above Sea Level —

Mikhailov, V. V. (see **Baldin, A. M.**) — 213

Mikheeva, M. N. (see **Alekseevskii, N. E.**) — 810

Mishakova, A. P. (see **Alpers, V. V.**) — 768L.

Mishin, G. I. (see **Lun'kin, Iu. P.**) — 939L

Mitin, N. A. (see **Grigorev, E. L.**) — 10

Mitin, R. V. (see **Fogel', Ia. M.**) — 359.

Moiseev-Olkhovskii, I. I. A Method of Obtaining Non-stationary Solutions of Boltzmann's Kinetic Equation — 183.

Mokhov, V. N. (see **M. G. Urin**) — 738.

Morozov, A. I. Interaction between a Moving Current-Carrying Wire and a Conducting Wall — 920L.

Mukhin, A. I., E. B. Ozerov, and B. M. Pontecorvo. The Scattering of π^+-Mesons on Hydrogen. I. Angular Distributions at Energies of 176, 200, 240, 270, and 307 Mev — 237.

— **and B. M. Pontecorvo.** Scattering of π^+-Mesons by Hydrogen. II. Discussion and Interpretation of the Results — 373.

— (see **Ignatenko, A. E.**) — 351.

Murzin, V. S. (see **Isaev, P. S.**) — 591L.

Neganov, B. S. (see **Mescheriakov, M. G.**) — 60, 79.

Nemilov, Iu. A. and V. F. Litvin. Excitation Function for the $Si^{28}(dp)Si^{29}$ Reaction — 606L.

Neudachin, V. G. Accuracy of Isobaric Spin for the $lf_{7/2}$ Shell — 756L.

— "Seniority" Quantum Number Selection Rules in Nuclear Reactions — 751L.

Niang, Chuan Chen-(Kuan Shen-nian) (see **Kuznetsov, E. V.**) — 773L.

Nikishov, A. I. (see **Maksimenko, V. M.**) — 614L.

Nikolaev, F. A. (see **Bogdankevich, O. V.**) — 320.

Nikol'skii, S. I. and I. E. Satsevich. Influence of the Earth's Magnetic Field on the Space-Distribution of Particles in Extensive Air Showers — 589L.

— (see **Dobrovol'skii, S. P.**) — 799.

Nizametdinova, M. (see **Azimov, S. A.**) — 632.

Nosov, V. G. Energy Dependence of the Fission Width — 263L.

Novikov, G. I. (see **Kondrat'ev, L. N.**) — 645.

Novozhilov, Iu. V. Quantum Field Theory with Causal Operators* — 553.

— The Variational Principle and the Virial Theorem for the Continuous Dirac Spectrum — 928L.

Nurushev, S. B. (see **Mescheriakov, M. G.**) — 337.

Obukhov, Iu. V. (see **Balats, M. Ia.**) — 436L.

Ochkur, V. I. and Iu. V. Petrov. Calculation of Elastic Scattering of Slow Electrons in Hydrogen by the Integral Equation Method — 144L.

Okun', L. B. On the Probabilities of Σ-Particle Decay — 284L.

Orlov, Iu. V. Internal Bremsstrahlung in Electric Monopole $0^+ \rightarrow 0^+$ Nuclear Transitions — 944L.

Orlova, M. P. (see **Borovik-Romanov, A. S.**) — 531.

Osipenkov, V. T. (see **Ivanov, V. G.**) — 922L.

— (see **Dzhelepov, V. P.**) — 864

Ostroumov, V. I. and N. A. Perfilov. Angular Distribution of Uranium Fission Fragments Produced by High-Energy Neutrons — 603L.

Ozerov, E. B. (see **Ignatenko, A. E.**) — 351.

— (see **Mukhin, A. I.**) — 237.

Parfanovich, D. M., N. V. Rabin, and A. M. Semchinova. Interaction of Nitrogen Nucleus with Nuclei in an Emulsion. — 99

Pavlovskii, E. S. (see **Kompaneetz, A. S.**) — 328.

Pekar, S. I. Invalidity of the Fermi-Dirac Distribution for Electrons of Semiconductor and Crystal Phosphor Impurity Centers — 271L.

— (see **Krivoglaz, M. A.**) — 286L.

Perfilov, N. A. (see **Lozhkin, O. V.**) — 790

— (see **Ostroumov, V. I.**) — 603L.

Peshkov, V. P. and V. N. Kachinskii. Measurement of the Saturated Vapor Pressure of a He^3-He^4 Mixture

with a High He^3 Concentration – 607L.
Petrov, Iu. V. (see **Ochkur, V. I.**) – 144L.
Petrov, N. I. (see **Dzhelepov, V. P.**) – 864
— (see **Ivanov, V. G.**) – 922L.
Pevzner, M. I. (see **Gurevich, I. I.**) – 278L.
P'ianov, I. I. (see **Ivanova, N. S.**) – 367.
Pitaevskii, L. P. On the Derivation of a Formula for the Energy Spectrum of Liquid He^4– 439L.
Pligin, Iu. S. (see **Meshkovskii, A. G.**) – 404.
Pliutto, A. A. (see **Kvartskhava, I. F.**) – 623.
Podgoretskii, M. I. (see **Azimov, S. A.**) – 632.
Pokrovskii, V. L. A Theorem on the Equality of the Cross Sections for Photoproduction of Charged π-Mesons on Nuclei with Isotopic Spin Zero – 459L.
— **and Iu. B. Rumer.** Note on the Theorem of Pauli on the Relation of Spin and Statistics – 264L.
Polovin, R. V. Nonlinear Theory of Longitudinal Plasma Oscillations – 290L.
— Radiative Corrections to the Scattering of Electrons and Positrons – 385.
Pomeranchuk, I. Ia. (see **Berestetskii, V. B.**) – 289L.
— (see **Ioffe, B. L.**) – 588L.
Pontecorvo, B. M. (see **Ignatenko, A. E.**) – 351.
— (see **Mukhin, A. I.**) – 237, 373.
Popov, Iu. A. Solution of the Fundamental Diffusion Equation for Cosmic Ray Particles Emitted by a Constant Energy Concentrated Pulsed Source – 85.
Prokhorov, A. M. (see **Manenkov, A. A.**) – 288L.
— (see **Veselago, V. G.**) – 750L.
Prokoshkin, Iu. D. Relation between the Angular Distributions of Particles and Their Decay Products – 618L.
Rabin, N. V. (see **Parfanovich, D. M.**) – 99.
Rabinovich, M. S. (see **Baldin, A. M.**) – 213
Raiskii, G. Remarks on Bilocal Field Theory – 577L.
Rashba, E. I. (see **Tolpygo, K. B.**) – 213.
Rebane, T. K. Application of the Lattice Model to Semiconductors of the Lead Sulphide Type – 273L.
Riabikov, S. V. (see **Birger, N. G.**) – 836
Rivin, A. I. Behavior of Particles with Nonzero Spin in Crossed Constant and Varying Magnetic Fields – 619L.
Rozental', I. L. A Quasi-Unidimensional Interpretation of the Hydrodynamic Theory of Multiple Particle Production – 217.
Rozentsweig, L. N. Obtaining Polarized Electron Beams – 455L.
— The Polarization of Neutrons from D(γ, n) Reaction – 280L.
— (see **Gerasimenko, V. I.**) – 509.
Rudik, A. P. (see **Ioffe, B. L.**) – 588L.
Rumer, Iu. B. (see **Pokrovskii, V. L.**) – 264L.
Rusakov, V. A. (see **Dzhelepov, V. P.**) – 864
— (see **Ivanov, V. G.**) – 922L.
Ryzhanov, S. G. Connection between α-Decay and Nuclear Deformation – 282L.
Samoilovich, A. G. and V. M. Kondratenko. On the Theory of Atomic Semiconductors – 481.
Sannikov, D. G. (see **Shirokov, Iu. M.**) – 13.
Satsevich, I. E. (see **Nikol'skii, S. I.**) – 589L.
Semchinova, A. M. (see **Parfanovich, D. M.**) – 99.
Semenenko, E.E. (see **Sudovtsov, A. I.**) – 592L.
Shabanskii, V. P. Transfer Processes in Conductors with Regard to Nonlinear Effects – 497.
Shabudin, A. F. (see **Mescheriakov, M. G.**) – 60, 79.
Shakhulov, O. A., N. A. Kebuladze, E. A. Andronikashvilli, and K. A. Abashidze. New Type of Disintegration of a Heavy Meson? – 281L.
Shalamov, Ia. Ia. (see **Meshkovskii, A. G.**) – 404.
Sharvin, Iu. V. (see **Balashova, B. M.**) – 54.
Shcherbakov, Iu. A. (see **Kozodaev, M. S.**) – 580L.
Shebanov, V. A. (see **Meshkovskii, A. G.**) – 404.
Shimanskaia, N. S. A Calorimetric Determination of the Mean Energy of the β-Spectra of P^{32}, S^{35}, Cu^{64}, W^{185} and Au^{198}– 355.
— Determination of the Branching Ratio in the Disintegration Scheme of Po^{210} – 165.
Shirokov, Iu. M. and D. G. Sannikov. On the Problem of Unquantized Relativistically Invariant Renormalized Equations for a Three-Dimensional Extended Particle – 13.
Shirokov, M. F. and V. B. Brodovskii. On the Equations of Motion of Finite Masses in the General Theory of Relativity* – 904
Shirokov, M. I. Concerning the Spin of the $\overset{\circ}{\Lambda}$-Particle – 620L.
Shmushkevich, I. M. Concerning the Impulse Approximation – 611L.
Shostakovich, N. V. (see **Alikhanian, A. I.**) – 817
Shvets, A. D. (see **Esel'son, B. N.**) – 774L.
Sidorov, V. M. Production of Positive Pions in (p-p) Collisions at 660 Mev – 22.
Simonov, Iu. N. (see **Kazarinov, Iu. M.**) – 161.
Sinel'nikov, K. D. (see **Esel'son, B. N.**) – 774L.
Sitenko, A. G. On the Theory of the Stripping Reaction – 492.
— Production of π-Meson Pairs on Nuclei by High Energy γ-Quanta – 269L.
— **and K. N. Stepanov.** On the Oscillations of an Electron Plasma in a Magnetic Field – 512.
Sitenko, T. N. (see **Liashenko, V. I.**) – 940L.
Skanavi, G. I. and A. I. Demeshina. Dielectric Properties of Bismuth Titanate – 524.
Skobelkin, V. I. Variational Principles in Hydrodynamics – 68.
Skorniakov, G. V. The Three Body Problem for Short Range Forces. II – 910
— **and K. A. Ter-Martirosian.** Three Body Problem for Short Range Forces. I. Scattering of Low Energy Neutrons by Deuterons – 648.

Slavatinskii, S. A. (see **Birger, N. G.**) — 872

Sliv, L. A. and I. M. Band. *K*-Shell Gamma Ray Internal Conversion Coefficients — 133L.

Smorodinskii, Ia. A. (see **Golubenkov, V. N.**) — 442L.

Sobel'man, I. I. Electron Broadening of Spectral Lines — 453L.

Sobolev, Iu. P. (see **Kondrat'ev, L. N.**) — 645.

Sokolov, A. A. and B. K. Kerimov. On the Damping Theory of Particle Scattering by a Fixed Center — 921L.

— **and I. M. Ternov.** On Polarization Effects in the Radiation of an Accelerated Electron — 396.

— **I. M. Ternov, and G. M. Strakhovskii.** Investigation of Stability of Electron Motion in Cyclic Accelerators when Quantum Effects are Included — 251.

Sokolov, I. A. (see **Kogan, A. V.**) — 767L.

Sokolov, L. I. (see **Meshkovskii, A. G.**) — 629.

Solov'eva, L. P. Nuclear Interactions with 220 Mev Deuterons — 923L.

— (see **Grigorev, E. L.**) — 801

Soroko, L. M. Elastic (p-p) - Scattering and Peculiarities of Interactions between Pions and Nucleons — 579L.

Stashkov, G. M. (see **Birger, N. G.**) — 872

Stepanov, A. F. (see **Kizel', V. A.**) — 458L.

Stepanov, K. N. (see **Sitenko, A. G.**) — 512.

Stepanova, G. I. (see **Lifshitz, I. M.**) — 151L.

Stoletov, G. D. (see **Mescheriakov, M. G.**) — 337.

Strakhovskii, G. M. (see **Sokolov, A. A.**) — 251.

Stratonovich, R. L. On Distributions in Representation Space — 891

Strizhak, V. I. Inelastic Scattering Cross Section of Nuclei for 2.5 Mev Neutrons — 769L.

Sudakov, V. V. Consequences of the Renormalizability of Quantum Electrodynamics and Meson Theory — 616L.

— **and K. A. Ter-Martirosian.** Consequences of Renormalizability of Pseudoscalar Meson Theory with Two Interaction Constants — 763L.

Sudovtsov, A. I. and E. E. Semenko. Peculiarities of the Temperature Dependence of the Electrical Resistance of Ferromagnetic Metals at Low Temperatures — 592L.

Suladze, K. V. (see **Kvartskhava, I. F.**) — 637.

Sulaev, R. M. (see **Kozodaev, M. S.**) — 580L.

Svidzinskii, A. V. Determination of the Green's Function in the Bloch-Nordsiek Model by Functional Integration — 179.

Tanatarov, L. V. (see **Kaganov, M. I.**) — 173.

Temkin, A. Ia. The Theory of Slowing Down of Neutrons — 757L.

Temko, S. V. On the Derivation of the Fokker-Planck Equation for a Plasma — 898

Teplov, I. B. Investigation of the (d,p) Reaction in Phosphorus and Chlorine — 31.

Terletskii, Ia. P. On a Rational System of Symbols for Fundamental Particles — 575L.

Ter-Martirosian, K. A. Charge Renormalization for an Arbitrary, not Necessarily Small, Value of e_0 — 443L.

— (see **Skorniakov, G. V.**) — 648.

— (see **Sudakov, V. V.**) — 763L.

Ternov, I. M. (see **Sokolov, A. A.**) — 251, 396.

Timan, B. L. (see **Gaek, Iu. V.**) — 578L.

Todes, O. M. (see **Zharhovskii, A. G.**) — 701.

Tolpygo, K. B. and A. M. Fedorchenko. The Interaction of an Electron Hole with the Lattice Vibrations in a Homopolar Crystal — 713

— **and E. I. Rashba.** Bipolar Diffusion of Current Carriers in the Presence of Deep Traps — 213.

— (see **Kucher, T. I.**) — 883

Tsetlin, M. L. (see **Gel'fand, I. M.**) — 947L.

Tsidil'kovskii, I. M. (see **Bass, F. G.**) — 565.

Tukish, E. I. (see **Dobrovol'skii, S. P.**) — 799

Tulinov, A. F. Investigation of Nuclear Energy Levels by Measuring the Angle of Emission of the Reaction Products — 596L.

Urin, M. G. and V. N. Mokhov. Polarization of Relativistic Protons in Coulomb Scattering — 738.

Vedenov, A. A. Contribution to the Theory of π-Meson Disintegration — 268L.

Veklenko, B. A. (see **Biberman, L. M.**) — 440L.

Verkin, B. I., I. M. Dmitrenko, and B. G. Lazarev. The Effect of Uniform Compression upon the Magnetic Properties of Bismuth at Low Temperatures — 432L.

Veselago, V. G. and A. M. Prokhorov. The HDSe Microwave Spectrum — 750L.

Vialov, G. N. Anamalous Magnetic Moments of Nucleons - 562.

Volokhova, T. I. Paramagnetic Relaxation in Monocrystals of Some Salts of the Iron Group Elements — 918L.

Vzorov, I. K. (see **Mescheriakov, M. G.**) — 60, 79.

Zamchalova, E. A. (see **Azimov, S. A.**) — 632.

Zatsepin, G. T. (see **Gushavina, O. A.**) — 690

Zel'dovich, Ia. B. Perturbation Theory for the One Dimensional Quantum Mechanical Problem and the Lagrange Method — 942L.

— The Magnetic Field in the Two-Dimensional Motion of a Conducting Turbulent Liquid — 460.

Zharkovskii, A. G. and O. M. Todes. Reflection of Waves from an Isotropic Inhomogeneous Layer — 701

Zhdanov, G. B. (see **Birger, N. G.**) — 872.

Zhdanova, N. F. Temperature Dependence of the Viscosity of Liquid Nitrogen at Constant Density — 19.

— Temperature Dependence of Viscosity of Liquid Argon — 749L.

Zinov'eva, K. N. The Coefficient of Volume Absorption of Second Sound and the Viscosity of the Normal Component of He II down to 0.83°K — 36.

Zrelov, V. P. (see **Mescheriankov, M. G.**) — 60, 79.

Analytic Subject Index to Volume 2

References with L are Letters to the Editor. Items are listed under the following categories:

Acoustics
Astrophysics
Atomic and Molecular Beams
Atomic Mass and Abundance
Atomic Structure and Spectra
Chemical Effects and Properties
Constants, Standards, and Units
Cosmic Radiation
Crystalline State
Dielectrics and Dielectric Properties
Diffraction
Diffusion
Editorial
Electrical Conductivity and Resistance
Electrical Discharges
Electrical Properties
Electromagnetic Theory and Electromagnetics
Electrons and Positrons
Elementary Particle Interactions
Errata
Field Theory
Films, Properties
Fluid Dynamics
Gamma Rays
Gases
Geophysics
Helium, Liquid
Imperfections in Solids
Ionization
Ions
Ions and Electrons, Mobility
Liquids
Luminescence
Magnetic Properties
Magnetic Resonance
Mathematical Methods
Mechanics
Mesons and Hyperons
Methods and Instruments
Microwaves
Miscellaneous
Molecular Aggregates
Molecular Structure and Spectra
Noise
Nuclear Fission
Nuclear Moments and Spin
Nuclear Photoeffects
Nuclear Reactions, General
Nuclear Reactions Induced by α-Particles and He^3
Nuclear Reactions Induced by Deuterons and Tritons
Nuclear Reactions Induced by Mesons
Nuclear Reactions Induced by Neutrons
Nuclear Reactions Induced by Protons
Nuclear Spectra
Nuclear Structure Theory
Optical Properties
Quantum Electrodynamics
Quantum Mechanics
Radiation
Radioactivity
Range and Energy Loss of Particles
Relativity and Gravitation
Scattering, General
Scattering of α-Particles
Scattering of Deuterons
Scattering of Electrons and Positrons
Scattering of Mesons
Scattering of Neutrons
Scattering of Protons
Statistical Mechanics and Thermodynamics
Superconductivity
Thermal Properties
X-Rays

Absorption of Radiation (see Radiation)
Acoustics
  A Method of Obtaining Nonstationary Solutions of Boltzmann's Kinetic Equation, I. I. Moiseev-Olkhovskii——183
  Reflection of Waves from an Isotropic Inhomogeneous Layer. A. G. Zharkovskii and O. M. Todes——701.
Afterglow (see Electrical Discharges)
Alloys (see Crystalline State)
Annihilation (see Electrons and Positrons)
Antiferroelectric Phenomena (see Dielectrics and Dielectric Properties)
Antiferromagnetism (see Magnetic Properties)
Arcs (see Electrical Discharges)
Astrophysics
  On Polarization Effects in the Radiation of an Accelerated Electron, A. A. Sokolov and I. M. Ternov——396.
  On the Equations of Motion of Finite Masses in the General Theory of Relativity*, M. F. Shirokov and V. B. Brodovskii—— 904
  On the Theory of the Stability of a Layer Located at a Superadiabatic Temperature Gradient in a Gravitational Field, V. N. Gribov and L. E. Gurevich——720.
  Solution of the Fundamental Diffusion Equation for Cosmic Ray Particles Emitted by a Constant Energy Concentrated Pulsed Source, Iu. A. Popov——85.
Atomic and Molecular Beams
  A Polarization Method for Measuring the Velocities of

Particles with Intrinsic Magnetic Moment, S. G. Kornilov—444L.
Electrodynamics of Charged Scalar Particles. P. Gor'kov and I. M. Khalatnikov— 777
Investigation of Two-Electron Capture in Collisions between Positive Carbon or Oxygen Ions and Gas Molecules, Ia. M. Fogel', R. V. Mitin, and A. G. Koval—359.
Synchrotron Oscillations in Strong Focusing Accelerators. I. Linear Theory, L. L. Gol'din and D. G. Koshkarev—681.
Atomic Mass and Abundance
A Possible Application of Cyclotron Resonance to Mass Spectrometry, V. N. Lazukin—266L.
Atomic Structure and Spectra
Electron Broadening of Spectral Lines, I. I. Sobel' man—453L.
Level Shifts in μ-Mesic Hydrogen and the Structure of the Proton, L. M. Afrikian—770L.
Auger Effect (ss Atomic Structure and Spectra)
Barkhausen Effect (see Magnetic Properties)
Boson Theory (see Field Theory)
Bremsstrahlung (see Radiation)
Broadening of Spectral Lines (see Atomic Structure and Spectra; Spectra, General)
Capture Cross Sections (see Electrons and Positrons; Nuclear Reactions, General; Radiation)
Cerenkov Effect (see Radiation)
Chemical Effects and Properties
Direct Measurement of Molecular Attraction of Solid Bodies. II. Method for Measuring the Gap. Results of Experiments, I. I. Abrikosova and B. V. Deriagin 2.
Chemiluminescence (see Luminescence)
Cold Emission (see Electrical Properties)
Compton Effect (see Radiation)
Conductivity, Electrical (see Electrical Conductivity and Resistance)
Constants, Standards and Units
K-Shell Gamma Ray Internal Conversion Coefficients, L. A. Sliv and I. M. Band—133L.
On a Certain Regularity of Decaying Unstable Particles, P. S. Isaev and V. S. Murzin—591L.
Cosmic Radiation
A Bubble Chamber for the Study of Cosmic Rays. E. V. Kuznetsov, M. F. Lomanov , G. A. Blinov, and Chaun Chen-Niang (Kuan shen-nian)—773L.
A Comparison of the Fermi-Landau Theory with Some Experimental Data on Cosmic Rays, O. A. Guzhavina, V. V. Guzhavin, and G. T. Zatsepin—690.
An Analysis of Some Cosmic Ray Meson-Production Events, II. N. G. Birger, V. V. Guseva, K. A. Kotel' nikov, V. M. Maksimenko, S. V. Riabikov, S. A. Slavatinskii, and G. M. Stashkov— 836
Cascade Showers Produced by Electrons and Photons in Light and Heavy Elements, I. P. Ivanenko—115.
Influence of the Earth's Magnetic Field on the Space-Distribution of Particles in Extensive Air Showers, S. I. Nikol'skii and I. E. Satsevich—589L.
Interaction of 5–50 BEV Cosmic Ray Particles with Be Nuclei. I. N. G. Birger, N. L. Grigorov, V. V. Guseva, G. B. Zhdanov, S. A. Slavatinskii, and G. M. Stashkov— 872
Investigation of α-Stars Induced by Negative π-Mesons S. A. Azimov, U. G. Guliamov, E. A. Zamchalova. M. Nizametdinova, M. I. Podgoretskii, and A. Iuldashev—632.
Investigation of High Energy Electron Showers by the "Emulsion Chamber" Technique. I. M. Gramenitskii—586L.
On the Composition of Primary Cosmic Rays. V. L. Ginzburg and M. I. Fradkin—462L.
On the Mass Spectrum of Charged Cosmic Ray Particles. A. I. Alikhanian, N. V. Shostakovich, A. T. Dadaian, V. N. Fedorov, and B. N. Deriagin— 817
On the Mechanism of Initiation of Boiling of Liquid Metastable Systems by Ionizing Radiation. G. A. Askar' ian—761L.
Solution of the Fundamental Diffusion Equation for Cosmic Ray Particles Emitted by a Constant Energy Concentrated Pulsed Source. Iu. A. Popov—85.
Spatial Distribution of the Particles of Extensive Air Showers Produced by Primary Cosmic Rays of Various Energies. S. P. Dobroval' skii, S. I. Nikol'skii, E. I. Tukish, and V. I. Iakovlev— 799
The Ionization Spectrum of Cosmic Rays 3250 m above Sea Level. A. G. Meshkovskii and L. I. Sokolov—629.
Cosmology (see Relativity and Gravitation)
Critical Potentials (see Atomic Structure and Spectra)
Cross Section (see Electrons and Positrons; Nuclear Reactions; Radiation; Scatter, General)
Crystal Counters (see Methods and Instruments)
Crystalline State (see also Electrical Properties; Magnetic Properties; Semiconductors, etc.)
Application of the Lattice Model to Semiconductors of the Lead Sulphide Type. T. K. Rebane—273L.
Contribution to the Theory of Phase Phenomena in Barium Titanate. L. P. Kholodenko— 847
Contribution to the Thermodynamical Theory of the Ferroelectric Properties of Barium Titanate. L. P. Kholodenko—188.
Dielectric Properties of Bismuth Titanate. G. I. Skanavi and A. I. Demeshina—524.
Discrete Energy Losses of Electrons Reflected from a MoO_2 Surface. N. B. Gornyi—131L.
Invalidity of the Fermi-Dirac Distribution for Electrons of Semiconductor and Crystal Phosphor Impurity Centers. S. I. Pekar—271L.
Many Electron Treatment of Motion of an Electron (Hole) in a Deformed Crystal. II. T. I. Kucher and K. B. Tolpygo— 883
Nuclear Magnetic Relaxation in Ionic Crystals, G. R. Khutsishvili—382.

  - On the Motion of Inclusions in a Solid. A. A. Chernov—585L.
  - Paramagnetic Relaxation in Monocrystals of Some Salts of the Iron Group Elements. T. I. Volokhova—918L
  - Relation between Neutron Scattering in Polycrystals and Specific Heat. M. V. Kazarnovskii—600L
  - Relation between the Parameters of Longitudinal and Transverse Optical Vibrations of Ions in Crystals, M. A. Krivoglaz and S. I. Pekar—286L.
  - Relaxation between Electrons and the Crystalline Lattice.* M. I. Kaganov, I. M. Lifshitz, and L. V. Tanatarov—173.
  - The Crystalline Structure of Hydrogen and Deuterium. V. S. Kogan, B. G. Lazarev, and R. F. Bulatova—593L.
  - The Effect of a Transverse Magnetic Field on the Thermal Conductivity of Metals. Z. Ia. Evseev—440L
  - The Effect of Ordering on the Energy Spectrum of Phonons. I. M. Lifshitz and G. I. Stepanova—151L
  - The Effect of Uniform Compression upon the Magnetic Properties of Bismuth at Low Temperatures. B. I. Verkin, I. M. Dmitrenko, and B. G. Lazarev—432L.
  - The Theory of Galvanomagnetic Effects in Metals. I. M. Lifshitz, M. Ia. Azbel', and M. I. Kaganov—41.
  - The Theory of Galvonomagnetic Phenomena in Semiconductors, M. I. Klinger—831
  - Theory of Classical Systems of Interacting Particles Obeying a Noncentral Interaction Law. I. A. E. Glauberman—169.
  - Theory of Diffuse Scattering of X-rays by Solid Solutions. I. M. A. Krivoglaz—293.
  - Theory of Localized Electron States in an Isotropic Homopolar Crystal. M. F. Deigen—424.
  - Transfer Processes in Conductors with Regard to Nonlinear Effects. V. P. Shabanskii—497.
- **Diamagnetism** (see **Magnetic Properties**)
- **Dielectrics and Dielectric Properties**
  - Contribution to the Theory of Phase Phenomena in Barium Titanate. L. P. Kholodenko—847
  - Contribution to the Thermodynamical Theory of the Ferroelectric Properties of Barium Titanate. L. P. Kholodenko—188.
  - Dielectric Properties of Alkali-Halide Single Crystals. B. N. Matsonashvili—952L
  - Dielectric Properties of Bismuth Titanate. G. I. Skanavi and A. I. Demashina—524.
  - On a Singularity of the Field of an Electromagnetic Wave Propagated in an Inhomogeneous Plasma. N. G. Denisov—544.
  - On the Possibility of Introducing an Effective Dielectric Constant at High Frequencies. E. A. Kaner and M. I. Kaganov—393.
  - Transfer Processes in Conductors with Regard to Nonlinear Effects. V. P. Shabanskii—497.
- **Diffraction**
  - Diffraction Scattering of High Energy Photons by Nuclei. V. B. Berestetskii and E. V. Kuznetsov—610L
  - Thermal Radiation of Good Conductors. M. L. Levin—225.
- **Diffusion**
  - On the Derivation of the Fokker-Planck Equation for a Plasma. S. V. Temko—898
  - On the Motion of Inclusions in a Solid. A. A. Chernov—585L.
- **Electrical Breakdown** (see **Dielectrics and Dielectric Properties; Electrical Discharges**)
- **Electrical Conductivity and Resistance** (see also **Electrical Properties; Semiconductors; Superconductivity**)
  - Dependence of the Life Time of Nonequilibrium Charge Carriers in Germanium on Temperature and Composition. E. I. Adirovich, G. M. Guro, and V. F. Kuleshov—202.
  - Electrical Explosion of Wires in Vacuum. I. F. Kvartskhava, V. V. Bondarenko, R. D. Meladze, and K. V. Suladze—637.
  - Galvanomagnetic Properties of Gold. N. E. Alekseevskii and Iu. P. Gaidukov—807
  - Investigation of the Effect of Pressure on the Galvanomagnetic Properties of Tellurium at Low Temperatures. N. E. Alekseevskii, N. B. Brandt and T. I. Kostina—813
  - On the Possibility of Introducing an Effective Dielectric Constant at High Frequencies. E. A. Kaner and M. I. Kaganov—393.
  - On the Theory of the Hall Effect in Ferromagnetics. N. S. Akulov and A. Cheremushkina—150L.
  - Oscillographic Determination of Energy of Electric Explosion of Wires. I. F. Kvartskhava, V. V. Bondarenko, A. A. Pliutto and A. A. Chernov—623.
  - Peculiarities of the Temperature Dependence of the Electrical Resistance of Ferromagnetic Metals at Low Temperatures. A. I. Sudovtsov and E. E. Semenko—592L.
  - Statistics of Electrons and Holes in a Homopolar Semiconductor Taking Into Account their Interaction with the Lattice Vibrations. V. L. Bonch-Bruevich—196.
  - Surface Electrical Conductivity of Germanium. V. I. Liashenko and T. N. Sitenko—940L.
  - The Theory of Galvanomagnetic Effects in Metals. I. M. Lifshitz, M. Ia. Azbel', and M. I. Kaganov—41.
  - Theory of Isothermal Galvanomagnetic and Thermomagnetic Effects in Semiconductors. F. G. Bass and I. M. Tsidil' kovskii—565.
  - Transfer Processes in Conductors with Regard to Nonlinear Effects. V. P. Shabanskii—497.
- **Electrical Discharges**
  - Electrical Explosion of Wires in Vaccum. I. F. Kvartskhava, V. V. Bondarenko, R. D. Meladze, and K. V. Suladze—637.
  - Nonlinear Theory of Longitudinal Plasma Oscillations. R. V. Polovin—290L.
  - Note on Waves in a Homogeneous Magnetoactive Plasma B. N. Gershman—582.
  - On the Hydrodynamic Description of Plasma Oscilla-

tions. B. B. Kadomtsev—926L.
Oscillographic Determination of Energy of Electric Explosion of Wires. I. F. Kvartskhava, V. V. Bondarenko, A. A. Pliutto, and A. A. Chernov—623.

Electrical Properties (see also Dielectrics and Dielectric Properties; Electrical Conductivity and Resistance; Semiconductors; Superconductivity)
Bipolar Diffusion of Current Carriers in the Presence of Deep Traps. K. B. Tolpygo, and E. I. Rashba—213.
Contribution to the Thermodynamical Theory of the Ferroelectric Properties of Barium Titanate. L. P. Kholodenko—188.
Electrical Explosion of Wires in Vacuum. I. F. Kvartskhava, V. V. Bondarenko, R. D. Meladze, and K. V. Suladze—637.
Galvanomagnetic Properties of Gold. N. E. Alekseevskii and Iu. P. Gaidukov—807.
Investigation of Stability of Electron Motion in Cyclic Accelerators when Quantum Effects are Included. A. A. Sokolov, I. M. Ternov and G. M. Strakhovskii—251.
Investigation of the Angular and Energy Distributions of Secondary Electrons from Cuprous Oxide. N. B. Gornyi—346.
Investigation of the Effect of Pressure on the Galvanomagnetic Properties of Tellurium at Low Temperatures. N. E. Alekseevskii, N. B. Brandt and T. I. Kostina—813.
Note on Waves in a Homogeneous Magnetoactive Plasma. B. N. Gershman—582.
On the Oscillations of an Electron Plasma in a Magnetic Field. A. G. Sitenko and K. N. Stepanov—512.
On the Possibility of Introducing an Effective Dielectric Constant at High Frequencies. E. A. Kaner and M. I. Kaganov—393.
Oscillographic Determination of Energy of Electric Explosion of Wires. I. F. Kvartskhava, V. V. Bondarenko, A. A. Pliutto, and A. A. Chernov—623.
Theory of Isothermal Galvanomagnetic and Thermomagnetic Effects in Semiconductors. F. G. Bass and I. M. Tsidil'kovskii—565.
Transfer Processes in Conductors with Regard to Nonlinear Effects. V. P. Shabanskii—497.

Electrodynamics (see Electromagnetic Theory and Electrodynamics)

Electromganetic Theory and Electrodynamics (see also Microwaves)
Anomalous Magnetic Moments of Nucleons. G. N. Vialov—562.
Interaction between a Moving Current-Carrying Wire and a Conducting Wall. A. I. Morozov—920L.
Investigation of Stability of Electron Motion in Cyclic Accelerators when Quantum Effects are Included. A. A. Sokolov, I. M. Ternov, and G. M. Strakhovskii—251.
Level Shifts in μ-Mesic Hydrogen and the Structure of the Proton. L. M. Afrikian—770L.
On a Singularity of the Filld of an Electromagnetic Wave Propagated in an Inhomogeneous Plasma. N. G. Denisov—544.
On Polarization Effects in the Radiation of an Accelerated Electron. A. A. Sokolov and I. M. Ternov—396.
On the Oscillations of an Electron Plasma in a Magnetic Field. A. G. Sitenko and K. N. Stepanov—512.
On the Possibility of Introducing an Effective Dielectric Constant at High Frequencies. E. A. Kaner and M. I. Kaganov—393.
On the Problem of Unquantized Relativistically Invariant Renormalized Equations for a Three-Dimensional Extended Particle. Iu. M. Shirokov and D. G. Sannikov—13.
Reflection of Waves from an Isotropic Inhomogeneous Layer. A. G. Zharkovskii and O. M. Todes—701.
Synchrotron Oscillations in Strong Focusing Accelerators. I. Linear Theory. L. L. Gol'din and D. G. Koshkarev—681.
The Lagrangian Function for a System of Identically Charged Particles. V. N. Golubenkov and Ia. I. Smorodinskii—442L.
The Photoproduction Cross Section for Positronium in an External Field Taking into Account Radiative Corrections. A. I. Alekseev—771L.
Thermal Radiation of Good Conductors. M. L. Levin—225.
Transformation Properties of the Electron-Positron Field Amplitudes. Iu. A Gol'fand—446L.

Electron Diffraction (see Scattering of Electrons and Positrons)

Electron Optics (see Electromagnetic Theory and Electrodynamics)

Electronic Tubes (see Methods and Instruments)

Electrons and Positrons (see also Electromagnetic Theory and Electrodynamics; Elementary Particle Interactions; Scattering of Electrons and Positrons)
Discrete Energy Losses of Electrons Reflected from a MoO_2 Surface. N. B. Gornyi—131L.
Investigation of High Energy Electron Showers by the "Emulsion Chamber" Technique. I. M. Gramenitskii—586L.
Investigation of Stability of Electron Motion in Cyclic Accelerators when Quantum Effects are Included. A. A. Sokolov, I. M. Ternov and G. M. Strahkovskii—251.
Honizational Slowing Down of High Energy Electron-Positron Pairs. V. B. Berestetskii and I. Ia. Pomeranchuk—609L.
K-Shell Gamma Ray Internal Conversion Coefficients L. A. Sliv and I. M. Band—133L.
Obtiining Polarized Electron Beams. L. N. Rosentsveig—455L.
Parapositronium Annihilation Probability, with Account of the First Radiative Corrections. A. I. Alekseev—261L.

Radiative Corrections to the Scattering of Electrons by Electrons and Positrons. R. V. Polovin—385.
Relaxation between Electrons and the Crystalline Lattice.* M. I. Kaganov, L. M. Lifshitz and L. V. Tanatarov—173.
Showers in Lead Produced by 369 ± 30 MEV electrons. V. G. Ivanov, N. I. Petrov, V.A. Rusakov, Iu. A. Budagov, and V. T. Osipenkov—934L.
The Establishment of Thermal Equilibrium between Quanta and Electrons. A. S. Kompaneets—730.
The Photoproduction Cross Section for Positronium in an External Field Taking into Account Radiative Corrections. A. I. Alekseev—771L.
The Role of Spin in the Radiation from a "Radiating" Electron. A. N. Matveev—409.
Theory of Localized Electron States in an Isotropic Homopolar Crystal. M. F. Deigen—424.
Transformation Properties of the Electron-Positron Field Amplitudes. Iu. A. Golfand—446L.

Electrons, Scattering of (see **Scattering of Electrons and Positrons**)

Electrons, Secondary (see **Electrical Properties**)

Electro-Optical Effects (see **Optical Properties**)

Electrostriction (see **Dielectrics and Dielectric Properties**)

Elemenatry Particle Interactions
A Comparison of the Fermi-Landau Theory with Some Experimental Data on Cosmic Rays. O. A. Guzhavina, V.V.Guzhavin and G. T. Zatsepin—690.
A Note on Mixed Meson Theory. A. D. Galanin and L. I. Lapidus—290L.
A Theorem on the Equality of the Cross Sections for Photoproduction of Charged π-Mesons on Nuclei with Isotopic Spin Zero. V. L. Pokrovskii—459L
Anomalous Magnetic Moments of Nucleons. G. N. Vialov—562.
Concerning the Spin of the Λ°-Particle. M. I. Shirokov-620L.
Consequences of Renormalizability of Pseudoscalar Meson Theory with Two Interaction Constants, V.V. Sudakov and K. A. Ter-Martirosian—763L.
Consequences of Renormalizablity of Quantum Electrodynamics and Meson Theory. V. V. Sudakov–616L.
Contribution to the Theory of π-Meson Disintegration. A. A. Vedenov—268L.
Dispersion Relations for Pions Scattered by Deuterons. B. L. Ioffe, I. Ia. Pomeranchuk, and A. P. Rudik—588L.
Elastic Scattering of 310 MEV π^{+}-Mesons from Protons. E. L. Grigorev and N. A. Mitin—10.
Elastic (p–p) Scattering and Peculiarities of Interaction between Pions and Nucleons. L. M. Soroko—579L.
Energy Dependence of the Fission Width. V. G. Nosov—263L.
Generalized Nonsingular Solutions for the Scalar Meson Field of a Point Charge in General Relativity Theory. Duan'—I–Shi— 935L.
Interaction between Negative Pions and Helium Nuclei at 330 mev energy. M. S. Kozodaev, R. M. Sulaev, A. I. Filippov, and Iu. A. Scherbakov—580L.
Investigation of α-Stars Induced by Negative π-Mesons. S. A. Azimov, U. G. Guliamov, E. A. Zamchalova, M. Nizametdinova, M. I. Podgoretskii, and A. Iuldashev—632.
Interaction of 230–250 mev Negative π-Mesons with Carbon and Lead Nuclei. V. P. Dzhelepov, V. G. Ivanov, M. S. Kozodaev, V. T. Osipenkov, N. I. Petrov, and V. A. Rusakov—864
Investigation of High-Energy Electron Showers by the "Emulsion Chamber" Technique. I. M. Gramenitskii—586L.
Isotopic Invariance and the Creation of Particles, L. I. Lapidus—740.
Level Shifss in μ-Mesic Hydrogen and the Structure of the Proton. L. M. Afrikian—770L.
Measurement of the Ionizing Power of Particles in a Bubble Chamber. G. A. Blinov, Iu. S. Krestnikov and M. F. Lomanov—661.
New Type of Disintegration of a Heavy Meson? O. A. Shakhulov, N. A. Kebuladze, E. A. Andronikashvili, and K. A. Abashidze—281L.
Nuclear Disintegrations Produced by 660 mev Protons in Photographic Emulsions. E. I. Grigor'ev and L. P. Solov'eva—801
On a Rational System of Symbols for Fundamental Particles. Ia. P. Terletskii—575L.
On K $\mu 3$–Decay. S. G. Matinian—434L.
On Quantities with Anomalous Parity and on a Possible Explanation of Parity Degeneracy of K-Mesons. I. M. Gel'fand and M. L. Tsetlin—947L.
On the Absorption of K-Mesons by Helium Nuclei. S. G. Matinian—431L.
On the Mass Spectrum of Charged Cosmic Ray Particles. A. I. Alikhanian, N. V. Shostakovich, A. T. Dadaian, V. N. Fedorov, and B. N. Deriagin—817
On the Problem of Unquantized Relativistically Invariant Renormalized Equations for a Three Dimensional Extended Particle. Iu. M. Shirokov and D. G. Sannikov—13.
On the Theory of the Stripping Reaction. A. G. Sitenko-492.
Parapositronium Annihilation Probability, with Account of the First Radiative Corrections. A. I. Alekseev—261L.
π^{+}-Meson Energy Spectrum for $pp \rightarrow np\, \pi^{+}$ Reaction at 556 and 657 mev. M. G. Meshcheriakov, V. P. Zrelov, B. S. Neganov, I. K. Vzorov, and A. F. Shabudin—60.
Polarization of Neutrons Scattered by Lead. A. I. Baz—259L.
Production of π-Meson Pairs on Nuclei By High Energy γ-Quanta. A. G. Sitenko—269L.
Production of Positive Pions in (p–p) Collisions at 660 mev. V. M. Sidorov—22.

Production of Positive π-Mesons in Various Nuclei by 660 mev Protons. A. G. Meshkovskii, Iu. S. Pligin, Ia. Ia. Shalamov, and V. A. Shebanov—842
Relation between the Angular Distributions of Particles and Their Decay Products. Iu. D. Prokoshkin—618L.
Remarks on the Theory of Scattering of Particles with a Given Total Angular Momentum. V. T. Khoziainov—137L.
Scattering Lengths of Slow Neutrons on Deuterons A. S. Davidov and G. F. Filippov—267L.
Selection Rules for Antiproton Annihilation into π-Mesons. L. M. Afrikian—135L.
The Dynamical Magnetic Moment of the Deuteron. A. M. Korolev—73.
The Polarization of Neutrons from the $D(\gamma, n)$ Reaction. L. N. Rosentsveig—280L.
The Production of Charged Mesons by the Bombardment of Beryllium and Carbon with 660 mev Protons. M. G. Meshcheriakov, I. K. Vzorov, V. P. Zrelov, B. S. Neganov, and A. F. Shabudin—79.
The Scattering of π^+-Mesons on Hydrogen. I. Angular Distributions at Energies of 176, 200, 240, 270, and 307 mev. A. I. Mukhin, E. B. Ozerov, and B. M. Pontecorvo—237.
Theory of Nonlocal Interaction. V. S. Barashenkov—709.
Two-Nucleon Potential of Intermolecular Type and Nuclear Saturation. D. D. Ivanenko and B. K. Kerimov—417.

Elements (see Atomic Mass and Abundance)
Energy Loss of Particles (see Range and Energy Loss)
Energy States of Atoms (See Atomic Structure and Spectra)
Energy States of Nucleus (see Nuclear Reactions; Nuclear Spectra; Nuclear Structure Theory)
Errata
Evaporation (see Liquids)
Excitation of Atoms (see Atomic Structure and Spectra)
Excitation of Nucleus (see Nuclear Reactions; Nuclear Spectra; Nuclear Structure)
Faraday Effect (see Optical Properties)
Ferroelectric Phenomena (see Dielectrics and Dielectric Properties)
Field Emission (see Electrical Properties)
Field Theory (see also Quantum Electrodynamics)
A Bubble Chamber for the Study of Cosmic Rays. E. V. Kuznetsov, M. F. Lomanov, G. A. Blinov, and Chaun Chen-Niang (Kuan Shen-nian)—773L.
A Dispersion Relation for All Scattering Angles. E. S. Fradkin—450L.
A Note on Mixed Meson Theory. A. D. Galanin and L. I. Lapidus—290L.
Anomalous Magnetic Moments of Nucleons. G. N. Vialov—562.
Atomic Self-consistent Field Equations. A. S. Kompaneets and E. S. Pavlovskii—328
Charge Renormalization for an Arbitrary, Not Necessarily Small Value of e_0. K. A. Ter-Martirosian—443L.
Concerning a Certain Possibility in Quantum Field Theory. Iu. M. Lomsadze—754L.
Concerning the Spin of the Λ^0-Particle. M. I. Shirokov—620L.
Consequences of Renormalizability of Pseudoscalar Meson Theory with Two Interaction Constants. V. V. Sudakov and K. A. Ter-Martirosian—763L.
Consequences of Renormalizability of Quantum Electrodynamics and Meson Theory. V. V. Sudakov—616L.
Determination of the Green's Function in the Bloch-Nordsieck Model by Functional Integration. A. V. Svidzinskii—179.
Dispersion Relations for Scattering and Photoproduction. B. L. Ioffe—534.
Generalized Nonsingular Solutions for the Scalar Meson Field of a Point Charge in General Relativity Theory. Duan'-I-Shi—935L.
Investigation of Stability of Electron Motion in Cyclic Accelerators when Quantum Effects are Included. A. A. Sokolov, I. M. Ternov, and G. M. Strakhovskii—251.
Level Shifts in μ-Mesic Hydrogen and the Structure of the Proton. L. M. Afrikian—770L.
Note on the Theorem of Pauli on the Relation of Spin and Statistics. V. L. Pokrovskii and Iu. B. Rumer—264L.
On a Singularity of the Field of an Electromagnetic Wave Propagated in an Inhomogeneous Plasma. N. G. Denisov—544.
On the Construction of the Scattering Matrix. I. Integral Causality Condition in Bogoliubov's Method. B. V. Medvedev—671.
On the Equations of Motion of Finite Masses in the General Theory of Relativity.* M. F. Shirokov and V. B. Bordovskii—904
On the Problem of Unquantized Relativistically Invariant Renormalized Equations for a Three-Dimensional Extended Particle. Iu. M. Shirokov and D. G. Sannikov—13.
Quantum Field Theory with Causal Operators.* Iu. V. Novozhilov—553.
Radiative Corrections to the Scattering of Electrons by Electrons and Positrons. R. V. Polovin—385.
Reduction of Wave Equations for Spin 0 and 1 to the Hamiltonian Form. F. I. Fedorov—139L.
Remarks on Bilocal Field Theory. G. Raiskii—577L.
Remarks on the Theory of Scattering of Particles with a Given Total Angular Momentum. V. T. Khoziainov—137L.
Spectral Representation of Green's Function in the Nonrelativistic Many Body Problem. V. L. Bonch-Bruevich—456L.
The Dynamical Magnetic Moment of the Deuteron. A. M. Korolev—73.

Theory of Nonlocal Interaction. V. S. Barashenkov—709.
Transformation Properties of the Electron-Positron Field Amplitudes. Iu. A. Gol'fand—446L.
Films, Properties
Paramagnetic Resonance and the Polarization of Nuclei in Thick Metal Foils. M. Ia. Azbel', V.I. Gerasimenko, and I. M. Lifshitz—276L.
Surface Electrical Conductivity of Germanium. V. I. Liashenko and T. N. Sitenko—940L.
Fine Structure (see **Atomic Structure and Spectra**)
Fission of Nucleus (see **Nuclear Fission**)
Fluctuation Phenomena (see **Noise**)
Fluid Dynamics
Isentropic Relativistic Gas Flows. F. I. Frankl'—401.
On Light Emission by a Shock Wave Front. Iu. P. Lun'kin and G. I. Mishin—939L.
On the Hydrodynamic Description of Plasma Oscillations. B. B. Kadomtsev—926L.
On the Theory of the Stability of a Layer Located at a Superadiabatic Temperature Gradient in a Gravitational Field. V. N. Gribov and L. E. Gurevich—720.
Temperature Dependence of Viscosity of Liquid Argon. N. F. Zhdanova—749L.
Variational Principles in Hydrodynamics. V. I. Skobelkin—68.
Fluorescence (see **Luminescence**)
Galvanomagnetic Effect (see **Magnetic Properties**)
Gamma Rays
Determination of the Branching Ratio in the Disintegration Scheme of Po^{210}. N. S. Shimanskaia—165.
Diffraction Scattering of High Energy Photons by Nuclei. V. B. Berestetskii and E. V. Kuznetsov—610L.
Gamma Quanta Emitted by I, Rh, and Co Nuclei in Thermal Neutron Capture. I. V. Estulin, L. F. Kalanin and A. S. Melioranskii—752L.
Inelastic Scattering of Photons by Indium-115 Nuclei. O. V. Bogdankevich, L. E. Lazareva, and F. A. Nikolaev—320.
Internal Bremsstrahlung in Electric Monopole $0^+ \to 0^+$ Nuclear Transitions. Iu. V. Orlov—944L.
K-Shell Gamma Ray Internal Conversion Coefficients. L. A. Sliv and I. M. Band—133L.
On the Total Energy of the β-Transition RaC—RaC′. A. V. Kogan and I. A. Sokolov—767L.
Photoprotons from A^{40}. A. P. Komar and I. P. Iavor—432L.
The Photoproduction Cross Section for Positronium in an External Field Taking into Account Radiative Corrections. A. I. Alekseev—771L.
Gases
A Method of Obtaining Nonstationary Solutions of Boltzmann's Kinetic Equation. I. I. Moiseev-Olkhovskii—183.
Dielectric Properties of Bismuth Titanate. G. I. Skanavi and A. I. Demeshina—524.
Measurement of the Saturated Vapor Pressure of a He^3–Ne^4 Mixture with a High He^3 Concentration. V. P. Peshkov and V. N. Kachinskii—607L.
Temperature Dependence of Viscosity of Liquid Argon. N. F. Zhdanova—749L.
Geophysics
Influence of the Earth's Magnetic Field on the Space distribution of Particles in Extensive Air Showers. S. I. Nikol'skii and I. E. Satsevich—589L.
On the Theory of the Stability of a Layer Located at a Superadiabatic Temperature Gradient in a Gravitational Field. V. N. Gribov and L. E. Gurevich—720.
Gravitation (see **Relativity and Gravitation**)
Gyromagnetization (see **Magnetic Properties**)
Hall Effect (see **Electrical Conductivity and Resistance; Semiconductors**)
Helium, Liquid
Density of the Normal Component for Solutions of the Isotopes of Helium. N. G. Berezniak and B. N. Esel'son—766L.
Measurement of the Saturated Vapor Pressure of a He^3–He^4 Mixture with a High He^3 Concentration. V. P. Peshkov and V. N. Kachinskii—607L.
On the Derivation of a Formula for the Energy Spectrum of Liquid He^4. L. P. Pitaevskii—439L.
Some Properties of Rotating He II. B. N. Esel'son, B. G. Lazarev, K. D. Sinel'nikov and A. D. Shvets—774L.
The Coefficient of Volume Absorption of Second Sound and the Viscosity of the Normal Component of Helium II down to 0.83° K. K. N. Zinov'eva—36
High Voltage Tubes and Machines (see **Methods and Instruments**)
Hyperfine Structure (see **Atomic Structure and Spectra; Nulcear Moments and Spin**)
Hyperons (see **Mesons and Hyperons**)
Imperfections in Solids
Invalidity of the Fermi-Dirac Distribution for Electrons of Semiconductor and Crystal, Phosphor Impurity Centers. S. I. Pekar—271L.
Many Electron Treatment of Motion of an Electron (Hole) in a Deformed Crystal. II. T. I. Kucher and K. B. Tolpygo—883
On the Motion of Inclusions in a Solid. A. A. Chernov—584L
Relation between Neutron Scattering in Polycrystals and Specific Heat. M. V. Kazarnovskii—600L.
Transfer Processes in Conductors with Regard to Nonlinear Effects. V. P. Shabanskii—497.
Inelastic Scattering (see **Nuclear Reactions; Scattering**)
Instruments (see **Methods and Instruments**)
Internal Conversion (see **Nuclear Spectra**)

Ionization (see also **Electrical Discharges, Range and Energy Loss of Particles**)
- Dielectric Properties of Bismuth Titanate. G. I. Skanavi and A. I. Demeshina—524.
- Electron Detachment from Negative Halogen Ions in Collisions with Inert-Gas Atoms and Hydrogen Molecules. Iu. F. Bydin and V. M. Dukel'skii—474.
- Interaction between Negative π-Mesons andHelium Nuclei at 330 mev Energy. M. S. Kozodaev, R. M. Sulaev, A. I. Filippov, and Iu. A. Shcherbakov—580L.
- Investigation of Two-Electron Capture in Collisions between Positive Carbon or Oxygen Ions and Gas Molecules. Ia. M. Fogel', R. V. Mitin, and A. G. Kaval'—359.
- Measurement of the Ionizing Power of Particles in a Bubble Chamber. G. A Blinov, Iu. S. Krestnikov and M. F. Lomanov—661.
- On a Singularity of the Field of an Electromagnetic Wave Propagated in an Inhomogeneous Plasma. N. G. Denisov—544.
- On the Mechanism of Initiation of Boiling of Liquid Metastable Systems by Ionizing Radiation. G. A. Askarian—761L.
- The Ionization Spectrum of Cosmic Rays 3250 m above Sea Level. A. G .Meshkovskii and L. I. Sokolov—629.

Ionization Potentials of Atoms (see **Atomic Structure and Spectra**)

Ions (see also **Electrical Discharges**)
- A Possible Application of Cyclotron Resonance to Mass Spectrometry. V. N. Lazukhin—266L.
- Electron Detachment from Negative Halogen Ions in Collisions with Inert-Gas Atoms and Hydrogen Molecules. Iu. F. Bydin and V. M. Dukel'skii—474.
- Investigation of Two-Electron Capture in Collisions between Positive Carbon or Oxygen Ions and Gas Molecules. Ia. Fogel', R. V. Mitin, and A. G. Koval'—359.
- Many-Electron Treatment of Motion of an Electron (Hole) in a Deformed Crystal. II. T. I. Kucher and K. B. Tolpygo—883
- On the Mechanism of Initiation of Boiling of Liquid Metastable Systems by Ionizing Radiation. G. A. Askar'ian —761L.

Ions and Electrons, Mobility
- On the Mechanism of Initiation of Boiling of Liquid Metastable Systems by Ionizing Radiation . G. A. Askar'ian—761L.
- Surface Electrical Conductivity of Germanium. V. I. Liashenko and T. N. Sitenko—940L.

Isobars (see **Atomic Mass and Abundance**)

Isomers, Nuclear (see **Nuclear Spectra**)

Isotopes (see **Atomic Mass and Abundance; Radioactivity**)

Kerr Effect (see **Optical Properties**)

Liquid Helium (see **Helium, Liquid**)

Liquids
- A Bubble Chamber for the Study of Cosmic Rays. E. V. Kuznetsov, M. F. Lomanov, G. A. Blinov, and Chaun Chen-Niang (Kuan Shen-nian)—773L.
- Concerning the Existence of a Transition Layer on a Liquid Surface . V. A. Kizel', and A. F. Stepanov—458L.
- Electron Scattering from Thermal Vibrations in a Liquid. A. I. Gubanov—465.
- On Light Emission by a Shock Wave Front. Iu. P. Lun'kin and G.I. Mishin—939L.
- On the Mechanism of Initiation of Boiling of Liquid Metastable Systems by Ionizing Radiation. G. A. Askar'ian—761L.
- Temperature Dependence of the Viscosity of Liquid Nitrogen at Constant Density. N. F. Zhdanova—19.
- Temperature Dependence of Viscosity of Liquid Argon. N. F. Zhdanova—749L.
- The Coefficient of Volume Absorption of Second Sound and the Viscosity of the Normal Component of Helium II down to 0.83° K. K. N. Zinov'eva —36.
- The Magnetic Field in a Conducting Turbulent Liquid During Two-Dimensional Motion. Ia. B. Zel'dovich—460

Luminescence
- On Polarization Effects in the Radiation of an Accelerated Electron. A. A. Sokolov and I. M. Ternov—396.

Magnetic Fields (see **Electromagnetic Theory and Electrodynamics**)

Magnetic Properties
- Anomalous Magnetic Moments of Nucleons. G. N. Vialov—562.
- Antiferromagnetism of Anhydrous Sulphates of Ni^{++} Fe^{++}, Co^{++}, Cu^{++}. A. S. Borovik-Romanov, V. R. Karasik, and N.M.Kreines—109L.
- Atomic Magnetic Moments of Ferromagnetic Metals and Alloys. F.M. Galperin— 147L.
- Ferromagnetic Superconductors. V. L. Ginzburg—153.
- Galvanomagnetic Properties of Gold. N. E. Alekseevskii, and Iu. P. Gaidukov—807.
- Investigation of the Effect of Pressure on the Galvanomagnetic Properties of Tellurium at Low Temperatures. N.E. Alekseevskii, N. B. Brandt, and T. I. Kostina— 813.
- Magnetic Properties of Cobalt and Manganese Carbonates. A. S. Borovik-Romanov and M. P. Orlova—531.
- On theMagnetization Mechanism of Some NiZn Ferrites in Very Weak Fields—L. A. Fomenko—931L.
- On the Theory of the Hall Effect in Ferromagnetics. N. S. Akulov and A. Cheremushkina—150L.
- Paramagnetic Relaxation in Monocrystals of Some Salts of the Iron Group Elements. T. I. Volokhova—918L.
- Peculiarities of the Temperature Dependence of the Electrical Resistance of Ferromagnetic Metals at Low Temperatures. A. I. Sudovtsov and E. E. Semenko—592L.
- Surface Electrical Conductivity of Germanium. V. I. Liashenko and T. N. Sitenko—940

The Effect of Ordering on the Energy Spectrum of Phonons. I. M. Lifshitz and G. I. Stepanova—151L.
The Effect of Uniform Compression upon the Magnetic Properties of Bismuth at Low Temperatures. B. I. Verkin, I. M. Dmitrenko, and B. G, Lazarev—432L.
The Magnetic Field in a Conducting Turbulent Liquid During Two-Dimensional Motion. Ia. B. Zel'dovich—460
Theory of Isothermal Galvanomagnetic and Thermomagnetic Effects in Semiconductors. F. G. Bass and I. M. Tsidil'kovskii—565.
Transfer Processes in Conductors with Regard to Nonlinear Effects. V. P. Shabanskii—497.

Magnetic Resonance
A Polarization Method for Measuring the Velocities of Particles with Intrinsic Magnetic Moment. S. G. Kornilov—444L.
Hyperfine Structure of the Paramagnetic Resonance Spectrum of $^{53}Cr^{3+}$ in Al_2O_3. A. A. Manenkov and A. M. Prokhorov—288L.
Nuclear Magnetic Relaxation in Ionic Crystals. G. R. Khutshishvili—382.
Paramagnetic Resonance and the Polarization of Nuclei in Thick Metal Foils. M. Ia. Azbel', V. I. Gerasimenko, and I. M. Lifshitz—276L.

Magneto-Optical Effects (see **Optical Properties**)

Magnetoresistance (see **Electrical Conductivity and Resistance; Semiconductors**)

Magnetostriction (see **Magnetic Properties**)

Mass Defects (see **Atomic Mass and Abundance**)

Mass Spectroscopy (see **Atomic Mass and Abundance; Methods and Instruments**)

Mathematical Methods
A Static Solution of the Nonlinear Meson Equation. V. G. Iaichnitsyn—925L.
Atomic Self-consistent Field Equations. A. S. Kompaneets and E. S. Pavlovskii—328
Calculation of Elastic Scattering of Slow Electrons in Hydrogen by the Integral Equation Method—144L.
Electrodynamics of Charged Scalar Particles. I. P. Gor'kov and I. M. Khalatnikov—777
Generalized Phase Analysis as a Corollary of the Unitary Property of the *S*-Matrix. Iu. A. Gol'fand—103.
On a Singularity of the Field of an Electromagnetic Wave Propagated in an Inhomogeneous Plasma. N. G. Denisov—544.
On Distributions in Representation Space. R. L. Stratonovich—891
On Evolution of Continued Integrals. I. M. Gel'fand and N. N. Chentsov—945L.
On Quantities with Anomalous Parity and on a Possible Explanation of Parity Degeneracy of K-Mesons. I. M. Gel'fand and M. L. Tsetlin—947L.
On the Derivation of the Fokker-Planck Equation for a Plasma. S. V. Temko—898
On the Relation between the Distribution of a Quasi-Monochromatic Stationary Process and the Distribution of its Envelope. Ia. I. Likhter—146L.
Perturbation Theory for the One-Dimensional Quantum Mechanical Problem and the Lagrange Method. Ia. B. Zel'dovich—942
Quantum Field Theory with Causal Operators. Iu. V. Novozhilov—553.
Reduction of Wave Equations for Spin 0 and 1 to the Hamiltonian Form. F. I. Fedorov—139L.
Spectral Representation of Green's Function in the Nonrelativistic Many Body Problem. V. L. Bonch-Bruevich—456L.
The Establishment of Thermal Equilibrium between Quanta and Electrons.* A. S. Kompaneets—736.
The Method of Envelopes for Investigating Free Oscillations in Accelerators.* A. M. Baldin, V. V. Mikhailov and M. S. Rabinovich—857
The Photoproduction Cross Section for Positronium in an External Field Taking into Account Radiative Corrections, A. I. Alekseev—771L.
The Three Body Problem for Short Range Forces. II. G. V. Skorniakov—910
Variational Principles in Hydrodynamics. V.I. Skobelkin—68.

Measurements (see **Methods and Instruments**)

Mechanics
Electrical Explosion of Wires in Vacuum. I. F. Kvartskhava, V. V. Bondarenko, R. D. Meladze, and K. V. Suladze—637.
On Theories of Multiple Meson Production. L. G. Iakovlev—141L.
Oscillographic Determination of Energy of Electric Explosion of Wires. I. F. Kvarstkhava, V.V. Bondarenko, A. A. Pliutto and A. A. Chernov—623.

Mechanics, Quantum (see **Quantum Mechanics**)

Mechanics, Quantum—Atomic Structure and Spectra; (see **Atomic Structure and Spectra**)

Mechanics, Quantum—Nuclear; (see **Nuclear Structure Theory**)

Mechanics, Quantum—Of Solid Bodies (see **Crystalline State**)

Mechanics, Statistical (see **Statistical Mechanics and Thermodyanmics**)

Meson Field Theory (see **Field Theory**)

Mesons and Hyperons (see also **Cosmic Radiation; Elementary Particle Interactions; Nuclear Reactions Induced by Mesons; Scattering of Mesons**)
An Analysis of Some Cosmic Ray-Meson-Production Events. II. N. G. Birger, V.V. Guseva, K. A. Kotel'nikov, N. M. Maksimenko, S. V. Riabikov, S. A. Slavatinskii, and G. M. Stashkov—836
A Comparison of the Fermi-Landau Theory with Some Experimental Data on Cosmic Rays. O. A. Guzhavina, V. V. Guzhavin, and G. T. Zatsepin—690.
A Note on Mixed Meson Theory. A. D. Galanin and L. I. Lapidus—290L.
A Quasi-Unidimensional Interpretation of the Hydrodynamic Theory of Multiple Particle Production. I. L. Rozental'—217.
A Static Solution of the Nonlinear Meson Equation.

V. G. Iaichnitsyn—925
A Theorem on the Equality of the Cross Sections for Photoproduction of Charged π-Mesons on Nuclei with Isotopic Spin Zero. V. L. Pokrovskii—459L.
Anomalous Magnetic Moments of Nucleons. G. M. Vialov—562.
Contribution to the Theory of π-Meson Disintegration. A. A. Vedenov—286L.
Correlative Phenomena in K-Meson Capture. V. B. Berestetskii and I. Ia. Pomeranchuk—289L.
Decay of a t'Meson. V. V. Alpers and A. P. Mishakova—768L.
Determination of the Spins of K-Particles and Hyperons. L. I. Lapidus—447L.
Dispersion Relations for Pions Scattered by Deuterons. B. L. Ioffe, I. Ia. Pomeranchuk, and A. P. Rudik—588L.
Dispersion Relations for Scattering and Photoproduction. B. L. Ioffe—534.
Elastic Scattering of 310 MEV π^+-Mesons from Protons. E. L. Grigorov and N. A. Mitin—10.
Energy Dependence of the Fission Width. V. G. Nosov—263L.
γ-γ –Angular Correlation in Transitions of Mesic Atoms. V. A. Dzhebashian—949
Interaction of 5–50 BEV Cosmic Ray Particles with Be Nuclei. I. N. G. Birger, N. L. Grigorov, V. V. Guseva, G. B. Zhdanov, S. A. Slavatinskii, and G. M. Stashkov—872
Interaction of π^-–Mesons with Lead, Copper, Oxygen and Beryllium Nuclei. A. E. Ignatenko, A. I. Mukhin, E. B. Ozerov and B. M. Pontecorvo—351.
Investigation of α –Stars Induced by Negative π-Mesons. S. A. Azimov, U. G. Guliamov, E. A. Zamchalova, M. Nizametdinova, M. I. Podgoretskii, and A. Iuldashev—632.
Isotopic Invariance and the Creation of Particles. L. I. Lapidus—740.
Level Shifts in μ-Mesic Hydrogen and the Structure of the Proton. L. M. Afrikian—770L.
Measurement of the Lifetimes of K-Mesons. M. Ia. Balats, P. I. Lebedev and Iu. V. Obiukov—436L.
Multiple Formation of Particles in 5.3 BEV Nucleon–Nucleon Collisions. V. M. Maksimenko and A. I. Nikishov—614L.
New Type of Disintegration of a Heavy Meson? O. A. Shakhulov, N. A. Kebuladze, E. A. Andronikashvilli and K. A. Abashidze—281L.
Nuclear Disintegrations Produced by 660 MEV Protons in Photographic Emulsions. E. L. Grigorev and L. P. Solov'eva—801
On a Certain Regularity of Decaying Unstable Particles. P. S. Isaev and V. S. Murzin—591L.
On $K_{\mu 3}$–Decay. S. G. Matinian—434L.
On Quantities with Anomalous Parity and on a Possible Explanation of Parity Degeneracy of K-Mesons. I. M. Gel'fand and M. L. Tsetlin—947L.
On the Absorption of K-Mesons by Helium Nuclei. G. Matinian—431L.
On Theories of Multiple Meson Production. L. G. Iakovlev—141L.
Photoproduction of π-Meson Pairs in Hydrogen and Deuterium Near Threshold and Isotopic Invariance. M. V. Dushin—274L.
π^+-Meson Energy Spectrum for $pp \to np\ \pi^+$–Reaction at 556 and 657 MEV. M. G. Meshcheriakov, V. P. Zrelov, B. S. Neganov, I. K. Vzorov, and A. F. Shabudin—60.
Production of Positive Pions in (p–p) Collisions at 660 MEV. V. M. Sidorov—22.
Production of Positive π-Mesons in Various Nuclei by 660 MEV Protons. A. G. Meshkovskii, Iu. S. Pligin, Ia. Ia. Shalamov, and V. A. Shebanov—842
Scattering of π^+ -Mesons by Hydrogen. II. Discussion and Interpretation of the Results. A. I. Mukhin and B. M. Pontecorvo—373.
Selection Rules for Antiproton Annihilation into π-Mesons. L. M. Afrikian—135L.
The Production of Charged Mesons by the Bombardment of Beryllium and Carbon with 660 MEV Protons. M. G. Meshcheriakov, I. K. Vzorov, V. P. Zrelov, B. S. Neganov, and A. F. Shabudin—79.
The Scattering of π^+-Mesons on Hydrogen. I. Angular Distributions at Energies of 176, 200, 240, 270, and 307 MEV. A. I. Mukhin, E. B. Ozerov, and B. M. Pontecorvo—237.
Metals (see Crystalline State)
Metastable Atoms (see Atomic Structure and Spectra)
Methods and Instruments
A Bubble Chamber for the Study of Cosmic Rays. E. V. Kuznetsov, M. F. Lomanov, G. A. Blinov, and Chaun Chen-Niang (Kuan Shen-nian)—773L.
A Method of Investigating of Radial-Phase Oscillations of Electrons in a Synchrotron. Iu. M. Ado—437L.
A New Impulse Technique for Ion Mass Measurements. S. G. Alikhanov—452L.
A Polarization Method for Measuring the Velocities of Particles with Intrinsic Magnetic Moment—S. G. Kornilov—444L.
A Possible Application of Cyclotron Resonance to Mass Spectrometry. V. N. Lazukin—266L.
Direct Measurement of Molecular Attraction of Solid Bodies II. Method for Measuring the Gap. Results of Experiments. I. I. Abrikosova and B. V. Deriagin—2.
Investigation of Stability of Electron Motion in Cyclic Accelerators when Quantum Effects are Included.

A. A. Sokolov, I. M. Ternov and G. M. Strakhovskii—251.
On the Mechanism of Initiation of Boiling of Liquid Metastable Systems by Ionizing Radiation—G. A. Askar'ian—761L.
π^+-Meson Energy Spectrum for $pp \to np\,\pi^+$-Reaction at 556 and 657 MEV. M. G. Meshcheriakov, V. P. Zrelov, B. S. Neganov, I. K. Vzorov and A. F. Shabudin—60.
Production of Positive π-Mesons in Hydrogen by 660 MEV Protons. A. G. Meshkovskii, Iu. S. Pligin, Ia. Ia. Shalamov, and V. A. Shebanov—404.
Synchrotron Oscillations in Strong Focusing Accelerators. I. Linear Theory. L. L. Gol'din and D. G. Koshkarev—681.
The Method of Envelopes for Investigating Free Oscillations in Accelerators.* A. M. Baldin, V. V. Mikhailov and M. S. Rabinovich—857

Microwaves
On the Possivility of Introducing an Effective Dielectric Constant at High Frequencies. E. A. Kaner and M. I. Kaganov—393.

Miscellaneous
Application of the Theory of Random Processes to Radiation Transfer Phenomena. L. M. Biberman and V. A. Veklenko—440L.
Interaction between a Moving Current-Carrying Wire and a Conducting Wall. A. I. Morozov—920L.
Temperature Dependence of Viscosity of Liquid Argon. N. F. Zhdanova—749L.
Two Electron Charge Exchange of α-Particles in Helium. V. I. Gerasimenko and L. N. Rozentsveig—509.

Molecular Aggregates
Direct Measurement of Molecular Attraction of Solid Bodies. II. Method for Measuring the Gap. Results of Experiments. I. I. Abrikosova and B. V. Deriagin—2.

Molecular Structure and Spectra
On Molecular Neutronoscopy. V. I. Gol'danskii—604L.
The HDSe Microwave Spectrum. V. G. Veselago and A. M. Prokhorov—750L.

Moments, Nuclear (see Nuclear Moments and Spin)

Neutrons (see Elementary Particle Interactions)

Noise
Relation between the Distribution of a Quasi-Stationary Process and the Distribution of its Envelope. Ia. I. Likhter—146L.
Synchrotron Oscillations in Strong Focussing Accelerators. I. Linear Theory. L. L. Gol'din and D. G. Koshkarev—681.

Nuclear Fission
Angular Distribution of Uranium Fission Fragments Produced by High-Energy Neutrons. V. I. Ostroumov and N. A. Perfilov—603L.
Connection between α-Decay and Nuclear Deformation. S. G. Ryzhanov—282L.
Heavy Nuclear Fragments from Disintegration Produced by Fast Protons in Nuclear Emulsions.* O. V. Lozhkin and N.A. Perfilov—790
Investigation of Nuclear Energy Levels by Measuring the Angle of Emission of the Reaction Products. A. F. Tulinov—596L.
Mean Excitation Energy of Fissioning Uranium Nuclei on Absorption of Slow π^--Mesons. N. S. Ivanova—597L.
The Cross Section for the Fission of Uranium Induced by High Energy Protons. N. S. Ivanova—365L.
Uranium Fission Induced by High Energy Protons. N. S. Ivanova and I. I. P'ianov—367L.

Nuclear Forces (see Elemenatry Particle Interactions; Field Theory; Nuclear Structure Theory)

Nuclear Induction (see Magnetic Resonance)

Nuclear Moments and Spin
Elastic (pp)—Scattering and Peculiarities of Interaction between Pions and Nucleons. L. M. Soroko—579L.
Investigation of the (d,p) Reaction in Phosphorus and Chlorine. I. B. Teplov—31.
Nuclear Magnetic Relaxation in Ionic Crystals. G. R. Khutsishvili—382.
On the Theory of the Stripping Reaction. A. G. Sitenko—482.
The Dynamical Magnetic Moment of the Deuteron. A. M. Korolev—73.
The Rolé of Spin in the Radiation from a "Radiating" Electron. A. N. Matveev—409.

Nuclear Photoeffects
A Theorem on the Equality of the Cross Sections for Photoproduction of Charged π-Mesons on Nuclei with Isotopic Spin Zero. V. L. Pokrovskii—459L.
Inelastic Scattering of Photons by Indium—115 Nuclei. O. V. Bogdankevich, L. E. Lazareva, and F. A. Nikolaev—320.
K-Shell Gamma Ray Internal Conversion Coefficients. L. A. Sliv and I. M. Band—133L.
μ-Pair Production in Nuclei by Gamma Rays. L. M. Afrikian—933L.
Photoproduction of π-Meson Pairs in Hydrogen and Deuterium Near Threshold and Isotopic Invariance. M. V. Dushin—274L.
Photoprotons from A^{40}. A. P. Komar and I. P. Iavor—432L.
The Internal Compton Effect. E. G. Melikian—930L.
The Photoproduction Cross Section for Positronium in an External Field Taking into Account Radiative Corrections. A. I. Alekseev—771L.
The Polarization of Neutrons from the $D\ (\gamma,n)$ Reaction L. N. Rosentsveig—280L.

Nuclear Reactions, General
A Quasi-Unidimensional Interpretation of the Hydro-

dynamic Theory of Multiple Particle Production. I. L.Rozental'—217.
Elastic (*pp*)–Scattering and Peculiarities of Interaction between Pions and Nucleons. L. M. Soroko—579L.
Inelastic Scattering of Photons by Indium—115 Nuclei. O. V. Bogdankevich, L. E. Lazareva, and F. A. Nikolaev—320.
Interaction between Negative Pions and Helium Nuclei at 330 MEV Energy. M. S. Kozodaev, R. M. Sulaev, A. I. Filippov and Iu A. Shcherbakov—580L.
Interaction of 5–50 BEV Cosmic Ray Particles with Be Nuclei. I. N. G. Birger, N. L. Grigorov, V. V. Guseva, G. B. Zhdanov, S. A. Slavatinskii, and G. M. Stashkov— 872.
Interaction of Nitrogen Nucleus with Nuclei in an Emulsion. D. M. Parfanovich, N. V. Rabin, and A. M. Semchinova—99.
Internal Bremmsstrahlung in Electric Monopole $0^+ \to 0^+$ Nuclear Transition. Iu. V. Orlov— 944L.
Investigation of Nuclear Energy Levels by Measuring the Angle of Emission of the Reaction Products. A. F. Tulinov—596L.
Investigation of the (*d,p*) Reaction in Phosphorus and Chlorine. I. B. Teplov—31.
K-Shell Gamma Ray Internal Conversion Coefficients. L. A. Sliv and I. M. Band—133L.
Multiple Formation of Particles in 5.3 BEV Nucleon-Nucleon Collisions. V. M. Maksimenko and A. I. Nikishov—614L.
On the Theory of the Stripping Reaction. A. G. Sitenko—492.
Production of Positive π-Mesons in Hydrogen by 660 MEV Protons. A. G. Meshkovskii, Iu. S. Pligin, Ia. Ia. Shalamov, and V. A. Shebanov—404.
"Seniority" Quantum Number Selecgion Rules in Nuclear Reactions, V.G. Neudachin—751L.
The Application of Nonself-Adjoint Operators to Scattering Theory. M. S. Livshits—91.

Nuclear Reactions Induced by α-Particles and He^3.
Elastic (*p–p*)–Scattering and Peculiarities of Interaction between Pions and Nucleons. L. M. Soroko—579L.
Investigation of Nuclear Energy Levels by Measuring the Angle of Emission of the Reaction Products: A. F. Tulinov—596L.
Two Electron Charge Exchange of α -Particles in Helium. V. I. Gerasimenko and L. N.Rosentsveig—509.

Nuclear Reactions Induced by Deuterons and Tritons
Dispersion Relations for Pions Scattered by Deuterons. B. L. Ioffe, I. Ia. Pomeranchuk, and A. P. Rudik—588L.
Excitation Function for the Si^{28} (*d,p*) Si^{29} Reaction. Iu. A. Nemilov and V. F. Litvin—606L.
Investigation of Nuclear Energy Levels by Measuring the Angle of Emission of the Reaction Products. A. F. Tulinov—596L.
Investigation of the Be^9 (*dn*) B^{10} Nuclear Reaction V.I. Mamasakhlisov—520.
Investigation of the (*d,p*) Reaction in Phosphorus and Chlorine. I. B. Teplov—31.
Nuclear Interactions with 220 MEV Deuterons. L. P. Solov'eva— 923L.
On the Theory of the Stripping Reaction. A. G. Sitenko—492.
·The Effect of Finiteness of Target-Nucleus Mass on Angular Distribution in (*d,p*) and (*d,n*) Reactions. D. P. Grechukhin—759L.

Nuclear Reactions Induced by Mesons (see also **Elementary Particle Interactions; Scattering of Mesons**)
An Analysis of Some Cosmic Ray Meson-Production Events. II. N.G. Birger, V.V. Guseva, K. A. Kotel' nikov, V. M. Maksimenko, S. V. Riabikov, S. A. Slavatinskii, and G. M. Stashkov— 836.
Interaction of Nitrogen Nucleus with Nuclei in an Emulsion. D. M. Parfanovich, N. V. Rabin, and A. M. Semchinova—99.
On a Certain Regularity of Decaying Unstable Particles. P. S. Isaev and V. S. Murzin—591L.
On the Probabilities of Σ-Particle Decay. L. B. Okun'-—284L.
"Seniority" Quantum Number Selection Rules in Nuclear Reactions. V. G. Neudachin—751L.
Spin-Orbit Interaction in Nuclear Magnetic Multipole Radiation. D. P. Grechukhin—448L.
The Dynamical Magnetic Moment of the Deuteron. A. M. Korolev—73.
The Three Body Problem for Short Range Forces. II. G. V. Skorniakov— 910.
Two-Nucleon Potential of Intermolecular Type and Nuclear Saturation. D. D. Ivanenko and B. K. Kerimov —417.

Optical Instruments (see **Methods and Instruments**)

Optical Properties (see also **Luminescence**)
Concerning the Existence of a Transition Layer on a Liquid Surface. V. A. Kizel', and A. F. Stepanov–458L.
On the Theory of Atomic Semiconductors. A. G. Samoilovich and V. M. Kondratenko—481.
Relation between the Parameter of Longitudinal and Transverse Optical Vibrations of Ions in Crystals. M. A. Krivoglaz and S. I. Pekar—286L.
The Optical Theorem and Elastic Scattering Through Small Angles. L. I. Lapidus— 937L.

Pair Production (see **Electrons and Positrons**)

Phosphors and Phosphorescence (see **Luminescence; Semiconductors**)

Photoconductivity (see **Electrical Conductivity and Resistance**)

Photodisintegration (see **Nuclear Photoeffects**)

Photoelectric Effect (see **Electrical Properties**)

Photography and Photographic Emulsions (see **Method**

and Instruments; Optical Properties)
Photometry (see Methods and Instruments; Optical Properties)
Photons (see Radiation)
Photovoltaic Effect (see Electrical Properties; Semiconductors)
Piezoelectric Effect (see Dielectrics and Dielectric Properties)
Polarization, Electrical (see Dielectrics and Dielectric Properties)
Positrons (see Electrons and Positrons)
Probability (see Mathematical Methods)
Protons (see Elementary Particle Interactions)
Quantum Electrodynamics (see also Field Theory)
Anomalous Magnetic Moments of Nucleons. G. N. Vialov—562.
Atomic Self-consistent Field Equations. A. S. Kompaneets and E. S. Pavlovskii—328.
Charge Renormalization for an Arbitrary, Not Necessarily Small Value of e_0. K. A. Ter-Martirosian—443L.
Compton Effect in the Extended Electron. V. S. Barashenkov—599L.
Concerning a Certain Possibility in Quantum Field Theory. Iu. M. Lomsadze—754L.
Consequences of Renormalizability of Quantum Electrodynamics and Meson Theory. V. V. Sudakov—616L.
Dispersion Relations for Pions Scattered by Deuterons. B. L. Ioffe, I. Ia. Pomeranchuk, and A. P. Rudik—588L.
Level Shifts in μ-Mesic Hydrogen and the Structure of the Proton. L. M. Afrikian—790L.
μ-Pair Production inNuclei by Gamma Rays. L. M. Afrikian—933L.
Multiple Formation of Particlesin 5.3 BEV Nucleon-Nucleon Collisions. V. M. Maksimenko and I. I. Nikishov—614L.
On a Certain Regularity of Decaying Unstable Particles. P. S. Isaev and V. S. Murzin—591L.
On Polarization Effects in the Radiation of an Accelerated Electron. A. A. Sokolov and I. M. Ternov—396.
Radiative Corrections to the Scattering of Electrons by Electrons and Positrons. R. V. Polovin—385.
Scattering of Fast Neutrons by a Nuclear Coulomb Field. Iu. A Aleksandrov and I. I. Bondarenko—612L.
The Internal Compton Effect. E. G. Melikian—930L.
The Photoproduction Cross Section for Positronium in an External Field Taking into Account Radiative Corrections. A. I. Alekseev—771L.
The Role of Spin in the Radiation from a "Radiating" Electron. A. N. Matveev—409.
Theory of Nonlocal Interaction. V. S. Barashenkov—709.
Transformation Properties of the Electron-Positron Field Amplitudes. Iu. A. Gol'fand—446L.
Quantum Mechanics
Anomalous Magnetic Moments of Nucleons. G. N. Vialov—562.
Behavior of Particles with Nonzero Spin in Crossed Constant and Varying Magnetic Fields. A. I. Rivin—619L.
Calculation of Elastic Scattering of Slow Electrons in Hydrogen by the Integral Equation Method—144L.
Concerning the Impulse Approximation. I. M. Shmushkevich—611L.
Concerning the Spin of the Λ°-Particle. M. I. Shirokov—620L.
Investigation of Stability of Electron Motion in Cyclic Accelerators when Quantum Effects are Included. A. A. Sokolov, I. M. Ternov, and G. M. Strakhovskii—251.
On Distributions in Representation Space. R. L. Stratonovich—891
On Quasi-Classical Quantization. V. S. Kudriavtsev—527.
On the Theory of the Stripping Reaction. A. G. Sitenko—492.
PerturbationTheory for the One-Dimensional Quantum Mechanical Problem and the Lagrange Method. Ia. B. Zel'dovich—942L.
Polarization of Nucleons Scattered by Carbon with Account of Nuclear Exchange. N. A. Guliev—142L.
Reduction of Wave Equations for Spin 0 and 1 to the Hamiltonian Form. F. I. Fedorov—139L.
The Application of Nonself-Adjoint Operators to Scattering Theory. M. S. Livshits—91.
The Establishment of Thermal Equilibrium between Quanta and Electrons. A. S. Kompaneets—730.
Dispersion Relations for Pions Scattered by Deuterons. B. L. Ioffe, I. Ia. Pomeranchuk and A. P. Rudik—588L.
Elastic (*pp*)–Scattering andPeculiarities of Interaction between Pions and Nucleons. L. M. Soroko—579L.
Interaction between Negative Pions and Helium Nuclei at 330 MEV Energy. M. S. Kozodaev, R. M. Sulaev, A. I. Filippov and Iu. A. Shcherbakov—580L.
Level Shifts in μ-Mesic Hydrogen and the Structure of the Proton. L. M. Afrikian 770L.
Mean Excitation Energy of Fissioning Uranium Nuclei on Absorption of Slow π^--Mesons. N. S. Ivanova—597L.
On the Absorption of K-Mesons by Helium Nuclei S. G. Matinian—431L.
The Scattering of π^+-Mesons on Hydrogen. I. Angular Distributions at Energies of 170, 200, 240, 270, and 307 MEV. A. I. Mukhin, E. B. Ozerov, and B. M. Pontecorvo—237.
Total Inelastic Cross Sections of 225 ± 10 MEV Negative π-Mesons with C, Al, Cu, Sn and Pb Nuclei. V. G. Ivanov, V. T. Osipenkov, N. I. Petrov, and V. A. Rusakov—922L.
Nuclear Reactions Induced by Neutrons

- A Comparison of the Fermi-Landau Theory with Some Experimental Data on Cosmic Rays. O. A. Guzhavina, V. V. Guzhavin, and G. T. Zatsepin—690.
- Angular Distribution of Uranium Fission Fragments Produced by High-Energy Neutrons. V. I. Ostroumov and N. A. Perfilov—603L.
- Gamma Quanta Emitted by I, Rh, and Co Nuclei in Thermal Neutron Capture. I. V. Estulin, L. F. Kalinin, and A. S. Melioranskii—752L.
- Inelastic Scattering Cross Sections for 2.5 MEV Neutrons. V. I. Strizhak—769L.
- Multiple Formation of Particles in 5.3 BEV Nucleon-Nucleon Collisions. V. M. Maksimenko and A. I. Nikishov—614L.
- On Molecular Neutronoscopy. V. I. Gol'danskii—604L.
- Relative Cross Sections for *n*–*p* Reactions Involving Nuclei with Several Stable Isotopes. V. N. Levkovskii—291L.
- The Theory of Slowing Down of Neutrons. A. Ia. Temkin—757L.

Nuclear Reactions Induced by Protons
- A Comparison of the Fermi-Landau Theory with Some Experimental Data on Cosmic Rays. O. A. Guzhavina, V. V. Guzhavin, and G. T. Zatsepin—690.
- An Analysis of Some Cosmic Ray Meson-Production Events. II. N. G. Birger, V. V. Guseva, K. A. Kotel'nikov, V. M. Maksimenko, S. V. Riabikov, S. A. Slavatinskii, and G. M. Stashkov—836.
- Heavy Nuclear Fragments from Disintegration Produced by Fast Protons in Nuclear Emulsions.* O. V. Lozhkin and N. A. Perfilov—
- Multiple Formation of Particles in 5.3 BEV Nucleon-Nucleon Collisions. V. M. Maksimenko and A. I. Nikishov—614L.
- Nuclear Disintegrations Produced by 660 MEV Protons in Photographic Emulsions. E. L. Grigorev and L. P. Solov'eva—807.
- Production of Positive π-Mesons in Hydrogen by 660 MEV Protons. A. G. Meshkovskii, Iu. S. Pligin, Ia. Ia. Shalamov, and V. A. Shebanov—404.
- Production of Positive π-Mesons in Various Nuclei by 660 MEV Protons. A. G. Meshkovskii, Iu. S. Pligin, Ia. Ia. Shalamov, and V. A. Shebanov—842.
- The Cross Section for the Fission of Uranium Induced By High Energy Protons. N. S. Ivanova—365.
- The Scattering of π^+-Mesons on Hydrogen. I. Angular Distributions at Energies of 176, 200, 240, 270 and 307 MEV. A. I. Mukhin, E. B. Ozerov, and B. M. Pontecorvo—237.
- Uranium Fission Induced by High Energy Protons. N. S. Ivanova and I. I. P'Ianov—367L.

Nuclear Scattering (see **Scattering**)

Nuclear Spectra (see also **Nuclear Reactions; Radioactivity**)
- Alpha Decay of Pu^{240}. L. N. Kondrat'ev, G. I. Novikov, Iu. P. Sobolev, and L. L. Gol'din—645.
- Excitation Function for the Si^{28} (d,p) Si^{29} Reaction. Iu. A. Nemilov and V. F. Litvin—606L.
- Expansion of Single Particle Wave Functions in Functions of the Relative Motion of the Nucleons. A. I. Baz—704.
- *y*—*y*—Angular Correlation in Transitions of Mesic Atoms. V. A. Dzhebashian—949L.
- Gamma Quanta Emitted by I, Rh and Co Nuclei in Thermal Neutron Capture. I. V. Estulin, L. F. Kalinkin, and A. S. Melioranskii—752L.
- Internal Bremsstrahlung in Electric Monopole $0^+ \rightarrow 0^+$ Nuclear Transitions. Iu. V. Orlov—944L.
- Investigation of the $(d.p)$ Reaction in Phosphorus and Chlorine. I. B. Teplov—31.
- On Molecular Neutronoscopy. V. I. Gol'danskii—604L.
- On the Total Energy of the β-Transition RaC—RaC′. A. V. Kogan and I. A. Sokolov—767L.
- "Repulsion" of Nuclear Levels. I. I. Gurevich and M. I. Pevzner—278L.
- Scattering of Fast Neutrons by a Nuclear Coulomb Field. Iu. A. Aleksandrov and I. I. Bondarenko—612L.
- Spin-Orbit Interaction in Nuclear Magnetic Multipole Radiation. D. P. Grechukhin—448L.

Nuclear Structure Theory (see also **Nuclear Reactions; Nuclear Spectra**)
- A Theorem on the Equality of the Cross Sections for Photoproduction of Charged π-Mesons on Nuclei with Isotopic Spin Zero. V. L. Prokrovskii—459L.
- Accuracy of Isobaric Spin for the *lf* 7/2 Shell. V. G. Neudachin—756L.
- Anomalous Magnetic Moments of Nucleons. G. M. Vialov—562.
- Excitation Function for the Si^{28} (d,p) Si^{29} Reaction. Iu. A. Nemilov and V. F. Litvin—606L.
- Excitation of Nuclear Vibrational Levels by Scattering of Fast Neutrons. E. V. Inopin—764L.
- Expansion of Single Particle Wave Functions in Functions of the Relative Motion of the Nucleons. A. I. Baz.—704.
- The Three Body Problem for Short Range Forces. II. G. V. Skorniakov—910.
- The Variational Principle and the Virial Theorem for the Continuous Dirac Spectrum. Iu. V. Novozhilov—928L.

Quenching of Radiation (see **Radiation**)

Radar (see **Methods and Instruments; Radiation**)

Radiation (see also **Range and Energy Loss of Particles**)
- A Calorimetric Determination of the Mean Energy of the β-Spectra of P^{32}, S^{35}, Cu^{64}, W^{185} and Au^{198}. N. S. Shimanskaia—355.
- Application of the Theory of Random Processes to Radiation Transfer Phenomena. L. M. Biberman and

P. A. Veklenko—440L.

Internal Bremsstrahlung in Electric Monopole $0^+ \to 0^+$ Nuclear Transitions. Iu. V. Orlov—949L.

Investigation of Nuclear Energy Levels by Measuring the Angle of Emission of the Reaction Products. A. F. Tulinov—596L.

Investigation of Stability of Electron Motion in Cyclic Accelerators when Quantum Effects are Included. A. A. Sokolov, I. M. Ternov, and G. M. Strakhovskii—251.

On the Composition of Primary Cosmic Rays. V. L. Ginzburg and M. I. Fradkin—462L.

The Role of Spin in the Radiation from a "Radiating" Electron. A. N. Matveev—409.

Thermal Radiation of Good Conductors. M. L. Levin—225.

Radioactivity (see also **Nuclear Spectra**)

A Calorimetric Determination of the Mean Energy of the β-Spectra of P^{32}, S^{35}, Cu^{64}, W^{185}, and Au^{198}. N. S. Shimanskaia—355.

Alpha Decay of Pu^{240}. L. N. Kondrat'ev, G. I. Novikov, Iu. P. Sobolev, and L. L. Gol'din—645.

Determination of the Branching Ratio in the Disintegration Scheme of Po^{210}. N. S. Shimanskaia—165.

On the Probabilities of Σ-Particle Decay. L. B. Okun'—284L.

On the Total Energy of the β-Transition RaC–RaC′. A. V. Kogan and I. A. Sokolov—767L.

Range and Energy Loss of Particles

Elastic (*p–p*)–Scattering and Peculiarities of Interaction between Pions and Nucleons. L. M. Soroko—597L.

Interaction between Negative Pions and Helium Nuclei at 330 MEV Energy. M. S. Kozodaev, R. M. Sulaev, A. I. Filippov, and Iu. A. Shcherbakov—580L.

Interaction of Nitrogen Nucleus with Nuclei in an Emulsion. D. M. Parfanovich, N. V. Rabin, and A. M. Semchinova—99.

Investigation of α-Stars Induced by Negative π-Mesons. S. A. Azimov, U. G. Guliamov, E. A. Zamchalova, M. Nizametdinova, M. I. Podgoretskii, and A. Iuldashev—632.

Investigation of Nuclear Energy Levels by Measuring the Angle of Emission of the Reaction Products. A. F. Tulinov—596L.

Ionizational Slowing Down of High Energy Electron-Positron Pairs. V. B. Berestetskii and I. Ia. Pomeranchuk—609L.

Mean Excitation Energy of Fissioning Uranium Nuclei on Absorption of Slow π^--Mesons. N. S. Ivanova—597L.

Measurement of the Ionizing Power of Particles in a Bubble Chamber. G. A. Blinov, Iu. S. Krestikov and M. F. Lomanov—661.

On the Mass Spectrum of Charged Cosmic Ray Particles. A. I. Alikhanian, N. V. Shostakovich, A. T. Dadaian, V. N. Fedorov, and B. N. Deriagin—817.

Radiative Corrections to the Scattering of Electrons by Electrons and Positrons. R. V. Polovin—385.

The Establishment of Thermal Equilibrium between Quanta and Electrons. A. S. Kompaneets—730.

Rectifiers (see **Electrical Conductivity and Resistance; Semiconductors**)

Relativity and Gravitation

Generalized Nonsingular Solutions for the Scalar Meson Field of a Point Charge in General Relativity Theory, Duan'–I–Shi—935L.

Isentropic Relativistic Gas Flows F. I. Frankl—401.

On the Equations of Motion of Finite Masses in the General Theory of Relativity.* M. F. Shirokov and V. B. Brodovskii—904.

Resistance, Electrical (see **Electrical Conductivity and Resistance**)

Resonance Radiation (see **Radiation**)

Scattering, General (see also **Elementary Particle Interactions; Nuclear Reactions; Range and Energy Loss of Particles**)

A Dispersion Relation for all Scattering Angles. E. S. Fradkin—450L.

Concerning the Impulse Approximation. I. M. Shmushkevich—611L.

Diffraction Scattering of High Energy Photons by Nuclei. V. B. Berestetskii and E. V. Kuznetsov—610L.

Elastic (*p–p*)–Scattering and Peculiarities of Interaction between Pions and Nucleons. L. M. Soroko—579L.

Elastic Scattering of 310 MEV π^+-Mesons from Protons. E. L. Grigorev and N. A. Mitin—10.

Electron Scattering from Thermal Vibrations in a Liquid. A. I. Gubanov—465.

Generalized Phase Analysis as a Corollary of the Unitary Property of the S-Matrix. Iu. A. Gol'fand—103.

Inelastic Scattering Cross Sections for 2.5 MEV Neutrons. V. I. Strizhak—769L.

Interaction between Negative Pions and Helium Nuclei at 330 MEV energy. M. S. Kozodaev, R. M. Sulaev, A. I. Filippov and Iu. A. Shcherbakov—580L.

On the Construction of the Scattering Matrix. I. Integral Causality Condition in Bogoliubov's Method. B. V. Medvedev—671.

On the Damping Theory of Particle Scattering by a Fixed Center. A. A. Sokolov, and B. K. Kerimov—921L.

Remarks on the Theory of Scattering of Particles with a Given Total Angular Momentum. V. T. Khoziainov—137L.

Scattering of π^--Mesons by Hydrogen. II. Discussion and Interpretation of the Results. A. I. Mukhin and

B. M. Pontecorvo—373.
The Application of Nonself-Adjoint Operators to Scattering Theory. M. S. Livshits—91.
The Optical Theorem and Elastic Scattering Through Small Angles. L. I. Lapidus—937L.
The Variational Principle and the Virial Theorem for the Continuous Dirac Spectrum. Iu. V. Novozhilov— 928L.
Theory of Diffuse Scattering of X-Rays by Solid Solutions. I. M. A. Krivoglaz—293.

Scattering of α-Particles
Interaction between Negative Pions and Helium Nuclei at 330 MEV Energy. M. S. Kozodaev, R. M. Sulaev, A. I. Filippov, and Iu. A. Shcherbakov—580L.

Scattering of Deuterons
On the Theory of the Stripping Reaction. A. G. Sitenko—492.
Three Body Problem for Short Range Forces. I. Scattering of Low Energy Neutrons by Deuterons. G. V. Skorniakov and K. A. Ter-Martirosian—646.

Scattering of Electrons and Positrons (see also **Electrons and Positrons**)
Calculation of Elastic Scattering of Slow Electrons in Hydrogen by the Integral Equation Method. V. I. Ochkur, and Iu. V. Petrov—144L.
Radiative Corrections to the Scattering of Electrons by Electrons and Positrons . R. V. Polovin—385.
The Theory of Collisions of Electrons with Atoms. G. F. Drukarev—309.

Scattering of Mesons (see also **Nuclear Reactions Induced by Mesons**)
Concerning the Spin of the Λ°-Particle. M. I. Shirokov—620L.
Dispersion Relations for Pions Scattered by Deuterons. B. L. Ioffe, I. Ia. Pomeranchuk, and A. P. Rudik—588L.
Dispersion Relations for Scattering and Photoproduction. B. L. Ioffe—534.
Elastic $(p-p)$–Scattering and Peculiarities of Interaction between Pions and Nucleons. L. M. Soroko—579L.
Elastic Scattering of 310 MEV π-Mesons from Protons. E. L. Grigor'ev and N. A. Mitin—10.
Interaction between Negative Pions and Helium Nuclei at 330 MEV Energy. M. S. Kozodaev, R. M. Sulaev, A. I . Filippov, and Iu. A. Shcherbakov—580L.
Interaction of π^--Mesons with Lead, Copper, Oxygen, and Beryllium Nuclei. A. E. Ignatenko, A. I. Mukhin, E. B. Ozerov, and B. M. Pontecorvo—351.
Interaction of 230–250 MEV Negative π-Mesons with Carbon and Lead Nuclei. V. P. Dzhelepov, V. G. Ivanov, M. S. Kozodaev, V. T. Osipenkov, N. I. Petrov, and V. A. Rusakov— 864
Isotopic Invariance and the Creation of Particles . L. I. Lapidus—740.
Level Shift in μ-Mesic Hydrogen and the Structure of the Proton. L. M. Afrikian—770L.
On the Damping Theory of Particle Scattering by a Fixed Center. A. A. Sokolov, and B. K. Kerimov—921L.
π^+-Meson Energy Spectrum for $pp \to np\pi^+$ Reaction at 556 and 657 MEV. M. G. Meshcheriakov, V. P. Zrelov, B. S. Neganov, I. K. Vzorov, and A. F. Shabudin—60.
Remarks on the Theory of Scattering of Particles with a Given Total Angular Momentum. V. T. Khoziainov—137L.
Scattering of π^+-Mesons by Hydrogen II. Discussion and Interpretation of the Results. A. I. Mukhin and B. M. Pontecorvo—373.
The Optical Theorem and Elastic Scattering through Small Angles. L. I. Lapidus— 937L.
The Scattering of π^+-Mesons on Hydrogen. I. Angular Distributions at Energies of 176, 200, 240, 270, and 307 MEV. A I. Mukhin, E. B. Ozerov, and B. M. Pontecorvo—237.
Total Inelastic Interaction Cross Sections of 225 ± 10 MEV Negative π-Mesons with C, Al, Cu, Sn and Pb Nuclei. V. G. Ivanov, V. T. Osipenkov, N. I. Petrov, and V. A. Rusakov— 922L.

Scattering of Neutrons (see also **Nuclear Reactions Induced by Neutrons**)
An Investigation of the Elastic Scattering of 590 MEV Neutrons by Neutrons. B. M. Golovin and V. P. Dzhelepov—303.
Elastic Scattering of Neutrons by 580 MEV Protons. Iu. M. Kazarinov and Iu. N. Simonov—161.
Excitation of Nuclear Vibrational Levels by Scattering of Fast Neutrons. E. V. Inopin—764L.
Inelastic Scattering Cross Sections of Nuclei for 2.5 MEV Neutrons. V. I. Strizhak—769L.
Isotopic Invariance and the Creation of Particles . L. I. Lapidus —740.
On the Theory of the Stripping Reaction. A. G. Sitenko—492.
Polarization of Neutrons Scattered by Lead. A. I. Baz—259L.
Polarization of Nucleons Scattered by Carbon with Account of Nuclear Exchange. N. A. Guliev—142L.
Relation between Neutron Scattering in Polycrystals and Specific Heat. M. V. Kazarnovskii—600L.
Scattering Lengths of Slow Neutrons on Deuterons. A. S. Davidov and G. F. Filippov—267L.
Scattering of Fast Neutrons by a Nuclear Coulomb Field. Iu . A. Aleksandrov and I. I. Bondarenko—612L.
The Optical Theorem and Elastic Scattering Through Snall Angles. L. I. Lapidus— 937L.
The Theory of Slowing Down of Neutrons. A. Ia. Tem-

kin—757L.

Scattering of Protons (see also **Nuclear Reactions Induced by Protons**)

Elastic $(p-p)$ –Scattering and Peculiarities of Interaction between Pions and Nucleons. L. M. Soroko—579L.

Isotopic Invariance and the Creation of Particles. L. I. Lapidus—740.

On the Theory of the Stripping Reaction, A. G. Sitenko—492.

π^+-Meson Energy Spectrum for $pp \to n\pi^+$ Reaction at 556 and 657 MEV. M. G. Meshcheriakov, V. P. Zrelov, B. S. Neganov, I. K. Vzorov, and A. F. Shabudin—60.

Polarization of Relativistic Protons in Coulomb Scattering. M. G. Urin and V. N. Mokhov-128.

Polarization of 660 MEV Protons Scattered by Nuclei. M. G. Meshcheriakov, S.B. Nurushev, and G. D. Stoletov—337.

Production of Positive Pions in $(p-p)$ Collisions at 660 MEV. V. M. Siderov—22.

The Optical Theorem and Elastic Scattering Through Small Angles. L. I. Lapidus—937L.

The Production of Charged Mesons by the Bombardment of Beryllium and Carbon with 660 MEV Protons. M. G. Meshcheriakov, I.K. Vzorov, V. P. Zrelov, B. S. Neganov, and A. F. SHabudin—79.

Scattering of Radiation (see **Radiation**)

Scintillation Counters (see **Methods and Instruments**)

Secondary Emission (see **Electrical Properties**)

Semiconductors

Application of the Lattice Model to Semiconductors of the Lead Sulphide Type. T.K. Rebane—273L.

Bipolar Diffusion of Current Carriers in the Presence of Deep Traps. K. B. Tolpygo, and E. I. Rashbov—213.

Dependence of the Life Time of Nonequilibrium Charge Carriers on Germanium on Temperature and Composition. E. I. Adirovich, G. M. Guro, and V. F. Kuleshov—202.

Invalidity of the Fermi-Dirac Distribution for Electrons of Semiconductor and Crystal Phosphor Impurity Centers. S. I. Pekar—271L.

Investigation of the Effect of Pressure on the Galvanomagnetic Properties of Tellurium at Low Temperatures. N. E. Alekseevskii, N. B. Brandt and T. I. Kostina— 813.

On the Theory of Atomic Semiconductors. A. G. Samoilovich and V. M. Kondratenko—481.

Statistics of Electrons and Holes in a Homopolar Semiconductor Taking into Account their Interaction with the Lattice Vibrations. V. L. Bonch-Bruevich—196.

The Effect of Uniform Compression upon the Magnetic Properties of Bismuth at Low Temperatures. B. I. Verkin, I. M. Dmitrenko, and B. G. Lazarev—432L.

The Interaction of an Electron Hole with the Lattice Vibrations in a Homopolar Crystal. K. B. Tolpygo and A. M. Fedorchenko—713.

The Theory of Galvanomagnetic Phenomena in Semiconductors. M. I. Klinger— 831.

Theory of Isothermal Galvanomagnetic and Thermomagnetic Effects in Semiconductors. F. G. Bass and I. M. Tsidil'kovskii—565.

Transfer Processes in Conductors with Regard to Nonlinear Effects. V. P. Shabanskii—497.

Solid State (see **Crystalline State**)

Solutions (see **Liquids**)

Sound (see **Acoustics**)

Spallation (see **Nuclear Reactions**)

Spark Discharge (see **Electrical Discharges**)

Spectra , Atomic (see **Atomic Structure and Spectra**)

Spectra, Nuclear (see **Nuclear Spectra**)

Spectroscopy Technique (see **Methods and Instruments**)

Spinor Fields (see **Field Theory**)

Stark Effect (see **Atomic Structure and Spectra**)

Statistical Mechanics and Thermodynamics)

A Method of Obtaining Nonstationary Solutions of Boltzmann's Kinetic Equation. I. I. Moiseev-Olkhovskii—183.

Application of the Theory of Random Processes to Radiation Transfer Phenomena. L.M. Biberman and B. A. Veklenko—440L.

Contribution to the ThermodynamicalTheory of the Ferro electric Properties of Barium Titanate. L.P. Kholodenko—188.

Effect of Multiple Thermal Ionization on the Specific Heat of Gases. Iu. V.Gaek and B. L. Timan—578L.

On Distributions in Representation Space. R. L. Stratonovich— 891.

On Light Emission by a Shock Wave Front. Iu. P. Lun'kin and G. I. Mishin— 939L.

On the Derivation of the Fokker-Planck Equation for a Plasma. S. V. Temko— 898.

On the Hydrodynamic Description of Plasma Oscillations. B.B. Kadomtsev— 926L.

On the Motion of Inclusions in a Solid. A. A. Chernov—585L.

Relation between Neutron Scattering in Polycrystals and Specific Heat. M.V. Kazarnovskii—600L.

The Establishment of Thermal Equilibrium between Quanta and Electrons. A. S. Kompaneets—730.

Theory of Classical Systems of Interacting Particles Obeying a Noncentral Interaction Law. I. A. E. Glauberman—169.

Transfer Processes in Conductors with Regard to Nonlinear Effects. V. P. Shabanskii—497.

Statistical Methods (see **Mathematical Methods**)

Superconductivity

An Experimental Manifestation of Instability of the Normal Phase in Superconductors. V. L. Ginzburg—594L.

- Critical Currents in Superconducting Tin Films. N. E. Alekseevskii and M. N. Mikheeva— 810.
- Ferromagnetic Superconductors. V. L. Ginzburg—153.
- Structure of the Intermediate State of Superconductors. B. M. Balashova and Iu. V. Sharvin—54.

Thermal Properties
- Antiferromagnetism of Anhydrous Sulphates of Ni^{++} Fe^{++}, Co^{++}, Cu^{++}. A. S. Borovik-Romanov, V. R. Karasik, and N. M. Kreines—1091.
- Electrical Explosion of Wires in Vacuum. I. F. Kvartskhava, V. V. Bondarenko, R. D. Meladze, and K. V. Suladze—637.
- On the Motion of Inclusions in a Solid. A. A. Chernov—585L.
- Oscillographic Determination of Energy of Electric Explosion of Wires. I. F. Kvartskhava, V. V. Bondarenko, A. A. Pliutto, and A. A. Chernov—623.
- Relation between Neutron Scattering in Polycrystals and Specific Heat. V.M. Kazarnovskii—600L.
- The Effect of a Transverse Magnetic Field on the Thermal Conductivity of Metals. Z. Ia. Evseev—440L.
- Theory of Isothermal Galvanomagnetic and Thermomagnetic Effects in Semiconductors. F. G. Bass and I. M. Tsidil'kovskii—565.
- Thermal Radiation of Good Conductors. M. L. Levin—235.
- Transfer Processes in Conductors with Regard to Nonlinear Effects. V.P. Shabanskii—497.

Thermionic Emission (see Electrical Properties)

Thermodynamics (see Statistical Mechanics and Thermodynamics)

Thermoelectric Effect (see Electrical Properties: Semiconductors)

Thermoluminescence (see Luminescence)

Total Cross Sections (see Electrons and Positrons: Nuclear Reactions)

Uncertainty Principle (see Quantum Mechanics)

Vacuum Tubes (see Methods and Instruments)

Viscosity (see Liquids)

Wave Mechanics (see Quantum Mechanics)

Work Function (see Electrical Properties)

X-Rays
- The Crystalline Structure of Hydrogen and Deuterium V. S. Kogan, B. G. Lazarev, and R. F. Bulatova—593L.
- Theory of Diffuse Scattering of X-Rays By Solid Solutions. I. M.A. Krivoglaz—293.

ERRATA TO VOLUME 4

	reads	should read
P. 218, column 2, Eq. (10)	$\ldots\ \xi(\sqrt{3}+2)\,(2-\sqrt{3})$	$\ldots\ \xi^{(\sqrt{2}+2)/(2-\sqrt{3})}\ldots$
P. 219, column 1, Eq. (11)	$\ldots\ (t\,\xi)^{\sqrt{3/2}}\ldots$	$\ldots\ (t\,\xi)]^{\sqrt{3/2}}\ldots$
P. 219, column 1, Eq. (12)	$y^2 = \rho^{2/3}$	$y^2 - \rho^{2/3} \gg 1$
P. 223, column 1, Eq. (45)	$\ldots\ (E_0\mu^{3/4})^{\sqrt{3/4}}$	$\ldots\ (E_0\,\mu^{3/4})^{\sqrt{3}/4}$
P. 223, column 2, Eq. (46)	$\ldots\ \mu^{3\sqrt{3/4}}\ \ldots$	$\ldots\ \mu^{3\sqrt{3/4}}\ \ldots$
P. 225, column 1, 3 lines above Eq. (1.1)	transversality	cross section
P. 225, column 1, 3 lines above Eq. (1.2)	transversality	cross section
P. 256, column 1, Eq. (37)	$\ldots\ \frac{55\sqrt{3}}{48}\ \ldots$	$\ldots\ \frac{55}{\sqrt{3}\,48}\ \ldots$
P. 289, column 2, Eq. (2)		$I=\sum_{n}\frac{1}{2n+1}A_n\sum_{\nu=-n}^{n}\frac{1}{1+i\omega\tau}Y_{n\nu}^{(n_1)}Y_{n\nu}(n_2)$
P. 377, column 1, last line	$\delta_{35}=\eta-21\times\eta^5$	$\delta_{35}-21\,\eta^5$
P. 436–7	Figures 2 and 3 should be exchanged.	
P. 449, column 1, last Eq.	$\ldots\ \mathrm{Y}_{lm\ \varphi\sigma\ \alpha}$	$\ldots\ \mathrm{Y}_{lm}\,\varphi_{\sigma\ \alpha}$
P. 449, column 2, Eq. (12)	$\ldots\ W\,(l,\ j,\ \sigma\,1\ ;\ j)\ldots$	$\ldots\ W\,(l,j,\sigma\,1;\sigma\,j)\ldots$
P. 451, column 1, Eq. (7)	$\ldots\ D^{(1)}_{\alpha\ \beta}\ (\mathrm{p},0,\ \lambda'\ \lambda)=\ldots$	$\ldots\ D^{(1)}_{\alpha\ \beta}\ (p,\omega_0,\lambda',\lambda)=\ldots$
P. 541, column 1, Eq. (28)	$M^{*\ \mathrm{monex}}_{++}$	$M^{*\mathrm{monex}}_{+}$
P. 543, column 2, Eq. (35)	$\ldots\ \int_{\rho^2-\tau^2+l_0^2}$	$\ldots\ \int_{\rho^2<\tau^2+l_0^2}\ldots$

CONTENTS— *continued*

Russian Reference

Letters to the Editor

Paramagnetic Relaxation in Monocrystals of Some Salts of the Iron Group Elements . . . T. I. Volokhova 918 31, 889
Interaction between a Moving Current-Carrying Wire and a Conducting Wall . . . A. I. Morozov 920 31, 1079
On the Damping Theory of Particle Scattering by a Fixed Center . . . A. A. Sokolov and B. K. Kerimov 921 31, 1080
Total Inelastic Interaction Cross Sections of 225 ± 10 mev Negative π-Mesons with C, Al, Cu, Sn, and Pb Nuclei . . . V. G. Ivanov, V. I. Osipenkov, N. I. Petrov, V. A. Rusakov 922 31, 1097
Nuclear Interactions with 220 mev Deuterons . . . L. P. Solov'eva 923 31, 1086
A Static Solution of the Nonlinear Meson Equation . . . V. G. Iaichnitsyn 925 31, 1082
On the Hydrodynamic Description of Plasma Oscillations . . . B. B. Kadomtsev 926 31, 1083
The Variational Principle and the Virial Theorem for the Continuous Dirac Spectrum . . . Iu. V. Novozhilov 928 31, 1084
The Internal Compton Effect . . . E. G. Melikian 930 31, 1088
On the Magnetization Mechanism of Some NiZn Ferrites in Very Weak Fields . . . L. A. Fomenko 931 31, 1092
μ-Pair Production in Nuclei by Gamma Rays . . . L. M. Afrikian 933 31, 1094
Showers in Lead Produced by 360 ± 30 mev Electrons . . . V. G. Ivanov, N. I. Petrov, V. A. Rusakov, Iu. A. Budagov, V. I. Osipenkov 934 31, 1095
Generalized Nonsingular Solutions for the Scalar Meson Field of a Point Charge in General Relativity Theory . . . Duan'–I–Shi 935 31, 1098
The Optical Theorem and Elastic Scattering Through Small Angles . . . L. I. Lapidus 937 31, 1099
On Light Emission by a Shock Wave Front . . . Iu. P. Lun'kin and G. I. Mishiv 939 31, 1105
Surface Electrical Conductivity of Germanium . . . 940 31, 905
Perturbation Theory for the One Dimensional Quantum Mechanical Problem and the Lagrange Method . . . Ia. B. Zel'dovich 942 31, 1101
Internal Bremsstrahlung in Electric Monopole $0^+ \to 0^+$ Nuclear Transitions . . . Iu. V. Orlov 944 31, 1103
The Numerical Calculation of Path Integrals . . . I. M. Gel'fand and N. N. Chentsov 945 31, 1106
On Quantities with Anomalous Parity and on a Possible Explanation of Parity Degeneracy of K-Mesons . . . I. M. Gel'fand and M. L. Tsetlin 947 31, 1107
γ–γ Angular Correlation in Transitions of Mesic Atoms . . . V. A. Dzhrbashiav 949 31, 1090
Dielectric Properties of Alkali-Halide Single Crystals . . . B. N. Matsonashvili 951 31, 1110

SOVIET PHYSICS JETP VOLUME 4, NUMBER 6 JULY, 1957

CONTENTS

Russian Reference

Electrodynamics of Charged Scalar Particles . . . . L. P. Gor'kov and I. M. Khalatnikov 777 31, 1062
Heavy Nuclear Fragments from Disintegration Produced by Fast Protons in Nuclear Emulsions . . . . O. V. Lozhkin and N. A. Perfilov 790 31, 913
Spatial Distribution of the Particles of Extensive Air Showers Produced by Primary Cosmic Rays of Various Energies . . . . S. P. Dobroval'skii, S. I. Nikol'skii, E. I. Tukish and V. I. Iakovlev 799 31, 939
Nuclear Disintegrations Produced by 660 mev Protons in Photographic Emulsions . . . . E. L. Grigor'ev and L. P. Solov'eva 801 31, 932
Galvanomagnetic Properties of Gold . . . . N. E. Alekseevskii and Iu. P. Gaidukov 807 31, 947
Critical Currents in Superconducting Tin Films . . . . N. E. Alekseevskii and M. N. Mikheeva 810 31, 951
Investigation of the Effect of Pressure on the Galvanomagnetic Properties of Tellurium at Low Temperatures . . . . N. E. Alekseevskii, N. B. Brandt and T. I. Kostina 813 31, 943
On the Mass Spectrum of Charged Cosmic Ray Particles . . . . A. I. Alikhanian, N. V. Shostakovich, A. T. Dadaian, V. N. Fedorov, B. N. Deriagin 817 31, 955
The Theory of Galvanomagnetic Phenomena in Semiconductors . . . . M. I. Klinger 831 31, 1055
An Analysis of Some Cosmic Ray Meson-Production Events. II. . . . . N. G. Birger, V. V. Guseva, K. A. Kotel'nikov, V. M. Maksimenko, S. V. Riabikov . . . . S. A. Slavatinskii, and G. M. Stashkov 836 31, 982
Production of Positive π-Mesons in Various Nuclei by 660 mev Protons . . . . A. G. Meshkovskii, Iu. S. Pligin, Ia. Ia. Shalamov and V. A. Shebanov 842 31, 987
On the Theory of Phase Phenomena in Barium Titanate . . . . L. P. Kholodenko 847 31, 1034
The Method of Envelopes for Investigating Free Oscillations in Accelerators . . . . A. M. Baldin, V. V. Mikhailov, M. S. Rabinovich 857 31, 993
Interaction of 230-250 mev Negative π-Mesons with Carbon and Lead Nuclei . . . . . V. P. Dzhelepov, V. G. Ivanov, M. S. Kozodaev, V. T. Osipenkov, N. I. Petrov . . . . and V. A. Rusakov 864 31, 923
Interaction of 5–50 bev Cosmic Ray Particles with BeNuclei. I. . . . . N. G. Birger, N. L. Griogorov, V. V. Guseva, G. B. Zhdanov S. A. Slavatinskii, and . . . . G. M. Stashkov 872 31, 971
Many Electron Treatment of Motion of an Electron (Hole) in a Deformed Crystal . . . . T. I. Kucher and K. B. Tolpygo 883 31, 1002
On Distributions in Representation Space . . . . R. L. Stratonovich 891 31, 1012
On the Derivation of the Fokker-Planck Equation for a Plasma . . . . S. V. Temko 898 31, 1021
On the Equations of Motion of Finite Masses in the General Theory of Relativity . . . . M. F. Shirokov and V. B. Brodovskii 904 31, 1027
The Three Body Problem for Short Range Forces. II. . . . . G. V. Skorniakov 910 31, 1046

(*Contents continued on inside back cover*)